ISSN 1007-9327 (print)
ISSN 2219-2840 (online)

World Journal of *Gastroenterology*

World J Gastroenterol 2024 March 21; 30(11): 1470-1643

Published by Baishideng Publishing Group Inc

World Journal of Gastroenterology

Contents

Weekly Volume 30 Number 11 March 21, 2024

EDITORIAL

REVIEW

MINIREVIEWS

ORIGINAL ARTICLE

Retrospective Study

Clinical Trials Study

World Journal of Gastroenterology

Weekly Volume 30 Number 11 March 21, 2024

Contents

World Journal of Gastroenterology

Weekly Volume 30 Number 11 March 21, 2024

Contents

ABOUT COVER

Editorial Board of *World Journal of Gastroenterology*, David L Morris, MD, FRCS (Ed), Professor, Department of Surgery, University of New South Wales, Sydney 2217, New South Wales, Australia. david.morris@unsw.edu.au

AIMS AND SCOPE

The primary aim of *World Journal of Gastroenterology* (*WJG*, *World J Gastroenterol*) is to provide scholars and readers from various fields of gastroenterology and hepatology with a platform to publish high-quality basic and clinical research articles and communicate their research findings online. *WJG* mainly publishes articles reporting research results and findings obtained in the field of gastroenterology and hepatology and covering a wide range of topics including gastroenterology, hepatology, gastrointestinal endoscopy, gastrointestinal surgery, gastrointestinal oncology, and pediatric gastroenterology.

INDEXING/ABSTRACTING

The *WJG* is now abstracted and indexed in Science Citation Index Expanded (SCIE), MEDLINE, PubMed, PubMed Central, Scopus, Reference Citation Analysis, China Science and Technology Journal Database, and Superstar Journals Database. The 2023 edition of Journal Citation Reports® cites the 2022 impact factor (IF) for *WJG* as 4.3; Quartile category: Q2. The *WJG*'s CiteScore for 2021 is 8.3.

RESPONSIBLE EDITORS FOR THIS ISSUE

NAME OF JOURNAL

World Journal of Gastroenterology

ISSN

ISSN 1007-9327 (print) ISSN 2219-2840 (online)

LAUNCH DATE

October 1, 1995

FREQUENCY

Weekly

PUBLICATION DATE

March 21, 2024

PUBLISHING PARTNER

Shanghai Pancreatic Cancer Institute and Pancreatic Cancer Institute, Fudan University
Biliary Tract Disease Institute, Fudan University

INSTRUCTIONS TO AUTHORS

https://www.wjgnet.com/bpg/gerinfo/204

GUIDELINES FOR ETHICS DOCUMENTS

https://www.wjgnet.com/bpg/GerInfo/287

GUIDELINES FOR NON-NATIVE SPEAKERS OF ENGLISH

https://www.wjgnet.com/bpg/gerinfo/240

PUBLICATION ETHICS

https://www.wjgnet.com/bpg/GerInfo/288

PUBLICATION MISCONDUCT

https://www.wjgnet.com/bpg/gerinfo/208

POLICY OF CO-AUTHORS

https://www.wjgnet.com/bpg/GerInfo/310

ARTICLE PROCESSING CHARGE

https://www.wjgnet.com/bpg/gerinfo/242

STEPS FOR SUBMITTING MANUSCRIPTS

https://www.wjgnet.com/bpg/GerInfo/239

ONLINE SUBMISSION

https://www.f6publishing.com

PUBLISHING PARTNER's OFFICIAL WEBSITE

https://www.shca.org.cn
https://www.zs-hospital.sh.cn

World Journal of Gastroenterology

Submit a Manuscript: https://www.f6publishing.com

World J Gastroenterol 2024 March 21; 30(11): 1470-1474

DOI: 10.3748/wjg.v30.i11.1470

ISSN 1007-9327 (print) ISSN 2219-2840 (online)

EDITORIAL

MicroRNAs in hepatocellular carcinoma treatment: Charting the path forward

Hong T Lin, Antonio F Alvarez Castaneda, Somashekar G Krishna, Khalid Mumtaz

Specialty type: Gastroenterology and hepatology

Provenance and peer review: Unsolicited article; Externally peer reviewed.

Peer-review model: Single blind

Peer-review report's scientific quality classification

Grade A (Excellent): 0
Grade B (Very good): 0
Grade C (Good): C, C, C
Grade D (Fair): 0
Grade E (Poor): 0

P-Reviewer: Huang M, China; Tang H, China

Received: November 21, 2023
Peer-review started: November 21, 2023
First decision: December 25, 2023
Revised: January 10, 2024
Accepted: February 28, 2024
Article in press: February 28, 2024
Published online: March 21, 2024

Hong T Lin, Antonio F Alvarez Castaneda, Somashekar G Krishna, Khalid Mumtaz, Division of Gastroenterology, Hepatology and Nutrition, Department of Medicine, The Ohio State University Wexner Medical Center, Columbus, OH 43210, United States

Corresponding author: Khalid Mumtaz, MBBS, Associate Professor, Doctor, Division of Gastroenterology, Hepatology and Nutrition, Department of Medicine, The Ohio State University Wexner Medical Center, 395 W 12th Ave, Columbus, OH 43210, United States. khalid.mumtaz@osumc.edu

Abstract

MicroRNAs (miRNAs) are recognized for their involvement in the regulation of gene expression and exhibit significant potential in both the prognostic assessment and treatment of hepatocellular carcinoma (HCC). HCC, like other tumors, seldom occurs in isolation; instead, it evolves within a microenvironment featuring oncogenic and tumor-suppressive elements. When combined with suitable delivery vehicles, miRNA technology provides the capability to directly engage with these elements, thereby hindering tumor formation and progression. Ongoing research in this domain holds the promise of enabling a more efficacious and multi-modal treatment approach for HCC in the near future.

Key Words: Hepatocellular carcinoma; Tumor microenvironment; MicroRNA; Mesenchymal stem cell; Exosome

Core Tip: MicroRNAs (miRNAs) constitute a family of molecules with dual roles in both the development and prevention of cirrhosis and hepatocellular carcinoma (HCC). Depending on the type of miRNA and the target of interest, they have the potential to promote or inhibit angiogenesis, facilitate or inhibit immune invasion, and enable or halt cell cycle progression amongst other effects. When paired with safe and effective delivery vehicles, specific miRNAs show promise as targeted therapies for treating HCC. Nonetheless, owing to the intricate interactions within *in vivo* systems and limitations of current retrospective studies, further research is imperative to ensure the safety and efficacy of miRNA in HCC therapy.

Citation: Lin HT, Castaneda AFA, Krishna SG, Mumtaz K. MicroRNAs in hepatocellular carcinoma treatment: Charting the path forward. *World J Gastroenterol* 2024; 30(11): 1470-1474
URL: https://www.wjgnet.com/1007-9327/full/v30/i11/1470.htm
DOI: https://dx.doi.org/10.3748/wjg.v30.i11.1470

INTRODUCTION

Hepatocellular carcinoma (HCC) comprises 75% of primary liver cancers and stands as the third most prevalent cause of cancer-related deaths globally[1,2]. Beyond the immeasurable human toll, HCC inflicts a substantial financial burden and costs the United States healthcare system over $405 million annually[3]. Common triggers for cirrhosis and consequent HCC include excessive alcohol consumption, metabolic syndrome (including metabolic-associated fatty liver disease), hepatitis B virus infection, hepatitis C virus infection, autoimmune liver diseases, and exposure to aflatoxin B1[1].

Until recently, treatment of HCC was rudimentary. Options such as surgical resection, radiofrequency ablation, chemoembolization, systemic therapy, and radiation therapy come with significant potential complications and broad systemic effects. For instance, while procedures such as transcatheter arterial embolization (TAE) and chemoembolization (TACE) have become the treatment of choice for unresectable HCC, they are associated with significant side effects such as hepatic failure and abscess formation, biliary tract disease, and necrotizing pancreatitis[4]. As TAE and TACE trigger hypoxia in embolized regions, they paradoxically stimulate angiogenesis[5] and may potentially worsen the cancer. In the early stages of HCC, surgical resection may be an option. However, this option is limited by recurrence due to inadequate margins and can only be done if a functional liver remnant can be left. Lastly, while liver transplantation offers a cure for cirrhosis and HCC, it is often inaccessible due to delayed diagnoses and graft shortages.

It's now known that factors within tumor macroenvironments and tumor microenvironments (TME) significantly influence the onset, progression, and prognosis of HCC[6]. Cancer, immune, and stromal cells communicate with each other to promote angiogenesis, invasion, and evasion of the body's immune system. This communication takes place through the release of various biologically active molecules (*e.g.*, enzymes, lipoproteins, and nucleic acids) into the TME and the extracellular matrix (ECM). Examples include angiogenesis-promoting factors such as platelet-derived growth factor and vascular endothelial growth factor, as well as various matrix metalloproteinases that remodel the ECM and aid cellular invasion[6].

An intriguing mode of intercellular communication occurs *via* exosomes. These are phospholipid-bound vesicles known for their capacity to transport diverse noncoding RNAs, among other active contents, while shielding them from nucleases and proteases present in the ECM[6,7]. One possible component of exosomes is microRNAs (miRNAs). MiRNAs hold particular interest due to their role in selective gene silencing and are capable of either promoting or inhibiting cancer progression depending on the tissue type, specific sequence, and originating cell[7]. They may prove valuable as biomarkers for diagnosing and prognosticating various cancers, such as HCC, and serve as therapeutic targets. However, much is still unknown about the role of miRNAs in the pathogenesis of cancer and how they are targeted to certain cell types in living systems. While theories have been postulated based on *in vitro* observations, little is known about their validity in *in vivo* systems. Furthermore, more studies are also required to identify other possible miRNAs related to HCC.

SIGNIFICANCE OF MIRNAS

The review paper titled "Function and biomedical implications of exosomal microRNAs delivered by parenchymal and nonparenchymal cells in hepatocellular carcinoma", published in *World Journal of Gastroenterology*, provides a comprehensive exploration of how elements within the TME, particularly exosomal miRNAs, are associated with HCC[8]. Through review of recent literature, it summarizes current understanding regarding the role of miRNAs in promoting, preventing, and predicting the prognosis of HCC.

The development of HCC is linked with loss of tumor suppressive miRNAs (Table 1). The authors commented on the association of deficiency of miR-122 and miR-192 with increased rates of HCC and observed that their restoration in *in vitro* systems resulted in the inhibition of HCC growth and activation, respectively. This is of particular interest because miR-122 has previously been shown to sensitize HCC cells to chemotherapy by inhibiting multidrug resistance-associated genes, the anti-apoptotic gene Bcl-w, as well as the cell cycle-related gene cyclin B1. As such, miR-122 has been classified as a tumor suppressor gene. While the exact mechanism remains unclear, it appears to serve as a regulator and correlates with liver-specific transcription factors such as hepatocyte nuclear factor 4 alpha[9].

The review also discusses the tumor-suppressive role of certain miRNAs. MiR-223, well known for its immune system-modulating activity, plays a distinct role in the pathogenesis of various liver diseases. Upregulation of miR-223 has been shown to protect against alcoholic liver disease (ALD) and metabolic-dysfunction-associated steatohepatitis (MASH). In ALD, it directly inhibits interleukin-6 (IL-6) expression and its downstream target p47phox. This leads to reduced neutrophil infiltration and reactive oxygen species production-factors that are significant drivers of the disease's pathophysiology[10]. In MASH, miR-223 similarly reduces the inflammatory cascade resulting from insults to the liver parenchyma due to metabolic syndrome. In HCC, miR-223 can induce tumor cell apoptosis, inhibit cancer spread, and reduce multidrug resistance through its effects on mammalian target of rapamycin, integrin αV, and multidrug resistance

Table 1 Current understanding of pro- and anti-tumor microRNAs in hepatocellular carcinoma and brief descriptions of their effects

MicroRNAs of interest in hepatocellular carcinoma		
Prevents HCC	**Dual influence**	**Promotes HCC**
miR-122 - inhibits HCC growth and enhances tumor cell susceptibility to chemotherapy	miR-192 - suppresses tumor when acting on the PABPC4 and TRIP13 genes. Promotes tumor when acting on SEMA3A	miR-155 - role in promoting inflammation and tumor growth through unclear mechanisms
miR-223 - anti-inflammatory effects and role in resolution of liver fibrosis		miR-21 - stimulates cancer-associated fibroblasts
miR-335-5p - inhibition of tumor growth and invasion		miR-20a-5p - suppresses expression of tumor suppressors
miR-320a - blocks activation of MAPK pathway		miR-103 - facilitates tumor metastasis by damaging the integrity of endothelial junctions
miR-150-3p - suppresses tumor migration and invasion		miR-210 - derived from HCC cells. Promotes angiogenesis
miR-214 - suppresses angiogenesis		miR-93-5p - facilitates HCC progression *via* inducing immune evasion
miR-148a-3p - inhibits HCC proliferation and invasiveness		miR-107 - promotes HCC progression by increasing epithelial-to-mesenchymal transition (however, this notably seems to act as a tumor suppressor in head and neck squamous cell carcinoma)
		miR-4739 - associated with poor HCC prognosis. Unclear mechanism

HCC: Hepatocellular carcinoma; PABPC4: Poly-A binding protein cytoplasmic 4; TRIP13: Thyroid receptor-interacting protein 13; SEMA3A: Semaphorin 3A.

protein 1 (MDRP1 or ABCB1)[11].

Oncogenic miRNAs have been discussed in this article as well as in previous literature. They exert their effects through a multitude of routes. Examples include promotion of angiogenesis or loss of epithelial cell polarity (*e.g.*, miR-210 and miR-107), immune evasion (*e.g.*, miR-93-5p), and through unknown mechanisms (*e.g.*, miR-4739)[8,12,13]. As will be discussed later, many of these miRNAs will have relevant interactions with other proteins as well.

Moreover, some miRNAs have been shown to exhibit both tumor suppressor and oncogene roles, with miR-192 serving as a key example. While miR-192 has demonstrated anti-tumor properties through its effect on the poly-A binding protein cytoplasmic 4 (PABPC4) and thyroid receptor-interacting protein 13 (TRIP13) genes, it has also been shown to function as an oncogene by inhibiting semaphorin 3A (SEMA3A), an inhibitor of tumor angiogenesis[14]. Thus, while this review paper proposes the administration of miR-192 as a therapy for HCC, further research is required to selectively target this molecule to the PABPC4 or TRIP13 genes rather than SEMA3A. Moreover, miR-192 has been found to have both beneficial and harmful effects on different organ systems, highlighting the need for careful consideration when selecting an appropriate delivery vehicle and target.

The authors further describe the prognostic role of specific miRNAs in the early detection of HCC. For instance, the deficiency of exosomal miR-122 has been observed in patients with ALD, MASH, and HCC. Conversely, levels of other miRNAs such as miR-155 are elevated in patients with ALD, autoimmune hepatitis, and HCC. Another miRNA, miR-34a, has been associated with cirrhosis and HCC progression[8]. As additional prognostic miRNAs are identified, their use in calculating HCC pre-test probability may be explored.

Several limitations in the cited studies are acknowledged in this article, including the inconsistency in experimental subjects and varied study designs. Also recognized is the low targeting efficacy and durability of exosomal systems when used for treatment. Other limitations of miRNA treatment include the lack of testing in *in vivo* systems, the potential toxicity of certain targeting systems, and the unintended silencing or activation of other genes. Additionally, there are immune-related implications of miRNA therapy. Systemic and poorly targeted miRNA infusion may trigger the release of cytokines and interferons *via* the activation of toll-like receptors[15].

Discussion of the therapeutic possibilities of miRNAs would not be complete without acknowledgment of the importance of delivery vehicles. Mesenchymal stem cells (MSCs) are multipotent stem cells and integral components of the TME. They are present in various locales such as the skin, bone marrow, intestines, adipose tissue, lungs, and liver. While they may serve both oncogenic and tumor-suppressive roles when acting on different pathways, MSCs have been shown to exhibit chemotactic abilities and the capability to migrate with signals such as chemokine ligand 15, tumor growth factor β, macrophage inflammatory protein 1δ (MIP-1δ), and MIP-3α[16]. When loaded with miRNAs like MiR-122, exosomes derived from MSCs offer unique vehicles for targeting HCC cells to inhibit growth and sensitize them to chemotherapy.

Concerns regarding the safety and effectiveness of exosome therapy are valid; the long-term side effects are unclear and there have been reports of infection and contamination with unapproved regenerative therapy in the United States. However, these adverse events were likely secondary to the stem cells carried within the exosomes as well as improper preparation and poor selection of surface targeting ligands. Multiple regulated small-scale studies on exosomal delivery systems have shown positive outcomes with a favorable side effect profile[17,18]. Exosomes are structurally simple and

are relatively inert as they are composed of lipids already present within cells. The imperative will be to determine a way of effectively synthesizing them in large volumes and to identify effective targeting ligands to selectively transport them to the desired location.

CONCLUSION

The field of molecular medicine, coupled with our deepening understanding of miRNAs, holds significant promise for the future of HCC treatment. As discussed above, specific miRNAs are found to have an association with tumor suppression and oncogenesis. Other miRNAs may individually have either tumor suppressive or tumor-promoting effects depending on the target that they are acting on. Future research in multifactorial *in vivo* systems, perhaps with miRNA epitope tagging, would assist in delineating the pathways and targets responsible for these effects. Further knowledge in this area would prove highly applicable to the selection of therapeutic miRNAs as well as an appropriate delivery vehicle. Another avenue of exploration may encompass interactions between miRNAs and other cellular proteins. For example, H19 (a long non-coding RNA) and circGPR37B (a circular RNA) have shown promise in reducing the effects of oncogenic miRNAs such as miR-107 and miR-4739, respectively[12,13].

Additionally, most of the clinical studies cited in the in-press article by Wang *et al*[8] are retrospective in nature, which makes them inherently susceptible to biases in case selection (*e.g.*, subclinical HCC may have differing levels of association with certain miRNAs). They also offer weaker causal relationships (*e.g.*, does increased expression of a miRNA increase the risk for HCC, or does HCC development cause an increase in the miRNA). Future prospective studies in patients with high HCC risk factors may provide a resource-effective avenue for investigating the role of miRNAs.

MiRNAs offer the potential to become valuable tools for HCC prognosis, diagnosis, and clinical risk assessment. By comprehending their multifaceted roles, we can manipulate specific miRNAs to mitigate and combat tumors. When integrated with an enhanced understanding of MSC and exosome systems, miRNA infusions may be used either independently or in conjunction with existing HCC treatment modalities to improve treatment outcomes. For example, manipulation of miRNAs involved in the promotion or inhibition of angiogenesis, such as miR-214 and miR-210, may offer a remedy for the paradoxical angiogenesis associated with embolization procedures as noted above. Similarly, the application of miRNAs involved in tumor growth may allow for neoadjuvant debulking and improve the success rate of surgical resection.

Ongoing research is crucial to address these knowledge gaps and assess the safety of miRNAs within intricate, complex *in vivo* systems. As we continue to unlock the potential of miRNAs and molecular medicine, we stand on the cusp of transforming the landscape of HCC treatment, offering new hope and possibilities for patients facing this deadly disease.

FOOTNOTES

Author contributions: Lin HT, Castaneda AFA, Krishna SG, and Mumtaz K have all contributed significantly to the writing of the manuscript; and all authors have read and approved the final manuscript.

Conflict-of-interest statement: All the authors report no relevant conflicts of interest for this article.

Country/Territory of origin: United States

ORCID number: Hong T Lin 0000-0002-1888-2860; Somashekar G Krishna 0000-0001-5748-7890; Khalid Mumtaz 0000-0001-7868-6514.

S-Editor: Wang JJ
L-Editor: A
P-Editor: Cai YX

REFERENCES

1 **McGlynn KA**, Petrick JL, El-Serag HB. Epidemiology of Hepatocellular Carcinoma. *Hepatology* 2021; **73** Suppl 1: 4-13 [PMID: 32319693 DOI: 10.1002/hep.31288]

2 **Ghouri YA**, Mian I, Rowe JH. Review of hepatocellular carcinoma: Epidemiology, etiology, and carcinogenesis. *J Carcinog* 2017; **16**: 1 [PMID: 28694740 DOI: 10.4103/jcar.JCar_9_16]

3 **Aly A**, Ronnebaum S, Patel D, Doleh Y, Benavente F. Epidemiologic, humanistic and economic burden of hepatocellular carcinoma in the USA: a systematic literature review. *Hepat Oncol* 2020; **7**: HEP27 [PMID: 32774837 DOI: 10.2217/hep-2020-0024]

4 **Tu J**, Jia Z, Ying X, Zhang D, Li S, Tian F, Jiang G. The incidence and outcome of major complication following conventional TAE/TACE for hepatocellular carcinoma. *Medicine (Baltimore)* 2016; **95**: e5606 [PMID: 27930585 DOI: 10.1097/MD.0000000000005606]

5 **Pleguezuelo M**, Marelli L, Misseri M, Germani G, Calvaruso V, Xiruochakis E, Manousou P, Burroughs AK. TACE versus TAE as therapy for hepatocellular carcinoma. *Expert Rev Anticancer Ther* 2008; **8**: 1623-1641 [PMID: 18925854 DOI: 10.1586/14737140.8.10.1623]

6 **Anderson NM**, Simon MC. The tumor microenvironment. *Curr Biol* 2020; **30**: R921-R925 [PMID: 32810447 DOI: 10.1016/j.cub.2020.06.081]

7 **Dai J**, Su Y, Zhong S, Cong L, Liu B, Yang J, Tao Y, He Z, Chen C, Jiang Y. Exosomes: key players in cancer and potential therapeutic strategy. *Signal Transduct Target Ther* 2020; **5**: 145 [PMID: 32759948 DOI: 10.1038/s41392-020-00261-0]

8 **Wang HC**, Yin WX, Jiang M, Han JY, Kuai XW, Sun R, Sun YF, Ji JL. Function and biomedical implications of exosomal microRNAs delivered by parenchymal and nonparenchymal cells in hepatocellular carcinoma. *World J Gastroenterol* 2023; **29**: 5435-5451 [PMID: 37900996 DOI: 10.3748/wjg.v29.i39.5435]

9 **Jopling C**. Liver-specific microRNA-122: Biogenesis and function. *RNA Biol* 2012; **9**: 137-142 [PMID: 22258222 DOI: 10.4161/rna.18827]

10 **Li M**, He Y, Zhou Z, Ramirez T, Gao Y, Ross RA, Cao H, Cai Y, Xu M, Feng D, Zhang P, Liangpunsakul S, Gao B. MicroRNA-223 ameliorates alcoholic liver injury by inhibiting the IL-6-p47(phox)-oxidative stress pathway in neutrophils. *Gut* 2017; **66**: 705-715 [PMID: 27679493 DOI: 10.1136/gutjnl-2016-311861]

11 **Ye D**, Zhang T, Lou G, Liu Y. Role of miR-223 in the pathophysiology of liver diseases. *Exp Mol Med* 2018; **50**: 1-12 [PMID: 30258086 DOI: 10.1038/s12276-018-0153-7]

12 **Nokkeaw A**, Thamjamrassri P, Chantaravisoot N, Tangkijvanich P, Ariyachet C. Long non-coding RNA H19 promotes proliferation in hepatocellular carcinoma cells *via* H19/miR-107/CDK6 axis. *Oncol Res* 2023; **31**: 989-1005 [PMID: 37744274 DOI: 10.32604/or.2023.030395]

13 **Dong ZR**, Cai JB, Shi GM, Yang YF, Huang XY, Zhang C, Dong RZ, Wei CY, Li T, Ke AW, Fan J. Oncogenic miR-93-5p/Gal-9 axis drives CD8 (+) T-cell inactivation and is a therapeutic target for hepatocellular carcinoma immunotherapy. *Cancer Lett* 2023; **564**: 216186 [PMID: 37105392 DOI: 10.1016/j.canlet.2023.216186]

14 **Ren FJ**, Yao Y, Cai XY, Fang GY. Emerging Role of MiR-192-5p in Human Diseases. *Front Pharmacol* 2021; **12**: 614068 [PMID: 33708127 DOI: 10.3389/fphar.2021.614068]

15 **Segal M**, Slack FJ. Challenges identifying efficacious miRNA therapeutics for cancer. *Expert Opin Drug Discov* 2020; **15**: 987-992 [PMID: 32421364 DOI: 10.1080/17460441.2020.1765770]

16 **Zhang X**, Li N, Zhu Y, Wen W. The role of mesenchymal stem cells in the occurrence, development, and therapy of hepatocellular carcinoma. *Cancer Med* 2022; **11**: 931-943 [PMID: 34981659 DOI: 10.1002/cam4.4521]

17 **Muthu S**, Bapat A, Jain R, Jeyaraman N, Jeyaraman M. Exosomal therapy-a new frontier in regenerative medicine. *Stem Cell Investig* 2021; **8**: 7 [PMID: 33969112 DOI: 10.21037/sci-2020-037]

18 **Nazari H**, Alborzi F, Heirani-Tabasi A, Hadizadeh A, Asbagh RA, Behboudi B, Fazeli MS, Rahimi M, Keramati MR, Keshvari A, Kazemeini A, Soleimani M, Ahmadi Tafti SM. Evaluating the safety and efficacy of mesenchymal stem cell-derived exosomes for treatment of refractory perianal fistula in IBD patients: clinical trial phase I. *Gastroenterol Rep (Oxf)* 2022; **10**: goac075 [PMID: 36518984 DOI: 10.1093/gastro/goac075]

World Journal of Gastroenterology

Submit a Manuscript: https://www.f6publishing.com

World J Gastroenterol 2024 March 21; 30(11): 1475-1479

DOI: 10.3748/wjg.v30.i11.1475

ISSN 1007-9327 (print) ISSN 2219-2840 (online)

EDITORIAL

Innovative pathways allow safe discharge of mild acute pancreatitis from the emergency room

Darshan J Kothari, Sunil G Sheth

Specialty type: Gastroenterology and hepatology

Provenance and peer review: Invited article; Externally peer reviewed.

Peer-review model: Single blind

Peer-review report's scientific quality classification

Grade A (Excellent): 0
Grade B (Very good): B
Grade C (Good): 0
Grade D (Fair): 0
Grade E (Poor): 0

P-Reviewer: Liu C, China

Received: November 27, 2023
Peer-review started: November 27, 2023
First decision: January 5, 2024
Revised: January 22, 2024
Accepted: February 27, 2024
Article in press: February 27, 2024
Published online: March 21, 2024

Darshan J Kothari, Division of Gastroenterology, Duke University Medical Center, Durham, NC 27710, United States

Sunil G Sheth, Division of Gastroenterology & Hepatology, Beth Israel Deaconess Medical Center, Harvard Medical School, Boston, MA 02215, United States

Corresponding author: Sunil G Sheth, AGAF, FACG, FASGE, MBBS, MD, Associate Professor, Division of Gastroenterology & Hepatology, Beth Israel Deaconess Medical Center, Harvard Medical School, 330 Brookline Ave, Boston, MA 02215, United States.
ssheth@bidmc.harvard.edu

Abstract

Acute pancreatitis (AP) is a leading cause of gastrointestinal-related hospitalizations in the United States, resulting in 300000 admissions per year with an estimated cost of over $2.6 billion annually. The severity of AP is determined by the presence of pancreatic complications and end-organ damage. While moderate/severe pancreatitis can be associated with significant morbidity and mortality, the majority of patients have a mild presentation with an uncomplicated course and mortality rate of less than 2%. Despite favorable outcomes, the majority of mild AP patients are admitted, contributing to healthcare cost and burden. In this Editorial we review the performance of an emergency department (ED) pathway for patients with mild AP at a tertiary care center with the goal of reducing hospitalizations, resource utilization, and costs after several years of implementation of the pathway. We discuss the clinical course and outcomes of mild AP patients enrolled in the pathway who were successfully discharged from the ED compared to those who were admitted to the hospital, and identify predictors of successful ED discharge to select patients who can potentially be triaged to the pathway. We conclude that by implementing innovative clinical pathways which are established and reproducible, selected AP patients can be safely discharged from the ED, reducing hospitalizations and healthcare costs, without compromising clinical outcomes. We also identify a subset of patients most likely to succeed in this pathway.

Key Words: Emergency department; Mild pancreatitis; Pathways; Hospitalization; Predictors

Core Tip: In this editorial we review the outcomes of an emergency department (ED) pathway for patients with mild acute pancreatitis. The goal of the pathway is to reduce hospitalizations, prevent iatrogenic complications and reduce costs, without affecting readmission rates or mortality. We discuss the clinical course and outcomes of mild acute pancreatitis patients enrolled in the pathway who were successfully discharged from the ED compared to those who were admitted to the hospital, and identify predictors of successful ED discharge to select patients who can potentially be triaged to the pathway.

Citation: Kothari DJ, Sheth SG. Innovative pathways allow safe discharge of mild acute pancreatitis from the emergency room. *World J Gastroenterol* 2024; 30(11): 1475-1479
URL: https://www.wjgnet.com/1007-9327/full/v30/i11/1475.htm
DOI: https://dx.doi.org/10.3748/wjg.v30.i11.1475

INTRODUCTION

Acute pancreatitis (AP) is an inflammatory condition of the pancreas caused by the activation of pancreatic enzymes resulting in digestion of the pancreatic parenchyma. Patients typically present with acute onset epigastric abdominal pain with nausea and vomiting[1]. Diagnosis of AP requires two of the following three criteria: (1) Classic abdominal pain; (2) serum amylase or lipase that is greater than three times the upper limit of normal; and/or (3) radiographic evidence of pancreatic inflammation. Further, severity of AP is determined by the presence of peripancreatic complications and/or end-organ damage (*i.e.*, renal failure, respiratory failure or altered mental status)[2,3]. Studies report that patients with severe AP can have a mortality of nearly 30% during the hospitalization however account for less than 25% of all AP. Conversely, the majority of patients with AP have mild presentations and generally have a low mortality rate[1].

MAIN TEXT

In the United States, the most common cause of AP is gallstones followed by alcohol use and contributes to nearly 300000 hospital admissions per year amounting to approximately $2.6 billion in aggregate costs per year[4]. Over the past two decades, the incidence of AP has increased amongst hospitalized patients with an estimated annual incidence ranging from 68 to 81 per 100000 persons[5]. Furthermore, despite the low mortality rate for patients with mild AP, traditionally, patients with mild AP are hospitalized with length of stay (LOS) of up to 3 d to 7 d[6-8]. Thus, patients with AP contribute to significant health care costs per year and opportunity exists to streamline care for patients with mild AP.

In an effort to reduce healthcare costs, Emergency Departments (ED) implement clinical pathways for common chief complaints and clinical conditions to streamline care. The goal of these pathways is to provide high-level care and identify those patients who need admission *vs* those who can be stabilized and safely discharged with outpatient management. Examples include chest pain with acute coronary syndromes, asthma, atrial fibrillation, seizures, congestive heart failure, hyperglycemia including diabetic ketoacidosis, and chronic obstructive pulmonary disease. In these scenarios, pathways include specialists that help direct care but also a direct transition to outpatient follow up. These pathways became the mainstay of therapy during the coronavirus disease 2019 pandemic when EDs were overcrowded and hospital beds were scarce. In these times, other conditions that were typically managed with admission were managed with ED stabilization and close outpatient follow up[9-16].

The traditional dogma for AP management includes hospital admission for fluid resuscitation, bowel rest, symptom management, and risk mitigation for recurrence (*i.e.*, cholecystectomy for biliary pancreatitis and alcohol cessation resources for alcoholic pancreatitis)[1,2]. Over the decades, studies and guidelines advance this management to improve care and reduce hospital LOS. Specifically, the American Gastroenterological Association (AGA) guidelines for early management of AP published in 2018 specifically advocate for goal directed fluid resuscitation and oral solid diet within 24 h of presentation[17]. Streamlined protocols in AP are aimed at reducing LOS and health care costs[18-21]. Some studies have explored the effect of such pathways on patient outcomes including mortality, sepsis, and LOS[22-25]. One study using a combined paging alert and web-based clinical decision-making tool and demonstrated a reduction in LOS and included all patients with AP regardless of severity and local complications[25]. Finally, with greater support for judicious use of fluids, as published in Waterfall trial in 2022, there is greater evidence to support streamlined care[26].

Furthermore, a 2014 Turkish study demonstrated that patients with mild AP could be safely discharged from the ED with intensive in-home therapy without a difference in readmission rates and with lower charges[27]. Although a novel approach, most health systems are not able to provide intensive home care and thus these results are not generalizable to most. Further, this study eliminated alcoholic pancreatitis, an important etiology to consider for United States patients. Given the low mortality rates for mild AP and accurate prediction scoring systems to identify patients with mild AP, patients with low-risk AP could potentially be managed safely within the confines of the ED with close outpatient follow up.

In a study published in 2018, we developed a clinical pathway for patients with mild AP with the aim to determine the feasibility of managing these patients in the ED with discharge after stabilization rather than admission[28]. The clinical pathway isolated patients with the mildest form of AP by excluding those with confirmed moderately-severe or severe AP, patients with persistent systemic inflammatory response, severe hyperglycemia, evidence of cholangitis or

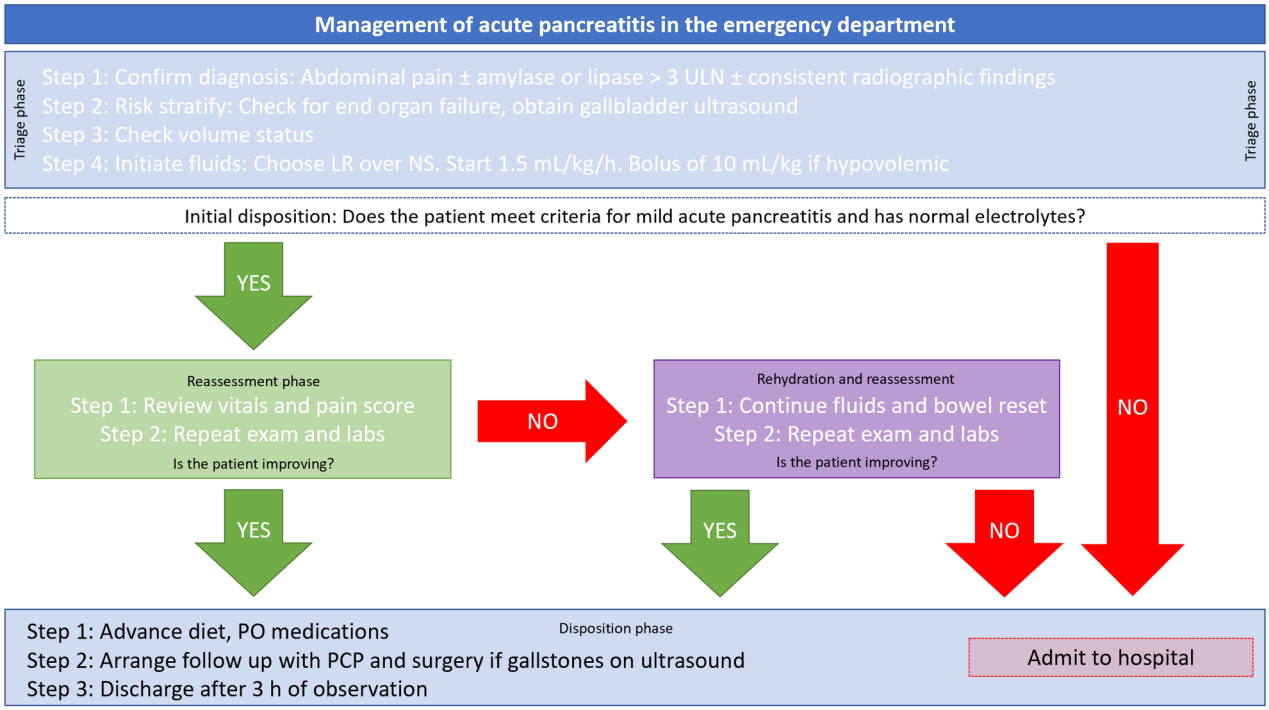

Figure 1 Example decision support tool for acute pancreatitis management in the emergency department. ULN: Upper limit of normal: NS: Normal saline; LR: Lactated ringers; PCP: Pseudotumoral chronic pancreatitis.

choledocholithiasis, or with patients with severe comorbidities (such as heart failure with reduced ejection fraction or end-stage renal failure on hemodialysis or peritoneal dialysis). Patients enrolled in the ED observation pathway, received structured hydration and reassessment in 8 h increments. Improvement was defined as lower pain scores, nausea controlled by medications, presence of hunger, and stable vital signs. When improved, patients would receive a solid fat diet and with continued improvement would be discharged with primary care or gastroenterology (GI) follow up. Patients with biliary pancreatitis in the absence of cholangitis or choledocholithiasis would have surgical follow up within 7 d of discharge to ensure close interval cholecystectomy. Patients who failed to improve would be admitted and follow standard of care.

In comparison to those admitted, we found that patients were typically younger, had lower prediction scores, and were more likely to have an idiopathic etiology for their pancreatitis. Patients in the observation pathway had a significantly lower LOS (22 h *vs* 87 h). In this study we also compared those patients in the observation pathway to a historical cohort of patients with similar presentations who would have met criteria for observation. In this comparison, patients' LOS were significantly longer in the historical cohort (72 h *vs* 23 h) and significantly greater patient charges in the historical cohort. Importantly, there was no difference in 30 d readmission rates and there were no deaths in either cohort. These findings suggested that a robust ED-based clinical pathway could be safe for the mildest form of AP.

In follow-up, we published longer-term data using the same ED-based clinical pathway in 2021[29]. In this study, the patients enrolled in the observation pathway continued to have a lower LOS and significantly fewer patient charges than those admitted and compared to those of a historical cohort without differences in readmission and without any related deaths. Compared to the initial study that had direct oversight by the GI team, the follow up study demonstrated that the ED providers could use the clinical pathway autonomously suggesting the ease of implementation and generalizability to institutions without GI providers. Using the availability data, we found that older age, greater medical comorbidity, and biliary pancreatitis were predictors for admission rather than observation whereas patients with idiopathic pancreatitis were nearly eight times more likely to be observed[30].

These studies demonstrate both the feasibility and durability of ED-based clinical observation pathways to support patients with mild AP using guideline based care while also providing safe discharge and avoiding unnecessary admission. In using such pathways, healthcare systems could reduce costs without compromising patient care or safety. In Figure 1, we provide a sample clinical decision tool as an example of a type of ED-based clinical pathway. In implementing such a pathway, we suggest assembling a group of stakeholders to include ED providers (physicians, midlevel providers, and nursing leadership), GI providers, hospital administrators and surgeons to sure that this pathway has support. Implicit in instituting such a pathway requires clear communication between the stakeholders to reduce risk of error and patient harm. In the studies we presented, we created a specific alert system to ensure that patients discharged from the ED on the pancreatitis pathway had adequate follow up with appropriated providers.

CONCLUSION

AP is an important contributor to healthcare burden in the United States and although some presentations are associated with a high mortality rate, the majority of patients have mild AP and thus a low mortality rate. As demonstrated by other clinical pathways for similarly morbid conditions such as asthma and atrial fibrillation, the mildest form of AP can safely manage in the ED with the implementation of guideline based clinical pathway.

FOOTNOTES

Author contributions: Kothari DJ and Sheth SG contributed equally to the manuscript; both the authors designed the study and write the manuscript.

Conflict-of-interest statement: The authors declare that they have no conflict of interest to disclose.

Country/Territory of origin: United States

ORCID number: Darshan J Kothari 0000-0002-6835-218X; Sunil G Sheth 0000-0003-0602-8509.

S-Editor: Chen YL
L-Editor: A
P-Editor: Cai YX

REFERENCES

1 **Forsmark CE**, Vege SS, Wilcox CM. Acute Pancreatitis. *N Engl J Med* 2016; **375**: 1972-1981 [PMID: 27959604 DOI: 10.1056/NEJMra1505202]
2 **Banks PA**, Bollen TL, Dervenis C, Gooszen HG, Johnson CD, Sarr MG, Tsiotos GG, Vege SS; Acute Pancreatitis Classification Working Group. Classification of acute pancreatitis--2012: revision of the Atlanta classification and definitions by international consensus. *Gut* 2013; **62**: 102-111 [PMID: 23100216 DOI: 10.1136/gutjnl-2012-302779]
3 **Working Group IAP/APA Acute Pancreatitis Guidelines**. IAP/APA evidence-based guidelines for the management of acute pancreatitis. *Pancreatology* 2013; **13**: e1-15 [PMID: 24054878 DOI: 10.1016/j.pan.2013.07.063]
4 **Peery AF**, Crockett SD, Murphy CC, Jensen ET, Kim HP, Egberg MD, Lund JL, Moon AM, Pate V, Barnes EL, Schlusser CL, Baron TH, Shaheen NJ, Sandler RS. Burden and Cost of Gastrointestinal, Liver, and Pancreatic Diseases in the United States: Update 2021. *Gastroenterology* 2022; **162**: 621-644 [PMID: 34678215 DOI: 10.1053/j.gastro.2021.10.017]
5 **Gapp J**, Hall AG, Walters RW, Jahann D, Kassim T, Reddymasu S. Trends and Outcomes of Hospitalizations Related to Acute Pancreatitis: Epidemiology From 2001 to 2014 in the United States. *Pancreas* 2019; **48**: 548-554 [PMID: 30946239 DOI: 10.1097/MPA.0000000000001275]
6 **Kulvatunyou N**, Watt J, Friese RS, Gries L, Green DJ, Joseph B, O'Keeffe T, Tang AL, Vercruysse G, Rhee P. Management of acute mild gallstone pancreatitis under acute care surgery: should patients be admitted to the surgery or medicine service? *Am J Surg* 2014; **208**: 981-7; discussion 986 [PMID: 25312841 DOI: 10.1016/j.amjsurg.2014.09.003]
7 **Lariño-Noia J**, Lindkvist B, Iglesias-García J, Seijo-Ríos S, Iglesias-Canle J, Domínguez-Muñoz JE. Early and/or immediately full caloric diet versus standard refeeding in mild acute pancreatitis: a randomized open-label trial. *Pancreatology* 2014; **14**: 167-173 [PMID: 24854611 DOI: 10.1016/j.pan.2014.02.008]
8 **Cavallini G**, Frulloni L, Bassi C, Gabbrielli A, Castoldi L, Costamagna G, De Rai P, Di Carlo V, Falconi M, Pezzilli R, Uomo G; ProInf-AISP Study Group. Prospective multicentre survey on acute pancreatitis in Italy (ProInf-AISP): results on 1005 patients. *Dig Liver Dis* 2004; **36**: 205-211 [PMID: 15046191 DOI: 10.1016/j.dld.2003.11.027]
9 **Capp R**, Sun B, Boatright D, Gross C. The impact of emergency department observation units on United States emergency department admission rates. *J Hosp Med* 2015; **10**: 738-742 [PMID: 26503082 DOI: 10.1002/jhm.2447]
10 **Baugh CW**, Venkatesh AK, Bohan JS. Emergency department observation units: A clinical and financial benefit for hospitals. *Health Care Manage Rev* 2011; **36**: 28-37 [PMID: 21157228 DOI: 10.1097/HMR.0b013e3181f3c035]
11 **Bellew SD**, Bremer ML, Kopecky SL, Lohse CM, Munger TM, Robelia PM, Smars PA. Impact of an Emergency Department Observation Unit Management Algorithm for Atrial Fibrillation. *J Am Heart Assoc* 2016; **5** [PMID: 26857070 DOI: 10.1161/JAHA.115.002984]
12 **Decker WW**, Smars PA, Vaidyanathan L, Goyal DG, Boie ET, Stead LG, Packer DL, Meloy TD, Boggust AJ, Haro LH, Laudon DA, Lobl JK, Sadosty AT, Schears RM, Schiebel NE, Hodge DO, Shen WK. A prospective, randomized trial of an emergency department observation unit for acute onset atrial fibrillation. *Ann Emerg Med* 2008; **52**: 322-328 [PMID: 18339449 DOI: 10.1016/j.annemergmed.2007.12.015]
13 **Atzema CL**, Austin PC, Miller E, Chong AS, Yun L, Dorian P. A population-based description of atrial fibrillation in the emergency department, 2002 to 2010. *Ann Emerg Med* 2013; **62**: 570-577.e7 [PMID: 23810031 DOI: 10.1016/j.annemergmed.2013.06.005]
14 **Scribano PV**, Wiley JF 2nd, Platt K. Use of an observation unit by a pediatric emergency department for common pediatric illnesses. *Pediatr Emerg Care* 2001; **17**: 321-323 [PMID: 11673706 DOI: 10.1097/00006565-200110000-00001]

15 **Grossman AM**, Volz KA, Shapiro NI, Salem R, Sanchez LD, Smulowitz P, Grossman SA. Comparison of 1-Day Emergency Department Observation and Inpatient Ward for 1-Day Admissions in Syncope Patients. *J Emerg Med* 2016; **50**: 217-222 [PMID: 26682847 DOI: 10.1016/j.jemermed.2015.06.013]

16 **Baugh CW**, Liang LJ, Probst MA, Sun BC. National cost savings from observation unit management of syncope. *Acad Emerg Med* 2015; **22**: 934-941 [PMID: 26204970 DOI: 10.1111/acem.12720]

17 **Crockett SD**, Wani S, Gardner TB, Falck-Ytter Y, Barkun AN; American Gastroenterological Association Institute Clinical Guidelines Committee. American Gastroenterological Association Institute Guideline on Initial Management of Acute Pancreatitis. *Gastroenterology* 2018; **154**: 1096-1101 [PMID: 29409760 DOI: 10.1053/j.gastro.2018.01.032]

18 **Fagenholz PJ**, Castillo CF, Harris NS, Pelletier AJ, Camargo CA Jr. Increasing United States hospital admissions for acute pancreatitis, 1988-2003. *Ann Epidemiol* 2007; **17**: 491-497 [PMID: 17448682 DOI: 10.1016/j.annepidem.2007.02.002]

19 **Fagenholz PJ**, Fernández-del Castillo C, Harris NS, Pelletier AJ, Camargo CA Jr. Direct medical costs of acute pancreatitis hospitalizations in the United States. *Pancreas* 2007; **35**: 302-307 [PMID: 18090234 DOI: 10.1097/MPA.0b013e3180cac24b]

20 **Rivers E**, Nguyen B, Havstad S, Ressler J, Muzzin A, Knoblich B, Peterson E, Tomlanovich M; Early Goal-Directed Therapy Collaborative Group. Early goal-directed therapy in the treatment of severe sepsis and septic shock. *N Engl J Med* 2001; **345**: 1368-1377 [PMID: 11794169 DOI: 10.1056/NEJMoa010307]

21 **Dellinger RP**, Levy MM, Rhodes A, Annane D, Gerlach H, Opal SM, Sevransky JE, Sprung CL, Douglas IS, Jaeschke R, Osborn TM, Nunnally ME, Townsend SR, Reinhart K, Kleinpell RM, Angus DC, Deutschman CS, Machado FR, Rubenfeld GD, Webb SA, Beale RJ, Vincent JL, Moreno R; Surviving Sepsis Campaign Guidelines Committee including the Pediatric Subgroup. Surviving sepsis campaign: international guidelines for management of severe sepsis and septic shock: 2012. *Crit Care Med* 2013; **41**: 580-637 [PMID: 23353941 DOI: 10.1097/CCM.0b013e31827e83af]

22 **Reddy N**, Wilcox CM, Tamhane A, Eloubeidi MA, Varadarajulu S. Protocol-based medical management of post-ERCP pancreatitis. *J Gastroenterol Hepatol* 2008; **23**: 385-392 [PMID: 18318823 DOI: 10.1111/j.1440-1746.2007.05180.x]

23 **Mao EQ**, Fei J, Peng YB, Huang J, Tang YQ, Zhang SD. Rapid hemodilution is associated with increased sepsis and mortality among patients with severe acute pancreatitis. *Chin Med J (Engl)* 2010; **123**: 1639-1644 [PMID: 20819621]

24 **Wu BU**, Hwang JQ, Gardner TH, Repas K, Delee R, Yu S, Smith B, Banks PA, Conwell DL. Lactated Ringer's solution reduces systemic inflammation compared with saline in patients with acute pancreatitis. *Clin Gastroenterol Hepatol* 2011; **9**: 710-717.e1 [PMID: 21645639 DOI: 10.1016/j.cgh.2011.04.026]

25 **Dimagno MJ**, Wamsteker EJ, Rizk RS, Spaete JP, Gupta S, Sahay T, Costanzo J, Inadomi JM, Napolitano LM, Hyzy RC, Desmond JS. A combined paging alert and web-based instrument alters clinician behavior and shortens hospital length of stay in acute pancreatitis. *Am J Gastroenterol* 2014; **109**: 306-315 [PMID: 24594946 DOI: 10.1038/ajg.2013.282]

26 **de-Madaria E**, Buxbaum JL, Maisonneuve P, García García de Paredes A, Zapater P, Guilabert L, Vaillo-Rocamora A, Rodríguez-Gandía MÁ, Donate-Ortega J, Lozada-Hernández EE, Collazo Moreno AJR, Lira-Aguilar A, Llovet LP, Mehta R, Tandel R, Navarro P, Sánchez-Pardo AM, Sánchez-Marin C, Cobreros M, Fernández-Cabrera I, Casals-Seoane F, Casas Deza D, Lauret-Braña E, Martí-Marqués E, Camacho-Montaño LM, Ubieto V, Ganuza M, Bolado F; ERICA Consortium. Aggressive or Moderate Fluid Resuscitation in Acute Pancreatitis. *N Engl J Med* 2022; **387**: 989-1000 [PMID: 36103415 DOI: 10.1056/NEJMoa2202884]

27 **Ince AT**, Senturk H, Singh VK, Yildiz K, Danalioğlu A, Cinar A, Uysal O, Kocaman O, Baysal B, Gürakar A. A randomized controlled trial of home monitoring versus hospitalization for mild non-alcoholic acute interstitial pancreatitis: a pilot study. *Pancreatology* 2014; **14**: 174-178 [PMID: 24854612 DOI: 10.1016/j.pan.2014.02.007]

28 **Kothari D**, Babineau M, Hall M, Freedman SD, Shapiro NI, Sheth SG. Preventing Hospitalization in Mild Acute Pancreatitis Using a Clinical Pathway in the Emergency Department. *J Clin Gastroenterol* 2018; **52**: 734-741 [PMID: 29095424 DOI: 10.1097/MCG.0000000000000954]

29 **Ahmed A**, Kothari DJ, Wardlaw S, Freedman SD, Sheth SG. Reducing Hospitalization in Mild Acute Pancreatitis: Results of Long-term Follow-up. *J Clin Gastroenterol* 2021; **55**: 180-186 [PMID: 32301837 DOI: 10.1097/MCG.0000000000001354]

30 **Anderson K**, Shah I, Yakah W, Cartelle AL, Zuberi SA, McHenry N, Horton L, Ahmed A, Freedman SD, Kothari DJ, Sheth SG. Prospective evaluation of an emergency department protocol to prevent hospitalization in mild acute pancreatitis: Outcomes and predictors of discharge. *Pancreatology* 2023; **23**: 299-305 [PMID: 36870814 DOI: 10.1016/j.pan.2023.02.006]

World Journal of Gastroenterology

Submit a Manuscript: https://www.f6publishing.com

World J Gastroenterol 2024 March 21; 30(11): 1480-1487

DOI: 10.3748/wjg.v30.i11.1480

ISSN 1007-9327 (print) ISSN 2219-2840 (online)

EDITORIAL

Current remarks and future directions on the interactions between metabolic dysfunction-associated fatty liver disease and COVID-19

Leonidas Brilakis, Eirini Theofilogiannakou, Panagis M Lykoudis

Specialty type: Gastroenterology and hepatology

Provenance and peer review: Invited article; Externally peer reviewed.

Peer-review model: Single blind

Peer-review report's scientific quality classification

Grade A (Excellent): A
Grade B (Very good): 0
Grade C (Good): 0
Grade D (Fair): 0
Grade E (Poor): 0

P-Reviewer: Tekin MS, Turkey

Received: December 29, 2023
Peer-review started: December 29, 2023
First decision: January 19, 2024
Revised: January 30, 2024
Accepted: March 4, 2024
Article in press: March 4, 2024
Published online: March 21, 2024

Leonidas Brilakis, Eirini Theofilogiannakou, Panagis M Lykoudis, School of Medicine, National & Kapodistrian University of Athens, Athens 11527, Greece

Panagis M Lykoudis, Division of Surgery & Interventional Science, University College London, London WC1E 6BT, United Kingdom

Corresponding author: Panagis M Lykoudis, MD, MSc, PhD, Lecturer, Division of Surgery & Interventional Science, University College London, Gower Street, London WC1E 6BT, United Kingdom. p.lykoudis@ucl.ac.uk

Abstract

During the outbreak of the coronavirus disease 2019 (COVID-19) pandemic, particular interest rose regarding the interaction between metabolic dysfunction-associated fatty liver disease (MAFLD) and the COVID-19 infection. Several studies highlighted the fact that individuals with MAFLD had higher probability of severe acute respiratory syndrome coronavirus 2 infection and more severe adverse clinical outcomes. One of the proposed mechanisms is the inflammatory response pathway, especially the one involving cytokines, such as interleukin 6, which appeared particularly elevated in those patients and was deemed responsible for additional insult to the already damaged liver. This should increase our vigilance in terms of early detection, close follow up and early treatment for individuals with MAFLD and COVID-19 infection. In the direction of early diagnosis, biomarkers such as cytokeratin-18 and scoring systems such as Fibrosis-4 index score are proposed. COVID-19 is a newly described entity, expected to be of concern for the years to come, and MAFLD is a condition with an ever-increasing impact. Delineating the interaction between these two entities should be brought into the focus of research. Reducing morbidity and mortality of patients with COVID-19 and MAFLD should be the ultimate objective, and the optimal way to achieve this is by designing evidence-based prevention and treatment policies.

Key Words: Metabolic dysfunction-associated fatty liver disease; COVID-19; Liver fibrosis; Cytokine storm; Drug induced liver injury

Core Tip: The intricate intertwining of metabolic dysfunction-associated fatty liver disease (MAFLD) and coronavirus disease 2019 (COVID-19) presents a critical nexus with severe clinical outcomes. The symbiotic impact of MAFLD increasing susceptibility to severe COVID-19, and the reciprocal exacerbation by the viral infection, mandate special attention. Early identification, vigilant monitoring and tailored evidence-based interventions, navigating both conditions, are pivotal in mitigating adverse effects. Investigating the molecular pathways underlying the synergistic effects of MAFLD and COVID-19, and the impact of specific COVID-19 treatment drugs on liver function and their potential exacerbation of MAFLD, stands as a promising research avenue that could unveil novel therapeutic targets.

Citation: Brilakis L, Theofilogiannakou E, Lykoudis PM. Current remarks and future directions on the interactions between metabolic dysfunction-associated fatty liver disease and COVID-19. *World J Gastroenterol* 2024; 30(11): 1480-1487
URL: https://www.wjgnet.com/1007-9327/full/v30/i11/1480.htm
DOI: https://dx.doi.org/10.3748/wjg.v30.i11.1480

INTRODUCTION

As the world encounters the enduring impact of coronavirus disease 2019 (COVID-19), the interplay between this viral pandemic and metabolic dysfunction-associated fatty liver disease (MAFLD) emerges as a topic for comprehensive research. While MAFLD has a remarkable prevalence among COVID-19 patients and is expected to be increased even more by 2030 due to obesity and metabolic syndrome persistently growing, the topical question that rises is whether concurrent obesity and MAFLD epidemics could be contributing factors to the exacerbation and prevalence of the ongoing COVID-19 pandemic[1,2]. In addition to the metabolic syndrome, MAFLD might influence the severity of viral infections, potentially impacting conditions like COVID-19 or even representing an independent risk factor. *Vice versa*, severe acute respiratory syndrome coronavirus 2 (SARS-CoV-2) infection exacerbates MAFLD and induces liver injury through various mechanisms.

In their consensus statement, Eslam *et al*[3] suggested that a positive diagnosis of MAFLD can be achieved through the confirmation of at least one criterion from each of the following two groups. The first group consists of the following: The presence of hepatic steatosis in adults, as it can be ascertained through imaging modalities such as ultrasound, magnetic resonance imaging or computerized tomography; blood biomarkers or blood test-based scoring systems; and liver histology. The second group consists of the following: Presence of overweight/obesity; type 2 diabetes mellitus; and evidence of metabolic dysregulation[3]. Metabolic dysregulation can be documented by the presence of at least two of the following metabolic risk abnormalities: (1) Waist circumference ≥ 102/88 cm in Caucasian men and women; (2) Blood pressure ≥ 130/85 mmHg or specific drug treatment; (3) Plasma triglycerides ≥ 150 mg/dL or specific drug treatment; (4) Plasma High Density Lipoprotein–cholesterol < 40 mg/dL for men and < 50 mg/dL for women or specific drug treatment; (5) Prediabetes; (6) Homeostasis model assessment of insulin resistance score ≥ 2.5; and (7) Plasma high-sensitivity C-reactive protein level > 2 mg/L[3]. Our ability to recognize individuals with MAFLD is very important as this condition is a favorable substrate for severe COVID-19 illness. In particular, Gao *et al*[4] reported that after adjustment for age and sex, patients with MAFLD had a 2.6-fold higher risk of severe COVID-19 illness over those without MAFLD. They also reported that MAFLD patients with elevated interleukin-6 (IL-6) Levels were at higher risk of severe COVID-19 illness over non-MAFLD patients[4].

THE IMPACT OF MAFLD ON COVID-19 DISEASE

Although there is an unmet need for further studies, it is a fact that COVID-19 affects liver function, which can be manifested straight from the onset of the disease, with mild and moderate elevations of alanine aminotransferase (ALT) and/or aspartate aminotransferase (AST)[2]. Tao *et al*[1] reported a negative impact of MAFLD on the course and clinical outcomes of COVID-19 illness but did not detect a statistically significant correlation[1].

The incidence of MAFLD in patients with COVID-19 has been noted as higher than in general population[1]. One possible explanation of the enhanced susceptibility to COVID-19 is the increased hepatic angiotensin-converting enzyme 2 (ACE2) and transmembrane serine protease 2 (TMPRSS2) expression in MAFLD patients, which are host cell proteins that contribute to SARS-CoV-2 infection[2,5,6]. In addition, COVID-19 patients with MAFLD under the age of 60 years have a higher risk of severe COVID-19 illness compared to those without MAFLD[5]. Due to liver's role in producing acute-phase reactants, coagulation factors and albumin, any dysfunction in the liver might affect the broader symptoms of COVID-19, potentially influencing conditions like acute respiratory distress syndrome (ARDS), coagulation disorders and multi-organ failure, aggravating the COVID-19 progression[2]. Therefore, MAFLD patients have higher risk of a poorer COVID-19 prognosis, higher prevalence of severe disease course, higher viral shedding time and more liver failure during hospitalization[7].

Notably, MAFLD is not a stand-alone disease. It can be characterized as the hepatic manifestation of metabolic syndrome and stands along with the obesity epidemic[5]. These comorbidities are associated with adverse clinical manifestation of type 2 diabetes and increased risk of severe infections, since obesity compromises the immune system due to chronic inflammation. It is essential to underline that increased liver steatosis is associated with a higher risk of

symptomatic COVID-19 in obese patients[7]. A pro-inflammatory state in MAFLD patients that aggravates COVID-19 illness, is also a result of excess of free fatty acids that enter the liver, activating Kupffer cells[1]. The already burdened immune system and its effects on liver, lead to a shift of Kupffer cells from an anti-inflammatory M2 state to a proinflammatory M1 state[1]. Consequently, this transition enhances the production of cytokines such as tumor necrosis factor-α and IL-6. Studies suggest that IL-6 plays a pivotal role in the cytokine 'storm', which could be a primary factor for the aggravation of COVID-19[1,4,7].

Research is needed to ascertain the exact role of fibrosis in the spectrum of outcomes in patients with MAFLD and COVID-19. Angulo *et al*[8] after highlighting the difficulty and the risks of liver biopsy, turned to the examination of a non-invasive model for the identification of liver fibrosis among MAFLD patients. They proposed a score that includes age, body mass index, AST/ALT ratio, platelet count, hyperglycemia and albumin, comprehensively known as the non-alcoholic fatty liver disease fibrosis score (NFS)[8]. In their study, Campos-Murguía *et al*[9], in the process of diagnosing liver fibrosis, instead of using a single score, used a two-score system simultaneously in order to better stratify high-risk patients with liver fibrosis. In this system, only individuals with intermediate or high risk of fibrosis-as calculated by NFS- had AST to platelet ratio index calculated[9]. It is suggested that the existence of MAFLD, and especially the coexistence with significant or advanced fibrosis, stimulates the virus-triggered cytokine storm. This is mainly explained by the hepatic production of pro-inflammatory cytokines that significantly contribute to the aggravation of COVID-19 disease[10]. In the same context, Hegyi *et al*[7] underlined fibrosis as an independent factor for severe COVID-19 illness, in addition to the existence of fatty liver[7]. Data provided by Targher *et al*[11] corroborate a correlation between MAFLD with higher Fibrosis-4 (FIB-4) and NFS scores, and severe course of COVID-19 disease[11]. The severity of COVID-19 notably escalates with the progression of liver fibrosis. A FIB-4 score higher than 2.67 was associated with the highest risk of developing severe COVID-19. Moreover, evidence was provided that the coexistence of MAFLD alongside with a neutrophil-to-lymphocyte ratio (NLR) over 2.8 correlated with an elevated risk of severe COVID-19 disease, compared to non-MAFLD individuals with a normal NLR[7,11]. Therefore, there is an urgent need to evaluate the existence of fibrosis and its degree as it seems to significantly affect the course of the disease.

EFFECTS OF COVID-19 ON MAFLD

Reversely, SARS-CoV-2 infection can promote the progression of MAFLD. SARS-CoV-2 demonstrates wide organotropism, including the liver[12]. Hepatic dysfunction, characterized by abnormalities in liver enzymes, is frequently observed in individuals with COVID-19, notably in severe cases across multiple studies[2,5]. Patients experiencing severe COVID-19 infection tend to exhibit significantly higher incidence of abnormal liver function tests, which are correlated with poorer outcomes[12,13]. Underlying liver conditions can exacerbate liver damage resulting from COVID-19, and multiple mechanisms could explain the abnormal liver dysfunction indicated in COVID-19 patients. Direct liver injury induced by SARS-CoV-2, systemic inflammatory response syndrome (SIRS) and cytokine storms, hypoxia, drug-induced liver injury (DILI), dysregulation of hepatic lipid metabolism and liver steatosis, and disruption in gut microbiota balance are only some of the postulated underlying mechanisms[5,12,14].

A variety of studies point out that SARS-CoV-2 can directly damage liver cells. ACE2 and TMPRSS2 are involved in the process of SARS-CoV-2 endocytosis[6]. Therefore, the presence of these receptors in the liver and bile ducts can cause cytopathic damage[2,12,13]. SARS-CoV-2 found in the gut lumen may migrate to the liver through the portal circulation, causing direct damage by actively replicating in hepatic cells *via* ACE2 receptors[15]. Liver cell apoptosis studies further support the indication of direct viral cytopathic effects as reported by Chen H and Chen Q[2].Other factors that lead to liver damage and therefore can worsen the progression of MAFLD are bi-nucleated cells, swollen mitochondria, and changes in canalicular structures[16,17]. A retrospective cohort study by Wong *et al*[18] also demonstrated that patients with prolonged viral presence were more likely to develop elevation of ALT/AST[18].

As an infectious condition, COVID-19 can provoke systemic inflammation and there is evidence that patients with severe COVID-19 may have cytokine storm syndrome[19]. This can lead to multi-organ dysfunction following liver damage. As liver steatosis is associated with markers of inflammation such as IL-6, MAFLD can be exacerbated by the inflammatory response of COVID-19[20]. Alongside the hyper-inflammatory state due to the co-existence of MAFLD and COVID-19 illness, patients with severe COVID-19 develop multi-organ failure, ARDS, shock and hypoxia[12]. Liver ischemia may lead to increased hypoxia-induced factors (HIFs). Higher levels of HIFs in COVID-19 patients could aggravate obesity and insulin resistance, and both aforementioned conditions constitute significant risk factors associated with MAFLD, as suggested by Tian *et al*[13]. It is important to mention that studies have shown that HIF-1α could promote MAFLD[2]. Moreover, increased production of HIF-2α could induce lipogenesis in the liver[2,14,21]. Therefore, SIRS and hypoxia in severe COVID-19 may exacerbate the progression of MAFLD.

During an infection, the activated innate immune response not only directly triggers and amplifies liver inflammation but also disrupts the regulation of lipid metabolism[22]. This lipid derangement can promote the development of liver fibrosis in MAFLD/non-alcoholic steatohepatitis (NASH) patients, as mentioned by Chen H and Chen Q[2]. Analysis of proteins and metabolites in COVID-19 patients have revealed dyslipidemia, characterized by lipid accumulation and decreased levels of apolipoproteins[23,24]. Unsaturated fatty acids might be released as a defense mechanism during a cytokine storm, which can occur in reaction to COVID-19[24]. This condition can lead to changes where proinflammatory lipids and lipid mediators alter the immune response[5].

In turn, viruses modify lipid metabolism to facilitate their replication, impacting the expression and function of vital enzymes in lipid biosynthesis[25]. These alterations in lipid metabolism can also relate to the host's response to an infection[25]. SARS-CoV-2 follows this pattern, inducing substantial changes in lipid metabolism post-infection[5,25]. In

particular, SARS-CoV-2 infection has been found to influence pathways involved in lipid synthesis and uptake, leading to increased accumulation of lipid droplets (LDs) within human cells. Interestingly, the virus utilizes these LDs to enhance its replication capacity[25]. Moreover, recent studies highlight the significance of ACE2 in maintaining metabolic balance [2]. However, SARS-CoV-2 infection impairs ACE2 expression, potentially inducing metabolic abnormalities[26]. This disruption in metabolic equilibrium due to ACE2 impairment may contribute to the progression of MAFLD in individuals affected by COVID-19[2].

Disruption of gut microbiome equilibrium might contribute to the severity of MAFLD during COVID-19. Growing evidence indicates that imbalances in the microbiota during COVID-19 correlate with disease severity and increased mortality[27]. The gastrointestinal tract serves as both the primary habitat for human microbiota and a target for SARS-CoV-2 infection due to its elevated expression of ACE2 and TMPRSS2[27]. Importantly, the intestine has a connection with the liver *via* the gut-liver axis, and intestinal microbiota significantly influences progression of MAFLD[28,29].

A variety of studies suggest an enrichment of opportunistic pathogens and a reduction of beneficial commensals in the intestinal microbiota of patients with severe COVID-19[30-33]. For example, a cohort study with 62 patients with COVID-19 found that anti-inflammatory bacteria such as *Roseburia* and *Faecalibacterium* decreased, while opportunistic pathogens such as *Clostridium* and *Streptococcus* increased in these patients[32]. These studies highlighted changes in gut microbiota linked to susceptibility to severe illness.

The relationship between gut microbiota and the liver appears to be strongly supported by evidence. Seventy percent of blood supply to the liver is provided by the portal vein which carries pathogens from the intestine, therefore liver acts as the primary defense against antigens originating from the gut. The balance and well-being of gut-liver axis heavily rely on the contribution of intestinal bacteria[28]. Therefore, disruptions in gut bacteria balance can lead to the passage of bacteria and endotoxins into the liver due to increased intestinal permeability, eventually triggering liver inflammation. This dysbiosis-induced hepatic inflammation, coupled with SIRS mentioned earlier in patients with severe COVID-19, can further aggravate MAFLD[2].

The liver, as the body's primary detoxifier, can be affected by numerous medications used to treat COVID-19[2]. Studies have demonstrated that treatment with antiviral drugs, such as lopinavir, ritonavir and remdesivir, and macrolides, used for superinfections, have the potential to cause DILI[2,34]. Lopinavir and ritonavir therapy in patients with COVID-19 is independently associated with elevated ALT/AST[2]. Hepatotoxicity has also been reported in association with antimalarial/antirheumatic drugs such as hydroxychloroquine, immunomodulatory drugs, corticosteroids and tocilizumab, as well as acetaminophen, commonly used as an antipyretic medication[2,35]. Importantly, corticosteroid therapy, currently recommended by the World Health Organization for patients with severe SARS-CoV-2 infection, is evidently linked to conditions such as steatosis or glycogenosis[36]. Therefore, amongst various drugs used to treat COVID-19, some can be harmful to the liver.

Underlying metabolic abnormalities and MAFLD have been identified as contributors to DILI[34]. MAFLD has the potential to increase the liver's sensitivity to hepatotoxicants like acetaminophen[34]. In addition, other compounds, such as corticoids, antiretroviral agents and methotrexate, appear to initiate the progression from simple fatty liver to NASH, or exacerbate pre-existing conditions like steatosis, necroinflammation and fibrosis[35]. Hence, in individuals with chronic liver disease, it's crucial to weigh the risk of potential liver injury when selecting medications for COVID-19 treatment and to carefully monitor these patients, as the use of drugs with elevated hepatotoxicity could potentially enhance the progression of MAFLD. Figure 1 provides an overview of the aforementioned interactions and highlights the bidirectional aggravating relationship.

TREATMENT CHALLENGES OF PATIENTS WITH COVID-19 AND MAFLD

Treatment of patients with COVID-19 and MAFLD is a very challenging task with significant implications. On the one hand, there is the need for appropriate treatment for COVID-19 and on the other, the need for the least possible burden on the already damaged liver. Given that many of the medications used to treat COVID-19 or its symptoms are harmful to or impair liver function, great care must be taken in their administration and close liver function monitoring is mandatory in order to deal with any adverse effects[37]. Hamid *et al*[38] highlighted the increased risk of drug-drug interactions and especially in liver transplant patients who are under immunosuppressive treatment. They also added that dexamethasone, which is effective in reducing mortality, does not appear to have an aggravating effect in patients with liver damage[38]. Elemam *et al*[12] emphasized the fact that the reduction in the drugs in COVID-19 patients with potential DILI, needs to be further evaluated[12]. Jeeyavudeen *et al*[5] reported medications such as dexamethasone, protease inhibitors, nucleoside analogue (remdesivir) and monoclonal antibodies to IL-6 as frequently used agents for COVID-19 treatment. Additionally, they proposed selection of medications according to disease severity, disease duration, ALT levels and cross-interactions with other treatments patients might be under. They also recommended close monitoring of liver function[5]. It can be argued that once research provides evidence for a more precise treatment algorithm for COVID-19, areas of clear overlap with MAFLD treatment will emerge, and more specific questions will need to be addressed.

TRIPLE NEXUS: CHRONIC HEPATITIS B AND C, MAFLD AND COVID-19

The triple association of chronic viral hepatitis B (CHB) and chronic viral hepatitis C (CHC), MAFLD, and COVID-19 introduces a complex interplay. Notably, there is a significant gap in the existing literature specifically addressing this

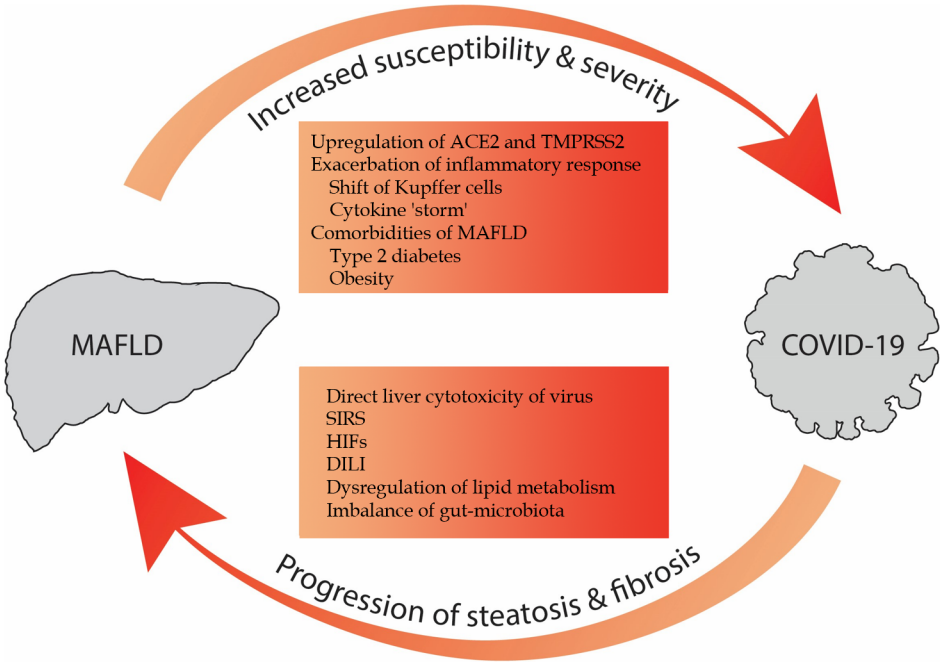

Figure 1 Interplay between coronavirus disease 2019 and metabolic dysfunction-associated fatty liver disease. Metabolic dysfunction-associated fatty liver disease (MAFLD) can increase the susceptibility and severity of coronavirus disease 2019 (COVID-19). Conversely, COVID-19 can promote the progression of preexisting MAFLD. MAFLD: Metabolic dysfunction-associated fatty liver disease; ACE2: Angiotensin-converting enzyme 2; TMPRSS2: Transmembrane protease serine 2; SIRS: Systematic inflammatory response syndrome; HIFs: Hypoxia-induced factors; DILI: Drug-induced liver injury; COVID-19: Coronavirus disease 2019.

triple association. The influence of pre-existing liver conditions on COVID-19-associated liver injury remains a topic of debate. Despite studies revealing the severity of COVID-19 in patients with chronic liver diseases (CLD), with MAFLD and alcoholic liver disease identified as independent risk factors for severe COVID-19, the relationship between COVID-19 and CLD caused by hepatitis C virus (HCV) and hepatitis B virus (HBV) has received less attention[5,18,39]. According to Elemam *et al*[12], there are conflicting results regarding the impact of viral hepatitis on COVID-19 outcomes[12]. Some studies suggest that individuals with viral hepatitis experienced more severe liver dysfunction due to pre-existing immune dysregulation, while other studies indicated that individuals with pre-existing liver disease or hepatitis B infection did not show more severe symptoms of COVID-19[12,18,39]. Postulated reasons for these discrepancies in literature, have been suggested by Lin *et al*[40] and include small sample size of patients with co-infection of HBV and COVID, heterogeneity of included patients and lack of thorough understanding of the complexity of enhanced liver injury caused by inflammatory response[40]. This conflicting evidence underscores the need for further research to elucidate the specific relationship between viral hepatitis and COVID-19-related liver injury. However, liver cirrhosis stands out as a critical factor contributing to severe outcomes in COVID-19, with CHB and CHC playing major roles in its development[5,12,38]. The World Gastroenterology Organisation underscores the need for more data to assess the risk of adverse outcomes in individuals with CHB or CHC without cirrhosis exposed to COVID-19[38]. While uncertainties persist about the susceptibility of patients with CHB or CHC to SARS-CoV-2-induced liver damage, those with advanced fibrosis or cirrhosis face a higher risk of severe outcomes, necessitating vigilant monitoring and tailored interventions[38].

The potential mechanisms underlying the association between viral hepatitis B and C with COVID-19 require thorough investigation and seem to be similar with those observed in the interplay between MAFLD and COVID-19. The enhanced liver injury induced by SARS-CoV-2 and HBV co-infection has been characterized as the hepatocyte type rather than the cholangiocyte type, emphasizing the primary involvement of hepatocytes in the pathogenesis[40]. One key aspect of this interaction is the inflammatory response and cytokine 'storm'. Inflammatory factors, including abnormal lactate dehydrogenase, D-dimer, and IL-6 production, may contribute significantly to liver injury following SARS-CoV-2 coinfection[40]. Thrombocytopenia, more pronounced in COVID-19 cases with HBV co-infection, indicates a potential role of inflammatory factors in liver injury[40,41]. Furthermore, DILI poses a significant concern[42]. Corticosteroids, commonly administered in severe COVID-19 cases, introduce a dual risk by not only suppressing the immune response but also activating HBV replication[42]. This activation occurs through the suppression of cytotoxic T cell function and direct stimulation of HBV genomic sequences[42]. Similarly, tocilizumab raises concerns as it can cause liver injury and induce reactivation of hepatotropic viruses[42].

Notably, while some studies indicate that related inflammatory factors contribute to abnormal liver function, the exact mechanisms of enhanced liver injury caused by the inflammatory response need further elucidation[40]. Some mechanistic insights revealed stable expression levels of HBV-associated markers during SARS-CoV-2 infection, suggesting that chronic HBV infection alone may not significantly increase the severity of COVID-19[43]. Nevertheless, caution is warranted, as reactivation of hepatitis B has been observed, particularly when corticosteroids are employed, emphasizing the need for continuous antiviral therapy to manage and prevent such occurrences[42]. Similarly, for

individuals co-infected with HCV and SARS-CoV-2, the continuation of antiviral therapy remains crucial[42]. Both the American Association for the Study of Liver Disease and the European Association for the Study of the Liver strongly recommend ongoing antiviral therapy in individuals diagnosed with COVID-19[42]. The parallel complexity seen in the MAFLD-COVID association prompts a closer examination of each potential mechanism to unveil common threads linking the diverse conditions of CHB/CHC and MAFLD to COVID-19 progression.

It is crucial to highlight that both CHB and CHC are frequently associated with hepatic steatosis, forming a connection with obesity, dyslipidemia and insulin resistance[44]. This shared link to metabolic factors is compounded by MAFLD as a common comorbidity, further emphasizing the interconnected nature of these conditions. This interplay highlights the need for comprehensive research to elucidate the complex dynamics of the triple association between CHB and CHC, MAFLD and COVID-19. While existing studies shed light on the impact of individual components, the triple association remains a relatively unexplored area in medical literature. Future investigations should aim to unravel the mechanisms underlying the interactions between these three entities. Understanding the synergistic effects could provide valuable insights into tailored interventions and preventive strategies.

CONCLUSION

In conclusion, the interaction of MAFLD and course of disease in patients with COVID-19 is particularly broad and there is a constant growing interest for research on this topic. Individuals with MAFLD have higher probability of SARS-COV-2 infection and more severe adverse clinical outcomes. Reversely, the disease from SARS-COV-2 can lead to triggering and progression of MAFLD. The multitude of already known mechanisms involved in this essential interaction need to be elucidated through focused research. Finally, it is imperative to quickly identify patients who combine the above two conditions and to apply tailored treatment, highly effective for COVID-19 and safe for the liver.

FOOTNOTES

Author contributions: Lykoudis PM designed the study and revised the draft; Brilakis L and Theofilogiannakou E performed the research and wrote the draft of the manuscript; All authors have read and approve the final manuscript.

Conflict-of-interest statement: Leonidas Brilakis, Eirini Theofilogiannakou and Panagis M Lykoudis have nothing to disclose.

Country/Territory of origin: Greece

ORCID number: Leonidas Brilakis 0009-0004-5042-3666; Eirini Theofilogiannakou 0009-0005-2151-4398; Panagis M Lykoudis 0000-0003-2170-0471.

S-Editor: Fan JR
L-Editor: A
P-Editor: Cai YX

REFERENCES

1 **Tao Z**, Li Y, Cheng B, Zhou T, Gao Y. Risk of Severe COVID-19 Increased by Metabolic Dysfunction-associated Fatty Liver Disease: A Meta-analysis. *J Clin Gastroenterol* 2021; **55**: 830-835 [PMID: 34406175 DOI: 10.1097/MCG.0000000000001605]

2 **Chen H**, Chen Q. COVID-19 Pandemic: Insights into Interactions between SARS-CoV-2 Infection and MAFLD. *Int J Biol Sci* 2022; **18**: 4756-4767 [PMID: 35874945 DOI: 10.7150/ijbs.72461]

3 **Eslam M**, Newsome PN, Sarin SK, Anstee QM, Targher G, Romero-Gomez M, Zelber-Sagi S, Wai-Sun Wong V, Dufour JF, Schattenberg JM, Kawaguchi T, Arrese M, Valenti L, Shiha G, Tiribelli C, Yki-Järvinen H, Fan JG, Grønbæk H, Yilmaz Y, Cortez-Pinto H, Oliveira CP, Bedossa P, Adams LA, Zheng MH, Fouad Y, Chan WK, Mendez-Sanchez N, Ahn SH, Castera L, Bugianesi E, Ratziu V, George J. A new definition for metabolic dysfunction-associated fatty liver disease: An international expert consensus statement. *J Hepatol* 2020; **73**: 202-209 [PMID: 32278004 DOI: 10.1016/j.jhep.2020.03.039]

4 **Gao F**, Zheng KI, Yan HD, Sun QF, Pan KH, Wang TY, Chen YP, Targher G, Byrne CD, George J, Zheng MH. Association and Interaction Between Serum Interleukin-6 Levels and Metabolic Dysfunction-Associated Fatty Liver Disease in Patients With Severe Coronavirus Disease 2019. *Front Endocrinol (Lausanne)* 2021; **12**: 604100 [PMID: 33763027 DOI: 10.3389/fendo.2021.604100]

5 **Jeeyavudeen MS**, Chaudhari R, Pappachan JM, Fouda S. Clinical implications of COVID-19 in patients with metabolic-associated fatty liver disease. *World J Gastroenterol* 2023; **29**: 487-502 [PMID: 36688018 DOI: 10.3748/wjg.v29.i3.487]

6 **Bertolini A**, van de Peppel IP, Bodewes FAJA, Moshage H, Fantin A, Farinati F, Fiorotto R, Jonker JW, Strazzabosco M, Verkade HJ, Peserico G. Abnormal Liver Function Tests in Patients With COVID-19: Relevance and Potential Pathogenesis. *Hepatology* 2020; **72**: 1864-

1872 [PMID: 32702162 DOI: 10.1002/hep.31480]
7 **Hegyi PJ**, Váncsa S, Ocskay K, Dembrovszky F, Kiss S, Farkas N, Erőss B, Szakács Z, Hegyi P, Pár G. Metabolic Associated Fatty Liver Disease Is Associated With an Increased Risk of Severe COVID-19: A Systematic Review With Meta-Analysis. *Front Med (Lausanne)* 2021; **8**: 626425 [PMID: 33777974 DOI: 10.3389/fmed.2021.626425]
8 **Angulo P**, Hui JM, Marchesini G, Bugianesi E, George J, Farrell GC, Enders F, Saksena S, Burt AD, Bida JP, Lindor K, Sanderson SO, Lenzi M, Adams LA, Kench J, Therneau TM, Day CP. The NAFLD fibrosis score: a noninvasive system that identifies liver fibrosis in patients with NAFLD. *Hepatology* 2007; **45**: 846-854 [PMID: 17393509 DOI: 10.1002/hep.21496]
9 **Campos-Murguía A**, Román-Calleja BM, Toledo-Coronado IV, González-Regueiro JA, Solís-Ortega AA, Kúsulas-Delint D, Cruz-Contreras M, Cruz-Yedra N, Cubero FJ, Nevzorova YA, Martínez-Cabrera CF, Moreno-Guillén P, Lozano-Cruz OA, Chapa-Ibargüengoitia M, Gulías-Herrero A, Aguilar-Salinas CA, Ruiz-Margáin A, Macías-Rodríguez RU. Liver fibrosis in patients with metabolic associated fatty liver disease is a risk factor for adverse outcomes in COVID-19. *Dig Liver Dis* 2021; **53**: 525-533 [PMID: 33551355 DOI: 10.1016/j.dld.2021.01.019]
10 **Sharma P**, Kumar A. Metabolic dysfunction associated fatty liver disease increases risk of severe Covid-19. *Diabetes Metab Syndr* 2020; **14**: 825-827 [PMID: 32540736 DOI: 10.1016/j.dsx.2020.06.013]
11 **Targher G**, Mantovani A, Byrne CD, Wang XB, Yan HD, Sun QF, Pan KH, Zheng KI, Chen YP, Eslam M, George J, Zheng MH. Risk of severe illness from COVID-19 in patients with metabolic dysfunction-associated fatty liver disease and increased fibrosis scores. *Gut* 2020; **69**: 1545-1547 [PMID: 32414813 DOI: 10.1136/gutjnl-2020-321611]
12 **Elemam NM**, Talaat IM, Maghazachi AA, Saber-Ayad M. Liver Injury Associated with COVID-19 Infection: Pathogenesis, Histopathology, Prognosis, and Treatment. *J Clin Med* 2023; **12** [PMID: 36902854 DOI: 10.3390/jcm12052067]
13 **Tian S**, Xiong Y, Liu H, Niu L, Guo J, Liao M, Xiao SY. Pathological study of the 2019 novel coronavirus disease (COVID-19) through postmortem core biopsies. *Mod Pathol* 2020; **33**: 1007-1014 [PMID: 32291399 DOI: 10.1038/s41379-020-0536-x]
14 **Chen J**, Chen J, Fu H, Li Y, Wang L, Luo S, Lu H. Hypoxia exacerbates nonalcoholic fatty liver disease *via* the HIF-2α/PPARα pathway. *Am J Physiol Endocrinol Metab* 2019; **317**: E710-E722 [PMID: 31430204 DOI: 10.1152/ajpendo.00052.2019]
15 **Portincasa P**, Krawczyk M, Smyk W, Lammert F, Di Ciaula A. COVID-19 and non-alcoholic fatty liver disease: Two intersecting pandemics. *Eur J Clin Invest* 2020; **50**: e13338 [PMID: 32589264 DOI: 10.1111/eci.13338]
16 **Fiel MI**, El Jamal SM, Paniz-Mondolfi A, Gordon RE, Reidy J, Bandovic J, Advani R, Kilaru S, Pourmand K, Ward S, Thung SN, Schiano T. Findings of Hepatic Severe Acute Respiratory Syndrome Coronavirus-2 Infection. *Cell Mol Gastroenterol Hepatol* 2021; **11**: 763-770 [PMID: 32992052 DOI: 10.1016/j.jcmgh.2020.09.015]
17 **Wang Y**, Liu S, Liu H, Li W, Lin F, Jiang L, Li X, Xu P, Zhang L, Zhao L, Cao Y, Kang J, Yang J, Li L, Liu X, Li Y, Nie R, Mu J, Lu F, Zhao S, Lu J, Zhao J. SARS-CoV-2 infection of the liver directly contributes to hepatic impairment in patients with COVID-19. *J Hepatol* 2020; **73**: 807-816 [PMID: 32437830 DOI: 10.1016/j.jhep.2020.05.002]
18 **Wong GL**, Yip TC, Wong VW, Tse YK, Hui DS, Lee SS, Yeoh EK, Chan HL, Lui GC. SARS-CoV-2 Viral Persistence Based on Cycle Threshold Value and Liver Injury in Patients With COVID-19. *Open Forum Infect Dis* 2021; **8**: ofab205 [PMID: 34099979 DOI: 10.1093/ofid/ofab205]
19 **Mehta P**, McAuley DF, Brown M, Sanchez E, Tattersall RS, Manson JJ; HLH Across Speciality Collaboration, UK. COVID-19: consider cytokine storm syndromes and immunosuppression. *Lancet* 2020; **395**: 1033-1034 [PMID: 32192578 DOI: 10.1016/S0140-6736(20)30628-0]
20 **Fricker ZP**, Pedley A, Massaro JM, Vasan RS, Hoffmann U, Benjamin EJ, Long MT. Liver Fat Is Associated With Markers of Inflammation and Oxidative Stress in Analysis of Data From the Framingham Heart Study. *Clin Gastroenterol Hepatol* 2019; **17**: 1157-1164.e4 [PMID: 30476583 DOI: 10.1016/j.cgh.2018.11.037]
21 **Gorden DL**, Myers DS, Ivanova PT, Fahy E, Maurya MR, Gupta S, Min J, Spann NJ, McDonald JG, Kelly SL, Duan J, Sullards MC, Leiker TJ, Barkley RM, Quehenberger O, Armando AM, Milne SB, Mathews TP, Armstrong MD, Li C, Melvin WV, Clements RH, Washington MK, Mendonsa AM, Witztum JL, Guan Z, Glass CK, Murphy RC, Dennis EA, Merrill AH Jr, Russell DW, Subramaniam S, Brown HA. Biomarkers of NAFLD progression: a lipidomics approach to an epidemic. *J Lipid Res* 2015; **56**: 722-736 [PMID: 25598080 DOI: 10.1194/jlr.P056002]
22 **Bai L**, Li H. Innate immune regulatory networks in hepatic lipid metabolism. *J Mol Med (Berl)* 2019; **97**: 593-604 [PMID: 30891617 DOI: 10.1007/s00109-019-01765-1]
23 **Bruzzone C**, Bizkarguenaga M, Gil-Redondo R, Diercks T, Arana E, García de Vicuña A, Seco M, Bosch A, Palazón A, San Juan I, Laín A, Gil-Martínez J, Bernardo-Seisdedos G, Fernández-Ramos D, Lopitz-Otsoa F, Embade N, Lu S, Mato JM, Millet O. SARS-CoV-2 Infection Dysregulates the Metabolomic and Lipidomic Profiles of Serum. *iScience* 2020; **23**: 101645 [PMID: 33043283 DOI: 10.1016/j.isci.2020.101645]
24 **Shen B**, Yi X, Sun Y, Bi X, Du J, Zhang C, Quan S, Zhang F, Sun R, Qian L, Ge W, Liu W, Liang S, Chen H, Zhang Y, Li J, Xu J, He Z, Chen B, Wang J, Yan H, Zheng Y, Wang D, Zhu J, Kong Z, Kang Z, Liang X, Ding X, Ruan G, Xiang N, Cai X, Gao H, Li L, Li S, Xiao Q, Lu T, Zhu Y, Liu H, Guo T. Proteomic and Metabolomic Characterization of COVID-19 Patient Sera. *Cell* 2020; **182**: 59-72.e15 [PMID: 32492406 DOI: 10.1016/j.cell.2020.05.032]
25 **Dias SSG**, Soares VC, Ferreira AC, Sacramento CQ, Fintelman-Rodrigues N, Temerozo JR, Teixeira L, Nunes da Silva MA, Barreto E, Mattos M, de Freitas CS, Azevedo-Quintanilha IG, Manso PPA, Miranda MD, Siqueira MM, Hottz ED, Pão CRR, Bou-Habib DC, Barreto-Vieira DF, Bozza FA, Souza TML, Bozza PT. Lipid droplets fuel SARS-CoV-2 replication and production of inflammatory mediators. *PLoS Pathog* 2020; **16**: e1009127 [PMID: 33326472 DOI: 10.1371/journal.ppat.1009127]
26 **Li Z**, Peng M, Chen P, Liu C, Hu A, Zhang Y, Peng J, Liu J, Li Y, Li W, Zhu W, Guan D, Chen H, Li J, Fan D, Huang K, Lin F, Zhang Z, Guo Z, Luo H, He X, Zhu Y, Li L, Huang B, Cai W, Gu L, Lu Y, Deng K, Yan L, Chen S. Imatinib and methazolamide ameliorate COVID-19-induced metabolic complications *via* elevating ACE2 enzymatic activity and inhibiting viral entry. *Cell Metab* 2022; **34**: 424-440.e7 [PMID: 35150639 DOI: 10.1016/j.cmet.2022.01.008]
27 **Wang B**, Zhang L, Wang Y, Dai T, Qin Z, Zhou F. Alterations in microbiota of patients with COVID-19: potential mechanisms and therapeutic interventions. *Signal Transduct Target Ther* 2022; **7**: 143 [PMID: 35487886 DOI: 10.1038/s41392-022-00986-0]
28 **Compare D**, Coccoli P, Rocco A, Nardone OM, De Maria S, Cartenì M, Nardone G. Gut--liver axis: the impact of gut microbiota on non alcoholic fatty liver disease. *Nutr Metab Cardiovasc Dis* 2012; **22**: 471-476 [PMID: 22546554 DOI: 10.1016/j.numecd.2012.02.007]
29 **Iruzubieta P**, Medina JM, Fernández-López R, Crespo J, de la Cruz F. A Role for Gut Microbiome Fermentative Pathways in Fatty Liver Disease Progression. *J Clin Med* 2020; **9** [PMID: 32392712 DOI: 10.3390/jcm9051369]
30 **Zuo T**, Zhang F, Lui GCY, Yeoh YK, Li AYL, Zhan H, Wan Y, Chung ACK, Cheung CP, Chen N, Lai CKC, Chen Z, Tso EYK, Fung KSC, Chan V, Ling L, Joynt G, Hui DSC, Chan FKL, Chan PKS, Ng SC. Alterations in Gut Microbiota of Patients With COVID-19 During Time of

Hospitalization. *Gastroenterology* 2020; **159**: 944-955.e8 [PMID: 32442562 DOI: 10.1053/j.gastro.2020.05.048]

31 **Gu S**, Chen Y, Wu Z, Gao H, Lv L, Guo F, Zhang X, Luo R, Huang C, Lu H, Zheng B, Zhang J, Yan R, Zhang H, Jiang H, Xu Q, Guo J, Gong Y, Tang L, Li L. Alterations of the Gut Microbiota in Patients With Coronavirus Disease 2019 or H1N1 Influenza. *Clin Infect Dis* 2020; **71**: 2669-2678 [PMID: 32497191 DOI: 10.1093/cid/ciaa709]

32 **Tao W**, Zhang G, Wang X, Guo M, Zeng W, Xu Z, Cao D, Pan A, Wang Y, Zhang K, Ma X, Chen Z, Jin T, Liu L, Weng J, Zhu S. Analysis of the intestinal microbiota in COVID-19 patients and its correlation with the inflammatory factor IL-18. *Med Microecol* 2020; **5**: 100023 [PMID: 34173452 DOI: 10.1016/j.medmic.2020.100023]

33 **Yeoh YK**, Zuo T, Lui GC, Zhang F, Liu Q, Li AY, Chung AC, Cheung CP, Tso EY, Fung KS, Chan V, Ling L, Joynt G, Hui DS, Chow KM, Ng SSS, Li TC, Ng RW, Yip TC, Wong GL, Chan FK, Wong CK, Chan PK, Ng SC. Gut microbiota composition reflects disease severity and dysfunctional immune responses in patients with COVID-19. *Gut* 2021; **70**: 698-706 [PMID: 33431578 DOI: 10.1136/gutjnl-2020-323020]

34 **Boeckmans J**, Rodrigues RM, Demuyser T, Piérard D, Vanhaecke T, Rogiers V. COVID-19 and drug-induced liver injury: a problem of plenty or a petty point? *Arch Toxicol* 2020; **94**: 1367-1369 [PMID: 32266419 DOI: 10.1007/s00204-020-02734-1]

35 **Ferron PJ**, Gicquel T, Mégarbane B, Clément B, Fromenty B. Treatments in Covid-19 patients with pre-existing metabolic dysfunction-associated fatty liver disease: A potential threat for drug-induced liver injury? *Biochimie* 2020; **179**: 266-274 [PMID: 32891697 DOI: 10.1016/j.biochi.2020.08.018]

36 **Nardo AD**, Schneeweiss-Gleixner M, Bakail M, Dixon ED, Lax SF, Trauner M. Pathophysiological mechanisms of liver injury in COVID-19. *Liver Int* 2021; **41**: 20-32 [PMID: 33190346 DOI: 10.1111/liv.14730]

37 **Hu X**, Sun L, Guo Z, Wu C, Yu X, Li J. Management of COVID-19 patients with chronic liver diseases and liver transplants. *Ann Hepatol* 2022; **27**: 100653 [PMID: 34929350 DOI: 10.1016/j.aohep.2021.100653]

38 **Hamid S**, Alvares da Silva MR, Burak KW, Chen T, Drenth JPH, Esmat G, Gaspar R, LaBrecque D, Lee A, Macedo G, McMahon B, Ning Q, Reau N, Sonderup M, van Leeuwen DJ, Armstrong D, Yurdaydin C. WGO Guidance for the Care of Patients With COVID-19 and Liver Disease. *J Clin Gastroenterol* 2021; **55**: 1-11 [PMID: 33230011 DOI: 10.1097/MCG.0000000000001459]

39 **Aslam J**, Qaisar F, Khaliq M, Khalid M, Sabeeh DE, Ali AY. Association between Chronic Liver Disease Caused by Viral Hepatitis, Hospitalisation for COVID-19 and Mortality. *J Coll Physicians Surg Pak* 2023; **33**: 647-652 [PMID: 37300260 DOI: 10.29271/jcpsp.2023.06.647]

40 **Lin Y**, Yuan J, Long Q, Hu J, Deng H, Zhao Z, Chen J, Lu M, Huang A. Patients with SARS-CoV-2 and HBV co-infection are at risk of greater liver injury. *Genes Dis* 2021; **8**: 484-492 [PMID: 33225036 DOI: 10.1016/j.gendis.2020.11.005]

41 **Liu R**, Zhao L, Cheng X, Han H, Li C, Li D, Liu A, Gao G, Zhou F, Liu F, Jiang Y, Zhu C, Xia Y. Clinical characteristics of COVID-19 patients with hepatitis B virus infection - a retrospective study. *Liver Int* 2021; **41**: 720-730 [PMID: 33351265 DOI: 10.1111/liv.14774]

42 **Li P**, Liu Y, Cheng Z, Yu X, Li Y. COVID-19-associated liver injury: Clinical characteristics, pathophysiological mechanisms and treatment management. *Biomed Pharmacother* 2022; **154**: 113568 [PMID: 36029543 DOI: 10.1016/j.biopha.2022.113568]

43 **Yu R**, Tan S, Dan Y, Lu Y, Zhang J, Tan Z, He X, Xiang X, Zhou Y, Guo Y, Deng G, Chen Y, Tan W. Effect of SARS-CoV-2 coinfection was not apparent on the dynamics of chronic hepatitis B infection. *Virology* 2021; **553**: 131-134 [PMID: 33276282 DOI: 10.1016/j.virol.2020.11.012]

44 **Gordon A**, McLean CA, Pedersen JS, Bailey MJ, Roberts SK. Hepatic steatosis in chronic hepatitis B and C: predictors, distribution and effect on fibrosis. *J Hepatol* 2005; **43**: 38-44 [PMID: 15876468 DOI: 10.1016/j.jhep.2005.01.031]

World Journal of Gastroenterology

Submit a Manuscript: https://www.f6publishing.com

World J Gastroenterol 2024 March 21; 30(11): 1488-1493

DOI: 10.3748/wjg.v30.i11.1488

ISSN 1007-9327 (print) ISSN 2219-2840 (online)

EDITORIAL

Routine utilization of machine perfusion in liver transplantation: Ready for prime time?

Alessandro Parente, Keyue Sun, Philipp Dutkowski, AM James Shapiro, Andrea Schlegel

Specialty type: Gastroenterology and hepatology

Provenance and peer review: Invited article; Externally peer reviewed.

Peer-review model: Single blind

Peer-review report's scientific quality classification

Grade A (Excellent): A
Grade B (Very good): 0
Grade C (Good): 0
Grade D (Fair): 0
Grade E (Poor): 0

P-Reviewer: Kalinowski P, Poland

Received: January 3, 2024
Peer-review started: January 3, 2024
First decision: January 19, 2024
Revised: January 30, 2024
Accepted: February 28, 2024
Article in press: February 28, 2024
Published online: March 21, 2024

Alessandro Parente, AM James Shapiro, Department of Surgery, Division of Transplantation, University of Alberta Hospital, Edmonton T6G 2B7, Canada

Keyue Sun, Immunity and Inflammation, Lerner Research Institute, Cleveland, OH 44195, United States

Philipp Dutkowski, Swiss Hepato-Pancreato-Biliary Center, Department of Visceral and Transplantation Surgery, University Hospital Zurich, Zurich 8091, Switzerland

Andrea Schlegel, Immunity and Inflammation, Digestive Disease and Surgery Institute, Cleveland, OH 44195, United States

Corresponding author: Alessandro Parente, FEBS, MD, PhD, Surgeon, Department of Surgery, Division of Transplantation, University of Alberta Hospital, No. 8440 112 St NW, Edmonton T6G 2B7, Canada. aleparen@gmail.com

Abstract

The last decade has been notable for increasing high-quality research and dramatic improvement in outcomes with dynamic liver preservation. Robust evidence from numerous randomized controlled trials has been pooled by meta-analyses, providing the highest available evidence on the protective effect of machine perfusion (MP) over static cold storage in liver transplantation (LT). Based on a protective effect with less complications and improved graft survival, the field has seen a paradigm shift in organ preservation. This editorial focuses on the role of MP in LT and how it could become the new "gold standard". Strong collaborative efforts are needed to explore its effects on long-term outcomes.

Key Words: Liver transplantation; Machine perfusion; Viability assessment; Hypothermic oxygenated perfusion; Normothermic machine perfusion

Core Tip: Machine perfusion (MP) has garnered the interest of the transplant community given its proven beneficial effects on the clinical outcomes after liver transplantation (LT). Herein, we discuss the historical background of MP in LT and the available clinical evidence. Furthermore, we highlighted the obstacles and the need for future research, in particular with respect to viability assessment and prolonged preservation times.

Citation: Parente A, Sun K, Dutkowski P, Shapiro AJ, Schlegel A. Routine utilization of machine perfusion in liver transplantation: Ready for prime time? *World J Gastroenterol* 2024; 30(11): 1488-1493
URL: https://www.wjgnet.com/1007-9327/full/v30/i11/1488.htm
DOI: https://dx.doi.org/10.3748/wjg.v30.i11.1488

INTRODUCTION

Machine perfusion (MP) technology is an old concept first introduced by Alexis Carrell and Charles Lindberg in the 1920's, then utilized first in clinical kidney transplantation in 1968[1], however static cold storage (SCS) appeared simpler and more practical, effectively hindering the progress in MP technology development for more than 3 decades. Recently, MP has emerged as one of the most promising approaches to improve post-transplant outcomes after liver transplantation (LT).

Two main ex-situ liver perfusion and one in-situ donor approach are increasingly used in clinical practice today[2]. The first ex-situ technique is known as hypothermic oxygenated perfusion (HOPE) using a highly oxygenated (pO_2: > 60 kPa) artificial solution at hypothermic temperatures (8-12 °C)[2]. The second perfusion technique, normothermic MP (NMP), uses a blood-based perfusates at 37 °C, thus recreating a near-physiologic environment. Both HOPE and NMP are mainly applied after SCS, however NMP-preservation is also started upfront after minimal SCS of 2-3 hrs or as described with "ischemia-free organ transplantation (IFOT)", as a technique avoiding all SCS[2]. In contrast, during in-situ normothermic regional perfusion (NRP) a veno-arterial extracorporeal membrane oxygenation technique is used to recirculate and oxygenate donor blood immediately after circulatory arrest in donation after circulatory death (DCD) donors[2].

The importance of oxygen was understood early with the use of HOPE in kidney transplants in 1968, however the earlier perfusion concepts in LT were simply hypothermic (HMP). Guarrera *et al*[3] presented the first clinical study in LT in 2010 with HMP using a homegrown device (Figure 1). NRP was used first in uncontrolled DCD in 2007[4] and NMP started later off in clinics in 2016[5].

The very first randomized controlled trial (RCT) with NMP and the Organox-Metra® device was published in 2018 by Nasralla *et al*[6]. The authors demonstrated less early allograft dysfunction (EAD) and lower peak aspartate aminotransferase levels during the first week after transplant in the recipient of NMP-treated grafts compared to SCS[6]. Only one year later, similar results in terms of EAD were illustrated by another single center RCT, however with much smaller number of patients[7].

Next, in 2021, another two important RCTs were published. The first was focused on HOPE in DCD livers and demonstrated a four times lower risk of non-anastomotic biliary strictures compared to SCS, together with lower EAD-rates, postreperfusion syndrome and retransplantation[8]. And the second RCT paralleled such results with HOPE and showed less 90-d post-operative complications, shorter intensive care and hospital stay compared to SCS in extended criteria donor livers after brain death (DBD)[9]. The following 2 years, the findings of these studies with HOPE were supported by further RCTs. The Bologna team showed that patients receiving HOPE-treated extended criteria DBD livers had significantly lower EAD-rates, better 1-year graft survival, less post-LT complications and lower hospital re-admission rates compared to SCS[10]. Authors from the United States published the results of another multicenter RCT using the portable OCS™ device provided by Transmedics for upfront NMP[11]. The NMP group in this study had significantly lower EAD-rates and less signs of ischemia-reperfusion injury on histopathology[11].

In the first half of 2023, two RCTs were published: The largest RCT ever conducted with HOPE and the first one with IFOT. In the former, the authors illustrated that, although the number of serious complications between HOPE and SCS was similar, a post hoc analysis revealed that liver-related serious complications occurred less frequently in the HOPE group compared to SCS. Notably, graft failure due to liver-related complications did not occur with HOPE but in 7% of SCS grafts (6 of 85)[12]. Subsequently, a Chinese group reported the results of the first RCT of DBD livers randomly assigned to SCS or IFOT, demonstrating significantly reduced EAD-rates, post-reperfusion syndrome, less non-anastomotic biliary stricture, and less cumulative post-operative complications at 12 months[13]. A group from Poland assessed the role of HOPE in their country. In low-risk DBD donors HOPE had no impact on outcomes, however authors demonstrated significantly lower EAD-rates and post-operative complications in donor livers with higher risk, *i.e.*, with a donor risk index of > 1.7)[14]. Two additional RCTs were recently presented with NMP and HOPE in the United States. NMP with the Organox-Metra® device had a positive effect on the post-reperfusion syndrome[15], and HOPE showed lower primary non function, less EAD rates and reduced biliary strictures[16].

Such RCTs were recently combined with other retrospective studies in several meta-analyses[17], summarizing the beneficial effects of MP over SCS[18,19]. Currently, there are no available RCTs comparing HOPE and NMP, however results of ongoing RCT are awaited (Clinicaltrials.gov: NCT04644744).

While there are no RCT with NRP available yet, this technology appears to be beneficial to reduce biliary complications, improve graft survival and increase organ utilization if combined with limited SCS up to 6-7 hrs[20-22]. It seems

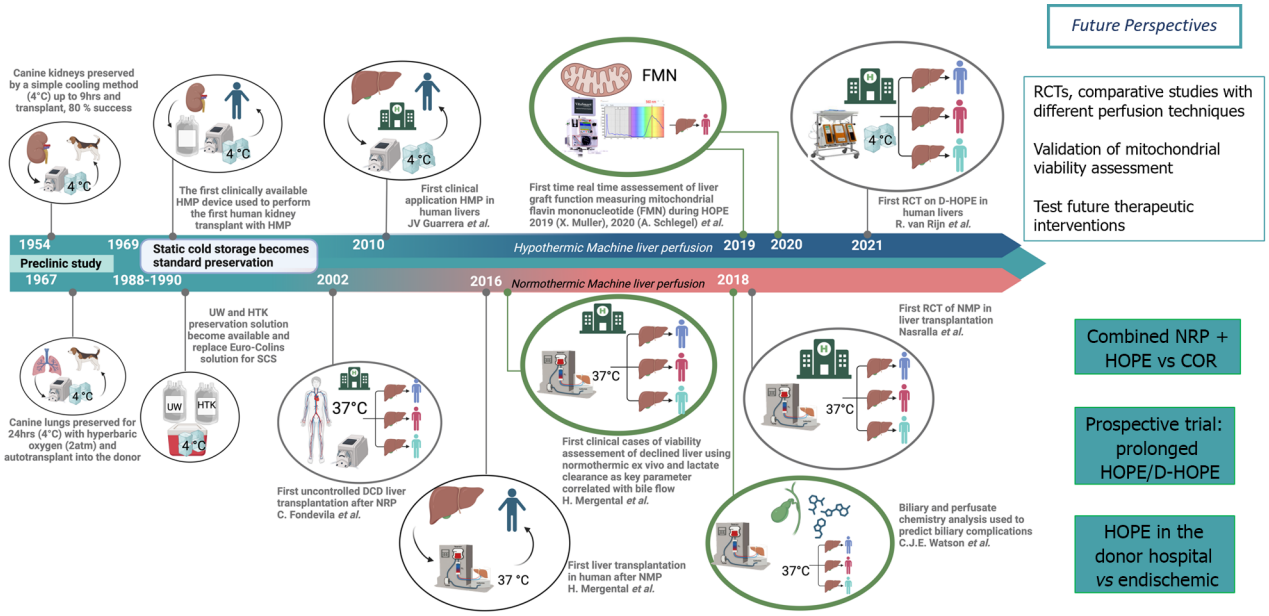

Figure 1 Overview on the history of organ and liver preservation. Key steps are highlighted for each time frame, with a final focus on the future research questions. HOPE: Hypothermic oxygenated perfusion; NRP: Normothermic regional perfusion; RCT: Randomized controlled trial; COR: Controlled oxygenated rewarming.

unlikely that a RCT would proceed as the clinical outcomes have been so positive to date-in fact it is currently mandated in France and other European countries that DCD donation should not proceed unless NRP is applied. Clinical studies demonstrated however several limitations, especially when donor warm ischemia time before or SCS after NRP are prolonged or when these grafts were used for retransplant candidates[23-26]. Perfusion technologies are not mutually exclusive, and indeed when looking at real-world data have been combined with satisfactory outcomes[27]. In particular, in Italy where the no-touch period following DCD donation is 20 min, combining NRP and HOPE has yielded good outcomes[28].

Despite its clinical benefits, MP is still not routinely used worldwide. There are several reasons behind this which have been identified as lack of funding, clarity as to what is research and what is accepted clinical care delivery, knowledge and availability of healthcare staff trained in the operation of this equipment[29,30]. In addition, it must be noted that the current available evidence is limited at one year follow-up. In fact, all RCTs and meta-analyses that have been published have reported their outcomes at one year. This appears to be one of the main limitations of the current available literature. As life expectancy of LT recipients continues to increase, exceeding 70% at 5 years[31], more evidence is needed to better understand the impact of MP on long-term outcomes after LT. Additionally, many RCTs have reported similar study endpoint outcome measures with however heterogenous definitions often lacking certain endpoints[18]. Future research will need to endeavor in more homogeneous outcome reporting to provide replicable data worldwide.

Perfusing marginal organ with the aim to increase liver utilization rates necessitate reliable viability tests. Although there are several biochemical factors that have been explored both for HOPE and NMP[32,33], there are no clear guidelines regarding a systematic viability assessment during liver perfusion and available parameters often lack sensitivity and acceptable positive predictive value to discriminate between livers of metabolically good quality and others with too high risk for failure in the recipient. Most viability parameters are usually measured in the perfusate, with arbitrary timepoints and cutoffs, reflecting a post ischemia-reperfusion injury downstream of instigating mitochondria in hepatocytes, including perfusate lactate, transaminases, cytokine, and lactate dehydrogenase. Bile chemistry is also applied to assist identification of livers at risk of ischemic cholangiopathy. The early occurring cellular damage during MP was recently assessed with proteomics analysis of bile collected during sequential HOPE, rewarming and subsequent NMP[34]. On the other hand, mitochondrial transition pore opening with danger signal release appears to be a more upfront parameter of liver injury[33,35,36]. There is evidence that MP could be utilized to reprogram mitochondrial metabolism during HOPE before normothermic reperfusion. The slow metabolism of succinate and concomitant ATP reloading are two protective mechanisms described with HOPE. A recent study has demonstrated that the analysis of flavin mononucleotide from complex I, perfusate nicotinamide adenine dinucleotide hydrogen, and mitochondrial CO_2 production during HOPE allows a more objective viability assessment of liver quality on a subcellular level which seems to be more reliable when compared to donor derived data, in particular for high-risk organs such as DCD[33].

In the real world, MP is used also for logistic reasons and prolonged liver preservation is increasingly used to enable timely LT with both NMP and HOPE[6,11,15,37]. A human liver graft was preserved for 3 d and successfully transplanted[38] and some discarded livers were preserved with MP up to 7 d with satisfactory viability parameters[39]. Although this approach might be of interest in the future to enable the modification of cellular metabolisms during ex-situ MP, its daily applicability is still limited to small number of cases and challenges with difficult devices required particularly for prolonged NMP[40].

Next to a prolonged *ex-situ* perfusion, super cooling and cryopreservation are potential but as yet untested clinically as additional technique to prolong organ preservation. A recent study has explored the concept of cryopreservation which enabled to preserve experimental kidney grafts for 100 d through vitrification and nanowarming[41]. Despite being compelling novel strategies, such techniques are currently limited to animal models or small studies and their potential future applications remains unclear.

CONCLUSION

In summary, within the past 5 years, increasing evidence has demonstrated the clinical benefits of MP in the setting of LT (Figure 1). We believe that this progress with MP technology and the clear beneficial effects will soon outpace and replace the standard SCS preservation for the human liver grafts, and now necessitates both a paradigm shift and rapid change in clinical practice to capitalize on these advances. This will pave the way for a new era in organ transplantation, leading to the application of MP routinely in clinical practice, in particular for marginal organs. However, several challenges remain and will need to be addressed in future research.

FOOTNOTES

Author contributions: Parente A and Schlegel A designed research; Parente A and Schlegel A wrote the manuscript; Sun K, Shapiro AMJ and Dutkowski P revised the manuscript. All authors approved the final version of the manuscript.

Conflict-of-interest statement: All authors declare no conflict of interest.

Country/Territory of origin: Canada

ORCID number: Alessandro Parente 0000-0001-5506-224X; Philipp Dutkowski 0000-0002-3016-604X; AM James Shapiro 0000-0002-6215-0990.

S-Editor: Qu XL
L-Editor: A
P-Editor: Cai YX

REFERENCES

1 **Belzer FO**, Ashby BS, Gulyassy PF, Powell M. Successful seventeen-hour preservation and transplantation of human-cadaver kidney. *N Engl J Med* 1968; **278**: 608-610 [PMID: 4866541 DOI: 10.1056/NEJM196803142781108]

2 **De Goeij FHC**, De Meijer V, Mergental H, Guarrera JV, Asthana S, Ghinolfi D, Boteon YL, Selzner N, Kalisvaart M, Pulitano C, Sonnenday C, Martins PN, Berlakovich G, Schlegel A. Challenges With the Implementation of Machine Perfusion in Clinical Liver Transplantation. *Transplantation* 2023 [PMID: 38057969 DOI: 10.1097/TP.0000000000004872]

3 **Guarrera JV**, Henry SD, Samstein B, Odeh-Ramadan R, Kinkhabwala M, Goldstein MJ, Ratner LE, Renz JF, Lee HT, Brown RS Jr, Emond JC. Hypothermic machine preservation in human liver transplantation: the first clinical series. *Am J Transplant* 2010; **10**: 372-381 [PMID: 19958323 DOI: 10.1111/j.1600-6143.2009.02932.x]

4 **Fondevila C**, Hessheimer AJ, Ruiz A, Calatayud D, Ferrer J, Charco R, Fuster J, Navasa M, Rimola A, Taurá P, Ginés P, Manyalich M, García-Valdecasas JC. Liver transplant using donors after unexpected cardiac death: novel preservation protocol and acceptance criteria. *Am J Transplant* 2007; **7**: 1849-1855 [PMID: 17564639 DOI: 10.1111/j.1600-6143.2007.01846.x]

5 **Ravikumar R**, Jassem W, Mergental H, Heaton N, Mirza D, Perera MT, Quaglia A, Holroyd D, Vogel T, Coussios CC, Friend PJ. Liver Transplantation After Ex Vivo Normothermic Machine Preservation: A Phase 1 (First-in-Man) Clinical Trial. *Am J Transplant* 2016; **16**: 1779-1787 [PMID: 26752191 DOI: 10.1111/ajt.13708]

6 **Nasralla D**, Coussios CC, Mergental H, Akhtar MZ, Butler AJ, Ceresa CDL, Chiocchia V, Dutton SJ, García-Valdecasas JC, Heaton N, Imber C, Jassem W, Jochmans I, Karani J, Knight SR, Kocabayoglu P, Malagò M, Mirza D, Morris PJ, Pallan A, Paul A, Pavel M, Perera MTPR, Pirenne J, Ravikumar R, Russell L, Upponi S, Watson CJE, Weissenbacher A, Ploeg RJ, Friend PJ; Consortium for Organ Preservation in Europe. A randomized trial of normothermic preservation in liver transplantation. *Nature* 2018; **557**: 50-56 [PMID: 29670285 DOI: 10.1038/s41586-018-0047-9]

7 **Ghinolfi D**, Rreka E, De Tata V, Franzini M, Pezzati D, Fierabracci V, Masini M, Cacciatoinsilla A, Bindi ML, Marselli L, Mazzotti V, Morganti R, Marchetti P, Biancofiore G, Campani D, Paolicchi A, De Simone P. Pilot, Open, Randomized, Prospective Trial for Normothermic Machine Perfusion Evaluation in Liver Transplantation From Older Donors. *Liver Transpl* 2019; **25**: 436-449 [PMID: 30362649 DOI: 10.1002/lt.25362]

8 **van Rijn R**, Schurink IJ, de Vries Y, van den Berg AP, Cortes Cerisuelo M, Darwish Murad S, Erdmann JI, Gilbo N, de Haas RJ, Heaton N, van Hoek B, Huurman VAL, Jochmans I, van Leeuwen OB, de Meijer VE, Monbaliu D, Polak WG, Slangen JJG, Troisi RI, Vanlander A, de Jonge J, Porte RJ; DHOPE-DCD Trial Investigators. Hypothermic Machine Perfusion in Liver Transplantation - A Randomized Trial. *N Engl J*

Med 2021; **384**: 1391-1401 [PMID: 33626248 DOI: 10.1056/NEJMoa2031532]

9 **Czigany Z**, Pratschke J, Froněk J, Guba M, Schöning W, Raptis DA, Andrassy J, Kramer M, Strnad P, Tolba RH, Liu W, Keller T, Miller H, Pavicevic S, Uluk D, Kocik M, Lurje I, Trautwein C, Mehrabi A, Popescu I, Vondran FWR, Ju C, Tacke F, Neumann UP, Lurje G. Hypothermic Oxygenated Machine Perfusion Reduces Early Allograft Injury and Improves Post-transplant Outcomes in Extended Criteria Donation Liver Transplantation From Donation After Brain Death: Results From a Multicenter Randomized Controlled Trial (HOPE ECD-DBD). *Ann Surg* 2021; **274**: 705-712 [PMID: 34334635 DOI: 10.1097/SLA.0000000000005110]

10 **Ravaioli M**, Germinario G, Dajti G, Sessa M, Vasuri F, Siniscalchi A, Morelli MC, Serenari M, Del Gaudio M, Zanfi C, Odaldi F, Bertuzzo VR, Maroni L, Laurenzi A, Cescon M. Hypothermic oxygenated perfusion in extended criteria donor liver transplantation-A randomized clinical trial. *Am J Transplant* 2022; **22**: 2401-2408 [PMID: 35671067 DOI: 10.1111/ajt.17115]

11 **Markmann JF**, Abouljoud MS, Ghobrial RM, Bhati CS, Pelletier SJ, Lu AD, Ottmann S, Klair T, Eymard C, Roll GR, Magliocca J, Pruett TL, Reyes J, Black SM, Marsh CL, Schnickel G, Kinkhabwala M, Florman SS, Merani S, Demetris AJ, Kimura S, Rizzari M, Saharia A, Levy M, Agarwal A, Cigarroa FG, Eason JD, Syed S, Washburn WK, Parekh J, Moon J, Maskin A, Yeh H, Vagefi PA, MacConmara MP. Impact of Portable Normothermic Blood-Based Machine Perfusion on Outcomes of Liver Transplant: The OCS Liver PROTECT Randomized Clinical Trial. *JAMA Surg* 2022; **157**: 189-198 [PMID: 34985503 DOI: 10.1001/jamasurg.2021.6781]

12 **Schlegel A**, Mueller M, Muller X, Eden J, Panconesi R, von Felten S, Steigmiller K, Sousa Da Silva RX, de Rougemont O, Mabrut JY, Lesurtel M, Cerisuelo MC, Heaton ND, Allard MA, Adam R, Monbaliu D, Jochmans I, Haring MPD, Porte RJ, Parente A, Muiesan P, Kron P, Attia M, Kollmann D, Berlakovich G, Rogiers X, Petterson K, Kranich AL, Amberg S, Müllhaupt B, Clavien PA, Dutkowski P. A multicenter randomized-controlled trial of hypothermic oxygenated perfusion (HOPE) for human liver grafts before transplantation. *J Hepatol* 2023; **78**: 783-793 [PMID: 36681160 DOI: 10.1016/j.jhep.2022.12.030]

13 **Guo Z**, Zhao Q, Jia Z, Huang C, Wang D, Ju W, Zhang J, Yang L, Huang S, Chen M, Zhu X, Hu A, Ma Y, Wu L, Chen Y, Han M, Tang Y, Wang G, Wang L, Li L, Xiong W, Zhang Z, Shen Y, Tang Z, Zhu C, Chen X, Hu X, Guo Y, Chen H, Zhang T, Zeng P, Lai S, Wang T, Chen Z, Gong J, Yu J, Sun C, Li C, Tan H, Liu Y, Dong Y, Liao B, Ren J, Zhou Z, Andrea S, Björn N, Cai C, Gong F, Rong J, Huang W, Guan X, Clavien PA, Stefan TG, Huang J, He X. A randomized-controlled trial of ischemia-free liver transplantation for end-stage liver disease. *J Hepatol* 2023; **79**: 394-402 [PMID: 37086919 DOI: 10.1016/j.jhep.2023.04.010]

14 **Grąt M**, Morawski M, Zhylko A, Rykowski P, Krasnodębski M, Wyporski A, Borkowski J, Lewandowski Z, Kobryń K, Stankiewicz R, Stypułkowski J, Hołówko W, Patkowski W, Mielczarek-Puta M, Struga M, Szczepankiewicz B, Górnicka B, Krawczyk M. Routine End-ischemic Hypothermic Oxygenated Machine Perfusion in Liver Transplantation From Donors After Brain Death: A Randomized Controlled Trial. *Ann Surg* 2023; **278**: 662-668 [PMID: 37497636 DOI: 10.1097/SLA.0000000000006055]

15 **Chapman WC**, Barbas AS, D'Alessandro AM, Vianna R, Kubal CA, Abt P, Sonnenday C, Barth R, Alvarez-Casas J, Yersiz H, Eckhoff D, Cannon R, Genyk Y, Sher L, Singer A, Feng S, Roll G, Cohen A, Doyle MB, Sudan DL, Al-Adra D, Khan A, Subramanian V, Abraham N, Olthoff K, Tekin A, Berg L, Coussios C, Morris C, Randle L, Friend P, Knechtle SJ. Normothermic Machine Perfusion of Donor Livers for Transplantation in the United States: A Randomized Controlled Trial. *Ann Surg* 2023; **278**: e912-e921 [PMID: 37389552 DOI: 10.1097/SLA.0000000000005934]

16 **Panayotova GG**, Lunsford KE, Quillin RC 3rd, Rana A, Agopian VG, Lee-Riddle GS, Markovic D, Paterno F, Griesemer AD, Amin A, Alonso D, Rocca JP, Borja-Cacho D, Hernandez-Alejandro R, Fung JJ, Pelletier SJ, Shah SA, Guarrera JV. Portable hypothermic oxygenated machine perfusion for organ preservation in liver transplantation: A randomized, open-label, clinical trial. *Hepatology* 2023 [PMID: 38090880 DOI: 10.1097/HEP.0000000000000715]

17 **Parente A**, Dondossola D, Dutkowski P, Schlegel A. Current evidence on the beneficial HOPE-effect based on systematic reviews and meta-analyses in liver transplantation. *J Hepatol* 2024; **80**: e116-e119 [PMID: 37952765 DOI: 10.1016/j.jhep.2023.10.033]

18 **Parente A**, Tirotta F, Pini A, Eden J, Dondossola D, Manzia TM, Dutkowski P, Schlegel A. Machine perfusion techniques for liver transplantation - A meta-analysis of the first seven randomized-controlled trials. *J Hepatol* 2023; **79**: 1201-1213 [PMID: 37302578 DOI: 10.1016/j.jhep.2023.05.027]

19 **Tingle SJ**, Dobbins JJ, Thompson ER, Figueiredo RS, Mahendran B, Pandanaboyana S, Wilson C. Machine perfusion in liver transplantation. *Cochrane Database Syst Rev* 2023; **9**: CD014685 [PMID: 37698189 DOI: 10.1002/14651858.CD014685.pub2]

20 **Hessheimer AJ**, de la Rosa G, Gastaca M, Ruíz P, Otero A, Gómez M, Alconchel F, Ramírez P, Bosca A, López-Andújar R, Atutxa L, Royo-Villanova M, Sánchez B, Santoyo J, Marín LM, Gómez-Bravo MÁ, Mosteiro F, Villegas Herrera MT, Villar Del Moral J, González-Abos C, Vidal B, López-Domínguez J, Lladó L, Roldán J, Justo I, Jiménez C, López-Monclús J, Sánchez-Turrión V, Rodríguez-Laíz G, Velasco Sánchez E, López-Baena JÁ, Caralt M, Charco R, Tomé S, Varo E, Martí-Cruchaga P, Rotellar F, Varona MA, Barrera M, Rodríguez-Sanjuan JC, Briceño J, López D, Blanco G, Nuño J, Pacheco D, Coll E, Domínguez-Gil B, Fondevila C. Abdominal normothermic regional perfusion in controlled donation after circulatory determination of death liver transplantation: Outcomes and risk factors for graft loss. *Am J Transplant* 2022; **22**: 1169-1181 [PMID: 34856070 DOI: 10.1111/ajt.16899]

21 **Hessheimer AJ**, Coll E, Torres F, Ruíz P, Gastaca M, Rivas JI, Gómez M, Sánchez B, Santoyo J, Ramírez P, Parrilla P, Marín LM, Gómez-Bravo MÁ, García-Valdecasas JC, López-Monclús J, Boscá A, López-Andújar R, Fundora-Suárez J, Villar J, García-Sesma Á, Jiménez C, Rodríguez-Laíz G, Lladó L, Rodríguez JC, Barrera M, Charco R, López-Baena JÁ, Briceño J, Pardo F, Blanco G, Pacheco D, Domínguez-Gil B, Sánchez Turrión V, Fondevila C. Normothermic regional perfusion vs. super-rapid recovery in controlled donation after circulatory death liver transplantation. *J Hepatol* 2019; **70**: 658-665 [PMID: 30582980 DOI: 10.1016/j.jhep.2018.12.013]

22 **Oniscu GC**, Mehew J, Butler AJ, Sutherland A, Gaurav R, Hogg R, Currie I, Jones M, Watson CJE. Improved Organ Utilization and Better Transplant Outcomes With In Situ Normothermic Regional Perfusion in Controlled Donation After Circulatory Death. *Transplantation* 2023; **107**: 438-448 [PMID: 35993664 DOI: 10.1097/TP.0000000000004280]

23 **Richards JA**, Gaurav R, Upponi SS, Swift L, Fear C, Webb GJ, Allison MED, Watson CJE, Butler AJ. Outcomes of livers from donation after circulatory death donors with extended agonal phase and the adjunct of normothermic regional perfusion. *Br J Surg* 2023; **110**: 1112-1115 [PMID: 37079886 DOI: 10.1093/bjs/znad099]

24 **Gaurav R**, Butler AJ, Kosmoliaptsis V, Mumford L, Fear C, Swift L, Fedotovs A, Upponi S, Khwaja S, Richards J, Allison M, Watson CJE. Liver Transplantation Outcomes From Controlled Circulatory Death Donors: SCS vs in situ NRP vs ex situ NMP. *Ann Surg* 2022; **275**: 1156-1164 [PMID: 35258511 DOI: 10.1097/SLA.0000000000005428]

25 **Antoine C**, Jasseron C, Dondero F, Savier E; French National Steering Committee of Donors After Circulatory Death. Liver Transplantation From Controlled Donors After Circulatory Death Using Normothermic Regional Perfusion: An Initial French Experience. *Liver Transpl* 2020; **26**: 1516-1521 [PMID: 32531132 DOI: 10.1002/lt.25818]

26 **Savier E**, Lim C, Rayar M, Orlando F, Boudjema K, Mohkam K, Lesurtel M, Mabrut JY, Pittau G, Begdadi N, Cherqui D, Adam R, Dondero

F, Sepulveda A, Soubrane O, Bucur P, Barbier L, Salame E, Jasseron C, Antoine C, Riou B, Scatton O. Favorable Outcomes of Liver Transplantation from Controlled Circulatory Death Donors Using Normothermic Regional Perfusion Compared to Brain Death Donors. *Transplantation* 2020; **104**: 1943-1951 [PMID: 32639402 DOI: 10.1097/TP.0000000000003372]

27 **van Leeuwen OB**, Bodewes SB, Lantinga VA, Haring MPD, Thorne AM, Brüggenwirth IMA, van den Berg AP, de Boer MT, de Jong IEM, de Kleine RHJ, Lascaris B, Nijsten MWN, Reyntjens KMEM, de Meijer VE, Porte RJ. Sequential hypothermic and normothermic machine perfusion enables safe transplantation of high-risk donor livers. *Am J Transplant* 2022; **22**: 1658-1670 [PMID: 35286759 DOI: 10.1111/ajt.17022]

28 **De Carlis R**, Schlegel A, Frassoni S, Olivieri T, Ravaioli M, Camagni S, Patrono D, Bassi D, Pagano D, Di Sandro S, Lauterio A, Bagnardi V, Gruttadauria S, Cillo U, Romagnoli R, Colledan M, Cescon M, Di Benedetto F, Muiesan P, De Carlis L. How to Preserve Liver Grafts From Circulatory Death With Long Warm Ischemia? A Retrospective Italian Cohort Study With Normothermic Regional Perfusion and Hypothermic Oxygenated Perfusion. *Transplantation* 2021; **105**: 2385-2396 [PMID: 33617211 DOI: 10.1097/TP.0000000000003595]

29 **Parente A**, Flores Carvalho M, Panconesi R, Boteon YL, De Carlis R, Dutkowski P, Muiesan P, Dondossola D, Schlegel A. Trends and Obstacles to Implement Dynamic Perfusion Concepts for Clinical Liver Transplantation: Results from a Global Web-Based Survey. *J Clin Med* 2023; **12** [PMID: 37297960 DOI: 10.3390/jcm12113765]

30 **Flores Carvalho M**, Boteon YL, Guarrera JV, Modi PR, Lladó L, Lurje G, Kasahara M, Dutkowski P, Schlegel A. Obstacles to implement machine perfusion technology in routine clinical practice of transplantation: Why are we not there yet? *Hepatology* 2024; **79**: 713-730 [PMID: 37013926 DOI: 10.1097/HEP.0000000000000394]

31 OPTN/SRTR 2020 Annual Data Report: Liver. *HRSA*.Available from: https://srtr.transplant.hrsa.gov/annual_reports/2020/Liver.aspx

32 **Mergental H**, Laing RW, Kirkham AJ, Perera MTPR, Boteon YL, Attard J, Barton D, Curbishley S, Wilkhu M, Neil DAH, Hübscher SG, Muiesan P, Isaac JR, Roberts KJ, Abradelo M, Schlegel A, Ferguson J, Cilliers H, Bion J, Adams DH, Morris C, Friend PJ, Yap C, Afford SC, Mirza DF. Transplantation of discarded livers following viability testing with normothermic machine perfusion. *Nat Commun* 2020; **11**: 2939 [PMID: 32546694 DOI: 10.1038/s41467-020-16251-3]

33 **Eden J**, Breuer E, Birrer D, Müller M, Pfister M, Mayr H, Sun K, Widmer J, Huwyler F, Ungethüm U, Humar B, Gupta A, Schiess S, Wendt M, Immer F, Elmer A, Meierhofer D, Schlegel A, Dutkowski P. Screening for mitochondrial function before use-routine liver assessment during hypothermic oxygenated perfusion impacts liver utilization. *EBioMedicine* 2023; **98**: 104857 [PMID: 37918219 DOI: 10.1016/j.ebiom.2023.104857]

34 **Thorne AM**, Wolters JC, Lascaris B, Bodewes SB, Lantinga VA, van Leeuwen OB, de Jong IEM, Ustyantsev K, Berezikov E, Lisman T, Kuipers F, Porte RJ, de Meijer VE. Bile proteome reveals biliary regeneration during normothermic preservation of human donor livers. *Nat Commun* 2023; **14**: 7880 [PMID: 38036513 DOI: 10.1038/s41467-023-43368-y]

35 **Eden J**, Dutkowski P. Prolonging Preservation or Assessment of Organ Quality-What is Key? *Transpl Int* 2023; **36**: 12174 [PMID: 38020743 DOI: 10.3389/ti.2023.12174]

36 **Sampaziotis F**, Muraro D, Tysoe OC, Sawiak S, Beach TE, Godfrey EM, Upponi SS, Brevini T, Wesley BT, Garcia-Bernardo J, Mahbubani K, Canu G, Gieseck R 3rd, Berntsen NL, Mulcahy VL, Crick K, Fear C, Robinson S, Swift L, Gambardella L, Bargehr J, Ortmann D, Brown SE, Osnato A, Murphy MP, Corbett G, Gelson WTH, Mells GF, Humphreys P, Davies SE, Amin I, Gibbs P, Sinha S, Teichmann SA, Butler AJ, See TC, Melum E, Watson CJE, Saeb-Parsy K, Vallier L. Cholangiocyte organoids can repair bile ducts after transplantation in the human liver. *Science* 2021; **371**: 839-846 [PMID: 33602855 DOI: 10.1126/science.aaz6964]

37 **Brüggenwirth IMA**, Mueller M, Lantinga VA, Camagni S, De Carlis R, De Carlis L, Colledan M, Dondossola D, Drefs M, Eden J, Ghinolfi D, Koliogiannis D, Lurje G, Manzia TM, Monbaliu D, Muiesan P, Patrono D, Pratschke J, Romagnoli R, Rayar M, Roma F, Schlegel A, Dutkowski P, Porte RJ, de Meijer VE. Prolonged preservation by hypothermic machine perfusion facilitates logistics in liver transplantation: A European observational cohort study. *Am J Transplant* 2022; **22**: 1842-1851 [PMID: 35315202 DOI: 10.1111/ajt.17037]

38 **Clavien PA**, Dutkowski P, Mueller M, Eshmuminov D, Bautista Borrego L, Weber A, Muellhaupt B, Sousa Da Silva RX, Burg BR, Rudolf von Rohr P, Schuler MJ, Becker D, Hefti M, Tibbitt MW. Transplantation of a human liver following 3 days of ex situ normothermic preservation. *Nat Biotechnol* 2022; **40**: 1610-1616 [PMID: 35641829 DOI: 10.1038/s41587-022-01354-7]

39 **Lau NS**, Ly M, Dennis C, Liu K, Kench J, Crawford M, Pulitano C. Long-term normothermic perfusion of human livers for longer than 12 days. *Artif Organs* 2022; **46**: 2504-2510 [PMID: 35929443 DOI: 10.1111/aor.14372]

40 **Eshmuminov D**, Becker D, Bautista Borrego L, Hefti M, Schuler MJ, Hagedorn C, Muller X, Mueller M, Onder C, Graf R, Weber A, Dutkowski P, Rudolf von Rohr P, Clavien PA. An integrated perfusion machine preserves injured human livers for 1 week. *Nat Biotechnol* 2020; **38**: 189-198 [PMID: 31932726 DOI: 10.1038/s41587-019-0374-x]

41 **Han Z**, Rao JS, Gangwar L, Namsrai BE, Pasek-Allen JL, Etheridge ML, Wolf SM, Pruett TL, Bischof JC, Finger EB. Vitrification and nanowarming enable long-term organ cryopreservation and life-sustaining kidney transplantation in a rat model. *Nat Commun* 2023; **14**: 3407 [PMID: 37296144 DOI: 10.1038/s41467-023-38824-8]

World Journal of Gastroenterology

Submit a Manuscript: https://www.f6publishing.com

World J Gastroenterol 2024 March 21; 30(11): 1494-1496

DOI: 10.3748/wjg.v30.i11.1494

ISSN 1007-9327 (print) ISSN 2219-2840 (online)

EDITORIAL

Advancements in Barrett's esophagus detection: The role of artificial intelligence and its implications

Sara Massironi

Specialty type: Gastroenterology and hepatology

Provenance and peer review: Invited article; Externally peer reviewed.

Peer-review model: Single blind

Peer-review report's scientific quality classification

Grade A (Excellent): A
Grade B (Very good): 0
Grade C (Good): 0
Grade D (Fair): 0
Grade E (Poor): 0

P-Reviewer: Haddadi S, Algeria

Received: January 7, 2024
Peer-review started: January 7, 2024
First decision: January 23, 2024
Revised: January 27, 2024
Accepted: February 27, 2024
Article in press: February 27, 2024
Published online: March 21, 2024

Sara Massironi, Division of Gastroenterology and Center for Autoimmune Liver Diseases, Department of Medicine and Surgery, Fondazione IRCCS San Gerardo dei Tintori, University of Milano-Bicocca, Monza 20900, Italy

Corresponding author: Sara Massironi, MD, PhD, Adjunct Professor, Division of Gastroenterology and Center for Autoimmune Liver Diseases, Department of Medicine and Surgery, Fondazione IRCCS San Gerardo dei Tintori, University of Milano-Bicocca, Via Pergolesi 33, Monza 20900, Italy. sara.massironi@libero.it

Abstract

Artificial intelligence (AI) is making significant strides in revolutionizing the detection of Barrett's esophagus (BE), a precursor to esophageal adenocarcinoma. In the research article by Tsai *et al*, researchers utilized endoscopic images to train an AI model, challenging the traditional distinction between endoscopic and histological BE. This approach yielded remarkable results, with the AI system achieving an accuracy of 94.37%, sensitivity of 94.29%, and specificity of 94.44%. The study's extensive dataset enhances the AI model's practicality, offering valuable support to endoscopists by minimizing unnecessary biopsies. However, questions about the applicability to different endoscopic systems remain. The study underscores the potential of AI in BE detection while highlighting the need for further research to assess its adaptability to diverse clinical settings.

Key Words: Barrett's esophagus; Artificial intelligence; Endoscopic images; Artificial intelligence model; Early cancer detection; Endoscopy

Core Tip: The use of artificial intelligence (AI) to detect Barrett's esophagus (BE) is a groundbreaking advancement in the field of gastroenterology. This innovative approach, which employs endoscopic images for training AI models, challenges the conventional distinction between endoscopic and histological BE. The results show good promise, with the AI system achieving high accuracy, sensitivity, and specificity in BE detection. This development has the potential to reduce unnecessary biopsies and streamline the diagnostic process. However, the adaptability of AI to different endoscopic systems remains a critical consideration, warranting further research for widespread clinical implementation.

Citation: Massironi S. Advancements in Barrett's esophagus detection: The role of artificial intelligence and its implications. *World J Gastroenterol* 2024; 30(11): 1494-1496
URL: https://www.wjgnet.com/1007-9327/full/v30/i11/1494.htm
DOI: https://dx.doi.org/10.3748/wjg.v30.i11.1494

INTRODUCTION

Barrett's esophagus (BE), a disease characterized by the transformation of the esophageal mucosa, poses a significant risk as a precursor to esophageal adenocarcinoma (EAC)[1,2]. In recent years, the prevalence of BE has increased not only in Western countries but also in Asia[2], highlighting the urgent need for efficient detection and diagnostic methods. Endoscopic surveillance and early detection of BE is crucial as it can significantly reduce the risk of EAC. However, current methods for diagnosing BE suffer from limitations, including inter-observer variability[3] and time-consuming procedures. Indeed, a large percentage of early EAC and BE-associated high-grade dysplasia goes undetected due to inadequate compliance with the Seattle protocol and errors in sample collection[4]. This is where artificial intelligence (AI) comes into play, which has the potential to fundamentally change the management of BE.

AI has already revolutionized various aspects of healthcare and is also making great strides in the field of gastroenterology and endoscopy. Researchers have explored the potential of AI in detecting and classifying various diseases such as intestinal polyps, gastric cancer, and inflammatory bowel diseases[5]. However, in the field of BE, training these AI models was challenging due to the lack of histologically confirmed BE images.

The research article by Tsai *et al*[6], published in the *World Journal of Gastroenterology*, is timely and pertinent. The authors' approach to addressing the gap in detection rates between endoscopic and histological BE is commendable. They utilized a dataset of 724 cases with endoscopic narrow-band imaging (NBI) and employed an AI system called 'EndoAID', which utilizes a deep learning algorithm specifically trained on NBI to accurately detect and classify BE, significantly enhancing early detection capabilities. The use of three senior endoscopists for image annotation adds a layer of robustness and credibility to the training process. The AI system was then tested on cases with and without histologically proven BE. The results showed that the AI model achieved an accuracy of 94.37% in detecting BE, with a sensitivity of 94.29% and a specificity of 94.44%. These results far outperform previous AI models and show great potential to improve BE detection.

Traditionally, AI models have heavily relied on histological images for training, limiting their adaptability to real-world endoscopic scenarios. However, in this groundbreaking research, the focus shifted towards utilizing endoscopic images for training. The profound significance of this shift lies in the realization that the features observed in endoscopic BE closely mirror those of histological BE. This discovery challenges the conventional demarcation between endoscopic and histologic BE and sheds light on a potential source of discrepancies – sampling or biopsy bias[4].

DATA SET COMPARED TO PREVIOUS STUDIES

In addition, this study included a significantly larger data set compared to previous studies, leading to more robust and reliable results.

The ultimate goal of this AI system is to serve as a valuable tool for endoscopists by providing timely reminders to consider a biopsy when BE is suspected during an endoscopy procedure. This functionality is expected to play a critical role in reducing unnecessary biopsies, which can be both invasive and costly[7]. In addition, it has the potential to streamline the diagnostic process and ultimately improve the overall efficiency and accuracy of BE detection. Moreover, early detection of BE is critical in reducing the incidence of esophago-gastric junction cancer as it allows for the timely identification and treatment of precancerous changes in the esophageal mucosa.

However, there are some limitations to this study. The data were collected in two medical centers in central Taiwan, which may not fully represent the different demographics and endoscopic systems worldwide.

In addition, the study focused exclusively on endoscopic images with NBI, raising the question of applicability to other types of endoscopic systems. Indeed, although NBI has proven its effectiveness in certain contexts, it is important to remember that different endoscopic systems may use different imaging technologies, each with its own strengths and limitations. As recently highlighted, the performance of computer-aided detection systems (CADe) for detecting polyps can vary significantly depending on the system used[8] and each system exhibited distinct performance characteristics, even when analyzing the same set of videos. Factors such as system updates and customizable detection thresholds played a significant role in determining the detection capabilities of these CADe systems. Therefore, further research is

warranted to assess how different endoscopic technologies and configurations may influence the performance of AI models in detecting BE. Such investigations will be crucial for ensuring the broad and effective deployment of AI in clinical practice.

CONCLUSION

In summary, this study represents an important milestone in the field of gastroenterology and AI. It demonstrates the potential of AI to improve the accuracy and efficiency of BE detection, potentially preventing progression to EAC. The advancement of AI promises to transform healthcare and improve patient outcomes across multiple medical specialties. The path to early cancer prevention is becoming clearer thanks to the power of AI.

FOOTNOTES

Author contributions: Massironi S authored the commentary article, contributing her expertise and insights to analyze the research findings, contextualize their significance in the field of gastroenterology, and articulate the implications of AI-assisted detection in Barrett's esophagus for the broader medical community.

Conflict-of-interest statement: Massironi S declares that there are no conflicts of interest regarding the publication of this article, with no financial, consultative, institutional, or other relationships that might lead to bias or a conflict of interest.

Country/Territory of origin: Italy

ORCID number: Sara Massironi 0000-0003-3214-8192.

S-Editor: Lin C
L-Editor: A
P-Editor: Cai YX

REFERENCES

1 **di Pietro M**, Alzoubaidi D, Fitzgerald RC. Barrett's esophagus and cancer risk: how research advances can impact clinical practice. *Gut Liver* 2014; **8**: 356-370 [PMID: 25071900 DOI: 10.5009/gnl.2014.8.4.356]
2 **Beydoun AS**, Stabenau KA, Altman KW, Johnston N. Cancer Risk in Barrett's Esophagus: A Clinical Review. *Int J Mol Sci* 2023; **24** [PMID: 37046992 DOI: 10.3390/ijms24076018]
3 **Berbís MA**, Aneiros-Fernández J, Mendoza Olivares FJ, Nava E, Luna A. Role of artificial intelligence in multidisciplinary imaging diagnosis of gastrointestinal diseases. *World J Gastroenterol* 2021; **27**: 4395-4412 [PMID: 34366612 DOI: 10.3748/wjg.v27.i27.4395]
4 **Zilberstein N**, Godbee M, Mehta NA, Waxman I. Advanced endoscopic imaging for detection of Barrett's esophagus. *Clin Endosc* 2024; **57**: 1-10 [PMID: 38178326 DOI: 10.5946/ce.2023.031]
5 **Stan-Ilie M**, Sandru V, Constantinescu G, Plotogea OM, Rinja EM, Tincu IF, Jichitu A, Carasel AE, Butuc AC, Popa B. Artificial Intelligence-The Rising Star in the Field of Gastroenterology and Hepatology. *Diagnostics (Basel)* 2023; **13** [PMID: 36832150 DOI: 10.3390/diagnostics13040662]
6 **Tsai MC**, Yen HH, Tsai HY, Huang YK, Luo YS, Kornelius E, Sung WW, Lin CC, Tseng MH, Wang CC. Artificial intelligence system for the detection of Barrett's esophagus. *World J Gastroenterol* 2023; **29**: 6198-6207 [PMID: 38186865 DOI: 10.3748/wjg.v29.i48.6198]
7 **Libanio D**, Antonelli G, Marijnissen F, Spaander MC, Hassan C, Dinis-Ribeiro M, Areia M. Combined gastric and colorectal cancer endoscopic screening may be cost-effective in Europe with the implementation of artificial intelligence: an economic evaluation. *Eur J Gastroenterol Hepatol* 2024; **36**: 155-161 [PMID: 38131423 DOI: 10.1097/MEG.0000000000002680]
8 **Troya J**, Sudarevic B, Krenzer A, Banck M, Brand M, Walter BM, Puppe F, Zoller WG, Meining A, Hann A. Direct comparison of multiple computer-aided polyp detection systems. *Endoscopy* 2024; **56**: 63-69 [PMID: 37532115 DOI: 10.1055/a-2147-0571]

World Journal of Gastroenterology

Submit a Manuscript: https://www.f6publishing.com

World J Gastroenterol 2024 March 21; 30(11): 1497-1523

DOI: 10.3748/wjg.v30.i11.1497

ISSN 1007-9327 (print) ISSN 2219-2840 (online)

REVIEW

MicroRNAs: A novel signature in the metastasis of esophageal squamous cell carcinoma

Qi-Ying Wei, Feng Jin, Zhong-Yu Wang, Bing-Jie Li, Wen-Bo Cao, Zhi-Yan Sun, Sai-Jun Mo

Specialty type: Gastroenterology and hepatology

Provenance and peer review: Invited article; Externally peer reviewed.

Peer-review model: Single blind

Peer-review report's scientific quality classification

Grade A (Excellent): 0
Grade B (Very good): B
Grade C (Good): 0
Grade D (Fair): 0
Grade E (Poor): 0

P-Reviewer: Motlagh B, Iran

Received: December 13, 2023
Peer-review started: December 13, 2023
First decision: December 28, 2023
Revised: January 12, 2024
Accepted: March 1, 2024
Article in press: March 1, 2024
Published online: March 21, 2024

Qi-Ying Wei, Feng Jin, Bing-Jie Li, Wen-Bo Cao, Department of Pathophysiology, School of Basic Medical Sciences, Zhengzhou University, Zhengzhou 450001, Henan Province, China

Zhong-Yu Wang, Department of Perioperative Medicine, The First Affiliated Hospital of Zhengzhou University, Zhengzhou 450052, Henan Province, China

Zhi-Yan Sun, Division of Special Service, Department of Basic Oncology, School of Basic Medicine, Zhengzhou University, Zhengzhou 450001, Henan Province, China

Sai-Jun Mo, Department of Basic Science of Oncology, School of Basic Medical Sciences, Zhengzhou University, Zhengzhou 450001, Henan Province, China

Corresponding author: Sai-Jun Mo, PhD, Associate Professor, Department of Basic Science of Oncology, School of Basic Medical Sciences, Zhengzhou University, No. 100 Science Avenue, Zhongyuan District, Zhengzhou 450001, Henan Province, China. sjmo@zzu.edu.cn

Abstract

Esophageal squamous cell carcinoma (ESCC) is a malignant epithelial tumor, characterized by squamous cell differentiation, it is the sixth leading cause of cancer-related deaths globally. The increased mortality rate of ESCC patients is predominantly due to the advanced stage of the disease when discovered, coupled with higher risk of metastasis, which is an exceedingly malignant characteristic of cancer, frequently leading to a high mortality rate. Unfortunately, there is currently no specific and effective marker to predict and treat metastasis in ESCC. MicroRNAs (miRNAs) are a class of small non-coding RNA molecules, approximately 22 nucleotides in length. miRNAs are vital in modulating gene expression and serve pivotal regulatory roles in the occurrence, progression, and prognosis of cancer. Here, we have examined the literature to highlight the intimate correlations between miRNAs and ESCC metastasis, and show that ESCC metastasis is predominantly regulated or regulated by genetic and epigenetic factors. This review proposes a potential role for miRNAs as diagnostic and therapeutic biomarkers for metastasis in ESCC metastasis, with the ultimate aim of reducing the mortality rate among patients with ESCC.

Key Words: MicroRNAs; Esophageal squamous cell carcinoma; Metastasis; Signaling pathway; Epigenetics mechanism

Core Tip: Esophageal squamous cell carcinoma (ESCC) is the sixth leading cause of cancer-related deaths globally predominantly due to metastasis. MicroRNAs (miRNAs), acting either as tumor suppressors or oncogenes, play crucial roles in the development and progression of tumors. We herein discussed the intimate correlations between miRNAs and ESCC metastasis, predominantly associated with genetic and epigenetic regulatory, and aimed to propose the potential role of miRNAs as diagnostic and therapeutic biomarkers for ESCC metastasis.

Citation: Wei QY, Jin F, Wang ZY, Li BJ, Cao WB, Sun ZY, Mo SJ. MicroRNAs: A novel signature in the metastasis of esophageal squamous cell carcinoma. *World J Gastroenterol* 2024; 30(11): 1497-1523
URL: https://www.wjgnet.com/1007-9327/full/v30/i11/1497.htm
DOI: https://dx.doi.org/10.3748/wjg.v30.i11.1497

INTRODUCTION

Esophageal cancer, the eighth most prevalent cancer worldwide, ranks as the sixth leading cause of cancer-related deaths [1]. There are two major histological types of esophageal cancer, which include esophageal squamous cell carcinoma (ESCC) and esophageal adenocarcinoma (EAC)[2]. Despite significant advancements in the treatment of ESCC treatment, both morbidity and mortality rates continue to rise annually. This is largely due to the advanced stage of the ESCC at diagnosis, combined with an increased propensity for metastasis[3,4]. When ESCC cells become metastatic and acquire the ability to invade surrounding tissues and enter the bloodstream or lymphatic system, they can travel to distant organs such as the liver, lungs, gastrointestinal tract, pancreas, and bones to establish secondary tumors[5].

Cancer metastasis is a complex process that encompasses a series of stages including local invasion (involving epithelial-to-mesenchymal transition, EMT), survival and entry into the bloodstream or lymphatic system (intravasation), exit from the bloodstream or lymphatic systems (extravasation), and proliferation at a new location (colonization). Examining this intricate process can offer valuable insights into the development of novel therapeutic strategies for cancer treatment. Numerous studies have demonstrated that a variety of signaling pathways, primarily receptor tyrosine kinase (RTK), transforming growth factor-β (TGF-β), Wnt/β-catenin, and the interleukin (IL)-6/Stat3 pathways, can partake in the process of cancer metastasis process[6-10]. Furthermore, evidence suggests that abnormally expressed microRNAs (miRNAs) can impact cancer metastasis by modulating these signaling pathways[7-10].

MiRNAs are endogenous short non-coding RNAs (approximately 22 nucleotides) that can regulate gene expression by inhibiting mRNA transcription or by promoting mRNA degradation through sequence- specific binding in the 3'-untranslated region (3' -UTR). They often function as master regulators of gene expression and play crucial roles in the development and progression of tumors by acting as either as tumor suppressors or oncogenes[11]. This review focuses on the role and mechanism of miRNAs in facilitating ESCC metastasis of ESCC, and also aims to highlight the potential use of miRNAs as diagnostic and therapeutic biomarkers in the management of ESCC metastasis.

THE ROLE OF MIRNAS IN THE METASTASIS OF ESCC METASTASIS

Tissues from cancer patients, cancer cell lines, and xenograft models are commonly employed to investigate the occurrence and mechanisms of cancer cell metastasis. In the tissues of cancer patients, lymph node metastasis (LNM), vessel invasion (VI), lymph node invasion (LNI), lymphatic invasion (LI), tumor nodes metastasis stage (TNM), and depth of invasion (DI), are often used to evaluate the metastatic characteristics of the cancer. In cancer cells, the cell invasion, migration and EMT often are commonly used to evaluate the ability of tumor cells to metastasize. In xenograft models, the location and quantity of tumor distribution are used to identify the metastatic potential of tumors. Thus, we assess the role and underlying mechanism of miRNA in the metastasis of ESCC by examining its metastatic behavior in tissues, cells, and xenograft models (Tables 1 and 2)[12-15].

Numerous studies have found that miRNAs, acting either as tumor suppressors or oncogenes, play crucial roles in the development and progression of tumors[13]. As tumor suppressors, some miRNAs can inhibit tumor occurrence and development by targeting genes that have the potential to promote oncogenesis and progression[16]. Conversely, as oncogenes, some miRNAs, often called oncomiRs, can promote tumor malignancy by suppressing the expression of genes that normally prevent cells from becoming cancerous[17]. Multiple studies over the past decade have highlighted the importance of miRNAs also acting as suppressors or oncogenes in ESCC metastasis.

MiRNAs act as tumor suppressors in ESCC metastasis

There is a significant reduction in the expression levels of tumor-suppressive miRNAs in both tissues and cells associated with ESCC. These miRNAs substantially influence the malignancy and metastatic potential of ESCC malignancy, including ESCC metastasis (Table 1). For example, miRNAs like miR-138, miR-193a-5p, miR-206, miR-451, and miR-718 are markedly decreased in ESCC-associated tissues, and these decreases are significantly correlated with LNM and the TNM stage[18-22]. Furthermore, the reduced expression of miRNAs, including but not limited to miR-100, miR-124, miR-125b, miR-126, miR-128-3p, and miR-129, are not only positively associated with ESCC metastasis in ESCC patient tissues,

Table 1 MicroRNAs act as suppressor in esophageal squamous cell carcinoma metastasis

miRNA	Metastasis studies in different sources			Ref.
Suppressor	Tissue	Cell	Xenograft	
miR-1	LNM, VI, TNM, advanced C stage	I		[148]
miR-10a	LNM, C stage	I, M, EMT	Tumor Me	[29]
miR-100	LNM	I, M		[24]
miR-100-5p	DI, LI, T stage			[149]
miR-101	LNM	I, M	Liver Me	[30]
miR-10527-5p	LNM, T stage, LI	I, M, EMT, LI		[9]
miR-107	NS (LNM)	I, M		[152]
miR-122		I, M, EMT		[116]
miR-124	LNM, Me	I, M		[25]
miR-124-3p	LNM, DI, DM, TNM	I, M, EMT		[31,156]
miR-125a-5p		I, M		[157]
miR-125b	LNM, TNM	I, M, EMT		[26]
miR-1254	VI, P stage			[159]
miR-126	LNM, TNM	I, M		[27]
miR-128-3p	LNM	I, M, EMT		[23]
miR-129	TNM	I, M		[28,143]
miR-129-2	LNM, DM, advance clinical TNM	I, M		[164]
MiR-129-2-3p		I, M		[166]
miR-1294	LNM, LI, VI	I, M		[84]
miR-130a-5p		I, M		[169]
miR-133a	LNM, P stage	I, M		[170]
miR-133b		I, M, EMT		[102]
miR-134	LNM, TNM	I, M		[32]
miR-136-5p	LNM, TNM	I, M		[168]
miR-137		I, M, EMT		[174]
miR-138	LNM, TNM			[18]
miR-140-3p	LNM, DM, TNM	I, EMT		[176]
miR-140	Me	I, M, EMT		[178]
miR-143	LNM, DI, VI, TNM	I, M		[13]
miR-143-3p		I, M		[180]
miR-144	Me, TNM	I, M	Liver Me	[33]
miR-145	LNM, DI, TNM	I, M, EMT		[182, 183]
miR-145-3p		I, M		[185]
miR-145-5p		I, M, EMT		[187]
miR-146a	NS (N stage), TNM	I, M, EMT		[189]
miR1469	LNM, DI			[191]
miR-148a		I, M, EMT		[193]
miR-149-5p		I, M		[10]
miR-150	LNM, LI, VI, TNM	I, M, EMT		[195]

miR-150-3p		I, M		[197]
miR-153		I, M, EMT		[94]
miR-181a-5p		I, M	DLA Me	[199]
miR-185	NS (LNM, DM, TNM)	I, M	Lung Me	[15]
miR-186-5p	NS (LNM), DM	I, M		[43]
miR-193a-5p	LNM, TNM			[19]
miR-193b		I, M		[104]
miR-195	LNM, VI, TNM	I, M		[202]
miR-198		I, M		[204]
miR-202	LNM	M		[206]
miR203	LNM, TNM	I, M, EMT	Lung Me	[34,81]
miR-203a-3p		I, M, EMT		[209]
miR-204-5p	LNM, DI	I, M, EMT		[210]
miR-205	LNM	I, M, EMT		[93,213]
miR206	LNM, TNM			[20]
miR-212-3p		I		[215]
miR-214	LNM, tumor stage	I, M, EMT		[216,217]
miR-214-3p		I, M		[219]
miR-216a/b	LNM, TNM			[220]
miR-217		I, M		[80]
miR-218	LNM, TNM	I, M		[221]
miR-26a	LNM, C stages	I, M	Liver Me	[33,223]
miR-27a	LNM	I		[103]
miR-27b-3p	LNM, TNM	I, M, EMT		[225]
miR-29b	LNM	I, M		[88]
miR-29c	MPI			[228]
miR-30a	LNM	I, M		[148]
miR-30b	NS (N stage)	I, M, EMT		[44]
miR30a-3p	LNM	I, M, EMT		[148]
miR-30c	T, N, M, stage	I, EMT		[95]
miR-30d	LNM, advanced TNM	I, M		[150]
miR-30e-5		I, M		[126]
miR-301a		I, M		[151]
miR-323a-3p		I, M	Lung Me	[153]
miR-326		I, M		[154]
miR-328		I, M	Liver Me	[155]
miR-33a-5p	LNM, TNM	I, M		[111]
miR-335-5p		I, M, EMT		[158]
miR-338-3p		I, M, EMT		[101]
miR-338-5p		I, M	Lung Me	[160]
miR-34a	LNM, TNM	I, M, EMT	Liver Me	[36,161]
miR-340-5p	LNM, TNM	I, M		[162]
miR-3612		I, M		[163]

miR-365		I, EMT		[165]
miR-370	LNM, tumor invasion			[167]
miR-370-3p	LNM, TNM	I, M		[168]
miR-375	LNM, LVI, DM, TNM	I, M, EMT	Tumor mobility, I	[37,38]
miR-377	LNM, TNM	I, M		[171]
miR378	LNM, TNM	I, M,		[172]
miR-378a-3p		I, M		[11]
miR-422a		I, M		[173]
miR-429	LNM, TNM	I, M, EMT		[175]
miR-4324	LNM, DI	I, M, EMT		[175]
miR-433-3p		I, M		[177]
miR-4429	LNM, TNM	I, M, EMT		[114]
miR-449a-5p	LNM, TNM			[179]
miR-451	LNM, TNM			[21]
miR-455-3p	LNM	I		[181]
miR-455-5p	LNM	I, M		[184]
miR-4766-5p		I, M, EMT		[186]
miR-485-5p	NS (LNM), TNM	I, M, EMT		[188]
miR-486-5p		I		[190]
miR-490-3p		I, M, EMT		[192]
miR-493		I, M		[145]
miR-497-5p		I, M		[194]
miR-498	NS (LNM, DM)	I, M		[196]
miR-508-3p		I, M		[198]
miR-515-3p	Me	I, M, EMT	Lung ME	[12]
miR-516b	LNM, DI, advanced TNM	I, M, EMT		[200]
miR-518b	LNM	I		[201]
miR-542-3p	NS (metastasis)	I, M		[47]
miR-574-3p	LNM, DI, TNM	I, M		[50]
miR-590	LNM, TNM	I, M, EMT		[51]
miR-595		I, M		[203]
miR-599		I, M, EMT		[205]
miR-615-5p	LNM, advanced TNM	I, M		[207]
miR-620		I, M, EMT	Lung ME	[208]
miR-622	N stage, TNM	I, M, EMT		[138]
miR-625	LNM, DM, advanced TNM	I		[211,212]
miR-630	LNM, P stage	I, M, EMT		[214]
miR-652	LNM, TNM	I, M	Multiple ME	[39]
miR-670-3p		I, M		[139]
miR-671-5p		I, M, EMT		[218]
miR-718	LNM, TNM			[22]
miR-765		I, M		[133]
miR-874-3p	LNM, C stage	I, M		[14]

miR-942-5p	TNM, C stage	I, M, EMT		[222]
miR-98	LNM, TNM	I, M		[216]
miR-99a		I, M, EMT		[224]
let-7	LNM			[226]
let-7a	TNM	I, M, EMT	LNM	[227]
let-7b-5p		I, M		[40]

LNM: Lymph node metastasis; VI: Vessel invasion; LVI: Lymphatic vessel invasion; LI: Lymphatic invasion; TNM: Tumor nodes metastasis stage; C stage: Clinical stage; P stage: Pathological stage; DI: Depth of invasion; DM: Distant metastasis; I: Invasion; M: Migration; EMT: Epithelial-mesenchymal transition; Me: Metastasis; DLA Me: Dilated lymphatic arteries metastasis; Multiple Me: Brain, bone, adrenal gland, lung, kidney, liver metastasis; MPI: Muscularis propria invasion.

but also promotes ESCC cell invasion, migration, and/or EMT processes[23-28]. Several studies have confirmed the inhibitory effects of some miRNAs on ESCC metastasis at the tissue, cell, and animal model levels, including miR-10a, miR-101, miR-124-3p, miR-134, miR-144, miR-203, miR-26a, miR-34a, miR-375, miR-515-3p, miR-652, and let-7b-5p[12,29-40]. Intriguingly, our research reveals that certain miRNAs, including miR-107, miR-146a, miR-185, miR-186-5p, miR-30b, miR-485-5p, miR-498, and miR-542-3p, among others, have minimal effects on ESCC metastasis in tissue samples. However, they can significantly suppress ESCC cell invasion and migration and have a considerable impact on metastasis in xenograft models[15,41-47].

The role of these miRNAs as tumor suppressors heavily relies on the tumor-promoting activities of their target genes. For instance, the significant downregulation of miR-101 in ESCC tissues correlates strongly with LNM. Moreover, miR-101 can suppress tumor metastasis both *in vitro* (in xenograft models) and *in vivo* (in ESCC cells). Notably, the inhibitory effect of miR-101 in ESCC migration and invasion is reversed *via* activation of its target genes, COX-2, MALAT1, or EZH2. These genes are identified as playing crucial roles in promoting tumor development and progression, although not exclusively in ESCC[30,48,49]. Another notable suppressor miRNA is miR-574-3p, whose reduced expression is negatively associated with LNM, TNM stage, and invasion depth. Inhibition of miR-574-3p promotes migration and invasion of ESCC cells *in vitro*. However, the knockdown of its target genes, FAM3C or MAPK1, can lessen the increase in migration and invasion observed following treatment with the miR-574-3p inhibitor. The majority of studies suggest that both FAM3C and MAPK1 promote malignant tumor development, including proliferation, invasion, and migration[50].

MiRNAs act as oncogenes in ESCC metastasis

Similar to cancer-suppressive miRNAs, oncomiRs have also been identified as promoters of ESCC tissue infiltration, as well as ESCC cell invasion, migration, and epithelial-mesenchymal transition (EMT) in ESCC (Table 2)[51-77]. The increased expressions of miR-10b-3p, miR-106b-5p, miR-25, miR-320b, miR-602, miR-9, and miR-99b/Let-7e/miR-125a not only show significant correlations with metastasis in ESCC patients, but these miRNAs are also known to increase the invasion, migration, and/or EMT of ESCC cells. Additionally, these miRNAs can promote the metastasis of transplanted tumors, primarily to the lungs[52-58]. Other miRNAs, including miR-1269, miR-17-5p, miR-18a-5p, miR-25-3p, miR-301, miR-373, miR-483-5p, miR-766-3p, and others, display oncogenic roles in metastasis, affecting both ESCC tissues and cells [59-67]. In addition, some miRNAs including but not limited to miR-103a-2-5p, miR-105-5p, miR-130b, miR-1323, miR-19b-3p, miR-196a, miR-23b-3p, and miR-301b display potent pro-metastatic functions, primarily pertaining to cellular activity[68-75].

The oncogenic potential of oncomiRs also hinges on their target genes, which typically act as tumor suppressors by preventing cells from becoming malignant. For instance, PTEN, a well-known tumor suppressor, is downregulated by several oncomiRs, including miR-1323, miR-25-3p, miR-301, miR-624-3p, miR-92a-3p, and others. The expression of these oncomiRs in ESCC tissues and/or cells is significantly upregulated and further research has shown that the effects of PTEN overexpression, including inhibition of cell migration and invasion, effects that can be partially reversed by the aforementioned oncomiRs[62,63,71,76,77]. Programmed cell death 4 (PDCD4), which functions as a tumor suppressor in ESCC, is a direct target of miR-320b. Exosomal miR-320b has been shown to promote LNM and lymphangiogenesis both *in vitro* and *in vivo*. Additional *in vitro* studies have confirmed that re-expression of PDCD4 can not only rescue its downregulation, but can also counteract lymphangiogenesis and LN metastasis mediated by exosomes with high levels of miR-320b[53].

THE GENETIC MECHANISM OF MIRNAS ON ESCC METASTASIS

Research evidence indicates that both genetic and epigenetic regulatory mechanisms of miRNAs play a crucial role in tumorigenesis and development, including metastasis in ESCC[54,78].

Tumor metastasis-associated genes (TMAGs) represent a category of genes that serve a vital function in the process of metastasis. This group includes metastasis suppressor genes (MSGs), and metastasis promoting genes (MPGs). MSGs and MPGs are primarily involved in various signaling pathways, including the RTK, transforming growth factor-β (TGF-β), Wnt/β-catenin, and interleukin (IL)-6/Stat3 pathways. They also target specific and key factors, including ZEB1/2,

Table 2 MicroRNAs act as oncogene in esophageal squamous cell carcinoma metastasis

miRNA	Metastasis studies in different sources			Ref.
oncomiR	Tissue	Cell	Xenograft	
miR-10b-3p	LNM, C stages	I, M, EMT	Lung, Liver Bone Me	[56,57]
miR-10b	NS (LNM)	I, M		[229]
miR-103a-2-5p		I		[68]
miR-105-5p		I, M		[69]
miR-106b-5p	TNM	I, M, EMT	Lung Me	[52]
miR-1179	Me TNM	I		[232]
miR-1269	LNM, TNM	I, M		[59]
miR-1290	LNM, tumor invasion, TNM	I, M		[113]
miR-130b		I, M		[70]
miR1323		I, M		[71]
miR-135b-5p	LNM	I, M		[236]
MiR-140-5p		I, M, EMT		[92]
miR-142-3p	LNM			[237]
miR-1470		M		[239]
miR-17-5p	LNM, TNM, DI	I, M		[60,240]
miR-17a	LNM, C stage			[242]
miR-18a	LNM, TNM	I, M		[61,244]
miR-181b-5p	Advance TNM	M		[107]
miR-181c-3p	DI, TNM			[246]
miR-19b	LNM, C stage			[242]
miR-19b-3p		I, M		[72]
miR-196a		I, M		[74]
miR-196a-3p		M		[74]
miR-20b-5p	LNM, C stage	I, M		[249]
miR200a		I, M		[87]
miR-21[1]	LNM, LI, VI, TNM	I, M, EMT		[282]
miR-221		I, M		[251]
miR-224	NR (LNM), TNM	I, M		[252]
miR-224-5p		I, M, EMT		[100]
miR-23a	NS	I, M	Lung Me	[140,254]
miR-23b-3p		I, M, EMT		[73]
MiR-23b-5p	Me	I, M	Lung Me	[257]
miR-25	LNM, TNM	I, M, EMT	Lung Me	[58]
miR-25-3p	LNM, TNM	I, M		[62]
miR-30d-5p	LNM, TNM, DI	I, M, EMT		[91,230]
miR-301	LNM, TNM	I, M		[63]
miR-301a-3p	LNM, tumor invasion, TNM			[231]
miR-301b		I, M		[75]
miR-31	N, M stage, TNM	I, M, EMT		[233]
miR-320b	LNM	I, M, EMT		[53]

miR-330-3p		I, M		[234]
miR-3656		I, M		[235]
miR-373	LNM, TNM	I, M		[64]
miR-425		I, M		[119]
miR-4286		I, M		[238]
miR-4443	TNM	I		[60]
miR-452-5p	LNM, DM	I, M		[241]
miR-483-3p		I, M, EMT		[243]
miR-483-5p	LNM, TNM	I, M		[65,66]
miR-506	LNM, TNM			[245]
miR-5692b	DI, TNM			[246]
miR-602	LNM, TNM	I, M	Lung, liver, bone, adrenal gland Me	[54]
miR-612	LNM, metastasis	I, M		[247]
miR-624-3p		I, M, EMT		[76]
miR-675-3p		I, M, EMT		[248]
miR-766-3p	LNM, TNM	I, M		[67]
miR-875-5p		I, M		[250]
miR-9	LNM	I, M, EMT	Lung Me	[85]
miR-92a	LNM, LNI	I, M		[86]
miR-92a-3p		I, M		[77]
miR-92b-3p		I, M		[253]
miR-935	Me			[255]
miR93		I, M		[256]

[1]NS (plasma).

LNM: Lymph node metastasis; VI: Vessel invasion; LNI: Lymph node invasion; LI: Lymphatic invasion; TNM: Tumor nodes metastasis stage; C stage: Clinical stage; DI: Depth of invasion; I: Invasion; M: Migration; Me: Metastasis; EMT: Epithelial-mesenchymal transition.

Snail1/2, E-cadherin, N-cadherin, C-myc, Vimentin, and MMPs, all of which are recognized as markers of tumor metastasis. Substantial evidence indicates that miRNAs exert their function on ESCC metastasis by targeting tumor suppressor genes or oncogenes, which belonging to the above-mentioned signaling pathways and their downstream signaling molecules[79].

MiRNAs directly target markers of tumor metastasis

Research indicates that miRNAs can regulate the metastasis of ESCC by directly targeting markers associated with tumor metastasis (Figures 1 and 2), including ZEB1/2, Snail1/2, E-cadherin, N-cadherin, C-myc, Vimentin, and members of the Matrix Metalloproteinase family (MMPs), *etc.*[12,26,78,80-84].

E-cadherin, predominantly found in epithelial tissues, is crucial for maintaining cell adhesion, polarity, and tissue architecture. Within the context of cancer metastasis, E-cadherin acts as a tumor suppressor. It serves as a critical biomarker and regulator of tumor metastasis, and its altered expression may indicate cancer progression. miR-9, miR-25, miR-92a, and miR-200a have been found to either directly or partially mediate tumor metastasis (including LNM, EMT, invasion, and migration) through E-cadherin[83,85-87].

The MMP family consists of enzymes mainly responsible for the degradation of extracellular matrix (ECM) components. In cancer, MMPs promote tumor growth, invasion, and metastasis by breaking down the ECM barriers, thereby facilitating cancer cell migration. Furthermore, they are involved in angiogenesis, a process of new blood vessel formation critical for tumor growth, survival, and metastasis. MMP2, MMP3, MMP9, and MMP13 are targets for miR-29b, miR-515-3p, miR-34a,and miR-375, respectively. These miRNAs are wholly or partly involved in ESCC metastasis[12,88-90].

Additionally, several transcription factors (TFs), particularly ZEB1/2 and Snail1/2, play critical roles in tumor metastasis. Their primary function is to downregulate the expression of epithelial markers (like E-cadherin) and upregulate the expression of mesenchymal markers (like N-cadherin and Vimentin), thereby driving the process of EMT process[81,82,91,92]. ZEB2, is a direct target of miR-140 and miR-205, and it reverses the effects of these miRNAs on EMT, migration, and invasion of ESCC cells[78,93]. miR-30c, miR-30d-5p, miR-203, and miR-153 are known to directly target

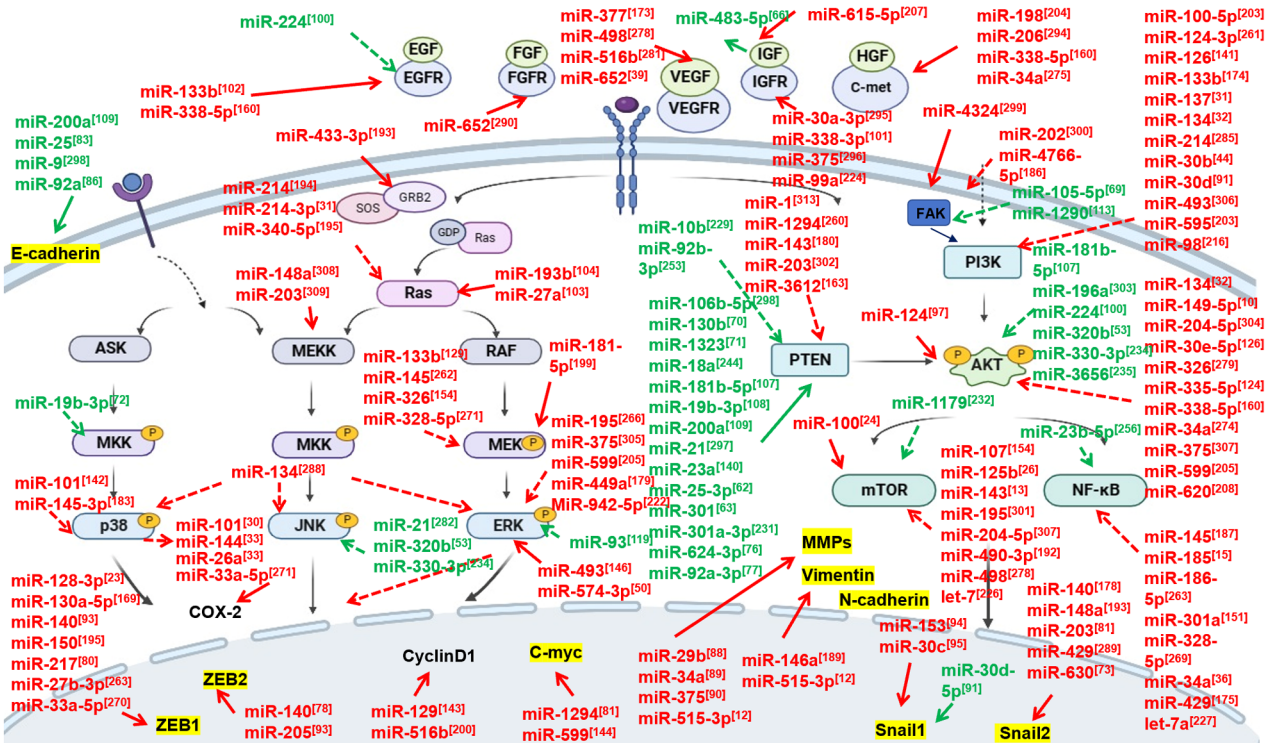

Figure 1 MicroRNAs targeting receptor tyrosine kinase signaling pathway in esophageal squamous cell carcinoma metastasis. The receptor tyrosine kinases (RTKs) signaling pathway effect many signals, including epidermal growth factor (EGF), fibroblast growth factor (FGF), vascular endothelial growth factor (VEGF), hepatocyte growth factor (HGF), insulin-like growth factor (IGF) and their receptors, as well as intracellular signaling pathways, such as mitogen-activated protein kinases (MAPKs) and phosphatidylinositol 3-kinase (PI3K). The dysregulation of miRNAs on the RTK signaling pathway is play important roles in ESCC metastasis[10,12,13,15,23,24,26,30-33,36,39,44,50,53,62,63,66,69,70-73,76-78,80,81,83,85,86,88-91,93,95,97,100-104,107-109,112,117,123,125,128,140-144,146,151,154,160,163,169,174,175,178-180,185-187,189,192,193,195,199,200,203-205,207,208,216,222,224,226,227,229,231,232,234,235,244,253,257,260-265,266,269-271,273,274,278,279,281,282,285,289-309,311]. ZEB1/2, Snail1/2, E-cadherin, N-cadherin, C-myc, Vimentin and MMPs are specific target and key factors for esophageal squamous cell carcinoma metastasis. “Green” and “Red” indicated oncomiRs and tumor-suppressive miRNAs, respectively. The dashed arrow and solid arrow indicated direct targeting effect and indirect targeting effect, respectively.

Snail1, a critical regulator of metastasis. Overexpression of these miRNAs, either individually or in combination, can counteract metastatic behaviors in whole or in part, thereby presenting a potential therapeutic strategy for mitigating cancer metastasis[82,91,94,95].

MiRNAs targeting RTK signaling pathway in ESCC metastasis

The RTKs signaling pathway serves as a central conduit for communication within and between cells, regulating a multitude of cellular functions including cell growth, differentiation, invasion, and migration[7]. This pathway comes into effect when specific signals, typically growth factors or hormones such as epidermal growth factor (EGF), fibroblast growth factor (FGF), vascular endothelial growth factor (VEGF), hepatocyte growth factor (HGF), and insulin-like growth factor (IGF), bind to their corresponding RTK on the cell surface. Upon activation, the RTK acts as a platform for various intracellular signaling pathways, but primarily, the mitogen-activated protein kinases (MAPKs) and phosphatidylinositol 3-kinase (PI3K) pathways. MAPK signaling, a common and highly conserved pathway, primarily includes extracellular signaling-associated kinases (ERK1/2), Jun amino-terminal kinases (JNK), and p38-MAPK. The PI3K/Akt pathway can be irregularly activated *via* several mechanisms, including various genomic alterations such as mutations in PTEN, Akt, and mTOR mechanism[7,71,96,97]. Dysregulation of the RTK signaling pathway is implicated in the malignant progression of ESCC, including metastasis[4,98,99].

Numerous miRNAs have been identified as crucial regulators in ESCC metastasis by targeting RTK signaling, suggesting a critical crosstalk between miRNAs and the RTK signaling is necessary for ESCC metastasis (Figure 1)[100,101]. Certain miRNAs exert control over ESCC metastasis by directly interacting with growth factors or growth factor receptors, such as RTKs, subsequently regulating their downstream signaling pathways and molecules. For instance, miR-133b can repress ESCC cell invasion and metastasis by targeting the EGFR, which inhibits the PI3K/AKT signaling pathway and curbs the expression of downstream molecules such as N-cadherin, MMP-2, MMP-9, and E-cadherin[102]. Similarly, the downregulation of miR-338-3p, whose target is the IGF1R, activates the Raf/MEK/ERK pathway and affects the expression levels of E-cadherin, N-cadherin, and vimentin, and thus promoting ESCC cell invasion, migration, and EMT in ESCC[101]. Certain miRNAs are known to directly target the downstream signaling of the RTK pathway to influence ESCC metastasis. For example, miR-27a and miR-193b, functioning as tumor suppressors, are downregulated in ESCC and suppress cell migration and invasion *via* the direct regulation of KRAS, which is linked to the MAPK/ERK signaling pathway[103,104]. The tumor suppressor protein PTEN is able to dephosphorylate Akt to lessen its activation, thus blocking all downstream signaling events controlled by Akt and acting as a negative regulator of PI3K. Numerous

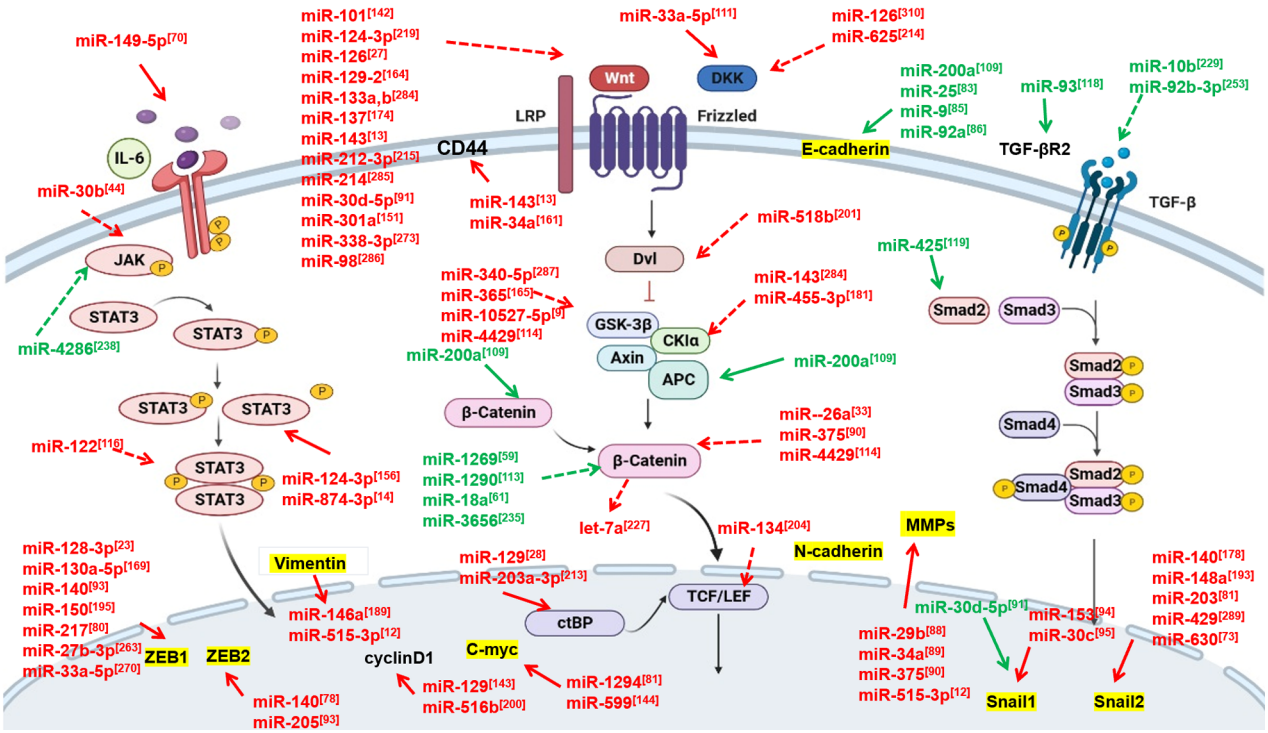

Figure 2 MicroRNAs targeting the pathways of Wnt/β-catenin, IL6/Stat3, and TGF-β in esophageal squamous cell carcinoma metastasis. In esophageal squamous cell carcinoma (ESCC), miRNAs serve as crucial effector to Wnt/β-catenin, IL-6/STAT3 and TGF-β signalings, which is consistently involved in cancer metastasis[9,12,14,23,27,28,33,44,59,61,70,73,78,80,81,83,85,86,88-91,93-95,109,111,113,114,116,118,119,142-144,151,156,161,164,165,169,174,178,181,189,193,195,200,201,204,209,211,215,219,227,229,235,238,253,263,270,273,284-287,289,310]. Wnt/β-catenin signaling includs Wnts, receptors (such as Frizzled, FZD and low-density lipoprotein receptor-related proteins, LRP), Dishevelled (Dsh/Dvl), β-catenin, glycogen synthase kinase 3β (GSK-3β), Axin, APC (adenomatous polyposis coli), IL-6 is known to activate the downstream JAK/STAT3 signaling, and canonical TGF-β pathway is mediated by SMAD2, SMAD3, and SMAD4. ZEB1/2, Snail1/2, E-cadherin, N-cadherin, C-myc, Vimentin and MMPs are specific target and key factors for ESCC metastasis. "Green" and "Red" indicated oncomiRs and tumor-suppressive miRNAs, respectively. The dashed arrow and solid arrow indicated direct targeting effect and indirect targeting effect, respectively.

miRNAs, including but not limited to miR-106b-5p, miR-130b, miR-1323, miR-18a, miR-181b-5p, miR-19b-3p, and miR-200a, exhibit a conspicuous overexpression and a negative association with LNM and/or TNM classification in ESCC. This overexpression fosters the progression of ESCC by facilitating cell invasion, metastasis, and/or EMT[52,71,105-109]. Furthermore, most of miRNAs whether indirectly or directly targeting PTEN can decrease the anticancer effect of PTEN, and promote the invasion and metastasis of ESCC[70,71,108].

MiRNAs targeting the Wnt/β-catenin signaling pathway in ESCC metastasis

The Wnt/β-catenin signaling pathway assumes a pivotal role in various physiological processes, such as cell proliferation, differentiation, migration, and apoptosis. This signaling pathway consists of several components, including Wnts, receptors (such as Frizzled, FZD and low-density lipoprotein receptor-related proteins, LRP), Dishevelled (Dsh/Dvl), β-catenin, glycogen synthase kinase 3β (GSK-3β), Axin, and APC (adenomatous polyposis coli). Research has shown that the Wnt/β-catenin signaling pathway is intricately linked with tumor development, partly as a significant contributor to the onset and metastasis of ESCC, including metastasis[98,110].

Studies suggest that miRNAs can directly or indirectly modulate various components of the Wnt/β-catenin pathway, thereby either activating or inhibiting ESCC metastasis (Figure 2). For instance, miR-33a-5p, which exhibits diminished expression in ESCC tissues and correlates with higher TNM staging and LNM, can directly target Dickkopf-related protein 1 (DKK1) thereby influencing the metastasis of ESCC *via* the Wnt/β-catenin pathway[111]. Additionally, a majority of miRNAs associated with ESCC were found to indirectly target molecules associated with the Wnt/β-catenin pathway. One such example is miR-340, which is significantly downregulated in ESCC tissues and is highly correlated with LNM and TNM stages. phosphoserine aminotransferase 1 (PSAT1), *via* the GSK3β/β-catenin/Cyclin D1 pathway, was identified as a direct target of miR-340, although it can also partially counteracts the miR-340 mediated inhibition of viability, invasion, and EMT in ESCC cells[112]. Beyond miR-200a, Numerous miRNAs, including suppressor miRNAs and oncomiRs, have been found to indirectly regulate β-catenin, playing a critical role in ESCC metastasis. For example, both of miR-1269 and miR-1290 act as oncomiRs, and are upregulated in ESCC tissues and cell lines. They are associated with positive LNM and/or advanced TNM stage, and their overexpression promotes the malignant transformation of ESCC cells, including migration and invasion, by directly targeting SRY-box transcription factor 6, interactive with β-catenin (SOX6)[59,113]. Furthermore, the downregulation of miR-4429 has been shown to foster ESCC cell invasion and migration by partially regulating β-catenin through the direct targeting of SRXN1[114].

MiRNAs targeting IL6/STAT3 signaling pathway in ESCC metastasis

IL-6, a pleiotropic cytokine, is implicated in a diverse array of pathological processes including chronic inflammation, autoimmune diseases, and tumors. and other diseases. IL-6 is known to activate the downstream JAK/STAT3 signaling pathway, a hallmark of many malignant tumors, thereby contributing to tumor onset and, progression, and metastasis [115]. In ESCC, miRNAs serve as crucial effectors to the IL-6/STAT3 pathway, which is consistently involved in cancer metastasis (Figure 2). One such instance is miR-149-5p, a direct target of IL-6. The overexpression of miR-149-5p suppresses IL-6 expression at both the mRNA and protein levels, thereby inhibiting the invasion and migration of ESCC cells[10]. Similarly, miR-874-3p, is found downregulated in ESCC tissues and cell lines and exhibits a statistically significant association with LNM and clinical stage. Its overexpression markedly suppresses migration and invasion in ESCC cells by directly targeting STAT3[14]. Intriguingly, several miRNAs, such as miR-30b and miR-122, have been found to modulate ESCC cell invasion, migration, and EMT by indirectly regulating JAK and STAT3, respectively[44,116].

MiRNAs targeting transforming growth factor-β signaling pathway in ESCC metastasis

The transforming growth factor-β (TGF-β) signaling pathway is a classical signal transduction pathway, encompassing both the conventional Smad-dependent pathway and the non-Smad-dependent pathways. The canonical pathway is mediated through the transcription factors SMAD2, SMAD3, and SMAD4, while the non-canonical pathways include MAPK, nuclear factor (NF)-κB, and PI3K/AKT/mTOR signaling, *etc*[8]. TGF-β signaling has been identified as a pivotal regulator in the modulation of the progression and metastasis of various types of cancer, including in ESCC. In the context of ESCC, our discussion primarily focuses on the role of the canonical pathway. TGF-β, induces EMT activation *via* the TGF-β/Smad signaling pathway[117].

In recent years, there has been a surge in investigations demonstrating that miRNAs play a pivotal role in the metastasis of ESCC through the modulation of the TGF-β pathway (Figure 2). For instance, miR-93-5p is highly expressed in ESCC cells and is known to enhance cell proliferation, migration, and invasion, while simultaneously suppressing apoptosis in ESCC cells. It achieves these effects by targeting and downregulating the expression of TGFβR2[118]. Similarly, miR-425 is overexpressed in both ESCC tissues and plasma, and positively influences cell migration and invasion. It functions as an oncogene by specifically targeting the 3'-untranslated region (3'-UTR) of SMAD2, thereby modulating its expression and subsequent cellular behavior[119].

EPIGENETICS EFFECTS ON MIRNAS IN ESCC METASTASIS

Epigenetics refers to the study of heritable changes in gene expression that occur without a change in DNA sequence. Epigenetic changes occur in extreme cases and contain several regulatory mechanisms, including noncoding RNAs (ncRNAs), DNA methylation, heterochromatin, polycomb and trithorax proteins and 3D genome architecture[120]. In recent years, accumulating evidences suggest that different expression patterns of ncRNA play increasingly important roles in cancer. ncRNAs are made of distinct classes, including noncoding RNA (lncRNA), miRNA, circRNA, rRNA, tRNA, and so on[121-123]. Among them, more exciting progress has been made in the study of the role and mechanism of lncRNA, circRNA and the impact of DNA methylation of miRNAs in tumor processes (Table 3).

The crosstalk between lncRNA and miRNA in ESCC metastasis

LncRNA are ncRNAs with lengths > 200 nucleotides. They represent diverse types of RNA molecules with limited or no protein-coding capability, and different biological functions depending on their subcellular location. Cytoplasmic lncRNAs exhibit vital roles in cancer, often acting as tumor suppressors or oncogenes through the modulation of miRNAs [124]. Recently, accumulated evidences has demonstrated that lncRNAs are involved in ESCC metastasis by acting as competing endogenous RNAs (ceRNAs) that "sponge" miRNAs to block their function, and then, up-regulate the downstream genes[125]. For example, lncRNA DLEU2, is up-regulated in EC tissues and associated with poor prognosis. The overexpression of this lncRNA DLEU2 increased the proliferation, migration and invasion abilities of ESCC by suppressing miR-30e-5p and then directly targeting E2F7. Another lncRNA, LncRNA-IUR up-regulates PTEN by "sponging" miR-21 and acting as a tumor suppressor in ESCC metastasis[126]. Antisense lncRNAs, a special type of lncRNA, are antisense RNAs with partial exon overlap with forward genes. They can also regulate gene expression by competitively binding to certain miRNA in ESCC metastasis, such as PSMA3-AS1, ZFAS1, TTN-AS1, NCK1-AS1, THAP9-AS1, FAM83A-AS1, OIP5AS1, DDX11-AS1, SLC2A1-AS1, and MAFG-AS1[48,91,124,127-133]. MAFG-AS1 is significantly up-regulated in ESCC tissues and cell lines, and accelerates ESCC cell proliferation, migration, invasion and aerobic glycolysis by competitively adsorbing miR-765, a negative modulator of PDX1 expression of PDX1. Overexpression of lncRNA HAND2-AS1 its overexpression inhibited cell proliferation, migration, and invasion by downregulation of miRNA-21 in ESCC cells[133,134].

The crosstalk between circRNA and miRNA in ESCC metastasis

CircRNAs also act as miRNA "sponges" and comprise a large class of endogenous non-coding RNA with covalently closed loops. CircRNAs have independent functions from the linear transcripts that are transcribed from identical genes [135]. Recently, it was demonstrated that numerous circRNAs are differentially expressed in ESCC, and their dysfunction is linked to ESCC metastasis. The typical circRNAs contain circHIPK3, circ2646, circOGDH, circ_0001273, circABCB10, circ_0001946, circLARP4, circ_0007624, circFoxo3[25,71,100,113,136-140]. circ-OGDH was upregulated in ESCC cells and its inhibition repressed cell proliferation, migration, and invasion, and reduced miR-615-5p-induced cellular glutamine

Table 3 The epigenetic regulation on microRNAs in esophageal squamous cell carcinoma metastasis

miRNA (Suppressor)	Epigenetic regulation	Ref.
miR-101	~/lncMALAT1	[48,49,142]
	lncXIST/~/EZH2	
	PSMA3-AS1/~/EZH2	
miR-122	LINC01410/~/ PKM2	[259]
miR-129	lncNEAT1/~/CtBP2;	[28,145]
	lnc XIST/~/CCND1	
miR-130a-5p	CCL18-induced lncHOTAIR/~/ZEB1	[169]
miR-133b	TTN-AS1/~/FSCN1	[102,128,129,261]
	NCK1-AS1/~/ENPEP	
	lncKCNQ1OT1/~/EGFRTHAP9-AS1/~/SOX4	
miR-145	lncROR/~/FSCN1	[262]
miR-140-5p	lncSNHG16/~/ZEB1	[92]
miR-186-5p	lncSNHG6/~/HIF-1α	[264]
miR-195	lncSNHG1/~/Cdc42	[265,266]
miR203	circ_0008717/~/Slug	[35,267]
	circPRMT5/~	
miR206	circ_0008726/~	[20]
miR-214	FAM83A-AS1/~/CDC25B	[130,268]
	LINC00963/~/RAB14	
miR-30a	OIP5AS1/~/VOPP1	[131]
miR-30d-5p	DDX11-AS1/~/SNAI1	[91]
miR-30e-5p	lncDLEU2/~/ E2F7	[126]
miR-301a	lncGAS5/~/CXCR4	[151]
miR-328	lncLOC146880/~/FSCN1	[269]
miR-33a-5p	lncDANCR/~/ZEB1	[270,271]
	lncCASC15/~/PTGS2	
miR-335-5p	lncTHAP9-AS1/~/SGMS2	[124]
miR-338-3p	lncBRAF/~/IGF1R	[101,273]
	lncSNHG17/~/SOX4	
miR-34a	lncMIR31HG/~/c-Met	[274]
miR-340-5p	LINC00662/~/HOXB2	[162]
miR-378a-3p	SLC2A1-AS1/~/Glut1	[132]
miR-498	lncTUG1/~/Cdc42	[46,294,278]
	AFAP1-AS1/~/VEGFA	
	lncTUG1/~/XBP1	
miR-508-3p	lncPCAT-1/~/ANXA10	[198]
miR-516b	lncJPX/~/VEGFA	[281]
miR-765	MAFG-AS1/~/PDX1	[135]
oncomiR		
miR-18a-5p	lncPART1/~/SOX6	[61]
miR-21	LncRNA-IUR/~/PTEN	[134,282]

	HAND2-AS1/~	
miR-1290	circ_0086414/~/SPARCL1circ_0001946/~/SOX6	[113,283]
miR1323	circLARP4/~/PTEN	[71]
miR-224	circ_0007624/~/CPEB3	[100]
miR-23a	circFoxo3/miR-23a	[140]
miR-125a-5p	lncHOTAIR/~/HK2	[258]
miR-124	circHIPK3/~/AKT3	[25,136]
	circ2646/~/PLP2	
miR-1294	circ 0004370/~/LASP1	[260]
miR-140-3p	circNTRK2/~/NRIP1	[176,222]
	circ0087378/~/E2F3	
miR-198	circLPAR3/~/C-met	[204]
miR-217	circZDHHC5/~/ZEB1	[80]
miR-27b-3p	circLONP2/~/ZEB1	[263]
miR-3612	circ_0006948/~/LASP1	[163]
miR-422a	circUBAP2/~/Rab10	[173]
miR-433-3p	circ_0023984/~/REV3L	[177]
miR-4766-5p	circPDE3B/~/LAMA1	[186]
miR-490-3p	circ_0006948/ ~/HMGA2	[192]
miR-497-5p	circ-AGFG1/~/SLC1A5	[194]
miR-595	circNRIP1/~/SEMA4D	[203]
miR-599	circHIPK3/~/c-myc	[144,205]
	circ_0030018/~/ENAH	
miR-615-5p	circOGDH/~/PDX1	[139]
miR-622	circ_0001273/~/SLC1A5	[138]
miR-670-3p	circABCB10/~	[139]
miR-874-3p	circ0000977/~	[272]
miR-126	DNMT1/~/ADAM9	[141]
miR-137	CTCF/(DNA methylation) /~/EZH2+PXN	[174]
miR-107	circSFMBT2/~/SLC1A5	[275,276]
	LINC00152/~/Rab10	
miR-149-5p	lnc GACAT3/~/FOXM1	[10,277]
	circ_0000654/~/IL-6	
miR-326	LINC01711/~/FSCN1	[154,279]
	circATIC/~/ID1	
miR-377	LncNEAT1/~/E2F3	[171,280]
	circ_0072088/~/VEGF	
miR-493	LINC00324/~/MAPK1	[145,146]
	circFIG4/~/E2F3	
miR-124-3p	lncZFAS1/~/STAT3	[31,156]
	DNMT1/~/BCAT1 ~/EZH2/H3K27me3	
miR-10b-3p	DNA methylation; Hypoxia	[56,57]
miR-320b	DGCR8+METTL3- N6 -methyladenosine (m6A)/~	[53]

miR-483-5p	Igf2 methylationgene promoter/Igf2/~/ARHGDIA	[66]
miR-602	CpG hypomethylation/~	[54]
miR-515-3p	Promoter hypomethylation	[12]

metabolism to regulate PDX1 expression[137]. circLARP4 expression was observably downregulated in ESCC, and its overexpression circLARP4 restrained cell proliferation and migration in ESCC cell. And circLARP4 was also able to act as a sponge for miR-1323 and negatively modulated miR-1323 *via* the PTEN/PI3K/AKT pathway in ESCC[71].

The crosstalk between DNA methylation and miRNA in ESCC metastasis

DNA methylation is a form of DNA chemical modification that can alter genetic expression without altering the DNA sequence. It is a common occurrence in malignancies and is implicated in tumor initiation and progress[31]. Methylation of the CPG island, usually located in the promoter region of genes, its methylation also plays an important role in ESCC metastasis by up-regulating expression of various miRNAs, includingmiR-483-5p, miR-602[54,66]. miR-483-5p was overexpressed in preoperative serum and cancer tissues and is significantly correlated with the TNM stage and LNM. Low methylation of the Igf2 gene promoter region may promote the expression of Igf2, which directly affects the expression of miR-483-5p and its target genes, including Rho GDP dissociation inhibitor α, activated leukocyte cell adhesion molecule, and suppressor of cytokine signaling 3[66]. miR-602 expression was also increased in human ESCC and significantly correlated with LNM and TNM stage, and showed positive effects on ESCC cell invasion and migration by targeting Fork head box (FOX)K2 (FOXK2). Additionally, direct evidence has shown that the overexpression of miR-602 in the ESCC tissues was correlated with promoter hypomethylation and that demethylation of the promoter genes could upregulate the expression of miR-602[54]. DNA methyltransferases (DNMTs) often are involved in DNA methylation, thereby often modifying gene function through the regulation of gene expression. In ESCC, miR-124-3p shows a high correlation with TNM stage and can directly targets the mRNA 3′UTR region of BCAT1. The expression of miR-124-3p itself is regulated by hypermethylation-silencing regulation mediated by DNA methyltransferase 1 (DNMT1)[31]. The DNMT1/miR-126 epigenetic circuit contributes to ESCC proliferation and migration *via* ADAM9/EGFR/AKT signaling: ADAM9 has been identified as a key target of miR-126 and ectopic expression of miR-126 or silencing of ADAM9 reduced ESCC cell proliferation and migration by inhibiting EGFR-AKT signaling; Downregulation of miR-126 was due to promoter hypermethylation of its host gene Egfl7, and DNMT1 was aberrantly upregulated in ESCC and is responsible for the hypermethylation of Egfl7; Intriguingly, overexpression of miR-126 suppressed DNMT1,was suppressed by overexpression of miR-126, indicating the existence of a regulatory feedback circuit[141].

Multiple epigenetic regulatory mechanisms and miRNA in ESCC metastasis

A more complex and dynamic epigenetic regulatory network of miRNA has been shown to be positively involved in ESCC metastasis. For example, one lncRNA, circRNA can "spong" several miRNAs. lncXIST, serves as oncogene and is significantly upregulated in ESCC tissues and cells, and is significantly associated with a poor prognosis in ESCC patients. Downregulation of lncXIST can inhibit ESCC cell proliferation, migration and invasion by elevating expression of miR-101 and decreasing the expression of EZH2. Downregulation of lncXIST also functions by inhibiting CCND1 expression *via* "sponging" of miR-129-5p[142,143]. circHIPK3 is highly expressed in ESCC tissues and cell lines and is associated with advanced TNM stage, LNM and tumor size. circHIPK3 can promote ESCC cell proliferation, invasion, and migration by modulating the miR-599/c-MYC axis, as well as *via* the regulation of ESCC cell proliferation, migration, and EMT by absorbing miR-124 *via* target AKT3[25,144]. Not more than that, the same miRNA can be regulated by different epigenetic mechanisms. For example, miR-493-5p, is dramatically downregulated in ESCC tissues and cells due to "sponging" from both circFIG4 and linc00324, both of which modulated ESCC progression including ESCC cell invasion and migration *via* targeting the miR-493-5p/E2F3 and miR-493-5p/MAPK1 axis, respectively[145-147]. Another example, miR-124-3p, was found to have positive correlations with ESCC invasion and migration, as well as EMT *via* the regulation of lncZFAS1 and through DNA methylation[31,127].

CONCLUSION

ESCC is a cancer that originates from the squamous epithelial cells lining the esophagus. It is notorious for its aggressive progression and high propensity for metastasis or dispersion to other regions of the body. In ESCC, metastasis contributes to approximately 90% of cancer-associated fatalities, primarily due to the resulting disruption of digestive function, complications arising from metastasis, an overall deterioration of health, and poor prognostic outcomes. The treatment of metastatic ESCC is intricate, possibly necessitating a combination of therapeutic modalities including surgery, radiation therapy, chemotherapy, and targeted treatments. However, these interventions frequently carry their own array of side effects and complications, and their efficacy can be restricted in the face of metastatic progression. As such, deciphering the mechanisms that underpin metastasis and pioneering effective measures for its prevention and treatment are pivotal objectives in ESCC research.

The metastatic process of ESCC is influenced by a variety of factors, including tumor characteristics, host factors, microenvironmental elements, as well as genetic and epigenetic variations. Growing evidence suggests that miRNA signatures represent an epigenetic mechanism that can profoundly impact various stages of metastasis by regulating gene

expression. This regulation occurs through multiple signaling pathways, primarily including the RTK, TGF-β, Wnt/β-catenin, and IL6/Stat3 pathways. Given their regulatory capabilities, miRNAs have surfaced as potential novel diagnostic, prognostic, and therapeutic markers for ESCC metastasis. In their capacity as diagnostic and prognostic markers, certain miRNAs are consistently overexpressed or underexpressed in ESCC tissues. These miRNAs show negative or positive associations with characteristics of metastasis, such as tumor invasive depth, lymphatic/vascular invasion, lymph node metastasis, and distant metastasis. Intriguingly, specific miRNAs have even been linked to metastatic potential, being associated with the propensity of a tumor to metastasize, the severity of metastasis, and the likely sites of metastatic spread. As therapeutic targets, miRNAs that suppress ESCC metastasis can be restored through the application of miRNA mimics, while those promoting ESCC metastasis can be suppressed using anti-miRNA molecules. The regulation of miRNAs is also influenced by other epigenetic factors, including lncRNAs, circRNAs, and DNA methylation. Additionally, miRNAs play a crucial role in molding the tumor microenvironment, affecting angiogenesis, and modulating the immune response to tumors. Given their central roles, miRNAs hold significant potential as metastatic biomarkers for both the diagnosis and therapy of ESCC.

Recent advancements in miRNA-based therapy revolve around two principal tactics: the suppression of oncogenic miRNAs to reinstate the activity of their targeted tumor suppressor genes, and the augmentation of tumor suppressor miRNAs to dampen the expression of the oncogenes they regulate. Although they are typically downregulated in cancers, enhancing the expression of tumor suppressor miRNAs can correct the aberrant overexpression of oncogenes they normally control. Additionally, the artificial introduction of tumor suppressor miRNAs can replenish deficient miRNA levels, thereby targeting and disrupting cellular pathways that contribute to tumor development and metastasis. At present, a variety of therapeutic strategies capitalizing on miRNA mimics or inhibitors are being intensively investigated. One such example is MRX34, a liposome-encapsulated miR-34 mimic that has been introduced into clinical trials for the treatment of patients with primary liver cancer or other malignancies involving the liver. Despite the significant therapeutic potential of miRNAs, several challenges loom must be addressed before their comprehensive integration into clinical practice. One of the foremost challenges in the field of miRNA therapy lies in the potential for off-target effects. These occur when the treatment unintentionally affects genes that have no direct connection to the disease being addressed, leading to unintended and potentially detrimental side effects. Such inadvertent gene regulation can be attributed to the inherent sequence similarities among miRNAs. Moreover, the expansive binding capacity of miRNAs exacerbates this issue; a single miRNA molecule may attach to multiple, disparate mRNAs, thereby simultaneously regulating a host of unrelated genes. This promiscuity in target selection underscores the complexity of achieving precise therapeutic outcomes with miRNA-based interventions. Another substantial challenge in miRNA therapy is achieving effective delivery and ensuring stability. The targeted transport of miRNAs or their inhibitors to designated tissues or cells without loss of function is an ongoing obstacle. Additionally, miRNAs are inherently unstable in the bloodstream due to rapid degradation by nucleases, which calls for the development of sophisticated systems capable of safeguarding these fragile therapeutic agents during delivery. Furthermore, the administration of exogenous miRNA or miRNA mimics may elicit an immune response that could undermine the safety and efficacy of the treatment. Determining the optimal dosage of miRNAs is equally critical, as incorrect dosing could compromise the therapeutic balance, impacting both treatment outcomes and patient well-being. Finally, there are still limitations in accurately predicting miRNA targets, understanding miRNA-mRNA interactions, and quantifying miRNA expression levels, all of which can impede the development of miRNA-based therapies.

As research advances and technology evolves, scientists and healthcare professionals are pioneering methods to navigate the complexities of miRNA therapy. For instance, the integration of large-scale functional screenings, sophisticated bioinformatics analyses, and strategic chemical modifications are being employed to attenuate off-target effects and bolster specificity. Moreover, an array of innovative delivery mechanisms, including nanocarriers, viral vectors, and exosome-based systems, are being utilized to shield miRNAs from enzymatic degradation and to ensure precise tissue-specific targeting with elevated efficiency. Enhancements in the structural design of miRNAs to assist in evasion of immune detection stand as a testament to the proactive measures being taken to preclude unsolicited immune responses. Additionally, gaining a nuanced understanding of the complex miRNA-mRNA interactions, as well as the epigenetic mechanisms at play, is necessary in order to illuminate new potential applications for miRNA-based interventions.

In summary, persistent explorations in the field of miRNA research are unlocking significant opportunities for improving diagnostic accuracy, refining prognostic predictions, and advancing the therapeutic strategies employed in the battle against cancer. With steadfast commitment to research, the future of miRNAs in medicine appears to be both promising and profound.

FOOTNOTES

Co-first authors: Qi-Ying Wei and Feng Jin.

Author contributions: Wei QY, Jin F and Mo SJ wrote this manuscript and created figures; Wang ZY, Li BJ, Cao WB, and Sun ZY consulted and analysis literature, and created tables; Wei QY and Jin F contributed equally to this work.

Supported by Foundation of Henan Educational Committee, No. 22A310024; and Natural Science Foundation for Young Teachers' Basic Research of Zhengzhou University, No. JC202035025.

Conflict-of-interest statement: Mo SJ has nothing to disclose.

Country/Territory of origin: China

ORCID number: Sai-Jun Mo 0000-0001-7375-3562.

S-Editor: Yan JP
L-Editor: A
P-Editor: Cai YX

REFERENCES

1 **Sheikh M**, Roshandel G, McCormack V, Malekzadeh R. Current Status and Future Prospects for Esophageal Cancer. *Cancers (Basel)* 2023; **15** [PMID: 36765722 DOI: 10.3390/cancers15030765]
2 **Yang J**, Liu X, Cao S, Dong X, Rao S, Cai K. Understanding Esophageal Cancer: The Challenges and Opportunities for the Next Decade. *Front Oncol* 2020; **10**: 1727 [PMID: 33014854 DOI: 10.3389/fonc.2020.01727]
3 **He S**, Xu J, Liu X, Zhen Y. Advances and challenges in the treatment of esophageal cancer. *Acta Pharm Sin B* 2021; **11**: 3379-3392 [PMID: 34900524 DOI: 10.1016/j.apsb.2021.03.008]
4 **Zheng S**, Liu B, Guan X. The Role of Tumor Microenvironment in Invasion and Metastasis of Esophageal Squamous Cell Carcinoma. *Front Oncol* 2022; **12**: 911285 [PMID: 35814365 DOI: 10.3389/fonc.2022.911285]
5 **Li Q**, Deng M, Xi M, Zhu Y, Hu Y. Characteristics and Treatment of Brain Metastases from Esophageal Squamous Cell Carcinoma. *J Cancer* 2018; **9**: 901-905 [PMID: 29581768 DOI: 10.7150/jca.21511]
6 **Suhail Y**, Cain MP, Vanaja K, Kurywchak PA, Levchenko A, Kalluri R, Kshitiz. Systems Biology of Cancer Metastasis. *Cell Syst* 2019; **9**: 109-127 [PMID: 31465728 DOI: 10.1016/j.cels.2019.07.003]
7 **Regad T**. Targeting RTK Signaling Pathways in Cancer. *Cancers (Basel)* 2015; **7**: 1758-1784 [PMID: 26404379 DOI: 10.3390/cancers7030860]
8 **Xie F**, Ling L, van Dam H, Zhou F, Zhang L. TGF-β signaling in cancer metastasis. *Acta Biochim Biophys Sin (Shanghai)* 2018; **50**: 121-132 [PMID: 29190313 DOI: 10.1093/abbs/gmx123]
9 **Xiao Z**, Feng X, Zhou Y, Li P, Luo J, Zhang W, Zhou J, Zhao J, Wang D, Wang Y, Tian Z, Zhao X. Exosomal miR-10527-5p Inhibits Migration, Invasion, Lymphangiogenesis and Lymphatic Metastasis by Affecting Wnt/β-Catenin Signaling *via* Rab10 in Esophageal Squamous Cell Carcinoma. *Int J Nanomedicine* 2023; **18**: 95-114 [PMID: 36636641 DOI: 10.2147/IJN.S391173]
10 **Xu Z**, Tie X, Li N, Yi Z, Shen F, Zhang Y. Circular RNA hsa_circ_0000654 promotes esophageal squamous cell carcinoma progression by regulating the miR-149-5p/IL-6/STAT3 pathway. *IUBMB Life* 2020; **72**: 426-439 [PMID: 31778020 DOI: 10.1002/iub.2202]
11 **Ding N**, Sun X, Wang T, Huang L, Wen J, Zhou Y. miR378a3p exerts tumor suppressive function on the tumorigenesis of esophageal squamous cell carcinoma by targeting Rab10. *Int J Mol Med* 2018; **42**: 381-391 [PMID: 29693138 DOI: 10.3892/ijmm.2018.3639]
12 **Hu HF**, Xu WW, Zhang WX, Yan X, Li YJ, Li B, He QY. Identification of miR-515-3p and its targets, vimentin and MMP3, as a key regulatory mechanism in esophageal cancer metastasis: functional and clinical significance. *Signal Transduct Target Ther* 2020; **5**: 271 [PMID: 33243974 DOI: 10.1038/s41392-020-00275-8]
13 **Ni Y**, Meng L, Wang L, Dong W, Shen H, Wang G, Liu Q, Du J. MicroRNA-143 functions as a tumor suppressor in human esophageal squamous cell carcinoma. *Gene* 2013; **517**: 197-204 [PMID: 23276710 DOI: 10.1016/j.gene.2012.12.031]
14 **Yuan RB**, Zhang SH, He Y, Zhang XY, Zhang YB. MiR-874-3p is an independent prognostic factor and functions as an anti-oncomir in esophageal squamous cell carcinoma *via* targeting STAT3. *Eur Rev Med Pharmacol Sci* 2018; **22**: 7265-7273 [PMID: 30468470 DOI: 10.26355/eurrev_201811_16261]
15 **Jing R**, Chen W, Wang H, Ju S, Cong H, Sun B, Jin Q, Chu S, Xu L, Cui M. Plasma miR-185 is decreased in patients with esophageal squamous cell carcinoma and might suppress tumor migration and invasion by targeting RAGE. *Am J Physiol Gastrointest Liver Physiol* 2015; **309**: G719-G729 [PMID: 26316588 DOI: 10.1152/ajpgi.00078.2015]
16 **Zhang B**, Pan X, Cobb GP, Anderson TA. microRNAs as oncogenes and tumor suppressors. *Dev Biol* 2007; **302**: 1-12 [PMID: 16989803 DOI: 10.1016/j.ydbio.2006.08.028]
17 **Hill M**, Tran N. miRNA interplay: mechanisms and consequences in cancer. *Dis Model Mech* 2021; **14** [PMID: 33973623 DOI: 10.1242/dmm.047662]
18 **Zheng S**, Zhang X, Wang X, Li J. Downregulation of miR-138 predicts poor prognosis in patients with esophageal squamous cell carcinoma. *Cancer Biomark* 2017; **20**: 49-54 [PMID: 28759955 DOI: 10.3233/CBM-170079]
19 **Guo Y**, Jin J, Li L, Zhang X, Dong X, He Y. Expression and role of microRNA-193a-5p in esophageal cancer. *Zhongliu* 2019; **39**: 784-794
20 **Han T**, Shi M, Chen G, Hao J. Circ_0008726 promotes malignant progression of ESCC cells through miR-206/HOXA13 pathway. *Gen Thorac Cardiovasc Surg* 2023; **71**: 33-45 [PMID: 36190650 DOI: 10.1007/s11748-022-01874-8]
21 **Zang W**, Wang Y, Du Y, Xuan X, Wang T, Li M, Ma Y, Li P, Chen X, Dong Z, Zhao G. Differential expression profiling of microRNAs and their potential involvement in esophageal squamous cell carcinoma. *Tumour Biol* 2014; **35**: 3295-3304 [PMID: 24272087 DOI: 10.1007/s13277-013-1432-5]
22 **Sun L**, Dong S, Dong C, Sun K, Meng W, Lv P, Yin H, Ming L, He F. Predictive value of plasma miRNA-718 for esophageal squamous cell carcinoma. *Cancer Biomark* 2016; **16**: 265-273 [PMID: 26756617 DOI: 10.3233/CBM-150564]
23 **Zhao L**, Li R, Xu S, Li Y, Zhao P, Dong W, Liu Z, Zhao Q, Tan B. Tumor suppressor miR-128-3p inhibits metastasis and epithelial-mesenchymal transition by targeting ZEB1 in esophageal squamous-cell cancer. *Acta Biochim Biophys Sin (Shanghai)* 2018; **50**: 171-180

[PMID: 29329360 DOI: 10.1093/abbs/gmx132]
24 **Zhang N**, Fu H, Song L, Ding Y, Wang X, Zhao C, Zhao Y, Jiao F. MicroRNA-100 promotes migration and invasion through mammalian target of rapamycin in esophageal squamous cell carcinoma. *Oncol Rep* 2014; **32**: 1409-1418 [PMID: 25109390 DOI: 10.3892/or.2014.3389]
25 **Yao D**, Lin S, Chen S, Wang Z. circHIPK3 regulates cell proliferation and migration by sponging microRNA-124 and regulating serine/threonine kinase 3 expression in esophageal squamous cell carcinoma. *Bioengineered* 2022; **13**: 9767-9780 [PMID: 35443871 DOI: 10.1080/21655979.2022.2060776]
26 **Mei LL**, Wang WJ, Qiu YT, Xie XF, Bai J, Shi ZZ. miR-125b-5p functions as a tumor suppressor gene partially by regulating HMGA2 in esophageal squamous cell carcinoma. *PLoS One* 2017; **12**: e0185636 [PMID: 28968424 DOI: 10.1371/journal.pone.0185636]
27 **Li H**, Meng F, Ma J, Yu Y, Hua X, Qin J, Li Y. Insulin receptor substrate-1 and Golgi phosphoprotein 3 are downstream targets of miR126 in esophageal squamous cell carcinoma. *Oncol Rep* 2014; **32**: 1225-1233 [PMID: 25017784 DOI: 10.3892/or.2014.3327]
28 **Li Y**, Chen D, Gao X, Li X, Shi G. LncRNA NEAT1 Regulates Cell Viability and Invasion in Esophageal Squamous Cell Carcinoma through the miR-129/CTBP2 Axis. *Dis Markers* 2017; **2017**: 5314649 [PMID: 29147064 DOI: 10.1155/2017/5314649]
29 **Liu Y**, Wang X, Jiang X, Yan P, Zhan L, Zhu H, Wang T, Wen J. Tumor-suppressive microRNA-10a inhibits cell proliferation and metastasis by targeting Tiam1 in esophageal squamous cell carcinoma. *J Cell Biochem* 2019; **120**: 7845-7857 [PMID: 30426564 DOI: 10.1002/jcb.28059]
30 **Shao Y**, Li P, Zhu ST, Yue JP, Ji XJ, He Z, Ma D, Wang L, Wang YJ, Zong Y, Wu YD, Zhang ST. Cyclooxygenase-2, a Potential Therapeutic Target, Is Regulated by miR-101 in Esophageal Squamous Cell Carcinoma. *PLoS One* 2015; **10**: e0140642 [PMID: 26556718 DOI: 10.1371/journal.pone.0140642]
31 **Zeng B**, Zhang X, Zhao J, Wei Z, Zhu H, Fu M, Zou D, Feng Y, Luo H, Lei Y. The role of DNMT1/hsa-miR-124-3p/BCAT1 pathway in regulating growth and invasion of esophageal squamous cell carcinoma. *BMC Cancer* 2019; **19**: 609 [PMID: 31226958 DOI: 10.1186/s12885-019-5815-x]
32 **Yuan Y**, Wang Q, Cao F, Han B, Xu L. MiRNA-134 suppresses esophageal squamous cell carcinoma progression by targeting FOXM1. *Int J Clin Exp Pathol* 2019; **12**: 2130-2138 [PMID: 31934035]
33 **Shao Y**, Li P, Zhu ST, Yue JP, Ji XJ, Ma D, Wang L, Wang YJ, Zong Y, Wu YD, Zhang ST. MiR-26a and miR-144 inhibit proliferation and metastasis of esophageal squamous cell cancer by inhibiting cyclooxygenase-2. *Oncotarget* 2016; **7**: 15173-15186 [PMID: 26959737 DOI: 10.18632/oncotarget.7908]
34 **Liu Z**, Huang Y, Han Z, Shen Z, Yu S, Wang T, Dong Z, Kang M. Exosome-mediated miR-25/miR-203 as a potential biomarker for esophageal squamous cell carcinoma: improving early diagnosis and revealing malignancy. *Transl Cancer Res* 2021; **10**: 5174-5182 [PMID: 35116367 DOI: 10.21037/tcr-21-1123]
35 **Wang T**, Wang J, Ren W, Chen S, Cheng YF, Zhang XM. CircRNA-0008717 promotes cell proliferation, migration, and invasion by regulating miR-203/Slug in esophageal cancer cells. *Ann Transl Med* 2020; **8**: 999 [PMID: 32953799 DOI: 10.21037/atm-20-5205]
36 **Cui XB**, Peng H, Li RR, Mu JQ, Yang L, Li N, Liu CX, Hu JM, Li SG, Wei Y, Laibo-Yin, Zhou H, Li F, Chen YZ. MicroRNA-34a functions as a tumor suppressor by directly targeting oncogenic PLCE1 in Kazakh esophageal squamous cell carcinoma. *Oncotarget* 2017; **8**: 92454-92469 [PMID: 29190930 DOI: 10.18632/oncotarget.21384]
37 **Hu C**, Lv L, Peng J, Liu D, Wang X, Zhou Y, Huo J. MicroRNA-375 suppresses esophageal cancer cell growth and invasion by repressing metadherin expression. *Oncol Lett* 2017; **13**: 4769-4775 [PMID: 28599478 DOI: 10.3892/ol.2017.6098]
38 **Li J**, Li X, Li Y, Yang H, Wang L, Qin Y, Liu H, Fu L, Guan XY. Cell-specific detection of miR-375 downregulation for predicting the prognosis of esophageal squamous cell carcinoma by miRNA in situ hybridization. *PLoS One* 2013; **8**: e53582 [PMID: 23301089 DOI: 10.1371/journal.pone.0053582]
39 **Gao P**, Wang D, Liu M, Chen S, Yang Z, Zhang J, Wang H, Niu Y, Wang W, Yang J, Sun G. DNA methylation-mediated repression of exosomal miR-652-5p expression promotes oesophageal squamous cell carcinoma aggressiveness by targeting PARG and VEGF pathways. *PLoS Genet* 2020; **16**: e1008592 [PMID: 32343702 DOI: 10.1371/journal.pgen.1008592]
40 **Zheng S**, Liu Q, Ma R, Tan D, Shen T, Zhang X, Lu X. Let-7b-5p inhibits proliferation and motility in squamous cell carcinoma cells through negative modulation of KIAA1377. *Cell Biol Int* 2019; **43**: 634-641 [PMID: 30958603 DOI: 10.1002/cbin.11136]
41 **Zhang P**, Zhang W, Jiang J, Shen Z, Chen S, Yu S, Kang M. MiR-107 inhibits the malignant biological behavior of esophageal squamous cell carcinoma by targeting TPM3. *J Gastrointest Oncol* 2022; **13**: 1541-1555 [PMID: 36092346 DOI: 10.21037/jgo-22-575]
42 **Liu H**, Ren G, Zhu L, Liu X, He X. The upregulation of miRNA-146a inhibited biological behaviors of ESCC through inhibition of IRS2. *Tumour Biol* 2016; **37**: 4641-4647 [PMID: 26508028 DOI: 10.1007/s13277-015-4274-5]
43 **Xu C**, Li B, Zhao S, Jin B, Jia R, Ge J, Xu H. MicroRNA-186-5p Inhibits Proliferation And Metastasis Of Esophageal Cancer By Mediating HOXA9. *Onco Targets Ther* 2019; **12**: 8905-8914 [PMID: 31802902 DOI: 10.2147/OTT.S227920]
44 **Meng L**, Wang F, Sun S, Zheng Y, Ding Z, Sun Y, Li B, Meng Q, Xu M. MicroRNA-30b targets CBX3 and regulates cell proliferation, apoptosis, and migration in esophageal squamous cell carcinoma *via* the JAK2/STAT3 signaling pathway. *Int J Clin Exp Pathol* 2017; **10**: 11828-11837 [PMID: 31966547]
45 **Han DL**, Wang LL, Zhang GF, Yang WF, Chai J, Lin HM, Fu Z, Yu JM. MiRNA-485-5p, inhibits esophageal cancer cells proliferation and invasion by down-regulating O-linked N-acetylglucosamine transferase. *Eur Rev Med Pharmacol Sci* 2019; **23**: 2809-2816 [PMID: 31002132 DOI: 10.26355/eurrev_201904_17556]
46 **Wang Z**, Liu J, Wang R, Wang Q, Liang R, Tang J. Long Non-Coding RNA Taurine Upregulated Gene 1 (TUG1) Downregulation Constrains Cell Proliferation and Invasion through Regulating Cell Division Cycle 42 (CDC42) Expression Via MiR-498 in Esophageal Squamous Cell Carcinoma Cells. *Med Sci Monit* 2020; **26**: e919714 [PMID: 32139664 DOI: 10.12659/MSM.919714]
47 **Sun J**, Deng Y, Shi J, Yang W. MicroRNA5423p represses OTUB1 expression to inhibit migration and invasion of esophageal cancer cells. *Mol Med Rep* 2020; **21**: 35-42 [PMID: 31939620 DOI: 10.3892/mmr.2019.10836]
48 **Qiu BQ**, Lin XH, Ye XD, Huang W, Pei X, Xiong D, Long X, Zhu SQ, Lu F, Lin K, Zhang XQ, Xu JJ, Sheng LL, Zhang XM, Zhang PF, Wu YB. Long non-coding RNA PSMA3-AS1 promotes malignant phenotypes of esophageal cancer by modulating the miR-101/EZH2 axis as a ceRNA. *Aging (Albany NY)* 2020; **12**: 1843-1856 [PMID: 32005028 DOI: 10.18632/aging.102716]
49 **Wang X**, Li M, Wang Z, Han S, Tang X, Ge Y, Zhou L, Zhou C, Yuan Q, Yang M. Silencing of long noncoding RNA MALAT1 by miR-101 and miR-217 inhibits proliferation, migration, and invasion of esophageal squamous cell carcinoma cells. *J Biol Chem* 2015; **290**: 3925-3935 [PMID: 25538231 DOI: 10.1074/jbc.M114.596866]
50 **Jin LL**, Zhang SJ, Lu GX, Lv F, Shang R, Yang J. miR-574-3p inhibits proliferation and invasion in esophageal cancer by targeting FAM3C and MAPK1. *Kaohsiung J Med Sci* 2020; **36**: 318-327 [PMID: 31880039 DOI: 10.1002/kjm2.12176]
51 **Guan H**, Liu J, Lv P, Zhou L, Zhang J, Cao W. MicroRNA590 inhibits migration, invasion and epithelialtomesenchymal transition of

esophageal squamous cell carcinoma by targeting lowdensity lipoprotein receptorrelated protein 6. *Oncol Rep* 2020; **44**: 1385-1392 [PMID: 32945478 DOI: 10.3892/or.2020.7692]

52 **Yang F**, Sun Z, Wang D, Du T. MiR-106b-5p regulates esophageal squamous cell carcinoma progression by binding to HPGD. *BMC Cancer* 2022; **22**: 308 [PMID: 35317779 DOI: 10.1186/s12885-022-09404-8]

53 **Liu T**, Li P, Li J, Qi Q, Sun Z, Shi S, Xie Y, Liu S, Wang Y, Du L, Wang C. Exosomal and intracellular miR-320b promotes lymphatic metastasis in esophageal squamous cell carcinoma. *Mol Ther Oncolytics* 2021; **23**: 163-180 [PMID: 34729394 DOI: 10.1016/j.omto.2021.09.003]

54 **Liu M**, Yu J, Wang D, Niu Y, Chen S, Gao P, Yang Z, Wang H, Zhang J, Zhang C, Zhao Y, Hu W, Sun G. Epigenetically Upregulated MicroRNA-602 Is Involved in a Negative Feedback Loop with FOXK2 in Esophageal Squamous Cell Carcinoma. *Mol Ther* 2019; **27**: 1796-1809 [PMID: 31401147 DOI: 10.1016/j.ymthe.2019.07.006]

55 **Ma J**, Zhan Y, Xu Z, Li Y, Luo A, Ding F, Cao X, Chen H, Liu Z. ZEB1 induced miR-99b/let-7e/miR-125a cluster promotes invasion and metastasis in esophageal squamous cell carcinoma. *Cancer Lett* 2017; **398**: 37-45 [PMID: 28408353 DOI: 10.1016/j.canlet.2017.04.006]

56 **Zhang Q**, Zhang J, Fu Z, Dong L, Tang Y, Xu C, Wang H, Zhang T, Wu Y, Dong C, Shao S, Wang G. Hypoxia-induced microRNA-10b-3p promotes esophageal squamous cell carcinoma growth and metastasis by targeting TSGA10. *Aging (Albany NY)* 2019; **11**: 10374-10384 [PMID: 31772141 DOI: 10.18632/aging.102462]

57 **Lu YF**, Yu JR, Yang Z, Zhu GX, Gao P, Wang H, Chen SY, Zhang J, Liu MY, Niu Y, Wei XM, Wang W, Ye FJ, Zhang LX, Zhao Y, Sun GG. Promoter hypomethylation mediated upregulation of MicroRNA-10b-3p targets FOXO3 to promote the progression of esophageal squamous cell carcinoma (ESCC). *J Exp Clin Cancer Res* 2018; **37**: 301 [PMID: 30514328 DOI: 10.1186/s13046-018-0966-1]

58 **Xu X**, Chen Z, Zhao X, Wang J, Ding D, Wang Z, Tan F, Tan X, Zhou F, Sun J, Sun N, Gao Y, Shao K, Li N, Qiu B, He J. MicroRNA-25 promotes cell migration and invasion in esophageal squamous cell carcinoma. *Biochem Biophys Res Commun* 2012; **421**: 640-645 [PMID: 22450326 DOI: 10.1016/j.bbrc.2012.03.048]

59 **Bai X**, Wang Q, Rui X, Li X, Wang X. Upregulation of miR-1269 Contributes to the Progression of Esophageal Squamous Cell Cancer Cells and Is Associated With Poor Prognosis. *Technol Cancer Res Treat* 2021; **20**: 1533033820985858 [PMID: 33416035 DOI: 10.1177/1533033820985858]

60 **Wang X**, Han J, Liu Y, Hu J, Li M, Chen X, Xu L. miR-17-5p and miR-4443 Promote Esophageal Squamous Cell Carcinoma Development by Targeting TIMP2. *Front Oncol* 2021; **11**: 605894 [PMID: 34778021 DOI: 10.3389/fonc.2021.605894]

61 **Zhao Y**, Zhang Q, Liu H, Wang N, Zhang X, Yang S. lncRNA PART1, manipulated by transcriptional factor FOXP2, suppresses proliferation and invasion in ESCC by regulating the miR18a5p/SOX6 signaling axis. *Oncol Rep* 2021; **45**: 1118-1132 [PMID: 33432363 DOI: 10.3892/or.2021.7931]

62 **Zhang L**, Tong Z, Sun Z, Zhu G, Shen E, Huang Y. MiR-25-3p targets PTEN to regulate the migration, invasion, and apoptosis of esophageal cancer cells *via* the PI3K/AKT pathway. *Biosci Rep* 2020; **40** [PMID: 32985648 DOI: 10.1042/BSR20201901]

63 **Wang B**, Hua P, Wang R, Li J, Zhang G, Jin C, Zhang Y. Inhibited MicroRNA-301 Restrains Angiogenesis and Cell Growth in Esophageal Squamous Cell Carcinoma by Elevating PTEN. *Nanoscale Res Lett* 2021; **16**: 3 [PMID: 33404856 DOI: 10.1186/s11671-020-03452-4]

64 **Liu W**, Li M, Chen X, Zhang D, Wei L, Zhang Z, Wang S, Meng L, Zhu S, Li B. MicroRNA-373 promotes migration and invasion in human esophageal squamous cell carcinoma by inhibiting TIMP3 expression. *Am J Cancer Res* 2016; **6**: 1-14 [PMID: 27073718]

65 **Chen Y**, Wang H, Zhu S, Lan X. miR-483-5p promotes esophageal cancer progression by targeting KCNQ1. *Biochem Biophys Res Commun* 2020; **531**: 615-621 [PMID: 32819715 DOI: 10.1016/j.bbrc.2020.07.037]

66 **Zhang H**, Shi X, Chang W, Li Y, Wang L. Epigenetic alterations of the Igf2 promoter and the effect of miR4835p on its target gene expression in esophageal squamous cell carcinoma. *Mol Med Rep* 2018; **17**: 2251-2256 [PMID: 29207103 DOI: 10.3892/mmr.2017.8134]

67 **Liu S**, Lin Z, Zheng Z, Rao W, Lin Y, Chen H, Xie Q, Chen Y, Hu Z. Serum exosomal microRNA-766-3p expression is associated with poor prognosis of esophageal squamous cell carcinoma. *Cancer Sci* 2020; **111**: 3881-3892 [PMID: 32589328 DOI: 10.1111/cas.14550]

68 **Gao DC**, Hou B, Zhou D, Liu QX, Zhang K, Lu X, Zhang J, Zheng H, Dai JG. Tumor-derived exosomal miR-103a-2-5p facilitates esophageal squamous cell carcinoma cell proliferation and migration. *Eur Rev Med Pharmacol Sci* 2020; **24**: 6097-6110 [PMID: 32572925 DOI: 10.26355/eurrev_202006_21505]

69 **He B**, Zhang K, Han X, Su C, Zhao J, Wang G, Zhang L, Hu W. Extracellular Vesicle-Derived miR-105-5p Promotes Malignant Phenotypes of Esophageal Squamous Cell Carcinoma by Targeting SPARCL1 *via* FAK/AKT Signaling Pathway. *Front Genet* 2022; **13**: 819699 [PMID: 35309127 DOI: 10.3389/fgene.2022.819699]

70 **Yu T**, Cao R, Li S, Fu M, Ren L, Chen W, Zhu H, Zhan Q, Shi R. MiR-130b plays an oncogenic role by repressing PTEN expression in esophageal squamous cell carcinoma cells. *BMC Cancer* 2015; **15**: 29 [PMID: 25637514 DOI: 10.1186/s12885-015-1031-5]

71 **Chen Z**, Yao N, Gu H, Song Y, Ye Z, Li L, Lu P, Shao Q. Circular RNA_LARP4 Sponges miR-1323 and Hampers Progression of Esophageal Squamous Cell Carcinoma Through Modulating PTEN/PI3K/AKT Pathway. *Dig Dis Sci* 2020; **65**: 2272-2283 [PMID: 31897898 DOI: 10.1007/s10620-019-05973-0]

72 **Zhang Y**, Lu W, Chen Y, Lin Y, Yang X, Wang H, Liu Z. The miR-19b-3p-MAP2K3-STAT3 feedback loop regulates cell proliferation and invasion in esophageal squamous cell carcinoma. *Mol Oncol* 2021; **15**: 1566-1583 [PMID: 33660414 DOI: 10.1002/1878-0261.12934]

73 **Zhang J**, Zhang Y, Tan X, Zhang Q, Liu C. MiR-23b-3p induces the proliferation and metastasis of esophageal squamous cell carcinomas cells through the inhibition of EBF3. *Acta Biochim Biophys Sin (Shanghai)* 2018; **50**: 605-614 [PMID: 29750239 DOI: 10.1093/abbs/gmy049]

74 **Hu CM**, Peng J, Lv L, Wang XH, Huo JR, Liu DL. MiR-196a promotes the proliferation and migration of esophageal cancer *via* the UHRF2/TET2 axis. *Mol Cell Biochem* 2022; **477**: 537-547 [PMID: 34826027 DOI: 10.1007/s11010-021-04301-3]

75 **Fu G**, Pei Z, Song N. Oncogenic microRNA-301b regulates tumor repressor dystrobrevin alpha to facilitate cell growth, invasion and migration in esophageal cancer. *Esophagus* 2021; **18**: 315-325 [PMID: 32737801 DOI: 10.1007/s10388-020-00764-3]

76 **He Y**, Mingyan E, Wang C, Liu G, Shi M, Liu S. CircVRK1 regulates tumor progression and radioresistance in esophageal squamous cell carcinoma by regulating miR-624-3p/PTEN/PI3K/AKT signaling pathway. *Int J Biol Macromol* 2019; **125**: 116-123 [PMID: 30508543 DOI: 10.1016/j.ijbiomac.2018.11.273]

77 **Li X**, Guo S, Min L, Guo Q, Zhang S. miR-92a-3p promotes the proliferation, migration and invasion of esophageal squamous cell cancer by regulating PTEN. *Int J Mol Med* 2019; **44**: 973-981 [PMID: 31257524 DOI: 10.3892/ijmm.2019.4258]

78 **Yang S**, Li X, Shen W, Hu H, Li C, Han G. MicroRNA-140 Represses Esophageal Cancer Progression *via* Targeting ZEB2 to Regulate Wnt/β-Catenin Pathway. *J Surg Res* 2021; **257**: 267-277 [PMID: 32862055 DOI: 10.1016/j.jss.2020.07.074]

79 **Iiizumi M**, Liu W, Pai SK, Furuta E, Watabe K. Drug development against metastasis-related genes and their pathways: a rationale for cancer therapy. *Biochim Biophys Acta* 2008; **1786**: 87-104 [PMID: 18692117 DOI: 10.1016/j.bbcan.2008.07.002]

80 **Wang Q**, Yang L, Fan Y, Tang W, Sun H, Xu Z, Zhou J, Zhang Y, Zhu B, Cao X. Circ-ZDHHC5 Accelerates Esophageal Squamous Cell Carcinoma Progression in vitro *via* miR-217/ZEB1 Axis. *Front Cell Dev Biol* 2020; **8**: 570305 [PMID: 33392180 DOI: 10.3389/fcell.2020.570305]

81 **Xiao JN**, Yan TH, Yu RM, Gao Y, Zeng WL, Lu SW, Que HX, Liu ZP, Jiang JH. Long non-coding RNA UCA1 regulates the expression of Snail2 by miR-203 to promote hepatocellular carcinoma progression. *J Cancer Res Clin Oncol* 2017; **143**: 981-990 [PMID: 28271214 DOI: 10.1007/s00432-017-2370-1]

82 **Li G**, Qi HW, Dong HG, Bai P, Sun M, Liu HY. Targeting deubiquitinating enzyme USP26 by microRNA-203 regulates Snail1's pro-metastatic functions in esophageal cancer. *Cancer Cell Int* 2020; **20**: 355 [PMID: 32760222 DOI: 10.1186/s12935-020-01441-2]

83 **Liu B**, Li X, Li C, Xu R, Sun X. miR-25 mediates metastasis and epithelial-mesenchymal-transition in human esophageal squamous cell carcinoma *via* regulation of E-cadherin signaling. *Bioengineered* 2019; **10**: 679-688 [PMID: 31679450 DOI: 10.1080/21655979.2019.1687391]

84 **Liu K**, Li L, Rusidanmu A, Wang Y, Lv X. Down-Regulation of MiR-1294 is Related to Dismal Prognosis of Patients with Esophageal Squamous Cell Carcinoma through Elevating C-MYC Expression. *Cell Physiol Biochem* 2015; **36**: 100-110 [PMID: 25925090 DOI: 10.1159/000374056]

85 **Song Y**, Li J, Zhu Y, Dai Y, Zeng T, Liu L, Wang H, Qin Y, Zeng M, Guan XY, Li Y. MicroRNA-9 promotes tumor metastasis *via* repressing E-cadherin in esophageal squamous cell carcinoma. *Oncotarget* 2014; **5**: 11669-11680 [PMID: 25375090 DOI: 10.18632/oncotarget.2581]

86 **Chen ZL**, Zhao XH, Wang JW, Li BZ, Wang Z, Sun J, Tan FW, Ding DP, Xu XH, Zhou F, Tan XG, Hang J, Shi SS, Feng XL, He J. microRNA-92a promotes lymph node metastasis of human esophageal squamous cell carcinoma *via* E-cadherin. *J Biol Chem* 2011; **286**: 10725-10734 [PMID: 21148309 DOI: 10.1074/jbc.M110.165654]

87 **Li P**, Liu X, Xing W, Qiu H, Li R, Liu S, Sun H. Exosome-derived miR-200a promotes esophageal cancer cell proliferation and migration *via* the mediating Keap1 expression. *Mol Cell Biochem* 2022; **477**: 1295-1308 [PMID: 35137328 DOI: 10.1007/s11010-022-04353-z]

88 **Qi Y**, Li X, Zhao S. miR-29b inhibits the progression of esophageal squamous cell carcinoma by targeting MMP-2. *Neoplasma* 2015; **62**: 384-390 [PMID: 25866219 DOI: 10.4149/neo_2015_046]

89 **Yang L**, Song X, Zhu J, Li M, Ji Y, Wu F, Chen Y, Cui X, Hu J, Wang L, Cao Y, Wei Y, Zhang W, Li F. Tumor suppressor microRNA-34a inhibits cell migration and invasion by targeting MMP-2/MMP-9/FNDC3B in esophageal squamous cell carcinoma. *Int J Oncol* 2017; **51**: 378-388 [PMID: 28534990 DOI: 10.3892/ijo.2017.4015]

90 **Osako Y**, Seki N, Kita Y, Yonemori K, Koshizuka K, Kurozumi A, Omoto I, Sasaki K, Uchikado Y, Kurahara H, Maemura K, Natsugoe S. Regulation of MMP13 by antitumor microRNA-375 markedly inhibits cancer cell migration and invasion in esophageal squamous cell carcinoma. *Int J Oncol* 2016; **49**: 2255-2264 [PMID: 27779648 DOI: 10.3892/ijo.2016.3745]

91 **Guo Y**, Sun P, Guo W, Yin Q, Han J, Sheng S, Liang J, Dong Z. LncRNA DDX11 antisense RNA 1 promotes EMT process of esophageal squamous cell carcinoma by sponging miR-30d-5p to regulate SNAI1/ZEB2 expression and Wnt/β-catenin pathway. *Bioengineered* 2021; **12**: 11425-11440 [PMID: 34866524 DOI: 10.1080/21655979.2021.2008759]

92 **Zhang K**, Chen J, Song H, Chen LB. SNHG16/miR-140-5p axis promotes esophagus cancer cell proliferation, migration and EMT formation through regulating ZEB1. *Oncotarget* 2018; **9**: 1028-1040 [PMID: 29416674 DOI: 10.18632/oncotarget.23178]

93 **Matsushima K**, Isomoto H, Yamaguchi N, Inoue N, Machida H, Nakayama T, Hayashi T, Kunizaki M, Hidaka S, Nagayasu T, Nakashima M, Ujifuku K, Mitsutake N, Ohtsuru A, Yamashita S, Korpal M, Kang Y, Gregory PA, Goodall GJ, Kohno S, Nakao K. MiRNA-205 modulates cellular invasion and migration *via* regulating zinc finger E-box binding homeobox 2 expression in esophageal squamous cell carcinoma cells. *J Transl Med* 2011; **9**: 30 [PMID: 21426561 DOI: 10.1186/1479-5876-9-30]

94 **Zuo J**, Wang D, Shen H, Liu F, Han J, Zhang X. MicroRNA-153 inhibits tumor progression in esophageal squamous cell carcinoma by targeting SNAI1. *Tumour Biol* 2016 [PMID: 27739030 DOI: 10.1007/s13277-016-5427-x]

95 **Ma T**, Zhao Y, Lu Q, Lu Y, Liu Z, Xue T, Shao Y. MicroRNA-30c functions as a tumor suppressor *via* targeting SNAI1 in esophageal squamous cell carcinoma. *Biomed Pharmacother* 2018; **98**: 680-686 [PMID: 29304493 DOI: 10.1016/j.biopha.2017.12.095]

96 **Huang Z**, Tian Z, Zhao Y, Zhu F, Liu W, Wang X. MAPK Signaling Pathway Is Essential for Female Reproductive Regulation in the Cabbage Beetle, Colaphellus bowringi. *Cells* 2022; **11** [PMID: 35626638 DOI: 10.3390/cells11101602]

97 **Guanen Q**, Junjie S, Baolin W, Chaoyang W, Yajuan Y, Jing L, Junpeng L, Gaili N, Zhongping W, Jun W. MiR-214 promotes cell meastasis and inhibites apoptosis of esophageal squamous cell carcinoma *via* PI3K/AKT/mTOR signaling pathway. *Biomed Pharmacother* 2018; **105**: 350-361 [PMID: 29864623 DOI: 10.1016/j.biopha.2018.05.149]

98 **An L**, Li M, Jia Q. Mechanisms of radiotherapy resistance and radiosensitization strategies for esophageal squamous cell carcinoma. *Mol Cancer* 2023; **22**: 140 [PMID: 37598158 DOI: 10.1186/s12943-023-01839-2]

99 **Kashyap MK**, Abdel-Rahman O. Expression, regulation and targeting of receptor tyrosine kinases in esophageal squamous cell carcinoma. *Mol Cancer* 2018; **17**: 54 [PMID: 29455652 DOI: 10.1186/s12943-018-0790-4]

100 **Cheng J**, Ma H, Yan M, Zhang Z, Xing W. Circ_0007624 suppresses the development of esophageal squamous cell carcinoma *via* targeting miR-224-5p/CPEB3 to inactivate the EGFR/PI3K/AKT signaling. *Cell Signal* 2022; **99**: 110448 [PMID: 35998761 DOI: 10.1016/j.cellsig.2022.110448]

101 **Song W**, Wang K, Yang X, Dai W, Fan Z. Long noncoding RNA BANCR mediates esophageal squamous cell carcinoma progression by regulating the IGF1R/Raf/MEK/ERK pathway *via* miR3383p. *Int J Mol Med* 2020; **46**: 1377-1388 [PMID: 32945416 DOI: 10.3892/ijmm.2020.4687]

102 **Xu H**, Miao J, Liu S, Liu H, Zhang L, Zhang Q. Long non-coding RNA KCNQ1 overlapping transcript 1 promotes the progression of esophageal squamous cell carcinoma by adsorbing microRNA-133b. *Clinics (Sao Paulo)* 2021; **76**: e2175 [PMID: 33909822 DOI: 10.6061/clinics/2021/e2175]

103 **Zhu L**, Wang Z, Fan Q, Wang R, Sun Y. microRNA-27a functions as a tumor suppressor in esophageal squamous cell carcinoma by targeting KRAS. *Oncol Rep* 2014; **31**: 280-286 [PMID: 24154848 DOI: 10.3892/or.2013.2807]

104 **Kang M**, Li Y, Zhu S, Zhang S, Guo S, Li P. MicroRNA-193b acts as a tumor suppressor gene in human esophageal squamous cell carcinoma *via* target regulation of KRAS. *Oncol Lett* 2019; **17**: 3965-3973 [PMID: 30881513 DOI: 10.3892/ol.2019.10039]

105 **Zhu Y**, Ma Y, Peng H, Gong L, Xiao M, Xiang L, He D, Cao K. MiR-130b promotes the progression of oesophageal squamous cell carcinoma by targeting SASH1. *J Cell Mol Med* 2019; **23**: 93-103 [PMID: 30443973 DOI: 10.1111/jcmm.13887]

106 **Noor MT**, Seehra N, Rajput J, Sharma R, Thakur BS. Evaluation of Roles of MicroRNA-21 and MicroRNA-18a in Esophageal Squamous Cell Carcinoma and Comparison of Their Changes in Expression Post-Chemoradiotherapy. *Gastroenterology Res* 2020; **13**: 107-113 [PMID: 32655727 DOI: 10.14740/gr1261]

107 **Wang Y**, Lu J, Chen L, Bian H, Hu J, Li D, Xia C, Xu H. Tumor-Derived EV-Encapsulated miR-181b-5p Induces Angiogenesis to Foster

Tumorigenesis and Metastasis of ESCC. *Mol Ther Nucleic Acids* 2020; **20**: 421-437 [PMID: 32244169 DOI: 10.1016/j.omtn.2020.03.002]
108 **Zeng Q**, Zhu Z, Song L, He Z. Transferred by exosomes-derived MiR-19b-3p targets PTEN to regulate esophageal cancer cell apoptosis, migration and invasion. *Biosci Rep* 2020; **40** [PMID: 33146702 DOI: 10.1042/BSR20201858]
109 **Yang B**, Liu Y, Li L, Deng H, Xian L. MicroRNA200a promotes esophageal squamous cell carcinoma cell proliferation, migration and invasion through extensive target genes. *Mol Med Rep* 2020; **21**: 2073-2084 [PMID: 32323771 DOI: 10.3892/mmr.2020.11002]
110 **Cui D**, Cheung AL. Roles of microRNAs in tumorigenesis and metastasis of esophageal squamous cell carcinoma. *World J Clin Oncol* 2021; **12**: 609-622 [PMID: 34513596 DOI: 10.5306/wjco.v12.i8.609]
111 **Song Q**, Liu H, Li C, Liang H. miR-33a-5p inhibits the progression of esophageal cancer through the DKK1-mediated Wnt/β-catenin pathway. *Aging (Albany NY)* 2021; **13**: 20481-20494 [PMID: 34426559 DOI: 10.18632/aging.203430]
112 **Yan S**, Jiang H, Fang S, Yin F, Wang Z, Jia Y, Sun X, Wu S, Jiang T, Mao A. MicroRNA-340 Inhibits Esophageal Cancer Cell Growth and Invasion by Targeting Phosphoserine Aminotransferase 1. *Cell Physiol Biochem* 2015; **37**: 375-386 [PMID: 26316084 DOI: 10.1159/000430361]
113 **Wang J**, Yao W, Li J, Zhang Q, Wei L. Identification of a novel circ_0001946/miR-1290/SOX6 ceRNA network in esophageal squamous cell cancer. *Thorac Cancer* 2022; **13**: 1299-1310 [PMID: 35411716 DOI: 10.1111/1759-7714.14381]
114 **Luo J**, Tian Z, Zhou Y, Xiao Z, Park SY, Sun H, Zhuang T, Wang Y, Li P, Zhao X. CircABCA13 acts as a miR-4429 sponge to facilitate esophageal squamous cell carcinoma development by stabilizing SRXN1. *Cancer Sci* 2023; **114**: 2835-2847 [PMID: 37017121 DOI: 10.1111/cas.15807]
115 **Johnson DE**, O'Keefe RA, Grandis JR. Targeting the IL-6/JAK/STAT3 signalling axis in cancer. *Nat Rev Clin Oncol* 2018; **15**: 234-248 [PMID: 29405201 DOI: 10.1038/nrclinonc.2018.8]
116 **Wang J**, Yu PY, Yu JP, Luo JD, Sun ZQ, Sun F, Kong Z, Wang JL. KIF22 promotes progress of esophageal squamous cell carcinoma cells and is negatively regulated by miR-122. *Am J Transl Res* 2021; **13**: 4152-4166 [PMID: 34150005]
117 **Hao Y**, Baker D, Ten Dijke P. TGF-β-Mediated Epithelial-Mesenchymal Transition and Cancer Metastasis. *Int J Mol Sci* 2019; **20** [PMID: 31195692 DOI: 10.3390/ijms20112767]
118 **Cai Y**, Ruan W, Ding J, Wei N, Wang J, Zhang H, Ma N, Weng G, Su WK, Lin Y, Zhu K. miR935p regulates the occurrence and development of esophageal carcinoma epithelial cells by targeting TGFβR2. *Int J Mol Med* 2021; **47** [PMID: 33448310 DOI: 10.3892/ijmm.2020.4836]
119 **Liu L**, Zhao Z, Zhou W, Fan X, Zhan Q, Song Y. Enhanced Expression of miR-425 Promotes Esophageal Squamous Cell Carcinoma Tumorigenesis by Targeting SMAD2. *J Genet Genomics* 2015; **42**: 601-611 [PMID: 26674378 DOI: 10.1016/j.jgg.2015.09.010]
120 **Recillas-Targa F**. Cancer Epigenetics: An Overview. *Arch Med Res* 2022; **53**: 732-740 [PMID: 36411173 DOI: 10.1016/j.arcmed.2022.11.003]
121 **Kazimierczyk M**, Wrzesinski J. Long Non-Coding RNA Epigenetics. *Int J Mol Sci* 2021; **22** [PMID: 34200507 DOI: 10.3390/ijms22116166]
122 **Ali Syeda Z**, Langden SSS, Munkhzul C, Lee M, Song SJ. Regulatory Mechanism of MicroRNA Expression in Cancer. *Int J Mol Sci* 2020; **21** [PMID: 32138313 DOI: 10.3390/ijms21051723]
123 **Denisenko O**. Epigenetics of Ribosomal RNA Genes. *Biochemistry (Mosc)* 2022; **87**: S103-SS31 [PMID: 35501990 DOI: 10.1134/S0006297922140097]
124 **Pan Q**, Li B, Zhang J, Du X, Gu D. LncRNA THAP9-AS1 accelerates cell growth of esophageal squamous cell carcinoma through sponging miR-335-5p to regulate SGMS2. *Pathol Res Pract* 2021; **224**: 153526 [PMID: 34273804 DOI: 10.1016/j.prp.2021.153526]
125 **Yang F**, Wen S, Zhang Y, Xu Y, Lv H, Zhu Y, Wang M, Su P, Huang C, Tian Z. Identifying potential metastasis-related long non-coding RNAs, microRNAs, and message RNAs in the esophageal squamous cell carcinoma. *J Cell Biochem* 2019; **120**: 13202-13215 [PMID: 30891809 DOI: 10.1002/jcb.28594]
126 **Lu T**, Wang R, Cai H, Cui Y. Long non-coding RNA DLEU2 promotes the progression of esophageal cancer through miR-30e-5p/E2F7 axis. *Biomed Pharmacother* 2020; **123**: 109650 [PMID: 31884338 DOI: 10.1016/j.biopha.2019.109650]
127 **Li Z**, Qin X, Bian W, Li Y, Shan B, Yao Z, Li S. Exosomal lncRNA ZFAS1 regulates esophageal squamous cell carcinoma cell proliferation, invasion, migration and apoptosis *via* microRNA-124/STAT3 axis. *J Exp Clin Cancer Res* 2019; **38**: 477 [PMID: 31775815 DOI: 10.1186/s13046-019-1473-8]
128 **Lin C**, Zhang S, Wang Y, Nice E, Guo C, Zhang E, Yu L, Li M, Liu C, Hu L, Hao J, Qi W, Xu H. Functional Role of a Novel Long Noncoding RNA TTN-AS1 in Esophageal Squamous Cell Carcinoma Progression and Metastasis. *Clin Cancer Res* 2018; **24**: 486-498 [PMID: 29101304 DOI: 10.1158/1078-0432.CCR-17-1851]
129 **He XY**, Wang XQ, Xiao QL, Liu D, Xu QR, Liu S. Long non-coding RNA NCK1-AS1 functions as a ceRNA to regulate cell viability and invasion in esophageal squamous cell carcinoma *via* microRNA-133b/ENPEP axis. *Cell Cycle* 2023; **22**: 596-609 [PMID: 36412985 DOI: 10.1080/15384101.2022.2138416]
130 **Jia J**, Li H, Chu J, Sheng J, Wang C, Jia Z, Meng W, Yin H, Wan J, He F. LncRNA FAM83A-AS1 promotes ESCC progression by regulating miR-214/CDC25B axis. *J Cancer* 2021; **12**: 1200-1211 [PMID: 33442418 DOI: 10.7150/jca.54007]
131 **Xu J**, Chen Z, Fang Z, Chen S, Guo Y, Liu X, Chen K. Long non-coding RNA OIP5-AS1 promotes the progression of esophageal cancer by regulating miR-30a/VOPP1 expression. *Oncol Lett* 2021; **22**: 651 [PMID: 34386073 DOI: 10.3892/ol.2021.12912]
132 **Liu H**, Zhang Q, Song Y, Hao Y, Cui Y, Zhang X, Qin Y, Zhu G, Wang F, Dang J, Ma S, Zhang Y, Guo W, Li S, Guan F, Fan T. Long non-coding RNA SLC2A1-AS1 induced by GLI3 promotes aerobic glycolysis and progression in esophageal squamous cell carcinoma by sponging miR-378a-3p to enhance Glut1 expression. *J Exp Clin Cancer Res* 2021; **40**: 287 [PMID: 34517880 DOI: 10.1186/s13046-021-02081-8]
133 **Qian CJ**, Xu ZR, Chen LY, Wang YC, Yao J. LncRNA MAFG-AS1 Accelerates Cell Migration, Invasion and Aerobic Glycolysis of Esophageal Squamous Cell Carcinoma Cells *via* miR-765/PDX1 Axis. *Cancer Manag Res* 2020; **12**: 6895-6908 [PMID: 32801913 DOI: 10.2147/CMAR.S262075]
134 **Yan Y**, Li S, Wang S, Rubegni P, Tognetti L, Zhang J, Yan L. Long noncoding RNA HAND2-AS1 inhibits cancer cell proliferation, migration, and invasion in esophagus squamous cell carcinoma by regulating microRNA-21. *J Cell Biochem* 2019; **120**: 9564-9571 [PMID: 30520131 DOI: 10.1002/jcb.28233]
135 **Kristensen LS**, Hansen TB, Venø MT, Kjems J. Circular RNAs in cancer: opportunities and challenges in the field. *Oncogene* 2018; **37**: 555-565 [PMID: 28991235 DOI: 10.1038/onc.2017.361]
136 **Zeng B**, Liu Z, Zhu H, Zhang X, Yang W, Li X, Cheng C. CircRNA_2646 functions as a ceRNA to promote progression of esophageal squamous cell carcinoma *via* inhibiting miR-124/PLP2 signaling pathway. *Cell Death Discov* 2021; **7**: 99 [PMID: 33976115 DOI: 10.1038/s41420-021-00461-9]
137 **Liang Z**, Zhao B, Hou J, Zheng J, Xin G. CircRNA circ-OGDH (hsa_circ_0003340) Acts as a ceRNA to Regulate Glutamine Metabolism and

Esophageal Squamous Cell Carcinoma Progression by the miR-615-5p/PDX1 Axis. *Cancer Manag Res* 2021; **13**: 3041-3053 [PMID: 33854374 DOI: 10.2147/CMAR.S290088]

138 **Wu B**, Chen Y, Xie X, Liang H, Peng F, Che W. Circ_0001273 downregulation inhibits the growth, migration and glutamine metabolism of esophageal cancer cells *via* targeting the miR-622/SLC1A5 signaling axis. *Thorac Cancer* 2022; **13**: 1795-1805 [PMID: 35567340 DOI: 10.1111/1759-7714.14458]

139 **Zhang WQ**, Liu KQ, Pei YX, Tan J, Ma JB, Zhao J. Circ-ABCB10 promotes proliferation and invasion of esophageal squamous cell carcinoma cells by modulating microRNA-670-3p. *Eur Rev Med Pharmacol Sci* 2020; **24**: 6088-6096 [PMID: 32572924 DOI: 10.26355/eurrev_202006_21504]

140 **Xing Y**, Zha WJ, Li XM, Li H, Gao F, Ye T, Du WQ, Liu YC. Circular RNA circ-Foxo3 inhibits esophageal squamous cell cancer progression *via* the miR-23a/PTEN axis. *J Cell Biochem* 2020; **121**: 2595-2605 [PMID: 31680314 DOI: 10.1002/jcb.29481]

141 **Liu R**, Gu J, Jiang P, Zheng Y, Liu X, Jiang X, Huang E, Xiong S, Xu F, Liu G, Ge D, Chu Y. DNMT1-microRNA126 epigenetic circuit contributes to esophageal squamous cell carcinoma growth *via* ADAM9-EGFR-AKT signaling. *Clin Cancer Res* 2015; **21**: 854-863 [PMID: 25512445 DOI: 10.1158/1078-0432.CCR-14-1740]

142 **Wu X**, Dinglin X, Wang X, Luo W, Shen Q, Li Y, Gu L, Zhou Q, Zhu H, Tan C, Yang X, Zhang Z. Long noncoding RNA XIST promotes malignancies of esophageal squamous cell carcinoma *via* regulation of miR-101/EZH2. *Oncotarget* 2017; **8**: 76015-76028 [PMID: 29100288 DOI: 10.18632/oncotarget.18638]

143 **Wang H**, Li H, Yu Y, Jiang Q, Zhang R, Sun H, Xing W, Li Y. Long non-coding RNA XIST promotes the progression of esophageal squamous cell carcinoma through sponging miR-129-5p and upregulating CCND1 expression. *Cell Cycle* 2021; **20**: 39-53 [PMID: 33345719 DOI: 10.1080/15384101.2020.1856497]

144 **Ba Y**, Liu Y, Li C, Zhu Y, Xing W. HIPK3 Promotes Growth and Metastasis of Esophageal Squamous Cell Carcinoma *via* Regulation of miR-599/c-MYC Axis. *Onco Targets Ther* 2020; **13**: 1967-1978 [PMID: 32189968 DOI: 10.2147/OTT.S217087]

145 **Huang Z**, Wang C, Zhao X. circFIG 4 drives the carcinogenesis and metastasis of esophagus cancer *via* the miR-493-5p/E2F3 axis. *Thorac Cancer* 2022; **13**: 783-794 [PMID: 35083866 DOI: 10.1111/1759-7714.14321]

146 **Sharma U**, Kaur Rana M, Singh K, Jain A. LINC00324 promotes cell proliferation and metastasis of esophageal squamous cell carcinoma through sponging miR-493-5p *via* MAPK signaling pathway. *Biochem Pharmacol* 2023; **207**: 115372 [PMID: 36493845 DOI: 10.1016/j.bcp.2022.115372]

147 **Liu W**, Li M, Chen X, Zhu S, Shi H, Zhang D, Cheng C, Li B. MicroRNA-1 suppresses proliferation, migration and invasion by targeting Notch2 in esophageal squamous cell carcinoma. *Sci Rep* 2018; **8**: 5183 [PMID: 29581534 DOI: 10.1038/s41598-018-23421-3]

148 **Qi B**, Wang Y, Chen ZJ, Li XN, Qi Y, Yang Y, Cui GH, Guo HZ, Li WH, Zhao S. Down-regulation of miR-30a-3p/5p promotes esophageal squamous cell carcinoma cell proliferation by activating the Wnt signaling pathway. *World J Gastroenterol* 2017; **23**: 7965-7977 [PMID: 29259372 DOI: 10.3748/wjg.v23.i45.7965]

149 **Chen C**, Yang C, Tian X, Liang Y, Wang S, Wang X, Shou Y, Li H, Xiao Q, Shu J, Sun M, Chen K. Downregulation of miR-100-5p in cancer-associated fibroblast-derived exosomes facilitates lymphangiogenesis in esophageal squamous cell carcinoma. *Cancer Med* 2023; **12**: 14468-14483 [PMID: 37184125 DOI: 10.1002/cam4.6078]

150 **Xie R**, Wu SN, Gao CC, Yang XZ, Wang HG, Zhang JL, Yan W, Ma TH. MicroRNA-30d inhibits the migration and invasion of human esophageal squamous cell carcinoma cells *via* the posttranscriptional regulation of enhancer of zeste homolog 2. *Oncol Rep* 2017; **37**: 1682-1690 [PMID: 28184915 DOI: 10.3892/or.2017.5405]

151 **Li W**, Zhao W, Lu Z, Zhang W, Yang X. Long Noncoding RNA GAS5 Promotes Proliferation, Migration, and Invasion by Regulation of miR-301a in Esophageal Cancer. *Oncol Res* 2018; **26**: 1285-1294 [PMID: 29386089 DOI: 10.3727/096504018X15166193231711]

152 **Sharma P**, Saini N, Sharma R. miR-107 functions as a tumor suppressor in human esophageal squamous cell carcinoma and targets Cdc42. *Oncol Rep* 2017; **37**: 3116-3127 [PMID: 28393193 DOI: 10.3892/or.2017.5546]

153 **Men Y**, Zhai Y, Wu L, Liu L, Zhang W, Jiang W, Bi N, Song Y, Hui Z, Wang L. MiR-323a-3p acts as a tumor suppressor by suppressing FMR1 and predicts better esophageal squamous cell carcinoma outcome. *Cancer Cell Int* 2022; **22**: 140 [PMID: 35351128 DOI: 10.1186/s12935-022-02541-x]

154 **Xu ML**, Liu TC, Dong FX, Meng LX, Ling AX, Liu S. Exosomal lncRNA LINC01711 facilitates metastasis of esophageal squamous cell carcinoma *via* the miR-326/FSCN1 axis. *Aging (Albany NY)* 2021; **13**: 19776-19788 [PMID: 34370713 DOI: 10.18632/aging.203389]

155 **Han N**, Zhao W, Zhang Z, Zheng P. MiR-328 suppresses the survival of esophageal cancer cells by targeting PLCE1. *Biochem Biophys Res Commun* 2016; **470**: 175-180 [PMID: 26773497 DOI: 10.1016/j.bbrc.2016.01.020]

156 **Tian Z**, Li Z, Zhu Y, Meng L, Liu F, Sang M, Wang G. Hypermethylation-mediated inactivation of miR-124 predicts poor prognosis and promotes tumor growth at least partially through targeting EZH2/H3K27me3 in ESCC. *Clin Exp Metastasis* 2019; **36**: 381-391 [PMID: 31197517 DOI: 10.1007/s10585-019-09974-1]

157 **Zhao Y**, Ma K, Yang S, Zhang X, Wang F, Liu H, Fan Q. MicroRNA-125a-5p enhances the sensitivity of esophageal squamous cell carcinoma cells to cisplatin by suppressing the activation of the STAT3 signaling pathway. *Int J Oncol* 2018; **53**: 644-658 [PMID: 29767234 DOI: 10.3892/ijo.2018.4409]

158 **Suyal G**, Pandey P, Saraya A, Sharma R. Tumour suppressor role of microRNA-335-5p in esophageal squamous cell carcinoma by targeting TTK (Mps1). *Exp Mol Pathol* 2022; **124**: 104738 [PMID: 34953918 DOI: 10.1016/j.yexmp.2021.104738]

159 **Takashima Y**, Komatsu S, Ohashi T, Kiuchi J, Nishibeppu K, Kamiya H, Arakawa H, Ishida R, Shimizu H, Arita T, Konishi H, Shiozaki A, Kubota T, Fujiwara H, Otsuji E. Plasma miR-1254 as a predictive biomarker of chemosensitivity and a target of nucleic acid therapy in esophageal cancer. *Cancer Sci* 2023; **114**: 3027-3040 [PMID: 37190912 DOI: 10.1111/cas.15830]

160 **Cui D**, Zhu Y, Yan D, Lee NPY, Han L, Law S, Tsao GSW, Cheung ALM. Dual inhibition of cMET and EGFR by microRNA-338-5p suppresses metastasis of esophageal squamous cell carcinoma. *Carcinogenesis* 2021; **42**: 995-1007 [PMID: 34089582 DOI: 10.1093/carcin/bgab046]

161 **Zuo J**, Zhu K, Wang Y, Yu Z. MicroRNA-34a suppresses invasion and metastatic in esophageal squamous cell carcinoma by regulating CD44. *Mol Cell Biochem* 2018; **443**: 139-149 [PMID: 29094237 DOI: 10.1007/s11010-017-3218-3]

162 **Zhang Z**, Liang X, Ren L, Zhang S, Li S, Wan T, Xu D, Lv S. LINC00662 promotes cell viability and metastasis in esophageal squamous cell carcinoma by sponging miR-340-5p and upregulating HOXB2. *Thorac Cancer* 2020; **11**: 2306-2315 [PMID: 32633082 DOI: 10.1111/1759-7714.13551]

163 **Tang R**, Zhou Q, Xu Q, Lu L, Zhou Y. Circular RNA circ_0006948 Promotes Esophageal Squamous Cell Carcinoma Progression by Regulating microRNA-3612/LASP1 Axis. *Dig Dis Sci* 2022; **67**: 2158-2172 [PMID: 34024023 DOI: 10.1007/s10620-021-07057-4]

164 **Kang M**, Li Y, Liu W, Wang R, Tang A, Hao H, Liu Z, Ou H. miR-129-2 suppresses proliferation and migration of esophageal carcinoma cells through downregulation of SOX4 expression. *Int J Mol Med* 2013; **32**: 51-58 [PMID: 23677061 DOI: 10.3892/ijmm.2013.1384]

165 **Sun C**, Zhang X, Chen Y, Jia Q, Yang J, Shu Y. MicroRNA-365 suppresses cell growth and invasion in esophageal squamous cell carcinoma by modulating phosphoserine aminotransferase 1. *Cancer Manag Res* 2018; **10**: 4581-4590 [PMID: 30410394 DOI: 10.2147/CMAR.S157858]

166 **Peng X**, Wu X, Wu G, Peng C, Huang B, Huang M, Ding J, Mao C, Zhang H. MiR-129-2-3p Inhibits Esophageal Carcinoma Cell Proliferation, Migration, and Invasion *via* Targeting DNMT3B. *Curr Mol Pharmacol* 2023; **16**: 116-123 [PMID: 35260066 DOI: 10.2174/1874467215666220308122716]

167 **Chen M**, Xia Y, Tan Y, Jiang G, Jin H, Chen Y. Downregulation of microRNA-370 in esophageal squamous-cell carcinoma is associated with cancer progression and promotes cancer cell proliferation *via* upregulating PIN1. *Gene* 2018; **661**: 68-77 [PMID: 29605603 DOI: 10.1016/j.gene.2018.03.090]

168 **Zhang Y**, Xiong W, Yang C, Li P, Tong H. Circ-FNDC3B Functions as an Oncogenic Factor in Esophageal Squamous Cell Carcinoma *via* Upregulating MYO5A by Absorbing miR-136-5p and miR-370-3p. *Biochem Genet* 2023; **61**: 1917-1936 [PMID: 36884165 DOI: 10.1007/s10528-023-10354-4]

169 **Wang W**, Wu D, He X, Hu X, Hu C, Shen Z, Lin J, Pan Z, He Z, Lin H, Wang M. CCL18-induced HOTAIR upregulation promotes malignant progression in esophageal squamous cell carcinoma through the miR-130a-5p-ZEB1 axis. *Cancer Lett* 2019; **460**: 18-28 [PMID: 31207321 DOI: 10.1016/j.canlet.2019.06.009]

170 **Li S**, Qin X, Li Y, Zhang X, Niu R, Zhang H, Cui A, An W, Wang X. MiR-133a suppresses the migration and invasion of esophageal cancer cells by targeting the EMT regulator SOX4. *Am J Transl Res* 2015; **7**: 1390-1403 [PMID: 26396670]

171 **Fang N**, Shi Y, Fan Y, Long T, Shu Y, Zhou J. Circ_0072088 Promotes Proliferation, Migration, and Invasion of Esophageal Squamous Cell Cancer by Absorbing miR-377. *J Oncol* 2020; **2020**: 8967126 [PMID: 33061973 DOI: 10.1155/2020/8967126]

172 **Jin W**, Wang L, Cheng S, Lv H. Prognostic value of microRNA-378 in esophageal cancer and its regulatory effect on tumor progression. *Exp Ther Med* 2021; **22**: 704 [PMID: 34007313 DOI: 10.3892/etm.2021.10136]

173 **Wu Y**, Zhi L, Zhao Y, Yang L, Cai F. Knockdown of circular RNA UBAP2 inhibits the malignant behaviours of esophageal squamous cell carcinoma by microRNA-422a/Rab10 axis. *Clin Exp Pharmacol Physiol* 2020; **47**: 1283-1290 [PMID: 32012318 DOI: 10.1111/1440-1681.13269]

174 **Xu S**, Li X, Li L, Wang Y, Geng C, Guo F, Zhang T, Du A, Lu Z, Hui H, Wang Q. CTCF-silenced miR-137 contributes to EMT and radioresistance in esophageal squamous cell carcinoma. *Cancer Cell Int* 2021; **21**: 155 [PMID: 33685449 DOI: 10.1186/s12935-020-01740-8]

175 **Wang Y**, Li M, Zang W, Ma Y, Wang N, Li P, Wang T, Zhao G. MiR-429 up-regulation induces apoptosis and suppresses invasion by targeting Bcl-2 and SP-1 in esophageal carcinoma. *Cell Oncol (Dordr)* 2013; **36**: 385-394 [PMID: 23999873 DOI: 10.1007/s13402-013-0144-6]

176 **Chen X**, Jiang J, Zhao Y, Wang X, Zhang C, Zhuan L, Zhang D, Zheng Y. Circular RNA circNTRK2 facilitates the progression of esophageal squamous cell carcinoma through up-regulating NRIP1 expression *via* miR-140-3p. *J Exp Clin Cancer Res* 2020; **39**: 133 [PMID: 32653032 DOI: 10.1186/s13046-020-01640-9]

177 **Li T**, Li S. Circ_0023984 Facilitates Esophageal Squamous Cell Carcinoma Progression by Regulating miR-433-3p/REV3L Axis. *Dig Dis Sci* 2022; **67**: 892-903 [PMID: 33725240 DOI: 10.1007/s10620-021-06916-4]

178 **Li W**, Jiang G, Zhou J, Wang H, Gong Z, Zhang Z, Min K, Zhu H, Tan Y. Down-regulation of miR-140 induces EMT and promotes invasion by targeting Slug in esophageal cancer. *Cell Physiol Biochem* 2014; **34**: 1466-1476 [PMID: 25322669 DOI: 10.1159/000366351]

179 **Jiang T**, Zhao R, Du Y, Shi Z, Cheng H. MiR-449a-5p regulates the proliferation of esophageal carcinoma cell by targeting B-cell lymphoma 2. *Transl Cancer Res* 2020; **9**: 7236-7247 [PMID: 35117327 DOI: 10.21037/tcr-20-2869]

180 **Liu H**, Zheng M, Zhao Y, Zhang S. miR-143 inhibits migration and invasion through regulating LASP1 in human esophageal cancer. *Int J Clin Exp Pathol* 2019; **12**: 466-476 [PMID: 31933851]

181 **Yang H**, Wei YN, Zhou J, Hao TT, Liu XL. MiR-455-3p acts as a prognostic marker and inhibits the proliferation and invasion of esophageal squamous cell carcinoma by targeting FAM83F. *Eur Rev Med Pharmacol Sci* 2017; **21**: 3200-3206 [PMID: 28770965]

182 **Jin W**, Luo W, Fang W, Wang Y, Wang L, Shen Q, Liu W, Zhang H. miR-145 expression level in tissue predicts prognosis of patients with esophageal squamous cell carcinoma. *Pathol Res Pract* 2019; **215**: 152401 [PMID: 31014553 DOI: 10.1016/j.prp.2019.03.029]

183 **Li Y**, Tang C, Huang S, He J, An J, Liu L, Lao S, Zhang J. MicroRNA -145 suppresses esophageal squamous cell carcinoma by targeting phospholipase C epsilon 1. *Zhonghua Shiyan Waike Zazhi* 2017; **34**: 1472-1475 [DOI: 10.3760/cma.j.issn.1001-9030.2017.09.011]

184 **Liu Y**, Tang Y, Li P. Inhibitory effect of microRNA-455-5p on biological functions of esophageal squamous cell carcinoma Eca109 cells *via* Rab31. *Exp Ther Med* 2018; **16**: 4959-4966 [PMID: 30542452 DOI: 10.3892/etm.2018.6820]

185 **Chen G**, Teng Z, Zhu Z, Li X. miR-145-3p Hampers the Malignant Progression of Esophageal Carcinoma *via* CXCL5 Downregulation. *Anal Cell Pathol (Amst)* 2022; **2022**: 5418356 [PMID: 35936390 DOI: 10.1155/2022/5418356]

186 **Zhou PL**, Wu Z, Zhang W, Xu M, Ren J, Zhang Q, Sun Z, Han X. Circular RNA hsa_circ_0000277 sequesters miR-4766-5p to upregulate LAMA1 and promote esophageal carcinoma progression. *Cell Death Dis* 2021; **12**: 676 [PMID: 34226522 DOI: 10.1038/s41419-021-03911-5]

187 **Mei LL**, Wang WJ, Qiu YT, Xie XF, Bai J, Shi ZZ. miR-145-5p Suppresses Tumor Cell Migration, Invasion and Epithelial to Mesenchymal Transition by Regulating the Sp1/NF-κB Signaling Pathway in Esophageal Squamous Cell Carcinoma. *Int J Mol Sci* 2017; **18** [PMID: 28832500 DOI: 10.3390/ijms18091833]

188 **Zhao R**, Shan Y, Zhou X, Zhang C, Zhao R, Zhao L, Shan B. MicroRNA4855p suppresses the progression of esophageal squamous cell carcinoma by targeting flotillin1 and inhibits the epithelialmesenchymal transition. *Oncol Rep* 2021; **45** [PMID: 33846817 DOI: 10.3892/or.2021.8044]

189 **Chang HY**, Lee CH, Li YS, Huang JT, Lan SH, Wang YF, Lai WW, Wang YC, Lin YJ, Liu HS, Cheng HC. MicroRNA-146a suppresses tumor malignancy *via* targeting vimentin in esophageal squamous cell carcinoma cells with lower fibronectin membrane assembly. *J Biomed Sci* 2020; **27**: 102 [PMID: 33248456 DOI: 10.1186/s12929-020-00693-4]

190 **Yi Y**, Lu X, Chen J, Jiao C, Zhong J, Song Z, Yu X, Lin B. Downregulated miR-486-5p acts as a tumor suppressor in esophageal squamous cell carcinoma. *Exp Ther Med* 2016; **12**: 3411-3416 [PMID: 27882172 DOI: 10.3892/etm.2016.3783]

191 **Liu J**, Wang C, Liu X, Wang Y, Liu H, Ren G, Zhu L, Sun Z, Chen Z. Low expression of miR-1469 predicts disease progression and unfavorable post-surgical clinical outcomes in patients with esophageal squamous cell cancer. *Oncol Lett* 2017; **13**: 4469-4474 [PMID: 28588716 DOI: 10.3892/ol.2017.5957]

192 **Pan Z**, Lin J, Wu D, He X, Wang W, Hu X, Zhang L, Wang M. Hsa_circ_0006948 enhances cancer progression and epithelial-mesenchymal transition through the miR-490-3p/HMGA2 axis in esophageal squamous cell carcinoma. *Aging (Albany NY)* 2019; **11**: 11937-11954 [PMID:

31881015 DOI: 10.18632/aging.102519]
193 **Xu F**, Zhang J. Long non-coding RNA HOTAIR functions as miRNA sponge to promote the epithelial to mesenchymal transition in esophageal cancer. *Biomed Pharmacother* 2017; **90**: 888-896 [PMID: 28441714 DOI: 10.1016/j.biopha.2017.03.103]
194 **Chen S**, Liu Z, Feng Q, Zhou J, Huang J, Yu J. Circular RNA circ-AGFG1 contributes to esophageal squamous cell carcinoma progression and glutamine catabolism by targeting microRNA-497-5p/solute carrier family 1 member 5 axis. *Anticancer Drugs* 2023; **34**: 195-206 [PMID: 36206112 DOI: 10.1097/CAD.0000000000001400]
195 **Yokobori T**, Suzuki S, Tanaka N, Inose T, Sohda M, Sano A, Sakai M, Nakajima M, Miyazaki T, Kato H, Kuwano H. MiR-150 is associated with poor prognosis in esophageal squamous cell carcinoma *via* targeting the EMT inducer ZEB1. *Cancer Sci* 2013; **104**: 48-54 [PMID: 23013135 DOI: 10.1111/cas.12030]
196 **Jin G**, Yang Y, Tuo G, Wang W, Zhu Z. LncRNA TUG1 promotes tumor growth and metastasis of esophageal squamous cell carcinoma by regulating XBP1 *via* competitively binding to miR-498. *Neoplasma* 2020; **67**: 751-761 [PMID: 32305055 DOI: 10.4149/neo_2020_190805N717]
197 **Osako Y**, Seki N, Koshizuka K, Okato A, Idichi T, Arai T, Omoto I, Sasaki K, Uchikado Y, Kita Y, Kurahara H, Maemura K, Natsugoe S. Regulation of SPOCK1 by dual strands of pre-miR-150 inhibit cancer cell migration and invasion in esophageal squamous cell carcinoma. *J Hum Genet* 2017; **62**: 935-944 [PMID: 28659612 DOI: 10.1038/jhg.2017.69]
198 **Zang B**, Zhao J, Chen C. LncRNA PCAT-1 Promoted ESCC Progression *via* Regulating ANXA10 Expression by Sponging miR-508-3p. *Cancer Manag Res* 2019; **11**: 10841-10849 [PMID: 31920393 DOI: 10.2147/CMAR.S233983]
199 **Wang M**, Huang C, Gao W, Zhu Y, Zhang F, Li Z, Tian Z. MicroRNA-181a-5p prevents the progression of esophageal squamous cell carcinoma in vivo and in vitro *via* the MEK1-mediated ERK-MMP signaling pathway. *Aging (Albany NY)* 2022; **14**: 3540-3553 [PMID: 35468097 DOI: 10.18632/aging.204028]
200 **Zhao Y**, Wang Y, Xing G. miR-516b functions as a tumor suppressor by directly modulating CCNG1 expression in esophageal squamous cell carcinoma. *Biomed Pharmacother* 2018; **106**: 1650-1660 [PMID: 30119241 DOI: 10.1016/j.biopha.2018.07.074]
201 Retraction statement: miR-518b is down-regulated, and involved in cell proliferation and invasion by targeting Rap1b in esophageal squamous cell carcinoma. *FEBS Lett* 2023; **597**: 2699 [PMID: 37823227 DOI: 10.1002/1873-3468.14743]
202 **Sun N**, Ye L, Chang T, Li X. microRNA-195-Cdc42 axis acts as a prognostic factor of esophageal squamous cell carcinoma. *Int J Clin Exp Pathol* 2014; **7**: 6871-6879 [PMID: 25400770]
203 **Zhou S**, Guo Z, Zhou C, Zhang Y, Wang S. circ_NRIP1 is oncogenic in malignant development of esophageal squamous cell carcinoma (ESCC) *via* miR-595/SEMA4D axis and PI3K/AKT pathway. *Cancer Cell Int* 2021; **21**: 250 [PMID: 33957921 DOI: 10.1186/s12935-021-01907-x]
204 **Shi Y**, Fang N, Li Y, Guo Z, Jiang W, He Y, Ma Z, Chen Y. Circular RNA LPAR3 sponges microRNA-198 to facilitate esophageal cancer migration, invasion, and metastasis. *Cancer Sci* 2020; **111**: 2824-2836 [PMID: 32495982 DOI: 10.1111/cas.14511]
205 **Wang C**, Tang D, Wang H, Hu G, Hu S, Li L, Min B, Wang Y. Circular RNA hsa_circ_0030018 acts as a sponge of miR-599 to aggravate esophageal carcinoma progression by regulating ENAH expression. *J Cell Biochem* 2020; **121**: 3730-3738 [PMID: 31736156 DOI: 10.1002/jcb.29507]
206 **Ma G**, Zhang F, Dong X, Wang X, Ren Y. Low expression of microRNA-202 is associated with the metastasis of esophageal squamous cell carcinoma. *Exp Ther Med* 2016; **11**: 951-956 [PMID: 26998018 DOI: 10.3892/etm.2016.3014]
207 **Yang B**, Xie R, Wu SN, Gao CC, Yang XZ, Zhou JF. MicroRNA-615-5p targets insulin-like growth factor 2 and exerts tumor-suppressing functions in human esophageal squamous cell carcinoma. *Oncol Rep* 2018; **39**: 255-263 [PMID: 29115555 DOI: 10.3892/or.2017.6079]
208 **Zhu Y**, Li F, Wan Y, Liang H, Li S, Peng B, Shao L, Xu Y, Jiang D. Cancer-Secreted Exosomal MiR-620 Inhibits ESCC Aerobic Glycolysis *via* FOXM1/HER2 Pathway and Promotes Metastasis. *Front Oncol* 2022; **12**: 756109 [PMID: 35651785 DOI: 10.3389/fonc.2022.756109]
209 **Jiang M**, Shi H, Xu Y, Bai W, Wang P, Ju Q. miR-203a-3p regulates the cellular processes of esophageal cancer cells *via* targeting CtBP2. *Transl Cancer Res* 2019; **8**: 2791-2802 [PMID: 35117036 DOI: 10.21037/tcr.2019.10.44]
210 **Zhang H**, Wu X, Sui Z, Ma Z, Gong L, Meng B, Tang P, Yu Z. High-mobility group AT-hook 2 promotes growth and metastasis and is regulated by miR-204-5p in oesophageal squamous cell carcinoma. *Eur J Clin Invest* 2021; **51**: e13563 [PMID: 33901298 DOI: 10.1111/eci.13563]
211 **Wang Z**, Qiao Q, Chen M, Li X, Wang Z, Liu C, Xie Z. miR-625 down-regulation promotes proliferation and invasion in esophageal cancer by targeting Sox2. *FEBS Lett* 2014; **588**: 915-921 [PMID: 24508466 DOI: 10.1016/j.febslet.2014.01.035]
212 **Li C**, Li DC, Che SS, Ma K, Wang YJ, Xia LH, Dai XM, Zhang GT, Shen Y, Jiao WJ, Tian KH. The decreased expression of miR-625 predicts poor prognosis of esophageal squamous cell carcinoma. *Int J Clin Exp Med* 2015; **8**: 9560-9564 [PMID: 26309624]
213 **Dong S**, Yin H, Lyu Y, Meng W, Dong C, He F. Expression and clinical significance of miRNA-205 in esophageal squamous cell carcinoma. *Disan Junyi Daxue Xuebao* 2016; **38**: 85-88
214 **Jin L**, Yi J, Gao Y, Han S, He Z, Chen L, Song H. MiR-630 inhibits invasion and metastasis in esophageal squamous cell carcinoma. *Acta Biochim Biophys Sin (Shanghai)* 2016; **48**: 810-819 [PMID: 27563011 DOI: 10.1093/abbs/gmw073]
215 **Wu Z**, Yu B, Jiang L. MiR-212-3p mediates apoptosis and invasion of esophageal squamous cell carcinoma through inhibition of the Wnt/β-catenin signaling pathway by targeting SOX4. *J Thorac Dis* 2020; **12**: 4357-4367 [PMID: 32944348 DOI: 10.21037/jtd-20-2558]
216 **Huang SD**, Yuan Y, Zhuang CW, Li BL, Gong DJ, Wang SG, Zeng ZY, Cheng HZ. MicroRNA-98 and microRNA-214 post-transcriptionally regulate enhancer of zeste homolog 2 and inhibit migration and invasion in human esophageal squamous cell carcinoma. *Mol Cancer* 2012; **11**: 51 [PMID: 22867052 DOI: 10.1186/1476-4598-11-51]
217 **Zhao H**, Diao C, Wang X, Xie Y, Liu Y, Gao X, Han J, Li S. LncRNA BDNF-AS inhibits proliferation, migration, invasion and EMT in oesophageal cancer cells by targeting miR-214. *J Cell Mol Med* 2018; **22**: 3729-3739 [PMID: 29896888 DOI: 10.1111/jcmm.13558]
218 **Li R**, Chai L, Lei L, Guo R, Wen X. MiR-671-5p sponging activity of circMMP1 promotes esophageal squamous cancer progression. *Thorac Cancer* 2023; **14**: 2924-2933 [PMID: 37635445 DOI: 10.1111/1759-7714.15078]
219 **Phatak P**, Burrows WM, Creed TM, Youssef M, Lee G, Donahue JM. MiR-214-3p targets Ras-related protein 14 (RAB14) to inhibit cellular migration and invasion in esophageal Cancer cells. *BMC Cancer* 2022; **22**: 1265 [PMID: 36471277 DOI: 10.1186/s12885-022-10304-0]
220 **Dong S**, Yin H, Dong C, Sun K, Lv P, Meng W, Ming L, He F. Predictive Value of Plasma MicroRNA-216a/b in the Diagnosis of Esophageal Squamous Cell Carcinoma. *Dis Markers* 2016; **2016**: 1857067 [PMID: 26989293 DOI: 10.1155/2016/1857067]
221 **Wang T**, Chen T, Niu H, Li C, Xu C, Li Y, Huang R, Zhao J, Wu S. MicroRNA-218 inhibits the proliferation and metastasis of esophageal squamous cell carcinoma cells by targeting BMI1. *Int J Mol Med* 2015; **36**: 93-102 [PMID: 25999024 DOI: 10.3892/ijmm.2015.2216]

222 **Zhang L**, Yu S, Yin X, Tu M, Cai L, Zhang Y, Yu L, Zhang S, Pan X, Huang Y. MiR-942-5p inhibits tumor migration and invasion through targeting CST1 in esophageal squamous cell carcinoma. *PLoS One* 2023; **18**: e0277006 [PMID: 36848349 DOI: 10.1371/journal.pone.0277006]

223 **Yang C**, Zheng S, Liu T, Liu Q, Dai F, Zhou J, Chen Y, Sheyhidin I, Lu X. Down-regulated miR-26a promotes proliferation, migration, and invasion *via* negative regulation of MTDH in esophageal squamous cell carcinoma. *FASEB J* 2017; **31**: 2114-2122 [PMID: 28174206 DOI: 10.1096/fj.201601237]

224 **Mei LL**, Qiu YT, Huang MB, Wang WJ, Bai J, Shi ZZ. MiR-99a suppresses proliferation, migration and invasion of esophageal squamous cell carcinoma cells through inhibiting the IGF1R signaling pathway. *Cancer Biomark* 2017; **20**: 527-537 [PMID: 28800315 DOI: 10.3233/CBM-170345]

225 **Han M**, Li N, Li F, Wang H, Ma L. MiR-27b-3p exerts tumor suppressor effects in esophageal squamous cell carcinoma by targeting Nrf2. *Hum Cell* 2020; **33**: 641-651 [PMID: 32419118 DOI: 10.1007/s13577-020-00329-7]

226 **Liu Q**, Lv GD, Qin X, Gen YH, Zheng ST, Liu T, Lu XM. Role of microRNA let-7 and effect to HMGA2 in esophageal squamous cell carcinoma. *Mol Biol Rep* 2012; **39**: 1239-1246 [PMID: 21598109 DOI: 10.1007/s11033-011-0854-7]

227 **Ling R**, Zhou Y, Zhou L, Dai D, Wu D, Mi L, Mao C, Chen D. Lin28/microRNA-let-7a promotes metastasis under circumstances of hyperactive Wnt signaling in esophageal squamous cell carcinoma. *Mol Med Rep* 2018; **17**: 5265-5271 [PMID: 29393461 DOI: 10.3892/mmr.2018.8548]

228 **Wang H**, Fu L, Wei D, Wang B, Zhang C, Zhu T, Ma Z, Li Z, Wu Y, Yu G. MiR-29c-3p Suppresses the Migration, Invasion and Cell Cycle in Esophageal Carcinoma *via* CCNA2/p53 Axis. *Front Bioeng Biotechnol* 2020; **8**: 75 [PMID: 32154226 DOI: 10.3389/fbioe.2020.00075]

229 **Tian Y**, Luo A, Cai Y, Su Q, Ding F, Chen H, Liu Z. MicroRNA-10b promotes migration and invasion through KLF4 in human esophageal cancer cell lines. *J Biol Chem* 2010; **285**: 7986-7994 [PMID: 20075075 DOI: 10.1074/jbc.M109.062877]

230 **Zhu Y**, Liu J, Fan L, Wang F, Bu L, Ma T, Du Y, Zhang C, Wang H, Sun G. Serum expression and significance of MicroRNA-30d-5p in esophageal squamous cell carcinoma. *Int J Clin Exp Pathol* 2017; **10**: 8677-8685 [PMID: 31966725]

231 **Shou Y**, Wang X, Chen C, Liang Y, Yang C, Xiao Q, Li H, Wang S, Shu J, Tian X, Chen K. Exosomal miR-301a-3p from esophageal squamous cell carcinoma cells promotes angiogenesis by inducing M2 polarization of macrophages *via* the PTEN/PI3K/AKT signaling pathway. *Cancer Cell Int* 2022; **22**: 153 [PMID: 35436935 DOI: 10.1186/s12935-022-02570-6]

232 **Jiang L**, Wang Y, Rong Y, Xu L, Chu Y, Zhang Y, Yao Y. miR-1179 promotes cell invasion through SLIT2/ROBO1 axis in esophageal squamous cell carcinoma. *Int J Clin Exp Pathol* 2015; **8**: 319-327 [PMID: 25755718]

233 **Gao Y**, Yi J, Zhang K, Bai F, Feng B, Wang R, Chu X, Chen L, Song H. Downregulation of MiR-31 stimulates expression of LATS2 *via* the hippo pathway and promotes epithelial-mesenchymal transition in esophageal squamous cell carcinoma. *J Exp Clin Cancer Res* 2017; **36**: 161 [PMID: 29145896 DOI: 10.1186/s13046-017-0622-1]

234 **Meng H**, Wang K, Chen X, Guan X, Hu L, Xiong G, Li J, Bai Y. MicroRNA-330-3p functions as an oncogene in human esophageal cancer by targeting programmed cell death 4. *Am J Cancer Res* 2015; **5**: 1062-1075 [PMID: 26045986]

235 **Jin Y**, Meng Q, Zhang B, Xie C, Chen X, Tian B, Wang J, Shih TC, Zhang Y, Cao J, Yang Y, Chen S, Guan X, Hong A. Cancer-associated fibroblasts-derived exosomal miR-3656 promotes the development and progression of esophageal squamous cell carcinoma *via* the ACAP2/PI3K-AKT signaling pathway. *Int J Biol Sci* 2021; **17**: 3689-3701 [PMID: 34671193 DOI: 10.7150/ijbs.62571]

236 **Chen J**. Downregulation of MicroRNA-135b-5p Inhibits Esophageal Cancer Cell Progression *via* Targeting GNG7. *J Biomater Tiss Eng* 2019; **9**: 1222-1231 [DOI: 10.1166/jbt.2019.2126]

237 **Lin RJ**, Xiao DW, Liao LD, Chen T, Xie ZF, Huang WZ, Wang WS, Jiang TF, Wu BL, Li EM, Xu LY. MiR-142-3p as a potential prognostic biomarker for esophageal squamous cell carcinoma. *J Surg Oncol* 2012; **105**: 175-182 [PMID: 21882196 DOI: 10.1002/jso.22066]

238 **Zhang M**, Tian H, Li R, Yan W, Xu R. MicroRNA-4286 promotes esophageal carcinoma development by targeting INPP4A to evoke the JAK2/STAT3 pathway activation. *Pharmazie* 2018; **73**: 342-348 [PMID: 29880087 DOI: 10.1691/ph.2018.7339]

239 **Mei LL**, Qiu YT, Wang WJ, Bai J, Shi ZZ. Overexpression of microRNA-1470 promotes proliferation and migration, and inhibits senescence of esophageal squamous carcinoma cells. *Oncol Lett* 2017; **14**: 7753-7758 [PMID: 29344220 DOI: 10.3892/ol.2017.7190]

240 **Gong T**, Zheng S, Huang S, Fu S, Zhang X, Pan S, Yang T, Sun Y, Wang Y, Hui B, Guo J. PTENP1 inhibits the growth of esophageal squamous cell carcinoma by regulating SOCS6 expression and correlates with disease prognosis. *Mol Carcinog* 2017; **56**: 2610-2619 [PMID: 28731203 DOI: 10.1002/mc.22705]

241 **Xu R**, Ding P, Zhao X, Li Z, Liu F, Gu L, Zheng Y, Sang M, Meng L. Circular RNA circ-TNRC6B inhibits the proliferation and invasion of esophageal squamous cell carcinoma cells by regulating the miR-452-5p/DAG1 axis. *Mol Oncol* 2023; **17**: 1437-1452 [PMID: 37014625 DOI: 10.1002/1878-0261.13432]

242 **Xu XL**, Jiang YH, Feng JG, Su D, Chen PC, Mao WM. MicroRNA-17, microRNA-18a, and microRNA-19a are prognostic indicators in esophageal squamous cell carcinoma. *Ann Thorac Surg* 2014; **97**: 1037-1045 [PMID: 24360091 DOI: 10.1016/j.athoracsur.2013.10.042]

243 **Ma J**, Hong L, Xu G, Hao J, Wang R, Guo H, Liu J, Zhang Y, Nie Y, Fan D. miR-483-3p plays an oncogenic role in esophageal squamous cell carcinoma by targeting tumor suppressor EI24. *Cell Biol Int* 2016; **40**: 448-455 [PMID: 26801660 DOI: 10.1002/cbin.10585]

244 **Qi J**, Fan W. miR-18a-5p and ATM Expression in Esophageal Squamous Cell Carcinoma and Their Correlations with Clinicopathological Features. *Comput Math Methods Med* 2022; **2022**: 5260608 [PMID: 36267307 DOI: 10.1155/2022/5260608]

245 **Li SP**, Su HX, Zhao D, Guan QL. Plasma miRNA-506 as a Prognostic Biomarker for Esophageal Squamous Cell Carcinoma. *Med Sci Monit* 2016; **22**: 2195-2201 [PMID: 27345473 DOI: 10.12659/msm.899377]

246 **Chen S**, Ainiwaer B, Qing S, Liu T, Ma Z, Shi Y, Pang X, Zhang W, Li X. [Expression levels of miR-181c-3p and miR-5692b in esophageal cancer and their clinical significance]. *Zhonghua Bing Li Xue Za Zhi* 2015; **44**: 905-909 [PMID: 26888510]

247 **Zhou P**, Dong H, He S, Fang L, Jiang N, Sun Q. miR612 is associated with esophageal squamous cell carcinoma development and metastasis, mediated through TP53. *Mol Med Rep* 2017; **16**: 1855-1863 [PMID: 28656264 DOI: 10.3892/mmr.2017.6808]

248 **Xiao Q**, Chen T, Wu Y, Wu W, Xu Y, Gong Z, Chen S. MicroRNA6753p promotes esophageal squamous cell cancer cell migration and invasion. *Mol Med Rep* 2018; **18**: 3631-3640 [PMID: 30106155 DOI: 10.3892/mmr.2018.9372]

249 **Yu J**, Chen S, Niu Y, Liu M, Zhang J, Yang Z, Gao P, Wang W, Han X, Sun G. Functional Significance and Therapeutic Potential of miRNA-20b-5p in Esophageal Squamous Cell Carcinoma. *Mol Ther Nucleic Acids* 2020; **21**: 315-331 [PMID: 32622332 DOI: 10.1016/j.omtn.2020.05.015]

250 **Kang N**, Ou Y, Wang G, Chen J, Li D, Zhan Q. miR-875-5p exerts tumor-promoting function *via* down-regulation of CAPZA1 in esophageal squamous cell carcinoma. *PeerJ* 2021; **9**: e10020 [PMID: 33505778 DOI: 10.7717/peerj.10020]

251 **Hao Z**, Tang L, Deng Y, Cai Y, Zhang N, Fu X, Li W. Up-regulation of miR-221 in early-stage esophageal squamous cell cancer and its

promotion effect on proliferation, migration and invasion of EC109 cells. *Zhongliu* 2016; **36**: 326-333 [DOI: 10.3781/j.issn.1000-7431.2016.33.865]

252 **He X**, Zhang Z, Li M, Li S, Ren L, Zhu H, Xiao B, Shi R. Expression and role of oncogenic miRNA-224 in esophageal squamous cell carcinoma. *BMC Cancer* 2015; **15**: 575 [PMID: 26245343 DOI: 10.1186/s12885-015-1581-6]

253 **Wang W**, Fu S, Lin X, Zheng J, Pu J, Gu Y, Deng W, Liu Y, He Z, Liang W, Wang C. miR-92b-3p Functions As A Key Gene In Esophageal Squamous Cell Cancer As Determined By Co-Expression Analysis. *Onco Targets Ther* 2019; **12**: 8339-8353 [PMID: 31686859 DOI: 10.2147/OTT.S220823]

254 **Shang M**, Weng L, Wu S, Liu B, Yin X, Wang Z, Mao A. HP1BP3 promotes tumor growth and metastasis by upregulating miR-23a to target TRAF5 in esophageal squamous cell carcinoma. *Am J Cancer Res* 2021; **11**: 2928-2943 [PMID: 34249436]

255 **Jin C**, Zuo S, Wang X, Diao C, Xie Y, Li S, Li X. Expression of microRNA-935 in esophageal squamous cell carcinoma tissues and cells and its effects on cell proliferation and invasion. *Zhonghua Shiyan Waike Zazhi* 2017; **34**: 1466-1468 [DOI: 10.3760/cma.j.issn.1001-9030.2017.09.009]

256 **Li C**, Ding C, Chen T, Chen J, Xu Z, Lei Z, Xu C, Zhao J. Micro ribonucleic acid-93 promotes proliferation and migration of esophageal squamous cell carcinoma by targeting disabled 2. *Thorac Cancer* 2015; **6**: 524-533 [PMID: 26273410 DOI: 10.1111/1759-7714.12242]

257 **Meng F**, Zhang X, Wang Y, Lin J, Tang Y, Zhang G, Qiu B, Zeng X, Liu W, He X. Hsa_circ_0021727 (circ-CD44) promotes ESCC progression by targeting miR-23b-5p to activate the TAB1/NFκB pathway. *Cell Death Dis* 2023; **14**: 9 [PMID: 36609391 DOI: 10.1038/s41419-022-05541-x]

258 **Ma J**, Fan Y, Feng T, Chen F, Xu Z, Li S, Lin Q, He X, Shi W, Liu Y, Liu Z, Zhu B, Cao X. HOTAIR regulates HK2 expression by binding endogenous miR-125 and miR-143 in oesophageal squamous cell carcinoma progression. *Oncotarget* 2017; **8**: 86410-86422 [PMID: 29156804 DOI: 10.18632/oncotarget.21195]

259 **Shi Z**, Jiang T, Cao B, Sun X, Liu J. CAF-derived exosomes deliver LINC01410 to promote epithelial-mesenchymal transition of esophageal squamous cell carcinoma. *Exp Cell Res* 2022; **412**: 113033 [PMID: 35041823 DOI: 10.1016/j.yexcr.2022.113033]

260 **Zhang Z**, Lin W, Gao L, Chen K, Yang C, Zhuang L, Peng S, Kang M, Lin J. Hsa_circ_0004370 promotes esophageal cancer progression through miR-1294/LASP1 pathway. *Biosci Rep* 2019; **39** [PMID: 30988074 DOI: 10.1042/BSR20182377]

261 **Cheng J**, Ma H, Yan M, Xing W. THAP9-AS1/miR-133b/SOX4 positive feedback loop facilitates the progression of esophageal squamous cell carcinoma. *Cell Death Dis* 2021; **12**: 401 [PMID: 33854048 DOI: 10.1038/s41419-021-03690-z]

262 **Shang M**, Wang X, Zhang Y, Gao Z, Wang T, Liu R. LincRNA-ROR promotes metastasis and invasion of esophageal squamous cell carcinoma by regulating miR-145/FSCN1. *Onco Targets Ther* 2018; **11**: 639-649 [PMID: 29430188 DOI: 10.2147/OTT.S157638]

263 **Zhu C**, Bi W, Li H, Wang W. CircLONP2 Accelerates Esophageal Squamous Cell Carcinoma Progression *via* Direct MiR-27b-3p-ZEB1 Axis. *Front Oncol* 2022; **12**: 822839 [PMID: 35865464 DOI: 10.3389/fonc.2022.822839]

264 **Du F**, Guo T, Cao C. Silencing of Long Noncoding RNA SNHG6 Inhibits Esophageal Squamous Cell Carcinoma Progression *via* miR-186-5p/HIF1α Axis. *Dig Dis Sci* 2020; **65**: 2844-2852 [PMID: 31853782 DOI: 10.1007/s10620-019-06012-8]

265 **Chen Y**, Sheng HG, Deng FM, Cai LL. Downregulation of the long noncoding RNA SNHG1 inhibits tumor cell migration and invasion by sponging miR-195 through targeting Cdc42 in oesophageal cancer. *Kaohsiung J Med Sci* 2021; **37**: 181-191 [PMID: 33171523 DOI: 10.1002/kjm2.12318]

266 **Shen S**, Li K, Liu Y, Liu X, Liu B, Ba Y, Xing W. Silencing lncRNA AGAP2-AS1 Upregulates miR-195-5p to Repress Migration and Invasion of EC Cells *via* the Decrease of FOSL1 Expression. *Mol Ther Nucleic Acids* 2020; **20**: 331-344 [PMID: 32199129 DOI: 10.1016/j.omtn.2019.12.036]

267 **Zhang LW**, Wang B, Yang JX, Yang H. Circ-PRMT5 stimulates migration in esophageal cancer by binding miR-203. *Eur Rev Med Pharmacol Sci* 2020; **24**: 9965-9972 [PMID: 33090401 DOI: 10.26355/eurrev_202010_23209]

268 **Liu HF**, Zhen Q, Fan YK. LINC00963 predicts poor prognosis and promotes esophageal cancer cells invasion *via* targeting miR-214-5p/RAB14 axis. *Eur Rev Med Pharmacol Sci* 2020; **24**: 164-173 [PMID: 31957829 DOI: 10.26355/eurrev_202001_19907]

269 **Tang J**, Xu H, Liu Q, Zheng J, Pan C, Li Z, Wen W, Wang J, Zhu Q, Wang Z, Chen L. LncRNA LOC146880 promotes esophageal squamous cell carcinoma progression *via* miR-328-5p/FSCN1/MAPK axis. *Aging (Albany NY)* 2021; **13**: 14198-14218 [PMID: 34016787 DOI: 10.18632/aging.203037]

270 **Zhang C**, Wang L, Yang J, Fu Y, Li H, Xie L, Cui Y. MicroRNA-33a-5p suppresses esophageal squamous cell carcinoma progression *via* regulation of lncRNA DANCR and ZEB1. *Eur J Pharmacol* 2019; **861**: 172590 [PMID: 31401160 DOI: 10.1016/j.ejphar.2019.172590]

271 **Zhou WZ**, Wang XW, Zhu J, Chen MZ, Jin H. LncRNA-CASC15 knockdown inhibits the progression of esophageal squamous cell carcinoma through targeting miR-33a-5p/PTGS2 axis. *Histol Histopathol* 2023; **38**: 223-232 [PMID: 36111503 DOI: 10.14670/HH-18-517]

272 **Li N**, Wu J, Hu B, Lu H, Gao J, Zhu L, Zheng D. Upregulation of hsa_circ_0000977 participates in esophageal squamous cancer progression by sponging miR-874-3p. *J Clin Lab Anal* 2022; **36**: e24458 [PMID: 35476874 DOI: 10.1002/jcla.24458]

273 **Chen W**, Wang L, Li X, Zhao C, Shi L, Zhao H, Huang C. LncRNA SNHG17 regulates cell proliferation and invasion by targeting miR-338-3p/SOX4 axis in esophageal squamous cell carcinoma. *Cell Death Dis* 2021; **12**: 806 [PMID: 34429400 DOI: 10.1038/s41419-021-04093-w]

274 **Chu J**, Jia J, Yang L, Qu Y, Yin H, Wan J, He F. LncRNA MIR31HG functions as a ceRNA to regulate c-Met function by sponging miR-34a in esophageal squamous cell carcinoma. *Biomed Pharmacother* 2020; **128**: 110313 [PMID: 32502839 DOI: 10.1016/j.biopha.2020.110313]

275 **Zhou Z**, Huang F. Long Non-Coding RNA LINC00152 Regulates Cell Proliferation, Migration And Invasion In Esophageal Squamous Cell Carcinoma Via miR-107/Rab10 Axis. *Onco Targets Ther* 2019; **12**: 8553-8567 [PMID: 31802892 DOI: 10.2147/OTT.S221515]

276 **Chang Z**, Fu Y, Jia Y, Gao M, Song L, Zhang W, Zhao R, Qin Y. Circ-SFMBT2 drives the malignant phenotypes of esophageal cancer by the miR-107-dependent regulation of SLC1A5. *Cancer Cell Int* 2021; **21**: 495 [PMID: 34530825 DOI: 10.1186/s12935-021-02156-8]

277 **Su M**, Tang J, Zhang B, Yang D, Wu Z, Wu J, Zhou Y, Liao Q, Wang H, Wang W, Xiao Y. LncRNA GACAT3 promotes esophageal squamous cell carcinoma progression through regulation of miR-149/FOXM1. *Cancer Cell Int* 2021; **21**: 478 [PMID: 34496842 DOI: 10.1186/s12935-021-02192-4]

278 **Shen W**, Yu L, Cong A, Yang S, Wang P, Han G, Gu B, Zhang W. Silencing lncRNA AFAP1-AS1 Inhibits the Progression of Esophageal Squamous Cell Carcinoma Cells *via* Regulating the miR-498/VEGFA Axis. *Cancer Manag Res* 2020; **12**: 6397-6409 [PMID: 32801880 DOI: 10.2147/CMAR.S254302]

279 **Zhang B**, Chu W, Li Z, Zhang Y, Zhen Q, Lv B, Liu J, Lu C, Zhao X. Circ-ATIC Serves as a Sponge of miR-326 to Accelerate Esophageal Squamous Cell Carcinoma Progression by Targeting ID1. *Biochem Genet* 2022; **60**: 1585-1600 [PMID: 35064360 DOI: 10.1007/s10528-021-10167-3]

280 **Du W**, Xu P, Yin H. LncRNA NEAT1 regulates the growth, migration, and invasion of the human esophageal cancer cells *via* the miR-377/

E2F3 axis. *Acta Biochim Pol* 2022; **69**: 731-736 [PMID: 36252156 DOI: 10.18388/abp.2020_5894]

281 **He Y**, Hua R, Yang Y, Li B, Guo X, Li Z. LncRNA JPX Promotes Esophageal Squamous Cell Carcinoma Progression by Targeting miR-516b-5p/VEGFA Axis. *Cancers (Basel)* 2022; **14** [PMID: 35681693 DOI: 10.3390/cancers14112713]

282 **Wang B**, Hua P, Zhang L, Li J, Zhang Y. LncRNA-IUR up-regulates PTEN by sponging miR-21 to regulate cancer cell proliferation and apoptosis in esophageal squamous cell carcinoma. *Esophagus* 2020; **17**: 298-304 [PMID: 32124090 DOI: 10.1007/s10388-020-00724-x]

283 **Jiang Q**, Wang H, Yuan D, Qian X, Ma X, Yan M, Xing W. Circular_0086414 induces SPARC like 1 (SPARCL1) production to inhibit esophageal cancer cell proliferation, invasion and glycolysis and induce cell apoptosis by sponging miR-1290. *Bioengineered* 2022; **13**: 12099-12114 [PMID: 35549806 DOI: 10.1080/21655979.2022.2073114]

284 **Kano M**, Seki N, Kikkawa N, Fujimura L, Hoshino I, Akutsu Y, Chiyomaru T, Enokida H, Nakagawa M, Matsubara H. miR-145, miR-133a and miR-133b: Tumor-suppressive miRNAs target FSCN1 in esophageal squamous cell carcinoma. *Int J Cancer* 2010; **127**: 2804-2814 [PMID: 21351259 DOI: 10.1002/ijc.25284]

285 **Li H**, Jia J, Yang L, Chu J, Sheng J, Wang C, Meng W, Jia Z, Yin H, Wan J, He F. LncRNA MIR205HG Drives Esophageal Squamous Cell Carcinoma Progression by Regulating miR-214/SOX4 Axis. *Onco Targets Ther* 2020; **13**: 13097-13109 [PMID: 33376358 DOI: 10.2147/OTT.S286627]

286 **Jin YY**, Chen QJ, Wei Y, Wang YL, Wang ZW, Xu K, He Y, Ma HB. Upregulation of microRNA-98 increases radiosensitivity in esophageal squamous cell carcinoma. *J Radiat Res* 2016; **57**: 468-476 [PMID: 27422937 DOI: 10.1093/jrr/rrw068]

287 **Wang X**, Fei X, Li C, Lu C, Chen H. MicroRNA-340-5p inhibits proliferation, migration and invasion of human esophageal squamous cell carcinoma cells by targeting inhibitors of DNA binding/differentiation 3. *Disan Junyi Daxue Xuebao* 2021; **42**: 1091-1097 [DOI: 10.16781/j.0258-879x.2021.10.1091]

288 **Wang WW**, Zhao ZH, Wang L, Li P, Chen KS, Zhang JY, Li WC, Jiang GZ, Li XN. MicroRNA-134 prevents the progression of esophageal squamous cell carcinoma *via* the PLXNA1-mediated MAPK signalling pathway. *EBioMedicine* 2019; **46**: 66-78 [PMID: 31383552 DOI: 10.1016/j.ebiom.2019.07.050]

289 **Zong M**, Liu Y, Zhang K, J Y, Chen L. The effects of miR-429 on cell migration and invasion by targeting Slug in esophageal squamous cell carcinoma. *Pathol Res Pract* 2019; **215**: 152526 [PMID: 31324391 DOI: 10.1016/j.prp.2019.152526]

290 **Zhen C**, Huang J, Lu J. MicroRNA-652 inhibits the biological characteristics of esophageal squamous cell carcinoma by directly targeting fibroblast growth factor receptor 1. *Exp Ther Med* 2019; **18**: 4473-4480 [PMID: 31777550 DOI: 10.3892/etm.2019.8072]

291 **Shi Q**, Wang Y, Mu Y, Wang X, Fan Q. MiR-433-3p Inhibits Proliferation and Invasion of Esophageal Squamous Cell Carcinoma by Targeting GRB2. *Cell Physiol Biochem* 2018; **46**: 2187-2196 [PMID: 29730656 DOI: 10.1159/000489548]

292 **Wang M**, Wang L, Zhang M, Li X, Zhu Z, Wang H. MiR-214 inhibits the proliferation and invasion of esophageal squamous cell carcinoma cells by targeting CDC25B. *Biomed Pharmacother* 2017; **95**: 1678-1683 [PMID: 28954387 DOI: 10.1016/j.biopha.2017.09.048]

293 **Wang X**, Gu M, Ju Y, Zhou J. PIK3C3 Acts as a Tumor Suppressor in Esophageal Squamous Cell Carcinoma and Was Regulated by MiR-340-5p. *Med Sci Monit* 2020; **26**: e920642 [PMID: 32207410 DOI: 10.12659/MSM.920642]

294 **Zhang J**, Fa X, Zhang Q. MicroRNA206 exerts antioncogenic functions in esophageal squamous cell carcinoma by suppressing the cMet/AKT/mTOR pathway. *Mol Med Rep* 2019; **19**: 1491-1500 [PMID: 30569129 DOI: 10.3892/mmr.2018.9775]

295 **Fan Y**, Bian X, Qian P, Wen J, Yan P, Luo Y, Wu J, Zhang Q. miRNA30a3p inhibits metastasis and enhances radiosensitivity in esophageal carcinoma by targeting insulinlike growth factor 1 receptor. *Mol Med Rep* 2019; **20**: 81-94 [PMID: 31115568 DOI: 10.3892/mmr.2019.10222]

296 **Kong KL**, Kwong DL, Chan TH, Law SY, Chen L, Li Y, Qin YR, Guan XY. MicroRNA-375 inhibits tumour growth and metastasis in oesophageal squamous cell carcinoma through repressing insulin-like growth factor 1 receptor. *Gut* 2012; **61**: 33-42 [PMID: 21813472 DOI: 10.1136/gutjnl-2011-300178]

297 **Li P**, Mao WM, Zheng ZG, Dong ZM, Ling ZQ. Down-regulation of PTEN expression modulated by dysregulated miR-21 contributes to the progression of esophageal cancer. *Dig Dis Sci* 2013; **58**: 3483-3493 [PMID: 24221338 DOI: 10.1007/s10620-013-2854-z]

298 **Zhang J**, Chen D, Liang S, Wang J, Liu C, Nie C, Shan Z, Wang L, Fan Q, Wang F. miR-106b promotes cell invasion and metastasis *via* PTEN mediated EMT in ESCC. *Oncol Lett* 2018; **15**: 4619-4626 [PMID: 29552108 DOI: 10.3892/ol.2018.7861]

299 **Zhou J**, Zhu J, Jiang G, Feng J, Wang Q. Downregulation of microRNA-4324 promotes the EMT of esophageal squamous-cell carcinoma cells *via* upregulating FAK. *Onco Targets Ther* 2019; **12**: 4595-4604 [PMID: 31354293 DOI: 10.2147/OTT.S198333]

300 **Meng X**, Chen X, Lu P, Ma W, Yue D, Song L, Fan Q. MicroRNA-202 inhibits tumor progression by targeting LAMA1 in esophageal squamous cell carcinoma. *Biochem Biophys Res Commun* 2016; **473**: 821-827 [PMID: 27045085 DOI: 10.1016/j.bbrc.2016.03.130]

301 **Li Y**, Wu D, Wang P, Li X, Shi G. miR-195 Regulates Proliferation and Apoptosis through Inhibiting the mTOR/p70s6k Signaling Pathway by Targeting HMGA2 in Esophageal Carcinoma Cells. *Dis Markers* 2017; **2017**: 8317913 [PMID: 28487599 DOI: 10.1155/2017/8317913]

302 **Takeshita N**, Mori M, Kano M, Hoshino I, Akutsu Y, Hanari N, Yoneyama Y, Ikeda N, Isozaki Y, Maruyama T, Akanuma N, Miyazawa Y, Matsubara H. miR-203 inhibits the migration and invasion of esophageal squamous cell carcinoma by regulating LASP1. *Int J Oncol* 2012; **41**: 1653-1661 [PMID: 22940702 DOI: 10.3892/ijo.2012.1614]

303 **Wang K**, Li J, Xiong G, He G, Guan X, Yang K, Bai Y. Negative regulation of lncRNA GAS5 by miR-196a inhibits esophageal squamous cell carcinoma growth. *Biochem Biophys Res Commun* 2018; **495**: 1151-1157 [PMID: 29170131 DOI: 10.1016/j.bbrc.2017.11.119]

304 **Tang J**, Li Z, Zhu Q, Wen W, Wang J, Xu J, Wu W, Zhu Y, Xu H, Chen L. miR-204-5p regulates cell proliferation, invasion, and apoptosis by targeting IL-11 in esophageal squamous cell carcinoma. *J Cell Physiol* 2020; **235**: 3043-3055 [PMID: 31544245 DOI: 10.1002/jcp.29209]

305 **Ren S**, Tan X, Fu MZ, Ren S, Wu X, Chen T, Latham PS, Lin P, Man YG, Fu SW. Downregulation of miR-375 contributes to ERBB2-mediated VEGFA overexpression in esophageal cancer. *J Cancer* 2021; **12**: 7138-7146 [PMID: 34729115 DOI: 10.7150/jca.63836]

306 **Bian W**, Li Y, Zhu H, Gao S, Niu R, Wang C, Zhang H, Qin X, Li S. miR-493 by regulating of c-Jun targets Wnt5a/PD-L1-inducing esophageal cancer cell development. *Thorac Cancer* 2021; **12**: 1579-1588 [PMID: 33793074 DOI: 10.1111/1759-7714.13950]

307 **Zhou Y**, Xu R, Luo J, Li X, Zhong Y, Sun Z. Dysregulation of miR-204-5p/APLN axis affects malignant progression and cell stemness of esophageal cancer. *Mutat Res* 2022; **825**: 111791 [PMID: 35930907 DOI: 10.1016/j.mrfmmm.2022.111791]

308 **Zhang BX**, Yu T, Yu Z, Yang XG. MicroRNA-148a regulates the MAPK/ERK signaling pathway and suppresses the development of esophagus squamous cell carcinoma *via* targeting MAP3K9. *Eur Rev Med Pharmacol Sci* 2019; **23**: 6497-6504 [PMID: 31378889 DOI: 10.26355/eurrev_201908_18533]

309 **Zong M**, Feng W, Wan L, Yu X, Yu W. miR-203 affects esophageal cancer cell proliferation, apoptosis and invasion by targeting MAP3K1. *Oncol Lett* 2020; **20**: 751-757 [PMID: 32566001 DOI: 10.3892/ol.2020.11610]

310 **Nie Z**, Weng W, Li J, Xu Y, Li Z. Down-regulation of miR-126 in esophageal carcinoma tissues and its inhibition effect on proliferation and

migration of esophageal carcinoma cell line EC109. *Zhongliu* 2015; **35**: 55-64 [DOI: 10.3781/j.issn.1000-7431.2015.33.578]

311 **Yao L**, Zhang Y, Zhu Q, Li X, Zhu S, Gong L, Han X, Lan M, Li S, Zhang W, Li Y. Downregulation of microRNA-1 in esophageal squamous cell carcinoma correlates with an advanced clinical stage and its overexpression inhibits cell migration and invasion. *Int J Mol Med* 2015; **35**: 1033-1041 [PMID: 25672418 DOI: 10.3892/ijmm.2015.2094]

World Journal of Gastroenterology

Submit a Manuscript: https://www.f6publishing.com

World J Gastroenterol 2024 March 21; 30(11): 1524-1532

DOI: 10.3748/wjg.v30.i11.1524

ISSN 1007-9327 (print) ISSN 2219-2840 (online)

MINIREVIEWS

Morphological and biochemical characteristics associated with autophagy in gastrointestinal diseases

Yi-Fan Chang, Jia-Jing Li, Tao Liu, Chong-Qing Wei, Li-Wei Ma, Vladimir N Nikolenko, Wei-Long Chang

Specialty type: Gastroenterology and hepatology

Provenance and peer review: Unsolicited article; Externally peer reviewed.

Peer-review model: Single blind

Peer-review report's scientific quality classification

Grade A (Excellent): 0
Grade B (Very good): B
Grade C (Good): 0
Grade D (Fair): 0
Grade E (Poor): 0

P-Reviewer: Machado NC, Brazil

Received: November 9, 2023
Peer-review started: November 9, 2023
First decision: December 15, 2023
Revised: January 5, 2024
Accepted: February 20, 2024
Article in press: March 21, 2024
Published online: March 21, 2024

Yi-Fan Chang, Tao Liu, Chong-Qing Wei, Wei-Long Chang, Department of Gastrointestinal Surgery, The First Affiliated Hospital of Zhengzhou University, Zhengzhou 450052, Henan Province, China

Jia-Jing Li, Department of Pathology, The First Affiliated Hospital of Zhengzhou University, Zhengzhou 450052, Henan Province, China

Li-Wei Ma, Department of Clinical Laboratory, The First Affiliated Hospital of Zhengzhou University, Zhengzhou 450052, Henan Province, China

Vladimir N Nikolenko, Department of Human Anatomy and Histology, I.M. Sechenov First Moscow State Medical University (Sechenov University), Moscow 119991, Russia

Corresponding author: Wei-Long Chang, PhD, Doctor, Department of Gastrointestinal Surgery, The First Affiliated Hospital of Zhengzhou University, No. 1 Jianshe East Road, Erqi District, Zhengzhou 450052, Henan Province, China. changwl365@foxmail.com

Abstract

Autophagy is a cellular catabolic process characterized by the formation of double-membrane autophagosomes. Transmission electron microscopy is the most rigorous method to clearly visualize autophagic engulfment and degradation. A large number of studies have shown that autophagy is closely related to the digestion, secretion, and regeneration of gastrointestinal (GI) cells. However, the role of autophagy in GI diseases remains controversial. This article focuses on the morphological and biochemical characteristics of autophagy in GI diseases, in order to provide new ideas for their diagnosis and treatment.

Key Words: Autophagy; Morphological study; Biochemical characteristics; Subcellular structure; Transmission electron microscopy; Gastrointestinal diseases

Core Tip: Autophagy, from a morphological standpoint, shares similarities with other biological processes such as phagocytosis and apoptosis. As an intracellular catabolic mechanism, autophagy, along with the ubiquitin-proteasome system, contributes to maintaining cellular homeostasis. Moreover, autophagy also assumes a role in programmed cell death when apoptosis is absent. Numerous studies have established the close association between autophagy and the physiological functions of different gastrointestinal (GI) cells. Morphological investigations have furnished substantial evidence highlighting autophagy's pro-survival role in benign conditions like intestinal ischemia-reperfusion injury, inflammatory bowel disease, and GI motility disorders. Further research into the involvement of autophagy in GI tumors is necessary to unravel these unresolved mysteries in the future.

Citation: Chang YF, Li JJ, Liu T, Wei CQ, Ma LW, Nikolenko VN, Chang WL. Morphological and biochemical characteristics associated with autophagy in gastrointestinal diseases. *World J Gastroenterol* 2024; 30(11): 1524-1532
URL: https://www.wjgnet.com/1007-9327/full/v30/i11/1524.htm
DOI: https://dx.doi.org/10.3748/wjg.v30.i11.1524

INTRODUCTION

Autophagy, as a cellular catabolic process, is closely related to the digestion, secretion, and regeneration of gastrointestinal (GI) cells. Morphological studies have shown that autophagy is similar to other biological phenomena such as phagocytosis and apoptosis, and it is involved in maintaining cellular homeostasis and programmed cell death, as well as cell growth, development, and differentiation. Autophagy has been found to play a pro-survival role in benign GI diseases like intestinal ischemia-reperfusion (I/R) injury, inflammatory bowel disease (IBD), and GI motility disorders. However, under pathological conditions, the role of autophagy in GI diseases varies, possibly due to the different degrees of autophagy or the presence of other factors. Therefore, more studies on the role of autophagy in GI tumors are required to address these unresolved questions in the future.

Autophagy occurs in all eukaryotic cells, including plant and animal cells, and is an evolutionarily conserved cellular catabolic process. The occurrence of autophagy cannot be separated from the existence of lysosomes. However, autophagy is rare in cells in a state of normal proliferation. Taking gastric tissue as an example, autolysosomes are difficult to observe by transmission electron microscopy (TEM) under normal circumstances[1]. Autophagy is elevated only when cells lack energy sources (starvation), face external stimuli (invasion by pathogens), and be in disease states (degenerative lesions, cancer, *etc*.). Thus, autophagy is also thought to often play a pro-survival role. However, in some cases, inhibiting autophagy can actually help to cure diseases. For example, studies have found that autophagy enhances the drug resistance of tumor cells to chemotherapy in kidney cancer, prostate cancer, and other cancers. The combination of autophagy inhibitor drugs and chemotherapy drugs can achieve good therapeutic effects. In addition, autophagy is also considered as a programmed death process. Excessive autophagy is thought to cause cell death. Thus, the effects of autophagy on cells in different states are complex (Figure 1).

AUTOPHAGY

Before the advent of electron microscopy, a variety of particle-containing vesicles could only be observed by ordinary light microscopy. Since 1933, the advent of TEM has accelerated the study of morphology to the subcellular level[2]. Compared with ordinary microscopes, electron microscopes can magnify tens of thousands of times, so submicroscopic structures within cells can be observed. Thus, electron microscopy is the "gold standard" for studying autophagic morphology. TEM images can provide information such as autophagosome integrity, changes in the number and volume of autophagic vesicles, and autophagosome-lysosomal interactions. In addition, this technique allows visualization of organelles inside autophagic chamber to distinguish whether autophagy is selective autophagy. Observing by TEM, we can clearly capture the moment of fusion of autophagosomes and lysosomes and the morphological changes of organelles during degradation.

The process of autophagy can be divided into five stages: Initiation, elongation, closure, fusion, and decomposition. Morphological studies of autophagy have found that a bilayer membrane structure derived from the endoplasmic reticulum without ribosomes is first formed in the cell, and the degenerate organelles form distinct aggregates, which are gradually surrounded by this bilayer membrane structure. The membrane of the autophagosome is continuously elongated and gradually envelops the aggregates. Eventually, autophagosomes fuse with lysosomes to release acid-lysozymes to break down the contents. Generally, typical features of different stages of autophagy can be observed simultaneously by TEM. According to the type of autophagic body contents, autophagy can be divided into selective autophagy and non-selective autophagy. Non-selective autophagy occurs when various organelles such as the endoplasmic reticulum and mitochondria accumulate in autophagosomes. When selective autophagy occurs, aggregation of only one type of content can be observed in autophagosomes. Common inclusions include mitochondria, lipids, and foreign pathogens (such as bacteria and viruses). Autophagy is also divided into macro-autophagy, micro-autophagy, and chaperone-mediated autophagy. The autophagy mentioned in this article mainly refers to macroscopic autophagy.

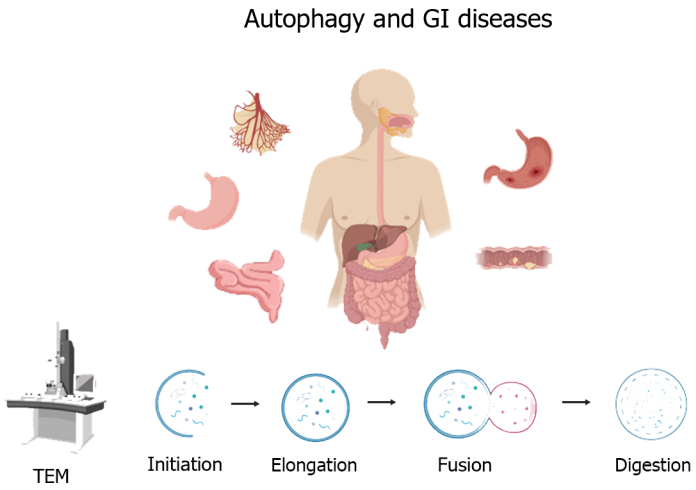

Figure 1 Overview of autophagy in gastrointestinal diseases. Created with MedPeer (www.medpeer.cn). TEM: Transmission electron microscopy; GI: Gastrointestinal.

AUTOPHAGY AND GI CELLS

The GI tract is the largest contact area with the external environment of the cavity organs. Many biochemical reactions occur in the GI tract every day. GI epithelial cells together with a variety of microorganisms constitute the first barrier of the human digestive system. GI cells are made up of three types of cells: Digestive cells (master cells and absorptive cells), secretory cells (goblet cells and Paneth cells), and regenerative cells (stem cells). Goblet cells are mucus-secreting cells that form a physical barrier between intestinal epithelial cells (IECs) and the external environment. One study found that autophagy produced a thicker, less penetrating mucus layer in mice, which enhanced intestinal anti-inflammatory function[3]. Mucus production protects gastric mucosal epithelial cells from chemicals (*e.g.*, alcohol and nonsteroidal anti-inflammatory drugs) and microorganisms. In that study, Naama *et al*[3] also found that autophagy relieves endoplasmic reticulum stress through autophagy-related protein Beclin1, thereby promoting goblet cell mucus secretion. Similarly, Paneth cells secrete antimicrobial proteins that are highly dependent on endoplasmic reticulum stress and autophagy levels[4]. Gorbunov *et al*[5] found that autophagy plays a role not only in secretory cells, but also in intestinal stem cells. Yang *et al*[6] demonstrated that autophagy is required for ileal stem cell maintenance and mammalian survival. In addition, recent studies have shown that autophagy is required to maintain increased enterocyte proliferation in honeybees[7].

According to reports, amino acid deficiency can regulate autophagy activity in IECs[8]. The researchers found that autophagic vacuoles increased by TEM and confocal microscopy[9]. In addition, exposure of IECs to hypoxia and lipopolysaccharide for 24 h not only increased the number of autophagic vesicles, but also significantly increased their diameter[10]. Interestingly, in the midgut epithelial cells of shrimp, approximately 40% of cells show signs of autophagy. The endoplasmic reticulum pool, electron transparent content, vacuoles, poly-vesicles, lamellar bodies, vesicles of autophagosome in lipids, and electron dense particles were observed. In addition, the researchers observed that degenerated mitochondria were mainly concentrated in autophagosomes (mitochondrial autophagy). A study has found that the reduction of intestinal cell volume in shrimp involves a programmed process that requires autophagy. In addition, UBA1 knockout significantly reduced the size of midgut cells, and double membrane autophagosomes containing mitochondria or ribosomes were observed in the cytoplasm[11].

AUTOPHAGY AND GI PHYSICAL BARRIER FUNCTION

GI epithelial cells constitute the first barrier to protect the alimentary tract from injury. The intestinal epithelial tight junction (TJ), which is the second line of defense in the intestinal mucosa, protects against permeation of luminal antigens, endotoxins, and bacteria into the blood stream. Recent research found that autophagy promotes membrane localization of occluding protein, a principal TJ component involved in TJ barrier enhancement, which could protect against inflammation-induced barrier loss[12]. Furthermore, Kim *et al*[13] discovered that protease-activated receptor 2 regulates autophagy and intestinal epithelial TJs, thus reducing intestinal epithelial permeability. Additionally, another study discovered that rapamycin (autophagy inducer) dramatically improved intestinal damage in benzo[a]pyrene induced intestinal epithelial TJ disruption[14]. In conclusion, the activation of autophagy plays an important role in maintaining intestinal barrier function against toxic chemicals, intestinal inflammation, and intestinal permeability.

The intestinal epithelium is frequently exposed to the invasion of many foreign pathogens, leading to increased permeability and intestinal barrier loss. When bacteria infect host cells, selective autophagy initially engulfs the pathogens to limit the access to nutrients. Although autophagy initially triggers an innate immune response that induces intestinal immune cells to produce interferon and clear harmful pathogens, some bacteria (such as *Escherichia coli*,

Salmonella, and *Listeria*) have evolved strategies to inhibit or escape it. For example, *Escherichia coli* hinders the autophagosome-lysosome fusion to inhibit autophagic flux, thus preventing the clearance of acidic hydrolase[15]. Besides that, Yang *et al*[16] suggested that *Salmonella* escapes host immune responses by inhibiting autophagy degradation. Previously, a large number of bacteria have been shown to evade NOD pathway-mediated intestinal immune surveillance by inhibiting autophagy[17,18]. Molecule evidence has been found that autophagy is involved in the secretion of membrane vesicles from *Listeria monocytogenes in vitro*[19]. In addition, one similar study discovered that *Fusobacterium* modulates autophagy to survive, thus aggravating experimental colitis *via* the miR-574-5p/CARD3 axis[20]. The latest findings show that bacterial extracellular vesicles induced mitophagy through mTOR pathways relieve oxidative stress in colonic epithelial cells[21]. Libertellenone T, a compound isolated from *Endolichenic fungus*, also induces autophagy to strengthen the epithelial barrier function of the colon[22].

In contrast, some viruses exploit autophagy for replication to survive inside intestinal cells. Recently, the effect of autophagy on SARS-CoV-2 infection has drawn much attention. Some studies showed that SARS-CoV-2 exploits host autophagy machinery for intestinal dissemination[23,24]. Furthermore, Cloherty *et al*[25] proofed that Berbamine, a selection of autophagy-blocking drugs, can suppress intestinal SARS-CoV-2 infection as well as prevent SARS-CoV-2-mediated disruption of the intestinal barrier *via* an autophagy-mediated BNIP3 mechanism. However, not all viruses have evolved such an escape mechanism. One study discovered that autophagy induced by urolithin A, an intestinal metabolite of ellagic acid, inhibits enterovirus 71 replication in infected cells[26]. In addition, another study discovered that the autophagy gene (ATG) *Epg5* plays an important role in intestinal antiviral signaling by modulating interferon-γ responses[27].

ATG MUTATIONS AND INTESTINAL INFLAMMATION

Autophagy dysfunction can lead to disruption of intestinal barrier function, triggering an immune response and leading to chronic intestinal inflammation. Genome-wide association studies have found that mutations in ATGs are associated with IBD. At present, many autophagy-related genes (such as *ATG16L1, ULK1, NOD2, LRRK2,* and *IRGM*) have been shown to be susceptibility genes for IBD[28,29]. One study found that ATG5 expression in intestinal myeloid cells modulates IL-12, thereby preventing uncontrolled IFN-γ-driven intestinal inflammation[30]. Furthermore, mice with specific deletion of ATG16L1 in IECs have aggravated intestinal injury[31]. ATG16L1^{T300A} is a single nucleotide polymorphism of the susceptibility gene for Crohn's disease (CD)[32]. Further studies have shown that autophagy disorder caused by the ATG16L1^{T300A} polymorphism contributes to the increased risk of CD through NF-κB-mediated inflammation[33]. In addition, researchers have found that ATG16L1 interferes with Paneth cell secretion of antimicrobial agents and dendritic cell antigen presentation, which leads to intestinal mucosal barrier dysfunction and the development of CD.

In recent years, more and more animal experiments have revealed the presence of a large number of autophagic vesicles accompanied by mitochondrial vacuolization in DSS-induced colitis. In Wistar rats, vitamin D has been shown to alleviate stress colitis through mTOR-STAT3 signaling and regulation of autophagy[34]. Similarly, we found that activation of estrogen receptor β, which is highly expressed in intestinal tissues, can inhibit colitis by promoting NLRP6-mediated autophagy[35]. In addition, Ma and collaborators demonstrated that Parkin loss may lead to high drug resistance in DSS-induced colitis[36].

AUTOPHAGY AND GI DISEASES

Intestinal I/R injury

Intestinal I/R injury is a common GI barrier dysfunction. The ultrastructural changes of the intestinal epithelium under the transmission electron microscope can provide information about the early changes of intestinal I/R, including the ischemia phase and reperfusion phase. One study showed that a large number of autophagosomes were found in the cytoplasm of colonic epithelial cells after 1 h of ischemia, with organelle damage, cytolysis, and lysosome formation[37]. However, in another study, a significant reduction in autophagic vacuoles was observed in intestinal tissues 4 h after reperfusion by TEM[38]. Another study found that the number of autophagosomes and autolysosomes increased at 4 h and decreased at 20 h after I/R upon electron microscopy analysis of intestinal epithelial tissues taken at 0, 4, and 20 h after I/R[39]. Thus, based on morphological evidence, autophagy has a conflicting role in the pathology of I/R-induced intestinal injury. In addition to TEM results, several studies have found that the autophagy-related marker LC3BII/I ratio and the mitophagy-related PINK1/Parkin pathway are significantly up-regulated during intestinal I/R injury[40-42]. Consistent with this, Liu *et al*[43] demonstrated in rat experiments that inhibition of autophagy alleviated intestinal I/R injury through the miR-146a/TXNIP axis. Similarly, upregulation of miR-182 in I/R mice leading to a significant reduction in autophagosomes has also found morphological evidence observed by TEM[44]. Studies have found that selenium nanoparticles can effectively alleviate intestinal epithelial barrier damage by inhibiting autophagy mediated by the TBC1D15/Rab7 signaling pathway[45]. In contrast to the above studies, activation of the AMPK/ SIRT1-autophagy pathway alleviated intestinal I/R injury[46,47]. These studies seem to suggest that autophagic changes during the ischemic phase play a more decisive role in the course of the disease. Therefore, studying the role of autophagy in intestinal I/R injury may require a more unified modeling approach and further analysis of the morphological changes of autophagy in different periods. Another common intestinal barrier dysfunction is necrotizing enterocolitis. The

ultrastructure of rapamycin-treated IEC-6 and Caco2 cells was observed by TEM, and the formation of autophagic vacuoles was significantly accumulated, which could be reduced by human β-defensin-3 (hBD3) treatment[48].

GI motility disorders

Functional dyspepsia (FD) is a common GI motility disorder, affecting 11.5%-29.2% of people worldwide. Interstitial cells of Cajal (ICC), especially muscle ICC (ICC-MY), are the key cells to GI motility. Early studies found that the impaired autophagy of ICC was closely related to gastric hypomotility in rats with gastroparesis[49], especially with the reduction and structural abnormalities of ICC-MY cells. Zhang *et al*[50] observed a large number of autophagosomes in the ultrastructure of ICC-MY in the FD model group by electron microscopy, and even degeneration or reduction of organelles. This suggests that increased autophagy and decreased differentiation of ICC-MY play an important role in FD. In addition, Drp-1 mediated mitophagy in ICC significantly promoted gastric motility in FD rats. Lee *et al*[51] also found that the traditional Chinese medicine compound Chaihu Shugan powder inhibits ICC autophagy through the PI3K/PDK1 pathway, thus playing a role in promoting GI motility. In addition, many studies have found that electroacupuncture can improve GI motility disorders by activating autophagy[52-54]. In addition, Fu *et al*[55] demonstrated that exosomes derived from patients with irritable bowel syndrome have an inhibitory effect on autophagy in human colonic epithelial cells by promoting ATG14. Although there are still many mysteries about how autophagy is impaired in GI motility disorders, with the further accumulation and analysis of morphological evidence, it is believed that more new regulatory mechanisms will be discovered in the future.

GI cancers

GI cancers have attracted much attention due to their high recurrence and metastasis rates, difficult diagnosis, and poor prognosis. More and more evidence has shown that although chemotherapy drugs are clinically effective, it has become a common phenomenon that many patients develop chemotherapy resistance in GI cancers during treatment.

Gastric cancer: Gastric cancer has attracted much attention due to its high recurrence and metastasis rates, difficult diagnosis, and poor prognosis. Common treatments include surgical resection, radiotherapy[56], and chemotherapy. *Helicobacter pylori* infection is a common cause in patients with gastric cancer. A study of *H. pylori*-positive human biopsy specimens revealed onion-like (autophagosome-like) structures containing intact bacteria as well as autolysosomes enclosing degraded material[57]. A number of studies have confirmed that autophagy is related to the chemoresistance in gastric cancer, including resistance to oxaliplatin, cisplatin, and paclitaxel[58-62]. It was found that in paclitaxel-pretreated BGC gastric cancer cells, typical double-membrane autophagic vacuoles and residual organelles around the nucleus could be clearly captured by TEM[62]. Further morphological studies revealed that overexpression of *SIRT5, Sec62,* and *TOB1* genes can induce autophagy in gastric cancer cells[63-65]. Of course, autophagy activation is not present in all drug-resistant gastric cancer cell lines. He *et al*[66] observed multiple autophagosomes (double-membrane structure) and autolysosomes (single-membrane structure) in the cytoplasm of BGC gastric cancer cells treated with 5-FU. Moreover, the ratio of autophagosome area to that of the cytoplasm was significantly different from that of the control group. However, in AGS cells treated with 5-FU, few autophagosomes and autolysosomes were observed by TEM. In addition, gastric cancer cell-derived exosomes (GC-Ex) have been found to have the ability to induce neutrophil autophagy[67]. The number of autophagosomes was increased in treated neutrophils. TEM and immunofluorescence staining showed that neutrophils treated with GC-Ex had more autophagosomes than those in the control group. Further study showed that FTO silencing reduced the number of autophagosomes in SGC-7901/DDP cells[68].

Colorectal cancer: Colorectal cancer (CRC) is the third most common malignancy and the second leading cause of cancer death in the world. Multiple clinicopathological studies have confirmed that several autophagy-related genes, such as *ATG9B, ATG4B*, and *ULK1*, are CRC prognostic markers[69-72]. Accumulating evidence suggests that cytoprotective autophagy not only increases cancer cell survival, but also enhances tumor drug resistance in CRC[73-75]. One study showed that inhibition of autophagy enhanced doxorubicin hydrochloride-induced apoptosis in human colon cancer cells [76]. Further studies found that MTOR signaling dependent mitochondrial dysfunction promotes colorectal cancer cell death[77]. Regulation of the Beclin1/Beclin2 signaling pathway may be the key to inducing autophagic death of colorectal cancer cells[78-80]. In addition, a study on the mechanism of lipopolysaccharide-induced injury in the colon adenoma cell lines Caco-2 and HT-29 showed that autophagic flow was blocked at the autolysosome stage *in vitro* and *in vivo*[81]. Moreover, Bacillus Calmette-Guerin has been shown to induce autophagic cell death through TLR2 and TLR4 signaling pathways in a radiosensitive colorectal cell line[82]. In addition, Liu *et al*[83] found that induction of autophagy-related ferroptosis through the MEK1/2/ERK/c-FOS axis enhanced the sensitivity of colon cancer cells to chemotherapy. TEM showed mitochondrial destruction and increased number of autophagosomes in the diabetic group compared with the non-diabetic group[40].

Autophagy and GI drugs: Autophagy is closely related to the occurrence and development of GI cancer and drug resistance. A large number of studies have found that a variety of natural compounds can induce autophagy to exert anti-cancer effects. For example, salidroside was found to induce autophagy in AGS cells[84]. Moreover, autolysosome accumulation in gastric cancer cells treated with narcicycline and galangin was observed under the electron microscope. TEM showed that the number of autophagosomes increased in lutein-treated IEC-6 cells[8]. In addition, several Chinese herbs such as ononin, celastrol, licorice, and Jianpi-Qingchang decoction have been shown to protect IECs and treat experimental colitis by activating mitophagy[85-88]. Subsequently, Truzzi and colleagues demonstrated that stimulation of autophagy by a combination of spermidine and eugenol supplements reduced intestinal inflammatory parameters[89].

CONCLUSION

From the perspective of morphology, autophagy is similar to the biological phenomena such as phagocytosis and apoptosis. As an intracellular catabolic mechanism, autophagy and the ubiquitin-proteasome system jointly assume the role of maintaining cellular homeostasis. Not only that, autophagy also plays a role in programmed cell death in cells lacking apoptosis. Autophagy is inextricably linked to cell growth, development, and differentiation. A large number of studies have confirmed that autophagy is closely related to the physiological functions of the GI tract in different types of GI cells. Morphological studies have provided us with a large amount of evidence that autophagy plays a pro-survival role in benign diseases such as intestinal I/R injury, IBD, and GI motility disorders. However, under pathological conditions, the role of autophagy is not the same, which may be due to the different degrees of autophagy or the existence of other factors. Therefore, more studies on the role of autophagy in GI tumors are needed to solve these unsolved mysteries in the future.

FOOTNOTES

Co-first authors: Yi-Fan Chang and Jia-Jing Li.

Co-corresponding authors: Vladimir N Nikolenko and Wei-Long Chang.

Author contributions: Chang YF and Li JJ contributed equally to this work; Chang WL contributed to study conceptualization; Liu T, Wei CQ, Ma LW, and Nikolenko VN contributed to manuscript writing and editing; all authors have read and approved the final manuscript.

Supported by the National Natural Science Foundation of China, No. 81900533; Science and Technology Project of Henan Science and Technology Department, No. 232102520032.

Conflict-of-interest statement: The authors declare that they have no conflict of interest to disclose.

Country/Territory of origin: China

ORCID number: Yi-Fan Chang 0009-0001-2080-1644; Vladimir N Nikolenko 0000-0001-9532-9957; Wei-Long Chang 0009-0007-0822-0592.

S-Editor: Yan JP
L-Editor: Wang TQ
P-Editor: Cai YX

REFERENCES

1 **Jia Q**, Li L, Wang X, Wang Y, Jiang K, Yang K, Cong J, Cai G, Ling J. Hesperidin promotes gastric motility in rats with functional dyspepsia by regulating Drp1-mediated ICC mitophagy. *Front Pharmacol* 2022; **13**: 945624 [PMID: 36034863 DOI: 10.3389/fphar.2022.945624]
2 **Ruska E**. Nobel lecture. The development of the electron microscope and of electron microscopy. *Biosci Rep* 1987; **7**: 607-629 [PMID: 3322421 DOI: 10.1007/BF01127674]
3 **Naama M**, Telpaz S, Awad A, Ben-Simon S, Harshuk-Shabso S, Modilevsky S, Rubin E, Sawaed J, Zelik L, Zigdon M, Asulin N, Turjeman S, Werbner M, Wongkuna S, Feeney R, Schroeder BO, Nyska A, Nuriel-Ohayon M, Bel S. Autophagy controls mucus secretion from intestinal goblet cells by alleviating ER stress. *Cell Host Microbe* 2023; **31**: 433-446.e4 [PMID: 36738733 DOI: 10.1016/j.chom.2023.01.006]
4 **Lu R**, Zhang YG, Xia Y, Zhang J, Kaser A, Blumberg R, Sun J. Paneth Cell Alertness to Pathogens Maintained by Vitamin D Receptors. *Gastroenterology* 2021; **160**: 1269-1283 [PMID: 33217447 DOI: 10.1053/j.gastro.2020.11.015]
5 **Gorbunov NV**, Kiang JG. Up-regulation of autophagy in small intestine Paneth cells in response to total-body gamma-irradiation. *J Pathol* 2009; **219**: 242-252 [PMID: 19681094 DOI: 10.1002/path.2591]
6 **Yang Y**, White E. Autophagy in PDGFRA(+) mesenchymal cells is required for intestinal homeostasis and mammalian survival. *Autophagy* 2023; **19**: 726-728 [PMID: 35708538 DOI: 10.1080/15548627.2022.2090694]
7 **Guo Y**, Hu R, Li N, Wu J, Yu H, Tan J, Li Z, Xu S. Autophagy Is Required to Sustain Increased Intestinal Cell Proliferation during Phenotypic Plasticity Changes in Honey Bee (Apis mellifera). *Int J Mol Sci* 2023; **24** [PMID: 36768248 DOI: 10.3390/ijms24031926]
8 **Chang CJ**, Lin JF, Hsiao CY, Chang HH, Li HJ, Lee GA, Hung CF. Lutein Induces Autophagy *via* Beclin-1 Upregulation in IEC-6 Rat Intestinal Epithelial Cells. *Am J Chin Med* 2017; **45**: 1273-1291 [PMID: 28893091 DOI: 10.1142/S0192415X17500707]
9 **Shi H**, Zhao X, Ding Z, Han C, Jiang Y, Qian W, Lin R, Hou X. Na+/H+ Exchanger Regulates Amino Acid-Mediated Autophagy in Intestinal Epithelial Cells. *Cell Physiol Biochem* 2017; **42**: 2418-2429 [PMID: 28848079 DOI: 10.1159/000480184]
10 **Yamoto M**, Lee C, Chusilp S, Yazaki Y, Alganabi M, Li B, Pierro A. The role of autophagy in intestinal epithelial injury. *Pediatr Surg Int* 2019; **35**: 1389-1394 [PMID: 31555857 DOI: 10.1007/s00383-019-04566-2]
11 **Chang TK**, Shravage BV, Hayes SD, Powers CM, Simin RT, Wade Harper J, Baehrecke EH. Uba1 functions in Atg7- and Atg3-independent autophagy. *Nat Cell Biol* 2013; **15**: 1067-1078 [PMID: 23873149 DOI: 10.1038/ncb2804]

12 **Saha K**, Subramenium Ganapathy A, Wang A, Michael Morris N, Suchanec E, Ding W, Yochum G, Koltun W, Nighot M, Ma T, Nighot P. Autophagy Reduces the Degradation and Promotes Membrane Localization of Occludin to Enhance the Intestinal Epithelial Tight Junction Barrier against Paracellular Macromolecule Flux. *J Crohns Colitis* 2023; **17**: 433-449 [PMID: 36219473 DOI: 10.1093/ecco-jcc/jjac148]

13 **Kim Y**, Lee Y, Heo G, Jeong S, Park S, Yoo JW, Jung Y, Im E. Modulation of Intestinal Epithelial Permeability *via* Protease-Activated Receptor-2-Induced Autophagy. *Cells* 2022; **11** [PMID: 35269499 DOI: 10.3390/cells11050878]

14 **Li J**, Bai J, Si X, Jia H, Wu Z. Benzo[a]pyrene induces epithelial tight junction disruption and apoptosis *via* inhibiting the initiation of autophagy in intestinal porcine epithelial cells. *Chem Biol Interact* 2023; **374**: 110386 [PMID: 36754226 DOI: 10.1016/j.cbi.2023.110386]

15 **David L**, Taieb F, Pénary M, Bordignon PJ, Planès R, Bagayoko S, Duplan-Eche V, Meunier E, Oswald E. Outer membrane vesicles produced by pathogenic strains of Escherichia coli block autophagic flux and exacerbate inflammasome activation. *Autophagy* 2022; **18**: 2913-2925 [PMID: 35311462 DOI: 10.1080/15548627.2022.2054040]

16 **Yang L**, Wang JF, Liu N, Wang X, Wang J, Yang GH, Yang GY, Zhu YH. Lactobacillusjohnsonii L531 Protects against Salmonella Infantis-Induced Intestinal Damage by Regulating the NOD Activation, Endoplasmic Reticulum Stress, and Autophagy. *Int J Mol Sci* 2022; **23** [PMID: 36142312 DOI: 10.3390/ijms231810395]

17 **Liu W**, Zhou Y, Peng T, Zhou P, Ding X, Li Z, Zhong H, Xu Y, Chen S, Hang HC, Shao F. N(ε)-fatty acylation of multiple membrane-associated proteins by Shigella IcsB effector to modulate host function. *Nat Microbiol* 2018; **3**: 996-1009 [PMID: 30061757 DOI: 10.1038/s41564-018-0215-6]

18 **Ge P**, Lei Z, Yu Y, Lu Z, Qiang L, Chai Q, Zhang Y, Zhao D, Li B, Pang Y, Liu CH, Wang J. M. tuberculosis PknG manipulates host autophagy flux to promote pathogen intracellular survival. *Autophagy* 2022; **18**: 576-594 [PMID: 34092182 DOI: 10.1080/15548627.2021.1938912]

19 **Karthikeyan R**, Gayathri P, Ramasamy S, Suvekbala V, Jagannadham MV, Rajendhran J. Transcriptome responses of intestinal epithelial cells induced by membrane vesicles of Listeria monocytogenes. *Curr Res Microb Sci* 2023; **4**: 100185 [PMID: 36942003 DOI: 10.1016/j.crmicr.2023.100185]

20 **Wei S**, Zhang J, Wu X, Chen M, Huang H, Zeng S, Xiang Z, Li X, Dong W. Fusobacterium nucleatum Extracellular Vesicles Promote Experimental Colitis by Modulating Autophagy *via* the miR-574-5p/CARD3 Axis. *Inflamm Bowel Dis* 2023; **29**: 9-26 [PMID: 35998069 DOI: 10.1093/ibd/izac177]

21 **Marzoog TR**, Jabir MS, Ibraheem S, Jawad SF, Hamzah SS, Sulaiman GM, Mohammed HA, Khan RA. Bacterial extracellular vesicles induced oxidative stress and mitophagy through mTOR pathways in colon cancer cells, HT-29: Implications for bioactivity. *Biochim Biophys Acta Mol Cell Res* 2023; **1870**: 119486 [PMID: 37172765 DOI: 10.1016/j.bbamcr.2023.119486]

22 **Gamage CDB**, Kim JH, Yang Y, Taş İ, Park SY, Zhou R, Pulat S, Varlı M, Hur JS, Nam SJ, Kim H. Libertellenone T, a Novel Compound Isolated from Endolichenic Fungus, Induces G2/M Phase Arrest, Apoptosis, and Autophagy by Activating the ROS/JNK Pathway in Colorectal Cancer Cells. *Cancers (Basel)* 2023; **15** [PMID: 36672439 DOI: 10.3390/cancers15020489]

23 **Han L**, Zheng Y, Deng J, Nan ML, Xiao Y, Zhuang MW, Zhang J, Wang W, Gao C, Wang PH. SARS-CoV-2 ORF10 antagonizes STING-dependent interferon activation and autophagy. *J Med Virol* 2022; **94**: 5174-5188 [PMID: 35765167 DOI: 10.1002/jmv.27965]

24 **Gassen NC**, Papies J, Bajaj T, Emanuel J, Dethloff F, Chua RL, Trimpert J, Heinemann N, Niemeyer C, Weege F, Hönzke K, Aschman T, Heinz DE, Weckmann K, Ebert T, Zellner A, Lennarz M, Wyler E, Schroeder S, Richter A, Niemeyer D, Hoffmann K, Meyer TF, Heppner FL, Corman VM, Landthaler M, Hocke AC, Morkel M, Osterrieder N, Conrad C, Eils R, Radbruch H, Giavalisco P, Drosten C, Müller MA. SARS-CoV-2-mediated dysregulation of metabolism and autophagy uncovers host-targeting antivirals. *Nat Commun* 2021; **12**: 3818 [PMID: 34155207 DOI: 10.1038/s41467-021-24007-w]

25 **Cloherty APM**, Rader AG, Patel KS, Pérez-Vargas J, Thompson CAH, Ennis S, Niikura M, Wildenberg ME, Muncan V, Schreurs RRCE, Jean F, Ribeiro CMS. Berbamine suppresses intestinal SARS-CoV-2 infection *via* a BNIP3-dependent autophagy blockade. *Emerg Microbes Infect* 2023; **12**: 2195020 [PMID: 36951188 DOI: 10.1080/22221751.2023.2195020]

26 **Wang S**, Qiao J, Chen Y, Tian L, Sun X. Urolithin A inhibits enterovirus 71 replication and promotes autophagy and apoptosis of infected cells in vitro. *Arch Virol* 2022; **167**: 1989-1997 [PMID: 35790643 DOI: 10.1007/s00705-022-05471-1]

27 **Lee S**, Kalugotla G, Ingle H, Rodgers R, Wu C, Wang Y, Li Y, Yang X, Zhang J, Borella NR, Deng H, Droit L, Hill R, Peterson ST, Desai C, Lawrence D, Lu Q, Baldridge MT. Intestinal antiviral signaling is controlled by autophagy gene Epg5 independent of the microbiota. *Autophagy* 2022; **18**: 1062-1077 [PMID: 34520306 DOI: 10.1080/15548627.2021.1968607]

28 **Liu JZ**, van Sommeren S, Huang H, Ng SC, Alberts R, Takahashi A, Ripke S, Lee JC, Jostins L, Shah T, Abedian S, Cheon JH, Cho J, Dayani NE, Franke L, Fuyuno Y, Hart A, Juyal RC, Juyal G, Kim WH, Morris AP, Poustchi H, Newman WG, Midha V, Orchard TR, Vahedi H, Sood A, Sung JY, Malekzadeh R, Westra HJ, Yamazaki K, Yang SK; International Multiple Sclerosis Genetics Consortium; International IBD Genetics Consortium, Barrett JC, Alizadeh BZ, Parkes M, Bk T, Daly MJ, Kubo M, Anderson CA, Weersma RK. Association analyses identify 38 susceptibility loci for inflammatory bowel disease and highlight shared genetic risk across populations. *Nat Genet* 2015; **47**: 979-986 [PMID: 26192919 DOI: 10.1038/ng.3359]

29 **Chauhan S**, Mandell MA, Deretic V. IRGM governs the core autophagy machinery to conduct antimicrobial defense. *Mol Cell* 2015; **58**: 507-521 [PMID: 25891078 DOI: 10.1016/j.molcel.2015.03.020]

30 **Merkley SD**, Goodfellow SM, Guo Y, Wilton ZER, Byrum JR, Schwalm KC, Dinwiddie DL, Gullapalli RR, Deretic V, Jimenez Hernandez A, Bradfute SB, In JG, Castillo EF. Non-autophagy Role of Atg5 and NBR1 in Unconventional Secretion of IL-12 Prevents Gut Dysbiosis and Inflammation. *J Crohns Colitis* 2022; **16**: 259-274 [PMID: 34374750 DOI: 10.1093/ecco-jcc/jjab144]

31 **Foerster EG**, Tsang DKL, Goyal S, Robertson SJ, Robert LM, Maughan H, Streutker CJ, Girardin SE, Philpott DJ. ATG16L1 protects from interferon-γ-induced cell death in the small intestinal crypt. *Mucosal Immunol* 2023; **16**: 135-152 [PMID: 36792009 DOI: 10.1016/j.mucimm.2023.02.001]

32 **Baradaran Ghavami S**, Kabiri F, Nourian M, Balaii H, Shahrokh S, Chaleshi V, Sherkat G, Shalileh F, Asadzadeh Aghdaei H. Association between variants of the autophagy related gene ATG16L1 in inflammatory bowel diseases and clinical statues. *Gastroenterol Hepatol Bed Bench* 2019; **12**: S94-S100 [PMID: 32099608]

33 **Gao P**, Liu H, Huang H, Sun Y, Jia B, Hou B, Zhou X, Strober W, Zhang F. The Crohn Disease-associated ATG16L1(T300A) polymorphism regulates inflammatory responses by modulating TLR- and NLR-mediated signaling. *Autophagy* 2022; **18**: 2561-2575 [PMID: 35220902 DOI: 10.1080/15548627.2022.2039991]

34 **Abdelmalak MFL**, Abdelrahim DS, George Michael TMA, Abdel-Maksoud OM, Labib JMW. Vitamin D and lactoferrin attenuate stress-induced colitis in Wistar rats *via* enhancing AMPK expression with inhibiting mTOR-STAT3 signaling and modulating autophagy. *Cell Biochem Funct* 2023; **41**: 211-222 [PMID: 36588325 DOI: 10.1002/cbf.3774]

35 **Zilleruelo I**, Espinoza E, Ruiz I. Influence of the assessment of the severity on the frequency of adverse drug reactions (ADRs). *Int J Clin Pharmacol Ther Toxicol* 1987; **25**: 328-333 [PMID: 3623738]

36 **Ma Z**, Wu J, Wu Y, Sun X, Rao Z, Sun N, Fu Y, Zhang Z, Li J, Xiao M, Zeng Q, Han C, Ding D, Zhang H, Yuan H, Zhang J, Yang S, Chen Y. Parkin increases the risk of colitis by downregulation of VDR *via* autophagy-lysosome degradation. *Int J Biol Sci* 2023; **19**: 1633-1644 [PMID: 37056928 DOI: 10.7150/ijbs.77153]

37 **Grosche A**, Morton AJ, Graham AS, Sanchez LC, Blikslager AT, Polyak MM, Freeman DE. Ultrastructural changes in the equine colonic mucosa after ischaemia and reperfusion. *Equine Vet J Suppl* 2011; 8-15 [PMID: 21790749 DOI: 10.1111/j.2042-3306.2011.00402.x]

38 **Li Z**, Wang G, Feng D, Zu G, Li Y, Shi X, Zhao Y, Jing H, Ning S, Le W, Yao J, Tian X. Targeting the miR-665-3p-ATG4B-autophagy axis relieves inflammation and apoptosis in intestinal ischemia/reperfusion. *Cell Death Dis* 2018; **9**: 483 [PMID: 29706629 DOI: 10.1038/s41419-018-0518-9]

39 **Jiang M**, Wan S, Dai X, Ye Y, Hua W, Ma G, Pang X, Wang H, Shi B. Protective effect of ghrelin on intestinal I/R injury in rats. *Open Med (Wars)* 2022; **17**: 1308-1317 [PMID: 35937002 DOI: 10.1515/med-2022-0520]

40 **Zeng Z**, Liu HM, Zhang YY, Chen R, Sun T, Li W, Sun Q, Xia ZY, Meng QT. Aggravated intestinal ischemiareperfusion injury is associated with activated mitochondrial autophagy in a mouse model of diabetes. *Mol Med Rep* 2020; **22**: 1892-1900 [PMID: 32582983 DOI: 10.3892/mmr.2020.11270]

41 **Li S**, Zhou Y, Gu X, Zhang X, Jia Z. NLRX1/FUNDC1/NIPSNAP1-2 axis regulates mitophagy and alleviates intestinal ischaemia/reperfusion injury. *Cell Prolif* 2021; **54**: e12986 [PMID: 33432610 DOI: 10.1111/cpr.12986]

42 **Zhang Q**, Liu XM, Hu Q, Liu ZR, Liu ZY, Zhang HG, Huang YL, Chen QH, Wang WX, Zhang XK. Dexmedetomidine inhibits mitochondria damage and apoptosis of enteric glial cells in experimental intestinal ischemia/reperfusion injury *via* SIRT3-dependent PINK1/HDAC3/p53 pathway. *J Transl Med* 2021; **19**: 463 [PMID: 34772407 DOI: 10.1186/s12967-021-03027-6]

43 **Zhenzhen L**, Wenting L, Jianmin Z, Guangru Z, Disheng L, Zhiyu Z, Feng C, Yajing S, Yingxiang H, Jipeng L, Zhanhai W, Yan Z, Xin L, Yongqiang L, Yufang L. miR-146a-5p/TXNIP axis attenuates intestinal ischemia-reperfusion injury by inhibiting autophagy *via* the PRKAA/mTOR signaling pathway. *Biochem Pharmacol* 2022; **197**: 114839 [PMID: 34774846 DOI: 10.1016/j.bcp.2021.114839]

44 **Li Y**, Luo Y, Li B, Niu L, Liu J, Duan X. miRNA-182/Deptor/mTOR axis regulates autophagy to reduce intestinal ischaemia/reperfusion injury. *J Cell Mol Med* 2020; **24**: 7873-7883 [PMID: 32510855 DOI: 10.1111/jcmm.15420]

45 **Dou X**, Qiao L, Song X, Chang J, Pi S, Zhang X, Zeng X, Zhu L, Xu C. Biogenic selenium nanoparticles alleviate intestinal epithelial barrier injury by regulating mitochondria-lysosome crosstalk. *Food Funct* 2023; **14**: 4891-4904 [PMID: 37144827 DOI: 10.1039/d2fo03992c]

46 **Li B**, Li W, Zheng M, Wang Y, Diao Y, Mou X, Liu J. Corilagin alleviates intestinal ischemia/reperfusion injury by relieving oxidative stress and apoptosis *via* AMPK/Sirt1-autophagy pathway. *Exp Biol Med (Maywood)* 2023; **248**: 317-326 [PMID: 36680375 DOI: 10.1177/15353702221147560]

47 **Liu X**, Yang B, Tan YF, Feng JG, Jia J, Yang CJ, Chen Y, Wang MH, Zhou J. The role of AMPK-Sirt1-autophagy pathway in the intestinal protection process by propofol against regional ischemia/reperfusion injury in rats. *Int Immunopharmacol* 2022; **111**: 109114 [PMID: 35933747 DOI: 10.1016/j.intimp.2022.109114]

48 **Chen L**, Lv Z, Gao Z, Ge G, Wang X, Zhou J, Sheng Q. Human β-defensin-3 reduces excessive autophagy in intestinal epithelial cells and in experimental necrotizing enterocolitis. *Sci Rep* 2019; **9**: 19890 [PMID: 31882811 DOI: 10.1038/s41598-019-56535-3]

49 **Wei X**, Lin Y, Zhao D, Xiao X, Chen Q, Chen S, Peng Y. Electroacupuncture Relieves Suppression of Autophagy in Interstitial Cells of Cajal of Diabetic Gastroparesis Rats. *Can J Gastroenterol Hepatol* 2020; **2020**: 7920715 [PMID: 32211350 DOI: 10.1155/2020/7920715]

50 **Zhang LM**, Zeng LJ, Deng J, Zhang YQ, Wang YJ, Xie TY, Ling JH. Investigation of autophagy and differentiation of myenteric interstitial cells of Cajal in the pathogenesis of gastric motility disorders in rats with functional dyspepsia. *Biotechnol Appl Biochem* 2018; **65**: 533-539 [PMID: 29274173 DOI: 10.1002/bab.1635]

51 **Li L**, Jia Q, Wang X, Wang Y, Wu C, Cong J, Ling J. Chaihu Shugan San promotes gastric motility in rats with functional dyspepsia by regulating Drp-1-mediated ICC mitophagy. *Pharm Biol* 2023; **61**: 249-258 [PMID: 36655341 DOI: 10.1080/13880209.2023.2166966]

52 **Wang L**, Chen Y, Xu MM, Cao W, Zheng QH, Zhou SY, Yao JP, Xi MH, Qin HY, Li Y, Zhang W. Electroacupuncture Alleviates Functional Constipation in Mice by Activating Enteric Glial Cell Autophagy *via* PI3K/AKT/mTOR Signaling. *Chin J Integr Med* 2023; **29**: 459-469 [PMID: 36973529 DOI: 10.1007/s11655-023-3594-3]

53 **Song LZ**, Xu N, Yu Z, Yang H, Xu CC, Qiu Z, Dai JW, Xu B, Hu XM. The effect of electroacupuncture at ST25 on Parkinson's disease constipation through regulation of autophagy in the enteric nervous system. *Anat Rec (Hoboken)* 2023; **306**: 3214-3228 [PMID: 36655864 DOI: 10.1002/ar.25148]

54 **Yang J**, Wang L, Mei M, Guo J, Yang X, Liu S. Electroacupuncture repairs intestinal barrier by upregulating CB1 through gut microbiota in DSS-induced acute colitis. *Chin Med* 2023; **18**: 24 [PMID: 36894930 DOI: 10.1186/s13020-023-00733-9]

55 **Fu R**, Liu S, Zhu M, Zhu J, Chen M. Apigenin reduces the suppressive effect of exosomes derived from irritable bowel syndrome patients on the autophagy of human colon epithelial cells by promoting ATG14. *World J Surg Oncol* 2023; **21**: 95 [PMID: 36915121 DOI: 10.1186/s12957-023-02963-5]

56 **Shi X**, Zou J, Wang Y, Zhao J, Ye B, Qi Q, Liu F, Hu J, Li S, Tian Y. MST4 as a novel therapeutic target for autophagy and radiosensitivity in gastric cancer. *IUBMB Life* 2023; **75**: 117-136 [PMID: 36239138 DOI: 10.1002/iub.2682]

57 **Hu W**, Zhang L, Li MX, Shen J, Liu XD, Xiao ZG, Wu DL, Ho IHT, Wu JCY, Cheung CKY, Zhang YC, Lau AHY, Ashktorab H, Smoot DT, Fang EF, Chan MTV, Gin T, Gong W, Wu WKK, Cho CH. Vitamin D3 activates the autolysosomal degradation function against Helicobacter pylori through the PDIA3 receptor in gastric epithelial cells. *Autophagy* 2019; **15**: 707-725 [PMID: 30612517 DOI: 10.1080/15548627.2018.1557835]

58 **Ren J**, Hu Z, Niu G, Xia J, Wang X, Hong R, Gu J, Wang D, Ke C. Annexin A1 induces oxaliplatin resistance of gastric cancer through autophagy by targeting PI3K/AKT/mTOR. *FASEB J* 2023; **37**: e22790 [PMID: 36786694 DOI: 10.1096/fj.202200400RR]

59 **Wang J**, Sun Y, Zhang X, Cai H, Zhang C, Qu H, Liu L, Zhang M, Fu J, Zhang J, Wang J, Zhang G. Oxidative stress activates NORAD expression by H3K27ac and promotes oxaliplatin resistance in gastric cancer by enhancing autophagy flux *via* targeting the miR-433-3p. *Cell Death Dis* 2021; **12**: 90 [PMID: 33462197 DOI: 10.1038/s41419-020-03368-y]

60 **Dai X**, Chen Y, Chen N, Dou J, Zhuang H, Wang J, Zhao X, Zhang X, Zhao H. KLF5-mediated aquaporin 3 activated autophagy to facilitate cisplatin resistance of gastric cancer. *Immunopharmacol Immunotoxicol* 2023; **45**: 140-152 [PMID: 36083020 DOI: 10.1080/08923973.2022.2122498]

61 **Nong ZL**, Zhao K, Wang Y, Yu Z, Wang CJ, Chen JQ. CLIC1-mediated autophagy confers resistance to DDP in gastric cancer. *Anticancer Drugs* 2024; **35**: 1-11 [PMID: 37104099 DOI: 10.1097/CAD.0000000000001518]

62 **Yu YF**, Hu PC, Wang Y, Xu XL, Rushworth GM, Zhang Z, Wei L, Zhang JW. Paclitaxel induces autophagy in gastric cancer BGC823 cells. *Ultrastruct Pathol* 2017; **41**: 284-290 [PMID: 28691892 DOI: 10.1080/01913123.2017.1334019]

63 **Gu W**, Qian Q, Xu Y, Xu X, Zhang L, He S, Li D. SIRT5 regulates autophagy and apoptosis in gastric cancer cells. *J Int Med Res* 2021; **49**: 300060520986355 [PMID: 33530803 DOI: 10.1177/0300060520986355]

64 **Su S**, Shi YT, Chu Y, Jiang MZ, Wu N, Xu B, Zhou H, Lin JC, Jin YR, Li XF, Liang J. Sec62 promotes gastric cancer metastasis through mediating UPR-induced autophagy activation. *Cell Mol Life Sci* 2022; **79**: 133 [PMID: 35165763 DOI: 10.1007/s00018-022-04143-2]

65 **Zang WJ**, Hu YL, Qian CY, Feng Y, Liu JZ, Yang JL, Huang H, Zhu YZ, Xue WJ. HDAC4 promotes the growth and metastasis of gastric cancer *via* autophagic degradation of MEKK3. *Br J Cancer* 2022; **127**: 237-248 [PMID: 35637410 DOI: 10.1038/s41416-022-01805-7]

66 **He XX**, Huang CK, Xie BS. Autophagy inhibition enhanced 5FUinduced cell death in human gastric carcinoma BGC823 cells. *Mol Med Rep* 2018; **17**: 6768-6776 [PMID: 29512733 DOI: 10.3892/mmr.2018.8661]

67 **Zhang X**, Shi H, Yuan X, Jiang P, Qian H, Xu W. Tumor-derived exosomes induce N2 polarization of neutrophils to promote gastric cancer cell migration. *Mol Cancer* 2018; **17**: 146 [PMID: 30292233 DOI: 10.1186/s12943-018-0898-6]

68 **Zhang Y**, Gao LX, Wang W, Zhang T, Dong FY, Ding WP. M(6) A demethylase fat mass and obesity-associated protein regulates cisplatin resistance of gastric cancer by modulating autophagy activation through ULK1. *Cancer Sci* 2022; **113**: 3085-3096 [PMID: 35730319 DOI: 10.1111/cas.15469]

69 **Kim IS**, Cho SY, Yang M, Han S, Lee KH, Kim JY, Kim JM, Kang S, Jo EK, Ryu H. ATG9B Is a Poor Prognostic Marker Associated With Immune Evasion in Colon Adenocarcinoma. *Anticancer Res* 2023; **43**: 1943-1957 [PMID: 37097701 DOI: 10.21873/anticanres.16354]

70 **Hu WH**, Liu TT, Liu PF, Morgan P, Lin IL, Tsai WL, Cheng YY, Hsieh AT, Hu TH, Shu CW. ATG4B and pS383/392-ATG4B serve as potential biomarkers and therapeutic targets of colorectal cancer. *Cancer Cell Int* 2023; **23**: 63 [PMID: 37038218 DOI: 10.1186/s12935-023-02909-7]

71 **Lv P**, Wu Z, Lai L, Zhang Y, Pei B. The clinicopathological significance and potential function of ULK1 in colon cancer. *Biotechnol Genet Eng Rev* 2023; 1-14 [PMID: 37191026 DOI: 10.1080/02648725.2023.2210952]

72 **Bednarczyk M**, Muc-Wierzgoń M, Dzięgielewska-Gęsiak S, Fatyga E, Waniczek D. Transcription of Autophagy Associated Gene Expression as Possible Predictors of a Colorectal Cancer Prognosis. *Biomedicines* 2023; **11** [PMID: 36830954 DOI: 10.3390/biomedicines11020418]

73 **Yue Y**, Zhang Q, Wang X, Sun Z. STAT3 regulates 5-Fu resistance in human colorectal cancer cells by promoting Mcl-1-dependent cytoprotective autophagy. *Cancer Sci* 2023; **114**: 2293-2305 [PMID: 36788743 DOI: 10.1111/cas.15761]

74 **Manzoor S**, Saber-Ayad M, Maghazachi AA, Hamid Q, Muhammad JS. MLH1 mediates cytoprotective nucleophagy to resist 5-Fluorouracil-induced cell death in colorectal carcinoma. *Neoplasia* 2022; **24**: 76-85 [PMID: 34952246 DOI: 10.1016/j.neo.2021.12.003]

75 **Saini H**, Dave R, Chatterjee S, Mandloi A, Sharma H, Daiya A, Mukherjee S, Chowdhury R, Chowdhury S. Transcriptomic analysis reveals differential adaptation of colorectal cancer cells to low and acute doses of cisplatin. *Gene* 2023; **864**: 147304 [PMID: 36822527 DOI: 10.1016/j.gene.2023.147304]

76 **Tang H**, Wu D, Yang H, Yang J, Zhang Y, Li M, Liu H, Li Q. [Inhibition of autophagy enhances apoptosis induced by doxorubicin hydrochloride in human colon cancer cells]. *Xi Bao Yu Fen Zi Mian Yi Xue Za Zhi* 2022; **38**: 237-243 [PMID: 35365989]

77 **Zheng Y**, Yang W, Jia Y, Ji J, Wu L, Feng J, Li Y, Cheng Z, Zhang J, Li J, Dai W, Xu X, Wu J, Zhou Y, Guo C. Promotion of colorectal cancer cell death by ezetimibe *via* mTOR signaling-dependent mitochondrial dysfunction. *Front Pharmacol* 2023; **14**: 1081980 [PMID: 36843944 DOI: 10.3389/fphar.2023.1081980]

78 **Kong W**, Zhu H, Zheng S, Yin G, Yu P, Shan Y, Liu X, Ying R, Ma S. Larotrectinib induces autophagic cell death through AMPK/mTOR signalling in colon cancer. *J Cell Mol Med* 2022; **26**: 5539-5550 [PMID: 36251949 DOI: 10.1111/jcmm.17530]

79 **Xu W**, Nie C, Chen X. DUSP4 inhibits autophagic cell death and apoptosis in colorectal cancer by regulating BCL2-Beclin1/Bax signaling. *Mol Biol Rep* 2023; **50**: 3229-3239 [PMID: 36705792 DOI: 10.1007/s11033-023-08270-2]

80 **Qian J**, Cao Y, Zhang J, Li L, Wu J, Yu J, Huo J. Tanshinone IIA Alleviates the Biological Characteristics of Colorectal Cancer *via* Activating the ROS/JNK Signaling Pathway. *Anticancer Agents Med Chem* 2023; **23**: 227-236 [PMID: 35593352 DOI: 10.2174/1871520622666220421093430]

81 **Zhou M**, Xu W, Wang J, Yan J, Shi Y, Zhang C, Ge W, Wu J, Du P, Chen Y. Boosting mTOR-dependent autophagy *via* upstream TLR4-MyD88-MAPK signalling and downstream NF-κB pathway quenches intestinal inflammation and oxidative stress injury. *EBioMedicine* 2018; **35**: 345-360 [PMID: 30170968 DOI: 10.1016/j.ebiom.2018.08.035]

82 **Yuk JM**, Shin DM, Song KS, Lim K, Kim KH, Lee SH, Kim JM, Lee JS, Paik TH, Kim JS, Jo EK. Bacillus calmette-guerin cell wall cytoskeleton enhances colon cancer radiosensitivity through autophagy. *Autophagy* 2010; **6**: 46-60 [PMID: 19901560 DOI: 10.4161/auto.6.1.10325]

83 **Liu Z**, Xu Y, Liu X, Wang B. PCDH7 knockdown potentiates colon cancer cells to chemotherapy *via* inducing ferroptosis and changes in autophagy through restraining MEK1/2/ERK/c-Fos axis. *Biochem Cell Biol* 2022; **100**: 445-457 [PMID: 35926236 DOI: 10.1139/bcb-2021-0513]

84 **Rong L**, Li Z, Leng X, Li H, Ma Y, Chen Y, Song F. Salidroside induces apoptosis and protective autophagy in human gastric cancer AGS cells through the PI3K/Akt/mTOR pathway. *Biomed Pharmacother* 2020; **122**: 109726 [PMID: 31918283 DOI: 10.1016/j.biopha.2019.109726]

85 **Yu T**, Lu X, Liang Y, Yang L, Yin Y, Chen H. Ononin alleviates DSS-induced colitis through inhibiting NLRP3 inflammasome *via* triggering mitophagy. *Immun Inflamm Dis* 2023; **11**: e776 [PMID: 36840499 DOI: 10.1002/iid3.776]

86 **Chen D**, Ye L, Liu Y, Yu J, Ni S, Chen Y, Zhong J. Celastrol activates mitochondrial autophagy through Nur77-TRAF2-p62/SQSTM1 pathway in the treatment of experimental colitis. *Minerva Pediatr (Torino)* 2023; **75**: 760-762 [PMID: 37021620 DOI: 10.23736/S2724-5276.23.07258-0]

87 **Kong J**, Xiang Q, Shi G, Xu Z, Ma X, Wang Y, Xuan Z, Xu F. Licorice protects against ulcerative colitis *via* the Nrf2/PINK1-mediated mitochondrial autophagy. *Immun Inflamm Dis* 2023; **11**: e757 [PMID: 36705402 DOI: 10.1002/iid3.757]

88 **Qiao D**, Liu X, Zhang Y, Zhang Z, Tang Y, Chen Q, Shi Y, Chen Y, Tang Z, Dai Y. Jianpi-Qingchang decoction alleviates ulcerative colitis by modulating endoplasmic reticulum stress-related autophagy in intestinal epithelial cells. *Biomed Pharmacother* 2023; **158**: 114133 [PMID: 36521243 DOI: 10.1016/j.biopha.2022.114133]

89 **Truzzi F**, Whittaker A, D'Amen E, Valerii MC, Abduazizova V, Spisni E, Dinelli G. Spermidine-Eugenol Supplement Preserved Inflammation-Challenged Intestinal Cells by Stimulating Autophagy. *Int J Mol Sci* 2023; **24** [PMID: 36835540 DOI: 10.3390/ijms24044131]

World Journal of Gastroenterology

Submit a Manuscript: https://www.f6publishing.com

World J Gastroenterol 2024 March 21; 30(11): 1533-1544

DOI: 10.3748/wjg.v30.i11.1533

ISSN 1007-9327 (print) ISSN 2219-2840 (online)

ORIGINAL ARTICLE

Retrospective Study

Efficacy of radiofrequency ablation combined with sorafenib for treating liver cancer complicated with portal hypertension and prognostic factors

Li-Min Yang, Hong-Juan Wang, Shan-Lin Li, Guan-Hua Gan, Wen-Wen Deng, Yong-Sheng Chang, Lian-Feng Zhang

Specialty type: Gastroenterology and hepatology

Provenance and peer review: Unsolicited article; Externally peer reviewed.

Peer-review model: Single blind

Peer-review report's scientific quality classification

Grade A (Excellent): 0
Grade B (Very good): B, B
Grade C (Good): 0
Grade D (Fair): 0
Grade E (Poor): 0

P-Reviewer: Moore LW, United States; Mroweh M, France

Received: January 5, 2024
Peer-review started: January 5, 2024
First decision: January 23, 2024
Revised: February 18, 2024
Accepted: March 8, 2024
Article in press: March 8, 2024
Published online: March 21, 2024

Li-Min Yang, Hong-Juan Wang, Guan-Hua Gan, Wen-Wen Deng, Lian-Feng Zhang, Department of Gastroenterology, The First Affiliated Hospital of Zhengzhou University, Zhengzhou 450052, Henan Province, China

Shan-Lin Li, Department of Gastroenterology, Zhoukou Central Hospital of Henan Province, Zhoukou 466000, Henan Province, China

Yong-Sheng Chang, Department of Gastroenterology, The First Affiliated Hospital of Xinxiang Medical College, Xinxiang 453000, Henan Province, China

Corresponding author: Li-Min Yang, MD, Associate Chief Physician, Department of Gastroenterology, The First Affiliated Hospital of Zhengzhou University, No. 1 Jianshe East Road, Erqi District, Zhengzhou 450052, Henan Province, China. ylmsunny6153@126.com

Abstract

BACKGROUND

Patients with liver cancer complicated by portal hypertension present complex challenges in treatment.

AIM

To evaluate the efficacy of radiofrequency ablation in combination with sorafenib for improving liver function and its impact on the prognosis of patients with this condition.

METHODS

Data from 100 patients with liver cancer complicated with portal hypertension from May 2014 to March 2019 were analyzed and divided into a study group (n = 50) and a control group (n = 50) according to the treatment regimen. The research group received radiofrequency ablation (RFA) in combination with sorafenib, and the control group only received RFA. The short-term efficacy of both the research and control groups was observed. Liver function and portal hypertension were compared before and after treatment. Alpha-fetoprotein (AFP), glypican-3 (GPC-3), and AFP-L3 levels were compared between the two groups prior to and after treatment. The occurrence of adverse reactions in both groups was observed. The 3-year survival rate was compared between the two groups. Basic data were

compared between the survival and non-surviving groups. To identify the independent risk factors for poor prognosis in patients with liver cancer complicated by portal hypertension, multivariate logistic regression analysis was employed.

RESULTS

When comparing the two groups, the research group's total effective rate (82.00%) was significantly greater than that of the control group (56.00%; $P < 0.05$). Following treatment, alanine aminotransferase and aspartate aminotransferase levels increased, and portal vein pressure decreased in both groups. The degree of improvement for every index was substantially greater in the research group than in the control group ($P < 0.05$). Following treatment, the AFP, GPC-3, and AFP-L3 levels in both groups decreased, with the research group having significantly lower levels than the control group ($P < 0.05$). The incidence of diarrhea, rash, nausea and vomiting, and fatigue in the research group was significantly greater than that in the control group ($P < 0.05$). The 1-, 2-, and 3-year survival rates of the research group (94.00%, 84.00%, and 72.00%, respectively) were significantly greater than those of the control group (80.00%, 64.00%, and 40.00%, respectively; $P < 0.05$). Significant differences were observed between the survival group and the non-surviving group in terms of Child-Pugh grade, history of hepatitis, number of tumors, tumor size, use of sorafenib, stage of liver cancer, histological differentiation, history of splenectomy and other basic data ($P < 0.05$). Logistic regression analysis demonstrated that high Child-Pugh grade, tumor size (6–10 cm), history of hepatitis, no use of sorafenib, liver cancer stage IIIC, and previous splenectomy were independent risk factors for poor prognosis in patients with liver cancer complicated with portal hypertension ($P < 0.05$).

CONCLUSION

Patients suffering from liver cancer complicated by portal hypertension benefit from the combination of RFA and sorafenib therapy because it effectively restores liver function and increases survival rates. The prognosis of patients suffering from liver cancer complicated by portal hypertension is strongly associated with factors such as high Child-Pugh grade, tumor size (6-10 cm), history of hepatitis, lack of sorafenib use, liver cancer at stage IIIC, and prior splenectomy.

Key Words: Radiofrequency ablation; Sorafenib; Liver cancer; Portal hypertension; Efficacy; Prognosis analysis

Core Tip: The combination of radiofrequency ablation (RFA) and sorafenib shows promise in treating liver cancer with portal hypertension. This approach demonstrated improved short- and long-term efficacy, with significant reduction in portal vein pressure and enhancement of liver function. Patients treated with this combination had higher survival rates compared to those receiving RFA alone. Moreover, the study identified key prognostic factors, such as Child-Pugh grade, tumor size, history of hepatitis, and the use of sorafenib, providing valuable insights for managing liver cancer complicated by portal hypertension. These findings suggest that the RFA and sorafenib combination could be a beneficial therapeutic strategy, but further research with larger sample sizes is warranted to validate these outcomes.

Citation: Yang LM, Wang HJ, Li SL, Gan GH, Deng WW, Chang YS, Zhang LF. Efficacy of radiofrequency ablation combined with sorafenib for treating liver cancer complicated with portal hypertension and prognostic factors. *World J Gastroenterol* 2024; 30(11): 1533-1544

URL: https://www.wjgnet.com/1007-9327/full/v30/i11/1533.htm

DOI: https://dx.doi.org/10.3748/wjg.v30.i11.1533

INTRODUCTION

Liver cancer is categorized into two types: primary and metastatic liver cancer. Primary liver cancer is more common than primary liver cancer, and its incidence ranks fifth among malignant tumors. According to epidemiological surveys, there are more than 600000 new cases of liver cancer worldwide. Approximately 85% to 95% of primary liver cancers develop from liver cirrhosis, 15% to 20% of which are complicated with different degrees of portal hypertension[1,2]. The condition of patients suffering from liver cancer complicated with portal hypertension is relatively complex, and since there are no obvious symptoms in the initial stages, most patients visit the hospital when they are typically already in the middle or late stages and have missed the best time for surgical treatment. Moreover, patients suffering from liver cancer complicated with portal hypertension are in poor physical condition and cannot tolerate surgical operation[3,4]. The treatment principle of radiofrequency ablation (RFA) is to increase the temperature of liver tissue to > 60°C and maintain it at that temperature for a certain time to cause degeneration and irreversible necrosis of cellular proteins. Multiple earlier research studies have revealed that RFA effectively treats liver cancer, but studies on its application in patients

with liver cancer complicated with portal hypertension are rare[5,6]. Sorafenib, an oral tyrosine kinase inhibitor, can reduce visceral neovascularization and ameliorate portal hypertension *via* the inhibition of vascular endothelial growth factor receptor (VEGFR) and platelet-derived growth factor receptor (PDGFR) to inhibit neovascularization[7,8]. In the present research, RFA in combination with sorafenib was applied to treat patients suffering from liver cancer complicated by portal hypertension to study its mechanism of action and to analyze patient prognosis. This study provides a reference for the treatment of liver cancer complicated by portal hypertension. The report is detailed below.

MATERIALS AND METHODS

General information

Data from 100 patients with liver cancer complicated with portal hypertension from May 2014 to March 2019 were analyzed and divided into study groups (n = 50) and control groups (n = 50) according to the treatment regimen. The research group comprised 23 women and 27 men aged 44-69 (55.46 ± 6.31) years; portal hypertension symptoms: 30 patients with hemorrhage, 9 patients with ascites, and 11 patients with hemorrhage and ascites. The control group included 31 men and 19 women aged 40-69 (57.40 ± 5.69) years; portal hypertension symptoms were 22 hemorrhages, 13 ascites, and 15 hemorrhages and ascites. The two groups' general data were comparable (P > 0.05).

Inclusion criteria

(1) Patients who satisfied the relevant standards in the "Guidelines for the Diagnosis and Treatment of Primary Liver Cancer"[9]; (2) Patients were diagnosed with liver cancer complicated with portal hypertension by clinicopathological and imaging examinations, and gastroscopy revealed active gastroesophageal venous active bleeding and a hepatic venous pressure gradient > 5 mmHg; and (3) Complete clinical data.

Exclusion criteria

(1) Patients with diffuse liver cancer, extrahepatic metastasis, or history of liver cancer surgery; (2) Expected survival time < 3 months; (3) Patients suffering from other cancerous tumors; (4) Individuals suffering from systemic infections; (5) Individuals who experienced disturbance of consciousness; and (6) Patients who experienced allergies triggered by the drugs utilized in this study.

Methods

The enrolled patients were screened for one month at our hospital before being included in the study, and each included patient was numbered. The research group received RFA in combination with sorafenib, while the control group received RFA. All the data were collected after admission and were accessed for study purposes in January 2023.

RFA therapy

A radiofrequency therapeutic instrument (CTRF220, Covidien, United States) was used for treatment, the output power was 200 W, the frequency was set to 480 kHz, and the electrode diameter was set to 1.2 mm. Patients with multiple tumors were treated with a multihook probe. Patients were placed in the supine or prone position, and multislice spiral CT was used to locate the tumor site. The puncture point on the body surface and the puncture direction were selected, and the puncture site was anesthetized with 10 mL of 2% lidocaine. RFA treatment was performed according to the tumor size after the lesion was punctured with the ablation electrode needle, and the treatment time was 8-12 min. The ablation area was 1-2 cm larger than the lesion area to ensure that the tumor tissue could be completely ablated and that the infiltrated part was killed. After RFA treatment, a CT scan was again performed to observe the effect of tumor ablation.

Sorafenib treatment

Sorafenib (Chongqing Yaoyou Pharmaceutical Co., Ltd., SFDA approval number: H20203403) was given orally 14 days before RFA treatment (400 mg/time) twice daily. After oral administration of sorafenib, adverse reactions were assessed as per the Common Terminology Criteria for Adverse Events of National Cancer Institutes[10]. If there was no adverse reaction, the drug dose was maintained until 1-2 d before the operation; if there was an adverse reaction, the dose was halved; if there was a grade 3 or 4 adverse reaction, the drug was stopped, and RFA was performed after 1-2 d of drug withdrawal. If the Child-Pugh grade was A or B after RFA and there was no serious complication, sorafenib was given orally 3-7 d after the operation (400 mg once a day). If no symptoms of discomfort occurred, a dose of 400 mg/time was given 7 d later, two times a day. If there were grade 3-4 adverse reactions, the drug was suspended, and when the adverse reactions were reduced to grade 2 or below, the drug was restored to 400 mg/time, twice/day or 400 mg/time, once/day.

Observation indicators

(1) Short-term efficacy; (2) Comparison of liver function and portal hypertension status. The detection of aspartate aminotransferase (AST) and glutamate alanine aminotransferase (ALT) was performed *via* an automatic biochemical analyzer. The AST and ALT levels before and after treatment were compared between the two groups. The portal vein pressure was compared between the two groups; (3) Comparison of liver cancer markers The levels of alpha-fetoprotein (AFP), glypican-3 (GPC-3) and AFP-L3 were determined *via* ELISA. The levels of AFP, GPC-3 and AFP-L3 before and after treatment were compared between the two groups; (4) Adverse reactions; and (5) Comparison of the 3-year survival

rate between the two groups. Univariate analysis of the survival and non-surviving groups Basic data such as age, Child-Pugh grade, history of hepatitis, number of tumors, tumor size, use of sorafenib, stage of liver cancer, histological differentiation, and history of splenectomy were compared between the survival and non-surviving groups. Multivariate analysis of the survival and non-surviving groups. To analyze the independent risk factors for poor prognosis in patients with liver cancer complicated by portal hypertension, multivariate logistic regression was employed.

Efficacy evaluation criteria

The efficacy of the WHO solid tumor evaluation criteria[11] was used to evaluate the efficacy of the treatment. Complete remission (CR) was defined as follows: Tumor disappeared completely; partial response (PR): Tumor regression area > 50% and no new lesions; no response: Tumor regression area ≤ 50% or increased area ≤ 25%; and progressed disease: Increased area > 50%. The total effectiveness was calculated as CR + PR.

Statistical methods

SPSS 20.0 statistical software was used to analyze and process the collected data. The measurement data are presented as mean ± SD, and for comparisons between the groups, the independent sample *t* test was used, while the paired t test was used for comparisons within the groups prior to and following the treatment. Count data are presented as the frequency or composition ratio, and the χ^2 test was used for comparison. Logistic multivariate regression was used to analyze the independent risk factors for poor prognosis in patients suffering from liver cancer complicated by portal hypertension. A value of $P < 0.05$ indicated a statistically significant difference.

RESULTS

Comparing the clinical efficacy of the two treatments

The research group's total effective rate (82.00%) was greater than that of the control group (56.00%), with statistically significant differences between the two groups ($P < 0.05$). As illustrated in Table 1.

Comparing liver function and portal venous pressure between the two groups before and after treatment

Prior to treatment, there were no considerable differences in ALT or AST levels or portal venous pressure between the two groups ($P > 0.05$). Following treatment, the ALT and AST levels in both groups increased, and the portal venous pressure was reduced. The improvement in each index was greater in the research group than in the control group. The differences were statistically significant ($P < 0.05$). As illustrated in Table 2.

Comparison of liver cancer marker levels between the two groups before and after treatment

Prior to treatment, there was no considerable difference in the AFP, GPC-3, or AFP-L3 Levels ($P > 0.05$); following treatment, the AFP, GPC-3 and AFP-L3 Levels decreased in both groups, and the levels in the research group were significantly lower than those in the control group ($P < 0.05$). As illustrated in Table 3, Figure 1.

Comparing the adverse reactions between the two groups

Instances of diarrhea, rash, nausea, vomiting and fatigue were significantly greater in the research group than in the control group ($P < 0.05$). As demonstrated in Table 4.

Comparison of 1-, 2-, and 3-year survival rates between the two groups

The 1-, 2-, and 3-year survival rates of the research group (94.00%, 84.00%, and 72.00%, respectively) were significantly greater than those of the control group (80.00%, 64.00%, and 40.00%, respectively; $P < 0.05$). As illustrated in Table 5, Figure 2.

Univariate analysis of the survival group and non-surviving group

Significant differences were observed between the survival group and the non-surviving group in terms of basic data such as Child-Pugh grade, history of hepatitis, number of tumors, tumor size, use of sorafenib, stage of liver cancer, histological differentiation, and previous splenectomy ($P < 0.05$). As illustrated in Table 6.

Logistic multivariate regression analysis of poor prognosis in patients with liver cancer complicated with portal hypertension

The items with statistically significant differences in the above factors were included in the multivariate logistic regression model, with survival at three years of follow-up as the dependent variable and the items with statistically significant differences as the independent variable. The values were assigned as follows: Child-Pugh grade (grade A = 0, grade B = 1), history of hepatitis (none = 0, yes = 1), number of tumors (1 = 0, ≥ 2 = 1), tumor size (< 6 = 0, 6-10 = 1), use of sorafenib (yes = 0, no = 1), stage of liver cancer (III B = 0, III C = 1), histological differentiation (high = 0, low-moderator necrosis = 1), and previous splenectomy (none = 0, yes = 1). Logistic regression analysis demonstrated that high Child-Pugh grade, tumor size (6–10 cm), history of hepatitis, no use of sorafenib, liver cancer stage IIIC, and previous splenectomy were independent risk factors for poor prognosis in patients with liver cancer complicated with portal hypertension ($P < 0.05$). As demonstrated in Table 7.

Table 1 Comparison of the clinical efficacy of the two treatment regimens [*n* (%)]

Group	CR	PR	NR	PD	Total effective rate
Research group (n = 50)	7 (14.00)	34 (68.00)	6 (12.00)	3 (6.00)	41 (82.00)
Control group (n = 50)	4 (8.00)	24 (48.00)	17 (34.00)	5 (10.00)	28 (56.00)
χ^2 value					7.901
P value					0.005

CR: Complete remission; PR: Partial response; NR: No response; PD: Progressed disease.

Table 2 Comparison of liver function and portal venous pressure between the two groups before and after treatment (mean ± SD)

Group	ALT (U/L)		AST (U/L)		Portal venous pressure (cm H_2O)	
	Before treatment	After treatment	Before treatment	After treatment	Before treatment	After treatment
Research group (n = 50)	40.06 ± 6.15	71.45 ± 9.85[a]	53.16 ± 6.98	75.90 ± 10.09[a]	39.71 ± 7.56	28.93 ± 5.98[a]
Control group (n = 50)	40.99 ± 7.51	89.27 ± 11.26[a]	51.21 ± 9.32	95.45 ± 9.29[a]	39.83 ± 5.15	31.51 ± 5.88[a]
t value	0.676	8.425	1.184	10.076	0.089	2.174
P value	0.501	< 0.001	0.240	<0.001	0.929	0.032

[a]P < 0.05 when compared to the same group prior to treatment.
ALT: Alanine aminotransferase; AST: Aspartate aminotransferase.

Table 3 Comparison of liver cancer marker levels before and after treatment between the two groups (mean ± SD)

Group	AFP (ug/L)		GPC-3 (ng/mL)		AFP-L3 (ng/L)	
	Before treatment	After treatment	Before treatment	After treatment	Before treatment	After treatment
Research group (n = 50)	645.88 ± 56.05	463.12 ± 40.45[a]	11.52 ± 2.88	6.46 ± 1.43[a]	1751.54 ± 214.99	867.26 ± 153.14[a]
Control group (n = 50)	655.80 ± 53.69	563.21 ± 41.46[a]	11.89 ± 2.58	4.84 ± 1.26[a]	1787.74 ± 177.19	1179.48 ± 175.10[a]
t value	0.904	12.220	0.665	5.975	0.919	9.491
P value	0.368	< 0.001	0.508	< 0.001	0.360	< 0.001

[a]P < 0.05 when compared to the same group prior to treatment.
AFP: Alpha-fetoprotein; GPC-3: Glypican-3.

Table 4 Comparison of adverse reactions between the two groups [*n* (%)]

Group	Diaphragm injury	Diarrhea	Rash	Portal vein and biliary tract injury	Gastrointestinal bleeding	Nausea and vomiting	Fatigue
Research group (n = 50)	3 (6.00)	14 (28.00)	20 (40.00)	13 (26.00)	5 (10.00)	9 (18.00)	33 (66.00)
Control group (n = 50)	1 (2.00)	2 (4.00)	2 (4.00)	10 (20.00)	3 (6.00)	1 (2.00)	10 (20.00)
χ^2 value	1.042	10.714	18.881	0.508	0.543	7.111	21.583
P value	0.307	0.001	< 0.001	0.476	0.461	0.008	< 0.001

DISCUSSION

Currently, the occurrence of liver cancer is increasing annually, and approximately 70%-90% of liver cancer patients are complicated with cirrhosis[12,13]. The common causes of liver cancer complicated with portal hypertension are as follows: Liver cancer usually develops from cirrhosis, which can cause portal hypertension; the formation of arteriovenous fistula in the tumor body can lead to increased portal vein load; and impaired portal vein patency can increase

Table 5 Comparison of 1-, 2-, and 3-year survival rates between the two groups

Group	1-yr survival rate		2-yr survival rate		3-yr survival rate	
	Number of cases	Survival rate (%)	Number of cases	Survival rate (%)	Number of cases	Survival rate (%)
Research group (n = 50)	47	94.00	42	84.00	36	72.00
Control group (n = 50)	40	80.00	32	64.00	20	40.00
Log-χ^2 value	4.465		5.337		9.223	
P value	0.035		0.021		0.002	

Table 6 Univariate analysis of the survival group and death group [n (%)]

Item	Survival group (n = 56)	Death group (n = 44)	χ^2 value	P value
Age				
≤ 60 yr	43 (76.79)	29 (65.91)	1.446	0.229
> 60 yr	13 (23.21)	15 (34.09)		
Child-Pugh grade				
Grade A	45 (80.36)	23 (52.27)	8.931	0.003
Grade B	11 (19.64)	21 (47.73)		
History of hepatitis				
Yes	18 (32.14)	29 (65.91)	11.278	0.001
None	38 (67.86)	15(34.09)		
Number of tumors				
1	35 (62.50)	15 (34.09)	8.266	0.016
2	16 (28.57)	20 (45.45)		
3	5 (8.93)	9 (20.45)		
Tumor size (cm)				
< 6	49 (87.50)	15 (34.09)	30.506	<0.001
6-10	7 (12.50)	29 (65.91)		
Use of sorafenib				
Yes	36 (64.29)	14 (31.82)	10.390	0.001
No	20 (35.71)	30 (68.18)		
Stage of liver cancer				
IIIB	47 (83.93)	20 (45.45)	16.496	< 0.001
IIIC	9 (16.07)	24 (54.55)		
Histological differentiation				
High	28 (50.00)	14 (31.82)	6.810	0.033
Low-moderate	18 (32.14)	12 (27.27)		
Necrosis	10 (17.86)	18 (40.91)		
Previous splenectomy				
Yes	18 (32.14)	30 (68.18)	12.822	< 0.001
None	38 (67.86)	14 (31.82)		

Table 7 Logistic multivariate regression analysis of poor prognosis in patients with liver cancer complicated with portal hypertension

Item	β	SE	Wald	*P* value	Exp (B)	95%CI
High Child-Pugh grade	1.470	0.738	3.970	0.046	4.349	1.024-18.469
History of hepatitis	2.286	0.803	8.098	0.004	9.833	2.037-47.463
Tumor size (6-10 cm)	2.399	0.788	9.268	0.002	11.008	2.350-51.567
No use of sorafenib	2.483	0.829	8.963	0.003	11.981	2.357-60.884
Liver cancer of stage IIIC	1.900	0.719	6.988	0.008	6.683	1.634-27.329
Previous splenectomy	1.629	0.741	4.835	0.028	5.101	1.194-21.800
Constant	6.685	1.486	20.226	< 0.001	0.001	

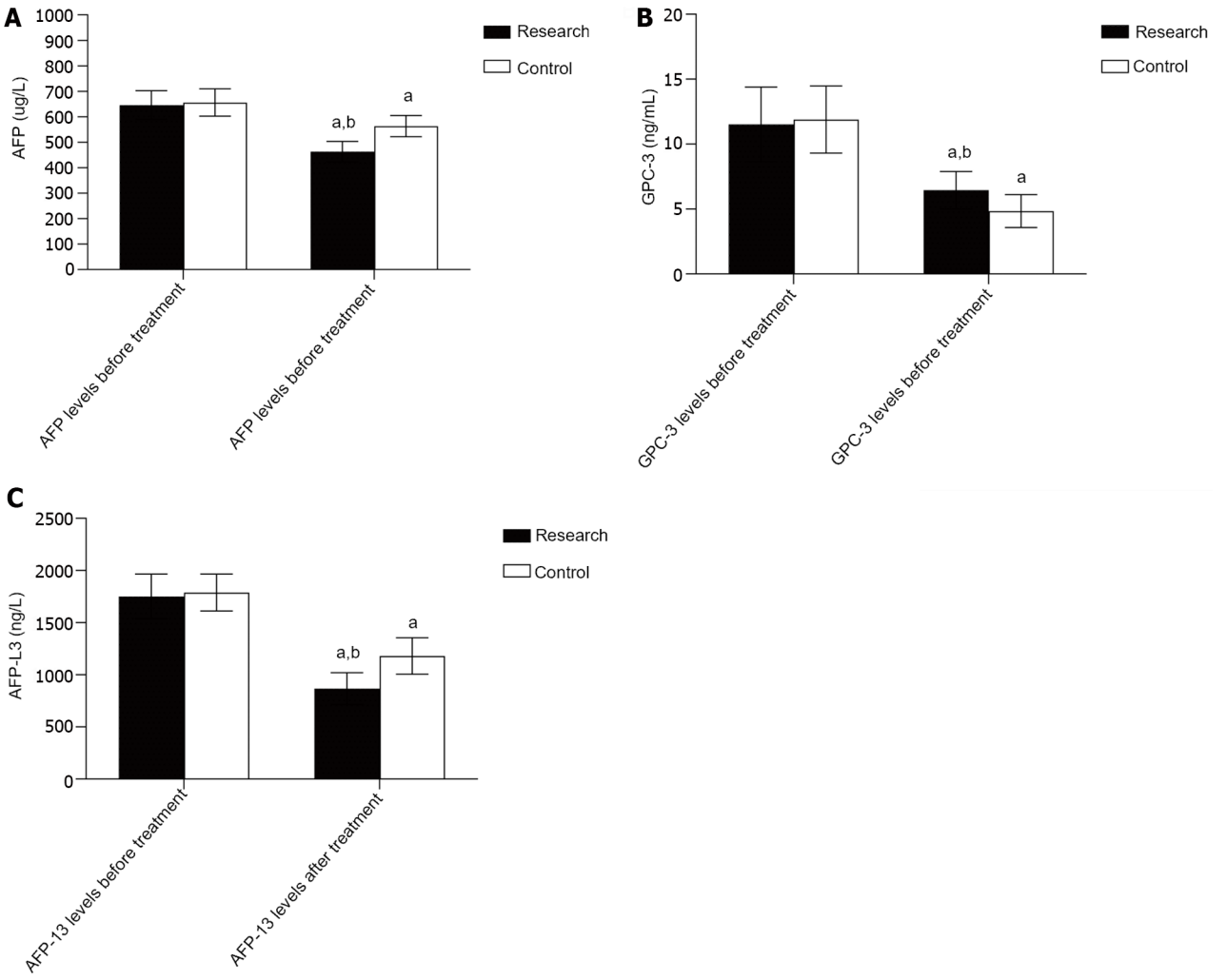

Figure 1 Comparison of alpha-fetoprotein, glypican-3 and alpha-fetoprotein-L3 levels before and after treatment between the two groups.
A: Alpha-fetoprotein (AFP); B: Glypican-3; C: AFP-L3 levels before and after treatment between the two groups. [a]*P* < 0.05 compared with the same group before treatment; [b]*P* < 0.05 compared with the control group after treatment. AFP: Alpha-fetoprotein; GPC-3: Glypican-3.

blood flow resistance. Patients suffering from liver cancer complicated with portal hypertension are at high risk of surgery, and hepatectomy can further lead to increased portal vein pressure. For this reason, the clinical treatment of patients with liver cancer complicated by portal hypertension relies mainly on alleviating portal vein symptoms. RFA is a kind of local ablation therapy. The treatment principle of RFA is to increase the temperature of liver tissue to > 60°C and maintain it at that temperature for a certain time to cause degeneration and irreversible necrosis of cellular proteins. It is suitable for patients with unresectable liver cancer complicated with portal hypertension. Sorafenib is a tyrosinase inhibitor that can reduce the generation of visceral neovascularization and ameliorate portal hypertension. Sorafenib can improve portal hypertension by improving hemodynamics, inhibiting the activation of HSCs, and reducing neovascularization. Several previous studies have applied sorafenib to patients suffering from liver cancer complicated with portal

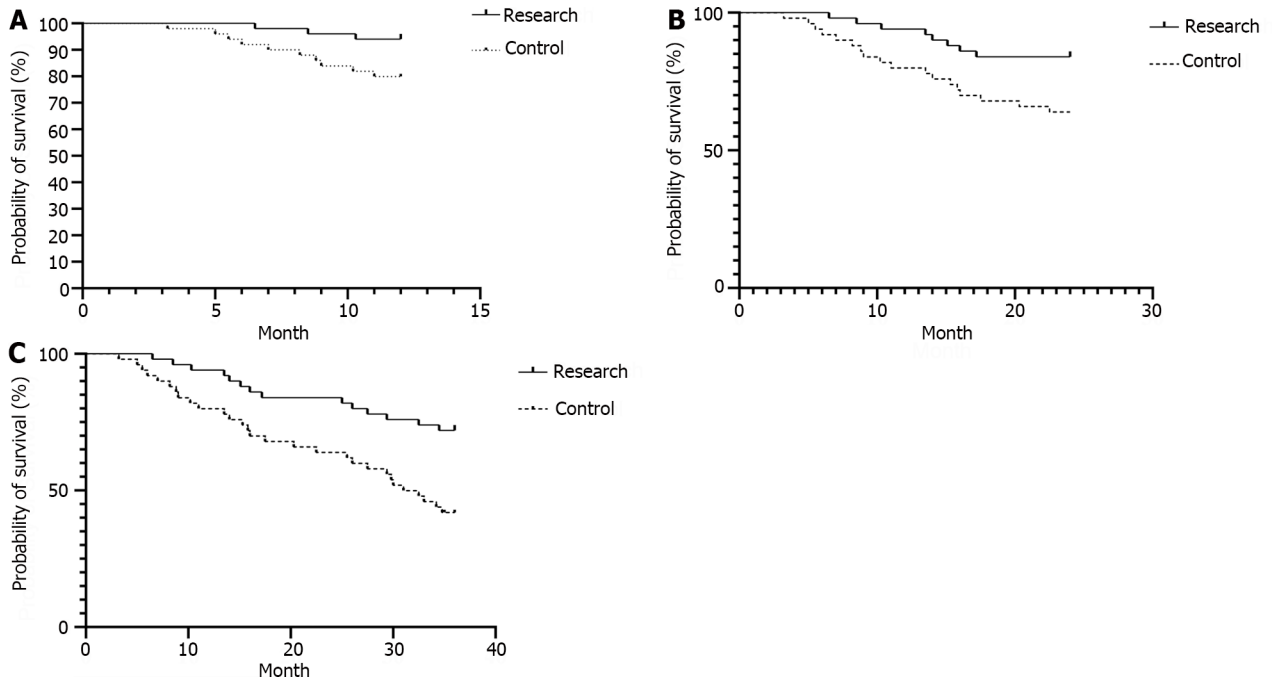

Figure 2 The 1-, 2-, and 3-year follow-up survival curves of the two groups. A: 1-year follow-up survival curves; B: 2-year follow-up survival curves for the two groups; C: 3-year follow-up survival curves for the two groups.

hypertension, and the effect of this treatment is good[14-16]. In the present study, the research group received RFA in combination with sorafenib, while the control group received RFA alone. The outcomes revealed that the research group's total effective rate (82.00%) was greater than that of the control group (56.00%). Following treatment, the ALT and AST levels of both groups were elevated, and the portal vein pressure was reduced. The degree of improvement for every index in the research group was substantially greater than that in the control group ($P < 0.05$). The results indicate that RFA in combination with sorafenib effectively treats liver cancer patients with portal hypertension and can effectively reduce portal vein pressure and improve liver function. This may be because, on the basis of RFA for the treatment of liver cancer, sorafenib, a molecularly targeted drug, blocks the further growth of tumor cells and inhibits the development of tumors and the generation of neovascularization. In addition, sorafenib improved portal hypertension, and the two treatment methods had synergistic effects; thus, the treatment effect was better.

AFP is a common marker of liver cancer and is strongly expressed in the serum of liver cancer patients and is directly associated with their prognosis[17,18]. GPC-3, a heparan sulfate glycoprotein, is expressed at low levels in normal liver tissues and nodular hyperplasia tissues and is overexpressed in patients with liver cancer. The specificity and sensitivity of the serum GPC-3 concentration for diagnosing liver cancer are greater than those of the AFP concentration[19,20]. AFP-L3 is a variant of AFP. According to relevant studies, the value of AFP-L3 in assessing the prognosis of liver cancer patients is greater than that of AFP, and high serum AFP-L3 levels can indicate the occurrence and poor prognosis of liver cancer[21,22]. According to the present research, the improved serum AFP, GPC-3, and AFP-L3 Levels in the present study were greater than those in the control group, implying that RFA in combination with sorafenib is capable of more efficiently protecting the liver function of patients suffering from liver cancer complicated with portal hypertension. Compared to those in the control group, the incidences of diarrhea, rash, nausea, vomiting, and fatigue in the research group were greater than those in the control group. These conditions are all typical adverse reactions to sorafenib, suggesting that changes in patients during the course of their clinical treatment should be closely monitored and that effective measures should be taken for patients with serious adverse reactions in time. In this study, the 1-, 2-, and 3-year survival rates of the individuals in the research group (94.00%, 84.00%, 72.00%) were greater than those of the individuals in the control group (80.00%, 64.00%, 40.00%), indicating that the long-term efficacy of RFA in combination with sorafenib for treating liver cancer patients with portal hypertension is better. Sorafenib can dramatically increase the survival duration of patients who have advanced liver cancer, according to numerous earlier studies[23-25]. The outcomes of the present research are in line with these findings and are related to the antitumor effect of sorafenib and the effect of reducing portal hypertension.

The observed efficacy of combined therapy involving RFA and sorafenib in the treatment of liver cancer complicated by portal hypertension can be attributed to the synergistic actions of these modalities, each targeting specific aspects of disease pathophysiology. RFA, a local ablation therapy, exerts its effects by inducing thermal damage to liver tissue, leading to cellular degeneration and irreversible necrosis. This approach is particularly advantageous in patients with unresectable liver cancer complicated by portal hypertension, where surgical intervention may not be feasible due to the patient's clinical condition. The localized tissue destruction achieved through RFA contributes to a reduction in tumor burden, thereby alleviating portal vein pressure and improving liver function, as evidenced by the observed reduction in transaminase levels and portal venous pressure in the study population.

Concurrently, the incorporation of sorafenib, an oral tyrosine kinase inhibitor, complements the effects of RFA by targeting critical molecular pathways involved in neovascularization and tumor progression. The mechanism of action of sorafenib includes the inhibition of VEGFR and PDGFR, which are known to play pivotal roles in the promotion of tumor angiogenesis and vascular remodeling. By disrupting these signaling pathways, sorafenib not only impedes tumor neovascularization but also exerts modulatory effects on portal hypertension, thereby contributing to the overall improvement in clinical outcomes observed in the present study.

Moreover, the synergy between RFA and sorafenib may extend beyond their individual mechanisms of action. It is plausible that the localized tissue injury caused by RFA creates an environment conducive to the antitumor effects of sorafenib, potentially enhancing its penetration and efficacy within the tumor microenvironment. This interplay between the two treatment modalities underscores the importance of combination strategies in addressing the complex interplay of factors associated with liver cancer complicating portal hypertension, with the potential to offer a more comprehensive and efficacious approach to disease management.

In the present research, all patients underwent a three-year follow-up to observe their prognosis, and based on their survival status, they were separated into a survival group and a death group. The basic data of the patients were analyzed *via* univariate analysis. Considerable differences were found in Child-Pugh grade, history of hepatitis, number of tumors, tumor size, use of sorafenib, stage of liver cancer, histological differentiation, previous splenectomy, and other basic data between the survival and death groups ($P < 0.05$), suggesting that Child-Pugh grade, history of hepatitis, number of tumors, tumor size, use of sorafenib, stage of liver cancer, histological differentiation and previous splenectomy are strongly associated with the prognosis of liver cancer patients complicated with portal hypertension. Logistic multivariate regression analysis demonstrated that high Child-Pugh grade, tumor size (6–10 cm), history of hepatitis, no use of sorafenib, liver cancer stage IIIC, and previous splenectomy were independent risk factors for poor prognosis in patients with liver cancer complicated with portal hypertension. A high Child-Pugh grade, large tumor diameter, history of hepatitis, and liver cancer stage IIIC indicate severe disease, so the prognosis is poor. The patients who did not use sorafenib composed the control group in this research, and the treatment effect in the control group was worse than that in the research group; thus, the prognosis was poor. Patients with portal hypertension often exhibit hypersplenism, and a history of previous splenectomy indicates that portal hypertension is more serious in these patients, so the prognosis is poor. It is suggested that effective treatment and nursing measures be taken to improve the prognosis of patients with high Child-Pugh grade, large tumor size (6-10 cm), history of hepatitis, no use of sorafenib, liver cancer of stage IIIC, or previous splenectomy.

The findings of this study contribute to elucidating the efficacy and potential challenges associated with combined therapy comprising RFA and sorafenib for the treatment of liver cancer complicated by portal hypertension. While the results indicate a promising improvement in patient outcomes, it is essential to acknowledge the observed increase in adverse reactions, particularly in the form of diarrhea, rash, nausea, vomiting, and fatigue, within the research group. These adverse reactions have been documented as common side effects of sorafenib therapy. Therefore, in light of these findings, it is imperative to address potential strategies for mitigating these adverse events to ensure the overall well-being and treatment adherence of patients.

The management of adverse reactions related to sorafenib therapy is paramount for ensuring the continued effectiveness of the treatment approach. Given the adverse reactions identified in the research group, it is crucial for health care providers to proactively monitor and manage these side effects to optimize patient tolerance and compliance. Strategies for mitigation may include personalized patient education on potential side effects, proactive symptom management, dose adjustments based on individual tolerability, and prompt intervention for severe adverse events. Additionally, comprehensive supportive care measures, such as nutritional support and psychological counseling, can play a significant role in contributing to the overall well-being of patients receiving this combined therapeutic approach.

Furthermore, future research endeavors should focus on investigating novel approaches to reduce the incidence and severity of these adverse events, potentially through the exploration of alternative dosing regimens, the use of adjunctive medications for symptom management, or the identification of predictive markers for susceptibility to specific adverse reactions. By addressing these challenges, health care providers can work toward optimizing the therapeutic benefits of RFA in combination with sorafenib while minimizing the impact of treatment-associated adverse reactions on patient quality of life.

It is also necessary to acknowledge the limitation of the sample size, which underscores the need for a more comprehensive investigation to establish stronger conclusions. While the present study offers valuable insights, a larger-scale investigation is warranted to reinforce the robustness and generalizability of the findings. Therefore, conducting a study with a larger sample size would address this limitation and ensure broader applicability of the results, enhancing the overall strength of the conclusions.

CONCLUSION

In conclusion, RFA in combination with sorafenib can successfully enhance patient liver function with good short- and long-term efficacy and has clinical therapeutic potential in the treatment of liver cancer complicated by portal hypertension. The disadvantage of the present research is the small sample size, which may produce a risk of selection bias; therefore, further research should be conducted with a larger sample size.

ARTICLE HIGHLIGHTS

Research background

Liver cancer, frequently arising from cirrhosis, presents with accompanying portal hypertension in a substantial portion of cases. Current treatments are limited due to the challenging nature of surgical interventions and poor physical tolerance of affected patients. Radiofrequency ablation (RFA) is a known therapeutic approach, but its application in liver cancer complicated by portal hypertension has been insufficiently explored.

Research motivation

Given the complexity and limited treatment options for patients with liver cancer and portal hypertension, investigating novel therapeutic strategies is crucial. Understanding the potential benefits of combining RFA with sorafenib in this context could offer improved efficacy and survival outcomes.

Research objectives

This study aimed to assess the effectiveness of RFA in combination with sorafenib for patients with liver cancer complicated by portal hypertension, discern prognostic factors, and evaluate their impact on patient outcomes. The study also sought to analyze the potential synergistic effects of both treatments and their impact on liver function and survival rates.

Research methods

A total of 100 patients were analyzed and categorized into a research group (RFA with sorafenib) and a control group (RFA alone). Short-term efficacy, liver function, portal hypertension, cancer markers, adverse reactions, and survival rates were assessed. Multivariate logistic regression analysis was employed to identify independent risk factors for poor patient prognosis.

Research results

The combined RFA and sorafenib treatment demonstrated a significantly higher total effective rate compared to RFA alone, effectively reducing portal vein pressure, improving liver function, and lowering liver cancer markers. Patients in the combined treatment group exhibited higher survival rates at 1-, 2-, and 3-year follow-ups, highlighting the potential long-term benefits of this approach.

Research conclusions

The combination of RFA and sorafenib yields promising results in treating liver cancer with portal hypertension, offering improved short- and long-term efficacy. Prognostic factors such as Child-Pugh grade, tumor size, history of hepatitis, and the use of sorafenib were identified as significant predictors of patient outcomes, providing valuable insights for clinical management.

Research perspectives

These findings underscore the potential clinical therapeutic value of combining RFA with sorafenib for liver cancer complicated by portal hypertension. However, further research with larger sample sizes is warranted to validate these outcomes and establish guidelines for optimizing treatment protocols and patient care.

FOOTNOTES

Co-corresponding authors: Li-Min Yang and Lian-Feng Zhang.

Author contributions: Yang LM and Zhang LF contributed equally to this work and are co-corresponding authors, including those involved in the design of the study, the acquisition and analysis of the data from the experiments, and the writing of the manuscript. Yang LM, Zhang LF and Wang HJ designed the experiment and conducted the clinical data collection; Li SL and Gan GH performed the postoperative follow-up and recorded the data; Deng WW and Chang YS conducted a number of collations and statistical analyses; all the authors read and approved the final manuscript.

Institutional review board statement: This study was approved by the Ethics Committee of the First Affiliated Hospital of Zhengzhou University, and the need to provide informed consent was waived.

Informed consent statement: After review by the Ethics Committee, a waiver of informed consent was granted for this subject.

Conflict-of-interest statement: The author(s) declare no potential conflicts of interest with respect to the research, authorship, and/or publication of this article.

Data sharing statement: All the data generated or analyzed during this study are included in this published article.

Country/Territory of origin: China

ORCID number: Li-Min Yang 0000-0001-5724-379X; Lian-Feng Zhang 0000-0003-0245-3751.

S-Editor: Lin C
L-Editor: A
P-Editor: Cai YX

REFERENCES

1 **Anwanwan D**, Singh SK, Singh S, Saikam V, Singh R. Challenges in liver cancer and possible treatment approaches. *Biochim Biophys Acta Rev Cancer* 2020; **1873**: 188314 [PMID: 31682895 DOI: 10.1016/j.bbcan.2019.188314]
2 **Xu F**, Jin T, Zhu Y, Dai C. Immune checkpoint therapy in liver cancer. *J Exp Clin Cancer Res* 2018; **37**: 110 [PMID: 29843754 DOI: 10.1186/s13046-018-0777-4]
3 **Shen ZF**, Liang X. Current status of radical laparoscopy for treating hepatocellular carcinoma with portal hypertension. *World J Clin Cases* 2021; **9**: 2419-2432 [PMID: 33889608 DOI: 10.12998/wjcc.v9.i11.2419]
4 **Azoulay D**, Ramos E, Casellas-Robert M, Salloum C, Lladó L, Nadler R, Busquets J, Caula-Freixa C, Mils K, Lopez-Ben S, Figueras J, Lim C. Liver resection for hepatocellular carcinoma in patients with clinically significant portal hypertension. *JHEP Rep* 2021; **3**: 100190 [PMID: 33294830 DOI: 10.1016/j.jhepr.2020.100190]
5 **Bai XM**, Cui M, Yang W, Wang H, Wang S, Zhang ZY, Wu W, Chen MH, Yan K, Goldberg SN. The 10-year Survival Analysis of Radiofrequency Ablation for Solitary Hepatocellular Carcinoma 5 cm or Smaller: Primary versus Recurrent HCC. *Radiology* 2021; **300**: 458-469 [PMID: 34003058 DOI: 10.1148/radiol.2021200153]
6 **Lawal G**, Xiao Y, Rahnemai-Azar AA, Tsilimigras DI, Kuang M, Bakopoulos A, Pawlik TM. The Immunology of Hepatocellular Carcinoma. *Vaccines (Basel)* 2021; **9** [PMID: 34696292 DOI: 10.3390/vaccines9101184]
7 **Zhang FW**, Guo PX, Wang X. The analysis of short and long term efficacy of sorafenib combined with TACE in patients with hepatocellular carcinoma complicated with microvascular invasion. *Shanxi Yiyao Zazhi* 2020; **49**: 798-802
8 **Scheiner B**, Pomej K, Kirstein MM, Hucke F, Finkelmeier F, Waidmann O, Himmelsbach V, Schulze K, von Felden J, Fründt TW, Stadler M, Heinzl H, Shmanko K, Spahn S, Radu P, Siebenhüner AR, Mertens JC, Rahbari NN, Kütting F, Waldschmidt DT, Ebert MP, Teufel A, De Dosso S, Pinato DJ, Pressiani T, Meischl T, Balcar L, Müller C, Mandorfer M, Reiberger T, Trauner M, Personeni N, Rimassa L, Bitzer M, Trojan J, Weinmann A, Wege H, Dufour JF, Peck-Radosavljevic M, Vogel A, Pinter M. Prognosis of patients with hepatocellular carcinoma treated with immunotherapy - development and validation of the CRAFITY score. *J Hepatol* 2022; **76**: 353-363 [PMID: 34648895 DOI: 10.1016/j.jhep.2021.09.035]
9 Chinese guidelines for diagnosis and treatment of primary lung cancer 2018 (English version). *Chin J Cancer Res* 2019; **31**: 1-28 [PMID: 30996564 DOI: 10.21147/j.issn.1000-9604.2019.01.01]
10 **Freites-Martinez A**, Santana N, Arias-Santiago S, Viera A. Using the Common Terminology Criteria for Adverse Events (CTCAE - Version 5.0) to Evaluate the Severity of Adverse Events of Anticancer Therapies. *Actas Dermosifiliogr (Engl Ed)* 2021; **112**: 90-92 [PMID: 32891586 DOI: 10.1016/j.ad.2019.05.009]
11 **Wahl RL**, Jacene H, Kasamon Y, Lodge MA. From RECIST to PERCIST: Evolving Considerations for PET response criteria in solid tumors. *J Nucl Med* 2009; **50** Suppl 1: 122S-150S [PMID: 19403881 DOI: 10.2967/jnumed.108.057307]
12 **Mohr R**, Özdirik B, Lambrecht J, Demir M, Eschrich J, Geisler L, Hellberg T, Loosen SH, Luedde T, Tacke F, Hammerich L, Roderburg C. From Liver Cirrhosis to Cancer: The Role of Micro-RNAs in Hepatocarcinogenesis. *Int J Mol Sci* 2021; **22** [PMID: 33540837 DOI: 10.3390/ijms22031492]
13 **Moon AM**, Singal AG, Tapper EB. Contemporary Epidemiology of Chronic Liver Disease and Cirrhosis. *Clin Gastroenterol Hepatol* 2020; **18**: 2650-2666 [PMID: 31401364 DOI: 10.1016/j.cgh.2019.07.060]
14 **Hidaka H**, Uojima H, Nakazawa T, Shao X, Hara Y, Iwasaki S, Wada N, Kubota K, Tanaka Y, Shibuya A, Kanoh Y, Kokubu S, Koizumi W. Portal hemodynamic effects of lenvatinib in patients with advanced hepatocellular carcinoma: A prospective cohort study. *Hepatol Res* 2020; **50**: 1083-1090 [PMID: 32515895 DOI: 10.1111/hepr.13531]
15 **Ma R**, Chen J, Liang Y, Lin S, Zhu L, Liang X, Cai X. Sorafenib: A potential therapeutic drug for hepatic fibrosis and its outcomes. *Biomed Pharmacother* 2017; **88**: 459-468 [PMID: 28122312 DOI: 10.1016/j.biopha.2017.01.107]
16 **Cerrito L**, Annicchiarico BE, Iezzi R, Gasbarrini A, Pompili M, Ponziani FR. Treatment of hepatocellular carcinoma in patients with portal vein tumor thrombosis: Beyond the known frontiers. *World J Gastroenterol* 2019; **25**: 4360-4382 [PMID: 31496618 DOI: 10.3748/wjg.v25.i31.4360]
17 **Liu S**, Wang M, Zheng C, Zhong Q, Shi Y, Han X. Diagnostic value of serum glypican-3 alone and in combination with AFP as an aid in the diagnosis of liver cancer. *Clin Biochem* 2020; **79**: 54-60 [PMID: 32087138 DOI: 10.1016/j.clinbiochem.2020.02.009]
18 **Özdemir F**, Baskiran A. The Importance of AFP in Liver Transplantation for HCC. *J Gastrointest Cancer* 2020; **51**: 1127-1132 [PMID: 32845425 DOI: 10.1007/s12029-020-00486-w]
19 **Liu Y**, Tan M, Fang C, Chen X, Liu H, Feng Y, Zhang Y, Min W. A novel multifunctional gold nanorod-mediated and tumor-targeted gene silencing of GPC-3 synergizes photothermal therapy for liver cancer. *Nanotechnology* 2021; **32**: 175101 [PMID: 33445163 DOI: 10.1088/1361-6528/abdbed]
20 **Makkouk A**, Yang XC, Barca T, Lucas A, Turkoz M, Wong JTS, Nishimoto KP, Brodey MM, Tabrizizad M, Gundurao SRY, Bai L, Bhat A, An Z, Abbot S, Satpayev D, Aftab BT, Herrman M. Off-the-shelf Vδ1 gamma delta T cells engineered with glypican-3 (GPC-3)-specific chimeric antigen receptor (CAR) and soluble IL-15 display robust antitumor efficacy against hepatocellular carcinoma. *J Immunother Cancer* 2021; **9** [PMID: 34916256 DOI: 10.1136/jitc-2021-003441]

21 **Park SJ**, Jang JY, Jeong SW, Cho YK, Lee SH, Kim SG, Cha SW, Kim YS, Cho YD, Kim HS, Kim BS, Park S, Bang HI. Usefulness of AFP, AFP-L3, and PIVKA-II, and their combinations in diagnosing hepatocellular carcinoma. *Medicine (Baltimore)* 2017; **96**: e5811 [PMID: 28296720 DOI: 10.1097/MD.0000000000005811]

22 **Zhou JM**, Wang T, Zhang KH. AFP-L3 for the diagnosis of early hepatocellular carcinoma: A meta-analysis. *Medicine (Baltimore)* 2021; **100**: e27673 [PMID: 34713864 DOI: 10.1097/MD.0000000000027673]

23 **Ren Z**, Xu J, Bai Y, Xu A, Cang S, Du C, Li Q, Lu Y, Chen Y, Guo Y, Chen Z, Liu B, Jia W, Wu J, Wang J, Shao G, Zhang B, Shan Y, Meng Z, Gu S, Yang W, Liu C, Shi X, Gao Z, Yin T, Cui J, Huang M, Xing B, Mao Y, Teng G, Qin Y, Xia F, Yin G, Yang Y, Chen M, Wang Y, Zhou H, Fan J; ORIENT-32 study group. Sintilimab plus a bevacizumab biosimilar (IBI305) versus sorafenib in unresectable hepatocellular carcinoma (ORIENT-32): a randomised, open-label, phase 2-3 study. *Lancet Oncol* 2021; **22**: 977-990 [PMID: 34143971 DOI: 10.1016/S1470-2045(21)00252-7]

24 **Kudo M**, Ueshima K, Ikeda M, Torimura T, Tanabe N, Aikata H, Izumi N, Yamasaki T, Nojiri S, Hino K, Tsumura H, Kuzuya T, Isoda N, Yasui K, Aino H, Ido A, Kawabe N, Nakao K, Wada Y, Yokosuka O, Yoshimura K, Okusaka T, Furuse J, Kokudo N, Okita K, Johnson PJ, Arai Y; TACTICS study group. Randomised, multicentre prospective trial of transarterial chemoembolisation (TACE) plus sorafenib as compared with TACE alone in patients with hepatocellular carcinoma: TACTICS trial. *Gut* 2020; **69**: 1492-1501 [PMID: 31801872 DOI: 10.1136/gutjnl-2019-318934]

25 **He M**, Li Q, Zou R, Shen J, Fang W, Tan G, Zhou Y, Wu X, Xu L, Wei W, Le Y, Zhou Z, Zhao M, Guo Y, Guo R, Chen M, Shi M. Sorafenib Plus Hepatic Arterial Infusion of Oxaliplatin, Fluorouracil, and Leucovorin *vs* Sorafenib Alone for Hepatocellular Carcinoma With Portal Vein Invasion: A Randomized Clinical Trial. *JAMA Oncol* 2019; **5**: 953-960 [PMID: 31070690 DOI: 10.1001/jamaoncol.2019.0250]

World Journal of Gastroenterology

Submit a Manuscript: https://www.f6publishing.com

World J Gastroenterol 2024 March 21; 30(11): 1545-1555

DOI: 10.3748/wjg.v30.i11.1545

ISSN 1007-9327 (print) ISSN 2219-2840 (online)

ORIGINAL ARTICLE

Clinical Trials Study

Effect of *Aspergillus niger* prolyl endopeptidase in patients with celiac disease on a long-term gluten-free diet

Juan Pablo Stefanolo, Verónica Segura, Martina Grizzuti, Abel Heredia, Isabel Comino, Ana Florencia Costa, Roberto Puebla, María Paz Temprano, Sonia Isabel Niveloni, Gabriel de Diego, María E Oregui, Edgardo Gustavo Smecuol, Mauricio C de Marzi, Elena F Verdú, Carolina Sousa, Julio César Bai

Specialty type: Gastroenterology and hepatology

Provenance and peer review: Invited article; Externally peer reviewed.

Peer-review model: Single blind

Peer-review report's scientific quality classification

Grade A (Excellent): 0
Grade B (Very good): B
Grade C (Good): 0
Grade D (Fair): 0
Grade E (Poor): 0

P-Reviewer: de Moraes JB, Brazil

Received: December 8, 2023
Peer-review started: December 8, 2023
First decision: December 21, 2023
Revised: December 31, 2023
Accepted: February 18, 2024
Article in press: February 18, 2024
Published online: March 21, 2024

Juan Pablo Stefanolo, Roberto Puebla, María Paz Temprano, Sonia Isabel Niveloni, Edgardo Gustavo Smecuol, Small Bowel Section, Department of Medicine, Gastroenterology Hospital of Buenos Aires "Dr. C. Bonorino Udaondo", Buenos Aires 1264, Argentina

Verónica Segura, Abel Heredia, Isabel Comino, Carolina Sousa, Department of Microbiology and Parasitology, Faculty of Pharmacy, University of Seville, Seville 41080, Spain

Martina Grizzuti, Ana Florencia Costa, María E Oregui, Julio César Bai, Department of Medicine, Dr. C. Bonorino Udaondo Gastroenterology Hospital, Buenos Aires 1264, Argentina

Gabriel de Diego, Mauricio C de Marzi, Basic and Applied Research Group in Immunology and Bioactives (GIBAIB), Institute of Ecology and Sustainable Development (INEDES), National University of Lujan, Luján 6700, Buenos Aires, Argentina

Elena F Verdú, Department of Medicine, Farncombe Family Digestive Health Research Institute, McMaster University, Hamilton L8S 4L8, Ontario, Canada

Julio César Bai, Facultad de Medicina, Universidad del Salvador, Buenos Aires C1051ABB, Argentina

Corresponding author: Julio César Bai, MD, Emeritus Professor of Medicine, Facultad de Medicina, Universidad del Salvador, 640 Rodriguez Peña, Buenos Aires C1051ABB, Argentina. jbai@intramed.net

Abstract

BACKGROUND

The gluten-free diet (GFD) has limitations, and there is intense research in the development of adjuvant therapies.

AIM

To examine the effects of orally administered *Aspergillus niger* prolyl endopeptidase protease (AN-PEP) on inadvertent gluten exposure and symptom prevention in adult celiac disease (CeD) patients following their usual GFD.

METHODS

This was an exploratory, double-blind, randomized, placebo-controlled trial that

enrolled CeD patients on a long-term GFD. After a 4-wk run-in period, patients were randomized to 4 wk of two AN-PEP capsules (GliadinX; AVI Research, LLC, United States) at each of three meals per day or placebo. Outcome endpoints were: (1) Average weekly stool gluten immunogenic peptides (GIP) between the run-in and end of treatments and between AN-PEP and placebo; (2) celiac symptom index (CSI); (3) CeD-specific serology; and (4) quality of life. Stool samples were collected for GIP testing by ELISA every Tuesday and Friday during run-ins and treatments.

RESULTS

Forty patients were randomized for the intention-to-treat analysis, and three were excluded from the per-protocol assessment. Overall, 628/640 (98.1%) stool samples were collected. GIP was undetectable (< 0.08 μg/g) in 65.6% of samples, and no differences between treatment arms were detected. Only 0.5% of samples had GIP concentrations sufficiently high (> 0.32 μg/g) to potentially cause mucosal damage. Median GIP concentration in the AN-PEP arm was 44.7% lower than in the run-in period. One-third of patients exhibiting GIP > 0.08 μg/g during run-in had lower or undetectable GIP after AN-PEP treatment. Compared with the run- in period, the proportion of symptomatic patients (CSI > 38) in the AN-PEP arm was significantly lower ($P < 0.03$). AN-PEP did not result in changes in specific serologies.

CONCLUSION

This exploratory study conducted in a real-life setting revealed high adherence to the GFD. The AN-PEP treatment did not significantly reduce the overall GIP stool concentration. However, given the observation of a significantly lower prevalence of patients with severe symptoms in the AN-PEP arm, further clinical research is warranted.

Key Words: Celiac disease; *Aspergillus niger* prolyl endoprotease; Gluten immunogenic peptides; Trial; Symptoms; Real-life trial

Core Tip: In treated celiac disease (CeD) patients, exposure to gluten due to both voluntary and involuntary dietary lapses is prevalent and often leads to persistent symptoms despite adherence to a gluten-free diet. The potential of oral administration of *Aspergillus niger* prolyl endopeptidase (AN-PEP) in preventing the effects of inadvertent gluten exposure, as confirmed by gluten immunogenic peptide (GIP) stool excretion, and reducing CeD-specific symptoms in adults remains uncertain. Our study findings indicate that while AN-PEP did not significantly reduce overall GIP stool excretion, it notably lowered the prevalence of severe symptoms compared to the placebo arm.

Citation: Stefanolo JP, Segura V, Grizzuti M, Heredia A, Comino I, Costa AF, Puebla R, Temprano MP, Niveloni SI, de Diego G, Oregui ME, Smecuol EG, de Marzi MC, Verdú EF, Sousa C, Bai JC. Effect of *Aspergillus niger* prolyl endopeptidase in patients with celiac disease on a long-term gluten-free diet. *World J Gastroenterol* 2024; 30(11): 1545-1555
URL: https://www.wjgnet.com/1007-9327/full/v30/i11/1545.htm
DOI: https://dx.doi.org/10.3748/wjg.v30.i11.1545

INTRODUCTION

Celiac disease (CeD) is a systemic autoimmune disorder that primarily affects the small intestine and is caused by gluten exposure in genetically susceptible people[1]. Currently, its only treatment is a strict gluten-free diet (GFD), which results in gradual improvement of symptoms and mucosal damage[2]. Gluten elimination is a difficult, time-consuming, and expensive process for patients[3]. Despite a GFD being notably effective in the long term for most patients, some may be considered non-responsive or experience symptom relapse and/or persistent enteropathy despite long-term adherence to a GFD[1,2]. Exposure to gluten caused by voluntary and involuntary dietary lapses is common and is thought to be responsible for most cases of persistent symptoms, low quality of life (QoL), intestinal mucosal damage, and the risk of complications[4-6]. Such dietary exposure to gluten has been objectively demonstrated by the excretion of gluten immunogenic peptides (GIP)[7,8].

The burden of following a GFD has led to the exploration of various potential therapies to be used alongside the GFD [2,9]. Mammalian enzymes cannot effectively break down proline and glutamine-rich protein sequences, resulting in incomplete degradation of gluten in the intestinal lumen. This exposes the intestinal mucosa to immunogenic gluten peptides, which in CeD will reactivate the disease and gluten-specific T cells[10,11]. Several microbial peptidases have been identified as potentially useful for detoxifying cereal prolamins[12-14]. The different proteases differ in affinities and hydrolysis specificity, as well as in their optimal pHs. One of the first peptidases studied *in vitro* and *in vivo* in pre-clinical studies was a prolyl endopeptidase from the *Aspergillus niger* (*A. niger*) fungus (AN-PEP)[10,15-17]. AN-PEP is optimally active at low pH values typically found in the stomach and is resistant to degradation by pepsin[13,17]. A study

conducted in a dynamic system that resembles the human gastrointestinal tract revealed that AN-PEP can accelerate gluten degradation[18]. A study using a challenge meal with gluten plus AN-PEP found a high rate of hydrolysis with a reduction of gluten-immunogenic peptides in the stomach before reaching the small intestine[12]. A clinical challenge study conducted over a 2-wk period showed that AN-PEP was well tolerated but had no significant advantages over placebo on clinical features or biomarkers[19]. Given that AN-PEP has been approved for marketing as an alimentary supplement, no additional clinical studies have been conducted to demonstrate whether it could be efficacious in other clinical stages of the disease, such as symptomatic patients likely exposed to real-life contamination. Therefore, we explored whether oral administration of AN-PEP prevents the effects of the commonly occurring involuntary gluten exposure, as verified by GIP stool excretion, and the reduction of CeD-specific symptoms in adult CeD patients who continued their usual GFD.

MATERIALS AND METHODS

Study design and enzymatic treatment

This was a real-life exploratory pilot study following a prospective, double-blind, randomized, placebo-controlled design that enrolled adult patients with CeD on a GFD for more than 2 years. Consecutive patients attending our Celiac Disease Clinic at the C. Bonorino Udaondo Gastroenterology Hospital were invited to be screened. CeD patients were enrolled if they met the following criteria: (1) A well-established histological (Marsh's type 3) and serologic diagnosis of CeD; (2) self-considering to be adherent with the GFD for more than 2 years; (3) having at least one bowel movement/day or every other day; (4) being able to provide serum samples at enrollment and the end of the study period; (5) being able to collect and store samples frozen, and transport stool samples to our institution in specially provided containers; and (6) having the ability to respond to symptom and QoL questionnaires. Patients who were unwilling to participate, intentionally ingested gluten, had uncontrolled concomitant disorders (*e.g.*, type I diabetes, hypothyroidism), had type II refractory CeD, or were taking drugs that could potentially affect stool GIP excretion (laxatives, probiotics, *etc*.) were excluded from the study. Patients who met the inclusion and exclusion criteria underwent clinical evaluation, completed the celiac symptom index (CSI) clinical questionnaire and the Short Form-36 (SF-36) QoL questionnaire, and provided blood samples for clinical biochemical and serological determinations at baseline and at the end of the study. After a 4-wk run-in period to achieve stable dietary adherence, patients were assigned to a 4-wk treatment period in which they consumed either two capsules during each of the three main meals/day of AN-PEP (325 mg/capsule containing 70% AN-PEP, 30% maltodextrin, and citric acid) (GliadinX; AVI Research, LLC, New York, NY, United States), or placebo (maltodextrin, citric acid, and microcrystalline cellulose) for 4 consecutive weeks (Figure 1). The protease is an enzyme preparation of prolyl-oligopeptidase produced with a genetically modified *A. niger* strain. This enzyme's composition and production process have been previously reported[19,20]. The dose of AN-PEP administered was the highest dose employed in the study König *et al*[16], which provides 174000 protease picomol IU/meal, where the authors demonstrated that AN-PEP significantly degraded most gluten in the stomach before it entered the duodenum. Other studies have shown that degradation of gluten proteins in the insoluble fraction became evident after 30 min at pH 4, the optimum pH for AN-PEP activity, with the strongest effect observed at a concentration of 20 propyl peptidase units/g gluten[21,22].

CSI questionnaire

The presence and intensity of symptoms were assessed at the time of randomization and at the end of the study using the CSI questionnaire. The CSI is a well-validated questionnaire of 36 items, developed in 2009 by an expert committee and, subsequently, internally and externally validated[23]. The CSI questionnaire includes 16 items, with 11 items evaluating "specific symptoms" related to CeD and five evaluating "general health" parameters. Participants rate each item on a Likert scale ranging from 1 to 5, where 1 represents no symptoms and 5 indicates the highest intensity for the given symptom. In previous comparative clinical studies, we have considered scores > 38 on the CSI to be indicative of a highly symptomatic clinical level of CeD[24]. By assessing symptom presence and intensity using the CSI, we were able to evaluate the impact of the enzyme treatment on symptom improvement and overall patient well-being throughout the study.

Self-administered quality-of-life questionnaire

The impact of the enzyme treatment on patients' QoL was evaluated by assessing parameters and gastrointestinal symptoms using the SF-36 health survey[24]. The SF-36 includes eight sub-dimension measures of functioning and wellness: Physical functioning, role limitations due to physical problems, bodily pain, general health, vitality, social functioning, role limitations due to emotional problems, and mental health. We measured these sub-dimensions at randomization and at the end of the trial and transformed the raw scores into a scale ranging from 0 to 100. A score of 0 indicates the poorest health and QoL, while a score of 100 represents optimal health and QoL. This assessment allowed us to evaluate the impact of the enzyme treatment on various aspects of the patient's well-being and overall QoL.

Stool collection and GIP measurement

During the study, patients were instructed to collect stool samples twice a week (on Tuesdays and Fridays) throughout the two 4-wk periods (run-in and treatment) in both arms. The samples were immediately placed in sealed containers and frozen at -10 °C until they were delivered to our laboratory. Upon arrival at the laboratory, the samples were stored at -20

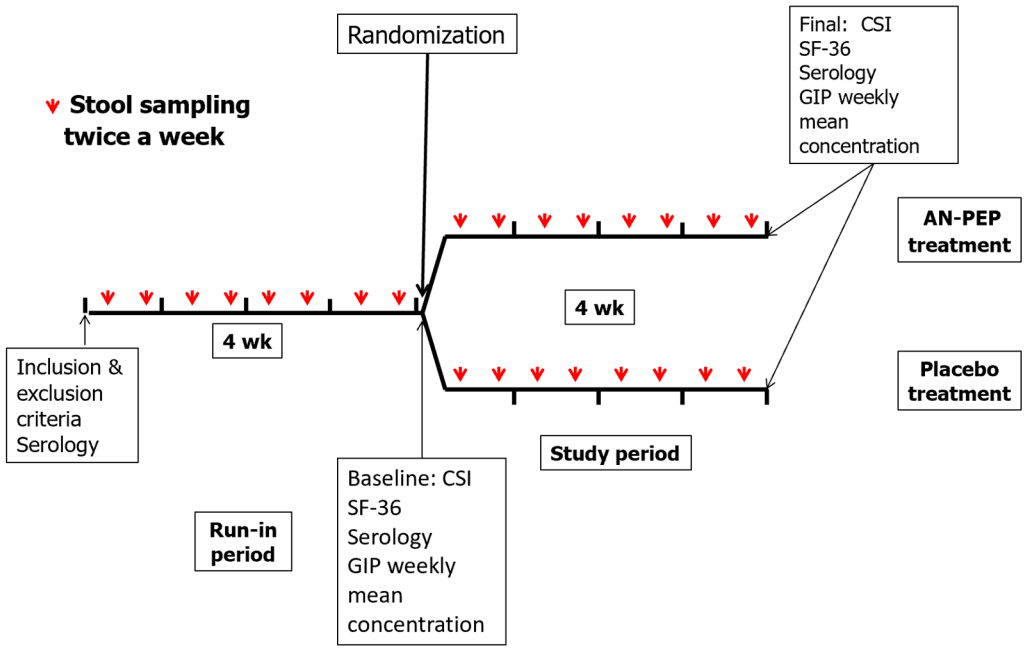

Figure 1 Study design. AN-PEP: *Aspergillus niger* prolyl endopeptidase protease; CSI: Celiac symptom index; GIP: Gluten immunogenic peptides; SF-36: Short Form-36 health survey questionnaire.

°C until they were tested for GIP measurement. To quantify GIP in the stool samples, a commercial ELISA kit (iVYLISA GIP-Stool; Biomedal S.L., Sevilla, Spain) was used following the manufacturer's instructions. This kit has been previously reported in the literature[8,25-27]. The detection limit of GIP is 0.08 μg/g of stool. Stool GIP testing was performed in duplicate, and the average concentration of eight measurements from both the run-in and treatment periods was reported. In the study, all analyses were conducted by operators who were deliberately blind to the clinical status of the patients and the type of treatment they were undergoing.

Celiac disease-specific serology

Serum samples were kept frozen at -20 °C until the assay was performed in only a single lab. The CeD-related tests and cut-offs were: (1) IgA tissue transglutaminase antibodies (tTG IgA) by ELISA (QUANTA LiteTM, h-tTG IgA; Inova Diagnostic Inc., San Diego, CA, United States); and (2) IgA antibodies reacting with deamidated gliadin-derived peptides (IgA DGP) (QUANTA LiteTM, IgA DGP; Inova Diagnostic Inc.) were performed at enrollment and at the end of the trial. Cut-off for both tests was 20 U/mL.

Study ethics, data analysis and safety issues

The study was approved by Dr. C. Bonorino Udaondo Gastroenterology Hospital's institutional ethical committee and the local research committee (CODEI). All patients were required to provide written informed consent. Patients were enrolled between October 2020 and July 2022. The study's results were blinded to the researchers performing clinical and biochemical analyses and collecting reports (CSI and SF-36 questionnaires). The study was registered at ClinicalTrials.gov under the number NCT04788797.

Based on the very limited availability of previous studies on AN-PEP and the evidence of gluten exposure in real life (determined by the excretion of stool GIP), this was an exploratory study. While we initially aimed at recruiting 80 patients, the long quarantine imposed in Argentina during the coronavirus disease 2019 (COVID-19) pandemic forced us to reset our aim to n = 40. Patients returning > 30% of capsules administered at the randomization were part of the per-protocol (PP) evaluation. After a 4-wk run-in period, patients were allocated to one of the two treatments (AN-PEP or placebo). A block randomization method (blocks of four subjects each) elaborated by an independent statistician was administered by an independent person who was not involved in the study analysis or an author of the study. The order of blocks was also randomized. Stata 14 (Stata Corp, College Station, TX, United States) was used for the statistical analysis. According to the data distribution, continuous variables were reported as median and 25%-75% percent interquartile range (IQR) or range. The comparison of results between treatment arms was conducted using the Mann-Whitney test. For assessing the differences within the same patients before and after treatment (paired samples), a Wilcoxon test was used. Proportions between groups were compared using the Chi-square test, while comparisons of proportions within the same patients before and after treatment (paired samples) were performed using the McNemar test. P values less than 0.05 were considered statistically significant. Outcome measurements were analyzed by intent-to-treat (ITT) analysis (all patients completing the run-in and treatment periods) and PP. For any safety concerns, all patients were in contact with expert monitors (AFC, MG, and JCB). If a safety issue was present, a self-reported form for safety concerns should have been completed.

RESULTS

Study population and compliance with AN-PEP administration

Figure 2 displays the flowchart illustrating trial progression. Due to limitations imposed by the COVID-19 pandemic on the activity of the ambulatory clinic for CeD patients, the enrollment period for the trial was from October 2020 to July 2022. Out of the initial 66 screened patients, 20 were excluded because they did not meet the inclusion and exclusion criteria. Additionally, six out of the remaining 46 enrolled patients did not initiate sample collection during the run-in period due to concerns about adhering to the protocol, leading to their exclusion from the study. Ultimately, 40patients completed the study for the ITT analysis. According to our pre-established guidelines, three patients were excluded from the final analysis because they returned more than 30% of the administered capsules. Table 1 presents the demographic information of the patients enrolled in the ITT analysis, while Table 2 provides the corresponding data for the PP analysis. No significant differences were observed between the AN-PEP and placebo-treated groups in terms of sex, age at enrollment, or duration of following a GFD. During and after the trial, no patients reported any abnormal symptom perception resulting from the use of AN-PEP or placebo.

Stool gluten immunogenic peptides

Throughout the trial, 628 (98.1%) samples were successfully collected. All analyses were conducted by investigators who were kept blind to the clinical status of the patients and the allocated treatment. A high proportion of samples from run-ins and treatment periods (65.6%) showed undetectable levels of gluten immunogenic peptides (GIP) (< 0.08 μg/g), indicating high adherence to the GFD. No significant differences in GIP levels were observed between the treatment arms in either the ITT or PP analyses. Three patients were excluded from the ITT analysis due to returning more than 30% of the capsules at the end of the trial, and none had a positive GIP. There were no differences in GIP between ITT and PP analyses. By using the information obtained in the PP, we observed that in the placebo arm, 52 out of 164 (31.7%) and 47 out of 165 (28.5%) stool samples collected tested positive for GIP during the run-in and placebo periods, respectively. Among these patients, 58.7% tested positive for GIP in both periods, 17.7% tested negative in both, 11.8% tested positive at the run-in and negative during the placebo, and 11.8% tested positive and negative, respectively. When comparing run-in and treatment periods in the placebo arm, 15% (3/20) of patients had GIP below 0.08 μg/g while 30% maintained high values at both time points and 25% (5/20) increased GIP during treatment with placebo. For the AN-PEP arm, 61 out of 151 (40.4%) samples tested positive for GIP during the run-in, while 54 out of 148 (36.5%) collected samples tested positive during the treatment period (data not shown). A more detailed analysis revealed that 17.7% (3/17) of patients exhibited no detectable stool GIP at both time points (run-in and AN-PEP administration), 29.4% (5/17) had reduced weekly GIP during AN-PEP and 17.7% (3/17) had unchanged GIP during both periods (data not shown). The average stool GIP per period for both arms is shown in Tables 1 and 2. During the run-in period, a noteworthy observation was that six patients (31.6%) in the AN-PEP arm exhibited an average stool GIP per period exceeding 0.08 μg/g. Among these cases, five patients had more than a 50% reduction or undetectable GIP. In contrast, among the four patients with high median concentrations (> 0.08 μg/g) at run-in in the placebo arm, only one patient experienced a decrease in GIP (data not shown). Overall, only 0.5% of all samples had average stool GIP concentrations greater than 0.32 μg/g, a threshold considered capable of causing mucosal damage. No patients were found to have a weekly average stool GIP concentration exceeding 0.64 μg/g.

Symptoms report using the CIS

The effects of AN-PEP on symptoms were analyzed based on the median CSI scores between the run-in periods and both treatments, as well as between the arms. Additionally, the proportion of cases with the highest CSI scores (> 38 points) was also examined. At randomization, no significant differences in median scores were observed between the placebo and AN-PEP arms, although patient scores in the AN-PEP arm were slightly higher than those in the placebo arm (Tables 1 and 2). Following treatment, there was a greater reduction in the median CSI score in the AN-PEP arm (12.5%) compared to the placebo arm (8.5%), although this difference was not statistically significant. The most notable finding was the decrease in the number of patients with the highest CSI scores (> 38 points) in the AN-PEP arm compared to those receiving placebo, which was statistically significant ($P < 0.03$) (Tables 1 and 2).

Outcome of celiac disease-related serology

We also examined the impact of treatment on the concentrations of IgA tTG and IgA DGP autoantibodies before and after the intervention. In the placebo group, seven patients tested positive for IgA tTG at enrollment, and this number decreased to five after treatment. In the AN-PEP group, eight patients tested positive at enrollment, and this slightly decreased to seven after treatment. Regarding IgA DGP antibodies, the positivity rate was lower, with two patients in both the placebo and AN-PEP arms having high concentrations at enrollment, which increased to three and two patients, respectively, after treatment. However, as expected because of the short duration of the study, there were no significant differences observed when comparing the median serum concentrations of both antibodies between baseline and final measurements within the same treatment arm or between the placebo and AN-PEP arms (Tables 1 and 2).

QoL and safety

The study also examined the impact of treatments on the QoL of patients using the SF-36 questionnaire, considering eight dimensions. Data for the ITT are reported in Table 3. At baseline, there were no significant differences in scores between arms across all dimensions for the ITT and PP analyses. After the treatment period, the placebo arm showed a significant improvement in general health, pain, and emotional limitations both in the ITT and PP analyses ($P < 0.05$ for all

Table 1 Patient data collected in the study in the intention-to-treat analysis

Item	Overall population	Placebo treatment	AN-PEP treatment
Number of patients	40	21	19
Age in yr, median (range)	40.5 (29-47)	42.0 (32-48)	39.0 (28-46)
Females, *n* (%)	33.0 (82.5)	18.0 (85.7)	15.0 (78.9)
CeD serology in U/mL, median (IQR)			
IgA DGP at baseline	3.0 (1.3-5.0)	2.0 (1.0-5.0)	4.0 (2.0-5.0)
End of study	3 (2-6)	3 (2-5)	3 (2-6)
IgA tTG at baseline	17 (7-44)	10 (5-30)	17 (8-49)
End of study	12 (6-50)	11 (6-15)	17 (8-70)
SCI global score at randomization median score (IQR)	36 (32-44)	35 (30-44)	40 (33-44)
End of the study median score (IQR)	34 (28-40)	32 (29-39)	35 (28-41)
SCI scores > 38 at randomization, *n* (%)	19 (47.5)	8 (38.1)	11 (57.9)
End of the study, *n* (%)	12 (30.0)	6 (28.6)	6 (31.6)[a]
Stool GIP. Median and CI (IQR) of the average concentration for period (μg/g)			
Run-in period	0.37 (0-0.83)[d]	0.34 (0-0.68)[b]	0.42 (0-0.93)[c]
Treatment period	0.21 (0-0.79)[d]	0.19 (0.11-0.79)[b]	0.22 (0-0.89)[c]

[a]Comparison with run-in (McNemar test): $P < 0.03$.
[b]Comparison with run-in values P (Wilcoxon): $P = 0.79$.
[c]Comparison with run-in values P (Wilcoxon): $P = 0.19$.
[d]Comparison with run-in values P (Wilcoxon): $P = 0.29$.
CeD: Celiac disease; CI: Confidence interval; CSI: Celiac symptom index; DGP: Deamidated gliadin peptide antibodies; GIP: Gliadin immunogenic peptides; IQR: Interquartile range; tTG: Tissue transgluteminase antibodies.

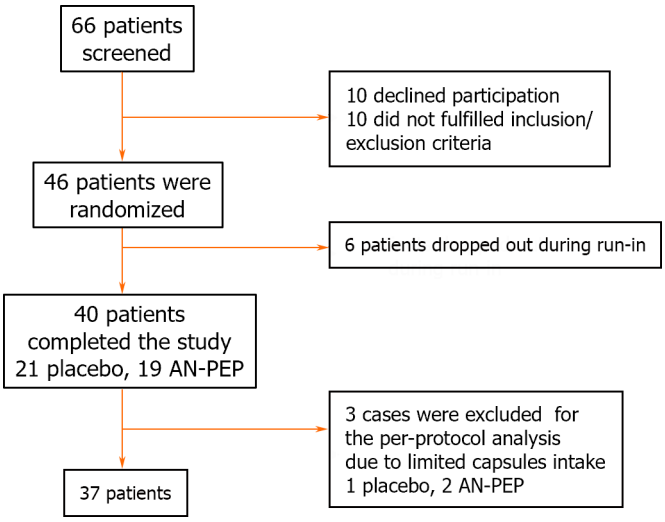

Figure 2 Flowchart of enrolled patients. AN-PEP: *Aspergillus niger* prolyl endopeptidase protease.

dimensions). In contrast, compared to the baseline assessment, patients in the AN-PEP arm had higher scores for pain ($P < 0.05$), but a higher score for vitality ($P < 0.005$), as assessed by both ITT and PP analyses. Neither AN-PEP nor placebo elicited any reported adverse events or concerns from the patients, indicating that the treatment doses were well-tolerated. Additionally, all three cases that were excluded from the ITT analysis tested negative for GIP. In these cases, the omissions in adhering to the trial were attributed to the individuals' intense working activity outside of their homes rather than any issues related to the treatment itself.

Table 2 Per-protocol data and analysis

Item	Overall population	Placebo treatment	AN-PEP treatment
Number of patients	37	20	17
Age in yr, median (range)	40 (29-46)	41 (31-48)	39 (28-45)
Females, *n* (%)	31 (83.8)	17 (85.0)	14 (82.3)
CeD serology in AU/mL, median (IQR)			
IgA DGP at baseline	3 (1-5)	2 (1-5)	3 (1-5)
At end of study	3 (2-6)	3 (2-5)	3 (2-6)
IgA tTG at baseline	17 (7-43)	13 (6-36)	17 (11-48)
End of study	12 (6-48)	11 (5-20)	17 (7-62)
SCI global score at randomization median score (IQR)	36.0 (31.0-44.0)	35.0 (30.0-45.5)	40.0 (33.0-44.0)
End of the study median score (IQR)	33.0 (28.0-39.0)	32.0 (28.5-37.5)	35.0 (28.0-41.0)
SCI scores > 38 at randomization, *n* (%)	17 (45.9)	7 (35.0)	10 (58.8)
End of study, *n* (%)	10 (27.0)	5 (25.0)	5 (29.4)[a]
Stool GIP median and CI (IQR) of the average concentration for period, μg/g			
Run-in period	0.40 (0-0.86)	0.37 (0-0.73)	0.55 (0-0.93)
Treatment period	0.30 (0.10-0.80)[b]	0.25 (0.11-0.79)[c]	0.32 (0-0.89)[d]

[a]Comparison with run-in (McNemar test): $P < 0.03$.
[b]Comparison with run-in values P (Wilcoxon): $P = 0.43$.
[c]Comparison with run-in values P (Wilcoxon): $P = 0.79$.
[d]Comparison with run-in values P (Wilcoxon): $P = 0.33$.
CeD: Celiac disease; CSI: Celiac symptom index; DGP: Deamidated gliadin peptide antibodies; GIP: Gliadin immunogenic peptides; IQR: Interquartile range; tTG: Tissue transgluteminase antibodies.

DISCUSSION

The primary objective of this exploratory study was to investigate the effects of AN-PEP, a proline-specific endoprotease, at a dose of 650 mg per meal, three times a day (during breakfast, lunch, and dinner) for 4 consecutive weeks, on involuntary gluten exposure in patients following a long-term GFD. A placebo arm was included for comparison. By replicating a real-life situation, the study expands on previous challenge studies to address the common issue of dietary contamination occurring in diagnosed patients on a long-term GFD[8,25-28]. In the AN-PEP arm, there was an observable reduction in the average stool GIP concentration during the treatment period compared with the 4-wk run-in phase. Patients in the placebo arm also exhibited a decrease in GIP. While the magnitude of reduction in GIP tended to be higher in patients receiving AN-PEP (47.6%) *vs* placebo (44.1%), this difference did not reach statistical significance. Interestingly, during the run-in period, approximately 35.3% of patients in the AN-PEP arm had GIP levels exceeding 0.08 μg/g. After undergoing protease treatment, five out of these six patients experienced a 50% reduction or more in GIP after AN-PEP, while only one out of four patients in the placebo group experienced such a reduction.

Neither AN-PEP nor placebo elicited any reported adverse events or concerns from the patients, indicating that the treatment doses were well-tolerated. Additionally, all three cases that were excluded from the ITT analysis tested negative for GIP. In these cases, the omissions in adhering to the trial were attributed to the individuals' intense working schedules rather than issues related to the treatment itself. Although CSI scores did not show a significant reduction between active treatment and placebo, the proportion of patients with the highest CSI score, which is considered indicative of the most symptomatic clinical course, was significantly reduced by AN-PEP. No changes were detected in specific CeD serology between treatment arms. Compared with the run-in period, patients in the placebo arm reported improved QoL scores in the areas of general health, while those in the AN-PEP arm had better scores for vitality and severe abdominal pain. These differences could be attributed to inherent limitations associated with questionnaires, such as subjectivity, and other external factors influencing QoL. Before this study, AN-PEP had demonstrated promising potential for degrading gluten in various *in vitro* and *ex vivo* laboratory models, as well as in gluten challenge trials.

However, testing AN-PEP in patients on long-term GFD who could be exposed to real-life dietary contamination has never been investigated[17-20]. While important in the daily management of CeD, a "real-life" design is not devoid of limitations, as real-life variability and trial effects cannot be controlled[8,29,30]. Indeed, this could explain our finding of an overall lower GIP when compared with the run-in period. Thus, and in contrast to findings from our previous studies [8], the level of GIP never reached one that could be associated with mucosal damage[27]. This discrepancy could be attributed to trial timing, which primarily took place during the COVID-19 pandemic when our country was characterized by high viral infection rates and prolonged isolation and lockdown. Consequently, the enforced stay-at-home

Table 3 Quality of life data from the Short Form-36 questionnaire on the intention-to-treat analysis

Item	Placebo arm		AN-PEP arm	
	At baseline	Final	At baseline	Final
Number of patients	21		19	
General health				
Median score (IQR)	65 (50-72)	70 (50-80)[b]	50 (35-75)	50 (40-80)
Pain				
Median score (IQR)	80 (42-90)	90 (50-80)[b]	80 (45-90)	67.5 (47.5-90.0)[a]
Vitality				
Median score (IQR)	60 (45-65)	60 (50-70)	40 (30-60)	55 (40-65)[c]
Mental health				
Median score (IQR)	68 (52-72)	68 (56-80)	68 (40-72)	64 (48-80)
Physical function				
Median score (IQR)	95 (75-100)	95 (75-100)	95 (85-100)	100 (90-100)
Social function				
Median score (IQR)	75 (50-100)	100 (62.5-100.0)	50 (37-100)	75 (50-100)
Physical limitations				
Median score (IQR)	100 (50-100)	100 (75-100)	100 (25-100)	75 (25-100)
Emotional limitations				
Median score (IQR)	50 (0-100)	100 (66-100)[b]	66.7 (0-100)	66.7 (0-100)

[a]*vs* placebo: $P < 0.05$.
[b]Run-in *vs* treatment: $P < 0.05$.
[c]Run-in *vs* treatment: $P < 0.005$.
AN-PEP: *Aspergillus niger* prolyl endopeptidase protease; IQR: Interquartile range.

measures during this time may have contributed to improved adherence to the GFD, as has been suggested by a recent study[31].

The relationship between the dose of AN-PEP, its enzymatic activity, the ratio of the protease administered per the total gluten intake, and the kinetics of substrate cleavage is a crucial aspect to consider. Previous studies have emphasized the importance of the dose-substrate relationship, contact time, and pH conditions in achieving optimal cleavage of gluten by peptidases[32]. König *et al*[16] conducted a study demonstrating the effective cleavage of gliadin peptides by AN-PEP shortly after its co-administration with gluten in a challenging study, even under varying caloric densities and acidic conditions. In our study, we opted for an AN-PEP dose that was twice the highest concentration previously demonstrated to effectively cleave gliadin in healthy individuals subjected to gluten challenges[21]. In essence, our assessment indicates that the observed gluten intake levels suggest a predominant trend of relatively low gluten exposure among the trial participants. However, it is important to underline that these individuals were concurrently receiving substantial doses of AN-PEP treatment. The study also investigated the impact of enzyme treatment on symptom intensity, as assessed by CSI score. Various factors have been associated with persistent symptoms in patients following a GFD, including involuntary and voluntary gluten exposure, irritable bowel syndrome, bacterial overgrowth syndrome, and a high intake of FODMAPs[1-5]. The most relevant and clinically interesting finding in the study was the significant reduction in the number of patients with the highest CSI scores (> 38 points) in the AN-PEP arm. This reduction could have been caused by a decrease in gluten exposure or through the action of the protease, and this cannot be identified with our design. While in a small number of patients, the observation that those with higher GIP experienced a > 50% reduction or non-detectable GIP after AN-PEP treatment supports the hypothesis of improved gluten degradation, as we did not observe a similar reduction in the placebo arm. Whether minor amounts of gluten exposure can contribute to symptom persistence is unclear, but hypersensitive patients have been reported[1]. Further research is needed to better understand the mechanisms underlying symptom persistence and the potential effects of AN-PEP treatment in larger trials with longer follow-up periods. Finally, while some parameters of QoL improved during AN-PEP *vs* placebo, we did not detect changes in CeD-specific serological tests.

One advantage of the present study was the attempt to mimic real-life conditions typically encountered by patients on lifelong GFD who are exposed to unpredictable gluten contamination. As previously discussed, this design is also susceptible to limitations; thus, while real-life studies are necessary for better long-term management of CeD, results need to be interpreted with caution as they lack the same level of control as gluten challenge studies[29,30]. Together, both

designs can provide complementary and powerful clinical and pathophysiological insights. However, we believe that the duration of treatment (4 wk) might not suffice to detect significant modifications in outcome parameters, particularly in specific-serology testing.

CONCLUSION

In summary, AN-PEP treatment did not significantly reduce the overall GIP stool concentration. However, our results support the idea that AN-PEP has a positive impact on symptom intensity and on some aspects of QoL during a long-term GFD. More research is needed to unravel the underlying mechanisms this, as well as in larger populations with longer follow-ups to confirm these findings. These studies will help us better implement adjunct therapies for the GFD in CeD.

ACKNOWLEDGMENTS

The authors thank Dr. Daniel Flores and Mrs. Karina Canguillen for their assistance with the independent design and administration of the randomization.

ARTICLE HIGHLIGHTS

Research background

The impact of *Aspergillus niger* proline-specific endoprotease (AN-PEP) on gluten exposure resulting from inadvertent dietary lapses in celiac disease (CeD) patients adhering to a gluten-free diet (GFD) in real-life scenarios remains unknown.

Research motivation

Early-stage research has hinted at AN-PEP's potential therapeutic role in breaking down gluten before it reaches the intestinal mucosa, potentially serving as an adjunct for managing gluten exposure. Despite AN-PEP's approval as a dietary supplement, there is a lack of appropriate clinical studies to confirm its efficacy in detoxifying gluten immunogenic peptides (GIP).

Research objectives

To examine the effects of orally administered AN-PEP on inadvertent gluten exposure and symptom prevention in adult CeD patients following their usual GFD in a real-life scenario.

Research methods

This exploratory trial employed a double-blind, randomized, placebo-controlled design involving CeD participants on a long-term GFD. After a 4-wk run-in phase, individuals were randomly assigned to receive either two AN-PEP capsules per meal for 4 wk or a placebo. The study main outcome endpoints were to compare the average weekly stool GIP and the celiac symptom index between run-in and treatment phases and between AN-PEP and placebo arms.

Research results

In this exploratory study, participants showed strong adherence to the GFD. While AN-PEP treatment did not decrease overall stool GIP concentration, the group receiving AN-PEP exhibited a significantly lower prevalence of severe symptoms compared to the placebo group.

Research conclusions

Despite the lack of reduction in stool GIP due to AN-PEP administration in this real-life setting, the significant decrease in the number of symptomatic patients suggests the need for further investigation and more extensive studies.

Research perspectives

Subsequent studies could delve into whether AN-PEP administration showcases a protective effect against gluten exposure using different research models. Additionally, these studies could aim to elucidate the reasons behind the observed reduction in symptomatic patients to better understand the potential mechanisms at play.

FOOTNOTES

Author contributions: Stefanolo JP contributed to the study's design, collected the patients, performed statistical analysis of the data and critical review of the manuscript; Segura V, Heredia A, and Comino I performed the gluten immunogenic peptides stool tests; Grizutti

M, Costa AF, and Oregui ME collected the patients and performed data acquisition; Temprano MP performed the dietary assessment; Puebla R, de Diego G, and de Marzi MC produced the biochemical determinations and performed the serology; Niveloni SI and Smecuol EG contributed to the data acquisition; Bai JC planned the study; Bai JC, Verdú EF, and Sousa C contributed to the study design, data analysis, and writing of the manuscript; All authors read and approved the final manuscript.

Supported by the Asociación de Celíacos y Sensibles al Gluten de Madrid, No. ACM2020); and Research Committee Argentine Society of Gastroenterology, No. 2020.

Institutional review board statement: The study was reviewed and approved by Dr. C. Bonorino Udaondo Gastroenterology Hospital's institutional ethical committee (CEI) and the local research committee (CODEI).

Clinical trial registration statement: The study was registered at ClinicalTrials.gov. The registration identification number is NCT04788797.

Informed consent statement: All study participants, or their legal guardian, provided informed written consent prior to study enrollment.

Conflict-of-interest statement: The authors have no conflicts of interest to declare.

Data sharing statement: No additional data are available.

CONSORT 2010 statement: The authors have read the CONSORT 2010 statement, and the manuscript was prepared and revised according to the CONSORT 2010 statement.

Country/Territory of origin: Argentina

ORCID number: Juan Pablo Stefanolo 0000-0003-0679-3470; Ana Florencia Costa 0000-0002-0082-5630; María Paz Temprano 0000-0003-2257-7858; Sonia Isabel Niveloni 0000-0002-1534-1604; Edgardo Gustavo Smecuol 0000-0002-4451-819X; Elena F Verdú 0000-0001-6346-2665; Carolina Sousa 0000-0002-9235-9496; Julio César Bai 0000-0003-4159-0185.

S-Editor: Chen YL
L-Editor: Filipodia
P-Editor: Cai YX

REFERENCES

1 **Catassi C**, Verdu EF, Bai JC, Lionetti E. Coeliac Disease, Seminar. *The Lancet* 2022; **399**: 2413-2426 [DOI: 10.1016/s0140-6736(22)00794-2]
2 **Makharia GK**, Singh P, Catassi C, Sanders DS, Leffler D, Ali RAR, Bai JC. The global burden of coeliac disease: opportunities and challenges. *Nat Rev Gastroenterol Hepatol* 2022; **19**: 313-327 [PMID: 34980921 DOI: 10.1038/s41575-021-00552-z]
3 **Al-Toma A**, Volta U, Auricchio R, Castillejo G, Sanders DS, Cellier C, Mulder CJ, Lundin KEA. European Society for the Study of Coeliac Disease (ESsCD) guideline for coeliac disease and other gluten-related disorders. *United European Gastroenterol J* 2019; **7**: 583-613 [PMID: 31210940 DOI: 10.1177/2050640619844125]
4 **Kelly CP**, Bai JC, Liu E, Leffler DA. Advances in diagnosis and management of celiac disease. *Gastroenterology* 2015; **148**: 1175-1186 [PMID: 25662623 DOI: 10.1053/j.gastro.2015.01.044]
5 **Rubio-Tapia A**, Hill ID, Semrad C, Kelly CP, Greer KB, Limketkai BN, Lebwohl B. American College of Gastroenterology Guidelines Update: Diagnosis and Management of Celiac Disease. *Am J Gastroenterol* 2023; **118**: 59-76 [PMID: 36602836 DOI: 10.14309/ajg.0000000000002075]
6 **Husby S**, Murray JA, Katzka DA. AGA Clinical Practice Update on Diagnosis and Monitoring of Celiac Disease-Changing Utility of Serology and Histologic Measures: Expert Review. *Gastroenterology* 2019; **156**: 885-889 [PMID: 30578783 DOI: 10.1053/j.gastro.2018.12.010]
7 **Coto L**, Mendia I, Sousa C, Bai JC, Cebolla A. Determination of gluten immunogenic peptides for the management of the treatment adherence of celiac disease: A systematic review. *World J Gastroenterol* 2021; **27**: 6306-6321 [PMID: 34712034 DOI: 10.3748/wjg.v27.i37.6306]
8 **Stefanolo JP**, Tálamo M, Dodds S, de la Paz Temprano M, Costa AF, Moreno ML, Pinto-Sánchez MI, Smecuol E, Vázquez H, Gonzalez A, Niveloni SI, Mauriño E, Verdu EF, Bai JC. Real-World Gluten Exposure in Patients With Celiac Disease on Gluten-Free Diets, Determined From Gliadin Immunogenic Peptides in Urine and Fecal Samples. *Clin Gastroenterol Hepatol* 2021; **19**: 484-491.e1 [PMID: 32217152 DOI: 10.1016/j.cgh.2020.03.038]
9 **Kivelä L**, Caminero A, Leffler DA, Pinto-Sanchez MI, Tye-Din JA, Lindfors K. Current and emerging therapies for coeliac disease. *Nat Rev Gastroenterol Hepatol* 2021; **18**: 181-195 [PMID: 33219355 DOI: 10.1038/s41575-020-00378-1]
10 **Piper JL**, Gray GM, Khosla C. Effect of prolyl endopeptidase on digestive-resistant gliadin peptides in vivo. *J Pharmacol Exp Ther* 2004; **311**: 213-219 [PMID: 15143130 DOI: 10.1124/jpet.104.068429]
11 **Shan L**, Marti T, Sollid LM, Gray M, Khosla C. Comparative biochemical analysis of three bacterial prolyl endopeptidases: implications for coeliac sprue. *Biochem J* 2004; **383**: 311-318 [DOI: 10.1042/BJ20040907]
12 **Salden BN**, Monserrat V, Troost FJ, Bruins MJ, Edens L, Bartholomé R, Haenen GR, Winkens B, Koning F, Masclee AA. Randomised

clinical study: Aspergillus niger-derived enzyme digests gluten in the stomach of healthy volunteers. *Aliment Pharmacol Ther* 2015; **42**: 273-285 [PMID: 26040627 DOI: 10.1111/apt.13266]

13 **Gass J**, Khosla C. Prolyl endopeptidases. *Cell Mol Life Sci* 2007; **64**: 345-355 [PMID: 17160352 DOI: 10.1007/s00018-006-6317-y]

14 **Wei G**, Helmerhorst EJ, Darwish G, Blumenkranz G, Schuppan D. Gluten Degrading Enzymes for Treatment of Celiac Disease. *Nutrients* 2020; **12**: 2095 [PMID: 32679754 DOI: 10.3390/nu12072095]

15 **Edens L**, Dekker P, van der Hoeven R, Deen F, de Roos A, Floris R. Extracellular prolyl endoprotease from Aspergillus niger and its use in the debittering of protein hydrolysates. *J Agric Food Chem* 2005; **53**: 7950-7957 [PMID: 16190655 DOI: 10.1021/jf050652c]

16 **König J**, Holster S, Bruins MJ, Brummer RJ. Randomized clinical trial: Effective gluten degradation by Aspergillus niger-derived enzyme in a complex meal setting. *Sci Rep* 2017; **7**: 13100 [PMID: 29026170 DOI: 10.1038/s41598-017-13587-7]

17 **Montserrat V**, Bruins MJ, Edens L, Koning F. Influence of dietary components on Aspergillus niger prolyl endoprotease mediated gluten degradation. *Food Chem* 2015; **174**: 440-445 [PMID: 25529703 DOI: 10.1016/j.foodchem.2014.11.053]

18 **Mitea C**, Havenaar R, Drijfhout JW, Edens L, Dekking L, Koning F. Efficient degradation of gluten by a prolyl endoprotease in a gastrointestinal model: implications for coeliac disease. *Gut* 2008; **57**: 25-32 [PMID: 17494108 DOI: 10.1136/gut.2006.111609]

19 **Tack GJ**, van de Water JM, Bruins MJ, Kooy-Winkelaar EM, van Bergen J, Bonnet P, Vreugdenhil AC, Korponay-Szabo I, Edens L, von Blomberg BM, Schreurs MW, Mulder CJ, Koning F. Consumption of gluten with gluten-degrading enzyme by celiac patients: a pilot-study. *World J Gastroenterol* 2013; **19**: 5837-5847 [PMID: 24124328 DOI: 10.3748/wjg.v19.i35.5837]

20 **EFSA Panel on Dietetic Products**, Nutrition and Allergies (NDA), Turck D, Bresson JL, Burlingame B, Dean T, Fairweather-Tait S, Heinonen M, Hirsch-Ernst KI, Mangelsdorf I, McArdle HJ, Naska A, Neuhäuser-Berthold M, Nowicka G, Pentieva K, Sanz Y, Siani A, Sjödin A, Stern M, Tomé D, Vinceti M, Willatts P, Engel KH, Marchelli R, Pöting A, Poulsen M, Schlatter J, Gelbmann W, Van Loveren H. Safety of proline-specific oligopeptidase as a novel food pursuant to Regulation (EC) No 258/97. *EFSA J* 2017; **15**: e04681 [PMID: 32625399 DOI: 10.2903/j.efsa.2017.4681]

21 **Stepniak D**, Spaenij-Dekking L, Mitea C, Moester M, de Ru A, Baak-Pablo R, van Veelen P, Edens L, Koning F. Highly efficient gluten degradation with a newly identified prolyl endoprotease: implications for celiac disease. *Am J Physiol Gastrointest Liver Physiol* 2006; **291**: G621-G629 [PMID: 16690904 DOI: 10.1152/ajpgi.00034.2006]

22 **Janssen G**, Christis C, Kooy-Winkelaar Y, Edens L, Smith D, van Veelen P, Koning F. Ineffective degradation of immunogenic gluten epitopes by currently available digestive enzyme supplements. *PLoS One* 2015; **10**: e0128065 [PMID: 26030273 DOI: 10.1371/journal.pone.0128065]

23 **Leffler DA**, Dennis M, Edwards George J, Jamma S, Cook EF, Schuppan D, Kelly CP. A validated disease-specific symptom index for adults with celiac disease. *Clin Gastroenterol Hepatol* 2009; **7**: 1328-1334, 1334.e1 [PMID: 19665584 DOI: 10.1016/j.cgh.2009.07.031]

24 **Nachman F**, del Campo MP, González A, Corzo L, Vázquez H, Sfoggia C, Smecuol E, Sánchez MI, Niveloni S, Sugai E, Mauriño E, Bai JC. Long-term deterioration of quality of life in adult patients with celiac disease is associated with treatment noncompliance. *Dig Liver Dis* 2010; **42**: 685-691 [PMID: 20399159 DOI: 10.1016/j.dld.2010.03.004]

25 **Comino I**, Fernández-Bañares F, Esteve M, Ortigosa L, Castillejo G, Fambuena B, Ribes-Koninckx C, Sierra C, Rodríguez-Herrera A, Salazar JC, Caunedo Á, Marugán-Miguelsanz JM, Garrote JA, Vivas S, Lo Iacono O, Nuñez A, Vaquero L, Vegas AM, Crespo L, Fernández-Salazar L, Arranz E, Jiménez-García VA, Antonio Montes-Cano M, Espín B, Galera A, Valverde J, Girón FJ, Bolonio M, Millán A, Cerezo FM, Guajardo C, Alberto JR, Rosinach M, Segura V, León F, Marinich J, Muñoz-Suano A, Romero-Gómez M, Cebolla Á, Sousa C. Fecal Gluten Peptides Reveal Limitations of Serological Tests and Food Questionnaires for Monitoring Gluten-Free Diet in Celiac Disease Patients. *Am J Gastroenterol* 2016; **111**: 1456-1465 [PMID: 27644734 DOI: 10.1038/ajg.2016.439]

26 **Cebolla Á**, Moreno ML, Coto L, Sousa C. Gluten Immunogenic Peptides as Standard for the Evaluation of Potential Harmful Prolamin Content in Food and Human Specimen. *Nutrients* 2018; **10**: E1927 [PMID: 30563126 DOI: 10.3390/nu10121927]

27 **Costa AF**, Sugai E, Temprano MP, Niveloni SI, Vázquez H, Moreno ML, Domínguez-Flores MR, Muñoz-Suano A, Smecuol E, Stefanolo JP, González AF, Cebolla-Ramirez A, Mauriño E, Verdú EF, Bai JC. Gluten immunogenic peptide excretion detects dietary transgressions in treated celiac disease patients. *World J Gastroenterol* 2019; **25**: 1409-1420 [PMID: 30918433 DOI: 10.3748/wjg.v25.i11.1409]

28 **Fernández-Bañares F**, Beltrán B, Salas A, Comino I, Ballester-Clau R, Ferrer C, Molina-Infante J, Rosinach M, Modolell I, Rodríguez-Moranta F, Arau B, Segura V, Fernández-Salazar L, Santolaria S, Esteve M, Sousa C; CADER study group. Persistent Villous Atrophy in De Novo Adult Patients With Celiac Disease and Strict Control of Gluten-Free Diet Adherence: A Multicenter Prospective Study (CADER Study). *Am J Gastroenterol* 2021; **116**: 1036-1043 [PMID: 33491958 DOI: 10.14309/ajg.0000000000001139]

29 **Skodje GI**, van Megen F, Stendahl M, Henriksen C, Lundin KEA, Veierød MB. Detection of gluten immunogenic peptides and the Celiac Disease Adherence Test to monitor gluten-free diet: a pilot study. *Eur J Clin Nutr* 2022; **76**: 902-903 [PMID: 35001079 DOI: 10.1038/s41430-021-01054-6]

30 **Camm AJ**, Fox KAA. Strengths and weaknesses of 'real-world' studies involving non-vitamin K antagonist oral anticoagulants. *Open Heart* 2018; **5**: e000788 [PMID: 29713485 DOI: 10.1136/openhrt-2018-000788]

31 **Azoulay L**. Rationale, Strengths, and Limitations of Real-World Evidence in Oncology: A Canadian Review and Perspective. *Oncologist* 2022; **27**: e731-e738 [PMID: 35762676 DOI: 10.1093/oncolo/oyac114]

32 **Monzani A**, Lionetti E, Felici E, Fransos L, Azzolina D, Rabbone I, Catassi C. Adherence to the Gluten-Free Diet during the Lockdown for COVID-19 Pandemic: A Web-Based Survey of Italian Subjects with Celiac Disease. *Nutrients* 2020; **12**: 3467 [PMID: 33198212 DOI: 10.3390/nu12113467]

World Journal of Gastroenterology

Submit a Manuscript: https://www.f6publishing.com

World J Gastroenterol 2024 March 21; 30(11): 1556-1571

DOI: 10.3748/wjg.v30.i11.1556

ISSN 1007-9327 (print) ISSN 2219-2840 (online)

ORIGINAL ARTICLE

Clinical Trials Study

Effects of *Lactobacillus paracasei* N1115 on gut microbial imbalance and liver function in patients with hepatitis B-related cirrhosis

Yan-Chao Hu, Xiang-Chun Ding, Hui-Juan Liu, Wan-Long Ma, Xue-Yan Feng, Li-Na Ma

Specialty type: Gastroenterology and hepatology

Provenance and peer review: Unsolicited article; Externally peer reviewed.

Peer-review model: Single blind

Peer-review report's scientific quality classification

Grade A (Excellent): 0
Grade B (Very good): 0
Grade C (Good): C
Grade D (Fair): 0
Grade E (Poor): 0

P-Reviewer: Wierzbicka A, Poland

Received: December 17, 2023
Peer-review started: December 17, 2023
First decision: December 25, 2023
Revised: January 8, 2024
Accepted: March 4, 2024
Article in press: March 4, 2024
Published online: March 21, 2024

Yan-Chao Hu, Xiang-Chun Ding, Hui-Juan Liu, Wan-Long Ma, Xue-Yan Feng, Li-Na Ma, Department of Infectious Disease, General Hospital of Ningxia Medical University, Yinchuan 750004, Ningxia Hui Autonomous Region, China

Xiang-Chun Ding, Infectious Disease Clinical Research Center of Ningxia, Yinchuan 750004, Ningxia Hui Autonomous Region, China

Corresponding author: Xiang-Chun Ding, MD, Doctor, Department of Infectious Disease, General Hospital of Ningxia Medical University, No. 804 Shengli Street, Yinchuan 750004, Ningxia Hui Autonomous Region, China. 13619511768@163.com

Abstract

BACKGROUND

Hepatitis B cirrhosis (HBC) is a chronic disease characterized by irreversible diffuse liver damage and aggravated by intestinal microbial imbalance and metabolic dysfunction. Although the relationship between certain single probiotics and HBC has been explored, the impact of the complex ready-to-eat *Lactobacillus paracasei* N1115 (LP N1115) supplement on patients with HBC has not been determined.

AIM

To compare the changes in the microbiota, inflammatory factor levels, and liver function before and after probiotic treatment in HBC patients.

METHODS

This study included 160 HBC patients diagnosed at the General Hospital of Ningxia Medical University between October 2018 and December 2020. Patients were randomly divided into an intervention group that received LP N1115 supplementation and routine treatment and a control group that received routine treatment only. Fecal samples were collected at the onset and conclusion of the 12-wk intervention period. The structure of the intestinal microbiota and the levels of serological indicators, such as liver function and inflammatory factors, were assessed.

RESULTS

Following LP N1115 intervention, the intestinal microbial diversity significantly increased in the intervention group ($P < 0.05$), and the structure of the intestinal microbiota was characterized by an increase in the proportions of probiotic

microbes and a reduction in harmful bacteria. Additionally, the intervention group demonstrated notable improvements in liver function indices and significantly lower levels of inflammatory factors ($P < 0.05$).

CONCLUSION

LP N1115 is a promising treatment for ameliorating intestinal microbial imbalance in HBC patients by modulating the structure of the intestinal microbiota, improving liver function, and reducing inflammatory factor levels.

Key Words: Hepatitis B cirrhosis; N1115 ready-to-eat lactobacillus; Inflammation; Liver function; Lachnospiraceae incertae sedis; Probiotic

Core Tip: Intestinal microbial imbalance and metabolic dysfunction may accelerate the process of liver cirrhosis. We explored the role of probiotic intervention in patients with hepatitis B cirrhosis in this study. After an intervention with the N1115 ready-to-eat *Lactobacillus* supplement, we found the following significant changes: an increase in gut microbial diversity, structural changes in the microbiota favoring the growth of probiotic microbes, improvements in liver function, and decreases in inflammatory factor levels. We conclude that supplementation with the N1115 ready-to-eat *Lactobacillus* product may be a beneficial intervention in patients with cirrhosis.

Citation: Hu YC, Ding XC, Liu HJ, Ma WL, Feng XY, Ma LN. Effects of *Lactobacillus paracasei* N1115 on gut microbial imbalance and liver function in patients with hepatitis B-related cirrhosis. *World J Gastroenterol* 2024; 30(11): 1556-1571
URL: https://www.wjgnet.com/1007-9327/full/v30/i11/1556.htm
DOI: https://dx.doi.org/10.3748/wjg.v30.i11.1556

INTRODUCTION

Liver cirrhosis (LC) is a severe chronic liver disease characterized by extensive hepatocyte degeneration, fibrosis, and nodular regeneration caused by various factors[1]. In China, 85% of cirrhosis and hepatocellular carcinoma (HCC) cases are attributed to hepatitis B virus (HBV) infection[2]. Approximately 257 million people are infected with HBV annually worldwide, leading to approximately 887000 deaths annually, approximately 30% of which result from LC[2]. Decompensated hepatitis B cirrhosis (HBC) often leads to multiple-organ dysfunction, such as gastrointestinal bleeding, hepatic encephalopathy, spontaneous bacterial peritonitis (SBP), primary liver cancer (PLC), and hepatorenal syndrome, often necessitating liver transplantation for survival[3].

Patients with LC often experience varying degrees of intestinal flora imbalance. The intestinal microbiota not only directly affects intestinal health but also influences liver metabolism and immunity. The gut microbiota plays a critical role in the development of various chronic liver diseases, including nonalcoholic fatty liver disease (NAFLD), alcoholic liver disease (ALD), LC, and PLC. Alterations in the gut microbiota can lead to immune dysregulation, intestinal barrier dysfunction, and systemic inflammation through the gut-liver axis, thus promoting disease progression. The gut microbiota is closely associated with LC complications and liver disease[4-11]. Given the growing understanding of intestinal flora imbalance in patients with LC, modulating the gut microbiota has emerged as a new therapeutic approach for the treatment of LC. Probiotics, which promote the growth of beneficial bacteria and reduce the growth of harmful bacteria, have particularly gained attention for their therapeutic effects on various liver diseases[12,13]. For instance, supplementation with *Lactobacillus casei* (*L. casei*) can improve lipid metabolism and regulate intestinal flora disorders in patients with alcoholic liver injury[14]. However, *L. rhamnosus* and its culture medium can ameliorate alcohol-induced liver function damage and steatosis[15]. Supplementation with *Lactobacillus*, *Bifidobacterium*, *Escherichia coli*, *Clostridium butyricum*, *Streptococcus salivarius*, and VSL#3 strains has shown promise in improving hepatic encephalopathy[16,17]. Although numerous studies have confirmed the effectiveness of probiotics in the treatment of liver disease in animal models and hospitalized patients, controversies remain, and limited options are available for probiotic selection in patients with hepatitis B virus-induced LC (HBC), necessitating further investigation of their efficacy[18].

N1115 is a ready-to-eat supplement containing fructooligosaccharides (FOS), lactitol, *Lactobacillus paracasei N1115* (LP N1115), *L. plantarum*, *Bifidobacterium bifidobacterium*, and *L. acidophilus*, with LP N1115 accounting for > 80% of its composition. LP N1115 is isolated from traditional fermented dairy products and has probiotic effects, such as acid resistance, bile salt tolerance, and promotion of intestinal cell growth[19]. In combination with FOS, LP N1115 promotes recovery of the p38 mitogen-activated protein kinase pathway, enhances the expression of cohesin-1, improves intestinal barrier function, and preserves histological integrity[20]. The combinedapplication of LP N1115 and FOS reduces endotoxin levels, inhibits the activation of the lipopolysaccharide (LPS)/Toll-like receptor 4 (TLR4) signaling pathway, decreases the release of inflammatory factors, and alleviates NAFLD-related insulin resistance in mice[21]. Stadlbauer *et al* demonstrated that *L. casei* preparations regulated the expression of TLR4, promoted interleukin (IL)-10 secretion, and restored neutrophil phagocytic ability in patients with ALD[22]. However, it remains unclear whether the complex ready-to-eat LP N1115 supplement can modulate the prognosis of patients with HBC by regulating the gut microbiota.

Based on the aforementioned background, this study recruited 160 HBC patients and evaluated them by comparing the changes in microbiota before and after probiotic treatment as well as the changes in the levels of inflammatory factors and liver function to assess whether LP N1115 had beneficial effects on the gut microbiota in HBC patients.

MATERIALS AND METHODS

Study participants

A total of 160 patients diagnosed with HBC and treated at the General Hospital of Ningxia Medical University between October 2018 and December 2020 were enrolled in this study. Patients were randomly divided into two groups. The intervention group consisted of 86 patients who received LP N1115 supplementation in addition to general treatment for 3 months. Stool samples were collected at baseline and at the end of the intervention (54 patients did not provide stool samples after the intervention owing to the use of antibiotics or proton pump inhibitors during LP N1115 treatment). The nonintervention group consisted of 74 patients who received general treatment only. The diagnosis of HBC was based on the guidelines for the prevention and treatment of chronic hepatitis B (2019 edition) issued by the Chinese Society of Hepatology and Chinese Society of Infectious Diseases[23]. The exclusion criteria were as follows: (1) Patients with alcoholic, autoimmune, or fatty liver disease, with acquired immunodeficiency, or with other viral liver diseases or other liver diseases; (2) patients with hypertension, diabetes, obesity, metabolic syndrome, inflammatory bowel disease, autoimmune disease (such as rheumatoid arthritis or multiple sclerosis) or various tumors; (3) patients who had not used antibiotics, microecological agents, or proton pump inhibitors within 2 wk before enrollment; and (4) pregnant and lactating women. This study was approved by the Medical Ethics Committee of the General Hospital of Ningxia Medical University (approval number: 2016-252), and all participants provided informed consent.

Clinical data

The Laboratory Department of the General Hospital of Ningxia Medical University conducted blood tests for high-sensitivity C-reactive protein (CRP), endotoxin, total bilirubin (TBIL), creatinine (Cr), albumin (Alb), prothrombin time (PT), and the prothrombin international standard ratio (INR). Abdominal color Doppler ultrasound was performed in the Department of Ultrasound at Ningxia Medical University.

The Child-Turcotte-Pugh (CTP)[24] scoring system was used as a clinical classification standard to quantitatively assess liver reserve function in patients with LC.

The Model for End-Stage Liver Disease (MELD) score was used to assess disease severity. The formula was as follows: r = 0.378 Ln [bilirubin (mg/dL)] + 1.12 Ln (INR) + 0.95 Ln [Cr (mg/dL)] + 0.64 (cause: Biliary or alcoholic 0, others 1). A higher R value indicated a greater risk and lower survival rate.

The prognostic index (PI)[25], which is based on serum CRP levels and white blood cell (WBC) counts, primarily reflects acute inflammation in the body. A CRP level of ≤ 10 mg/L and WBC count of ≤ 11 × 10^9/L score 0 points; CRP ≤ 10 mg/L and WBC count > 11 × 10^9/L score 1 point; CRP > 10 mg/L and WBC count ≤ 11 × 10^9/L score 1 point; CRP > 10 mg/L and WBC count > 11 × 10^9/L score 1 point; and CRP > 10 mg/L and WBC count > 11 × 10^9/L score 2 points.

Selection ofprobiotics

The probiotic used in this study was LP N1115, which was produced by Shijiazhuang Junlebao Dairy Co., Ltd. (Shijiazhuang City, China) and contains fructooligosaccharides, the food additive lactitol, LP N1115, *L. plantarum*, *Bifidobacterium bifidum*, and *L. acidophilus*. The dosage of active *Lactobacillus* added was ≥ 5 × 10^{10} CFU per bag, with each bag weighing 2 g. The probiotic was administered by mixing an appropriate amount of warm water or milk with the recommended dosage of one bag twice a day. The storage instructions recommend keeping the probiotics in a cool, dry, or refrigerated place.

Collection of feces

Fresh fecal samples were collected from the participants and promptly placed in liquid nitrogen tanks for preservation during transportation to the laboratory. The collection process involved weighing the fecal samples and repackaging them in sterile centrifuge tubes. Three samples were collected from each participant. The subpacked specimens were rapidly transferred to a low-temperature refrigerator at -80 °C for frozen storage. The entire collection and repackaging process was completed within 30 min.

DNA extraction and sequencing of the fecal microbiota

All the samples were subjected to the same procedures for DNA extraction and polymerase chain reaction (PCR) amplification by the same laboratory staff. The samples were suspended in 790 μL of sterile lysis buffer [4 M guanidine thiocyanate, 10% N-lauroyl sarcosine, and 5% N-lauroyl sarcosine in 0.1 M phosphate buffer (pH 8.0)] in a 2 mL screw-cap tube containing 1 g of glass beads (0.1 mm; BioSpec Products, Inc., United States). This mixture was vortexed vigorously and thenincubated at 70 °C for 1 h. After incubation, the mixture was subjected to bead beating for 10 min at maximum speed. Bacterial DNA was extracted using an E.Z.N.A.® Stool DNA Kit (Omega Biotek, Inc., GA) following the manufacturer's instructions, which excluded lysis steps; the extracted DNA was stored at -20 °C for further analysis.

The extracted DNA from each sample was used as the template for amplifying the V3-V4 region of the 16S rRNA gene. The primers F1 and R2 (*5′-CCTTCGGGNGGCWGCAG-3′* and *5′-GACTACHVGGGTATCTAATCC-3′*) corresponding to positions 341 to 805 of the *Escherichia coli* 16S rRNA gene were used to amplify the V3-V4 region of each fecal sample by

PCR. PCRs were run on an EasyCycler 96 PCR system (Analytik Jena Corp., AG). The products from different samples were indexed and mixed at equal ratios for sequencing using the MiSeq platform (Illumina, Inc., United States) according to the manufacturer's instructions.

Bioinformatic analysis

Clean data were extracted from the raw data using USEARCH software (version 11.0.667). The quality-filtered sequences were clustered into unique sequences and sorted in order of decreasing abundance to identify representative sequences using UPARSE according to the UPARSE operational taxonomic unit (OTU) analysis pipeline, and singletons were omitted from this step. OTUs were classified based on 97% similarity after chimeric sequences were removed using UPARSE (version 7.1; http://drive5.com/uparse/) and annotated using the SILVA reference database (SSU138) in qiime2-2020.11. Taxonomic analysis was performed on the representative sequences of the OTUs, and the community composition at each taxonomic level (domain, kingdom, phylum, class, order, family, genus, and species) was determined for each sample.

Statistical analysis

The Mann-Whitney U test (Wilcoxon rank-sum test) was used to compare the levels of CRP, endotoxin, and CTP between the two groups. The MELD score and PI were compared before and after treatment. $P < 0.05$ indicated statistical significance. The chi-square test was used to compare the incidence of ascites.

Bacterial α diversity was assessed using the Shannon, Simpson, Chao1, and The ACE estimator (ACE) indices. The Wilcoxon rank-sum test was also used to assess the α diversity among the different groups. The nonparametric factorial Kruskal-Wallis rank-sum test was used to detect differences in microbial abundances. Linear discriminant analysis (LDA) effect size (LEfSe) was used to detect taxa with differential abundance among the groups (LEfSe1.1, https://github.com/SegataLab/Lefse).

RESULTS

Baseline characteristics of the participants and changes in clinical indicators before and after treatment in the intervention group and nonintervention group

The baseline characteristics of the participants, including their clinical and biochemical characteristics, are summarized in Table 1. Before the intervention, no significant differences in age, sex, TBIL level, Cr level, PT time, WBC count, or platelet count were observed between the intervention and nonintervention groups. There were significant alterations observed in the levels of Alb, Cr, PT, INR, and CRP before and after treatment in the intervention group. Conversely, no notable changes were found in clinical parameters before or after treatment in the nonintervention group (Table 2).

Evaluation of liver function before and after treatment

The CTP and MELD scores were used to assess liver function before and after treatment in the intervention and nonintervention groups, respectively. The results showed that after treatment, the CTP score of the intervention group was better than that before treatment, with a decrease in the proportion of patients with CTP grade C disease from 25.68% to 12.16%. In contrast, the proportion of patients with CTP grade C disease in the nonintervention group increased from 31.08% to 33.78% (Figure 1A-D). Survival curves revealed that the probability of recurrence of ascites in the intervention group was significantly lower than that in the nonintervention group (Figure 1E).

The CTP grade in the intervention group significantly decreased after treatment ($P = 0.007$), whereas that in the nonintervention group did not significantly change ($P = 0.489$). The MELD score, which reflects the severity of end-stage liver disease, was not significantly different between the intervention and nonintervention groups before treatment, whereas after treatment, the MELD score of the intervention group was significantly lower than that of the nonintervention group ($P = 0.017$), indicating that the severity of liver disease was lower in the intervention group than in the nonintervention group (Figure 2).

Changes in inflammatory indices before and after treatment

The results showed no significant differences in CRP levels or PI between the intervention and nonintervention groups at baseline, whereas after the intervention, there were significant differences ($P < 0.001$ and $P = 0.001$, respectively). Compared with those in the pretreatment group, the CRP level and PI in the intervention group decreased significantly after treatment ($P < 0.001$ and $P = 0.006$, respectively), whereas there was no significant reduction in the nonintervention group after treatment ($P = 0.823$ and $P = 0.306$, respectively). The endotoxin levels were significantly lower after treatment in the intervention group ($P = 0.007$) (Figure 3).

Changes in the incidence of ascites before and after treatment

There was no significant difference in the incidence of ascites between the intervention and nonintervention groups before treatment ($P = 1.0$). After treatment with LP N1115, the incidence of ascites in the intervention group was significantly lower than that before treatment, whereas there was no significant change in the nonintervention group. The incidence of massive ascites decreased from 6.76% to 2.7%in the intervention group, whereas it increased from 8.11% to 12.16% in the nonintervention group. The incidence of ascites after treatment was significantly lower in the intervention group than in the nonintervention group ($P = 0.001$) (Figure 4).

Table 1 Baseline characteristics of the subjects

Characteristic	Treat (*n* = 86)	Untreat (*n* = 74)	*P* value
Age (yr), median (IQR)	58 (51.25, 64.75)	60 (51, 70)	0.219
Sex, *n* (%)			0.176
Male	68 (79.07)	53 (71.62)	
Female	18 (20.93)	21 (28.38)	
TBIL (3.0-22.0 μmol/L)	29.26 (21.025, 43.095)	33.875 (26.168, 53.657)	0.117
Alb (35.0-50.0 g/L)	32.75 (25, 39.6)	30.745 (26.575, 34.825)	0.341
Cr (58-110 μmol/L)	64.5 (54.45, 75.325)	60.55 (51.35, 76.925)	0.498
WBC (3.5-9.5 × 10^9/L)	3.89 (2.728, 5.578)	3.88 (2.9075, 5.06)	0.855
PLT (125.0-350.0 × 10^{12}/L)	78 (43.25, 110.25)	69 (48.25, 111.5)	0.943
PT (9.4-12.5 s)	16.15 (14.6, 18.125)	16.25 (14.625, 18.275)	0.986
INR (0.85-1.14)	1.345 (1.216, 1.518)	1.36 (1.193, 1.505)	0.907
CRP (< 10)	4.75 (1.74, 12.8)	4.995 (1.72, 9.403)	0.836

TBIL: Total bilirubin; Alb: Albumin; Cr: Creatinine; WBC: White blood cell; PLT: Platelet; PT: Prothrombin time; INR: International standard ratio; CRP: C-reactive protein.

Table 2 Changes in clinical indicators before and after treatment were compared between the intervention group and the nonintervention group

Characteristics	Treat		*P* value	Untreat		*P* value
	Before	After		Before	After	
TBIL (μmol/L), median (IQR)	29.26 (21.025, 43.095)	27.515 (18.237, 44.22)	0.707	33.875 (26.168, 53.657)	33.3 (20.8, 57.315)	0.637
Alb (g/L), median (IQR)	32.75 (25, 39.6)	37.85 (31.635, 43.773)	0.007	30.745 (26.575, 34.825)	29.9 (26.775, 38.025)	0.625
Cr (μmol/L), median (IQR)	64.5 (54.45, 75.325)	0.85 (48.425, 69.325)	0.03	60.55 (51.35, 76.925)	61.9 (51.4, 82.125)	0.689
WBC (10^9/L), median (IQR)	3.89 (2.7275, 5.5775)	3.505 (2.383, 5.155)	0.321	3.88 (2.9075, 5.06)	4.115 (3, 5.493)	0.439
PLT (10^{12}/L), median (IQR)	78 (43.25, 110.25)	71.5 (50.25, 123.25)	0.760	69 (48.25, 111.5)	69 (48.25, 103.75)	0.833
PT (s), median (IQR)	16.15 (14.6, 18.125)	15.05 (13.35, 16.6)	0.003	16.25 (14.625, 18.275)	15.95 (14, 17.75)	0.342
INR, median (IQR)	1.345 (1.216, 1.518)	1.29 (1.123, 1.408)	0.018	1.36 (1.193, 1.505)	1.315 (1.185, 1.448)	0.526
CRP, median (IQR)	4.75 (1.74, 12.8)	1.845 (0.775, 4.343)	0.005	4.995 (1.72, 9.403)	1.985 (2.035, 1.015)	0.822

TBIL: Total bilirubin; Alb: Albumin; Cr: Creatinine; WBC: White blood cell; PLT: Platelet; PT: Prothrombin time; INR: International standard ratio; CRP: C-reactive protein.

Changes in the intestinalflora before and after treatment in the intervention group

Venn diagram of the OTU distribution: The microbiota in a total of 118 fecal samples collected from the intervention group were tested, including 86 samples collected before the intervention and 32 samples after the intervention. A Venn diagram showed that there were 1744 OTUs shared in the samples before and after treatment, while 1541 OTUs were specifically detected before treatment, and 372 OTUs were specifically detected after treatment (Figure 5).

Alpha diversity analysis: Alpha diversity was used to assess the richness (Chao1 and ACE) and diversity (Shannon and Simpson indices) of the gut microbiota. Alpha-diversity analysis of the intervention group revealed changes in the bacterial richness and diversity before and after treatment. The richness of the intestinal flora tended to increase after the intervention, but the difference was not significant ($P > 0.05$). The Simpson index was significantly lower after the intervention than before the intervention ($P < 0.05$), indicating that the diversity of the intestinal flora tended to increase after intervention with probiotics (Figure 6).

Composition of the intestinal flora before and after probiotic treatment: At the phylum level, Firmicutes, Bacteroidetes, Proteobacteria, Actinobacteria and Fusobacteria were the main phyla identified both before and after treatment. However, the proportion of each phylum changed after the treatment: the proportion of Bacteroidetes (25.2%-35.3%)

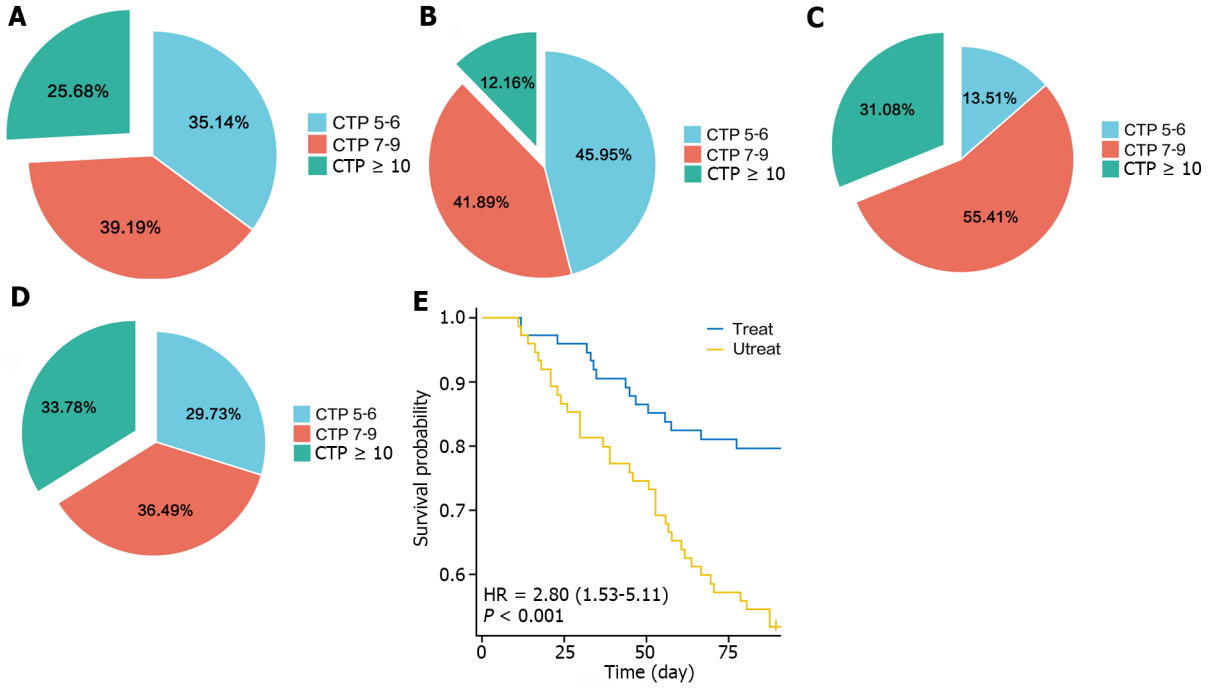

Figure 1 Proportions of Child-Turcotte-Pugh grades A, B, and C before and after treatment in the intervention and nonintervention groups and Kaplan-Meier survival curves. A: The proportion of Child-Turcotte-Pugh (CTP) grades A, B, and C before treatment in the intervention group; B: The proportions of patients with CTP grades A, B, and C in the intervention group after treatment with Lactobacillus paracasei N1115; C: The proportions of patients with CTP grades A, B, and C in the nonintervention group before treatment; D: The proportions of patients with CTP grades A, B, and C in the nonintervention group after treatment; E: The probability of recurrence of ascites in the intervention and nonintervention groups. CTP: Child-Turcotte-Pugh.

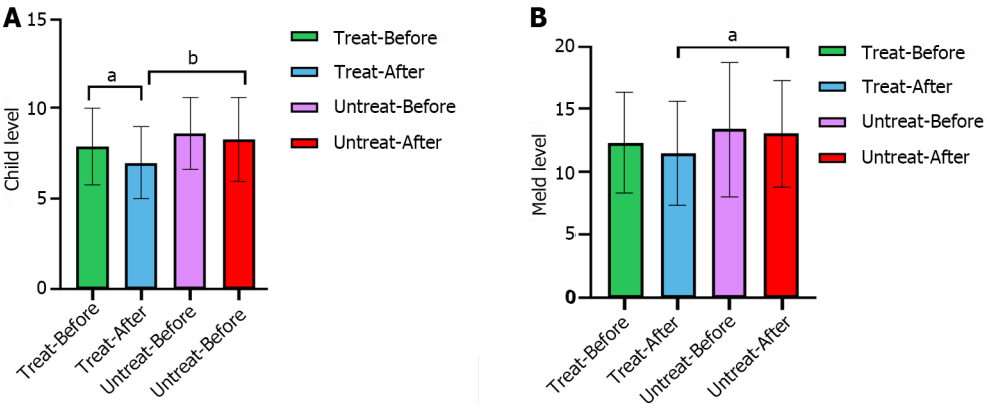

Figure 2 Comparison of liver function indices between the intervention and nonintervention groups before and after treatment. A: A comparison of Child-Turcotte-Pugh grades between the two groups; B: A comparison of Model for End-Stage Liver Disease scores between the two groups. [a]*P* < 0.01, [b]*P* < 0.001.

increased significantly, and those of Firmicutes (61.8%-51.7%) and Proteobacteria (10.5%-5.6%) decreased significantly (Table 3 and Figure 7).

The main genera identified before and after treatment were *Bacteroides*, *Faecalibacterium*, *Lachnospiraceae incertae sedis*, and *Ruminococcaceae*_unclassified. However, after treatment, the proportions of the potentially pathogenic bacteria Enterobacteriaceae_unclassified (2.6%-0.7%), *Escherichia*, *Shigella* (5%-1.8%), and *Streptococcus* (1.8%-0.6%) decreased in abundance. In contrast, the proportions of *Bacteroides* (19.8%-28.4%), *Bifidobacterium* (1.6%-4%), *Ruminococcus* (0.7%-1.5%), *Prevotella* (2.4%-4.9%), and *Lachnospiraceae incertae sedis* (4.8%-5.0%) increased (Table 3 and Figure 8).

Comparison of the abundance of flora before and after treatment: LEfSe analysis was used to identify the key phylotypes with significant differences in abundance before and after treatment. LEfSe analysis revealed that, compared to those before treatment, the proportions of Firmicutes (LDA = 4.74, $P = 0.05$), *Clostridium* (LDA = 3.8, $P = 0.03$), *Pseudobutyrivibrio* (LDA = 3.5, $P = 0.03$), and *Anaerostipes* (LDA = 3.46, $P = 0.01$) significantly decreased after treatment. In contrast, the proportions of Bacteroidetes (LDA = 4.66, $P = 0.01$), *Bifidobacterium* (LDA = 4.47, $P = 0.04$), Veillonellaceae (LDA = 4.0, $P = 0.01$), Lachnospiraceae (LDA = 3.95, $P = 0.001$) and *Eggerthella* (LDA = 3.47, $P = 0.01$) significantly

Table 3 Proportions of intestinal flora at the phylum and genus levels in all subjects in the intervention group before and after treatment

Phylum of bacteria (%)	GR	ZL	*P* value
Firmicutes	61.8	51.7	0.046
Bacteroidetes	25.2	35.5	0.008
Proteobacteria	10.5	5.6	0.468
Actinobacteria	1.7	4	0.057
Fusobacteria	0.3	0.8	0.494
Bacteroides	19.8	28.4	0.014
Faecalibacterium	22	17.8	0.803
Lachnospiraceae_Incertae_Sedis	4.8	5	0.001
Ruminococcaceae_uncultured	5.4	2.6	0.027
Escherichia-Shigella	5	1.8	0.348
Subdoligranulum	4.5	2.3	0.561
Prevotella	2.4	4.9	0.211
Veillonella	3	1.3	0.315
Bifidobacterium	1.6	3.9	0.039
Enterobacteriaceae_unclassified	2.6	0.7	0.629
Anaerostipes	1	0.6	0.007

GR: Before treatment with *Lactobacillus paracasei* N1115 (LP N1115); ZL: 3 months after treatment with LP N1115.

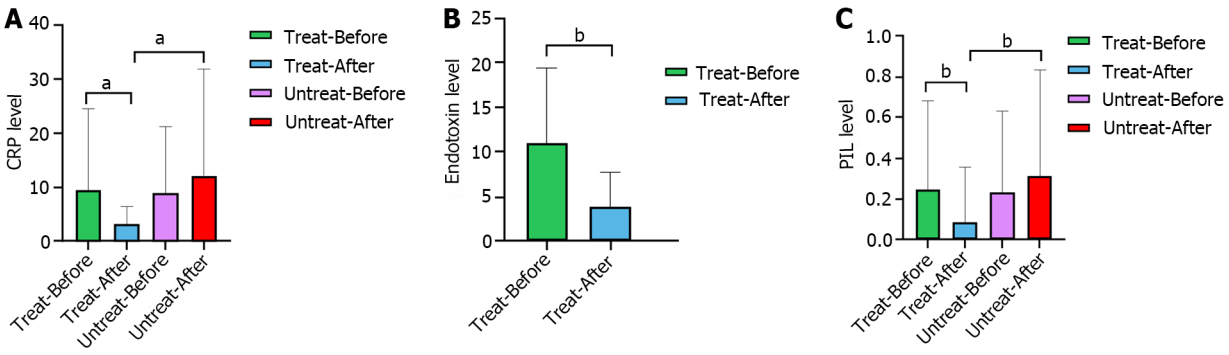

Figure 3 Comparison of inflammatory indices between the intervention and nonintervention groups before and after treatment. A: A comparison of C-reactive protein levels between the two groups; B: A comparison of endotoxin levels between the two groups; C: A comparison of the prognostic index between the two groups. $^{a}P < 0.001$, $^{b}P < 0.01$. CRP: C-reactive protein; PI: prognostic index.

increased after treatment (Figure 8).

Correlation analysis between differential flora and CTP classification: To further understand the relationship between the differential bacteria and the patient's CTP classification of liver function, we performed a correlation analysis between the differential flora and the CTP classification. There was no correlation between the occurrence of *Veillonella*, *Streptococcus*, or *Lachnospiraceae incertae sedis* and the CTP classification before treatment.However, after treatment, there was a positive correlation (Table 4).

DISCUSSION

Intestinal flora imbalance in patients with decompensated LC has garnered significant attention[8]. Studies have indicated that the intestinal microbiota may contribute to the progression of HBV-related chronic liver disease to severe liver failure by promoting the accumulation of inflammatory factors and pathogenic metabolites[26]. An imbalanced

Table 4 Correlations between genus and Child-Turcotte-Pugh classification score before and after intervention

	GR		ZL	
	r	*P* value	*r*	*P* value
Bacteroides	-0.436	0.013	-0.004	0.981
Lachnospiraceae_Incertae_Sedis	0.312	0.082	0.353	0.048
Veillonella	0.272	0.132	0.449	0.01
Streptococcus	0.143	0.433	0.354	0.047
Escherichia-Shigella	0.275	0.128	0.016	0.929
Prevotella	0.22	0.226	0.069	0.706
Enterobacteriaceae_unclassified	0.366	0.04	0.198	0.277
Firmicutes/Bacteroidetes	0.299	0.097	0.253	0.126

GR: Before treatment with *Lactobacillus paracasei* N1115 (LP N1115); ZL: 3 months after treatment with LP N1115.

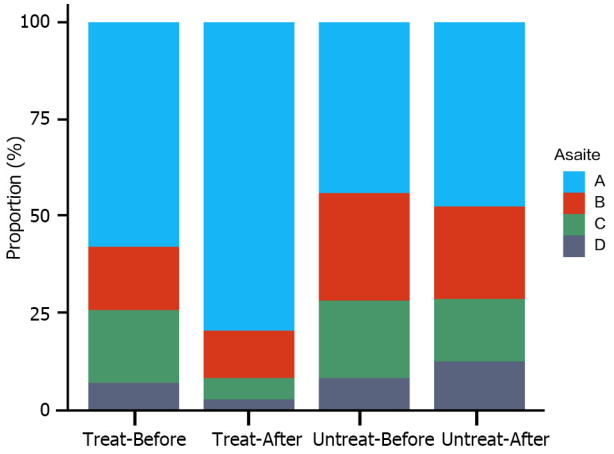

Figure 4 Occurrence of ascites before and after treatment in the intervention and non-intervention groups. A: No ascites; B: Small ascites; C: Moderate ascites; D: Large ascites.

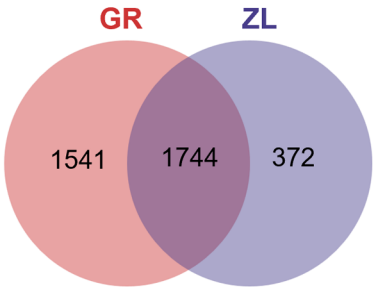

Figure 5 Venn analysis of the distribution of operational taxonomic units. GR: Before treatment with *Lactobacillus paracasei* N1115 (LP N1115); ZL: 3 months after treatment with LP N1115.

intestinal ecology in patients with LC can lead to impaired intestinal barrier function and microbial translocation, which in turn contributes to the development of SBP[27]. Moreover, intestinal flora imbalance after disruption of intestinal barrier function results in increased levels of *Klebsiella* and *Proteus* spp., which, through the production of ammonia and endotoxins, directly causes hepatic encephalopathy owing to an increase in blood ammonia levels[28]. Patients with HCC often exhibit elevated levels of gram-negative bacteria commonly found in the gut microbiome, such as *Escherichia coli*, and decreased levels of beneficial bacteria, including *Lactobacillus*, *Bifidobacterium*, and *Enterococcus*. This imbalance is primarily caused by increased intestinal permeability, leading to bacterial translocation and endotoxin accumulation, which in turn results in intestinal bacterial overgrowth and alterations in the composition of the intestinal microbiota[29].

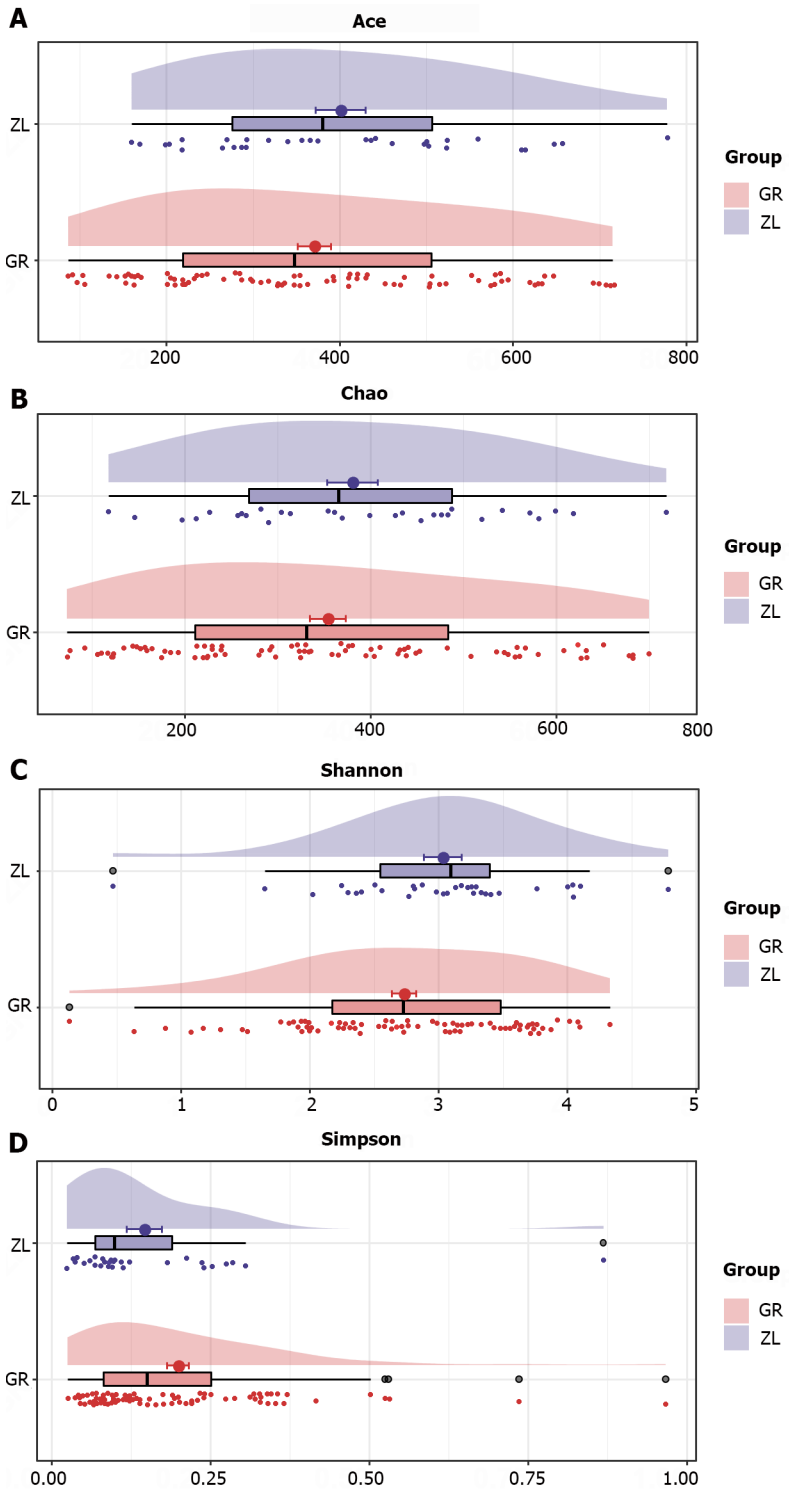

Figure 6 Comparison of gut microbiota abundance and diversity before and after intervention in patients. A: Differences in the Ace index between groups; B: Differences in the Chao index between groups; C: Differences in the Shannon index between groups; D: Differences in the Simpson index between groups. GR: Before treatment with *Lactobacillus paracasei* N1115 (LP N1115); ZL: 3 months after treatment with LP N1115.

A previous study involving patients with HBC demonstrated no significant differences in alpha diversity among patients with HBV-related chronic diseases, HBC, or HCC[30]. However, in the present study, the results indicated an increasing trend in gut microbiota diversity after treatment.

L. paracasei ameliorated diarrhea by inhibiting activation of the NF-κB-MLCK pathway and increasing the abundance of gut microbiota that produce short-chain fatty acids (SCFA)[31]. Lp N1115 was able to enhance the contentof Lactobacillus and maintain fecal pH levels. Its beneficial effects on gut development were more obvious in 6-12-month-old infants [32]. These findings suggest that intervention with the N1115 ready-to-eat *Lactobacillus* supplement may have a modulatory effect on gut microbiota dysbiosis in patients with LC. The increased diversity of the gut microbiota after treatment may help restore a healthy gut state. However, further studies are required to validate and explore the effect-

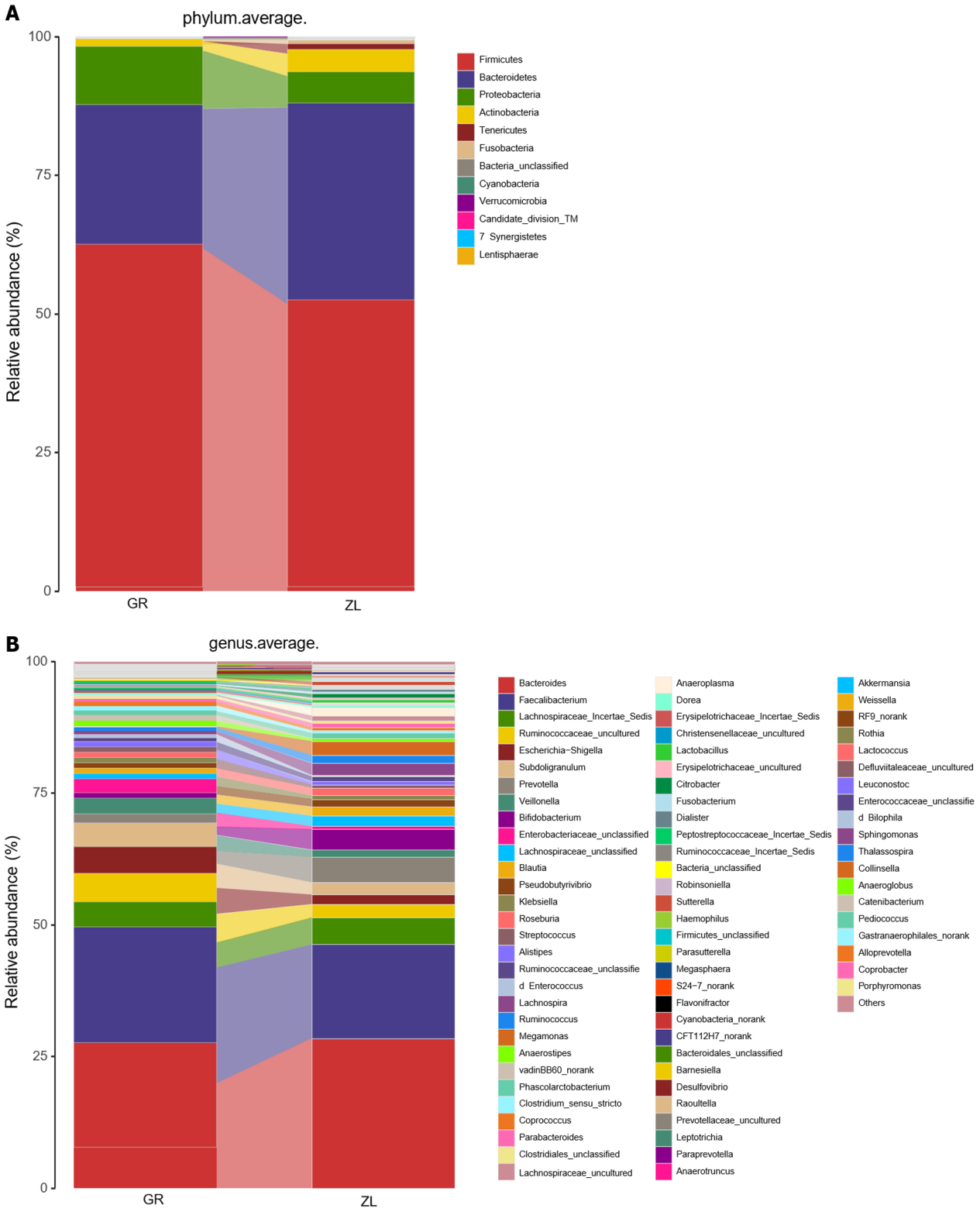

Figure 7 Plots of the relative abundance of the gut microbiota at the phylum and genus levels before and after treatment in all patients. A: Plots of the relative abundance of the gut microbiota at the phylum levels before and after treatment in all patients; B: Plots of the relative abundance of gut microbiota at the genus levels before and after treatment in all patients. GR: Before treatment with *Lactobacillus paracasei* N1115 (LP N1115); ZL: 3 months after treatment with LP N1115.

iveness and mechanisms of this intervention.

Although numerous studies have confirmed the efficacy of probiotics in animal models and in the treatment of hospitalized patients with liver disease, several controversies remain. The choice between single or combined probiotics as well as the efficacy of different bacterial combinations in different probiotics for chronic liver disease require further investigation. Interestingly, we found a close relationship among dysbiosis, inflammatory markers, and liver function. The partial recovery of inflammatory marker levels and liver function in patients after LP N1115 intervention was even more

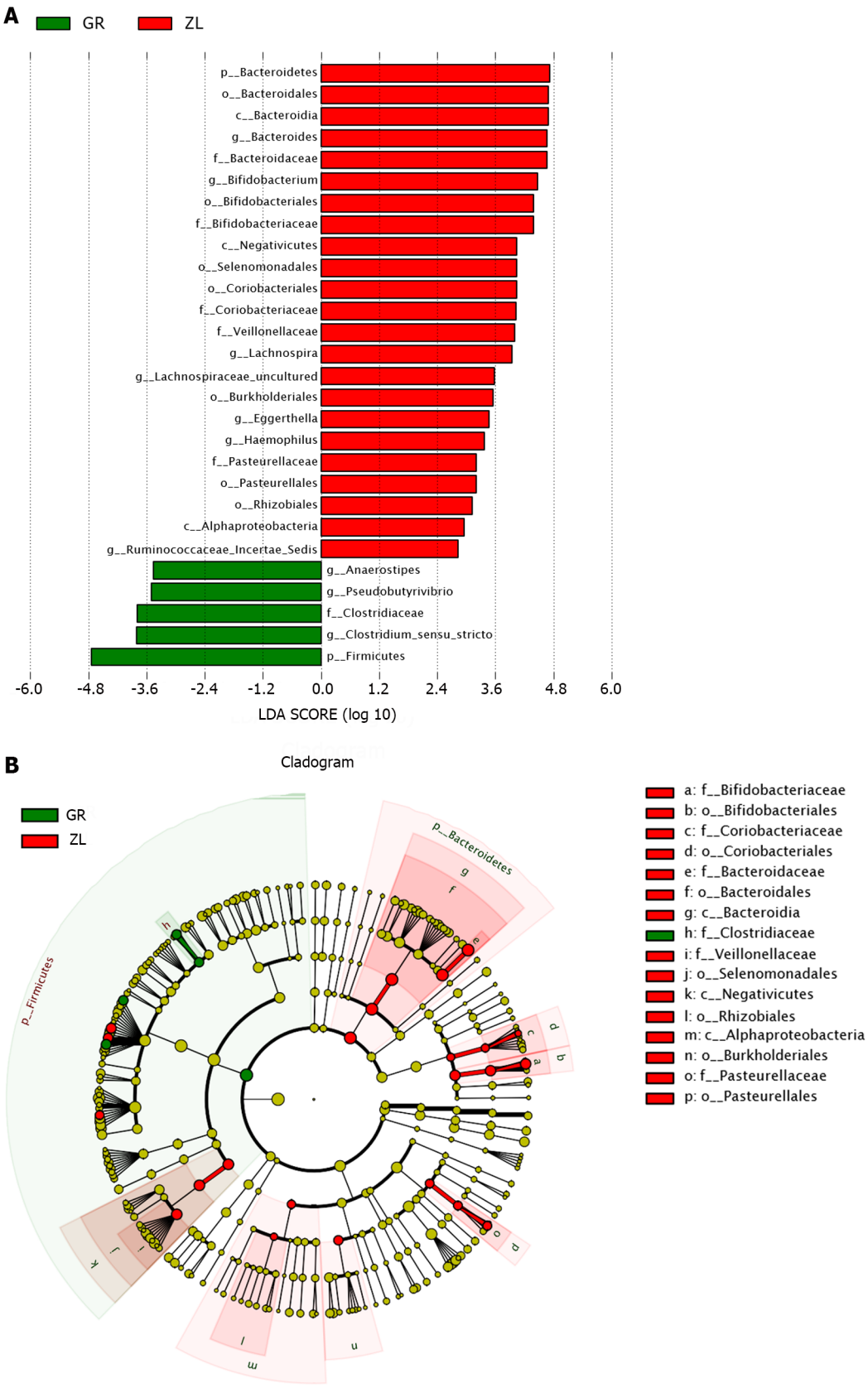

Figure 8 Histogram of linear discriminant analysis effect size distribution; evolutionary subplots were analyzed. A: Histogram of linear discriminant analysis effect size distribution; The evolutionary subplots were analyzed. TLEfse analyzed the LDA histogram; B: Histogram of linear discriminant analysis effect size distribution; The evolutionary subplots were analyzed. LEfse analyzed LDA evolutionary cladistics. GR: Before treatment with *Lactobacillus paracasei* N1115 (LP N1115); ZL: 3 months after treatment with LP N1115.

surprising. Our study demonstrated a significant decrease in CRP levels and a lower CRP level in the intervention group than in the nonintervention group after treatment. Moreover, endotoxin synthesis decreased in the intervention group. The PI, which reflects acute inflammation in the body, significantly decreased in the intervention group after treatment and was significantly lower than that in the nonintervention group, suggesting improved acute inflammation in the intervention group after treatment, whereas the nonintervention group receiving conventional treatment exhibited no significant changes. Patients with HBC often experience bacterial translocation and increased endotoxin levels, leading to changes in intestinal permeability and increased activation of the LPS/TLR4 signaling pathway in the liver[4,33]. TLR4 activation triggers the production of proinflammatory, antiviral, and antibacterial cytokines. The levels of IL-10 and tumor necrosis factor-α are significantly greater in HBC patients than in control individuals, and increased endotoxin expression promotes factor synthesis through signaling pathways[19,34,35]. *L. casei* preparations can regulate TLR4 expression and IL-10 secretion. Therefore, we propose that LP N1115inhibits the activation of the LPS/TLR4 signaling pathway, reduces the release of inflammatory factors, and effectively alleviates the inflammatory state of patients when combined with conventional treatment[36].

However, whether there is a correlation between intestinal flora imbalance and liver function needs to be further explored. The main pathophysiological changes in patients with LC are liver function impairment and portal hypertension, which are crucial factors to consider when evaluating disease conditions and prognosis. Widely used evaluation systems, such as the CTP classification and MELD score, are commonly used both domestically and internationally. An imbalance in the gut microbiota can trigger an inflammatory response and exacerbate liver fibrosis by activating TLRs, thereby promoting the progression of cirrhosis to decompensation and liver failure[27]. Probiotics have been found to reduce liver function damage and improve the levels of markers, such as alanine aminotransferase, aspartate aminotransferase, cholesterol, low-density lipoprotein, and triglycerides, and waist circumference in children with NAFLD[37]. One study showed that Bullavirinae, Felixounavirus, Streptococcus, Escherichia and Pseudomonas phages were positively linked with the MELD, whereas Faecalibacterium phages were negatively linked with the MELD [38]. In this study, we aimed to further understand the effects of LP N1115, a ready-to-eat *Lactobacillus* supplement, on liver function. We compared the CTP and MELD scores between the intervention and nonintervention groups before and after the intervention. The results showed a significant improvement in the CTP classification score and a decrease in the MELD score after the intervention. We further validated liver function by assessing the incidence of ascites. The incidence of ascites in patients treated with LP N1115 was significantly lower, including a lower incidence of massive ascites, than that in patients who did not receive the N1115 intervention and who only received conventional treatment during the same period. Therefore, LP N1115 is highly important for improving liver function and liver reserve function in patients.

In patients with HBC, an increase in the proportion of Enterobacteriaceae, Fusobacteriaceae, and alkali-producing bacteria in the gut was observed, accompanied by a decrease in the abundance of Ruminococcaceae and Pilospirillaceae. Many bacteria from the Ruminococcaceae and Pilospirillaceae families possess bile acid hydrolases that are closely associated with the production of secondary bile acids[27]. Bile acids can disrupt the gut barrier and immune function, affecting the regulation of the intestinal flora structure. At the phylum level, the dominant species remained consistent before and after treatment, although the proportion of each phylum changed. After treatment, the abundance of some potentially pathogenic bacteria decreased, whereas that of beneficial bacteria increased. LEfSe analysis revealed significant differences in the abundance of *Bacteroides*, *Bifidobacterium*, Lachnospirillaceae, and *Eggerthella* after treatment. These results are consistent with the relative abundance map of the dominant species, suggesting that LP N1115 effectively regulates the homeostasis of the intestinal flora. Surprisingly, we found a significant difference in *Lachnospiraceae incertae sedis* levels after N1115 intervention, which was positively correlated with the CTP classification score. Previous studies by Bajaj *et al*[8] indicated that beneficial bacteria, such as Spirillaceae and Verrucomicrobacteriaceae, decrease in abundance in the intestines of patients with LC, whereas harmful bacteria, such as Enterobacteriaceae and Bacteroidaceae, increase in abundance. Triclospira, a member of *Lachnospiraceae incertae sedis*, produces anti-inflammatory SCFA that help maintain water and electrolyte balance, improve intestinal mucosa function and morphology, inhibit tumor cell proliferation, induce macrophage apoptosis, inhibit histone deacetylation, promote the migration of regulatory T cells, and induce the production of anti-inflammatory IgA by mucosal B cells[39,40]. *Lachnospiraceae incertae sedis* possesses bile salt hydrolase, which is involved in secondary bile acid production. Bile acids can directly damage bacterial outer membranesand exert bactericidal effects. These bacteria can also generate nitric oxide and IL-18 through the "bile acid-G protein-coupled receptor (targeting of bile acid receptor 5) TGR5-farnesoid X receptor-camp" pathway, thereby influencing the intestinal flora *via* the immune system, which plays a crucial role in maintaining the balance of the intestinal flora[39,41]. Additionally, the liver secretes bile acids into the intestine through the biliary tract, which can affect the composition and abundance of the intestinal flora. LC is often accompanied by bile acid excretion disorders. Patients with decompensated cirrhosis may develop portal hypertension, leading to intestinal mucosal congestion, edema, impaired small intestinal motility, and intestinal content retention. Complications such as esophageal and gastric fundus variceal bleeding are accompanied by intestinal mucosal ischemia/reperfusion injury, leading to bacterial overgrowth and translocation to the small intestine[42]. Qin *et al*[42] reported that the intestinal flora of patients with LC contained a high proportion of oral bacteria, such as *Streptococcus* and *Veillonella*, indicating that the oral microbial flora invades the gut and contributes to LC deterioration. Reduced gastric acid secretion and altered bile acid secretion in patients with LC may facilitate the translocation of oral bacteria to the gut. Similarly, we observed an increased proportion of *Streptococcus* and *Veillonella* before the intervention, although this difference was not correlated with the CTP classification score. However, after the intervention, the proportion of patients who died decreased and was positively correlated with the CTP classification score. Therefore, we believe that LP N1115 may influence the level of intestinal bile acid by regulating the level of *Lachnospiraceae incertae sedis*, reducing the translocation of *Streptococcus* and *Veillonella* to the intestine, and assisting conventional treatment to improve inflammation levels and liver function in patients with hepatobiliary diseases, thereby significantly affecting patient prognosis.

Wang *et al*[43] discovered that patients with hepatitis B-decompensatedcirrhosis exhibited a significant reduction in the abundance of Firmicutes, Trichospirillum, *Dorea*, and *Dialister*. Conversely, there was a significant increase in the abundance of *Streptococcus*, *Fusobacterium*, *Veillonella*, and *Haemophilus spp*. In our analysis of patients with HBC at the phylum level, we observed a relatively high proportion of Firmicutes before the intervention, which decreased after the intervention, demonstrating slight differences from previous studies. We think that a phylum-based analysis is generally not applicable to patients with cirrhosis because of the inclusion of pathogenic groups, such as staphylococci and Enterococcaceae, within Firmicutes, which are more abundant in severely ill individuals. Following the intervention with LP N1115, the proportions of cocci and Enterococcaceae within the phylum Firmicutes decreased.

This study is limited by its small sample size, single- center analysis, absence of an intervention treatment in the control group and no additional stratification. Therefore, whether the effects of the N1115 ready-to-eat *Lactobacillus* supplement on the intestinal flora are limited by differences in region and dietary habits is unknown; additionally, whether the changes in the intestinal flora in patients with different complications are consistent needs to be further explored. Our future work will involve designing larger multicenter trials.

CONCLUSION

In conclusion, we propose that LP N1115 modulates intestinal bile acid levels by regulating the abundance of *Lachnospiraceae incertae sedis*, consequently reducing the translocation of *Streptococcus* and *Veillonella* to the intestine. This intervention can effectively complement conventional treatments, leading to improvements in inflammation and liver function in HBC patients. As a potential therapeutic target, it is crucial to consider the timing, duration, and dosage of this intervention. Therefore, conductinglarge-scale, multicenter, randomized, placebo-controlled trials investigating the microbiome and metabolomics of LP N1115-treated patients with HBC in the future would provide valuable insights.

ARTICLE HIGHLIGHTS

Research background

Hepatitis B cirrhosis (HBC) is a prevalent chronic disease associated with significant morbidity and mortality. Numerous studies have consistently demonstrated the occurrence of intestinal flora dysbiosis in patients diagnosed with HBC. Alterations in the composition of the intestinal flora can disrupt immune regulation, impair intestinal barrier function, and induce systemic inflammatory changes *via* the gut-liver axis, thereby hastening the progression of cirrhosis. Interventions utilizing microecological preparations hold immense significance in enhancing prognosis.

Research motivation

Although numerous individual probiotics have been documented in relation to HBC, the impact of the N1115 compound ready-to-eat *Lactobacillus* supplement in patients with HBC remains uncertain.

Research objectives

The primary objective was to assess the impact of the N1115 ready-to-consume lactic acid bacterial supplement on hepatic function, inflammation, and ascites in patients with HBC. This study aimed to investigate the therapeutic potential of the intestinal microecology in managing HBC. HBC patients were administered the N1115 ready-to-eat lactic acid bacterial supplement for 3 months, which resulted in a significant increase in intestinal microbial diversity and notable alterations in the composition of the intestinal microbiota. There was a remarkable improvement in liver function parameters and a decrease in the levels of inflammatory markers among the patients. This investigation offers novel insights into optimizing interventions targeting the intestinal microflora in individuals with HBC.

Research methods

This study included 160 HBC patients who were diagnosed at the General Hospital of Ningxia Medical University between October 2018 and December 2020. Patients were randomly divided into an intervention group that received *Lactobacillus paracasei* N1115 (LP N1115) supplementation along with routine treatment and a control group that received routine treatment only. Fecal samples were collected at the onset and conclusion of the 12-wk intervention period. The structure of the intestinal microbiota and the levels of serological indicators, such as liver function and inflammatory factors, were assessed.

Research results

The patients were assessed after 3 months of treatment with the N1115 ready-to-eat *Lactobacillus* supplement: (1) There were significant changes in the levels of albumin, creatinine, prothrombin time, international standard ratio, and C-reactive protein and in the Child-Turcotte-Pugh and Model for End-Stage Liver Disease scores before and after treatment in the intervention group; (2) the probability of recurrence of ascites in the intervention group was significantly lower than that in the nonintervention group; and (3) the diversity of the intestinal flora tended to increase after intervention with probiotics. At the phylum level, the proportion of Bacteroidetes increased significantly, and those of Firmicutes and Proteobacteria decreased significantly. At the genus level, the proportions of the potentially pathogenic bacteria

Enterobacteriaceae_unclassified, Escherichia, Shigella, and Streptococcus decreased. In contrast, the proportions of Bacteroides, Bifidobacterium, Ruminococcus, Prevotella, and Lachnospiraceae incertae sedis increased.

Research conclusions

LP N1115 supplementation is promising for ameliorating intestinal microbial imbalance in patients with HBC by modulating the structure of the intestinal microbiota, improving liver function, and reducing inflammatory factor levels.

Research perspectives

Future studies should prioritize investigating the structural and metabolic alterations in the composition of intestinal biota among patients with various complications of HBC, along with elucidating their underlying mechanisms. To address these inquiries, our research group intends to conduct large-scale, long-term clinical trials.

ACKNOWLEDGEMENTS

We thank all the patients who participated in this study and the physicians in the Department of Infectious Diseases, General Hospital, Ningxia Medical University. We also thank Shanghai Mobio Biomedical Technology Co. for their technical support.

FOOTNOTES

Author contributions: Ding XC is the guarantor and designed the study; Hu YC participated in the acquisition, analysis, and interpretation of the data and drafted the initial manuscript; Liu HJ, Ma WL, and Feng XY participated in the acquisition and analysis of the data; and Ding XC and Ma LN critically revised the article for important intellectual content.

Supported by The Health System Research Project of Ningxia Hui Autonomous Region of China, No. 2022-NWKY-061.

Institutional review board statement: The study was reviewed and approved by the Hungarian National Review Board and the Institutional Review Board of the Ningxia Medical University.

Clinical trial registration statement: This study is registered at http://www.chictr.org.cn. The registration identification number is ChiCTRIIR17011061.

Informed consent statement: All study participants, or their legal guardian, provided informed written consent prior to study enrollment.

Conflict-of-interest statement: The authors declare that they have no conflict of interest.

Data sharing statement: Technical appendix, statistical code, and dataset available from the corresponding author at [13619511768@163.com]. Participants consent for data sharing was not obtained but the presented data are anonymized and risk of identification is low. No additional data are available.

CONSORT 2010 statement: The authors have read the CONSORT 2010 statement, and the manuscript was prepared and revised according to the CONSORT 2010 statement.

Country/Territory of origin: China

ORCID number: Yan-Chao Hu 0000-0002-5570-5222; Xiang-Chun Ding 0000-0003-0283-9419; Hui-Juan Liu 0009-0001-2741-9659; Wan-Long Ma 0009-0007-3658-1571; Xue-Yan Feng 0009-0000-5773-0862; Li-Na Ma 0000-0002-6244-7997.

S-Editor: Qu XL
L-Editor: A
P-Editor: Cai YX

REFERENCES

1 **Ginès P**, Krag A, Abraldes JG, Solà E, Fabrellas N, Kamath PS. Liver cirrhosis. *Lancet* 2021; **398**: 1359-1376 [PMID: 34543610 DOI: 10.1016/S0140-6736(21)01374-X]

2 **Yang F**, Ma L, Yang Y, Liu W, Zhao J, Chen X, Wang M, Zhang H, Cheng S, Shen F, Wang H, Zhou W, Cao G. Contribution of Hepatitis B Virus Infection to the Aggressiveness of Primary Liver Cancer: A Clinical Epidemiological Study in Eastern China. *Front Oncol* 2019; **9**: 370 [PMID: 31179237 DOI: 10.3389/fonc.2019.00370]

3 **Fouts DE**, Torralba M, Nelson KE, Brenner DA, Schnabl B. Bacterial translocation and changes in the intestinal microbiome in mouse models of liver disease. *J Hepatol* 2012; **56**: 1283-1292 [PMID: 22326468 DOI: 10.1016/j.jhep.2012.01.019]

4 **Lee NY**, Yoon SJ, Han DH, Gupta H, Youn GS, Shin MJ, Ham YL, Kwak MJ, Kim BY, Yu JS, Lee DY, Park TS, Park SH, Kim BK, Joung HC, Choi IS, Hong JT, Kim DJ, Han SH, Suk KT. Lactobacillus and Pediococcus ameliorate progression of non-alcoholic fatty liver disease through modulation of the gut microbiome. *Gut Microbes* 2020; **11**: 882-899 [PMID: 31965894 DOI: 10.1080/19490976.2020.1712984]

5 **Duseja A**, Acharya SK, Mehta M, Chhabra S; Shalimar, Rana S, Das A, Dattagupta S, Dhiman RK, Chawla YK. High potency multistrain probiotic improves liver histology in non-alcoholic fatty liver disease (NAFLD): a randomised, double-blind, proof of concept study. *BMJ Open Gastroenterol* 2019; **6**: e000315 [PMID: 31423319 DOI: 10.1136/bmjgast-2019-000315]

6 **Bajaj JS**. Altered Microbiota in Cirrhosis and Its Relationship to the Development of Infection. *Clin Liver Dis (Hoboken)* 2019; **14**: 107-111 [PMID: 31632660 DOI: 10.1002/cld.827]

7 **Chen Y**, Yang F, Lu H, Wang B, Chen Y, Lei D, Wang Y, Zhu B, Li L. Characterization of fecal microbial communities in patients with liver cirrhosis. *Hepatology* 2011; **54**: 562-572 [PMID: 21574172 DOI: 10.1002/hep.24423]

8 **Bajaj JS**, Heuman DM, Hylemon PB, Sanyal AJ, White MB, Monteith P, Noble NA, Unser AB, Daita K, Fisher AR, Sikaroodi M, Gillevet PM. Altered profile of human gut microbiome is associated with cirrhosis and its complications. *J Hepatol* 2014; **60**: 940-947 [PMID: 24374295 DOI: 10.1016/j.jhep.2013.12.019]

9 **Acharya C**, Bajaj JS. Altered Microbiome in Patients With Cirrhosis and Complications. *Clin Gastroenterol Hepatol* 2019; **17**: 307-321 [PMID: 30099098 DOI: 10.1016/j.cgh.2018.08.008]

10 **Brescia P**, Rescigno M. The gut vascular barrier: a new player in the gut-liver-brain axis. *Trends Mol Med* 2021; **27**: 844-855 [PMID: 34229973 DOI: 10.1016/j.molmed.2021.06.007]

11 **Wang R**, Tang R, Li B, Ma X, Schnabl B, Tilg H. Gut microbiome, liver immunology, and liver diseases. *Cell Mol Immunol* 2021; **18**: 4-17 [PMID: 33318628 DOI: 10.1038/s41423-020-00592-6]

12 **Pessione E**. Lactic acid bacteria contribution to gut microbiota complexity: lights and shadows. *Front Cell Infect Microbiol* 2012; **2**: 86 [PMID: 22919677 DOI: 10.3389/fcimb.2012.00086]

13 **Shin D**, Chang SY, Bogere P, Won K, Choi JY, Choi YJ, Lee HK, Hur J, Park BY, Kim Y, Heo J. Beneficial roles of probiotics on the modulation of gut microbiota and immune response in pigs. *PLoS One* 2019; **14**: e0220843 [PMID: 31461453 DOI: 10.1371/journal.pone.0220843]

14 **Ren T**, Huang C, Cheng M. Dietary blueberry and bifidobacteria attenuate nonalcoholic fatty liver disease in rats by affecting SIRT1-mediated signaling pathway. *Oxid Med Cell Longev* 2014; **2014**: 469059 [PMID: 25544867 DOI: 10.1155/2014/469059]

15 **Zhang M**, Wang C, Zhao H, Zhao C, Chen Y, Wang Y, McClain C, Feng W. Enhanced AMPK phosphorylation contributes to the beneficial effects of Lactobacillus rhamnosus GG supernatant on chronic-alcohol-induced fatty liver disease. *J Nutr Biochem* 2015; **26**: 337-344 [PMID: 25622859 DOI: 10.1016/j.jnutbio.2014.10.016]

16 **Holte K**, Krag A, Gluud LL. Systematic review and meta-analysis of randomized trials on probiotics for hepatic encephalopathy. *Hepatol Res* 2012; **42**: 1008-1015 [PMID: 22548675 DOI: 10.1111/j.1872-034X.2012.01015.x]

17 **Lunia MK**, Sharma BC, Sharma P, Sachdeva S, Srivastava S. Probiotics prevent hepatic encephalopathy in patients with cirrhosis: a randomized controlled trial. *Clin Gastroenterol Hepatol* 2014; **12**: 1003-8.e1 [PMID: 24246768 DOI: 10.1016/j.cgh.2013.11.006]

18 **Ren YD**, Ye ZS, Yang LZ, Jin LX, Wei WJ, Deng YY, Chen XX, Xiao CX, Yu XF, Xu HZ, Xu LZ, Tang YN, Zhou F, Wang XL, Chen MY, Chen LG, Hong MZ, Ren JL, Pan JS. Fecal microbiota transplantation induces hepatitis B virus e-antigen (HBeAg) clearance in patients with positive HBeAg after long-term antiviral therapy. *Hepatology* 2017; **65**: 1765-1768 [PMID: 28027582 DOI: 10.1002/hep.29008]

19 **Acharya C**, Bajaj JS. Gut Microbiota and Complications of Liver Disease. *Gastroenterol Clin North Am* 2017; **46**: 155-169 [PMID: 28164848 DOI: 10.1016/j.gtc.2016.09.013]

20 **Yao F**, Jia R, Huang H, Yu Y, Mei L, Bai L, Ding Y, Zheng P. Effect of Lactobacillus paracasei N1115 and fructooligosaccharides in nonalcoholic fatty liver disease. *Arch Med Sci* 2019; **15**: 1336-1344 [PMID: 31572482 DOI: 10.5114/aoms.2019.86611]

21 **Yao FF**, Zheng PY, Huang H, Bai LM, Ding YR, Mei L, Liu SM. [Effects of Lactobacillus paracasei N1115 combined with fructooligosaccharides on non-alcoholic fatty liver disease induced by high-fat diet in mice]. *Zhonghua Gan Zang Bing Za Zhi* 2017; **25**: 927-933 [PMID: 29325294 DOI: 10.3760/cma.j.issn.1007-3418.2017.12.008]

22 **Stadlbauer V**, Mookerjee RP, Hodges S, Wright GA, Davies NA, Jalan R. Effect of probiotic treatment on deranged neutrophil function and cytokine responses in patients with compensated alcoholic cirrhosis. *J Hepatol* 2008; **48**: 945-951 [PMID: 18433921 DOI: 10.1016/j.jhep.2008.02.015]

23 **Chinese Society of Infectious Diseases**; Chinese Medical Association; Chinese Society of Hepatology, Chinese Medical Association. [The guidelines of prevention and treatment for chronic hepatitis B (2019 version)]. *Zhonghua Gan Zang Bing Za Zhi* 2019; **27**: 938-961 [PMID: 31941257 DOI: 10.3760/cma.j.issn.1007-3418.2019.12.007]

24 **Zuberi BF**, Rasheed T, Ali FS, Bader N, Sadaf R. Assessment of frailty in cirrhosis using bedside measures and its correlation with Child-Turcotte-Pugh, MELD & MELD-Na Scores. *Pak J Med Sci* 2022; **38**: 1086-1092 [PMID: 35799712 DOI: 10.12669/pjms.38.5.5545]

25 **Yang KL**, Chen JB, Zhu YQ, Zhou ZG, Chen MS. Inflammation Prognostic Score and its Correlation with the Prognosis of Radiofrequency Ablation in Liver Cancer. *Guangdong Yixue* 2018; **33**: 2294-2299 [DOI: 10.13820/j.cnki.gdyx.20180809.014]

26 **Wang WW**, Zhang Y, Huang XB, You N, Zheng L, Li J. Fecal microbiota transplantation prevents hepatic encephalopathy in rats with carbon tetrachloride-induced acute hepatic dysfunction. *World J Gastroenterol* 2017; **23**: 6983-6994 [PMID: 29097871 DOI: 10.3748/wjg.v23.i38.6983]

27 **Oikonomou T**, Papatheodoridis GV, Samarkos M, Goulis I, Cholongitas E. Clinical impact of microbiome in patients with decompensated cirrhosis. *World J Gastroenterol* 2018; **24**: 3813-3820 [PMID: 30228776 DOI: 10.3748/wjg.v24.i34.3813]

28 **Häussinger D**, Schliess F. Pathogenetic mechanisms of hepatic encephalopathy. *Gut* 2008; **57**: 1156-1165 [PMID: 18628377 DOI: 10.1136/gut.2007.122176]

29 **Milosevic I**, Vujovic A, Barac A, Djelic M, Korac M, Radovanovic Spurnic A, Gmizic I, Stevanovic O, Djordjevic V, Lekic N, Russo E, Amedei A. Gut-Liver Axis, Gut Microbiota, and Its Modulation in the Management of Liver Diseases: A Review of the Literature. *Int J Mol Sci* 2019; **20** [PMID: 30658519 DOI: 10.3390/ijms20020395]

30 **Zeng Y**, Chen S, Fu Y, Wu W, Chen T, Chen J, Yang B, Ou Q. Gut microbiota dysbiosis in patients with hepatitis B virus-induced chronic liver disease covering chronic hepatitis, liver cirrhosis and hepatocellular carcinoma. *J Viral Hepat* 2020; **27**: 143-155 [PMID: 31600845 DOI: 10.1111/jvh.13216]

31 **Ren S**, Wang C, Chen A, Lv W, Gao R. The Probiotic Lactobacillus paracasei Ameliorates Diarrhea Cause by Escherichia coli O(8) *via* Gut Microbiota Modulation(1). *Front Nutr* 2022; **9**: 878808 [PMID: 35662940 DOI: 10.3389/fnut.2022.878808]

32 **Li P**, Ren Z, Zhou J, Zhao A, Wang S, Xun Y, Jiang H, Wang P, Yuan Q, Zhang Y. Effect of Lacticaseibacillus paracasei N1115 on Immunomodulatory and Gut Microbial Composition in Young Children: A Randomized, Placebo-Controlled Study. *Nutrients* 2023; **15** [PMID: 37111189 DOI: 10.3390/nu15081970]

33 **Fukui H**. Gut Microbiome-based Therapeutics in Liver Cirrhosis: Basic Consideration for the Next Step. *J Clin Transl Hepatol* 2017; **5**: 249-260 [PMID: 28936406 DOI: 10.14218/JCTH.2017.00008]

34 **Moratalla A**, Gómez-Hurtado I, Moya-Pérez Á, Zapater P, Peiró G, González-Navajas JM, Gómez Del Pulgar EM, Such J, Sanz Y, Francés R. Bifidobacterium pseudocatenulatum CECT7765 promotes a TLR2-dependent anti-inflammatory response in intestinal lymphocytes from mice with cirrhosis. *Eur J Nutr* 2016; **55**: 197-206 [PMID: 25657013 DOI: 10.1007/s00394-015-0837-x]

35 **Fukui H**. Gut-liver axis in liver cirrhosis: How to manage leaky gut and endotoxemia. *World J Hepatol* 2015; **7**: 425-442 [PMID: 25848468 DOI: 10.4254/wjh.v7.i3.425]

36 **Bajaj JS**, Sikaroodi M, Shamsaddini A, Henseler Z, Santiago-Rodriguez T, Acharya C, Fagan A, Hylemon PB, Fuchs M, Gavis E, Ward T, Knights D, Gillevet PM. Interaction of bacterial metagenome and virome in patients with cirrhosis and hepatic encephalopathy. *Gut* 2021; **70**: 1162-1173 [PMID: 32998876 DOI: 10.1136/gutjnl-2020-322470]

37 **Albillos A**, de Gottardi A, Rescigno M. The gut-liver axis in liver disease: Pathophysiological basis for therapy. *J Hepatol* 2020; **72**: 558-577 [PMID: 31622696 DOI: 10.1016/j.jhep.2019.10.003]

38 **Famouri F**, Shariat Z, Hashemipour M, Keikha M, Kelishadi R. Effects of Probiotics on Nonalcoholic Fatty Liver Disease in Obese Children and Adolescents. *J Pediatr Gastroenterol Nutr* 2017; **64**: 413-417 [PMID: 28230607 DOI: 10.1097/MPG.0000000000001422]

39 **Keitel V**, Reinehr R, Gatsios P, Rupprecht C, Görg B, Selbach O, Häussinger D, Kubitz R. The G-protein coupled bile salt receptor TGR5 is expressed in liver sinusoidal endothelial cells. *Hepatology* 2007; **45**: 695-704 [PMID: 17326144 DOI: 10.1002/hep.21458]

40 **Wahlström A**, Sayin SI, Marschall HU, Bäckhed F. Intestinal Crosstalk between Bile Acids and Microbiota and Its Impact on Host Metabolism. *Cell Metab* 2016; **24**: 41-50 [PMID: 27320064 DOI: 10.1016/j.cmet.2016.05.005]

41 **Quan M**, Xing HC. Intestinal flora research progress associated with chronic liver disease. *Zhonguo Ganzangbing Zazhi (Dianziban)***11**: 26-30

42 **Qin N**, Yang F, Li A, Prifti E, Chen Y, Shao L, Guo J, Le Chatelier E, Yao J, Wu L, Zhou J, Ni S, Liu L, Pons N, Batto JM, Kennedy SP, Leonard P, Yuan C, Ding W, Hu X, Zheng B, Qian G, Xu W, Ehrlich SD, Zheng S, Li L. Alterations of the human gut microbiome in liver cirrhosis. *Nature* 2014; **513**: 59-64 [PMID: 25079328 DOI: 10.1038/nature13568]

43 **Wang YX**, Li W, Cheng DY, Liu SA, Zhang S, Han M, Zhu M, Sun J, Xing HC. Characteristics of intestinal flora of patients with hepatitis B related decompensated cirrhosis. *Zhonghua Shiyan He Linchuang Ganranbing Zazhi (Dianziban)* 2019; **13**: 110-116

World Journal of Gastroenterology

Submit a Manuscript: https://www.f6publishing.com

World J Gastroenterol 2024 March 21; 30(11): 1572-1587

DOI: 10.3748/wjg.v30.i11.1572

ISSN 1007-9327 (print) ISSN 2219-2840 (online)

ORIGINAL ARTICLE

Prospective Study

Washed microbiota transplantation for Crohn's disease: A metagenomic, metatranscriptomic, and metabolomic-based study

Shi-Ju Chen, Da-Ya Zhang, Xia Wu, Fa-Ming Zhang, Bo-Ta Cui, Yi-Hao Huang, Zu-Lun Zhang, Rui Wang, Fei-Hu Bai

Specialty type: Gastroenterology and hepatology

Provenance and peer review: Unsolicited article; Externally peer reviewed.

Peer-review model: Single blind

Peer-review report's scientific quality classification
Grade A (Excellent): A
Grade B (Very good): 0
Grade C (Good): 0
Grade D (Fair): 0
Grade E (Poor): 0

P-Reviewer: Snyder AM, United States

Received: January 7, 2024
Peer-review started: January 7, 2024
First decision: February 1, 2024
Revised: February 7, 2024
Accepted: March 6, 2024
Article in press: March 6, 2024
Published online: March 21, 2024

Shi-Ju Chen, Da-Ya Zhang, Graduate School, Hainan Medical University, Haikou 571199, Hainan Province, China

Xia Wu, Fa-Ming Zhang, Bo-Ta Cui, Yi-Hao Huang, Zu-Lun Zhang, Rui Wang, Department of Microbiota Medicine & Medical Center for Digestive Diseases, The Second Affiliated Hospital of Nanjing Medical University, Nanjing 210011, Jiangsu Province, China

Fei-Hu Bai, Department of Gastroenterology, The Second Affiliated Hospital of Hainan Medical University, Haikou 570216, Hainan Province, China

Corresponding author: Fei-Hu Bai, PhD, Chief Doctor, Professor, Department of Gastroenterology, The Second Affiliated Hospital of Hainan Medical University, No. 368 Yehai Avenue, Longhua District, Haikou 570216, Hainan Province, China.
baifeihu_hy@163.com

Abstract

BACKGROUND

Fecal microbiota transplantation (FMT) is a promising therapeutic approach for treating Crohn's disease (CD). The new method of FMT, based on the automatic washing process, was named as washed microbiota transplantation (WMT). Most existing studies have focused on observing the clinical phenomena. However, the mechanism of action of FMT for the effective management of CD-particularly in-depth multi-omics analysis involving the metagenome, metatranscriptome, and metabolome-has not yet been reported.

AIM

To assess the efficacy of WMT for CD and explore alterations in the microbiome and metabolome in response to WMT.

METHODS

We conducted a prospective, open-label, single-center clinical study. Eleven CD patients underwent WMT. Their clinical responses (defined as a decrease in their CD Activity Index score of > 100 points) and their microbiome (metagenome, metatranscriptome) and metabolome profiles were evaluated three months after the procedure.

RESULTS

Seven of the 11 patients (63.6%) showed an optimal clinical response three months post-WMT. Gut microbiome diversity significantly increased after WMT, consistent with improved clinical symptoms. Comparison of the metagenome and metatranscriptome analyses revealed consistent alterations in certain strains, such as *Faecalibacterium prausnitzii*, *Roseburia intestinalis*, and *Escherichia coli*. In addition, metabolomics analyses demonstrated that CD patients had elevated levels of various amino acids before treatment compared to the donors. However, levels of vital amino acids that may be associated with disease progression (*e.g.*, L-glutamic acid, gamma-glutamyl-leucine, and prolyl-glutamine) were reduced after WMT.

CONCLUSION

WMT demonstrated therapeutic efficacy in CD treatment, likely due to the effective reconstruction of the patient's microbiome. Multi-omics techniques can effectively help decipher the potential mechanisms of WMT in treating CD.

Key Words: Crohn's disease; Clinical trials; Fecal microbiota transplant; Metagenome; Metatranscriptome; Metabolome

Core Tip: Fecal microbiota transplantation (FMT) is a promising therapeutic approach for treating Crohn's disease (CD). The new method of FMT, based on the automatic washing process, was named as washed microbiota transplantation (WMT). However, most existing studies have focused on observing clinical phenomena. In the present study, we found that the efficacy of WMT in CD may be due to the effective remodeling of the intestinal micro-ecological balance of patients through the combined in-depth analysis of metagenomic, metatranscriptomic, and metabolomic technologies. Multi-omics techniques can effectively help decipher the underlying mechanism of WMT for CD.

Citation: Chen SJ, Zhang DY, Wu X, Zhang FM, Cui BT, Huang YH, Zhang ZL, Wang R, Bai FH. Washed microbiota transplantation for Crohn's disease: A metagenomic, metatranscriptomic, and metabolomic-based study. *World J Gastroenterol* 2024; 30(11): 1572-1587

URL: https://www.wjgnet.com/1007-9327/full/v30/i11/1572.htm

DOI: https://dx.doi.org/10.3748/wjg.v30.i11.1572

INTRODUCTION

The global incidence of Crohn's disease (CD), a type of inflammatory bowel disease (IBD), has been steadily rising over recent years. The prevalence rate has increased from 79.5 cases per 100000 individuals in 1990 to 84.3 per 100000 in 2017 [1]. This increase poses a significant risk to human health. The pathogenesis of CD is still not completely understood. However, it is widely believed that the onset of CD is influenced by genetic, environmental, and gut microbiota dysbiotic factors, especially the abnormal activation of the gastrointestinal immune system by disorders involving the gut microbiota, which have emerged as a research hotspot in recent years. CD patients have distinct differences in their gut microbiota compared to healthy individuals, including a general decrease in species diversity and abundance of certain commensal and beneficial bacteria (*e.g.*, *Firmicutes* and *Bacteroides* spp.), accompanied by increased *Proteobacteria*. The pathotype adherent-invasive *Escherichia coli* (*E. coli*), in the phylum Aspergillus, has been identified as an important risk factor for CD[2]. It potentially contributes to inflammation by producing α-hemolysin, which can lead to the destruction of the intestinal mucosa[3]. On the other hand, *Ruminococcus gnavus* may be involved in CD development by producing a glucorhamnan polysaccharide that acts on toll-like receptor 4 to induce an inflammatory response[4].

The utilization of fecal microbiota transplantation (FMT) has shown potential as an effective treatment option for CD. The new method of FMT, based on the automatic washing process, was named washed microbiota transplantation (WMT)[5] in the consensus statement from the FMT-standardization Study Group in 2019[6]. Washed preparation of fecal microbiota improves transplantation-related safety, quantitative methods, and delivery of the microbiota suspension[5, 7]. WMT has been used to effectively re-establish intestinal microecology and holds promise for treating CD. Interestingly, in comparison to manual FMT, WMT has significantly enhanced the safety of CD treatment, as evidenced by a decrease in adverse events from 21.7% (15/69) to 4.0% (35/882)[7]. Clinical responses to WMT in IBD treatment are primarily associated with successful *Akkermansia* fixation, and *F. prausnitzii* has been found to have a strong symbiotic relationship with it[8]. In addition, when the optimal timing of the second FMT was sought, it was determined that 125 d was the median time needed to maintain a clinical response to the first FMT[9].

A recent meta-analysis comprising 12 studies on 228 CD patients who underwent FMT revealed that 57% of patients achieved clinical remission between 2 and 4 wk after treatment[10]. However, most published studies are currently limited to observations of clinical phenomena, as the mechanisms of action by which FMT is effective in treating CD have not yet been fully identified, particularly regarding more extensive changes in the microbiome and metabolome. This identification is critical for expanding the high-quality evidence base for FMT in CD treatment.

In the first decade of microbiome research, microbial composition and genome structure were mainly elucidated using DNA sequencing techniques such as 16S rDNA and metagenomic sequencing[11]. Recently, researchers have employed transcriptomic sequencing to analyze bacterial communities to explore dynamic microbiome and gene expression. This approach can elucidate variations in microbiome function in specific environments and interactions with the host. It can also help to understand microbiome configurations across the transition from healthy to diseased states[11]. However, neither changes in the active gut microbiota (from metatranscriptomics) nor changes in fecal metabolites have been reported in CD patients treated with FMT. Therefore, this study aimed to reveal the multi-omics mechanism of WMT for the effective treatment of CD by evaluating and analyzing the metagenomic (DNA), metatranscriptomic (RNA), and metabolomic aspects of stool specimens before and after CD patients received WMT.

MATERIALS AND METHODS

The study was a prospective, open-label, and single-center clinical trial conducted at the Second Affiliated Hospital of Nanjing Medical University. All the participants willingly agreed to participate in the research and provided written informed consent. The institution's Institutional Review Board approved the study protocol (NCT01793831). The study protocol complied with the ethical guidelines of the 1975 Declaration of Helsinki and was approved by the Ethics Committee of the Second Affiliated Hospital of Nanjing Medical University (2022-KY-161-01).

Patient recruitment

Adult CD patients with a CD Activity Index (CDAI) score ≥ 150 were recruited from the Second Affiliated Hospital of Nanjing Medical University between March 2022 and March 2023. Exclusion criteria were applied as follows: (1) Patients who had used antibiotics, gastric acid suppressants (*e.g.*, proton pump inhibitors), probiotics, and other medications that may interfere with the gut microbiota in the three months prior to the recruitment; (2) patients requiring antibiotics during hospitalization; (3) patients who had changed their medication in the four weeks prior to recruitment; (4) patients who had comorbidities, such as infectious diseases identified by examination that included (but were not limited to) bacterial infections [including *Clostridioides difficile* (*C. difficile*)], fungal infections, and viral infections; (5) pregnant women, or women of childbearing age planning to conceive; (6) presence of contraindications to gastrointestinal endoscopy or anesthesia; and (7) any other conditions deemed by the investigator to be unsuitable for inclusion in the study.

Patient assessment

Montreal classification[12,13] was used to count the CD patients included in the study. The Montreal classification is based on the age at diagnosis (A1: < 16, A2: 17-40, A3: > 40), disease location (L1: Ileal, L2: Colonic, L3: Ileocolonic, L4: Upper gastrointestinal), and the disease behavior (B1: Non-stricturing/non-penetrating, B2: Stricturing, B3:penetrating, P: Perianal disease modifier). All the patients were assessed for CDAI and Harvey-Bradshaw Index (HBI) scores as well as clinically relevant indices (including general health, stool frequency, level of abdominal pain, presence of complications related to CD, abdominal masses, and Simple Endoscopy Score (SES) CD score by colonoscopy) before the WMT. Patients were also evaluated-three months post-WMT-for their CDAI and HBI scores and any modifications in their treatment medications and hospitalization. Patients were consistently monitored for any adverse events (AE) from when they underwent WMT until three months post-treatment. Stool samples were collected one week before and three months after WMT treatment for metagenomic, metatranscriptomic sequencing, and metabolomic testing.

Research program and WMT process

WMT donors were selected from the universal stool bank (China Microbiota Transplantation Systemm, CMTS). The donor screening criteria have been described in detail in the Nanjing Consensus[6]. The donors in the present study were six individuals (four males and two females) between the ages of 18 and 25. No donors were related to the participating patients.

The steps for the preparation of washed microbiota suspensions were as follows: (1) An automatic purification system (GenFMTer, FMT Medical, Nanjing, China) was used to enrich the microbiota; (2) the fecal microbiota suspension was transferred to tubes for centrifugation and the supernatant was discarded (this step was repeated three times using sterile saline to make the suspension); and (3) the volume ratio of final precipitation/vector solution was 1:2 for making fresh suspensions[6]. The washed preparation of fecal microbiota changes the transplantation-related safety, quantitative method, and delivery[7]. Moreover, the "one-hour FMT protocol" was used to ensure that the interval between defecation and infusion of the fresh bacteria into the intestinal tract of patients was less than one hour[14]. Washed microbiota suspensions (1U) were delivered through either colonic or mid-gut transendoscopic enteral tubing (TET) once daily for two days (methods for colonic[15] and mid-gut[16] TET have been reported in detail in previous studies). Colonic TET offers a new and convenient method of delivering WMT that is painless and easily reproducible, resulting in high patient satisfaction[14].

Assessment of efficacy

The primary outcome was the clinical response (a decrease in CDAI score > 100) three months after WMT. Secondary outcome included clinical remission (CDAI < 150), improvement in HBI, SES CD score, reduction in the various inflammatory markers [erythrocyte sedimentation rate (ESR), high-sensitivity C-reactive protein (hs-CRP), fecal calprotectin], and improvement in different clinical symptoms three months after WMT. In particular, mucosal healing after WMT can

be evaluated in patients willing to undergo colonoscopy three months after WMT.

Security assessment

The follow-up was conducted one week, one month, three months, and six months after WMT to assess the potential AE and concomitant medication changes. The correlation between AE and WMT was classified as either "unrelated," "possible," "probably," or "definitive"[17].

Patient and donor fecal sample collection

The stool samples from patients and donors were collected and delivered to the laboratory within one hour and stored at -80 °C until processing. The samples were collected one week before WMT and three months after WMT. A total of 22 fecal samples were collected, of which 16 were from eight CD patients (including five responders and three non-responders), and six were from the six donors. All the samples were subjected to metagenomic, metatranscriptomic, and untargeted metabolomic analysis.

DNA/RNA extraction and metagenomic/metatranscriptomic sequencing

Total gut microbiota genomic DNA was extracted from the 22 thawed stool samples using the QIAGEN DNeasy PowerSoil Pro Kit (Qiagen, Germany) according to the manufacturer's instructions. Total RNA was extracted from the samples using the QIAGEN RNeasy PowerMicrobiome Kit (Qiagen, Germany), employs the RiboMinus™ Transcriptome Isolation Kit (Invitrogen, United States), that utilizes rRNA-complementary probes to bind and remove rRNA. Subsequently, the mRNA was randomly divided into various short fragments of 250-300 bp with divalent cations in the NEB Fragmentation Buffer, and the first strand of cDNA was then synthesized using the fragmented RNA as a template and random oligonucleotides as potential primers. The DNA obtained by both methods was sequenced using the Illumina NovaSeq PE150 platform. The above experiments were performed at Institute of Microbiology, Chinese Academy of Sciences, Beijing, China.

Species annotation and functional analysis

The rRNA reads were removed using Bowtie2, based on the sortmerna-4.3 version of the rRNA database. The sequences were assembled using the MEGAHIT software, and gene prediction was conducted with Prodigal. The various redundant genes were removed from multiple samples using cd-hit. The obtained reference sequences and the reads were then compared to the reference sequences using the software BBMap Suite to calculate abundance. Both metagenome and metatranscriptome were analyzed using the software kraken2[18] to obtain abundance tables of species across different taxonomic levels. Intergroup differences were examined using linear discriminant analysis effect size (LEfSe).

Identification and quantification of metabolites in fecal samples

The chromatographic separation of the target compounds was performed on a Waters ACQUITY UPLC BEH Amide (2.1 mm × 50.0 mm, 1.7 μm) liquid chromatography column using a Vanquish (Thermo Fisher Scientific) ultra-performance liquid chromatograph[19]. The liquid chromatographic phase A consisted of an aqueous phase containing 25 mmol/L ammonium acetate and 25 mmol/L ammonia, whereas the phase B was acetonitrile. The temperature of the sample tray was maintained at 4 °C, and the injection volume was 2 μL. The Orbitrap Exploris 120 mass spectrometer, controlled by Thermo's Xcalibur software (version 4.4), could acquire primary and secondary mass spectrometry data. The raw data was converted into mzXML format by ProteoWizard software and then processed by an in-house written R package (kernel XCMS) for peak identification, extraction, alignment, and integration[20]. The substance annotation was then performed by matching it with the self-built secondary mass spectrometry database of BiotreeDB (V2.1), and the cut-off value for algorithm scoring was set to 0.3.

Metabolite analysis of fecal samples

The data were log-transformed and centered (CTR) formatted using SIMCA software (V16.0.2, Sartorius Stedim Data Analytics AB, Umea, Sweden). After that, it was subjected to automated modeling analysis[21], and a Score scatter plot of the PCA model was obtained. For each set of comparisons, we calculated the Euclidean distance matrix for determining the quantitative values of the differential metabolites and clustered differential metabolites in a complete chaining approach, and these metabolites were subsequently presented in a heat map.

Heat mapping of metabolite and microbial species correlation in fecal samples

Based on the non-parametric test method, paired Wilcoxon tests were employed to obtain significant differences in metabolite level ($P < 0.05$), RNA level species annotated with LEfSe LDA greater than two, and significant differences ($P < 0.05$) in species annotated with LEfSe LDA. The correlation coefficients, R, were calculated with a P value using the Spearman method to create the heatmap.

Statistical analysis

The descriptive statistics included reporting the means and standard deviations for continuous variables and the frequencies and percentages for categorical variables. The data were examined using IBM SPSS 26.0. Wilcoxon signed-rank tests were employed to analyze paired data. P values < 0.05 were considered as significantly different.

RESULTS

Clinical outcome

The baseline characteristics of patients are depicted in Table 1 (Supplementary Table 1 for specific parameters). We found that seven of the 11 patients met the primary endpoint of CDAI improvement-a clinical response rate of 63.6%. All the responders achieved clinical remission. The remaining four non-responders experienced symptoms of disease within three months of treatment and returned to the hospital. The seven patients who reached the primary observation endpoint were followed up 3-6 months after the treatment. Among these, one patient experienced increased abdominal pain and was readmitted to the hospital. Two patients in remission requested a repeat WMT to consolidate their treatment. The remaining four patients remained in clinical remission. The different parameters in responders and non-responders three months after WMT-including CDAI, HBI, stool frequency, abdominal pain, CRP, ESR, and fecal calprotectin-are shown in Table 2.

Based on a decrease of more than 100 points in their CDAI score, the patients were categorized into responders (n = 7) and non-responders (n = 4). After three months of WMT, responders exhibited significant improvements in HBI, CDAI, and bowel frequency (P < 0.05). In addition, abdominal pain, hs-CRP, and ESR decreased to varying degrees, although the reduction was not statistically significant. The fecal calprotectin levels in responders remained constant before and after the treatment (Table 2). However, non-responders did not experience any improvement in CD-related clinical symptoms and inflammatory indexes; in some cases, their condition even deteriorated compared to the baseline period (Supplementary Table 2). Consistent with the clinical symptoms and laboratory indices, four patients in the responder group displayed a trend of decreasing SES CD scores compared with the previous period. Conversely, the non-responder group showed increased SES CD scores during the same period.

AEs

The incidence of AEs was 2/22 (9.1%). One patient experienced constipation (possibly related, mild) within one week of transplantation, which improved rapidly with laxative medication. In the other patient, a mild increase in defecation (possibly related, mild) was observed on the second day after transplantation and was not treated. Both patients' symptoms resolved spontaneously within 24 hours. Two other patients experienced painful episodes of urticaria and gout after treatment. Because these patients had previously relapsed with similar conditions, the treating physicians did not consider them to be transplant-related. All of these AE were clarified as short-term AE according to the cut-pont of 1 month-post WMT[22]. No severe AEs and long-term AE occurred during treatment and follow-up.

MICROBIOME AND METABOLOMIC ANALYSIS

Differences in the gut microbiome and metabolome between patients with mildly active CD and donors

Metagenomic species-level annotation showed that CD patients had significantly decreased Shannon and Simpson indices compared to donors prior to WMT, indicating lower alpha diversity (ANOVA, P < 0.01; P < 0.05) (Figure 1A). Regarding β-diversity, we constructed a principal coordinate analysis plot of the categorical distances between the samples (Jaccard index in Figure 1B), revealing a significant separation between the two groups, with the donor group exhibiting a more compact clustering. At the metabolome level, a significant separation between the two groups was visible in the Score scatter plot of the PCA model. The donor group exhibited a significantly closer clustering than the CD group (Figure 1C). Differences in the amino acids composition of fecal samples were found between patients with baseline CD patients and donors (Figure 1D). Amino acids levels in the feces of CD patients were higher than those of donors.

LEfSe was employed in the metagenomic analysis to screen the two groups for the differential species based on LDA ≥ 2 and P < 0.05. The three species with the highest abundance in the patient group before the transplantation were *Collinsella aerofaciens* (LDA = 4.901 P < 0.05), *Erysipelotrichaceae bacteriumI46* (LDA = 3.745, P < 0.05), and *Clostridium scindens* (LDA = 3.697, P < 0.01). In contrast, the three species with the highest abundance in the donor group were *F. prausnitzii* (LDA = 5.002, P < 0.01), *Anaerostipes hadrus* (*A. hadrus*, LDA = 4.259, P < 0.01), and *Bacteroides vulgatus* (LDA = 4.104, P < 0.01), respectively (Supplementary Figure 1).

The same LEFSe was employed in the metatranscriptomic analysis to screen for the differential species between baseline and donor in CD patients based on LDA ≥ 2 and P < 0.05. The top three species with the highest baseline abundance in CD patients were observed to be *Phocaeicola coprophilus* (LDA = 4.43, P < 0.01), *Bacteroides fragilis* (LDA = 4.178, P < 0.01) and *Bacteroides* sp. *PHL 2737* (LDA = 4.035, P < 0.01). The three species with the highest abundance in the donor group were *Bifidobacterium bifidum* (LDA = 4.746, P < 0.05), *A. hadrus* (LDA = 4.638, P < 0.01), and *Blautia producta* (LDA = 4.518, P < 0.01) (Supplementary Figure 2). Interestingly, when analyzed in comparison with the metagenome assay results, elevated expression of *F. prausnitzii*, *A. hadrus*, and *R. intestinalis* in the donor group was found to be almost identical to the metatranscriptomic assay results (Supplementary Table 3).

The diversity of gut microbiome increased in responders after WMT, and the diversity was associated with clinical symptoms

According to the metagenomic species level annotation, there was a significant increase in alpha diversity (as indicated by the observed species and chao1 index) in the responder group after WMT compared to the baseline (ANOVA, both P < 0.01) (Figure 2A). However, the non-responder group did not show any notable alterations in observed species and chao1

Table 1 Baseline characteristics of the study participants, *n* (%)

Characteristic	*n* (%)
Age (SD)	35.6 (9.4)
Male	8 (81.8)
Female	3 (18.2)
Age at diagnosis (Montreal classification)	
A1 (age < 16 yr)	1 (9.1)
A2 (age 17-40 yr)	9 (81.8)
A3 (age > 40 yr)	1 (9.1)
Location (Montreal classification)	
L1 (terminal ileum disease)	5 (45.5)
L2 (colonic disease)	3 (27.3)
L3 (ileocolonic disease)	3 (27.3)
L4 (upper GI)	0 (0.0)
Behavior (Montreal classification)	
B1 (inflammatory)	3 (27.3)
B2 (stricturing)	4 (36.4)
B3 (penetrating)	2 (18.2)
B2 + B3	2 (18.2)
Perianal disease	4 (36.4)
Duration of disease, mean (SD), yr	8.8 (6.9)
Medication at the time of WMT	
None	2 (18.2)
Mesalamines	7 (63.6)
Steroids	1 (9.1)
Immunomodulators	3 (27.3)
Biologics therapy	1 (9.1)
Bowel surgery	2 (18.2)
Anal surgery	4 (36.4)
Smoking status	
Current	0 (0.0)
Ex-smoker	2 (18.2)
Never smoker	9 (81.8)
Disease severity	
Mild	11 (100.0)
Moderate	0 (0.0)
Severe	0 (0.0)
Route of WMT	
Mid-gut TET	4 (36.4)
Colonic TET	7 (63.6)

GI: Gastrointestinal; WMT: Washed microbiota transplantation; TET: Transendoscopic enteral tubing.

Table 2 Clinical outcomes baseline and post-3 month washed microbiota transplantation

Variable	Responders[1]				Non-responders[1]			
	n	Baseline, mean ± SD	3-month post-WMT, mean ± SD	*P* value	*n*	Baseline, mean ± SD	3-month post-WMT, mean ± SD	*P* value
HBI (three-month post-WMT)	7	5.7 ± 0.8	2.4 ± 0.5	0.014	4	5.0 ± 0.0	7.0 ± 2.3	0.157
CDAI (three-month post-WMT)	7	196.5 ± 21.7	76.4 ± 29.5	0.018	4	190.0 ± 13.3	238.5 ± 50.1	0.068
Stool frequency (number/d)	7	1.7 ± 1.0	0.6 ± 0.5	0.023	4	1.5 ± 0.6	3.5 ± 2.4	0.180
Pain (scale 0-3)	7	0.7 ± 0.5	0.3 ± 0.5	0.083	4	0.5 ± 0.6	0.5 ± 0.6	1.000
hs-CRP (mg/L)	7	3.6 ± 6.1	2.1 ± 2.0	0.500	4	14.8 ± 15.8	29.6 ± 19.0	0.144
ESR (mm/h)	7	15.9 ± 17.0	10.9 ± 11.2	0.340	4	43.3 ± 31.6	54.0 ± 33.0	0.273
Fecal calprotectin (ug/g)	6	367.6 ± 159.9	374.2 ± 290.4	0.753	4	391.6 ± 120.9	561.2 ± 140.2	0.144
SES CD score	4	5.3 ± 2.1	3.3 ± 2.5	0.285	4	9.3 ± 7.4	17.5 ± 7.1	0.068

[1]Values compared by Wilcoxon signed-rank tests.

Clinical outcomes of responders' baseline and post-washed microbiota transplantation (WMT) and non-responders' baseline and post-WMT. The data are presented as means ± SD. WMT: Washed microbiota transplantation; HBI: Harvey-Bradshaw index; CDAI: Crohn's Disease Activity Index; hs-CRP: High-sensitivity C-reactive protein; ESR: Erythrocyte sedimentation rate; SES: Simple Endoscopic Score; CD: Crohn's disease.

index following WMT compared to the baseline (ANOVA, both $P < 0.05$) (Figure 2B).

When analyzing the disparities in post-transplant microbiome diversity, the responder group presented a significant increase in observed species and chao1 index compared to the non-responder group. (ANOVA, both $P < 0.05$) (Figure 2C). Examining the disparity in species abundance at the DNA and RNA levels in both groups showed a marked resemblance between the two differential microbiomes (Figure 2D). There was a decrease in *F. prausnitzii* and *Phocaeicola vulgatus* and an increase in *E. coli*.

Changes in microbiome and metabolome before and after WMT in responders

A thorough comparison of DNA levels between the baseline responder group, post-transplantation responders, and donors exhibited that the transfer of *F. prausnitzii* can be identified in both donor and responder samples, with corresponding variations observed in RNA levels (Figure 3A). The fecal metabolites L-glutamic acid, gamma-glutamyl-leucine, and prolyl-glutamine were significantly higher than the donors before WMT but decreased after WMT (Figure 3B). Furthermore, a number of metabolites exhibit a similar pattern of alteration (Figure 3C).

At the DNA level, the comparison between the community species pre-and post-WMT revealed an increase in *Desulfovibrio piger* (*D. piger*) and *Clostridiales bacteriumCCNA10*, and a decrease in *Paraclostridium bifermentans* (*P. bifermentans*), *Bradyrhizobium sp 6 2017*, and *Bradyrhizobium sp SK17* (Figure 3D), according to the results from the comparative LEfSe analyses. Interestingly, the most significant changes at the RNA level included a decrease in *C. difficile* and a significant increase in *Prevotella copri* (*P. copri*) (Figure 3E). Analysis of fecal metabolites showed a significant decrease in several metabolites, such as isonicotinic acid, lutein, and norvaline (Supplementary Figure 3). Heatmaps were plotted to show differential species (RNA levels) and differential metabolite correlations before and after WMT in the responding group, as shown in Figure 3F.

DISCUSSION

In this prospective study on the effectiveness of WMT for CD, 63.6% of patients experienced notable improvements in CDAI (of more than 100 points) three months after WMT. This treatment efficacy was higher than in a previously reported study[10]. Although inflammatory indicators such as SES CD, fecal calprotectin, hs-CRP, and ESR decreased in the responding group, the small sample size prevented the identification of statistically differences ($P > 0.05$). Therefore, randomized controlled trials with larger sample sizes are needed for further validation of these findings.

We thoroughly analyzed fecal samples obtained from patients before and after WMT-and from donors-for metagenomic, metatranscriptomic, and non-targeted metabolomic assays. To our knowledge, this is the first time that metatranscriptomic and metabolomic techniques have been used to analyze pre- and post-transplant fecal samples in a study of FMT for CD. Metagenomic-based species annotation studies revealed that patient clinical phenotypes were significantly associated with alpha diversity (Figure 1A; Figure 2A-C). For example, the alpha diversity of the donor gut microbiome was significantly higher than that of baseline patients. The alpha diversity of the post-WMT responders was

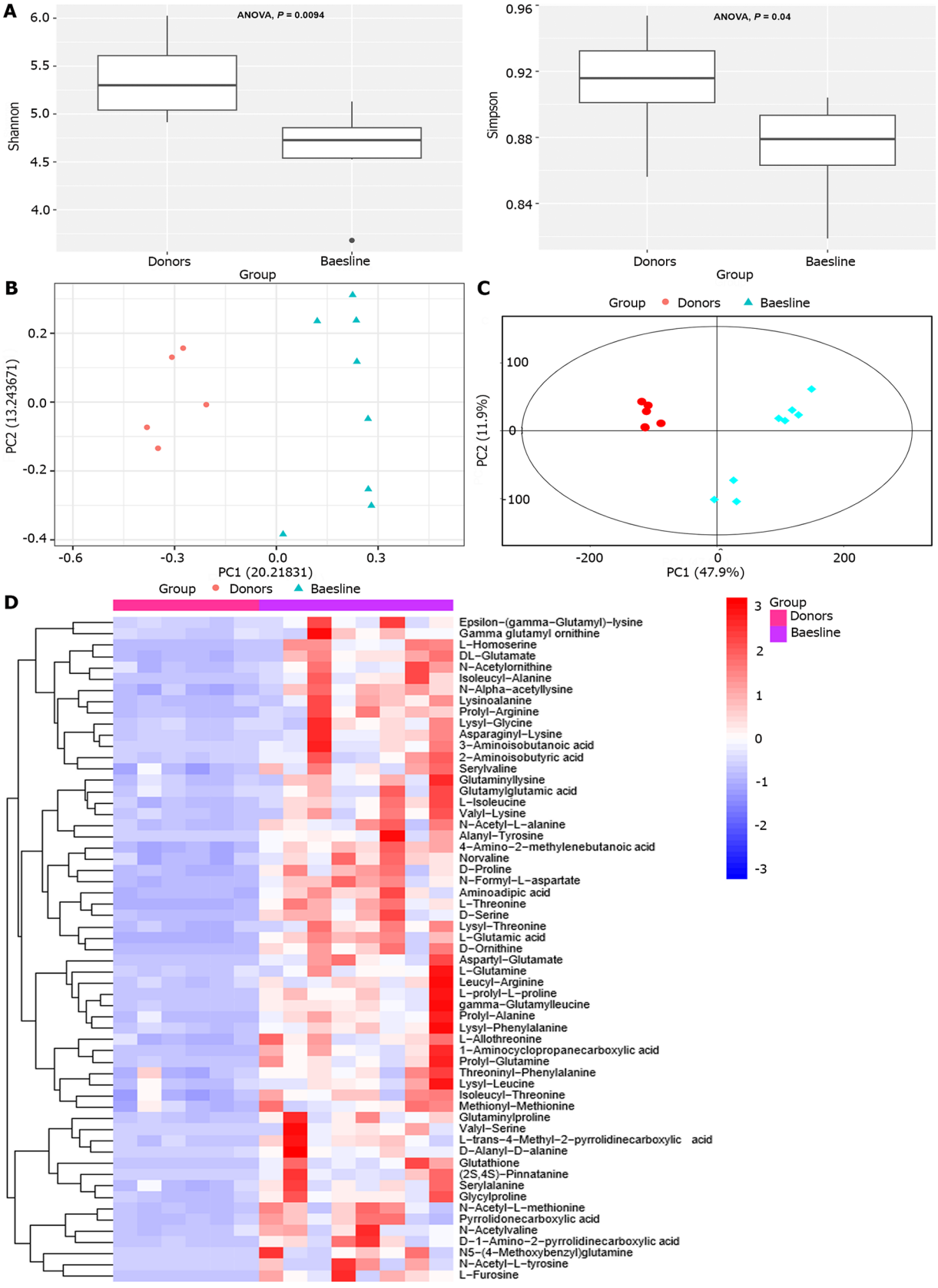

Figure 1 Mildly active Crohn's disease patients differed from the donors in alpha and beta diversity and metabolites. A: Baseline Crohn's disease (CD) patients exhibited significantly lower gut microbiome Shannon's and Simpson's index than the donors; B: Comparison of beta diversity of the microbial communities between baseline CD patients and donors. The Jaccard distances from principal coordinate analyses of abundance are depicted as donors (red) and baseline CD patients (blue). The donors' samples were more tightly clustered than the baseline samples; C: The PCA score plot clearly discriminated between donors (red) and baseline CD patients (blue), where donors' samples were more tightly clustered than baseline CD patients' samples; D: The heat map depicts the intensity of amino acid in the feces of CD patients and donors.

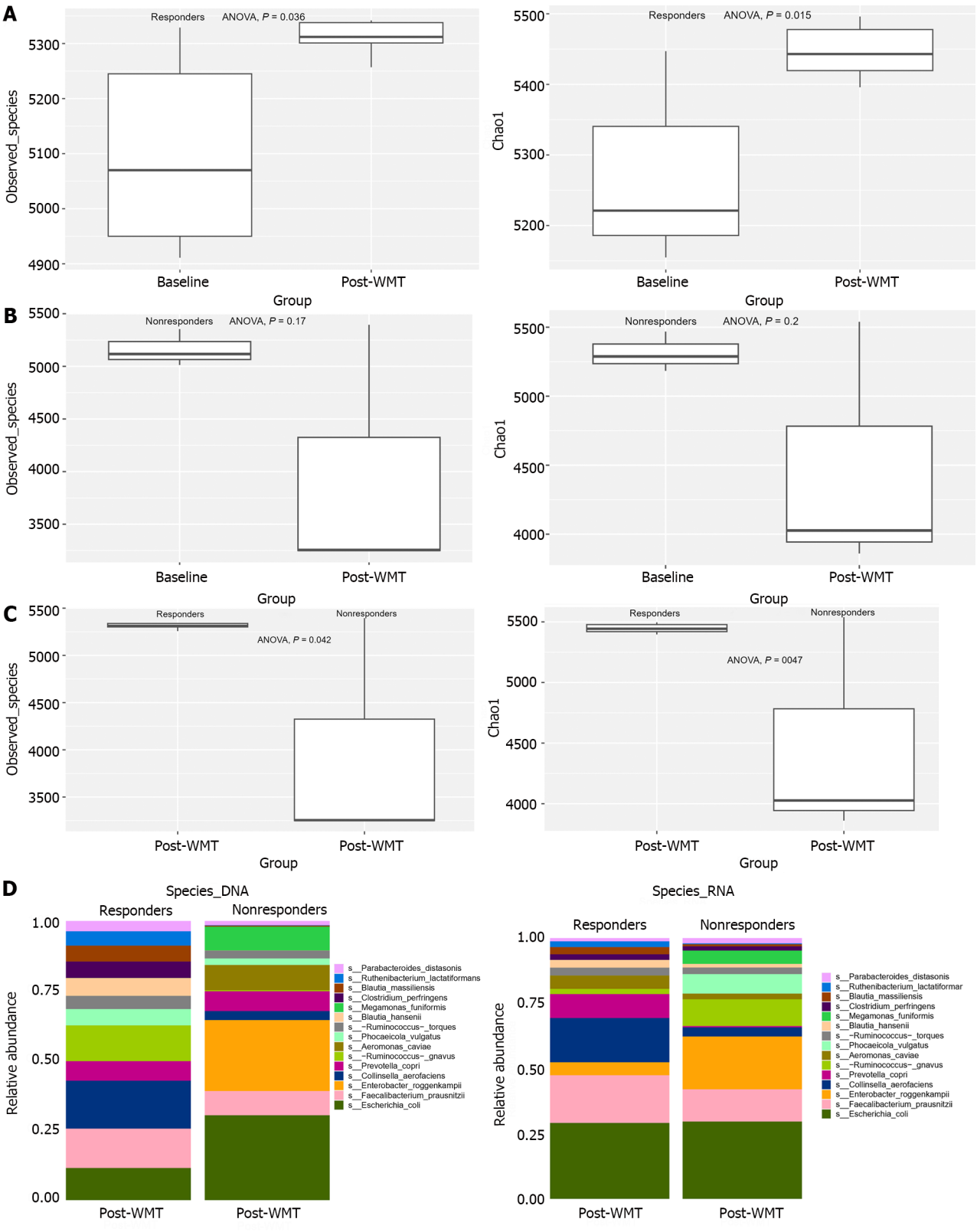

Figure 2 Patients' clinical symptoms were correlated with the composition of the gut microbiota and alpha diversity. A: The observed species and chao1 index of the gut microbiota were significantly increased in the responders after transplantation; B: The observed species and chao1 index of the gut microbiota of the non-responders did not change significantly before and after washed microbiota transplantation (WMT); C: The observed species and chao1 index significantly larger in the responders than non-responders post-transplantation; D: Similar differences in species-rich changes at both DNA and RNA levels were observed between the responders and non-responders after WMT treatment. WMT: Washed microbiota transplantation.

significantly higher than that of the baseline. However, the alpha diversity of the non-responders was not significantly altered pre- and post-WMT. These findings were consistent with those reported in previous studies[23]. In terms of beta diversity, it was observed that there was a distinct separation between the donor group and the baseline patients, and the samples were clustered more tightly between the donor groups, which also aligns with previous reports[24]. A similar phenomenon was observed in metabolomic analyses (Figure 1C).

The microbiome characteristics of the baseline CD patient samples were also analyzed. The significant reductions in *R. intestinalis*, *F. prausnitzii*, and *Akkermansia muciniphila* in the DNA-level species-richness-based differential analyses (Supplementary Figure 1) were very similar to the results of other recently reported studies of CD patients and healthy controls[25]. However, despite the presence of a gene in the DNA, its functionality and transcriptional activity are not guaranteed as they rely on the type and quantity of RNA transcribed from it[26]. The metatranscriptome can offer improved "resolution" for species identification compared to the metagenome[11]. In this study, we compared the metagenomic and metatranscriptomic analyses and observed that the changes in certain strains were consistent. When studying the species differences between the donors and baseline CD patients, it was discovered that *F. prausnitzi*, *A. hadrus*, and *R. intestinalis* were significantly more abundant in the donors than in baseline CD patients based on both DNA and RNA species annotation (Supplementary Table 3). All three bacteria are producers of short-chain fatty acid (SCFA)[25]. SCFA is an important metabolite for maintaining intestinal homeostasis and is thought to have some therapeutic potential for IBD[27]. *F. prausnitzi* and *R. intestinalis* are recognized as beneficial bacteria in IBD and can exert anti-inflammatory effects through the regulation of multiple pathways[25,28]. When comparing the differences in bacterial microbiomes between the responder and non-responder groups post-transplantation, an increase in SCFA-producing bacteria[25], such as *F. prausnitzii* and *Phocaeicola vulgatus*, as well as a decrease in the potentially pathogenic bacterium *E. coli*, were also found in the responder group at both the DNA and RNA levels (Figure 2D).

The effectiveness of WMT lies in its ability to restore the patient's microbial balance effectively. We observed that, whether based on investigation of DNA or RNA levels, the abundance of *F. prausnitzii* showed a remarkable increase after transplantation in the responders compared to baseline and was higher than in the non-responders group (Figures 2D and 3A). It was observed that *Ruminococcus gnavus*, a well-established CD causative agent[4], significantly decreased in the responders after transplantation at the RNA level. However, contrasting results were observed at the DNA level. (Figure 3A). Thus, RNA-based transcriptional activity of the bacterial population could be more relevant to the clinical outcomes.

Furthermore, a significant increase in the abundance of *D. piger* in the responding group (based on DNA levels) was noted in this study. Around 50% of individuals carry sulfate-reducing bacteria (SRB) in their gut. Specifically, *D. piger* was reported to be the most common SRB in a cohort of healthy adults in the United States[29]. In addition, prior studies have shown that a higher abundance of *D. piger* is resistant to invasion by *Salmonella enteritidis* in a chick preclinical model [30]. Moreover, the abundance of potentially pathogenic bacteria, such as *P. bifermentans* and *Bradyrhizobium sp 6 2017*, was significantly reduced in the responder group after the transplantation. *P. bifermentans* was the first strain reported to cause worsening of the pathological scores in a mouse model of ulcerative colitis[31]. In another elegant study, *Bradyrhizobium enterica* (*B. enterica*) nucleotide sequences were identified by PCR from the biopsy specimens of patients with umbilical cord colitis, thereby suggesting that *B. enterica* may be an opportunistic human pathogen[32].

Interestingly, the decreased abundance of *C. difficile* and increased abundance of *P. copri* was predominantly found at the RNA level (Figure 3E). *C. difficile* is an opportunistic pathogen with increased abundance in the intestines of dysbiotic intestinal hosts and is a leading pathogen in pseudomembranous colitis. Several previous studies have shown a significant decrease in *P. copri* in pediatric CD patients and in a canine model of CD[33], whereas *P. copri* abundance was significantly increased after WMT intervention. Based on these findings, it can be suggested that WMT can improve patients' clinical outcomes by optimizing microbiome structure, boosting the presence of helpful bacteria, and reducing the colonization of pathogenic bacteria.

Increased levels of many amino acids were observed in the baseline samples collected from CD patients (Figure 1D). Previous studies have shown that there is a noticeable increase in specific metabolites related to glutathione metabolism (including glutamate, glycine, cysteine, and pyroglutamate) in the urine of pediatric IBD patients[34], and it has also been suggested that CD patients tend to have enhanced fecal amino acids[35]. Furthermore, various studies in preclinical models have indicated that bacterial urease expression can effectively transfer host-sourced nitrogen to the gut microbiota to facilitate amino acid synthesis during gut microbiota dysregulation and inflammation[35].

Interestingly, several amino acids (including L-glutamic acid, gamma-glutamyl-leucine, and prolyl-glutamine) were elevated in the baseline samples compared to the donors but decreased significantly after WMT (Figure 3B). Among these, glutamic acid has been recognized as an inflammatory marker in an immunocompromised mouse model of a specific type of ulcerative colitis[36]. Moreover, another study indicates that increased levels of gamma-glutamyl-leucine-a biologically active peptide implicated in inflammation, oxidative stress, and glucose management-are causally associated with cardiometabolic risk[37]. In addition, the down-regulation of prolyl-glutamine has been linked with immune enhancement in mice[38]. We have illustrated the presence of several metabolites showing similar patterns (Figure 3C). One of these metabolites, N1-methyl-2-pyridone-5-carboxamide (M2Py), is known to be a uremic toxin[39]. The reduction in M2Py levels after transplantation through WMT suggests that WMT could be a potentially effective approach in protecting the renal function of patients suffering from renal failure[40]. In addition, the levels of many anti-inflammatory substances (including isonicotinic acid, lupulone, and norvaline) were elevated in the responders after WMT. The combination of isoniazid and salazosulfapyridine has demonstrated anti-colitis effects in preclinical experiments by suppressing the pathology of inflammation and fibrosis in a model of colitis[41]. Lupulone, a component found in hops extracts, is recognized for its significant role in exhibiting antimicrobial effects and its potential as an antioxidant, anti-inflammatory, and antibacterial agent[42]. Norvaline demonstrates anti-inflammatory properties by inhibiting arginase, and its effectiveness in reducing inflammation is partially due to its ability to suppress inhibited

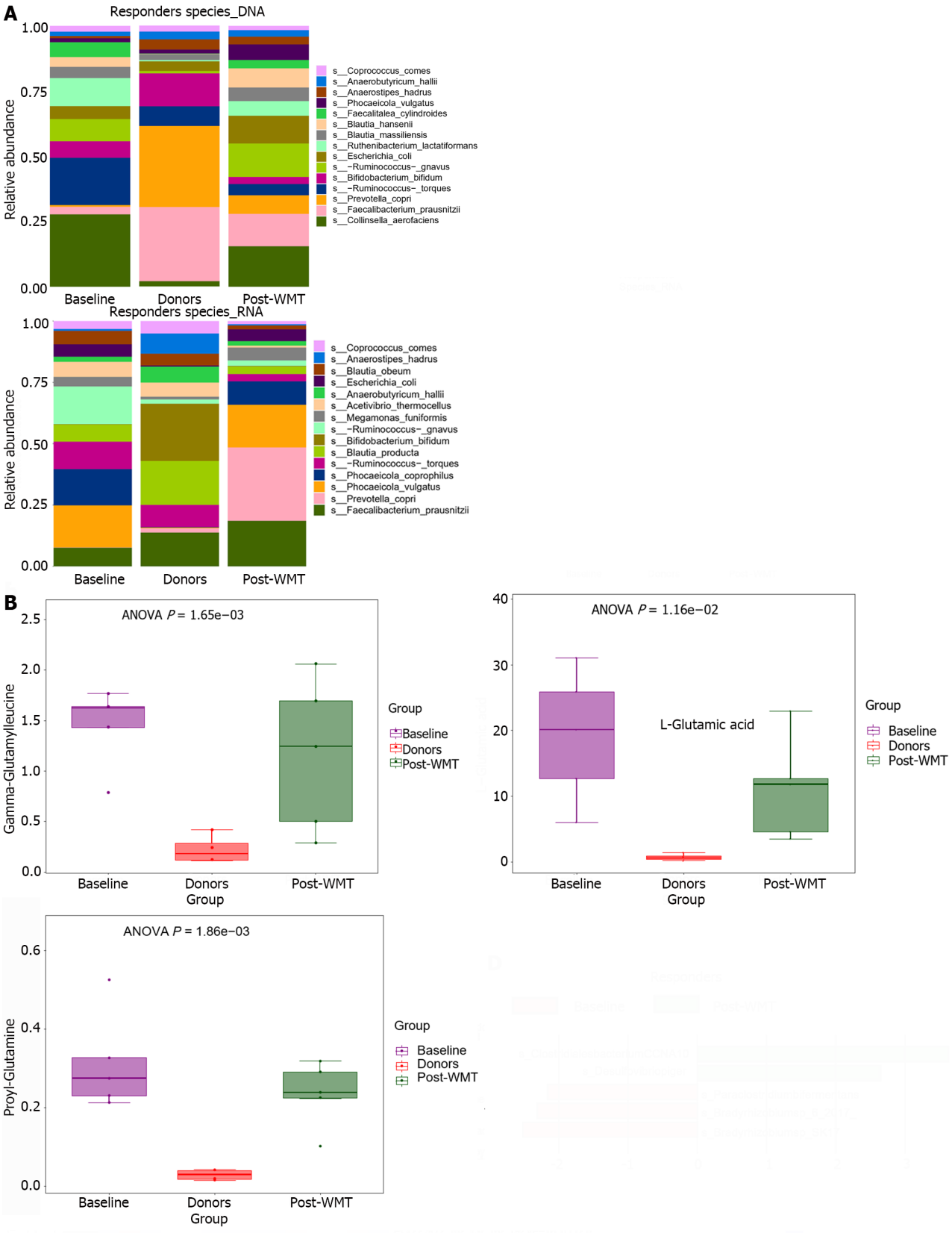
A
Responders species_DNA
Relative abundance
1.00
0.75
0.50
0.25
0.00
Baseline
Donors
Post-WMT
s__Coprococcus_comes
s__Anaerobutyricum_hallii
s__Anaerostipes_hadrus
s__Phocaeicola_vulgatus
s__Faecalitalea_cylindroides
s__Blautia_hansenii
s__Blautia_massiliensis
s__Ruthenibacterium_lactatiformans
s__Escherichia_coli
s__-Ruminococcus-_gnavus
s__Bifidobacterium_bifidum
s__-Ruminococcus-_torques
s__Prevotella_copri
s__Faecalibacterium_prausnitzii
s__Collinsella_aerofaciens
Responders species_RNA
Relative abundance
1.00
0.75
0.50
0.25
0.00
Baseline
Donors
Post-WMT
s__Coprococcus_comes
s__Anaerostipes_hadrus
s__Blautia_obeum
s__Escherichia_coli
s__Anaerobutyricum_hallii
s__Acetivibrio_thermocellus
s__Megamonas_funiformis
s__-Ruminococcus-_gnavus
s__Bifidobacterium_bifidum
s__Blautia_producta
s__-Ruminococcus-_torques
s__Phocaeicola_coprophilus
s__Phocaeicola_vulgatus
s__Prevotella_copri
s__Faecalibacterium_prausnitzii
B
ANOVA P = 1.65e−03
Gamma-Glutamylleucine
2.5
2.0
1.5
1.0
0.5
0.0
Baseline
Donors
Post-WMT
Group
Group
Baseline
Donors
Post-WMT
ANOVA P = 1.16e−02
L-Glutamic acid
40
30
20
10
0
Baseline
Donors
Post-WMT
Group
Group
Baseline
Donors
Post-WMT
ANOVA P = 1.86e−03
Proyl-Glutamine
0.6
0.4
0.2
0.0
Baseline
Donors
Post-WMT
Group
Group
Baseline
Donors
Post-WMT

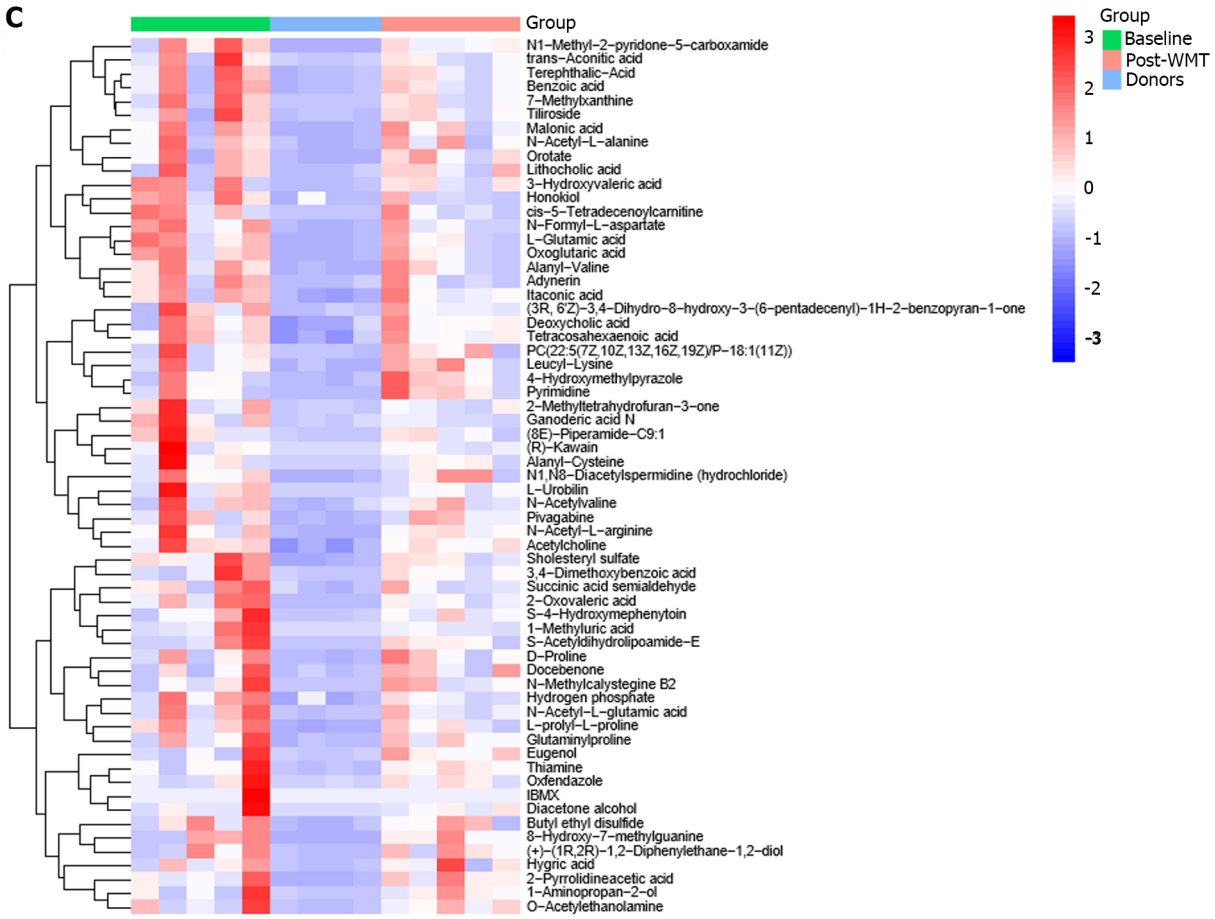
C
Group
N1-Methyl-2-pyridone-5-carboxamide
trans-Aconitic acid
Terephthalic-Acid
Benzoic acid
7-Methylxanthine
Tiliroside
Malonic acid
N-Acetyl-L-alanine
Orotate
Lithocholic acid
3-Hydroxyvaleric acid
Honokiol
cis-5-Tetradecenoylcarnitine
N-Formyl-L-aspartate
L-Glutamic acid
Oxoglutaric acid
Alanyl-Valine
Adynerin
Itaconic acid
(3R, 6'Z)-3,4-Dihydro-8-hydroxy-3-(6-pentadecenyl)-1H-2-benzopyran-1-one
Deoxycholic acid
Tetracosahexaenoic acid
PC(22:5(7Z,10Z,13Z,16Z,19Z)/P-18:1(11Z))
Leucyl-Lysine
4-Hydroxymethylpyrazole
Pyrimidine
2-Methyltetrahydrofuran-3-one
Ganoderic acid N
(8E)-Piperamide-C9:1
(R)-Kawain
Alanyl-Cysteine
N1,N8-Diacetylspermidine (hydrochloride)
L-Urobilin
N-Acetylvaline
Pivagabine
N-Acetyl-L-arginine
Acetylcholine
Sholesteryl sulfate
3,4-Dimethoxybenzoic acid
Succinic acid semialdehyde
2-Oxovaleric acid
S-4-Hydroxymephenytoin
1-Methyluric acid
S-Acetyldihydrolipoamide-E
D-Proline
Docebenone
N-Methylcalystegine B2
Hydrogen phosphate
N-Acetyl-L-glutamic acid
L-prolyl-L-proline
Glutaminylproline
Eugenol
Thiamine
Oxfendazole
IBMX
Diacetone alcohol
Butyl ethyl disulfide
8-Hydroxy-7-methylguanine
(+)-(1R,2R)-1,2-Diphenylethane-1,2-diol
Hygric acid
2-Pyrrolidineacetic acid
1-Aminopropan-2-ol
O-Acetylethanolamine
Group
Baseline
Post-WMT
Donors
3
2
1
0
-1
-2
-3

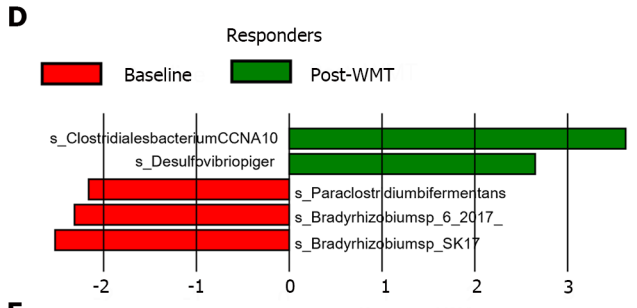
D
Responders
Baseline
Post-WMT
s_ClostridialesbacteriumCCNA10
s_Desulfovibriopiger
s_Paraclostridiumbifermentans
s_Bradyrhizobiumsp_6_2017_
s_Bradyrhizobiumsp_SK17
-2
-1
0
1
2
3
Species_RNA

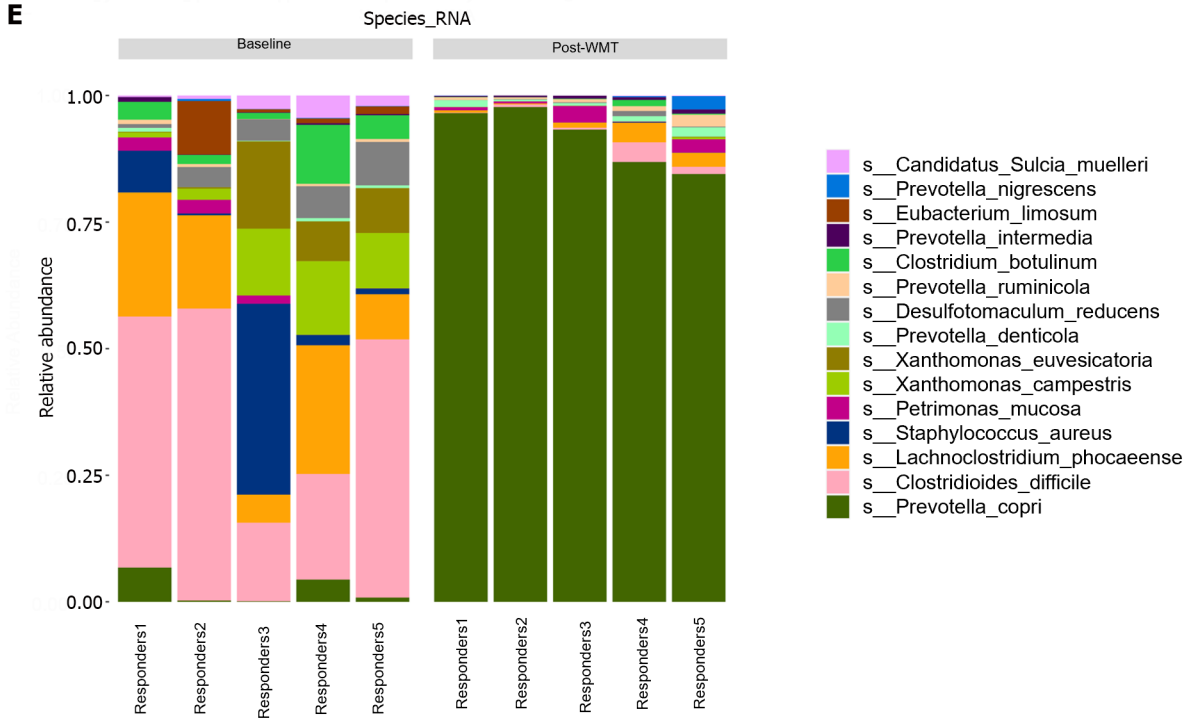
E
Baseline
Post-WMT
1.00
0.75
0.50
0.25
0.00
Relative abundance
Responders1
Responders2
Responders3
Responders4
Responders5
Responders1
Responders2
Responders3
Responders4
Responders5
s__Candidatus_Sulcia_muelleri
s__Prevotella_nigrescens
s__Eubacterium_limosum
s__Prevotella_intermedia
s__Clostridium_botulinum
s__Prevotella_ruminicola
s__Desulfotomaculum_reducens
s__Prevotella_denticola
s__Xanthomonas_euvesicatoria
s__Xanthomonas_campestris
s__Petrimonas_mucosa
s__Staphylococcus_aureus
s__Lachnoclostridium_phocaeense
s__Clostridioides_difficile
s__Prevotella_copri

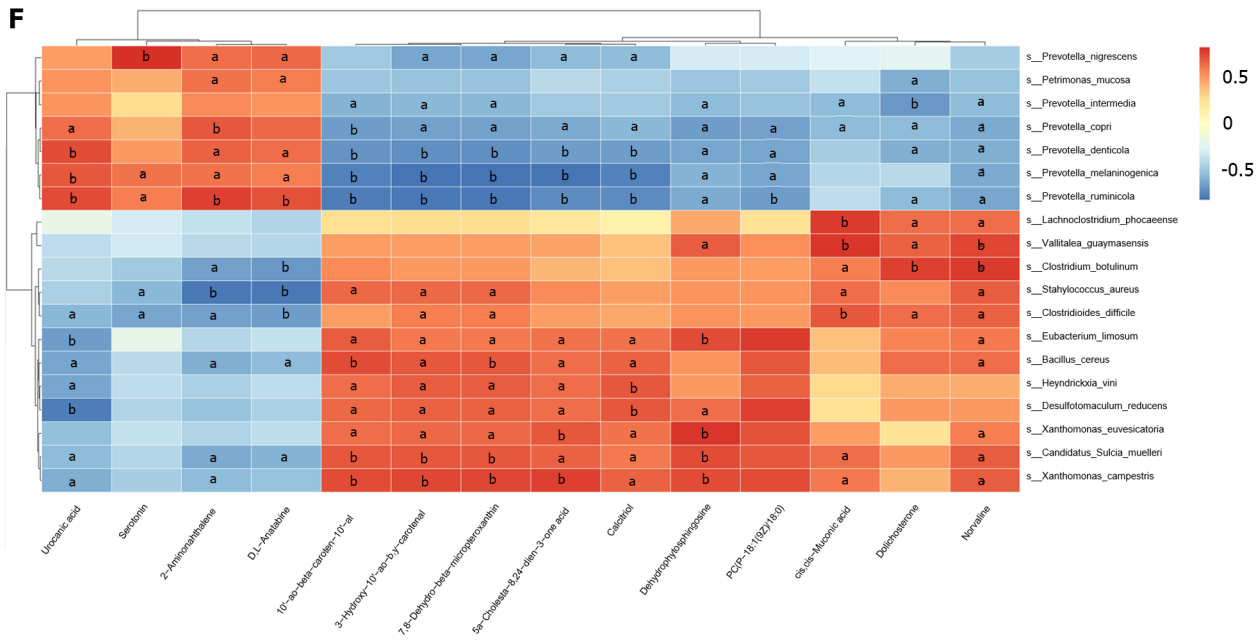

Figure 3 Changes in microbiome and metabolome before and after WMT in responders. A: The transfer of *Faecalibacterium prausnitzii* from the donor to the responders can be detected at both the DNA and RNA levels; B: Demonstration of several fecal metabolites that were significantly higher than those of the donors before the washed microbiota transplantation (WMT) and declined after the WMT; C: Heat map of the selected metabolite intensities between the responder group before and after WMT treatment and the donor trio; D: A plot of the difference in linear discriminant analysis effect size of the species level at the DNA level in the responders before and after the WMT revealed statistically significant differences ($P < 0.05$); E: The species changes at the RNA level before and after WMT in the responders; F: Correlation heatmap analysis of the differential metabolites in differential species (RNA levels) before and after WMT in the responder group. $^{a}P < 0.05$, $^{b}P < 0.01$. WMT: Washed microbiota transplantation.

p70s6k[43].

Correlation heatmap display analyses were performed for both differential metabolites and differential species at the RNA level pre-and post-WMT in the responders (Figure 3F). It was observed that species such as *Eubacterium limosum* and *Bacillus cereus* were positively correlated with the metabolite norvaline, which is associated with anti-inflammatory properties. In addition, previous studies have indicated that *Eubacterium spp.* and *Bacillus cereus* can exhibit significant anti-inflammatory effects related to intestinal inflammation[25,44]. Several species within the *genus Prevotella*, including *P. copri*, are negatively correlated with the immune-related metabolite dehydrophytosphingosine[45] but positively correlated with the anti-inflammatory metabolite norvaline[43] and urocanic acid[46].

A limitation of this study is its small sample size, which is related to our strict inclusion criteria. To minimize the interference of drugs on the results of microbiome testing, we excluded patients who had used drugs (such as antibiotics, proton pump inhibitors, and probiotics) within three months before recruitment and three months after WMT. We also excluded some patients with moderately to severely active CD. Nonetheless, although not designed as a randomized controlled trial, this study closely integrates microbiomics and metabolomic analyses, providing new evidence for understanding FMT in treating CD and thus advancing the field of microbiota medicine[47].

CONCLUSION

This study demonstrates that WMT is effective in CD treatment. The clinical phenotype of the patients was closely related to the altered diversity of the gut microbiota, and metagenomic and metatranscriptomic techniques were effective and complementary in improving the "resolution" of the active microbiome, which could potentially have significant implications. To better understand the role of the microbiome in WMT treatment and uncover the underlying mechanisms, it remains crucial to utilize additional genomic techniques such as macro-proteomics and culture genomics in future studies.

ARTICLE HIGHLIGHTS

Research background

Incidence of Crohn's disease (CD) is increasing every year, posing a serious threat to human health. Fecal microbial transplantation (FMT) is a promising therapeutic approach for the treatment of CD. The new methodology of FMT, based on the automatic washing process, was named as washed microbiota transplantation (WMT).

Research motivation
Most existing studies have focused on observing clinical phenomena. However, a combined multi-omics (metagenomic, metatranscriptomic, and metabolomic) analysis of FMT for the effective treatment of CD has not been reported.

Research objectives
To examine the effects of two consecutive fixed WMT doses on clinical and endoscopic outcomes in CD patients. A secondary aim was to explore alterations in the microbiome and metabolome in response to WMT.

Research methods
WMT was administered to 11 patients with active CD. Their clinical response (defined as a decrease in CD activity index score > 100 points) was assessed three months after transplantation. Fecal samples collected 1 wk before and 3 months after WMT were subjected to combined metagenomic, metatranscriptomic, and metabolomic analyses.

Research results
Seven of 11 patients (63.6%) demonstrated response 3 months after WMT. There was a significant increase in the diversity of the gut microbiota after WMT, consistent with improved clinical symptoms. A comparison of metagenomic and metatranscriptomic analyses revealed constant changes in certain strains, such as Faecalibacterium prausnitzii, Roseburia intestinalis, and Escherichia coli. Metabolomic analysis of the responder group identified certain amino acids that may be associated with disease progression (*e.g.*, L-glutamic acid, gamma-glutamyl-leucine, and prolyl-glutamine) that were higher in the pre-transplant than in the donor but lower in the post-transplant.

Research conclusions
WMT has shown efficacy in CD treatment, possibly due to the effective reconstitution of the patient's microbiome. Combined metagenomic, metatranscriptomic, and metabolomic analyses can effectively help decipher the underlying mechanisms of WMT for CD.

Research perspectives
The exact mechanism by which FMT treats CD still needs to be better understood. Future studies need to clarify the underlying mechanisms by utilizing additional histological techniques (*e.g.*, macro-proteomics and culture genomics *etc.*).

FOOTNOTES

Co-first authors: Shi-Ju Chen and Da-Ya Zhang.

Author contributions: Chen SJ and Zhang DY contributed equally to this work; Chen SJ, Zhang DY, Wu X, Zhang FM, Cui BT, and Bai FH participated in the design of this study and performed the statistical analysis; Chen SJ, Zhang DY, Wu X, and Bai FH drafted the manuscript; Huang YH, Zhang ZL and Wang R recruited participants and participated in the data collection; all authors read and approved the final manuscript.

Supported by the Innovation Platform for Academicians of Hainan Province, No. YSPTZX202313; Hainan Province Clinical Medical Center, No. 2021818; Hainan Provincial Health Industry Research Project, No. 22A200078; Hainan Provincial Postgraduate Innovation Research Project, No. Qhyb2022-133; Hainan Medical University Graduate Student Innovative Research Project, No. HYYB2022A18; and Nanjing Medical University Fan Daiming Research Funds for Holistic Integrative Medicine, No. 2020-3HIM.

Institutional review board statement: The study was reviewed and approved by the Second Affiliated Hospital of Nanjing Medical University Institutional Review Board [Approval No. (2022-KY-161-01)].

Clinical trial registration statement: This study is registered at ClinicalTrials.gov. The registration identification number is NCT01793831.

Informed consent statement: All study participants, or their legal guardian, provided informed written consent prior to study enrollment.

Conflict-of-interest statement: Zhang FM conceived the concept of GenFMTer and transendoscopic enteral tubing and devices related to them; the remaining authors declare that the research was conducted in the absence of any commercial or financial relationships that could be construed as a potential conflict of interest.

Data sharing statement: The datasets generated and/or analysed during the current study are available in the NCBI BioProject database (PRJNA1069244) and MetaboLights repository (MTBLS9421).

CONSORT 2010 statement: The authors have read the CONSORT 2010 Statement, and the manuscript was prepared and revised according to the CONSORT 2010 Statement.

Country/Territory of origin: China

ORCID number: Da-Ya Zhang 0000-0001-6133-8919; Xia Wu 0000-0002-0959-308X; Fa-Ming Zhang 0000-0003-4157-1144; Bo-Ta Cui 0000-0002-9238-7788; Fei-Hu Bai 0000-0002-1560-6131.

S-Editor: Chen YL
L-Editor: A
P-Editor: Cai YX

REFERENCES

1 **GBD 2017 Inflammatory Bowel Disease Collaborators**. The global, regional, and national burden of inflammatory bowel disease in 195 countries and territories, 1990-2017: a systematic analysis for the Global Burden of Disease Study 2017. *Lancet Gastroenterol Hepatol* 2020; **5**: 17-30 [PMID: 31648971 DOI: 10.1016/S2468-1253(19)30333-4]
2 **O'Brien CL**, Bringer MA, Holt KE, Gordon DM, Dubois AL, Barnich N, Darfeuille-Michaud A, Pavli P. Comparative genomics of Crohn's disease-associated adherent-invasive Escherichia coli. *Gut* 2017; **66**: 1382-1389 [PMID: 27196580 DOI: 10.1136/gutjnl-2015-311059]
3 **Mirsepasi-Lauridsen HC**, Vallance BA, Krogfelt KA, Petersen AM. Escherichia coli Pathobionts Associated with Inflammatory Bowel Disease. *Clin Microbiol Rev* 2019; **32** [PMID: 30700431 DOI: 10.1128/CMR.00060-18]
4 **Pal D**, Naskar M, Bera A, Mukhopadhyay B. Chemical synthesis of the pentasaccharide repeating unit of the O-specific polysaccharide from Ruminococcus gnavus. *Carbohydr Res* 2021; **507**: 108384 [PMID: 34229203 DOI: 10.1016/j.carres.2021.108384]
5 **Zhang T**, Lu G, Zhao Z, Liu Y, Shen Q, Li P, Chen Y, Yin H, Wang H, Marcella C, Cui B, Cheng L, Ji G, Zhang F. Washed microbiota transplantation vs. manual fecal microbiota transplantation: clinical findings, animal studies and *in vitro* screening. *Protein Cell* 2020; **11**: 251-266 [PMID: 31919742 DOI: 10.1007/s13238-019-00684-8]
6 **Fecal Microbiota Transplantation-standardization Study Group**. Nanjing consensus on methodology of washed microbiota transplantation. *Chin Med J (Engl)* 2020; **133**: 2330-2332 [PMID: 32701590 DOI: 10.1097/CM9.0000000000000954]
7 **Lu G**, Wang W, Li P, Wen Q, Cui B, Zhang F. Washed preparation of faecal microbiota changes the transplantation related safety, quantitative method and delivery. *Microb Biotechnol* 2022; **15**: 2439-2449 [PMID: 35576458 DOI: 10.1111/1751-7915.14074]
8 **Zhang T**, Li P, Wu X, Lu G, Marcella C, Ji X, Ji G, Zhang F. Alterations of Akkermansia muciniphila in the inflammatory bowel disease patients with washed microbiota transplantation. *Appl Microbiol Biotechnol* 2020; **104**: 10203-10215 [PMID: 33064186 DOI: 10.1007/s00253-020-10948-7]
9 **Li P**, Zhang T, Xiao Y, Tian L, Cui B, Ji G, Liu YY, Zhang F. Timing for the second fecal microbiota transplantation to maintain the long-term benefit from the first treatment for Crohn's disease. *Appl Microbiol Biotechnol* 2019; **103**: 349-360 [PMID: 30357440 DOI: 10.1007/s00253-018-9447-x]
10 **Zhou S**, Cui Y, Zhang Y, Zhao T, Cong J. Fecal microbiota transplantation for induction of remission in Crohn's disease: a systematic review and meta-analysis. *Int J Colorectal Dis* 2023; **38**: 62 [PMID: 36882658 DOI: 10.1007/s00384-023-04354-4]
11 **Bashiardes S**, Zilberman-Schapira G, Elinav E. Use of Metatranscriptomics in Microbiome Research. *Bioinform Biol Insights* 2016; **10**: 19-25 [PMID: 27127406 DOI: 10.4137/BBI.S34610]
12 **Gajendran M**, Loganathan P, Catinella AP, Hashash JG. A comprehensive review and update on Crohn's disease. *Dis Mon* 2018; **64**: 20-57 [PMID: 28826742 DOI: 10.1016/j.disamonth.2017.07.001]
13 **Satsangi J**, Silverberg MS, Vermeire S, Colombel JF. The Montreal classification of inflammatory bowel disease: controversies, consensus, and implications. *Gut* 2006; **55**: 749-753 [PMID: 16698746 DOI: 10.1136/gut.2005.082909]
14 **Zhang F**, Cui B, He X, Nie Y, Wu K, Fan D; FMT-standardization Study Group. Microbiota transplantation: concept, methodology and strategy for its modernization. *Protein Cell* 2018; **9**: 462-473 [PMID: 29691757 DOI: 10.1007/s13238-018-0541-8]
15 **Zhang T**, Long C, Cui B, Buch H, Wen Q, Li Q, Ding X, Ji G, Zhang F. Colonic transendoscopic tube-delivered enteral therapy (with video): a prospective study. *BMC Gastroenterol* 2020; **20**: 135 [PMID: 32375675 DOI: 10.1186/s12876-020-01285-0]
16 **Long C**, Yu Y, Cui B, Jagessar SAR, Zhang J, Ji G, Huang G, Zhang F. A novel quick transendoscopic enteral tubing in mid-gut: technique and training with video. *BMC Gastroenterol* 2018; **18**: 37 [PMID: 29534703 DOI: 10.1186/s12876-018-0766-2]
17 **Kelly CR**, Kunde SS, Khoruts A. Guidance on preparing an investigational new drug application for fecal microbiota transplantation studies. *Clin Gastroenterol Hepatol* 2014; **12**: 283-288 [PMID: 24107393 DOI: 10.1016/j.cgh.2013.09.060]
18 **Wood DE**, Lu J, Langmead B. Improved metagenomic analysis with Kraken 2. *Genome Biol* 2019; **20**: 257 [PMID: 31779668 DOI: 10.1186/s13059-019-1891-0]
19 **Wang JL**, Zhang T, Shen XT, Liu J, Zhao DL, Sun YW, Wang L, Liu YJ, Gong XY, Liu YX, Zhu ZJ, Xue FZ. Serum metabolomics for early diagnosis of esophageal squamous cell carcinoma by UHPLC-QTOF/MS. *Metabolomics* 2016; **12**: 116 [DOI: 10.1007/s11306-016-1050-5]
20 **Smith CA**, Want EJ, O'Maille G, Abagyan R, Siuzdak G. XCMS: processing mass spectrometry data for metabolite profiling using nonlinear peak alignment, matching, and identification. *Anal Chem* 2006; **78**: 779-787 [PMID: 16448051 DOI: 10.1021/ac051437y]
21 **Wiklund S**, Johansson E, Sjöström L, Mellerowicz EJ, Edlund U, Shockcor JP, Gottfries J, Moritz T, Trygg J. Visualization of GC/TOF-MS-based metabolomics data for identification of biochemically interesting compounds using OPLS class models. *Anal Chem* 2008; **80**: 115-122 [PMID: 18027910 DOI: 10.1021/ac0713510]
22 **Marcella C**, Cui B, Kelly CR, Ianiro G, Cammarota G, Zhang F. Systematic review: the global incidence of faecal microbiota transplantation-related adverse events from 2000 to 2020. *Aliment Pharmacol Ther* 2021; **53**: 33-42 [PMID: 33159374 DOI: 10.1111/apt.16148]
23 **Cheng F**, Huang Z, Wei W, Li Z. Fecal microbiota transplantation for Crohn's disease: a systematic review and meta-analysis. *Tech Coloproctol* 2021; **25**: 495-504 [PMID: 33759066 DOI: 10.1007/s10151-020-02395-3]

24 **Goyal A**, Yeh A, Bush BR, Firek BA, Siebold LM, Rogers MB, Kufen AD, Morowitz MJ. Safety, Clinical Response, and Microbiome Findings Following Fecal Microbiota Transplant in Children With Inflammatory Bowel Disease. *Inflamm Bowel Dis* 2018; **24**: 410-421 [PMID: 29361092 DOI: 10.1093/ibd/izx035]

25 **Wu R**, Xiong R, Li Y, Chen J, Yan R. Gut microbiome, metabolome, host immunity associated with inflammatory bowel disease and intervention of fecal microbiota transplantation. *J Autoimmun* 2023; **141**: 103062 [PMID: 37246133 DOI: 10.1016/j.jaut.2023.103062]

26 **Mallick H**, Ma S, Franzosa EA, Vatanen T, Morgan XC, Huttenhower C. Experimental design and quantitative analysis of microbial community multiomics. *Genome Biol* 2017; **18**: 228 [PMID: 29187204 DOI: 10.1186/s13059-017-1359-z]

27 **Parada Venegas D**, De la Fuente MK, Landskron G, González MJ, Quera R, Dijkstra G, Harmsen HJM, Faber KN, Hermoso MA. Short Chain Fatty Acids (SCFAs)-Mediated Gut Epithelial and Immune Regulation and Its Relevance for Inflammatory Bowel Diseases. *Front Immunol* 2019; **10**: 277 [PMID: 30915065 DOI: 10.3389/fimmu.2019.00277]

28 **Vich Vila A**, Imhann F, Collij V, Jankipersadsing SA, Gurry T, Mujagic Z, Kurilshikov A, Bonder MJ, Jiang X, Tigchelaar EF, Dekens J, Peters V, Voskuil MD, Visschedijk MC, van Dullemen HM, Keszthelyi D, Swertz MA, Franke L, Alberts R, Festen EAM, Dijkstra G, Masclee AAM, Hofker MH, Xavier RJ, Alm EJ, Fu J, Wijmenga C, Jonkers DMAE, Zhernakova A, Weersma RK. Gut microbiota composition and functional changes in inflammatory bowel disease and irritable bowel syndrome. *Sci Transl Med* 2018; **10** [PMID: 30567928 DOI: 10.1126/scitranslmed.aap8914]

29 **Rey FE**, Gonzalez MD, Cheng J, Wu M, Ahern PP, Gordon JI. Metabolic niche of a prominent sulfate-reducing human gut bacterium. *Proc Natl Acad Sci U S A* 2013; **110**: 13582-13587 [PMID: 23898195 DOI: 10.1073/pnas.1312524110]

30 **Wu S**, Cong G, Zhang Q, Yao H, Wang Z, Kang K, He X, Shi S. Infection Heterogeneity and Microbiota Differences in Chicks Infected by Salmonella enteritidis. *Microorganisms* 2021; **9** [PMID: 34442784 DOI: 10.3390/microorganisms9081705]

31 **Kutsuna R**, Tomida J, Morita Y, Kawamura Y. Paraclostridium bifermentans exacerbates pathosis in a mouse model of ulcerative colitis. *PLoS One* 2018; **13**: e0197668 [PMID: 29782507 DOI: 10.1371/journal.pone.0197668]

32 **Bhatt AS**, Freeman SS, Herrera AF, Pedamallu CS, Gevers D, Duke F, Jung J, Michaud M, Walker BJ, Young S, Earl AM, Kostic AD, Ojesina AI, Hasserjian R, Ballen KK, Chen YB, Hobbs G, Antin JH, Soiffer RJ, Baden LR, Garrett WS, Hornick JL, Marty FM, Meyerson M. Sequence-based discovery of Bradyrhizobium enterica in cord colitis syndrome. *N Engl J Med* 2013; **369**: 517-528 [PMID: 23924002 DOI: 10.1056/NEJMoa1211115]

33 **Maldonado-Contreras A**, Ferrer L, Cawley C, Crain S, Bhattarai S, Toscano J, Ward DV, Hoffman A. Dysbiosis in a canine model of human fistulizing Crohn's disease. *Gut Microbes* 2020; **12**: 1785246 [PMID: 32730134 DOI: 10.1080/19490976.2020.1785246]

34 **Martin FP**, Su MM, Xie GX, Guiraud SP, Kussmann M, Godin JP, Jia W, Nydegger A. Urinary metabolic insights into host-gut microbial interactions in healthy and IBD children. *World J Gastroenterol* 2017; **23**: 3643-3654 [PMID: 28611517 DOI: 10.3748/wjg.v23.i20.3643]

35 **Ni J**, Shen TD, Chen EZ, Bittinger K, Bailey A, Roggiani M, Sirota-Madi A, Friedman ES, Chau L, Lin A, Nissim I, Scott J, Lauder A, Hoffmann C, Rivas G, Albenberg L, Baldassano RN, Braun J, Xavier RJ, Clish CB, Yudkoff M, Li H, Goulian M, Bushman FD, Lewis JD, Wu GD. A role for bacterial urease in gut dysbiosis and Crohn's disease. *Sci Transl Med* 2017; **9** [PMID: 29141885 DOI: 10.1126/scitranslmed.aah6888]

36 **Jodeleit H**, Winkelmann P, Caesar J, Sterz S, Holdt LM, Beigel F, Stallhofer J, Breiteneicher S, Bartnik E, Leeuw T, Siebeck M, Gropp R. Head-to-head study of oxelumab and adalimumab in a mouse model of ulcerative colitis based on NOD/Scid IL2Rγnull mice reconstituted with human peripheral blood mononuclear cells. *Dis Model Mech* 2021; **14** [PMID: 33293281 DOI: 10.1242/dmm.046995]

37 **Wu Q**, Li J, Zhu J, Sun X, He D, Cheng Z, Zhang X, Xu Y, Chen Q, Zhu Y, Lai M. Gamma-glutamyl-leucine levels are causally associated with elevated cardio-metabolic risks. *Front Nutr* 2022; **9**: 936220 [PMID: 36505257 DOI: 10.3389/fnut.2022.936220]

38 **Wu X**, Cao J, Li M, Yao P, Li H, Xu W, Yuan C, Liu J, Wang S, Li P, Wang Y. An integrated microbiome and metabolomic analysis identifies immunoenhancing features of Ganoderma lucidum spores oil in mice. *Pharmacol Res* 2020; **158**: 104937 [PMID: 32464331 DOI: 10.1016/j.phrs.2020.104937]

39 **Carrey EA**, Smolenski RT, Edbury SM, Laurence A, Marinaki AM, Duley JA, Zhu L, Goldsmith DJ, Simmonds HA. Origin and characteristics of an unusual pyridine nucleotide accumulating in erythrocytes: positive correlation with degree of renal failure. *Clin Chim Acta* 2003; **335**: 117-129 [PMID: 12927693 DOI: 10.1016/s0009-8981(03)00294-8]

40 **Zhong HJ**, Xie X, Chen WJ, Zhuang YP, Hu X, Cai YL, Zeng HL, Xiao C, Li Y, Ding Y, Xue L, Chen M, Zhang J, Wu Q, He XX. Washed microbiota transplantation improves renal function in patients with renal dysfunction: a retrospective cohort study. *J Transl Med* 2023; **21**: 740 [PMID: 37858192 DOI: 10.1186/s12967-023-04570-0]

41 **Yaghoubi A**, Davoodi J, Asgharzadeh F, Rezaie S, Nazari E, Khazaei M, Soleimanpour S. Therapeutic effect of an anti-tuberculosis agent, isoniazid, and its nano-isoform in ulcerative colitis. *Int Immunopharmacol* 2021; **96**: 107577 [PMID: 33812254 DOI: 10.1016/j.intimp.2021.107577]

42 **Li Y**, Dalabasmaz S, Gensberger-Reigl S, Heymich ML, Krofta K, Pischetsrieder M. Identification of colupulone and lupulone as the main contributors to the antibacterial activity of hop extracts using activity-guided fractionation and metabolome analysis. *Food Res Int* 2023; **169**: 112832 [PMID: 37254407 DOI: 10.1016/j.foodres.2023.112832]

43 **Ming XF**, Rajapakse AG, Carvas JM, Ruffieux J, Yang Z. Inhibition of S6K1 accounts partially for the anti-inflammatory effects of the arginase inhibitor L-norvaline. *BMC Cardiovasc Disord* 2009; **9**: 12 [PMID: 19284655 DOI: 10.1186/1471-2261-9-12]

44 **Sheng K**, Xu Y, Kong X, Wang J, Zha X, Wang Y. Probiotic Bacillus cereus Alleviates Dextran Sulfate Sodium-Induced Colitis in Mice through Improvement of the Intestinal Barrier Function, Anti-Inflammation, and Gut Microbiota Modulation. *J Agric Food Chem* 2021; **69**: 14810-14823 [PMID: 34677958 DOI: 10.1021/acs.jafc.1c03375]

45 **Kunisawa J**, Kiyono H. Immunological function of sphingosine 1-phosphate in the intestine. *Nutrients* 2012; **4**: 154-166 [PMID: 22666543 DOI: 10.3390/nu4030154]

46 **Albert E**, Walker J, Thiesen A, Churchill T, Madsen K. cis-Urocanic acid attenuates acute dextran sodium sulphate-induced intestinal inflammation. *PLoS One* 2010; **5**: e13676 [PMID: 21060867 DOI: 10.1371/journal.pone.0013676]

47 **Zhang F**, Wang W, Nie Y, Li J, He X. From microbial technology to microbiota medicine as a clinical discipline: Sustainable development goal. *Microb Biotechnol* 2023; **16**: 1705-1708 [PMID: 37452703 DOI: 10.1111/1751-7915.14317]

World Journal of Gastroenterology

Submit a Manuscript: https://www.f6publishing.com

World J Gastroenterol 2024 March 21; 30(11): 1588-1608

DOI: 10.3748/wjg.v30.i11.1588

ISSN 1007-9327 (print) ISSN 2219-2840 (online)

ORIGINAL ARTICLE

Basic Study

Silent information regulator sirtuin 1 ameliorates acute liver failure *via* the p53/glutathione peroxidase 4/gasdermin D axis

Xing-Nian Zhou, Quan Zhang, Hong Peng, Yu-Jie Qin, Yu-Hong Liu, Lu Wang, Ming-Liang Cheng, Xin-Hua Luo, Hong Li

Specialty type: Gastroenterology and hepatology

Provenance and peer review: Unsolicited article; Externally peer reviewed.

Peer-review model: Single blind

Peer-review report's scientific quality classification

Grade A (Excellent): 0
Grade B (Very good): B
Grade C (Good): C, C
Grade D (Fair): 0
Grade E (Poor): 0

P-Reviewer: Motlagh B, Iran; Wang M, China; Xia B, China

Received: October 5, 2023
Peer-review started: October 5, 2023
First decision: December 6, 2023
Revised: December 20, 2023
Accepted: February 18, 2024
Article in press: February 18, 2024
Published online: March 21, 2024

Xing-Nian Zhou, Quan Zhang, Yu-Jie Qin, Yu-Hong Liu, Lu Wang, Ming-Liang Cheng, Hong Li, Department of Infectious Diseases, The Affiliated Hospital of Guizhou Medical University, Guizhou Medical University, Guiyang 550004, Guizhou Province, China

Hong Peng, Xin-Hua Luo, Hong Li, Department of Infectious Diseases, Guizhou Provincial People's Hospital, Guiyang 550001, Guizhou Province, China

Corresponding author: Hong Li, PhD, Chief Physician, Department of Infectious Diseases, The Affiliated Hospital of Guizhou Medical University, Guizhou Medical University, No. 28 Guiyi Road, Guiyang 550004, Guizhou Province, China. 625062102@qq.com

Abstract

BACKGROUND

Acute liver failure (ALF) has a high mortality with widespread hepatocyte death involving ferroptosis and pyroptosis. The silent information regulator sirtuin 1 (SIRT1)-mediated deacetylation affects multiple biological processes, including cellular senescence, apoptosis, sugar and lipid metabolism, oxidative stress, and inflammation.

AIM

To investigate the association between ferroptosis and pyroptosis and the upstream regulatory mechanisms.

METHODS

This study included 30 patients with ALF and 30 healthy individuals who underwent serum alanine aminotransferase (ALT) and aspartate aminotransferase (AST) testing. C57BL/6 mice were also intraperitoneally pretreated with SIRT1, p53, or glutathione peroxidase 4 (GPX4) inducers and inhibitors and injected with lipopolysaccharide (LPS)/D-galactosamine (D-GalN) to induce ALF. Gasdermin D (GSDMD)$^{-/-}$ mice were used as an experimental group. Histological changes in liver tissue were monitored by hematoxylin and eosin staining. ALT, AST, glutathione, reactive oxygen species, and iron levels were measured using commercial kits. Ferroptosis- and pyroptosis-related protein and mRNA expression was detected by western blot and quantitative real-time polymerase chain reaction. SIRT1, p53, and GSDMD were assessed by immunofluorescence analysis.

RESULTS

Serum AST and ALT levels were elevated in patients with ALF. SIRT1, solute carrier family 7a member 11 (SLC7A11), and GPX4 protein expression was decreased and acetylated p5, p53, GSDMD, and acyl-CoA synthetase long-chain family member 4 (ACSL4) protein levels were elevated in human ALF liver tissue. In the p53 and ferroptosis inhibitor-treated and GSDMD$^{-/-}$ groups, serum interleukin (IL)-1β, tumour necrosis factor alpha, IL-6, IL-2 and C-C motif ligand 2 levels were decreased and hepatic impairment was mitigated. In mice with GSDMD knockout, p53 was reduced, GPX4 was increased, and ferroptotic events (depletion of SLC7A11, elevation of ACSL4, and iron accumulation) were detected. *In vitro*, knockdown of p53 and overexpression of GPX4 reduced AST and ALT levels, the cytostatic rate, and GSDMD expression, restoring SLC7A11 depletion. Moreover, SIRT1 agonist and overexpression of SIRT1 alleviated acute liver injury and decreased iron deposition compared with results in the model group, accompanied by reduced p53, GSDMD, and ACSL4, and increased SLC7A11 and GPX4. Inactivation of SIRT1 exacerbated ferroptotic and pyroptotic cell death and aggravated liver injury in LPS/D-GalN-induced *in vitro* and *in vivo* models.

CONCLUSION

SIRT1 activation attenuates LPS/D-GalN-induced ferroptosis and pyroptosis by inhibiting the p53/GPX4/GSDMD signaling pathway in ALF.

Key Words: Silent information regulator sirtuin 1; Ferroptosis; Pyroptosis; p53/glutathione peroxidase 4/gasdermin D; Acute liver failure

Core Tip: In this study, we investigated the involvement of ferroptosis and pyroptosis in acute liver failure (ALF) using lipopolysaccharide/D-galactosamine-induced ALF model mice. Our results showed that silent information regulator sirtuin 1 activation alleviated ALF through p53/glutathione peroxidase 4/gasdermin D, which mediated the ferroptosis and pyroptosis crosstalk. Our study established a link between ferroptosis and pyroptosis and the upstream regulatory mechanisms. These results may lead to the identification of potential therapeutic targets for ALF.

Citation: Zhou XN, Zhang Q, Peng H, Qin YJ, Liu YH, Wang L, Cheng ML, Luo XH, Li H. Silent information regulator sirtuin 1 ameliorates acute liver failure *via* the p53/glutathione peroxidase 4/gasdermin D axis. *World J Gastroenterol* 2024; 30(11): 1588-1608
URL: https://www.wjgnet.com/1007-9327/full/v30/i11/1588.htm
DOI: https://dx.doi.org/10.3748/wjg.v30.i11.1588

INTRODUCTION

Acute liver failure (ALF) is a rare and severe consequence of abrupt hepatocyte injury, with a mortality rate of up to 30% [1]. ALF is caused by various factors, including drugs, toxins, virus, and metabolic diseases. The central event in ALF is the excessive and uncontrolled mass death of hepatocytes through necrosis and apoptosis, which can cause DNA damage and oxidation stress, accompanied by an inflammatory storm[2,3]. Accumulating evidence has suggested that ferroptosis and pyroptosis, which are novel programmed modes of cell death that are distinct from necrosis, apoptosis, and autophagy, play critical roles in ALF by each mediating different immunological effects and inflammatory responses[4-6].

Ferroptosis is characterized by intracellular iron overload, decreased glutathione peroxidase 4 (GPX4) activity, and accumulation of lipid reactive oxygen species (ROS)[7]. Solute carrier family 7a member 11 (SLC7A11), a component of the system XC^- antiporter located in the cell membrane, is involved in glutathione (GSH) synthesis[8]. Jiang *et al*[9] showed that transcriptional suppression of SLC7A11 by p53 resulted in inhibited cystine uptake and sensitized cells to ferroptosis. p53 plays a critical role in the cellular response to various stresses, including DNA damage, hypoxia, nutrition starvation, and oncogene activation[10]. Additionally, p53 promotes ferroptosis by inhibiting cystine metabolism and ROS activity[9,11].

Pyroptosis is a form of lytic cell death induced by pathogen infection or an endogenous challenge[12]. When cells receive internal and external danger signals, pattern recognition receptors initiate various inflammasomes to activate caspase 1, leading to cleavage of the pyroptosis executor gasdermin D (GSDMD) into the active N terminal and inactive C terminal. The active N terminal fragment translocates from the cytosol into the medial cell membrane, forming a large number of sieve membrane pores, resulting in the release of cell contents, including interleukin (IL)-1β and IL-18, into the extracellular space. Recruitment of immune cells for targeted migration to the injury site mediates secondary immune damage[13]. Our previous study showed that GSDMD-mediated pyroptosis of hepatocytes played an important role in the pathogenesis of ALF[14]. Furthermore, GSDMD knockout reduced hepatocyte death and inflammatory responses, thus alleviating ALF. However, the relationship between ferroptosis and pyroptosis in ALF is unknown.

Silent information regulator sirtuin 1 (SIRT1), which is an NAD+-dependent protein deacetylase, regulates the acetylation of specific transcription factors and proteins, including p53. SIRT1 is involved in various functions, such as energy metabolism, stress responses, inflammation, and redox homeostasis[15,16]. Deacetylation of p53 by SIRT1 may act as a protective shield in sepsis-induced liver injury[17].

In the present study, we investigated the involvement of ferroptosis and pyroptosis in ALF using lipopolysaccharide (LPS)/D-galactosamine (D-GalN)-induced ALF model mice. Our study established an association between ferroptosis and pyroptosis and the upstream regulatory mechanisms. These results may lead to the identification of potential therapeutic targets for ALF.

MATERIALS AND METHODS

Patients

Samples from 30 patients with ALF and 30 healthy individuals were collected from the Affiliated Hospital of Guizhou Medical University. ALF was diagnosed by following the definition in the 2017 EASL ALF Guidelines[18]. Whole livers of seven patients with ALF and donor trimmed portions from three liver transplant recipients were collected. This study was approved by the Ethics Committee of the Affiliated Hospital of Guizhou Medical University (2018 Lun Audit No. 036) and complied with the ethical guidelines of the 1975 Declaration of Helsinki. The tissue donors and/or their families provided informed consent for the use of human residual material for research purposes.

Mouse model and drug treatment

Male C57BL/6 mice (8-10 wk, 22-26 g) were purchased from SPF Biotechnology Co. (Beijing, China). Male GSDMD systemic knockout (GSDMD$^{-/-}$) mice (C57BL/6J strain, 6-8 wk) were a generous gift from Shao Feng's Laboratory, Beijing Institute of Life Sciences, China. All animals were kept in the Laboratory Animal Centre of Guizhou Medical University (laboratory animal production license No. SYXK (Guizhou) 2023-0002, and laboratory animal use license No. SYXK (Guizhou) 2023-0002). The animal experimental methods designed in this study were reviewed and approved by the Animal Ethics Committee of Guizhou Medical University. The mice were maintained in a 12-h light-dark cycle environment and had free access to water and food. The mice acclimated to the environment for 1 wk before the experiments.

The mice were randomly divided into the following nine experimental groups (n = 10 per group): Vehicle (phosphate-buffered saline), resveratrol [a SIRT1 activator; MedChemExpress, New Jersey, United States; 30 mg/kg, intraperitoneal injection (i.p.) for 14 d], EX527 (a SIRT1 inhibitor; Sigma, St. Louis, Missouri, United States; 5 mg/kg, i.p. for 14 d), pifithrin-α (a p53 inhibitor; MedChemExpress; 2.2 mg/kg, i.p. for 3 d), nutlin-3α (a p53 inducer; MedChemExpress; 12 mg/kg, i.p. for 7 d), liproxstatin-1 (a ferroptosis inhibitor; MedChemExpress; 10 mg/kg, i.p. for 14 d), RAS-selective lethal 3 (RSL3) (a ferroptosis inducer; Sigma; 2 mg/kg, i.p. for 7 d), GSDMD$^{-/-}$, and ALF model. The mice were pre-treated as described above before establishing the model.

To establish the ALF model, all groups except for the vehicle group, were injected with LPS (Sigma; 10 μg/kg, i.p.) and D-GalN (Sigma; 300 mg/kg, i.p.). After 48 h, survival was recorded and the surviving mice were sacrificed. Blood was collected from the eyeball vein and centrifuged at 3000 × g/min for 15 min. The serum was separated and stored at -80 °C. Liver tissues were harvested by portal vein perfusion. Some of the specimens were fixed using paraformaldehyde for 48 h, and a pathological examination was performed. The remaining tissues were quickly stored at -80 °C.

Iron assay

Liver tissues and cells were homogenized in an ice bath using the Iron Assay Kit (BC4355; Solarbio, Beijing, China). The samples were centrifuged at 4000 × g at 4 °C and the supernatants were removed. The supernatants were added to a 96-well plate, and the absorbance was measured at 520 nm with a microplate reader.

Hematoxylin and eosin staining

Liver tissues were fixed in 4% paraformaldehyde for 24 h and dehydrated with a concentration gradient of ethanol solutions, followed by paraffin embedding. Tissue sections were cut, de-waxed, rehydrated, and stained with hematoxylin and eosin (HE). The sections were subjected to microscope analysis.

Immunofluorescence analysis

Liver tissues were collected and routinely embedded in optimal cutting temperature compound. The sections were dewaxed three times for 30 min each and dehydrated three times for 30 min each, followed by three washes with phosphate-buffered saline. Liver sections were stained with antibodies against SIRT1 (ab110304; Abcam), p53 (80077-1-RR; Proteintech), and GSDMD (ab219800; Abcam) overnight at 4 °C. After extensive washing, the sections were incubated with the respective fluorescent secondary antibodies (ab150115 and ab150077; Abcam) for 2 h at room temperature.

Short interfering RNA transfection

SIRT1, p53, GPX4, and negative control (NC) short interfering (siRNAs) were obtained from GeneChem (China). HL7702 cells were transfected with siRNAs using Lipofectamine 3000 (Invitrogen, United States) by following the manufacturer's instructions. After 6 h, the culture medium was replaced with fresh complete medium and the cells were cultured for 48 h.

Alanine aminotransferase and aspartate aminotransferase assays

The levels of alanine aminotransferase (ALT) and aspartate aminotransferase (AST) in serum were assessed using the ALT Kit (E-BC-K235-M; Elabscience, China) and AST Kit (E-BC-K236-M; Elabscience, China) by following the manufacturers' instructions.

ROS assay

ROS activity in cells was measured with a fluorescent probe (DCFH-DA) (Beyotime, Shanghai, China). HL7702 cells in a six-well plate were treated with D-GalN/LPS (D-GalN 15 mmol/L + LPS 100 μg/mL) for 24 h, and DCFH-DA (2 μL/well) was added for 30 min at 37 °C. The cells were washed three times with serum-free medium. DCFH-DA was measured by flow cytometric analysis.

Quantitative real-time polymerase chain reaction

Liver tissue was lysed with Trizol (Omega, United States). Total RNA was extracted and tested for concentration and purity. The RNA was reverse transcribed using a reverse transcription kit (Takara, Japan) to synthesize cDNA. Expression levels of mRNA were evaluated using the SYBR Green detection system (Takara, Japan). All samples were measured in triplicate and gene expression was normalized with glyceraldehyde 3-phosphate dehydrogenase (GAPDH) mRNA levels. The primer sequences were as follows: GAPDH, (forward) *AGGTCGGTGTGAACGGATTTG* and (reverse) *GGGGTCGTTGATGGCAACA*; p53, (forward) *CCCCTGCATCTT TTGTCCCT* and (reverse) *AGCTGGCAGAATAGCTTATTGAG*; GPX4, (forward) *TGTGCATC CCGCGATGATT* and (reverse) *CCCTGTACTTATCCAGGCAGA*; GSDMD, (forward) *ATGCC ATCGGCCTTTGAGAAA* and (reverse) *AGGCTGTCCACCGGAATGA*; SLC7A11, (forward) *GGCACCGTCATCGGATCAG* and (reverse) *CTCCACAGGCAGACCAGAAAA*; and acyl-CoA synthetase long-chain family member 4 (ACSL4), (forward) *CCTGAGGGGCTTGAAATTCAC* and (reverse) *GTTTCGGTGTGAACGGATTTG*.

Western blot analysis

Liver tissues and cells were rinsed twice with phosphate-buffered saline buffer and lysed on ice with RIPA lysis solution (Solarbio). The protein samples were separated on 10% sodium dodecyl sulfate-polyacrylamide gels and transferred to polyvinylidene fluoride membranes (Millipore, United States). The membranes were incubated with mouse anti-Sirt1 (1:1000; Abcam; ab110304), mouse anti-p53 (1:1000; Abcam; ab26), rabbit anti-p53 (acetyl K382) (1:1000; Abcam; ab75754), mouse anti-GPX4 (1:2000; Proteintech; 67763-1-Ig), rabbit anti-GSDMD (1:1000; Abcam; ab129800), rabbit anti-SLC7A11 (1:2000; Origene; TA351958), and rabbit anti-ACSL4 (1:2000; Origene; TA349566) antibodies overnight at 4 °C. The membranes were incubated with secondary anti-mouse (1:5000; Proteintech; SA00001-1) or anti-rabbit horseradish peroxidase-conjugated antibodies (1:5000; Proteintech; SA00001-2) for 2 h at room temperature. The signals were visualized using enhanced chemiluminescence reagent (CLiNX; Chemiscop, Shanghai, China).

Statistical analysis

Statistical analyses were conducted using Prism 8.3.0 (GraphPad, United States). Values are expressed as the mean ± SD of at least three independent experiments. The normality and the homogeneity of variance were checked by the Shapiro-Wilk test before Student's *t*-test and one-way analysis of variance. Student's *t*-test was used to compare data between two groups, while one-way analysis of variance analysis was used for comparison among multiple groups. Statistical significance was considered if P value was < 0.05.

RESULTS

Ferroptosis and pyroptosis are triggered in liver tissue in patients with ALF

To examine the potential role of ferroptosis and pyroptosis in ALF, we first examined the inflammatory status, liver function biomarkers, and markers for ferroptosis and pyroptosis in the serum or liver tissue samples from patients with ALF. We found that AST, ALT, and inflammatory factor levels were increased in human ALF serum (Figure 1A). Iron staining showed iron accumulation in liver tissue in patients with ALF (Figure 1B and C). Additionally, the ferroptotic markers GPX4 and SLC7A11 showed decreased protein expression, whereas p53 and ACSL4 proteins, which are positive regulators of ferroptosis, were elevated in human ALF liver tissue (Figure 1D). In line with previous studies[14], GSDMD, which is a key regulatory factor of pyroptosis, was increased in human ALF tissue (Figure 1E). We also found that p53 and acetylated p53 (Ac-p53) were elevated and SIRT1 was decreased in human ALF tissue (Figure 1F).

Inhibition of p53/GPX4/GSDMD-mediated ferroptosis and the pyroptosis pathway protects mice against LPS/D-GalN-induced ALF

We observed an induction of ferroptosis and pyroptosis in human ALF liver tissues, accompanied by increased p53 protein expression. To further examine the mechanism of ferroptosis and pyroptosis in ALF, we inhibited ferroptosis and pyroptosis in mice with ALF induced by LPS/D-GalN. Untreated mice were first pretreated with pifithrin-α and liproxstatin-1, which inhibits GPX4 consumption[19,20]. GSDMD$^{-/-}$ mice were used as another experimental group. HE staining of liver sections showed that mice pre-treated with pifithrin-α or liproxstatin-1 and GSDMD$^{-/-}$ mice had less structural damage in liver tissue, and most liver lobules were structurally intact compared with those in the ALF model group. These mice also showed a prolonged survival compared with those in the ALF model group (Figure 2A and B).

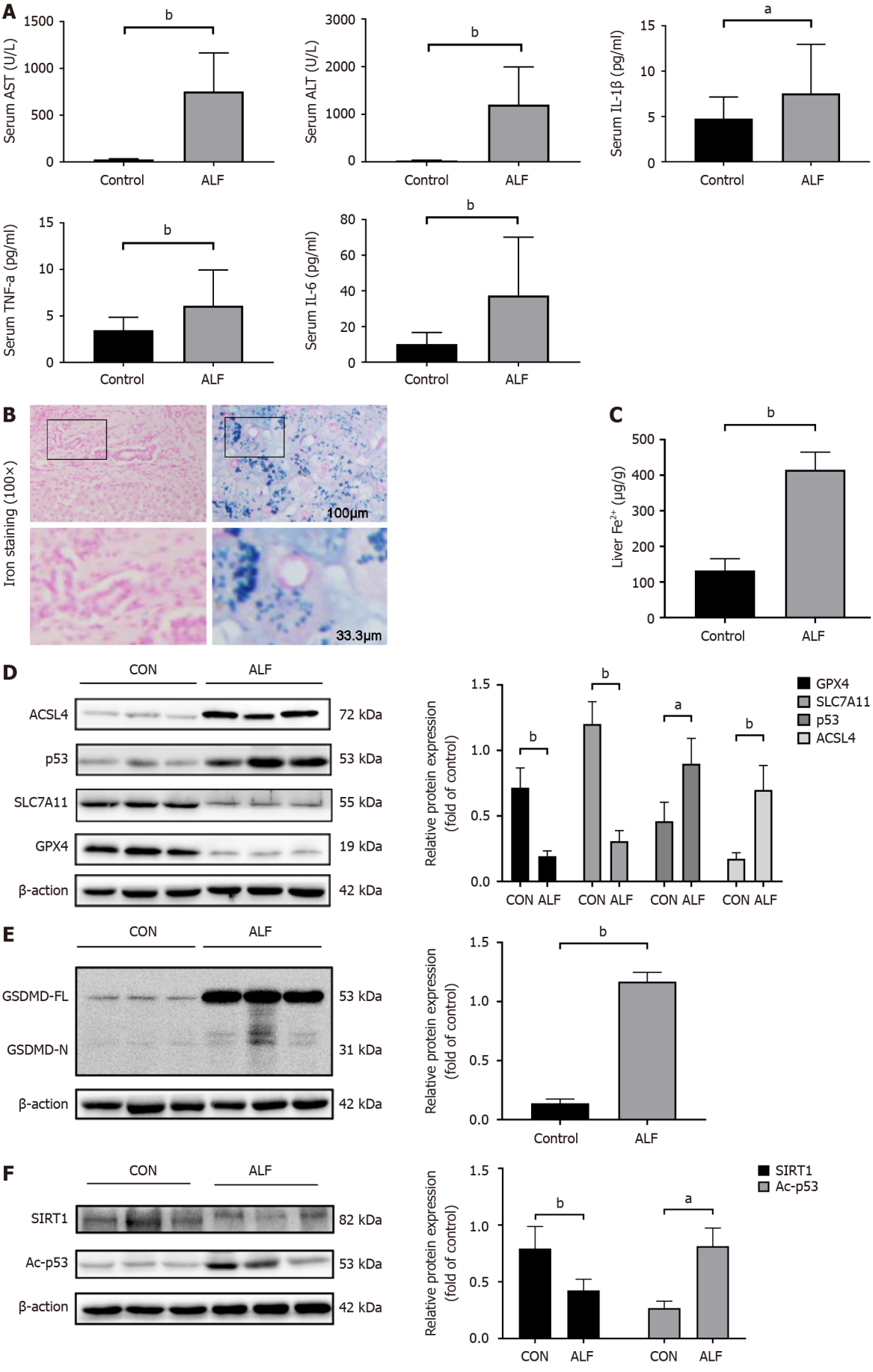

Figure 1 Ferroptosis and pyroptosis occur in human acute liver failure. A: The levels of aspartate aminotransferase, alanine aminotransferase, tumour

necrosis factor alpha, interleukin (IL)-1β, and IL-6 were changed in serum samples of healthy individuals and patients with acute liver failure (ALF) (n = 30 in each group); B: Iron staining (scale bar: 100 μm and 33.3 μm) of normal liver tissue and ALF liver tissue; C: Detection of iron in normal liver tissue and ALF; D: Western blot analyses of glutathione peroxidase 4, solute carrier family 7a member 11, p53, and acyl-CoA synthetase long-chain family member 4 proteins were performed in healthy individuals and patients with ALF. Data are presented as the mean ± SD of three independent experiments; E: Western blot analysis of gasdermin D protein expression (n = 3); F: Western blot analysis of silent information regulator sirtuin 1 and Ac-p53 protein expression in healthy individuals and patients with ALF (n = 3). $^{a}P < 0.05$, $^{b}P < 0.01$. ALF: Acute liver failure; AST: Aspartate aminotransferase; ALT: Alanine aminotransferase; IL: Interleukin; GPX4: Glutathione peroxidase 4; SLC7A11: Solute carrier family 7a member 11; ACSL4: Acyl-CoA synthetase long-chain family member 4; GSDMD: Gasdermin D; SIRT1: Silent information regulator sirtuin 1.

Furthermore, mice pre-treated with pifithrin-α or liproxstatin-1 and GSDMD$^{-/-}$ mice showed a reduction in elevated serum levels of IL-1β, tumour necrosis factor alpha (TNF-α), IL-6, IL-2, and C-C motif ligand 2 (CCL2), which are inflammatory factors associated with pyroptosis, compared with those in the ALF model group (Figure 2C). Western blot analysis and quantitative real-time polymerase chain reaction (qRT-PCR) showed that mice pre-treated with pifithrin-α and liproxstatin-1 had reduced protein and mRNA levels of GSDMD and ferroptotic markers (ACSL4 and p53) compared with those in the ALF model group. We also found that GSDMD$^{-/-}$ mice showed increased GPX4 and SLC7A11 and decreased p53 and ACSL4 expression, accompanied by a decrease in iron accumulation (Figure 2D-G). Notably, p53 protein levels were markedly lower in GSDMD$^{-/-}$ mice than in ALF mice, but they were not affected by liproxstatin-1. However, p53 mRNA levels in the liproxstatin-1 group were downregulated (Figure 2D). An immunofluorescence assay showed a decrease in GSDMD expression in the groups treated with pifithrin-α and liproxstatin-1 (Supplementary Figure 1A).

To gain insight into the potential mechanisms of ferroptosis and pyroptosis in ALF induced by LPS/D-GalN, HL7702 cells transfected with siRNA targeting p53 and plasmid overexpressing GPX4 were stimulated with LPS/D-GalN for 24 h. We then detected the cellular AST and ALT contents. We found that LPS/D-GalN significantly increased AST and ALT, while knocking down p53 and overexpressing GPX4 reduced AST and ALT (Figure 3A and B). We further examined iron, ROS, GSH, and lipid peroxidation products, and found that knocking down p53 and overexpressing GPX4 significantly reduced GSH, malondialdehyde, and ROS contents compared with those in the AFL model group (Figure 3C-E). Western blot analysis and qRT-PCR showed that when p53 was knocked down and GPX4 was overexpressed, SLC7A11 protein and mRNA expression levels were restored compared with control levels. This change occurred at the same time as a decrease in ACSL4 expression (Figure 3F-H). Notably, GSDMD expression was also reduced in the sh-p53 group compared with the sh-NC group. To evaluate the relationships between p53, GPX4, and GSDMD, we overexpressed GPX4 in HL7702 cells, and found that AST and ALT levels were increased (Supplementary Figure 1A). Furthermore, with GPX4 overexpression, iron, ROS, and GSH contents and ferroptotic events were higher than those in the control group (Supplementary Figure 2A). Western blot analysis and qRT-PCR showed that SLC7A11 protein and mRNA levels were downregulated, while p53, ACSL4, and GSDMD protein and mRNA levels were upregulated in the GPX4 knockdown group compared with the sh-NC group (Supplementary Figure 2B and C).

GPX4 and GSDMD play a prominent role in the occurrence of ferroptosis and pyroptosis. p53 promotes ferroptosis by inhibiting cystine metabolism and ROS activity. However, the relationships between p53, GPX4, and GSDMD are unknown. These results showed that the suppression of ferroptosis and pyroptosis attenuated LPS/D-GalN-induced hepatocyte injury by inhibiting the p53/GPX4/GSDMD signaling pathway and lipid peroxidation.

Upregulation of p53 downregulates SLC7A11 and GPX4, leading to ferroptosis and triggering of pyroptosis

To further validate our hypothesis, we used nutlin-3α and RSL3 (ferroptosis inducer, which also causes GPX4 inactivation)[21,22] in ALF model mice. HE staining of liver tissue showed that the administration of nutlin-3α dramatically aggravated liver injury in ALF model mice to the same extent as that with RSL3 (Figure 4A). Furthermore, both treatments shortened the survival time of mice (Figure 4B). We also found that nutlin-3α and RSL3 worsened the inflammatory response in ALF model mice (Figure 4C). GPX4 and SLC7A11 were significantly decreased after nutlin-3α treatment, and ACSL4 protein levels were elevated (Figure 4D). Notably, p53 protein levels were upregulated slightly after RSL3 treatment, but this was not significant (Figure 4D). Western blot analysis showed that GSDMD and GSDMD-N protein levels were significantly higher in the nutlin-3α and RSL3 groups than in the ALF model group (Figure 4E), accompanied by increased iron deposition (Figure 4F). Immunofluorescence staining showed that nutlin-3α and RSL3 significantly exacerbated GSDMD expression in liver tissue, which suggested that inducing ferroptosis aggravated pyroptosis (Supplementary Figure 1B). Taken together, these data indicate that p53 upregulation may cause SLC7A11 and GPX4 downregulation, leading to ferroptosis, which in turn triggers pyroptosis to amplify the inflammatory response. This process may form a positive feedback loop, resulting in the deterioration of ALF.

The SIRT1-mediated p53/GPX4/GSDMD signaling pathway is dependent on p53 deacetylation in LPS/D-GalN-induced ALF

We found that SIRT1 levels were downregulated in human ALF, while Ac-p53 and p53 Levels were increased (Figure 1D and E). Previous studies have shown that SIRT1 inhibits p53 deacetylation. Our results confirmed that p53/GPX4/GSDMD mediated ferroptosis and pyroptosis. Therefore, we next pre-treated mice with EX527 and resveratrol. HE staining showed that the structure of the liver lobules was severely destroyed by the infiltration of inflammatory cells in the EX527 group compared with the ALF model group. In contrast, resveratrol treatment attenuated LPS/D-GalN-induced acute liver injury (Figure 5A) and prolonged the survival time of mice (Figure 5B). Multi-factor kits showed that

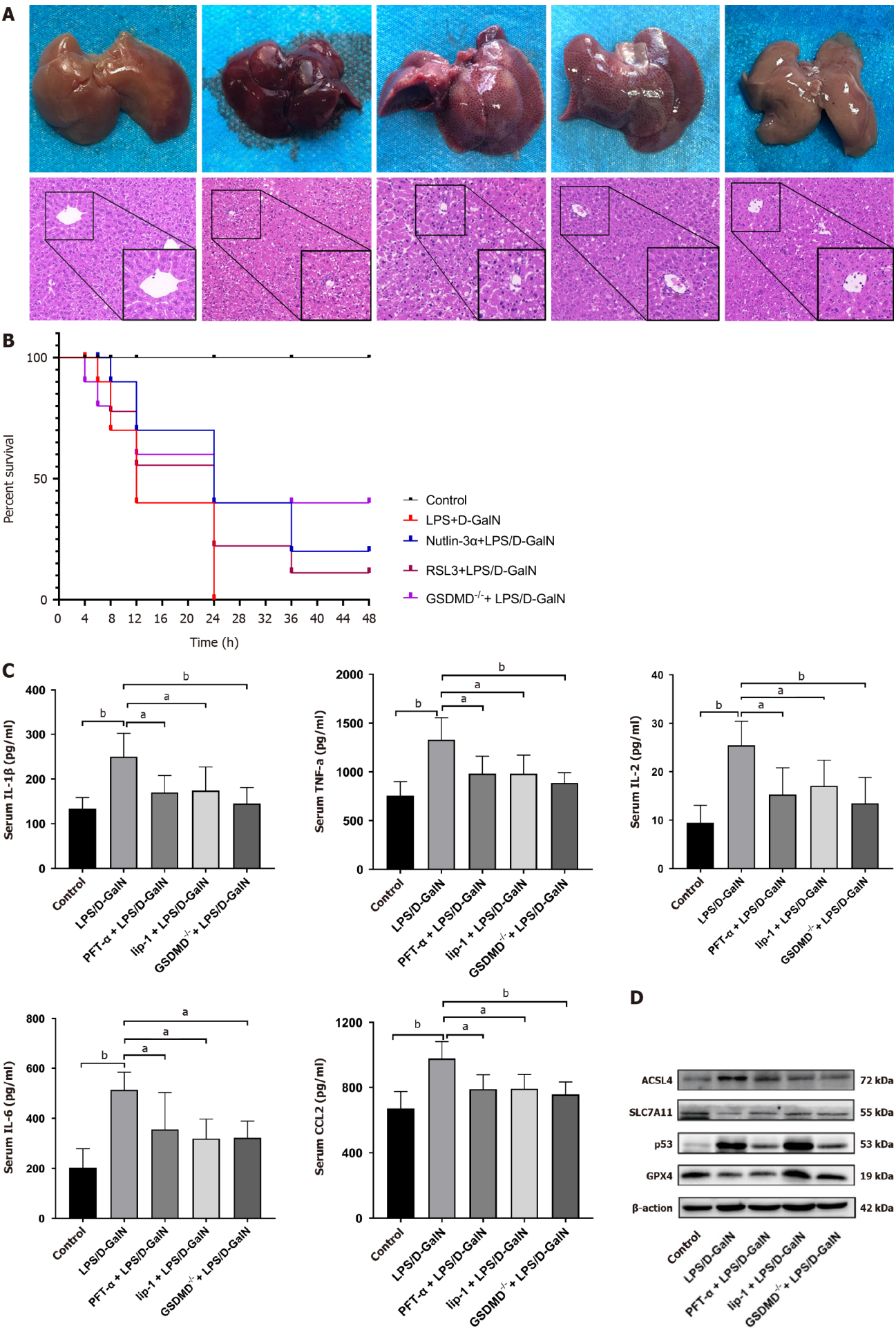
A
B
Percent survival
Time (h)
Control
LPS+D-GalN
Nutlin-3α+LPS/D-GalN
RSL3+LPS/D-GalN
GSDMD-/-+ LPS/D-GalN
C
Serum IL-1β (pg/ml)
Serum TNF-α (pg/ml)
Serum IL-2 (pg/ml)
Serum IL-6 (pg/ml)
Serum CCL2 (pg/ml)
Control
LPS/D-GalN
PFT-α + LPS/D-GalN
Iip-1 + LPS/D-GalN
GSDMD-/- + LPS/D-GalN
D
ACSL4
SLC7A11
p53
GPX4
β-action
72 kDa
55 kDa
53 kDa
19 kDa
42 kDa

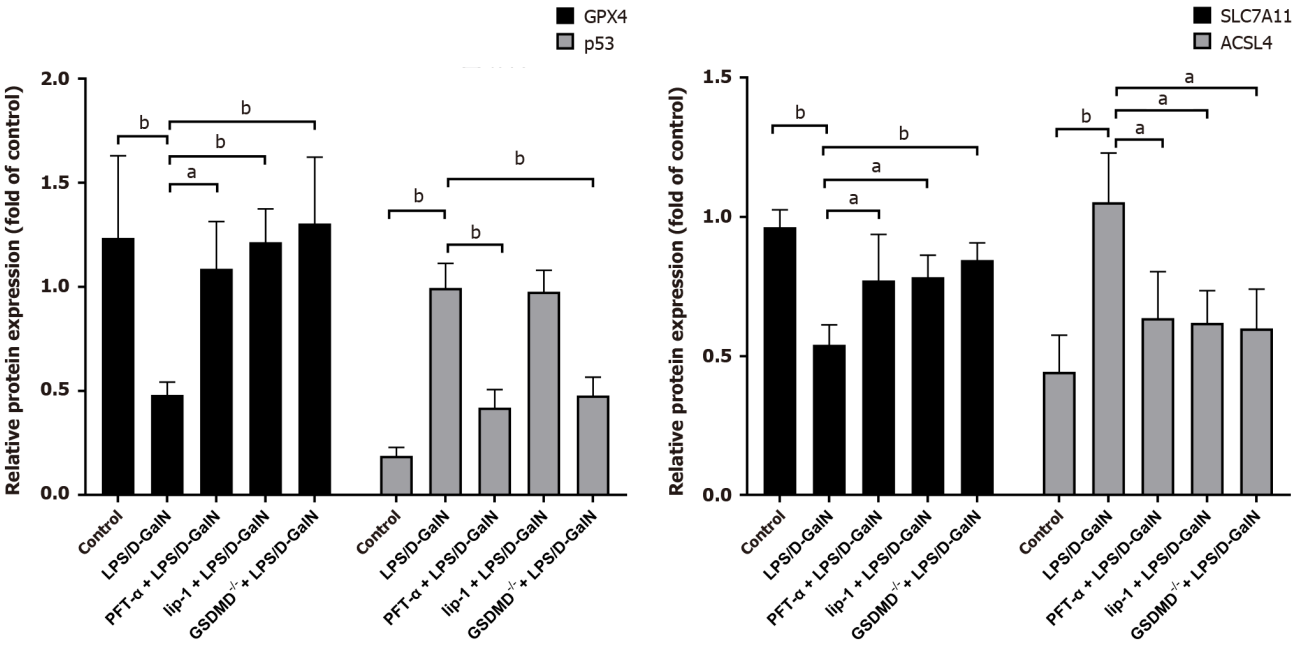
GPX4
p53
Relative protein expression (fold of control)
2.0
1.5
1.0
0.5
0.0
b
a
Control
LPS/D-GalN
PFT-α + LPS/D-GalN
Iip-1 + LPS/D-GalN
GSDMD-/- + LPS/D-GalN
SLC7A11
ACSL4
Relative protein expression (fold of control)
1.5
1.0
0.5
0.0

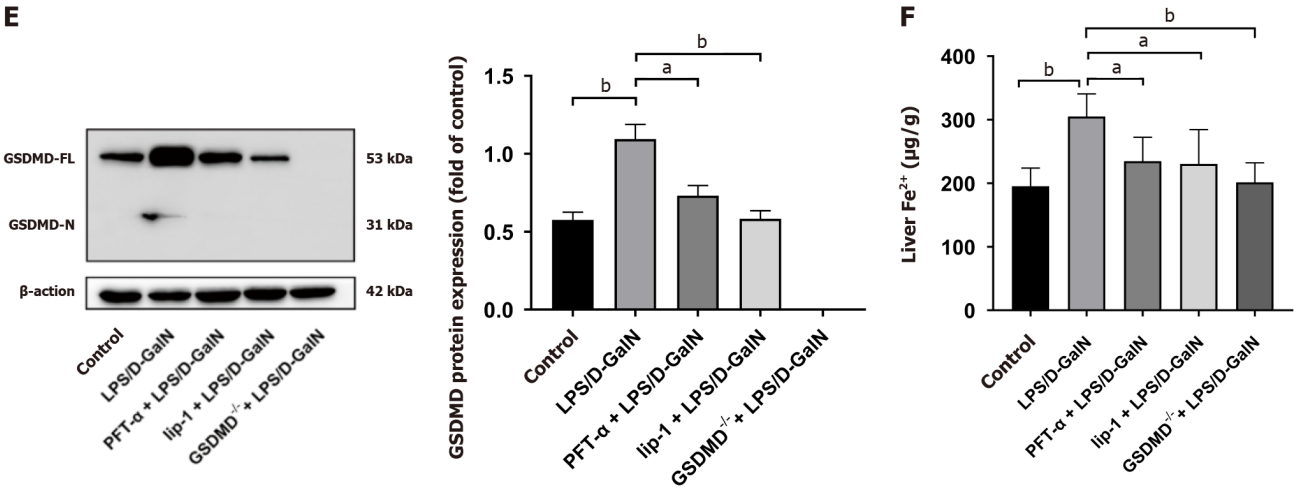
E
GSDMD-FL
GSDMD-N
β-action
53 kDa
31 kDa
42 kDa
GSDMD protein expression (fold of control)
1.5
1.0
0.5
0.0
F
Liver Fe2+ (μg/g)
400
300
200
100
0
Control
LPS/D-GalN
PFT-α + LPS/D-GalN
Iip-1 + LPS/D-GalN
GSDMD-/- + LPS/D-GalN

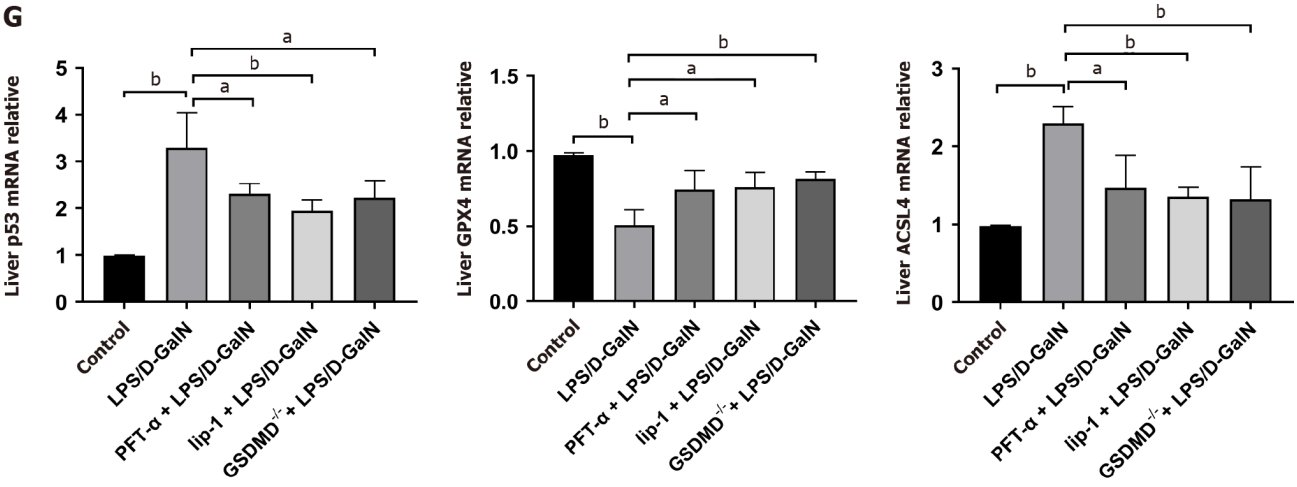
G
Liver p53 mRNA relative
5
4
3
2
1
0
Liver GPX4 mRNA relative
1.5
1.0
0.5
0.0
Liver ACSL4 mRNA relative
3
2
1
0
Control
LPS/D-GalN
PFT-α + LPS/D-GalN
Iip-1 + LPS/D-GalN
GSDMD-/- + LPS/D-GalN

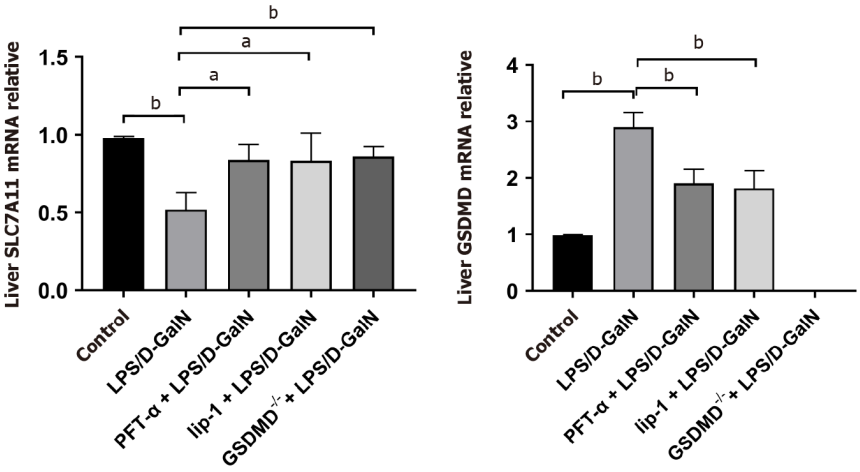

Figure 2 Inhibition of the p53/glutathione peroxidase 4/gasdermin D signaling pathway attenuates acute liver failure *in vivo*. A: Macroscopic examinations of mouse livers and microscopic examinations of liver sections stained with hematoxylin and eosin (100 ×); B: Administration of pifithrin-α and liproxstatin-1 and gasdermin D (GSDMD) knockout improved the median survival in mice treated with D-galactosamine/lipopolysaccharide; C: Detection of interleukin (IL)-1β, tumour necrosis factor alpha, IL-6, IL-2, and C-C motif ligand 2 in mouse serum with multi-factor kit. Data are presented as the mean ± SD of five independent experiments; D: Western blot analyses of p53, glutathione peroxidase 4 (GPX4), solute carrier family 7a member 11, Acyl-CoA synthetase long-chain family member 4 (ACSL4), and GSDMD proteins (n = 3 in each group). Data are presented as the mean ± SD of three independent experiments; E: Western blot analyses of GSDMD protein expression (n = 3 in each group). Data are presented as the mean ± SD of three independent experiments; F: IIron detection with an iron kit. Data are presented as the mean ± SD of five independent experiments; G: Quantitative real-time polymerase chain reaction analyses of p53, GPX4, SLC7A11, ACSL4, and GSDMD mRNA expression (n = 3 in each group). Data are presented as the mean ± SD of three independent experiments. $^{a}P < 0.05$, $^{b}P < 0.01$. ALF: Acute liver failure; AST: Aspartate aminotransferase; ALT: Alanine aminotransferase; IL: Interleukin; GPX4: Glutathione peroxidase 4; SLC7A11: Solute carrier family 7a member 11; ACSL4: Acyl-CoA synthetase long-chain family member 4; GSDMD: Gasdermin D; SIRT1: Silent information regulator sirtuin 1; LPS: Lipopolysaccharide; D-GalN: D-galactosamine.

EX527 exacerbated the inflammatory response (serum IL-1β, TNF-α, IL-6, IL-2, and CCL2 levels in mice), while resveratrol had the opposite effect (Figure 5C). Western blot analysis showed that, in liver tissue of resveratrol-treated mice with ALF, SIRT1 activation increased p53 acetylation, with no significant changes in p53 protein levels (Figure 5D). When SIRT1 was inhibited, GPX4 and SLC7A11 expression was decreased and ACSL4 expression was upregulated (Figure 5E). GSDMD and GSDMD-N expression was increased, especially GSDMD-N (Figure 6A), and iron accumulation was enhanced (Figure 6B). We found that resveratrol, as a SIRT1 inducer, increased SIRT1 expression. In contrast, EX527 decreased SIRT1 level (Figure 6C and D). We further performed immunofluorescence experiments, which showed no significant change in p53 protein expression in the resveratrol or EX527 treatment groups compared with the ALF model group (Figure 6E and F), which is consistent with our results mentioned above (Figure 5D). Overall, these data demonstrate that SIRT1 exerts protection against ALF by inhibiting p53 deacetylation, thereby inhibiting the GPX4/GSDMD signaling pathway.

SIRT1 attenuates hepatocyte ferroptosis and pyroptosis via a p53/GPX4/GSDMD-dependent mechanism

To further investigate the functional role of SIRT1 in hepatocyte ferroptosis and pyroptosis, we knocked down and overexpressed SIRT1 in HL7702 cells. ALT and AST levels were lower in the SIRT1 overexpression group and higher in the SIRT1 knockdown group than in the ALF model and knockdown groups (Figure 7A and B). Ferroptotic events (elevation of ROS activity and iron accumulation) were detected in the SIRT1 overexpression group (Figure 7C and D). Western blot analysis showed that Ac-p53 protein levels were significantly decreased in the SIRT1 overexpression group, while p53 did not change (Figure 7E). We next examined ferroptosis- and pyroptosis-related proteins (GPX4, SLC7A11, ACSL4, and GSDMD). We found that upregulation of SIRT1 increased GPX4 and SLC7A11 protein expression and decreased ACSL4 and GSDMD protein expression (Figure 7F and G). Furthermore, knockdown of SIRT1 inhibited the deacetylation and degradation of p53 and downregulated the levels of SLC7A11 and GPX4 (Figure 7F and G). These data show that SIRT1 overexpression alleviated ALF in HL7702 cells *via* a p53/GPX4/GSDMD-dependent mechanism.

DISCUSSION

ALF is a life-threatening disease with high morbidity and mortality rates. The most effective treatment for ALF at present is liver transplantation[23]. However, liver transplants are not widely available because of the lack of donors and the high cost of medical care[18]. ALF is characterized by extensive hepatocellular cell death, leading to massive loss of parenchymal cells, with the release of cell contents, cell swelling, and inflammation. Emerging evidence has indicated that ferroptosis and pyroptosis, two newly identified forms of non-apoptotic cell death, play a crucial role in liver disease[24, 25], but their precise role in ALF is unknown. In this study, we provided evidence that ferroptosis and pyroptosis occurred in ALF and established an association between them. We found that SIRT1 activation or inhibition of the p53/

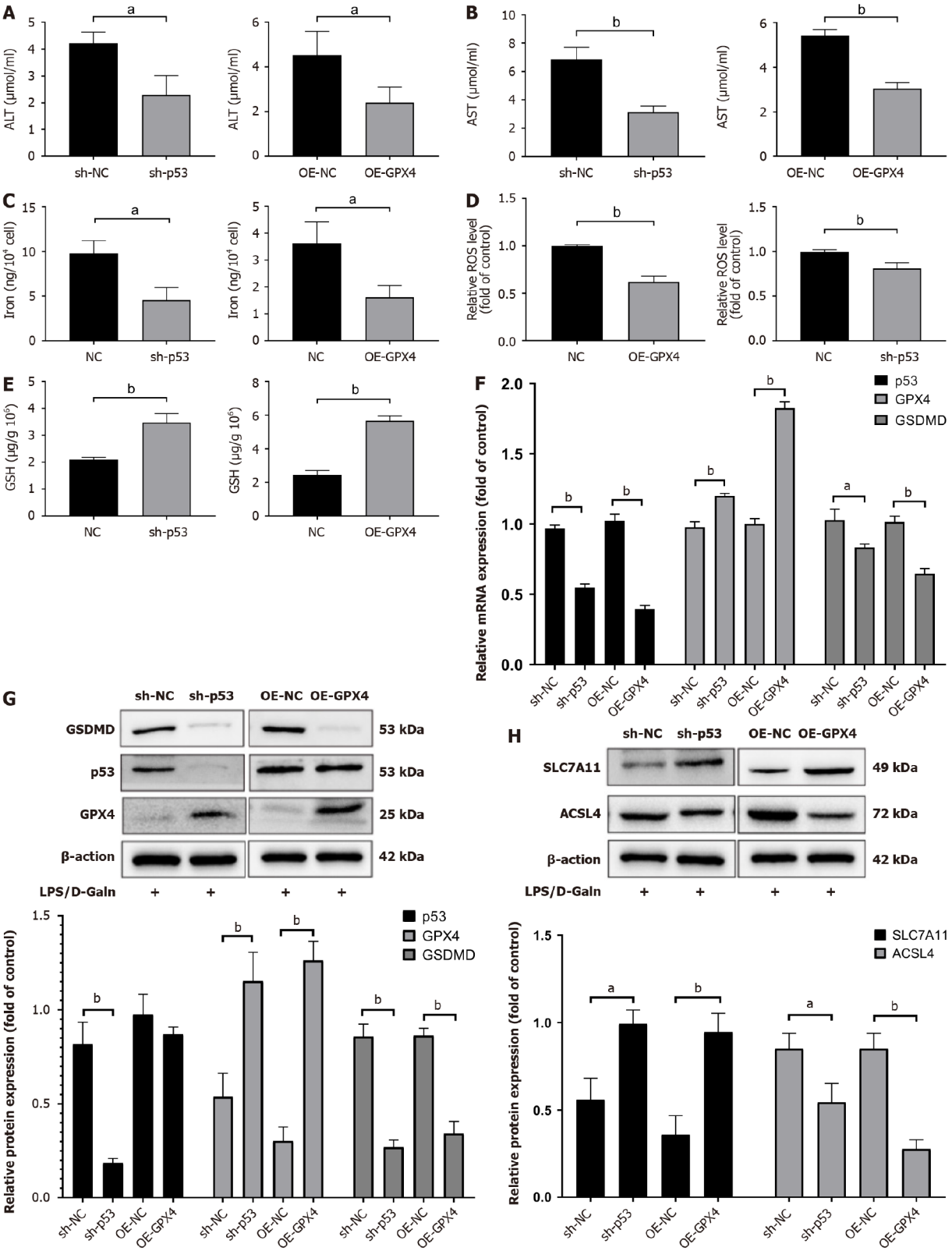

Figure 3 Inhibition of the p53/glutathione peroxidase 4/gasdermin D signaling pathway exacerbates acute liver injury *in vitro*. A and B: The levels of alanine aminotransferase and aspartate aminotransferase were changed in HL7702 cells (n = 3); C-E: The levels of iron, reactive oxygen species, and glutathione were changed in HL7702 cells (n = 3); F: Quantitative real-time polymerase chain reaction analyses of p53, glutathione peroxidase 4 (GPX4), solute carrier family 7a member 11 (SLC7A11), Acyl-CoA synthetase long-chain family member 4 (ACSL4), and gasdermin D (GSDMD) mRNA expression (n = 3 in each group); G: Western blot analyses of p53, GPX4, and GSDMD protein expression (n = 3 in each group); H: Western blot analyses of SLC7A11 and ACSL4 protein expression (n = 3 in each group). $^{a}P < 0.05$, $^{b}P < 0.01$. ALF: Acute liver failure; AST: Aspartate aminotransferase; ALT: Alanine aminotransferase; IL: Interleukin; GPX4: Glutathione peroxidase 4; SLC7A11: Solute carrier family 7a member 11; ACSL4: Acyl-CoA synthetase long-chain family member 4; GSDMD: Gasdermin D; SIRT1: Silent information regulator sirtuin 1; LPS: Lipopolysaccharide; D-GalN: D-galactosamine.

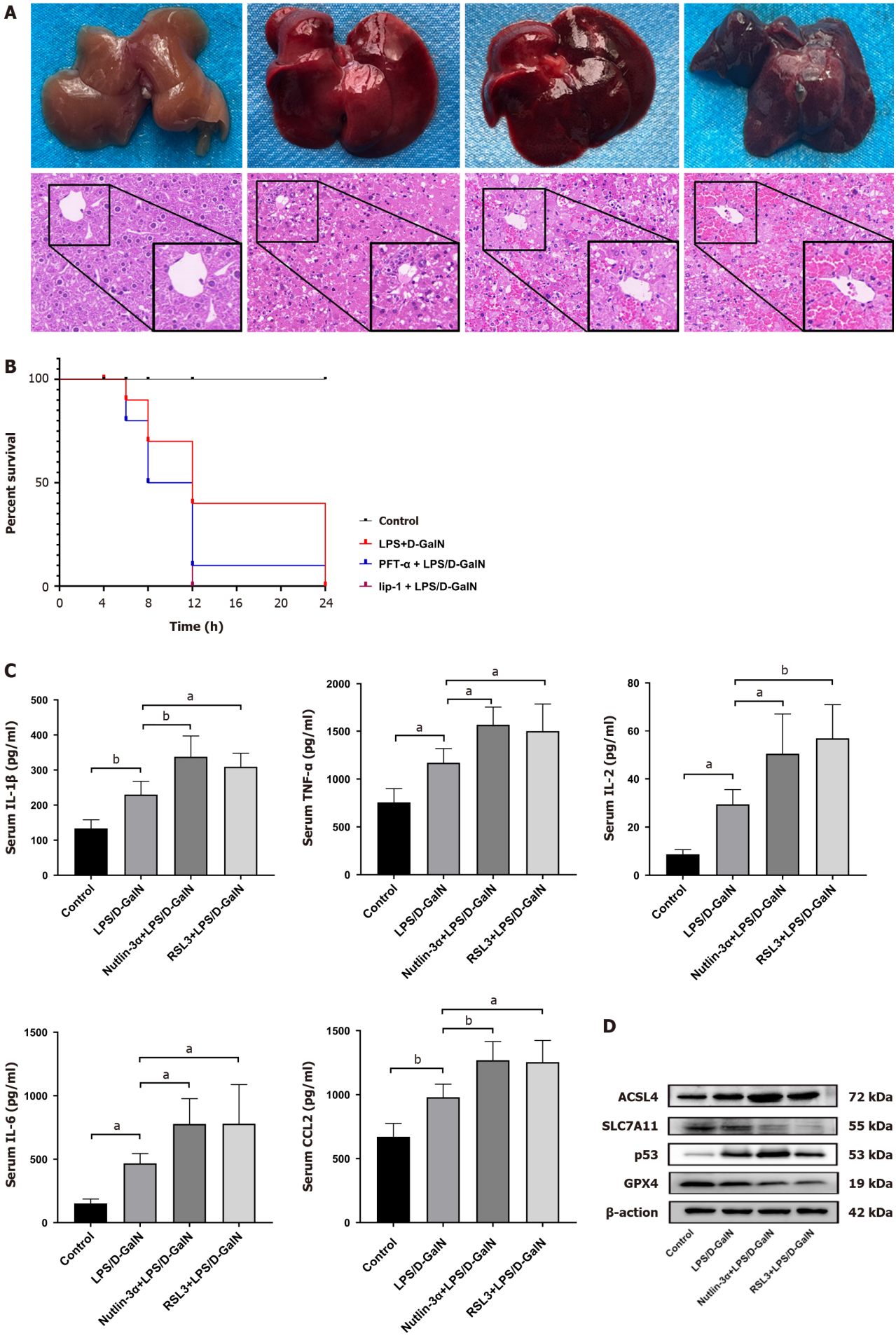
A
B
Percent survival
100
50
0
0
4
8
12
16
20
24
Time (h)
Control
LPS+D-GalN
PFT-α + LPS/D-GalN
lip-1 + LPS/D-GalN
C
Serum IL-1β (pg/ml)
Serum TNF-α (pg/ml)
Serum IL-2 (pg/ml)
Serum IL-6 (pg/ml)
Serum CCL2 (pg/ml)
Control
LPS/D-GalN
Nutlin-3α+LPS/D-GalN
RSL3+LPS/D-GalN
a
b
D
ACSL4
SLC7A11
p53
GPX4
β-action
72 kDa
55 kDa
53 kDa
19 kDa
42 kDa

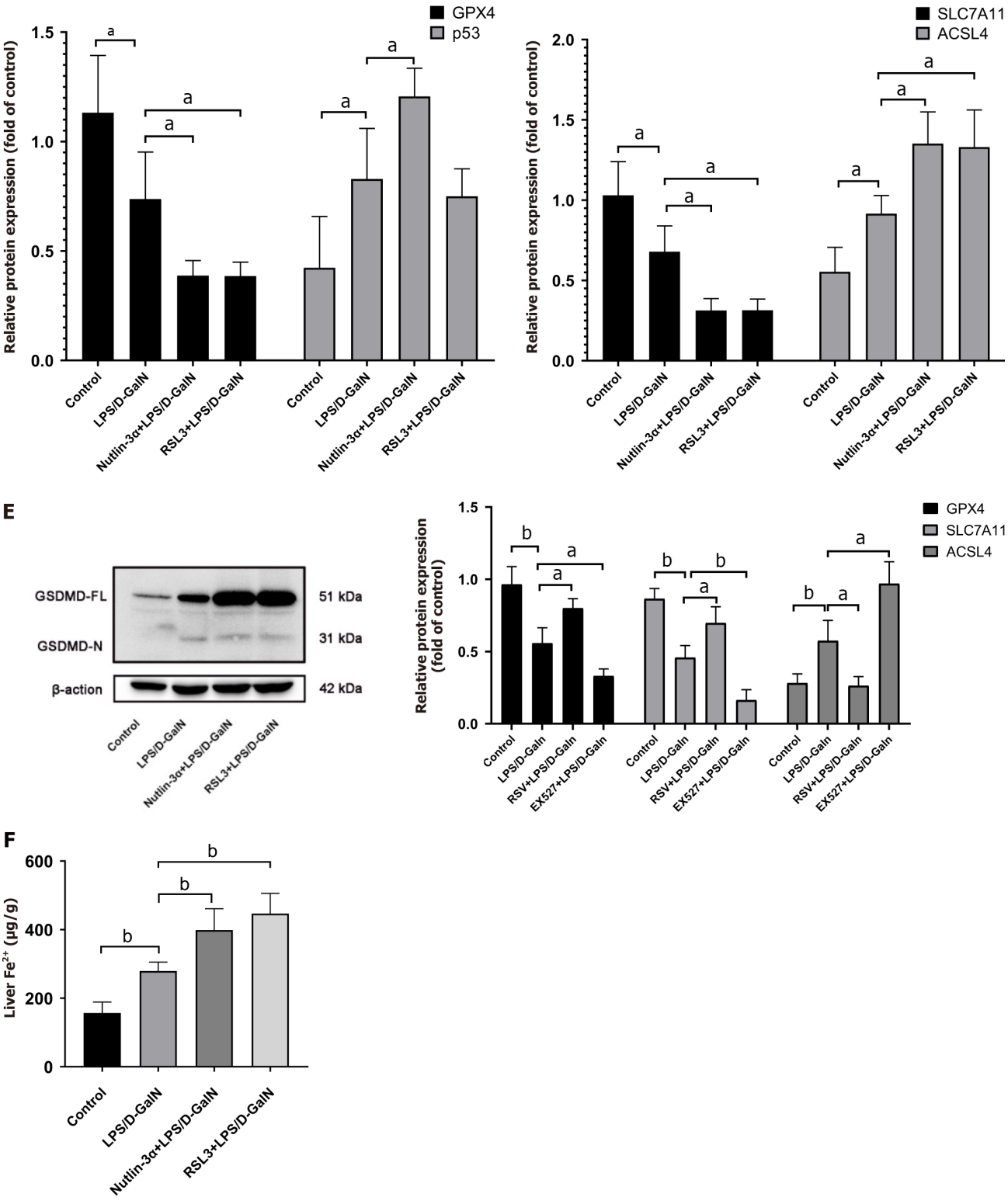

Figure 4 Activation of the p53/glutathione peroxidase 4/gasdermin D signaling pathway exacerbates alanine aminotransferase. A: Macroscopic examinations of mouse livers and microscopic examinations of liver sections stained with hematoxylin and eosin (100 ×); B: Administration of nutlin-3α and RAS-selective lethal 3 shortened the survival time of mice treated with lipopolysaccharide/D-galactosamine; C: Detection of interleukin (IL)-1β, tumour necrosis factor alpha, IL-6, IL-2, and C-C motif ligand 2 in mouse serum with multi-factor kit; D: Western blot analyses of p53, glutathione peroxidase 4, solute carrier family 7a member 11, acyl-CoA synthetase long-chain family member 4, and gasdermin D (GSDMD) protein expression (n = 3 in each group); E: Western blot analyses of GSDMD protein expression (n = 3 in each group); F: Iron detection with an iron kit. $^{a}P < 0.05$, $^{b}P < 0.01$. ALF: Acute liver failure; AST: Aspartate aminotransferase; ALT: Alanine aminotransferase; IL: Interleukin; GPX4: Glutathione peroxidase 4; SLC7A11: Solute carrier family 7a member 11; ACSL4: Acyl-CoA synthetase long-chain family member 4; GSDMD: Gasdermin D; SIRT1: Silent information regulator sirtuin 1; LPS: Lipopolysaccharide; D-GalN: D-galactosamine; RSL3: RAS-selective lethal 3.

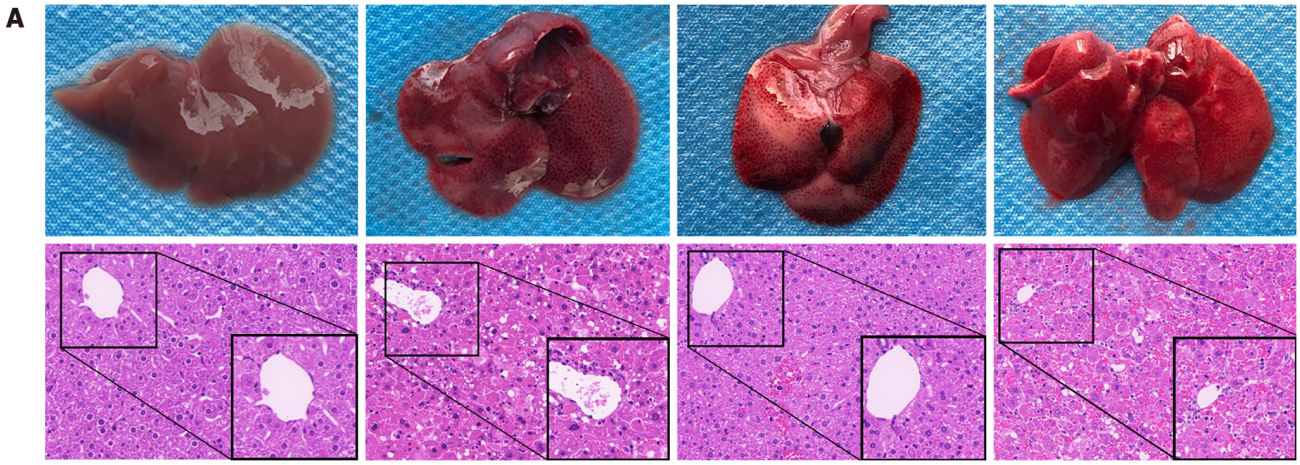
A

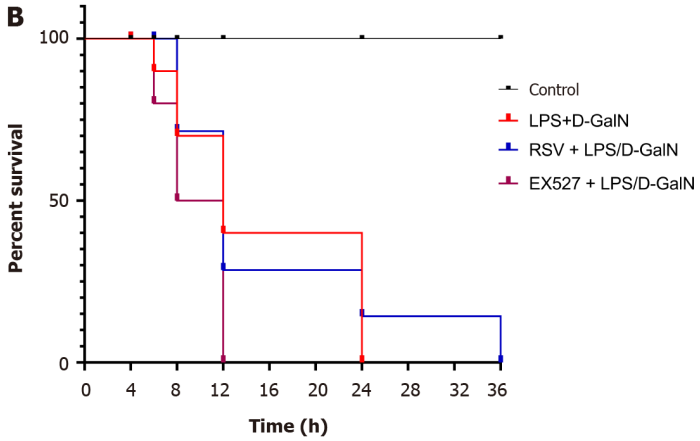
B
Percent survival
Time (h)
Control
LPS+D-GalN
RSV + LPS/D-GalN
EX527 + LPS/D-GalN

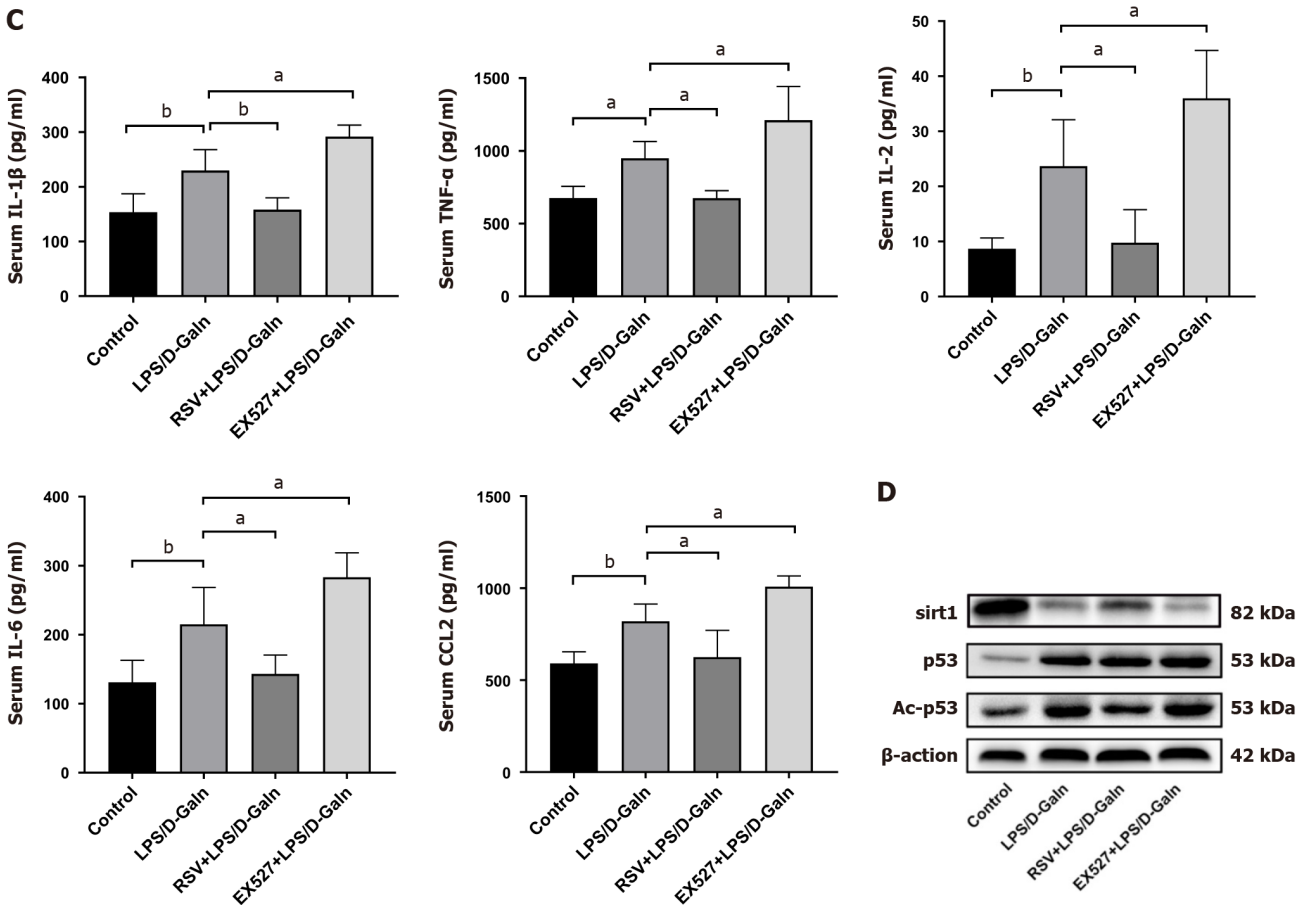
C
Serum IL-1β (pg/ml)
Serum TNF-α (pg/ml)
Serum IL-2 (pg/ml)
Serum IL-6 (pg/ml)
Serum CCL2 (pg/ml)
Control
LPS/D-GalN
RSV+LPS/D-GalN
EX527+LPS/D-GalN
D
sirt1
p53
Ac-p53
β-action
82 kDa
53 kDa
53 kDa
42 kDa

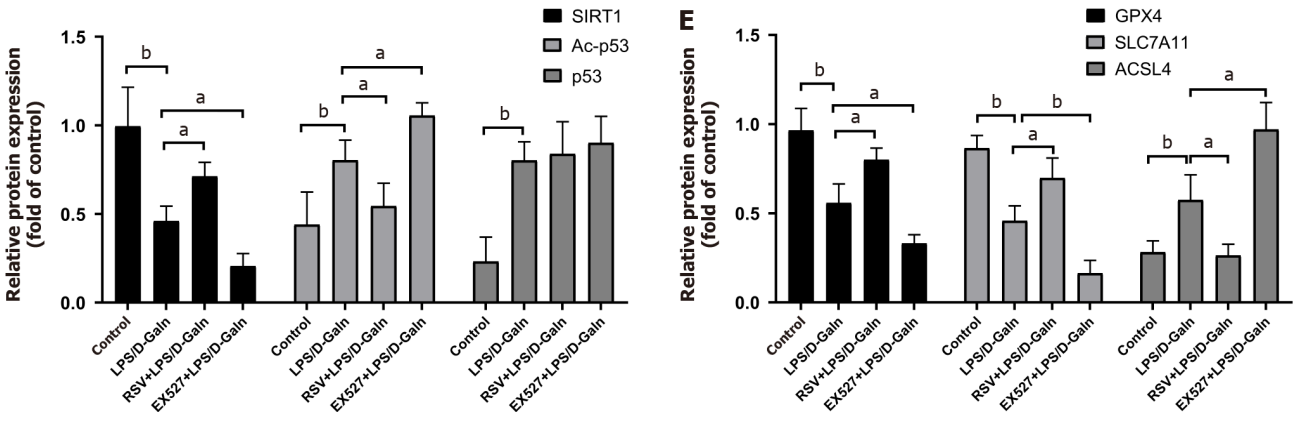

Figure 5 Silent information regulator sirtuin 1 interdicts the glutathione peroxidase 4/gasdermin D signaling pathway by intercepting p53 deacetylation. A: Macroscopic examinations of mouse livers and microscopic examinations of liver sections stained with hematoxylin and eosin (100 ×); B: Survival time of mice after resveratrol and EX527 treatments; C: Multi-factor kit for the Detection of interleukin (IL)-1β, tumour necrosis factor alpha, IL-6, IL-2, and C-C motif ligand 2 in mouse serum with multi-factor kit; D and E: Western blot analyses of silent information regulator sirtuin 1, acetylated p53, p53, glutathione peroxidase 4, solute carrier family 7a member 11, and Acyl-CoA synthetase long-chain family member 4 protein expression (n = 3 in each group). $^{a}P < 0.05$, $^{b}P < 0.01$. ALF: Acute liver failure; AST: Aspartate aminotransferase; ALT: Alanine aminotransferase; IL: Interleukin; GPX4: Glutathione peroxidase 4; SLC7A11: Solute carrier family 7a member 11; ACSL4: Acyl-CoA synthetase long-chain family member 4; GSDMD: Gasdermin D; SIRT1: Silent information regulator sirtuin 1; LPS: Lipopolysaccharide; D-GalN: D-galactosamine; RSL3: RAS-selective lethal 3; RSV: Resveratrol.

GPX4/GSDMD signaling pathway attenuated LPS/D-GalN-induced ferroptosis and pyroptosis in ALF (Figure 8).

In this study, we found that the activity of the enzymatic biomarkers ALT and AST was markedly increased in human ALF, accompanied by elevated inflammatory factors, such as TNF-α, IL-1β, and IL-6. Furthermore, we found that the ferroptosis-related antioxidant proteins GPX4 and SLC7A11 were reduced and iron deposition was aggravated. Additionally, GSDMD expression was increased.

The pathogenesis of ALF induced by LPS/D-GalN in mice is similar to that of fulminant hepatitis in humans[26,27]. Only some evidence has indicated that ferroptosis and pyroptosis occur in LPS/D-GalN-induced ALF, and inhibition of ferroptosis and pyroptosis attenuates ALF[28,29]. However, the association between ferroptosis and pyroptosis is unclear.

GPX4 and GSDMD play a prominent role in the occurrence of ferroptosis and pyroptosis. GSH biosynthesis and proper functioning of GPX4 are critical for inhibiting ferroptosis, and conditions that culminate in GPX4 inhibition/destabilization sensitize cells to ferroptosis or even trigger ferroptotic cell death[19,21,30]. GSDMD, a mediator of pyroptosis, is cleaved by inflammasome-activated caspase-1 and LPS-activated caspase-11/4/5 into active GSDMD-N and inactive GSDMD-C. Deletion of GSDMD completely abolishes cell pyroptosis[31,32]. An increasing number of studies have suggested that there is an interaction between ferroptosis and pyroptosis. The knockout of caspase-11, which is involved in the non-classical pathway of pyroptotic cell death, in myeloid cells conferred similar protection in septic myeloid cell–specific GPX4-knockout mice, which were susceptible to lethal infection[33]. The caspase-1-dependent NLRP3 inflammasome was also inhibited by GPX4, indicating that GPX4 has a broad role in inhibiting pyroptosis[33]. However, the association between ferroptosis and pyroptosis in ALF is unclear. The present study provided evidence that bridged the gap between ferroptosis and pyroptosis, and showed that blocking the p53/GPX4/GSDMD pathway regulated ferroptosis and pyroptosis in ALF. Inhibiting p53 and enhancing GPX4 in ALF model mice with drugs reduced AST and ALT levels and inflammatory reactions compared with the ALF model group, and ferroptotic events (depletion of GPX4, GSH, and SLC7A11, and iron accumulation) were reversed. Additionally, GSDMD-N protein levels were significantly decreased, consistent with the immunofluorescence results (Supplementary Figure 1). Notably, deletion of GSDMD decreased p53 expression and upregulated GPX4, which indicated crosstalk between ferroptosis and pyroptosis. The knockdown of GPX4 increased AST and ALT levels, accompanied by significantly increased ferroptotic markers and GSDMD (Supplementary Figure 2). Together, these results suggested that blocking the p53/GPX4/GSDMD signaling pathway alleviated ferroptosis and pyroptosis in ALF, and a positive feedback loop may exist.

In our study, we found that increased or decreased GPX4 mRNA or protein expression did not affect p53, but it acted indirectly by regulating GSDMD, suggesting that GPX4 is a downstream regulator of p53. Chen *et al*[34] reported that p53 levels were unaffected by the loss of ACSL4 and GPX4, and p53-driven ferroptosis was induced in a GPX4-independent manner. Nevertheless, enhancement of GPX4 reduced p53 transcription, which was inconsistent with the Western blot results. This difference between mRNA and protein levels suggests that post-transcriptional regulation, translational efficiency, and post-translational modifications alter protein levels. One possible explanation for this difference is that reduced translational efficiency may be compensated for by increased transcriptional activity[35]. However, the mechanism underlying the differences in transcription and translation of p53 is unclear.

SIRT1 has been widely reported to play a protective role in various biological processes including nutrient starvation, DNA repair, aging, oxidative stress, and the inflammatory response[36,37]. One study suggested that negative regulation of SIRT1 increased pyroptosis (GSDMD) and aggravated the acute hepatic pro-inflammatory reaction[38]. This finding is consistent with another study, which showed that SIRT1 was suppressed in APAP-induced hepatotoxicity[39]. Treatment with resveratrol, a small-molecule SIRT1 activator, shows a protective effect in mouse liver ischemia–reperfusion injury [40,41]. Similarly, in our study, we found that SIRT1 was decreased and p53 and Ac-p53 were increased in human ALF.

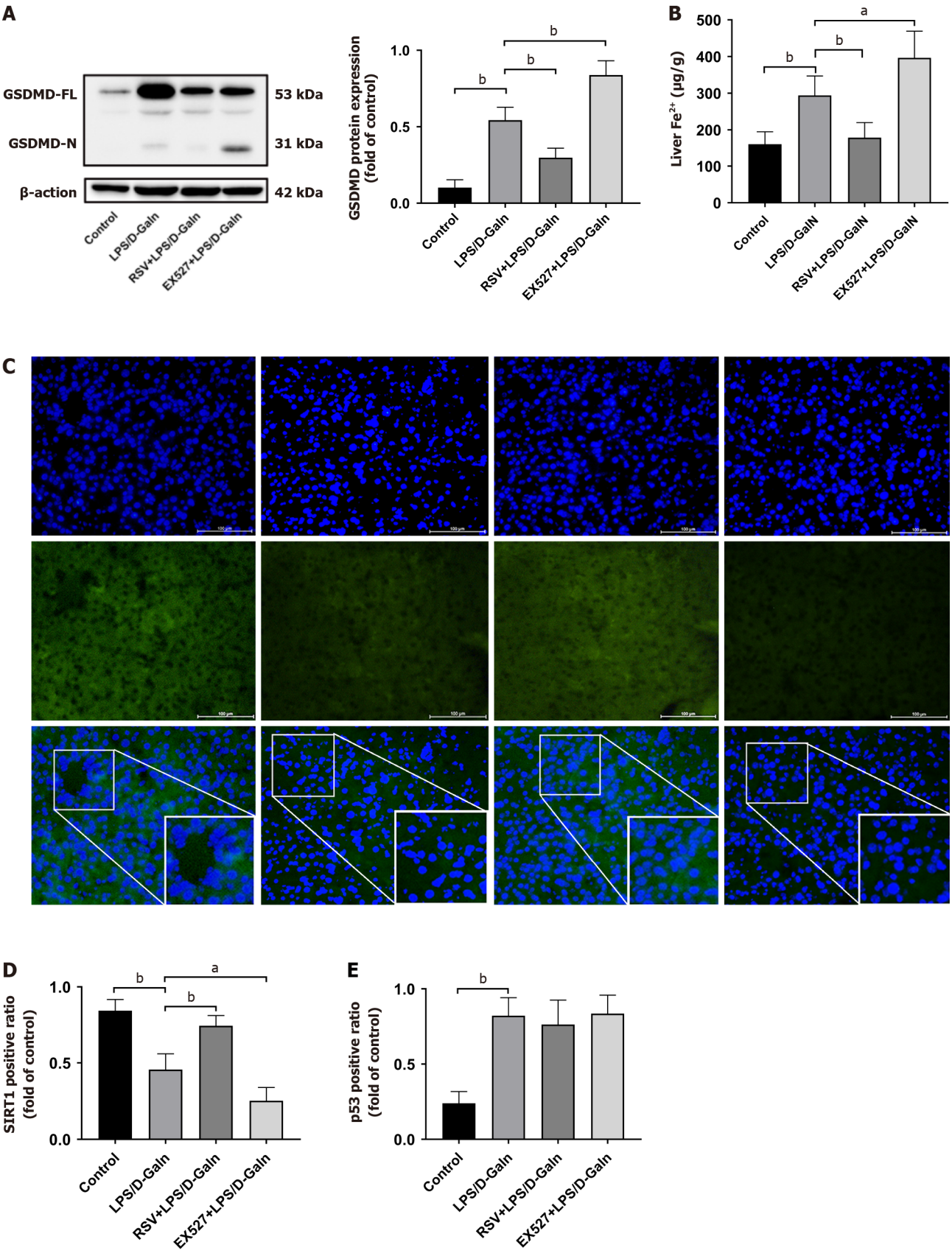
A
GSDMD-FL
GSDMD-N
β-action
53 kDa
31 kDa
42 kDa
Control
LPS/D-GalN
RSV+LPS/D-GalN
EX527+LPS/D-GalN
GSDMD protein expression (fold of control)
B
Liver Fe2+ (μg/g)
C
D
SIRT1 positive ratio (fold of control)
E
p53 positive ratio (fold of control)

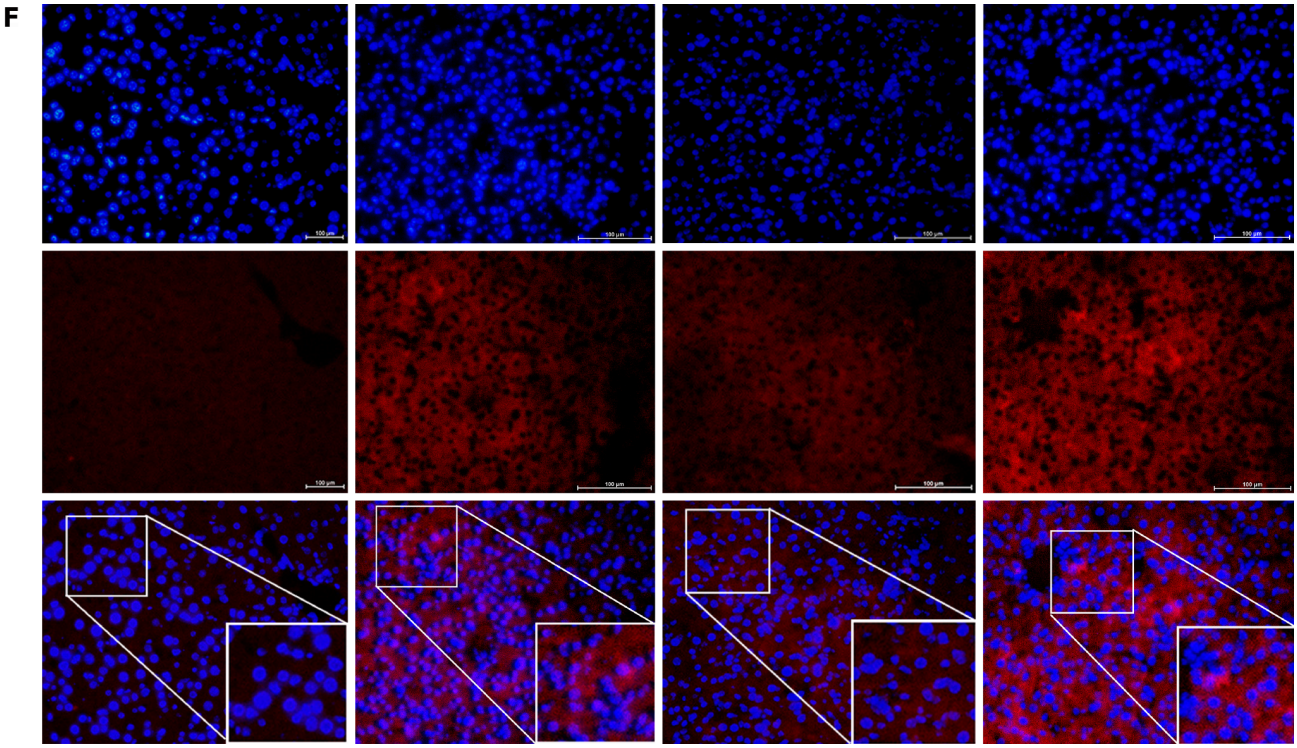

Figure 6 Silent information regulator sirtuin 1 interdicts the glutathione peroxidase 4/gasdermin D signaling pathway by intercepting p53 deacetylation. A: Western blot analyse of gasdermin D protein expression (n = 3 in each group); B: Iron detection with an iron kit; C: Silent information regulator sirtuin 1 (SIRT1) expression in liver tissue measured by immunofluorescence (100 ×); D: Percentage of SIRT1 immunofluorescence area; E: Percentage of p53 immunofluorescence area; F: p53 expression in liver tissue measured by immunofluorescence (100 ×). Data are presented as the mean ± SD of five independent experiments. $^{a}P < 0.05$, $^{b}P < 0.01$. ALF: Acute liver failure; AST: Aspartate aminotransferase; ALT: Alanine aminotransferase; IL: Interleukin; GPX4: Glutathione peroxidase 4; SLC7A11: Solute carrier family 7a member 11; ACSL4: Acyl-CoA synthetase long-chain family member 4; GSDMD: Gasdermin D; SIRT1: Silent information regulator sirtuin 1; LPS: Lipopolysaccharide; D-GalN: D-galactosamine; RSL3: RAS-selective lethal 3; RSV: Resveratrol.

SIRT1 is an NAD-dependent deacetylase that directly deacetylates p53 and mediates its function[37]. A study showed that SIRT1 overexpression abolished p53 acetylation levels and reduced the release of hepatic enzymes, hepatic oxidative, stress, and inflammation in non-alcoholic fatty liver disease[42]. Ma *et al*[43] demonstrated that SIRT1 inhibited ferroptosis-induced myocardial cell death through the p53/SLC7A11 axis in myocardial ischemia–reperfusion injury. Nevertheless, whether SIRT1 activation regulates p53 deacetylation to affect ferroptosis in ALF has not been shown. Our study showed that SIRT1 activation attenuated liver injury and the inflammatory response, accompanied by a reduction in ferroptosis and pyroptosis-related proteins in ALF. We demonstrated that SIRT1 activation inhibited p53/GPX4/GSDMD by inducing p53 acetylation, which attenuated LPS/D-GalN-induced ALF.

CONCLUSION

In conclusion, our study provides evidence that ferroptosis and pyroptosis are crucial modes of hepatocyte death in ALF, and the interactions between these modes of cell death advance the progression of ALF. SIRT1 plays an important role in ALF through p53/GPX4/GSDMD-mediated ferroptosis and pyroptosis. These results could provide new therapeutic targets to alleviate ALF. However, there are still many issues that need to be further investigated. First, p53 is a versatile protein with multiple roles in promoting physiological and pathological regulation. Although p53 can promote ferroptosis, it is also involved in several major functions, such as cell cycle arrest, DNA repair, angiogenesis, metastasis, and senescence. When p53 pro-death function is inhibited, its pro-survival function is concomitantly impaired. Therefore, how the unique p53-mediated pro-death function might be achieved is unclear. Second, our research was only limited to cellular and mouse models and has not been applied to clinical studies. Although we found decreased SIRT1 expression in human ALF liver tissue, whether an SIRT1 activator is effective for acute liver injury and failure in patients is unknown, and further safety and efficacy studies are required. Third, the mechanism of ALF may be associated with multiple modes of cell death, but our study was limited to ferroptosis and pyroptosis, and was not designed to examine other modes of death. The focus of our next study will be to further investigate the mechanism of ALF in depth.

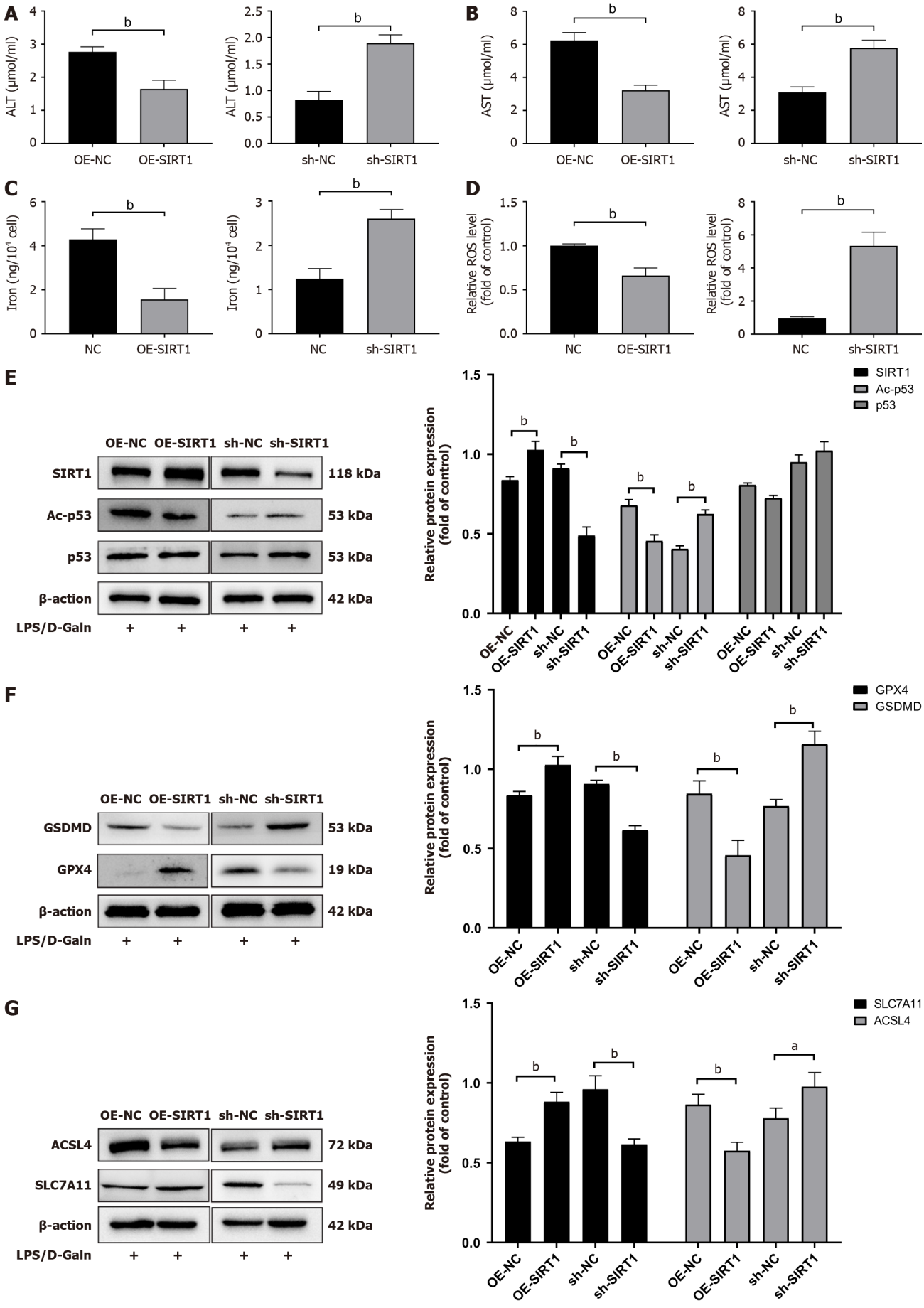

Figure 7 Silent information regulator sirtuin 1 attenuates hepatocyte ferroptosis and pyroptosis *via* a p53/glutathione peroxidase

4/gasdermin D dependent mechanism *in vitro*. A and B: The levels of aspartate aminotransferase and alanine aminotransferase were changed in serum samples of HL7702 cells (n = 3); C and D: The levels of iron and reactive oxygen species were changed in HL7702 cells (n = 3); E: Western blot analyses of silent information regulator sirtuin 1, p53, and acetylated p53 protein expression (n = 3 in each group); F: Western blot analyses of gasdermin D and glutathione peroxidase 4 protein expression (n = 3 in each group); G: Western blot analyses of solute carrier family 7a member 11 and Acyl-CoA synthetase long-chain family member 4 protein expression (n = 3 in each group). $^{a}P < 0.05$, $^{b}P < 0.01$. ALF: Acute liver failure; AST: Aspartate aminotransferase; ALT: Alanine aminotransferase; IL: Interleukin; GPX4: Glutathione peroxidase 4; SLC7A11: Solute carrier family 7a member 11; ACSL4: Acyl-CoA synthetase long-chain family member 4; GSDMD: Gasdermin D; SIRT1: Silent information regulator sirtuin 1; LPS: Lipopolysaccharide; D-GalN: D-galactosamine; RSL3: RAS-selective lethal 3; ROS: Reactive oxygen species.

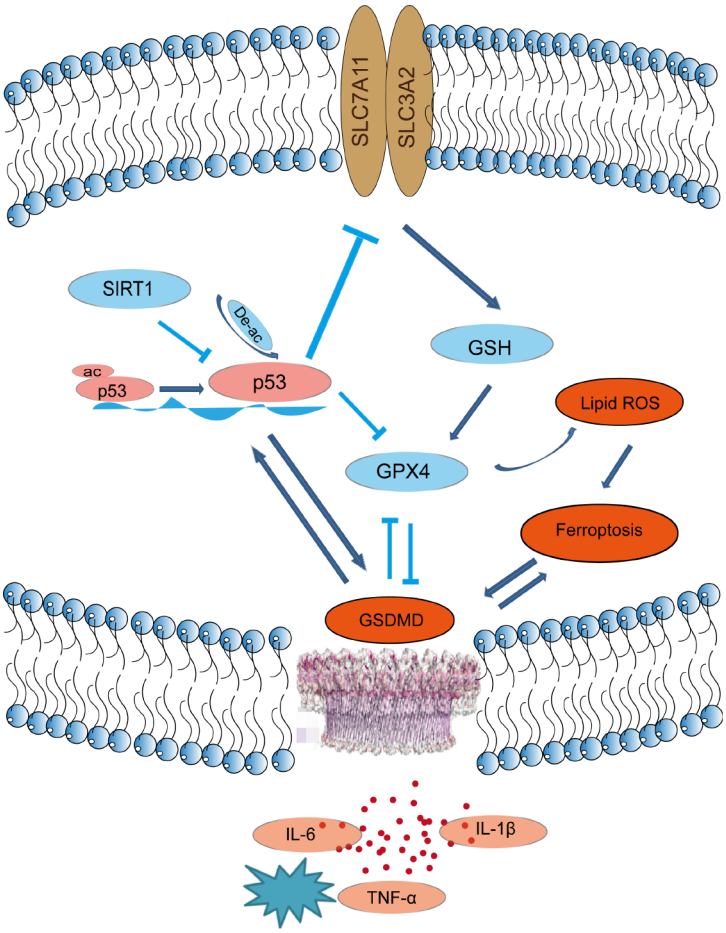

Figure 8 Silent information regulator sirtuin 1 activation ameliorates lipopolysaccharide/D-galactosamine-induced acute liver failure by inhibiting p53/glutathione peroxidase 4/gasdermin D to reduce ferroptosis and pyroptosis. Silent information regulator sirtuin 1 activation inhibits p53 deacetylation, thereby inhibiting the glutathione peroxidase 4 (GPX4)/gasdermin D (GSDMD) signaling pathway and reducing inflammatory response and iron deposition. Blocking the p53/GPX4/GSDMD signaling pathway attenuates ferroptosis and pyroptosis in acute liver failure. IL: Interleukin; GPX4: Glutathione peroxidase 4; SLC7A11: Solute carrier family 7a member 11; GSDMD: Gasdermin D; SIRT1: Silent information regulator sirtuin 1; ROS: Reactive oxygen species; GSH: Glutathione; TNF-α: Tumour necrosis factor alpha.

ARTICLE HIGHLIGHTS

Research background

Acute liver failure (ALF) has a high mortality with widespread hepatocyte death involving ferroptosis and pyroptosis, but their precise role in ALF is unknown. Silent information regulator sirtuin 1 (SIRT1)-mediated deacetylation influences multiple biological processes, including cellular senescence, apoptosis, sugar and lipid metabolism, oxidative stress, and inflammation. In this study, we examined the link between ferroptosis and pyroptosis and the upstream regulatory mechanisms.

Research motivation

The most effective treatment for ALF at present is liver transplantation. However, liver transplants are not widely available because of the lack of donors and the high cost of medical care. Therefore, therapies for ALF are imminent.

Research objectives
To explore the link between ferroptosis and pyroptosis and the upstream regulatory mechanisms.

Research methods
Animal and cellular models of ALF were developed. The levels of aspartate aminotransferase (AST) and alanine aminotransferase (ALT) were tested with automatic biochemistry instrument. Iron, reactive oxygen species, and glutathione levels were measured using commercial kits. SIRT1, p53, acetylated p53 (Ac-p53), glutathione peroxidase 4 (GPX4), gasdermin D (GSDMD), solute carrier family 7a member 11 (SLC7A11), and acyl-CoA synthetase long-chain family member 4 (ACSL4) protein expression levels were measured through Western blot analysis.

Research results
AST and ALT levels were elevated in the serum of ALF patients. SIRT1, SLC7A11, and GPX4 expressions were decreased and Ac-p53, p53, GSDMD, and ACSL4 levels were elevated in human ALF liver tissue. In p53 and ferroptosis inhibitor–treated and GSDMD$^{-/-}$ groups, serum interleukin (IL)-1β, tumour necrosis factor alpha, IL-6, IL-2, and C-C motif ligand 2 levels were decreased and hepatic impairment was mitigated. In mice with GSDMD knockout, p53 was reduced, GPX4 was increased, and ferroptotic events (depletion of SLC7A11, elevation of ACSL4, and iron accumulation) were detected.

Research conclusions
SIRT1 activation attenuates lipopolysaccharide/D-galactosamine-induced ferroptosis and pyroptosis by inhibiting the p53/GPX4/GSDMD signaling pathway in ALF.

Research perspectives
Our research is only limited to cellular and mouse models and has not been applied to clinical studies. Although we found decreased SIRT1 expression in human ALF liver tissue, whether SIRT1 activator is effective for acute liver injury and failure in patients is unknown, and further safety and efficacy studies are required.

ACKNOWLEDGEMENTS

We thank Ellen Knapp, PhD, for editing the English text of a draft of this manuscript.

FOOTNOTES

Co-first authors: Xing-Nian Zhou and Quan Zhang.

Co-corresponding authors: Hong Li and Xin-Hua Luo.

Author contributions: Li H and Luo XH designed the study; Zhou XN, Zhang Q, Peng H, Qin YJ, and Liu YH were involved in the data collection; Zhou XN, Qin YJ, and Liu YH analyzed the data; Zhou XN, Zhang Q, Luo XH, and Li H drafted the manuscript; all authors were involved in the critical review of the results and have contributed to, read, and approved the final manuscript. Zhou XN and Zhang Q contributed equally to this work as co-first authors. The reasons for designating Zhou XN and Zhang Q as co-first authors are threefold. First, the research was performed as a collaborative effort, and the designation of co-first authors authorship accurately reflects the distribution of responsibilities and burdens associated with the time and effort required to complete the study and the resultant paper. Zhou XN and Zhang Q co-designed this study and worked together to explore the feasibility, innovativeness, and scientific validity of this study. Second, Zhou XN and Zhang Q worked together to complete the cell and animal parts of this study. In the process of the study, we encountered heavy problems, but we did not abandon each other or give up the study, but inspired and promoted each other. Without each other, we would not have been able to complete the study successfully. Third, Zhou XN and Zhang Q wrote the paper together. We collected and analysed the data, and then plotted them into graphs. We reviewed the literature and learnt from each other, thus successfully completing this paper. In summary, we believe that designating Zhou XN and Zhang Q as co-first authors is fitting for our manuscript as it accurately reflects our team's collaborative spirit, equal contributions, and diversity. Luo XH and Li H contributed equally to this work as co-corresponding authors. Three aspects are described here to illustrate this. First, Luo XH and Li H jointly designed the study and completed the pilot experiments, which laid a solid foundation for the later experiments. Second, Luo XH and Li H worked together to help and solve the problems encountered during the study, thus facilitating the process of the study and finally completing it. When we encountered difficulties in our study and stopped moving forward, Luo XH and Li H provided us with valuable advice and research direction. When we wanted to give up, Luo XH and Li H inspired and motivated us. Under the leadership of Luo XH and Li H, we successfully achieved the current academic results. Third, Luo XH and Li H revised the current manuscript together, and Luo XH and Li H guided the framework structure of the paper. The paper could only be completed successfully under the tutelage of Luo XH and Li H. Luo XH and Li H played the roles of supervising, guiding, clearing doubts, and preaching throughout the study process.

Supported by National Natural Science Foundation of China, No. 82060123; Doctoral Start-up Fund of Affiliated Hospital of Guizhou Medical University, No. gysybsky-2021-28; Fund Project of Guizhou Provincial Science and Technology Department, No. [2020]1Y299; and Guizhou Provincial Health Commission, No. gzwjk2019-1-082.

Institutional review board statement: This study was reviewed and approved by the Ethics Committee of the Affiliated Hospital of

Guizhou Medical University.

Institutional animal care and use committee statement: All procedures involving animals were reviewed and approved by the Institutional Animal Care and Use Committee of the Affiliated Hospital of Guizhou Medical University.

Informed consent statement: All study participants or their legal guardian provided informed written consent about personal and medical data collection prior to study enrolment.

Conflict-of-interest statement: We have no financial relationships to disclose.

Data sharing statement: The data presented in this study are available from the corresponding author upon reasonable request.

ARRIVE guidelines statement: The authors have read the ARRIVE guidelines, and the manuscript was prepared and revised according to the ARRIVE guidelines.

Country/Territory of origin: China

ORCID number: Xing-Nian Zhou 0000-0002-7569-9747; Yu-Jie Qin 0000-0002-8674-7492; Yu-Hong Liu 0009-0005-6346-7999; Lu Wang 0009-0008-7403-3434; Ming-Liang Cheng 0000-0002-2525-3595; Xin-Hua Luo 0000-0002-1140-2588; Hong Li 0000-0003-0601-3198.

S-Editor: Qu XL
L-Editor: Wang TQ
P-Editor: Yuan YY

REFERENCES

1 **Stravitz RT**, Lee WM. Acute liver failure. *Lancet* 2019; **394**: 869-881 [PMID: 31498101 DOI: 10.1016/S0140-6736(19)31894-X]
2 **Luedde T**, Kaplowitz N, Schwabe RF. Cell death and cell death responses in liver disease: mechanisms and clinical relevance. *Gastroenterology* 2014; **147**: 765-783.e4 [PMID: 25046161 DOI: 10.1053/j.gastro.2014.07.018]
3 **Brenner C**, Galluzzi L, Kepp O, Kroemer G. Decoding cell death signals in liver inflammation. *J Hepatol* 2013; **59**: 583-594 [PMID: 23567086 DOI: 10.1016/j.jhep.2013.03.033]
4 **Green DR**. The Coming Decade of Cell Death Research: Five Riddles. *Cell* 2019; **177**: 1094-1107 [PMID: 31100266 DOI: 10.1016/j.cell.2019.04.024]
5 **Mancardi D**, Mezzanotte M, Arrigo E, Barinotti A, Roetto A. Iron Overload, Oxidative Stress, and Ferroptosis in the Failing Heart and Liver. *Antioxidants (Basel)* 2021; **10** [PMID: 34942967 DOI: 10.3390/antiox10121864]
6 **de Carvalho Ribeiro M**, Szabo G. Role of the Inflammasome in Liver Disease. *Annu Rev Pathol* 2022; **17**: 345-365 [PMID: 34752711 DOI: 10.1146/annurev-pathmechdis-032521-102529]
7 **Li J**, Cao F, Yin HL, Huang ZJ, Lin ZT, Mao N, Sun B, Wang G. Ferroptosis: past, present and future. *Cell Death Dis* 2020; **11**: 88 [PMID: 32015325 DOI: 10.1038/s41419-020-2298-2]
8 **Stockwell BR**, Jiang X, Gu W. Emerging Mechanisms and Disease Relevance of Ferroptosis. *Trends Cell Biol* 2020; **30**: 478-490 [PMID: 32413317 DOI: 10.1016/j.tcb.2020.02.009]
9 **Jiang L**, Kon N, Li T, Wang SJ, Su T, Hibshoosh H, Baer R, Gu W. Ferroptosis as a p53-mediated activity during tumour suppression. *Nature* 2015; **520**: 57-62 [PMID: 25799988 DOI: 10.1038/nature14344]
10 **Kastenhuber ER**, Lowe SW. Putting p53 in Context. *Cell* 2017; **170**: 1062-1078 [PMID: 28886379 DOI: 10.1016/j.cell.2017.08.028]
11 **Kang R**, Kroemer G, Tang D. The tumor suppressor protein p53 and the ferroptosis network. *Free Radic Biol Med* 2019; **133**: 162-168 [PMID: 29800655 DOI: 10.1016/j.freeradbiomed.2018.05.074]
12 **Jorgensen I**, Miao EA. Pyroptotic cell death defends against intracellular pathogens. *Immunol Rev* 2015; **265**: 130-142 [PMID: 25879289 DOI: 10.1111/imr.12287]
13 **Bergsbaken T**, Fink SL, Cookson BT. Pyroptosis: host cell death and inflammation. *Nat Rev Microbiol* 2009; **7**: 99-109 [PMID: 19148178 DOI: 10.1038/nrmicro2070]
14 **Li H**, Zhao XK, Cheng YJ, Zhang Q, Wu J, Lu S, Zhang W, Liu Y, Zhou MY, Wang Y, Yang J, Cheng ML. Gasdermin D-mediated hepatocyte pyroptosis expands inflammatory responses that aggravate acute liver failure by upregulating monocyte chemotactic protein 1/CC chemokine receptor-2 to recruit macrophages. *World J Gastroenterol* 2019; **25**: 6527-6540 [PMID: 31802832 DOI: 10.3748/wjg.v25.i44.6527]
15 **Sauve AA**, Wolberger C, Schramm VL, Boeke JD. The biochemistry of sirtuins. *Annu Rev Biochem* 2006; **75**: 435-465 [PMID: 16756498 DOI: 10.1146/annurev.biochem.74.082803.133500]
16 **Singh CK**, Chhabra G, Ndiaye MA, Garcia-Peterson LM, Mack NJ, Ahmad N. The Role of Sirtuins in Antioxidant and Redox Signaling. *Antioxid Redox Signal* 2018; **28**: 643-661 [PMID: 28891317 DOI: 10.1089/ars.2017.7290]
17 **Liu X**, Yang X, Han L, Ye F, Liu M, Fan W, Zhang K, Kong Y, Zhang J, Shi L, Chen Y, Zhang X, Lin S. Pterostilbene alleviates polymicrobial sepsis-induced liver injury: Possible role of SIRT1 signaling. *Int Immunopharmacol* 2017; **49**: 50-59 [PMID: 28550734 DOI: 10.1016/j.intimp.2017.05.022]

18 **Flamm SL**, Yang YX, Singh S, Falck-Ytter YT; AGA Institute Clinical Guidelines Committee. American Gastroenterological Association Institute Guidelines for the Diagnosis and Management of Acute Liver Failure. *Gastroenterology* 2017; **152**: 644-647 [PMID: 28056348 DOI: 10.1053/j.gastro.2016.12.026]

19 **Friedmann Angeli JP**, Schneider M, Proneth B, Tyurina YY, Tyurin VA, Hammond VJ, Herbach N, Aichler M, Walch A, Eggenhofer E, Basavarajappa D, Rådmark O, Kobayashi S, Seibt T, Beck H, Neff F, Esposito I, Wanke R, Förster H, Yefremova O, Heinrichmeyer M, Bornkamm GW, Geissler EK, Thomas SB, Stockwell BR, O'Donnell VB, Kagan VE, Schick JA, Conrad M. Inactivation of the ferroptosis regulator Gpx4 triggers acute renal failure in mice. *Nat Cell Biol* 2014; **16**: 1180-1191 [PMID: 25402683 DOI: 10.1038/ncb3064]

20 **Fan BY**, Pang YL, Li WX, Zhao CX, Zhang Y, Wang X, Ning GZ, Kong XH, Liu C, Yao X, Feng SQ. Liproxstatin-1 is an effective inhibitor of oligodendrocyte ferroptosis induced by inhibition of glutathione peroxidase 4. *Neural Regen Res* 2021; **16**: 561-566 [PMID: 32985488 DOI: 10.4103/1673-5374.293157]

21 **Yang WS**, SriRamaratnam R, Welsch ME, Shimada K, Skouta R, Viswanathan VS, Cheah JH, Clemons PA, Shamji AF, Clish CB, Brown LM, Girotti AW, Cornish VW, Schreiber SL, Stockwell BR. Regulation of ferroptotic cancer cell death by GPX4. *Cell* 2014; **156**: 317-331 [PMID: 24439385 DOI: 10.1016/j.cell.2013.12.010]

22 **Li S**, He Y, Chen K, Sun J, Zhang L, Yu H, Li Q. RSL3 Drives Ferroptosis through NF-κB Pathway Activation and GPX4 Depletion in Glioblastoma. *Oxid Med Cell Longev* 2021; **2021**: 2915019 [PMID: 34987700 DOI: 10.1155/2021/2915019]

23 **Rodgers SK**, Horrow MM. Acute (fulminant) liver failure: a clinical and imaging review. *Abdom Radiol (NY)* 2021; **46**: 3117-3127 [PMID: 33635361 DOI: 10.1007/s00261-021-02973-5]

24 **Chen J**, Li X, Ge C, Min J, Wang F. The multifaceted role of ferroptosis in liver disease. *Cell Death Differ* 2022; **29**: 467-480 [PMID: 35075250 DOI: 10.1038/s41418-022-00941-0]

25 **Aizawa S**, Brar G, Tsukamoto H. Cell Death and Liver Disease. *Gut Liver* 2020; **14**: 20-29 [PMID: 30917630 DOI: 10.5009/gnl18486]

26 **Silverstein R**. D-galactosamine lethality model: scope and limitations. *J Endotoxin Res* 2004; **10**: 147-162 [PMID: 15198850 DOI: 10.1179/096805104225004879]

27 **Wilhelm EA**, Jesse CR, Roman SS, Nogueira CW, Savegnago L. Hepatoprotective effect of 3-alkynyl selenophene on acute liver injury induced by D-galactosamine and lipopolysaccharide. *Exp Mol Pathol* 2009; **87**: 20-26 [PMID: 19344711 DOI: 10.1016/j.yexmp.2009.03.004]

28 **Wang Y**, Zhang H, Chen Q, Jiao F, Shi C, Pei M, Lv J, Wang L, Gong Z. TNF-α/HMGB1 inflammation signalling pathway regulates pyroptosis during liver failure and acute kidney injury. *Cell Prolif* 2020; **53**: e12829 [PMID: 32419317 DOI: 10.1111/cpr.12829]

29 **Huang S**, Wang Y, Xie S, Lai Y, Mo C, Zeng T, Kuang S, Deng G, Zhou C, Chen Y, Huang S, Gao L, Lv Z. Hepatic TGFβr1 Deficiency Attenuates Lipopolysaccharide/D-Galactosamine-Induced Acute Liver Failure Through Inhibiting GSK3β-Nrf2-Mediated Hepatocyte Apoptosis and Ferroptosis. *Cell Mol Gastroenterol Hepatol* 2022; **13**: 1649-1672 [PMID: 35202887 DOI: 10.1016/j.jcmgh.2022.02.009]

30 **Seibt TM**, Proneth B, Conrad M. Role of GPX4 in ferroptosis and its pharmacological implication. *Free Radic Biol Med* 2019; **133**: 144-152 [PMID: 30219704 DOI: 10.1016/j.freeradbiomed.2018.09.014]

31 **Shi J**, Zhao Y, Wang K, Shi X, Wang Y, Huang H, Zhuang Y, Cai T, Wang F, Shao F. Cleavage of GSDMD by inflammatory caspases determines pyroptotic cell death. *Nature* 2015; **526**: 660-665 [PMID: 26375003 DOI: 10.1038/nature15514]

32 **Wang K**, Sun Q, Zhong X, Zeng M, Zeng H, Shi X, Li Z, Wang Y, Zhao Q, Shao F, Ding J. Structural Mechanism for GSDMD Targeting by Autoprocessed Caspases in Pyroptosis. *Cell* 2020; **180**: 941-955.e20 [PMID: 32109412 DOI: 10.1016/j.cell.2020.02.002]

33 **Kang R**, Zeng L, Zhu S, Xie Y, Liu J, Wen Q, Cao L, Xie M, Ran Q, Kroemer G, Wang H, Billiar TR, Jiang J, Tang D. Lipid Peroxidation Drives Gasdermin D-Mediated Pyroptosis in Lethal Polymicrobial Sepsis. *Cell Host Microbe* 2018; **24**: 97-108.e4 [PMID: 29937272 DOI: 10.1016/j.chom.2018.05.009]

34 **Chen D**, Chu B, Yang X, Liu Z, Jin Y, Kon N, Rabadan R, Jiang X, Stockwell BR, Gu W. iPLA2β-mediated lipid detoxification controls p53-driven ferroptosis independent of GPX4. *Nat Commun* 2021; **12**: 3644 [PMID: 34131139 DOI: 10.1038/s41467-021-23902-6]

35 **Shu L**, Matveyenko AV, Kerr-Conte J, Cho JH, McIntosh CH, Maedler K. Decreased TCF7L2 protein levels in type 2 diabetes mellitus correlate with downregulation of GIP- and GLP-1 receptors and impaired beta-cell function. *Hum Mol Genet* 2009; **18**: 2388-2399 [PMID: 19386626 DOI: 10.1093/hmg/ddp178]

36 **Yang Y**, Liu Y, Wang Y, Chao Y, Zhang J, Jia Y, Tie J, Hu D. Regulation of SIRT1 and Its Roles in Inflammation. *Front Immunol* 2022; **13**: 831168 [PMID: 35359990 DOI: 10.3389/fimmu.2022.831168]

37 **Chen C**, Zhou M, Ge Y, Wang X. SIRT1 and aging related signaling pathways. *Mech Ageing Dev* 2020; **187**: 111215 [PMID: 32084459 DOI: 10.1016/j.mad.2020.111215]

38 **Kadono K**, Kageyama S, Nakamura K, Hirao H, Ito T, Kojima H, Dery KJ, Li X, Kupiec-Weglinski JW. Myeloid Ikaros-SIRT1 signaling axis regulates hepatic inflammation and pyroptosis in ischemia-stressed mouse and human liver. *J Hepatol* 2022; **76**: 896-909 [PMID: 34871625 DOI: 10.1016/j.jhep.2021.11.026]

39 **Wang C**, Liu T, Tong Y, Cui R, Qu K, Liu C, Zhang J. Ulinastatin protects against acetaminophen-induced liver injury by alleviating ferroptosis *via* the SIRT1/NRF2/HO-1 pathway. *Am J Transl Res* 2021; **13**: 6031-6042 [PMID: 34306342]

40 **Nakamura K**, Zhang M, Kageyama S, Ke B, Fujii T, Sosa RA, Reed EF, Datta N, Zarrinpar A, Busuttil RW, Araujo JA, Kupiec-Weglinski JW. Macrophage heme oxygenase-1-SIRT1-p53 axis regulates sterile inflammation in liver ischemia-reperfusion injury. *J Hepatol* 2017; **67**: 1232-1242 [PMID: 28842295 DOI: 10.1016/j.jhep.2017.08.010]

41 **Nakamura K**, Kageyama S, Ke B, Fujii T, Sosa RA, Reed EF, Datta N, Zarrinpar A, Busuttil RW, Kupiec-Weglinski JW. Sirtuin 1 attenuates inflammation and hepatocellular damage in liver transplant ischemia/Reperfusion: From mouse to human. *Liver Transpl* 2017; **23**: 1282-1293 [PMID: 28719070 DOI: 10.1002/lt.24821]

42 **Alshehri AS**, El-Kott AF, El-Kenawy AE, Khalifa HS, AlRamlawy AM. Cadmium chloride induces non-alcoholic fatty liver disease in rats by stimulating miR-34a/SIRT1/FXR/p53 axis. *Sci Total Environ* 2021; **784**: 147182 [PMID: 34088068 DOI: 10.1016/j.scitotenv.2021.147182]

43 **Ma S**, Sun L, Wu W, Wu J, Sun Z, Ren J. USP22 Protects Against Myocardial Ischemia-Reperfusion Injury *via* the SIRT1-p53/SLC7A11-Dependent Inhibition of Ferroptosis-Induced Cardiomyocyte Death. *Front Physiol* 2020; **11**: 551318 [PMID: 33192549 DOI: 10.3389/fphys.2020.551318]

World Journal of Gastroenterology

Submit a Manuscript: https://www.f6publishing.com

World J Gastroenterol 2024 March 21; 30(11): 1609-1620

DOI: 10.3748/wjg.v30.i11.1609

ISSN 1007-9327 (print) ISSN 2219-2840 (online)

ORIGINAL ARTICLE

Basic Study

Identification of an immune-related gene signature for predicting prognosis and immunotherapy efficacy in liver cancer *via* cell-cell communication

Jun-Tao Li, Hong-Mei Zhang, Wei Wang, Dong-Qing Wei

Specialty type: Gastroenterology and hepatology

Provenance and peer review: Invited article; Externally peer reviewed.

Peer-review model: Single blind

Peer-review report's scientific quality classification
Grade A (Excellent): A
Grade B (Very good): 0
Grade C (Good): 0
Grade D (Fair): 0
Grade E (Poor): 0

P-Reviewer: Rodrigues AT, Brazil

Received: December 13, 2023
Peer-review started: December 13, 2023
First decision: December 27, 2023
Revised: January 9, 2024
Accepted: March 4, 2024
Article in press: March 4, 2024
Published online: March 21, 2024

Jun-Tao Li, Hong-Mei Zhang, College of Mathematics and Information Science, Henan Normal University, Xinxiang 453007, Henan Province, China

Wei Wang, College of Computer and Information Engineering, Henan Normal University, Xinxiang 453007, Henan Province, China

Dong-Qing Wei, State Key Laboratory of Microbial Metabolism, and School of Life Sciences and Biotechnology, Shanghai Jiao Tong University, Shanghai 200240, China

Corresponding author: Hong-Mei Zhang, MPhil, Master's Student, College of Mathematics and Information Science, Henan Normal University, Jianshe East Road, Xinxiang 453007, Henan Province, China. zhanghmmail@163.com

Abstract

BACKGROUND

Liver cancer is one of the deadliest malignant tumors worldwide. Immunotherapy has provided hope to patients with advanced liver cancer, but only a small fraction of patients benefit from this treatment due to individual differences. Identifying immune-related gene signatures in liver cancer patients not only aids physicians in cancer diagnosis but also offers personalized treatment strategies, thereby improving patient survival rates. Although several methods have been developed to predict the prognosis and immunotherapeutic efficacy in patients with liver cancer, the impact of cell-cell interactions in the tumor microenvironment has not been adequately considered.

AIM

To identify immune-related gene signals for predicting liver cancer prognosis and immunotherapy efficacy.

METHODS

Cell grouping and cell-cell communication analysis were performed on single-cell RNA-sequencing data to identify highly active cell groups in immune-related pathways. Highly active immune cells were identified by intersecting the highly active cell groups with B cells and T cells. The significantly differentially expressed genes between highly active immune cells and other cells were subsequently selected as features, and a least absolute shrinkage and selection

operator (LASSO) regression model was constructed to screen for diagnostic-related features. Fourteen genes that were selected more than 5 times in 10 LASSO regression experiments were included in a multivariable Cox regression model. Finally, 3 genes (stathmin 1, cofilin 1, and C-C chemokine ligand 5) significantly associated with survival were identified and used to construct an immune-related gene signature.

RESULTS

The immune-related gene signature composed of stathmin 1, cofilin 1, and C-C chemokine ligand 5 was identified through cell-cell communication. The effectiveness of the identified gene signature was validated based on experimental results of predictive immunotherapy response, tumor mutation burden analysis, immune cell infiltration analysis, survival analysis, and expression analysis.

CONCLUSION

The findings suggest that the identified gene signature may contribute to a deeper understanding of the activity patterns of immune cells in the liver tumor microenvironment, providing insights for personalized treatment strategies.

Key Words: Liver cancer; Cell-cell communication; Gene signature; Prognosis; Immunotherapy; Single-cell RNA sequencing

Core Tip: In this study, CellChat was employed to infer cell-cell communication, thereby selecting highly active cell groups in immune-related pathways on single-cell RNA-sequencing data. Highly active immune cells were identified by intersecting these groups with B and T cells. Subsequently, significantly differentially expressed genes between highly active immune cells and the remaining cells were incorporated into the Lasso regression model. Ultimately, incorporating genes selected more than 5 times in 10 Lasso regression experiments into a multivariable Cox regression model, 3 genes (stathmin 1, cofilin 1, and C-C chemokine ligand 5) significantly associated with survival were identified to construct a gene signature.

Citation: Li JT, Zhang HM, Wang W, Wei DQ. Identification of an immune-related gene signature for predicting prognosis and immunotherapy efficacy in liver cancer *via* cell-cell communication. *World J Gastroenterol* 2024; 30(11): 1609-1620
URL: https://www.wjgnet.com/1007-9327/full/v30/i11/1609.htm
DOI: https://dx.doi.org/10.3748/wjg.v30.i11.1609

INTRODUCTION

Liver cancer, a malignant tumor with consistently high global incidence and mortality rates, has long been a focal point of medical research and clinical intervention[1,2]. In particular, within the rapidly advancing field of immunotherapy, immune checkpoint blockade (ICB) treatment has emerged as an innovative therapeutic approach, offering renewed hope for patients with liver cancer[3]. This strategy has achieved significant clinical efficacy by preventing tumor cells from suppressing the immune system and stimulating the body's own immune response[3-5]. However, only a small fraction of liver cancer patients benefit from this treatment, and the molecular basis underlying the control of immune responses and evasion has not been determined[6,7]. To better guide treatment strategies and predict patient prognosis, it is imperative to explore into the molecular mechanisms and immune characteristics of liver cancer.

The success of immunotherapy in liver cancer hinges on a comprehensive understanding of the tumor immune microenvironment, necessitating the exploration of high-throughput technologies to unravel intricate molecular interactions[8-10]. Using bulk RNA sequencing (RNA-seq) data, Tang *et al*[11] first screened gene modules partitioned by weighted gene co-expression network analysis that were most relevant to tumor immune phenotype genes. Subsequently, a tumor immune phenotype-related gene signature in liver cancer was identified through least absolute shrinkage and selection operator (LASSO) and univariate Cox regression analyses. Similarly, Wang *et al*[12] employed differential expression analysis and univariate Cox regression to identify differentially expressed genes associated with overall survival. These genes were further refined through LASSO regression to construct a novel immune-related prognostic model in hepatocellular carcinoma. Although bulk RNA-seq provides a global view of gene expression patterns, single-cell RNA-sequencing (scRNA-seq) offers the advantage of revealing heterogeneity within tumors at the single-cell level[10,13]. Therefore, the integration of bulk RNA-seq and scRNA-seq data holds great promise. Yang *et al*[14] utilized scRNA-seq data from liver cancer patients to identify tumor-associated endothelial cell (TEC) subpopulations and established a prognostic model for liver cancer by integrating the marker genes of these cells with bulk RNA-seq data. Li *et al*[15] accurately identified cell subpopulations related to liver cancer by integrating bulk and scRNA-seq data, introducing the cell group structure into the model construction process.

However, cellular crosstalk in the tumor microenvironment should also be considered, as it plays a crucial role in shaping the immune landscape of liver cancer[8,16,17]. The construction of a cell-cell communication network facilitates the identification of key participants in tumor-immune crosstalk. In this context, CellChat, a computational framework for

inferring cell-cell communication, provides a powerful means to identify the communication networks within the liver cancer microenvironment[18,19]. In CellChat, the dynamic process of intercellular communication is simulated using the law of mass action, and the inferred ligand-receptor pairs are systematically classified into functionally relevant signaling pathways[19]. The activity level of a cell group in immune-related pathways can be quantified by counting the number of times the cell group is used as a source and target.

In this study, we aimed to leverage the power of bulk RNA-seq and scRNA-seq data integration to identify a comprehensive immune-related gene signature in liver cancer. By focusing on the cell-cell communication network using the CellChat framework, we sought to unravel the intricate interplay among diverse cell groups within the liver cancer microenvironment. The identified gene signature holds promise for predicting liver cancer prognosis and understanding potential immunotherapeutic responses, providing valuable insights for personalized treatment strategies.

MATERIALS AND METHODS

Data collection and preprocessing

The liver cancer bulk RNA-seq data, which included 50 normal and 369 tumor samples, 368 of which included total survival time and status, were downloaded from The Cancer Genome Atlas (TCGA) database. The liver cancer scRNA-seq data were downloaded from the Gene Expression Omnibus database with the accession number GSE125449 and included 8853 cells and 7 cell types[20]: Cancer-associated fibroblast, tumor-associated macrophage, malignant cell, TEC, cells with an unknown entity but that express hepatic progenitor cell markers, T cell, and B cell. For bulk RNA-seq data, a logarithmic transformation with a base of 2 was first performed on the original count data. The expression values of genes with the same name were subsequently averaged. The R package Seurat was used for preprocessing the scRNA-seq data. Specifically, the NormalizeData and FindVariableFeatures functions were used to normalize the data and select 2000 highly variable genes, respectively. Standardization and principal component analysis were performed using the ScaleData and RunPCA functions, respectively. The first ten principal components were used to construct a shared nearest-graph through the FindNeighbors function. Two-dimensional cell visualization was achieved *via* the RunUMAP function.

Cell-cell communication inference

The Louvain algorithm, employed for cell grouping, was implemented through the function FindClusters in the R package Seurat, with the resolution parameter set to 0.5. Based on these cell grouping results, the cell-cell interaction network was inferred through CellChat. Specifically, the entire human ligand-receptor interaction database CellChatDB was chosen as the foundation for this article. CellChat utilizes the law of mass action to simulate ligand-receptor-mediated signal interactions, which can not only infer intercellular communication but also further classify significant ligand-receptor pairs into functionally related signaling pathways. Immune-related pathways were identified by searching for pathway functions on the official Kyoto Encyclopedia of Genes and Genomes website (https://www.kegg.jp). The number of times each cell group served as a source and target in immune-related pathways was counted, and the top 20% of cell groups were considered highly active. Highly active immune-related cells were identified by the intersection of the obtained highly active cell groups with T and B cells.

LASSO regression and Cox regression

Differential expression analysis was performed through the R package limma[21]. The significantly differentially expressed genes between highly active immune cells and other cells were selected using the criteria $|\log(\text{fold change})| > 1$ and $P < 0.05$. The genes shared between these genes and the bulk RNA-seq data were included in the following LASSO regression model for selecting diagnostic-related features:

$$\min_{w,b} \frac{1}{n}\sum_{i=1}^{n}\left(\ln(1+e^{w^T x_i+b}) - y_i(w^T x_i + b)\right) + \lambda \| w \|_1 \quad (1)$$

Where n represents the number of samples, $w = (w_1, w_2, \ldots w_m)^T$ is the coefficient vector corresponding to m shared genes, $x_i = (x_{i1}, x_{i2}, \ldots, x_{im})^T$ is the expression level of m genes in the i-th sample, b is the offset, λ represents the regularization parameter determined by 10-fold cross validation, and y_i represents the label corresponding to the i-th sample. If a sample was considered to be a tumor, this value was 1; otherwise, it was 0. Eighty percent of the samples were randomly selected as the training set for LASSO regression, while the remaining 20% of the samples were used as the test set to evaluate the effectiveness of the selected diagnostic-related features. The coefficient vector w and threshold b in Equation (1) were solved through the R package glmnet[22]. To avoid randomness in the experimental results, the dataset was divided 10 times by setting random seeds from 1 to 10. Genes that were selected more than 5 times were considered diagnostic-related features.

To comprehensively evaluate the impact of risk factors on patient survival, diagnostic-related features were included in the following multivariable Cox regression model:

$$\frac{h(t,x)}{h(t,0)} = \exp(\beta_1 x_1 + \beta_2 x_2 + \cdots + \beta_s x_s) \quad (2)$$

Table 1 Number of times cell groups served as a source and target in immune-related pathways

	Number of times														
Cell group	12	15	6	2	10	9	14	11	8	1	7	13	3	5	4
Frequency	195	195	100	84	76	72	65	50	48	44	41	35	26	22	9

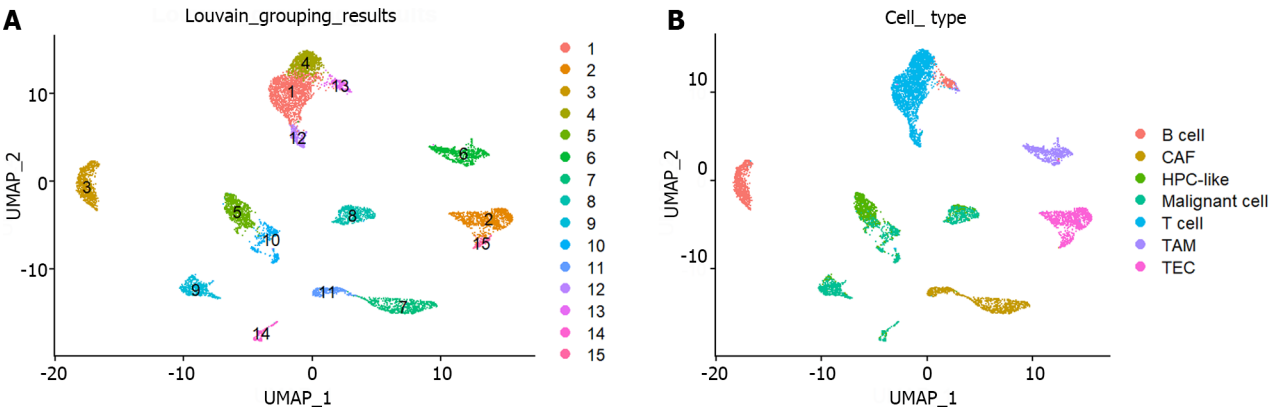

Figure 1 UMAP visualization of single-cell RNA sequencing data. A: UMAP visualization of 15 cell groups obtained through the Louvain algorithm; B: UMAP visualization of 7 cell types. CAF: Cancer-associated fibroblast; HPC: Hepatic progenitor cell; TAM: Tumor-associated macrophage; TEC: Tumor-associated endothelial cell.

Where $h(t,x)$ represents the risk function at time t, $h(t,0)$ denotes the baseline risk function, and $(\beta_1,\beta_2,\ldots,\beta_s)^T$ is the regression coefficient vector corresponding to s diagnostic-related features, which is solved through the R package survival.

Identification of a gene signature

After performing multivariable Cox regression analysis, genes significantly associated with survival were selected according to a criterion of $p < 0.05$ to identify the following gene signature:

$$Risk\ score = \sum_{j=1}^{t} coef(gene_j) * EXP(gene_j) \quad (3)$$

Where $gene_j$ represents the j-th gene among the t genes significantly associated with survival, $coef(gene_j)$ represents the coefficient of $gene_j$ when only genes significantly related to survival were included in the multivariable Cox regression, and $EXP(gene_j)$ represents the preprocessed expression values of $gene_j$. When $coef(gene_j)$ is greater than 0, the expression level of $gene_j$ increases, and the patient's survival risk increases; when the coefficient is less than 0, the expression level of this gene increases, and the survival risk decreases.

RESULTS

Identification of highly active immune cells

The preprocessed scRNA-seq data were divided into 15 cell groups using the Louvain algorithm. The UMAP visualization of 15 cell groups and 7 cell types was presented in Figure 1A and B, respectively. Subsequently, the communication network between cell groups was inferred through the CellChat, and 16 immune-related pathways were identified. The cell-cell communication within signal pathways inferred integrin beta2 and major histocompatibility class I were demonstrated as examples in Figure 2A and B, respectively. In Figure 2A, cell group 12 serves as the source targeting the other six cell groups, while in Figure 2B, it serves as the target for all cell groups. The number of times each cell group served as a source and target in immune-related pathways was statistically displayed in Table 1. The top 20% of the cell groups in descending order were identified as highly active cell groups, *i.e.*, cell groups 12, 15, and 6. A total of 240 highly active immune cells were identified by intersecting 1009 cells from cell groups 6, 12, and 15 with 3785 T cells and B cells, as shown in Figure 3. These cells are involved in multiple immune-related signaling pathways and play a critical role in regulating immune responses.

Gene screening and gene signature identification

Differential expression analysis was also conducted between 240 highly active immune cells and the remaining 8613 cells. Then, 50 significantly differentially expressed genes were identified, and 46 genes shared between them and bulk RNA-

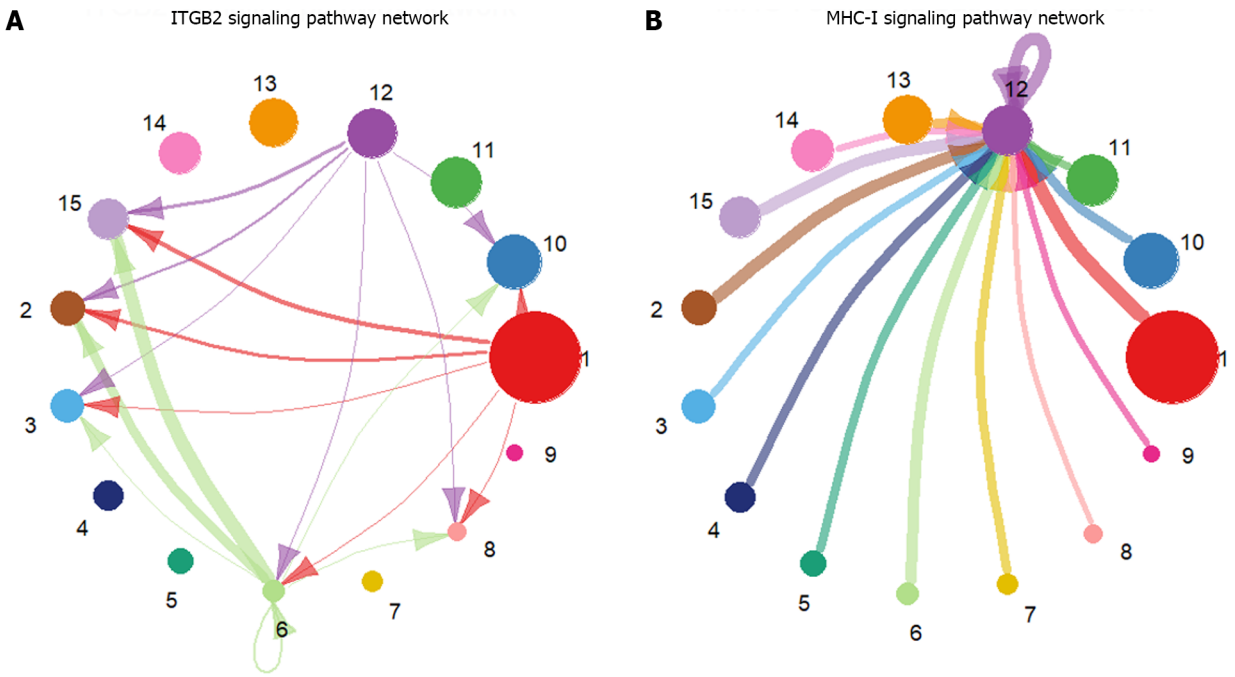

Figure 2 Circle plot of signaling pathway networks inferred by CellChat. A: Visualization of the inferred integrin beta2 signaling pathway network details; B: Visualization of the inferred major histocompatibility class I signaling pathway network details. The different colors of the circles represent different cell groups. The size of the circle is proportional to the number of cells in the cell group. The arrows point from the source to the target, and the colors of the edges are consistent with those of the signal source. The width of the edges represents the communication probability. ITGB2: Integrin beta2; MHC-I: Major histocompatibility class I.

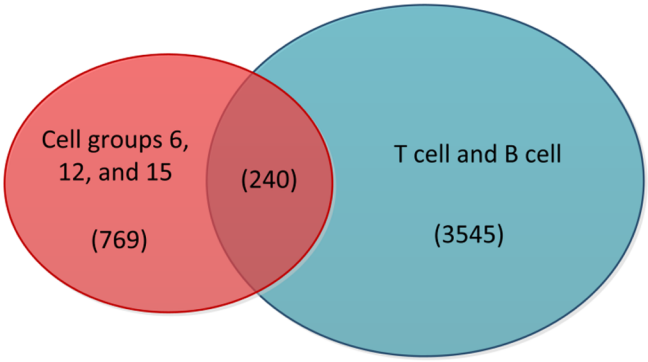

Figure 3 Venn diagram of highly active cells with T cells and B cells. The red portion in the diagram represents cells from cell groups 6, 12, and 15, while the blue portion represents T cells and B cells. The middle section indicates the intersection between the two, and the numbers in parentheses correspond to the cell counts in these three sections.

seq data were included in the LASSO regression model. Of these, 14 genes were identified as diagnostic-related genes because they were selected more than 5 times in 10 experiments. The average diagnostic accuracy on the test set over 10 experiments was 96.55%, indicating that the selected features were effective. Subsequently, multivariable Cox regression analysis was conducted, and 3 genes [stathmin 1 (*STMN1*), C-C chemokine ligand 5 (*CCL5*), and cofilin 1 (*CFL1*)] out of 14 were selected to construct a gene signature due to their significant correlation with patient survival. The coefficients and *P* values of the 14 diagnostic-related genes were listed in Table 2. Ultimately, the following gene signature was generated by incorporating only *STMN1*, *CCL5*, and *CFL1* into the multivariable Cox regression analysis model:

$$Risk\ score = 0.2754 * EXP(STMN1) - 0.2222 * EXP(CCL5) + 0.6458 * EXP(CFL1)$$

Patients with higher risk scores were considered to have worse prognoses. The samples were divided into high-risk and low-risk groups based on the median of this risk score.

Survival analysis and expression analysis

To assess the difference in survival between the high-risk and low-risk groups, Kaplan-Meier survival analysis was conducted, and the log-rank test was employed for statistical analysis. Figure 4 illustrated the significant difference between the high-risk and low-risk groups ($P < 0.0001$), with the median survival time of patients in the low-risk group being approximately three times longer than that in the high-risk group. These results indicated that the identified gene

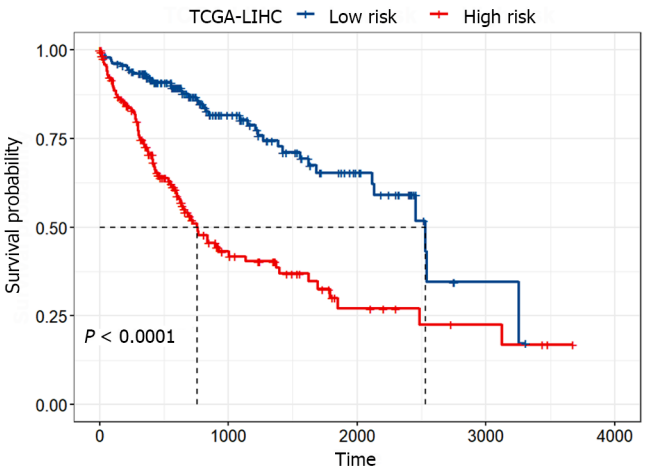

Figure 4 Kaplan-Meier survival curves of the high-risk and low-risk groups. The red and blue curves represent the high-risk and low-risk groups, respectively, which were divided according to the median risk score. The significance of the difference between the two was evaluated through the log-rank test. TCGA-LIHC: The Cancer Genome Atlas Liver Hepatocellular Carcinoma.

signature could significantly distinguish between patients with favorable and poor prognoses.

Furthermore, expression analysis of the individual genes constituting the gene signature was conducted in the high-risk and low-risk groups, as well as in tumor and normal samples; the results were presented in Figure 5. A *t* test was performed to assess whether there were significant differences between two groups of samples, and the obtained *P* values were displayed in all boxplots. The *STMN1* and *CFL1* genes had significantly greater expression in the high-risk group and tumor samples, while the *CCL5* gene had greater expression in the low-risk group and normal samples. Meta-analysis revealed that in liver cancer, *STMN1* and *CFL1* are considered oncogenes, and their upregulation is closely associated with poor prognosis[23,24]. The *CCL5*-high subtype is significantly correlated with immune cells and markedly improved overall survival[25]. This finding is consistent with the findings in Figure 5, providing additional confirmation for the reliability of the identified gene signature.

Immunocyte infiltration analysis

The relative infiltration of immune cells in the high-risk and low-risk groups was investigated using the single-sample gene set enrichment analysis algorithm[26]. This algorithm was implemented through the function GSVA in the R package GSVA. A reference gene set comprising 28 reported immune cell types was utilized for the analysis[27]. Figure 6 showed that out of the 28 immune cell types, 20 exhibited significant correlations with the risk groups. The Kruskal-Wallis test was used to evaluate significant differences between two groups. In particular, the infiltration levels in cell types activated B cell, effector memory CD8 T cell, eosinophil, immature B cell, mast cell, and type 1 T helper cell were significantly greater in the low-risk group than in the high-risk group. These results indicated that an immune-related gene signature identified through cell-cell communication plays a crucial role in stratifying the risk of liver cancer.

Tumor mutation burden analysis

Tumor mutation burden (TMB) was approved by the United States Food and Drug Administration in 2020 as a biomarker for predicting the response to immunotherapy[28]. To assess the relationship between the identified gene signature and the immune response, the TMB of the samples was computed using mutation data obtained from liver cancer patients downloaded from the TCGA database. Figure 7A illustrated the TMB distribution across all samples. Figure 7B and C showed the mutation landscapes of the high-risk and the low-risk groups, respectively. Among the top 10 mutated genes, 6 were common between the high-risk group and the low-risk group, but each gene had a different mutation type. Furthermore, the TMB in the high-risk and low-risk groups identified by the gene signature proposed in this article, as well as the groups identified by the gene signatures proposed by Tang *et al*[11] and Wang *et al*[12], were separately analyzed, as shown in Figure 7D-F. However, only the samples from the high-risk and low-risk groups defined by the proposed gene signature showed a significant difference in TMB ($P = 0.01106$). These results strongly demonstrated that the identified gene signature could predict the efficacy of immunotherapy.

Prediction of immunotherapy response

The TIDE algorithm, which simulates both the immune evasion mechanisms of immune function suppression and immune cell exclusion, more accurately predicts patient prognosis than individual biomarkers alone[29]. Currently, this algorithm has been widely applied for predicting patient responses to ICB therapy. In this article, the TIDE algorithm was used to analyze the response of liver cancer patients to immunotherapy using an online tool (http://tide.dfci.harvard.edu/). A higher TIDE score indicates that the patient is more prone to experiencing immune escape and is likely to exhibit poor efficacy in response to immunotherapy. The Pearson correlation coefficient between TIDE scores and Risks cores was calculated, and the significant correlation trends between the two were illustrated in Figure 8A.

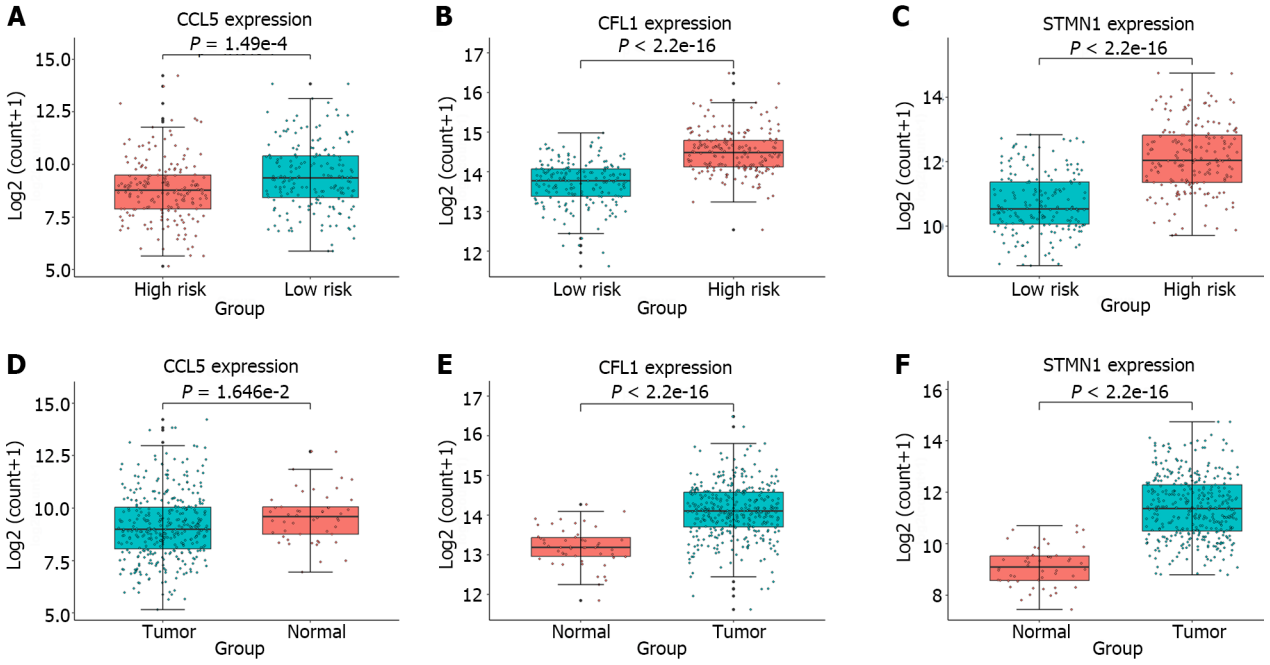

Figure 5 Box plots depicting the expression analysis of the genes employed in constructing the gene signature. A-C: Expression analysis of C-C chemokine ligand 5 (CCL5), cofilin 1 (CFL1), and stathmin 1 (STMN1) in the high-risk and low-risk groups; D-F: Expression analysis of CCL5, CFL1, and STMN1 in the tumor and normal groups. The high-risk and normal groups are represented by red boxes, while the low-risk and tumor groups are represented by blue boxes. The significant differences between groups were evaluated through t tests. CCL5: C-C chemokine ligand 5; CFL1: Cofilin 1; STMN1: Stathmin 1.

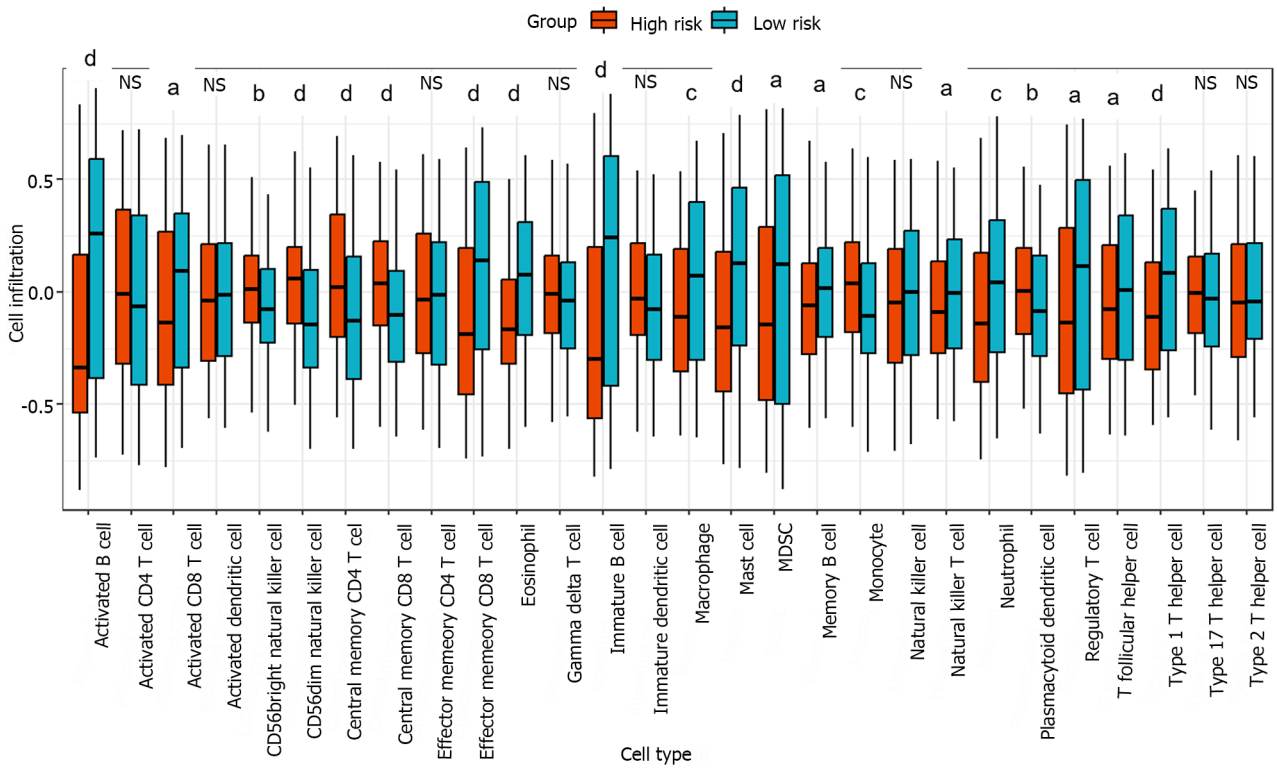

Figure 6 Box plot of the degree of immune cell infiltration in the high-risk and low-risk groups. The infiltration degree of 28 immune cell types in the high-risk and low-risk groups was analyzed, and the significant differences between the two groups were evaluated using the Kruskal-Wallis test. [a]*P* < 0.05; [b]*P* < 0.01; [c]*P* < 0.001; [d]*P* < 0.0001.

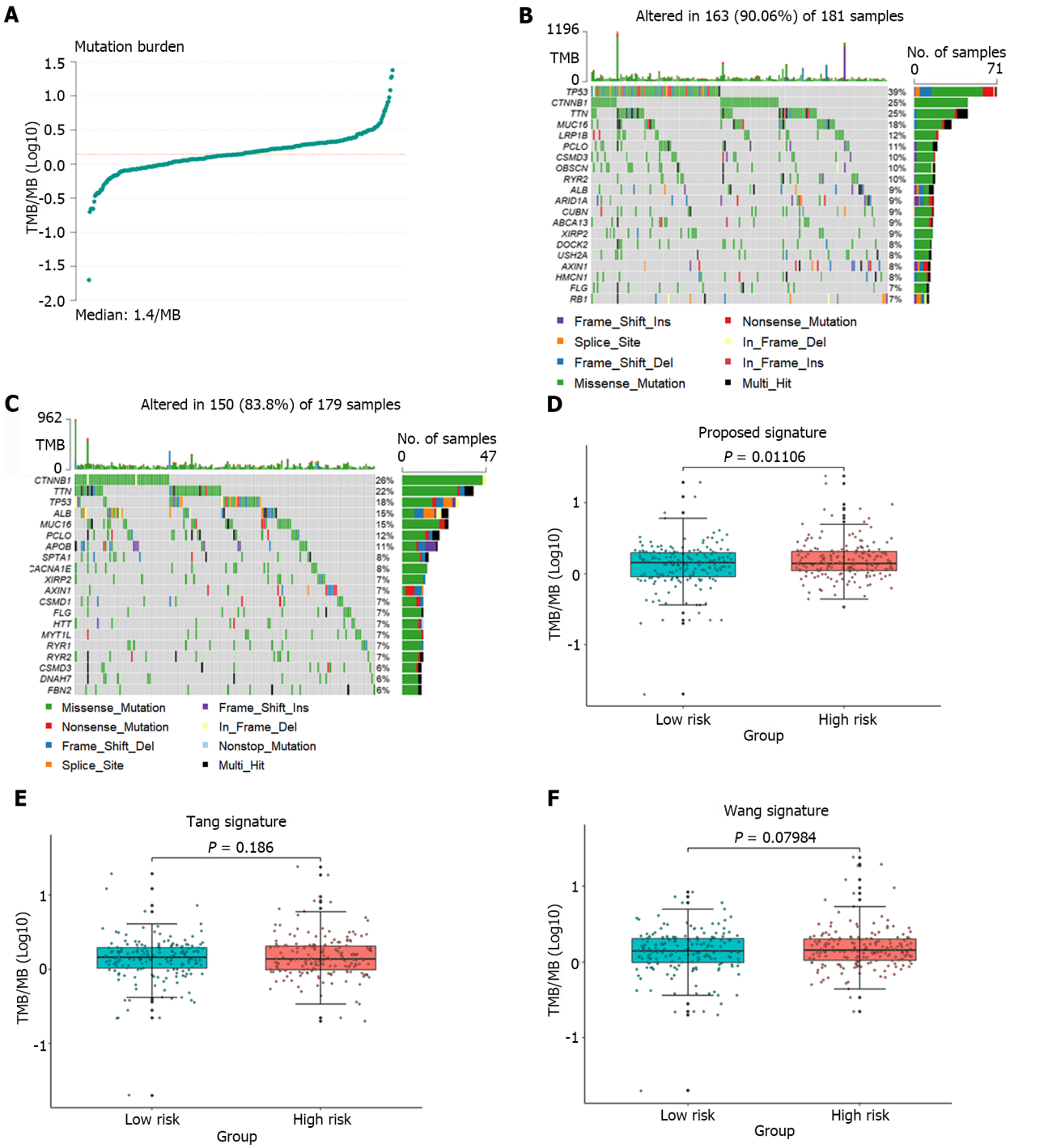

Figure 7 Analysis of the tumor mutation burden in the samples. A: The distribution of tumor mutation burden (TMB) for all samples; B and C: Waterfall plots depicting mutation landscapes in the high-risk and low-risk groups, respectively; D-F: A comparative analysis of TMB was conducted in the high-risk and low-risk groups identified by the gene signature identified in this article and the groups identified by the gene signature proposed by Tang *et al*[11] and Wang *et al*[12].

Furthermore, the TIDE scores corresponding to the high-risk and low-risk groups identified by the gene signature in this article, as well as the groups identified by the gene signatures reported by Tang *et al*[11] and Wang *et al*[12], are depicted in Figure 8B-D. The TIDE scores exhibited significant differences across all high-risk and low-risk groups, with the minimum *P* value observed among groups stratified by the proposed gene signature (*P* = 3.762e-10). Moreover, compared to those of the other two methods, the gene signature identified in this article requires the fewest genes. A significant correlation was observed between TIDE score and Risk scores, and a distinction was made between the high-risk and low-risk groups, suggesting that the identified gene signature could serve as a valuable tool for predicting the efficacy of immunotherapy.

Table 2 Coefficients and *P* values corresponding to diagnostic-related genes in multivariable Cox regression

Gene	Coefficient	*P* value
NUSAP1	-0.108515073	0.219706452
STMN1	0.367886836	0.006598885
UBE2C	-0.038808062	0.692223045
CKS1B	0.019614361	0.885123337
HMGB1	-0.036928764	0.841313659
CCL5	-0.351813314	0.000909645
DUT	-0.200404711	0.201189097
PFN1	0.156824573	0.389822262
ITM2A	-0.021567354	0.742760958
CCL4	0.146793282	0.182629575
CFL1	0.688652826	0.001683044
IL32	-0.054741614	0.491028415
MT2A	0.033545401	0.525093809
IFITM3	-0.053229362	0.706251853

NUSAP1: Nucleolar and spindle associated protein 1; STMN1: Stathmin 1; UBE2C: Ubiquitin conjugating enzyme E2 C; CKS1B: CDC28 protein kinase regulatory subunit 1B; HMGB1: High mobility group box 1; CCL5: C-C chemokine ligand 5; DUT: Deoxyuridine triphosphatase; PFN1: Profilin 1; ITM2A: Integral membrane protein 2A; CCL4: C-C chemokine ligand 4; CFL1: Cofilin 1; IL32: Interleukin 32; MT2A: Metallothionein 2A; IFITM3: Interferon induced transmembrane protein 3.

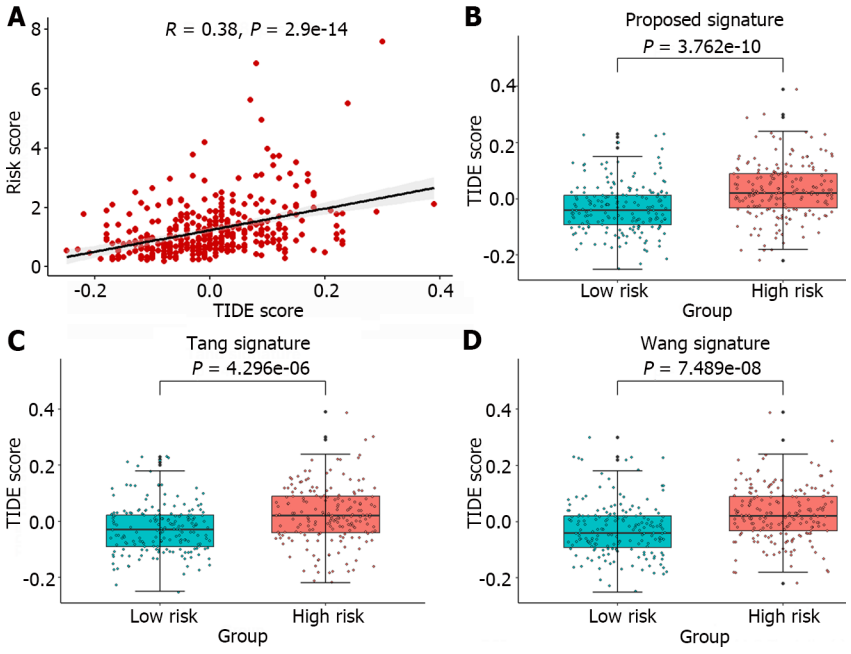

Figure 8 Analysis of predicted TIDE scores in the sample. A: Pearson correlation analysis between the sample risk score and TIDE score; B-D: A comparative analysis of the TIDE score was conducted for the high-risk and low-risk groups identified by the gene signature in this article and the groups identified by the gene signatures proposed by Tang *et al*[11] and Wang *et al*[12].

DISCUSSION

Our research demonstrated that utilizing cell-cell communication information to identify immune-related gene signature outperformed two other methods in terms of predictive performance. However, it's worth noting that we focused on cell-cell communication at the cell group level rather than at the level of individual cells. Investigating the interactions between cells at single-cell resolution and their impact on predicting patient prognosis and immunotherapeutic efficacy is

a direction for our future research.

CONCLUSION

In summary, our integrated analysis of bulk and scRNA-seq data, coupled with the exploration of the cell-cell communication network, has identified a comprehensive immune-related gene signature with clinical and therapeutic implications. The identified gene signature not only demonstrates potential as a prognostic tool for liver cancer but also provides invaluable insights into the dynamics of immune responses within the tumor microenvironment.

ARTICLE HIGHLIGHTS

Research background

Immunotherapy has provided hope to patients with advanced liver cancer, but only a small fraction of patients benefit from this treatment due to individual differences. Although several methods have been developed to predict the prognosis and immunotherapeutic efficacy in patients with liver cancer, the impact of cell-cell interactions in the tumor microenvironment has not been adequately considered.

Research motivation

Recent research has demonstrated the crucial role of cell-cell interactions in shaping the immune landscape of liver cancer.

Research objectives

This study aims to identify immune-related gene signatures through cell-cell interactions to predict prognosis and immunotherapeutic efficacy in liver cancer.

Research methods

In this study, CellChat was employed to infer cell-cell communication, thereby selecting highly active cell groups in immune-related pathways on single-cell RNA-sequencing (scRNA-seq) data. Highly active immune cells were identified by intersecting these groups with B and T cells. Subsequently, significantly differentially expressed genes between highly active immune cells and the remaining cells were incorporated into the Lasso regression model. Ultimately, incorporating genes selected more than 5 times in 10 Lasso regression experiments into a multivariable Cox regression model, 3 genes (stathmin 1, cofilin 1, and C-C chemokine ligand 5) significantly associated with survival were identified to construct a gene signature.

Research results

The immune-related gene signature composed of stathmin 1, cofilin 1, and C-C chemokine ligand 5 was identified through cell-cell communication. The identified gene signature has been validated to be superior to the other two methods through immunotherapy response prediction, tumor mutation burden analysis, and immune cell infiltration analysis, enabling better prediction of prognosis and immune therapy efficacy in liver cancer.

Research conclusions

This study suggest that the identified gene signature may contribute to a deeper understanding of the activity patterns of immune cells in the liver tumor microenvironment, providing insights for personalized treatment strategies.

Research perspectives

This article utilized cell-cell communication information and machine learning method, combined with Cox regression, to comprehensively analyze bulk and scRNA-seq data, identifying clinically and therapeutically relevant immune-related gene signature.

FOOTNOTES

Co-corresponding authors: Hong-Mei Zhang and Dong-Qing Wei.

Author contributions: Zhang HM and Wei DQ contributed equally to this work and should be considered co-corresponding authors. Li JT and Zhang HM conceived this study and implemented the experiments; Li JT and Wang W collected and preprocessed the data; Zhang HM and Wei DQ drafted and revised the manuscript.

Supported by Scientific and Technological Project of Henan Province, No. 212102210140.

Institutional review board statement: This study doesn't involve any human subjects.

Conflict-of-interest statement: All the authors report no relevant conflicts of interest for this article.

Country/Territory of origin: China

ORCID number: Jun-Tao Li 0000-0002-3288-4395; Hong-Mei Zhang 0009-0003-0914-1539; Wei Wang 0000-0002-9616-1145; Dong-Qing Wei 0000-0003-4200-7502.

S-Editor: Wang JJ
L-Editor: A
P-Editor: Cai YX

REFERENCES

1 **Sung H**, Ferlay J, Siegel RL, Laversanne M, Soerjomataram I, Jemal A, Bray F. Global Cancer Statistics 2020: GLOBOCAN Estimates of Incidence and Mortality Worldwide for 36 Cancers in 185 Countries. *CA Cancer J Clin* 2021; **71**: 209-249 [PMID: 33538338 DOI: 10.3322/caac.21660]
2 **Bakrania A**, Joshi N, Zhao X, Zheng G, Bhat M. Artificial intelligence in liver cancers: Decoding the impact of machine learning models in clinical diagnosis of primary liver cancers and liver cancer metastases. *Pharmacol Res* 2023; **189**: 106706 [PMID: 36813095 DOI: 10.1016/j.phrs.2023.106706]
3 **Villarruel-Melquiades F**, Mendoza-Garrido ME, García-Cuellar CM, Sánchez-Pérez Y, Pérez-Carreón JI, Camacho J. Current and novel approaches in the pharmacological treatment of hepatocellular carcinoma. *World J Gastroenterol* 2023; **29**: 2571-2599 [PMID: 37213397 DOI: 10.3748/wjg.v29.i17.2571]
4 **Fritz JM**, Lenardo MJ. Development of immune checkpoint therapy for cancer. *J Exp Med* 2019; **216**: 1244-1254 [PMID: 31068379 DOI: 10.1084/jem.20182395]
5 **Kalbasi A**, Ribas A. Tumour-intrinsic resistance to immune checkpoint blockade. *Nat Rev Immunol* 2020; **20**: 25-39 [PMID: 31570880 DOI: 10.1038/s41577-019-0218-4]
6 **Shen W**, Chen Y, Lei P, Sheldon M, Sun Y, Yao F, Ma L. Immunotherapeutic Approaches for Treating Hepatocellular Carcinoma. *Cancers (Basel)* 2022; **14** [PMID: 36291797 DOI: 10.3390/cancers14205013]
7 **Llovet JM**, Castet F, Heikenwalder M, Maini MK, Mazzaferro V, Pinato DJ, Pikarsky E, Zhu AX, Finn RS. Immunotherapies for hepatocellular carcinoma. *Nat Rev Clin Oncol* 2022; **19**: 151-172 [PMID: 34764464 DOI: 10.1038/s41571-021-00573-2]
8 **Donne R**, Lujambio A. The liver cancer immune microenvironment: Therapeutic implications for hepatocellular carcinoma. *Hepatology* 2023; **77**: 1773-1796 [PMID: 35989535 DOI: 10.1002/hep.32740]
9 **Thorgeirsson SS**, Lee JS, Grisham JW. Molecular prognostication of liver cancer: end of the beginning. *J Hepatol* 2006; **44**: 798-805 [PMID: 16488507 DOI: 10.1016/j.jhep.2006.01.008]
10 **Suvà ML**, Tirosh I. Single-Cell RNA Sequencing in Cancer: Lessons Learned and Emerging Challenges. *Mol Cell* 2019; **75**: 7-12 [PMID: 31299208 DOI: 10.1016/j.molcel.2019.05.003]
11 **Tang Y**, Guo C, Yang Z, Wang Y, Zhang Y, Wang D. Identification of a Tumor Immunological Phenotype-Related Gene Signature for Predicting Prognosis, Immunotherapy Efficacy, and Drug Candidates in Hepatocellular Carcinoma. *Front Immunol* 2022; **13**: 862527 [PMID: 35493471 DOI: 10.3389/fimmu.2022.862527]
12 **Wang Z**, Zhu J, Liu Y, Liu C, Wang W, Chen F, Ma L. Development and validation of a novel immune-related prognostic model in hepatocellular carcinoma. *J Transl Med* 2020; **18**: 67 [PMID: 32046766 DOI: 10.1186/s12967-020-02255-6]
13 **Yofe I**, Dahan R, Amit I. Single-cell genomic approaches for developing the next generation of immunotherapies. *Nat Med* 2020; **26**: 171-177 [PMID: 32015555 DOI: 10.1038/s41591-019-0736-4]
14 **Yang D**, Kuang T, Zhou Y, Su Y, Shen J, Yu B, Zhao K, Ding Y. Tumor-associated endothelial cell prognostic risk model and tumor immune environment modulation in liver cancer based on single-cell and bulk RNA sequencing: Experimental verification. *Int Immunopharmacol* 2023; **124**: 110870 [PMID: 37690233 DOI: 10.1016/j.intimp.2023.110870]
15 **Li J**, Zhang H, Mu B, Zuo H, Zhou K. Identifying phenotype-associated subpopulations through LP_SGL. *Brief Bioinform* 2023; **25** [PMID: 38008419 DOI: 10.1093/bib/bbad424]
16 **Zhou G**, Boor PPC, Bruno MJ, Sprengers D, Kwekkeboom J. Immune suppressive checkpoint interactions in the tumour microenvironment of primary liver cancers. *Br J Cancer* 2022; **126**: 10-23 [PMID: 34400801 DOI: 10.1038/s41416-021-01453-3]
17 **Zhang Q**, Lou Y, Bai XL, Liang TB. Immunometabolism: A novel perspective of liver cancer microenvironment and its influence on tumor progression. *World J Gastroenterol* 2018; **24**: 3500-3512 [PMID: 30131656 DOI: 10.3748/wjg.v24.i31.3500]
18 **Ma L**, Heinrich S, Wang L, Keggenhoff FL, Khatib S, Forgues M, Kelly M, Hewitt SM, Saif A, Hernandez JM, Mabry D, Kloeckner R, Greten TF, Chaisaingmongkol J, Ruchirawat M, Marquardt JU, Wang XW. Multiregional single-cell dissection of tumor and immune cells reveals stable lock-and-key features in liver cancer. *Nat Commun* 2022; **13**: 7533 [PMID: 36476645 DOI: 10.1038/s41467-022-35291-5]
19 **Jin S**, Guerrero-Juarez CF, Zhang L, Chang I, Ramos R, Kuan CH, Myung P, Plikus MV, Nie Q. Inference and analysis of cell-cell communication using CellChat. *Nat Commun* 2021; **12**: 1088 [PMID: 33597522 DOI: 10.1038/s41467-021-21246-9]
20 **Ma L**, Hernandez MO, Zhao Y, Mehta M, Tran B, Kelly M, Rae Z, Hernandez JM, Davis JL, Martin SP, Kleiner DE, Hewitt SM, Ylaya K, Wood BJ, Greten TF, Wang XW. Tumor Cell Biodiversity Drives Microenvironmental Reprogramming in Liver Cancer. *Cancer Cell* 2019; **36**: 418-430.e6 [PMID: 31588021 DOI: 10.1016/j.ccell.2019.08.007]
21 **Ritchie ME**, Phipson B, Wu D, Hu Y, Law CW, Shi W, Smyth GK. limma powers differential expression analyses for RNA-sequencing and

microarray studies. *Nucleic Acids Res* 2015; **43**: e47 [PMID: 25605792 DOI: 10.1093/nar/gkv007]

22 **Friedman J**, Hastie T, Tibshirani R. Regularization Paths for Generalized Linear Models *via* Coordinate Descent. *J Stat Softw* 2010; **33**: 1-22 [PMID: 20808728 DOI: 10.18637/jss.v033.i01]

23 **Zhang R**, Gao X, Zuo J, Hu B, Yang J, Zhao J, Chen J. STMN1 upregulation mediates hepatocellular carcinoma and hepatic stellate cell crosstalk to aggravate cancer by triggering the MET pathway. *Cancer Sci* 2020; **111**: 406-417 [PMID: 31785057 DOI: 10.1111/cas.14262]

24 **Li S**, Xu L, Wu G, Huang Z, Huang L, Zhang F, Wei C, Shen Q, Li R, Zhang L, Xu X. Remodeling Serine Synthesis and Metabolism *via* Nanoparticles (NPs)-Mediated CFL1 Silencing to Enhance the Sensitivity of Hepatocellular Carcinoma to Sorafenib. *Adv Sci (Weinh)* 2023; **10**: e2207118 [PMID: 37203277 DOI: 10.1002/advs.202207118]

25 **Xia Y**, Zhou L, Yang HC, Yu CW. Chemokine CCL5 immune subtypes of human liver cancer with prognostic significance. *Int Immunopharmacol* 2022; **113**: 109372 [PMID: 36332449 DOI: 10.1016/j.intimp.2022.109372]

26 **Barbie DA**, Tamayo P, Boehm JS, Kim SY, Moody SE, Dunn IF, Schinzel AC, Sandy P, Meylan E, Scholl C, Fröhling S, Chan EM, Sos ML, Michel K, Mermel C, Silver SJ, Weir BA, Reiling JH, Sheng Q, Gupta PB, Wadlow RC, Le H, Hoersch S, Wittner BS, Ramaswamy S, Livingston DM, Sabatini DM, Meyerson M, Thomas RK, Lander ES, Mesirov JP, Root DE, Gilliland DG, Jacks T, Hahn WC. Systematic RNA interference reveals that oncogenic KRAS-driven cancers require TBK1. *Nature* 2009; **462**: 108-112 [PMID: 19847166 DOI: 10.1038/nature08460]

27 **Charoentong P**, Finotello F, Angelova M, Mayer C, Efremova M, Rieder D, Hackl H, Trajanoski Z. Pan-cancer Immunogenomic Analyses Reveal Genotype-Immunophenotype Relationships and Predictors of Response to Checkpoint Blockade. *Cell Rep* 2017; **18**: 248-262 [PMID: 28052254 DOI: 10.1016/j.celrep.2016.12.019]

28 **Subbiah V**, Solit DB, Chan TA, Kurzrock R. The FDA approval of pembrolizumab for adult and pediatric patients with tumor mutational burden (TMB) ≥10: a decision centered on empowering patients and their physicians. *Ann Oncol* 2020; **31**: 1115-1118 [PMID: 32771306 DOI: 10.1016/j.annonc.2020.07.002]

29 **Jiang P**, Gu S, Pan D, Fu J, Sahu A, Hu X, Li Z, Traugh N, Bu X, Li B, Liu J, Freeman GJ, Brown MA, Wucherpfennig KW, Liu XS. Signatures of T cell dysfunction and exclusion predict cancer immunotherapy response. *Nat Med* 2018; **24**: 1550-1558 [PMID: 30127393 DOI: 10.1038/s41591-018-0136-1]

World Journal of Gastroenterology

Submit a Manuscript: https://www.f6publishing.com

World J Gastroenterol 2024 March 21; 30(11): 1621-1635

DOI: 10.3748/wjg.v30.i11.1621

ISSN 1007-9327 (print) ISSN 2219-2840 (online)

META-ANALYSIS

Effects of neoadjuvant chemotherapy *vs* chemoradiotherapy in the treatment of esophageal adenocarcinoma: A systematic review and meta-analysis

Armand Csontos, Alíz Fazekas, Lajos Szakó, Nelli Farkas, Csenge Papp, Szilárd Ferenczi, Szabolcs Bellyei, Péter Hegyi, András Papp

Specialty type: Gastroenterology and hepatology

Provenance and peer review: Invited article; Externally peer reviewed.

Peer-review model: Single blind

Peer-review report's scientific quality classification

Grade A (Excellent): A
Grade B (Very good): 0
Grade C (Good): 0
Grade D (Fair): 0
Grade E (Poor): 0

P-Reviewer: Haddadi S, Algeria

Received: December 23, 2023
Peer-review started: December 23, 2023
First decision: January 4, 2024
Revised: January 18, 2024
Accepted: March 4, 2024
Article in press: March 4, 2024
Published online: March 21, 2024

Armand Csontos, Csenge Papp, Szilárd Ferenczi, András Papp, Department of Surgery, University of Pécs, Medical School, Clinical Center, Pécs H-7624, Baranya, Hungary

Alíz Fazekas, Nelli Farkas, Institute of Bioanalysis, University of Pécs, Medical School, Pécs H-7624, Baranya, Hungary

Alíz Fazekas, Nelli Farkas, Péter Hegyi, Institute for Translational Medicine, University of Pécs, Medical School, Pécs H-7624, Baranya, Hungary

Lajos Szakó, Department of Emergency Medicine, Clinical Center, University of Pécs, Medical School, Pécs 7624, Baranya, Hungary

Szabolcs Bellyei, Department of Oncotherapy, University of Pécs, Medical School, Clinical Center, Pécs H-7624, Baranya, Hungary

Péter Hegyi, Centre for Translational Medicine, Semmelweis University, Budapest 1085, Hungary

Péter Hegyi, Institute of Pancreatic Diseases, Semmelweis University, Budapest H-1083, Hungary

Corresponding author: Armand Csontos, MD, Doctor, Department of Surgery, University of Pécs, Medical School, Clinical Center, Ifjúság Street 13, Pécs H-7624, Baranya, Hungary. csontos.armand@gmail.com

Abstract

BACKGROUND

Neoadjuvant therapy is an essential modality for reducing the clinical stage of esophageal cancer; however, the superiority of neoadjuvant chemotherapy (nCT) or neoadjuvant chemoradiotherapy (nCRT) is unclear. Therefore, a discussion of these two modalities is necessary.

AIM

To investigate the benefits and complications of neoadjuvant modalities.

METHODS

To address this concern, predefined criteria were established using the PICO

protocol. Two independent authors performed comprehensive searches using predetermined keywords. Statistical analyses were performed to identify significant differences between groups. Potential publication bias was visualized using funnel plots. The quality of the data was evaluated using the Risk of Bias Tool 2 (RoB2) and the GRADE approach.

RESULTS

Ten articles, including 1928 patients, were included for the analysis. Significant difference was detected in pathological complete response (pCR) [$P < 0.001$; odds ratio (OR): 0.27; 95%CI: 0.16-0.46], 30-d mortality ($P = 0.015$; OR: 0.4; 95%CI: 0.22-0.71) favoring the nCRT, and renal failure ($P = 0.039$; OR: 1.04; 95%CI: 0.66-1.64) favoring the nCT. No significant differences were observed in terms of survival, local or distal recurrence, or other clinical or surgical complications. The result of RoB2 was moderate, and that of the GRADE approach was low or very low in almost all cases.

CONCLUSION

Although nCRT may have a higher pCR rate, it does not translate to greater long-term survival. Moreover, nCRT is associated with higher 30-d mortality, although the specific cause for postoperative complications could not be identified. In the case of nCT, toxic side effects are suspected, which can reduce the quality of life. Given the quality of available studies, further randomized trials are required.

Key Words: Neoadjuvant; Chemotherapy; Chemoradiotherapy; Esophageal cancer; Adenocarcinoma

Core Tip: Neoadjuvant chemoradiation increases pathological complete response and 30-d mortality in patients with esophageal adenocarcinoma; however, it has no effect on long-term survival. It may be associated with side effects that can reduce the quality of life.

Citation: Csontos A, Fazekas A, Szakó L, Farkas N, Papp C, Ferenczi S, Bellyei S, Hegyi P, Papp A. Effects of neoadjuvant chemotherapy *vs* chemoradiotherapy in the treatment of esophageal adenocarcinoma: A systematic review and meta-analysis. *World J Gastroenterol* 2024; 30(11): 1621-1635

URL: https://www.wjgnet.com/1007-9327/full/v30/i11/1621.htm

DOI: https://dx.doi.org/10.3748/wjg.v30.i11.1621

INTRODUCTION

Epidemiology

Esophageal cancer (EC) is the eighth most prevalent cancer, with more than 500000 cases worldwide, and it is the sixth leading cause of tumor mortality. Squamous cell carcinoma (SCC) is still the leading subtype in the Asian EC Belt; however, in Western countries, such as North America, Oceania, and Western and Northern Europe, including Hungary, the incidence rate of adenocarcinoma (AC) has been increasing, surpassing that of SCC[1,2].

In the early stages, surgery can lead to full recovery; however, an advanced tumor stage at initial diagnosis can result in high morbidity and mortality rates[3]. Esophagectomy with radical lymphadenectomy is one of the most invasive gastrointestinal procedures. To improve treatment results, a multidisciplinary approach is important, including the application of the enhanced recovery after surgery protocol[4,5], the minimally invasive approach of esophagectomy[6], and neoadjuvant oncological therapy, which can decrease mortality by 25%-35% compared with that of surgery alone[7-9].

Impact of the topic

The superiority of neoadjuvant therapy has been proven in several meta-analyses[7-9]. Neoadjuvant chemotherapy (nCT) or preoperative neoadjuvant chemoradiotherapy (nCRT) can also improve oncologic endpoints[8-15], increase overall and progression-free surveillance, and pathological complete response (pCR); however, it may also be associated with numerous clinical or surgical side effects and impaired quality of life. Therefore, the cost-benefit balance of these modalities is still unclear, especially in cases of AC of the esophagus and esophagogastric junction (GEJ).

Literature background

Previous meta-analyses have numerous limitations, including patients with SCC and AC as a homogenous population. Therefore, the results cannot be clearly applied to either subtype.

Impact of our analysis

We performed a comprehensive, up-to-date investigation to determine whether nCT or nCRT yields more favorable results in the surgical treatment of AC of the esophagus and esophageal junction.

MATERIALS AND METHODS

Protocol registration

The objectives and methodologies of this meta-analysis were predefined in a protocol registered with PROSPERO[16]. The registration was accepted on November 01, 2023, under the number CRD42023478615.

Question of the review

To define the scope of this meta-analysis, we used the PICO protocol, focusing on patients with esophageal or cardiac AC, who received neoadjuvant therapy before surgery. Intervention assessed was preoperative nCT, which was compared to nCRT. We investigated the following outcomes: Survival, remission rate, mortality, short- and long-term clinical and surgical complications, and quality of life. First, we planned to investigate only randomized controlled trials (RCTs) to minimize the risk of bias; however, to achieve an adequate sample size and robust conclusions, propensity score matched and high-quality cohort studies were also included. Studies that did not strictly involve patients with AC were excluded.

Search strategy and search terms

We conducted a comprehensive search on September 15, 2023, using PubMed, Embase, Cochrane, Web of Science, and Scopus databases. We used previously defined search terms, including "neoadjuvant," "chemotherapy," "chemoradiotherapy," "esophageal cancer," "esophagectomy," and other random keywords, and their variants. The retrieved datasets were imported into the EndNote (ver. x9.3.3; Alfasoft AB, Göteborg, Sweden) library.

Selection process

Two independent authors conducted the selection process using EndNote software. The Cohen's kappa coefficients were calculated from these results. Discrepancies were resolved through consensus.

Data extraction

Data were extracted from text, figures, and tables of the included articles by two independent authors, with any discrepancies resolved through mutual agreement. Plot digitizer applications were used to collect data not provided in a numerical format[17]. Excel (Office 365, Microsoft, Redmond, WA, United States) datasheets were used to collect and organize the datasets. Descriptive data collected included study characteristics (author, year, type, and number of elements), patients demographics (age, sex, and performance), tumors (stage, location), and therapy (neoadjuvant regimen, surgical procedure). A meta-analysis was performed on outcomes with at least four homogeneous datasets. Outcomes, ineligible for statistical analysis, were qualitatively described. The outcomes assessed included pCR, surveillance (overall, progression-free, disease-free), mortality (30 or 90 d), tumor remission (local or distant), clinical complications (thromboembolism, respiratory and cardiac complications, renal failure, neutropenia) and surgical complication (anastomotic and chyle leakage, wound infection, bleeding, vocal cord paresis).

Statistical analysis

A random-effects meta-analysis was performed. Odds ratios (OR) with 95%CI were calculated to measure the effect size. To calculate the OR and pooled odds ratio, data for the total number of patients and those experiencing the event of interest in each group separately (referred as "raw data") was extracted or calculated from the studies, where it was available. The results are presented as the odds of an event of interest in the experimental group *vs* the control group. The results were considered statistically significant if the pooled CI did not contain a null value. We also performed a supplementary analysis. Using the WebPlotDigitizer online tool, we digitalized the Kaplan-Meier (KM) curves published in the involved studies. Then, by applying the methodology of Guyot *et al*[18,19], we estimated the individual patient time-to-event data. Finally, we plotted all the available KM curves in the same figure. Using the estimated raw data, we calculated the hazard ratio (HR) within the studies and the pooled HR. A less than one HR suggests a smaller risk in the experimental group. The HR result was considered significant if it was not included in the confidence interval.

We visualized the findings in forest plots. Where applicable-the study number was large enough and not too heterogeneous-we also reported the prediction intervals (*i.e.*, the expected range of effects of future studies) of the results. Additionally, between-study heterogeneity was described using Higgins and Thompson's (I^2) statistics (Higgins and Thompson[20], in 2002).

Publication bias was assessed by visual inspection of the funnel plots and calculation of the Harbord (modified Egger's) test *P* value[21] for the OR effect size. We assumed the presence of a possible small study bias if the *P* value was < 10%. However, we kept in mind that the test has limited diagnostic assessment (below 10 studies). Potential outlier publications were explored using different influence measures and plots following the recommendations of Harrer *et al* [22]. All statistical analyses were performed with R (R Core Team 2023, v4.3.0)[23] using the meta (Schwarzer 2023, v6.2.1) [24] package for basic meta-analysis calculations and plots, IPDfromKM for raw data simulations, and the dmetar (v0.0.9000)[25] package for additional influential analysis calculations and plots. To pool the effect size, the pooled OR based on raw data was calculated using the Mantel-Haenszel method[26,27]. The Exact Mantel-Haenszel method

(without continuity correction) was used to handle zero-cell counts[28,29]. We used the Hartung-Knapp adjustment[30,31] for the CIs. To estimate the heterogeneity variance measure for the raw data OR calculation, the Paule-Mandel method[32] (recommended by Veroniki *et al*[33]) was used with the Q profile method for the confidence interval. Prediction interval calculations were based on the t-distribution. In the case of 0 cell counts, individual study OR with 95%CI was calculated by adding 0.5, as continuity correction (it was used only for visualization on forest plot). The pooled HR was calculated using classical inverse-variance meta-analysis of log-transformed HR ratios using the REML heterogeneity variance estimator.

Descriptive analyses were performed by calculating the means, standard deviations, and percentages. The mean estimates from the median and range were calculated as follows[34]:

Risk of bias and certain of evidence

The Risk of Bias Tool 2 (RoB2) and GRADE approaches were used to assess the quality of the articles and our research.

RESULTS

Search process

A total of 1285 articles were identified from the five databases. After removing duplicates, 1141 articles were screened, after which 485 and 153 articles were selected based on title and abstract screening, respectively. Subsequently, 125 full-text reports were examined, and eight studies were included in the quantitative synthesis. Cohen's kappa indicated 99.74% substantial agreement (Cohen's k: 0.77). Some reports could not be retrieved as they were conference abstracts [28]. Articles were excluded based on predefined criteria (83 articles), including those covering only SCCs (9 articles) or mixed group of ACs and SCCs (23 articles), mentioning no pathological subtype (1 article), and being a preliminary trial (1 article). Two additional articles were included during the screening of previous reviews. Overall, the analysis included ten articles. More information is provided in Figure 1.

Characteristics of the studies

Ten articles, published between 2011 and 2018, were included in this meta-analysis. Seven studies were conducted in Europe, two in Australia, and one in the United States[35-44]. Of the 10 studies, two were RCTs[43,44], four were propensity score-matched cohort study[39-42], and four were cohort study based on prospective institutional databases (clinical cancer registry)[35-38]. Six studies were single-center trials[36,39,40,42-44]. The articles collectively included data from 1928 patients, with 956 and 972 patients the nCT and nCRT groups, respectively. All included patients had esophageal ACs. Additional details are provided in Table 1.

Characteristics of the patients

The estimated mean age of the patients in both the groups was 60 years. The age range was 12-84 and 19-83 years. The nCT and nCRT groups included 829 (91%) and 857 (94%) male patients, respectively. Based on the available data, 84%, 16% and < 0.1% of the patients had American Society of Anesthesiologists scores of I-II, III, and IV, respectively. The patients had coronary morbidity (18%), diabetes mellitus (16%), pulmonary morbidity, chronic obstructive pulmonary disease (9%), history of malignancy (6%), and history of smoking (42%). More detailed information is summarized in Supplementary Table 1.

Characteristics of the tumor and pathological approach

Based on the available data, 99% of the tumors were diagnosed in the lower third of the esophagus or the GEJ. Clinical T-stages 1-4 accounted for 1%, 16%, 80%, and 3% of the cases, respectively. Nodal involvement was observed in 367 (61%) and 350 patients (59%) in the nCT and nCRT groups, respectively. Tumor differentiation was good in 2% and 1%, moderate in 36% and 31%, and poor in 57% and 64% of patients in the nCT and nCRT groups, respectively. Margin negative resection (R0) was performed in 696 (81%) and 800 (92%) patients in the nCT and nCRT groups. Pathological T-stage 1-4 accounted for 13%, 15%, 22%, and 47% of the cases, respectively, whereas N-stages 0-3 accounted for 45%, 31%, 14%, and 9% of the cases, respectively. Tumor regression grade (TRG, Mandard) stages 1-4/5 (in the nCT and nCRT groups) accounted for 14% (6%-22%), 17% (7%-26%), 24% (18%-29%), and 42% (62%-22%) of the cases, respectively additional details are provided in Supplementary Table 2.

Characteristics of the neoadjuvant therapy

Neoadjuvant regimens were administered to patients in both groups. The most frequently used neoadjuvant drugs were cisplatin, 5-fluorouracil, and docetaxel. The CROSS protocol was the most commonly used protocol in the chemoradiation group. Additional details are provided in Table 2[7,8,10,45-48].

Characteristics of the surgical procedure

Based on the available data, Ivor-Lewis (transthoracic), Orringer (transhiatal), McKeown (thoraco-abdomino-cervical) esophagectomies, and total gastrectomy were performed in 67%, 23%, 5%, and 4% of the patients, respectively. Minimally invasive or hybrid surgery techniques were performed in 27% and 51% of the patients, respectively, and open surgery was performed in only 23% of the patients. Two-field lymphadenectomy was the standard procedure in 74% of the patients, whereas three-field lymphadenectomy was performed in only 5% of the patients. Additional details are

Table 1 Characteristic of the studies

Ref.	Design	Center	Country	Year	Number of patients	nCT	nCRT	AC, %
Stahl *et al*[44], 2017	RCT, Phase III	1	Germany	N/A	119	59	60	100
Burmeister *et al*[43], 2011	RCT, Phase II	1	Australia	N/A	75	36	39	100
Visser *et al*[42], 2018	PSM	1	Australia	2000-2017	262	131	131	100
Markar *et al*[41], 2017	PSM	10	United Kingdom	2001-2012	442	221	221	100
Goense *et al*[40], 2017	PSM	1	Netherlands	2006-2015	172	86	86	100
Favi *et al*[39], 2017	PSM	1	Germany	2011-2015	80	40	40	100
Anderegg *et al*[35], 2017	Cohort, PID	3	Netherlands	2005-2011	313	137	176	100
Spicer *et al*[38], 2016	Cohort, PID	3	United States	2002-2012	214	114	100	100
Luc *et al*[36], 2015	Cohort, PID	1	France	2000-2012	116	61	55	100
Münch *et al*[37], 2018	Cohort, PCCR	70	Germany	1998-2014	135	71	64	100

RCT: Randomized controlled trial; PSM: Propensity score matched cohort; PID: Prospective institutional databases; PCCR: Population-based clinical cancer registry; N/A: Not applicable; nCT: Neoadjuvant chemotherapy; nCRT: Neoadjuvant chemoradiotherapy; AC: Adenocarcinoma.

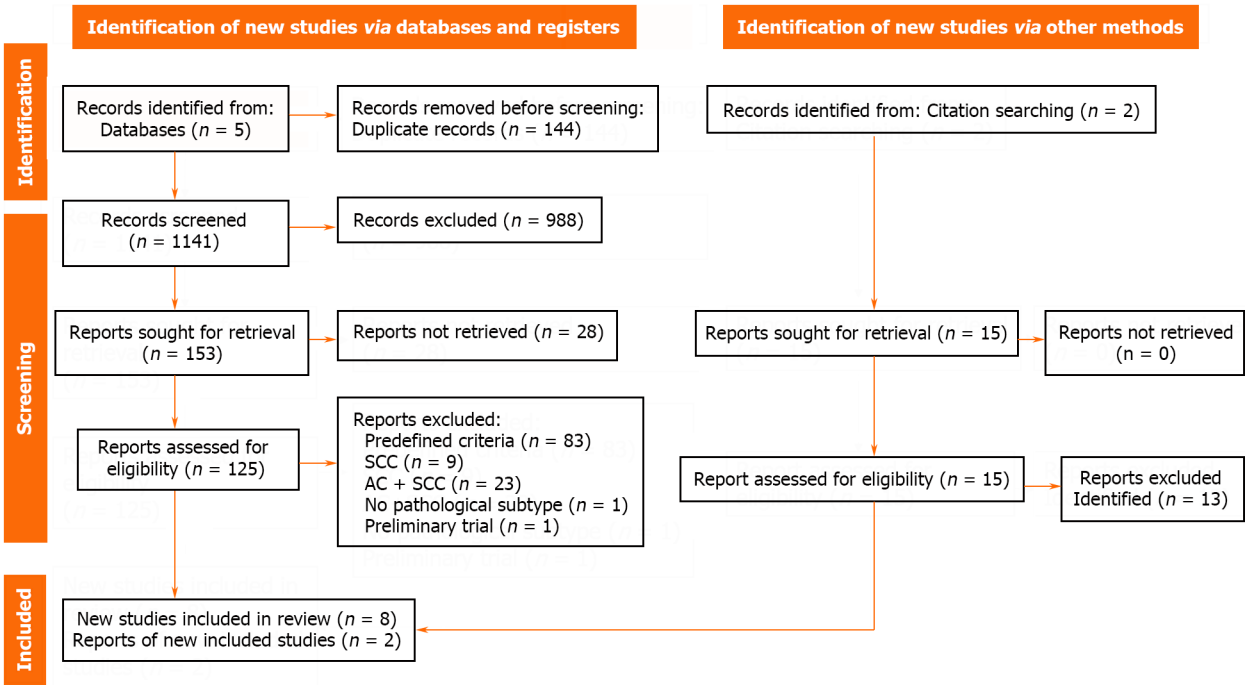

Figure 1 The preferred reporting items for systematic reviews and meta-analyses flow diagram flowchart shows the number of articles (*n*) in the different selection stages of the selection process. AC: Adenocarcinoma; SCC: Squamous cell carcinoma.

provided in Supplementary Table 3.

Pathological complete response

Data from eight studies, covering a total of 1547 patients, were analyzed[35,36,39-44]. The OR (pooled effect size) was 0.27 (95%CI: 0.16-0.46). A significant difference was observed, favoring nCRT over nCT ($P < 0.001$). Between-study heterogeneity, expressed as the I^2 value, was 0.29 (95%CI: 0-0.68; Figure 2).

Thirty-day mortality

Data from four studies, including 899 patients, were analyzed[38,40,41,43]. The OR was 0.4 (95%CI: 0.22-0.71). A significant difference was observed, favoring nCRT over nCT ($P = 0.015$), with no between-study heterogeneity (I^2 value:

Table 2 Characteristic of the neoadjuvant regimen, *n* (%)

Ref.	nCT	nCRT	
	Chemotherapy	Chemotherapy	Irradiation
Stahl *et al*[44], 2017	15 × weekly CFFa	15 × weekly CFFa followed by 3 wk course of CRT + 1 cycle CE	30 Gy in 15 fractions of 2 Gy in 3 wk
Burmeister *et al*[43], 2011	C (80 mg/m^2) + iv 5-FU (1000 mg/m^2/d) on days 1 and 21	CF + RT, 5-FU reduced to 800 mg/m^2/d (on day 21)	35 Gy in 15 fractions in 3 wk (on day 21)
Visser *et al*[42], 2018	OEO2	OEO2 + RT	35 Gy in 15 fractions or 45 Gy in 25 fractions
	MAGIC	DCF (2 cycles pre-operatively) + RT	45 Gy in 25 fractions
	DCF (2 cycles pre-operatively)	CROSS (since 2015)	41.4 Gy in 23 fractions of 1.8 Gy in 5 wk
	Cisplatin + 5-FU: 92 (70)	Cisplatin + 5-FU: 94 (72)	35 Gy: 69 (53)
	Epirubicin, cisplatin, 5-FU: 30 (23)	Epirubicin, cisplatin, 5-FU: 2 (2)	41 Gy: 14 (11)
	Carboplatin + paclitaxel: 0 (0)	Carboplatin + paclitaxel: 20 (15)	45 Gy: 40 (31)
	Other: 9 (7)	Other: 15 (11)	Other: 8 (6)
Markar *et al*[41], 2017	mainly MAGIC, OEO2 or OEO5 regimens[8,10,45]	CROSS regimen[7,46]	41.4 Gy in 23 fractions of 1.8 Gy in 5 wk
Goense *et al*[40], 2017	ECX	CROSS regimen[7,46]	41.4 Gy in 23 fractions of 1.8 Gy in 5 wk
Favi *et al*[39] , 2017	FLOT[47]	CROSS regimen[7,46]	41.4 Gy in 23 fractions of 1.8 Gy in 5 wk
Anderegg *et al*[35], 2017	ECX	CROSS regimen[7,46]	41.4 Gy in 23 fractions of 1.8 Gy in 5 wk
Spicer *et al*[38], 2016	Cornell: Platinum or taxane-based doublet, or both	concurrent ChT + RT	50.4 Gy
	McGill: DCF (3 cycles)[48]		
Luc *et al*[36], 2015	DCF (3 cycles pre- and postoperatively)	continuous iv 5-FU 750 mg/m^2/d on days 1–5 by, C 20 mg/m^2 on day 1	45 Gy for 5 d per week at 1.8 Gy/d (started on day 28 along with the second CT cycle)
Münch *et al*[37], 2018	N/A	N/A	N/A

OEO2: Two cycles of cisplatin and 5-fluoruracil (5-FU). OEO5: Five cycles of cisplatin and 5-FU. CFFa: 15 × weekly 5-FU (2000 mg/m^2, 24 h infusion)/Fa (500 mg/m^2, 2 h infusion) and biweekly cisplatin (50 mg/m^2, 1 h infusion), in 14 wk. MAGIC: Protocol epirubicin, cisplatin, and 5-FU for three cycles before andthree cycles after esophagectomy (EGJ Siewert II EAC and good vital status). DCF: Docetaxel 75 mg/m^2 (on day 1), cisplatin 75 mg/m^2 (on day 1), and 5-FU 750 mg/m^2/d by continuous infusion on days 2–5, (day 1 = day 22 = day 43). CROSS: With concurrent weekly administration of carboplatin (targeted at an area under the curve of 2 mg/mL per min) and paclitaxel (50 mg/m^2 of body-surface area). Forty-one four Gy in 23 fractions of 1.8 Gy in 5 wk. FLOT: 5-FU/leucovorin, oxaliplatin, and docetaxel 50 mg/m^2 every 2 wk. ECX: Pre- and postoperative 3-wk cycles epirubicin (50 mg/m^2) and cisplatin (60 mg/m^2), followed by 1000 mg/m^2 of capecitabine twice daily for 14 d or 625 mg/m^2 of capecitabine twice daily for 21 d. Adaptations to the regimen such as dose reduction or change of regimen to oxaliplatin or 5-FU were applied when necessary. C: Cisplatin; F: Fluorouracil; P: Paclitaxel; Fa: Folinic acid; E: Etoposide; N/A: Not applicable; nCT: Neoadjuvant chemotherapy; nCRT: Neoadjuvant chemoradiotherapy; AC: Adenocarcinoma; CRT: Chemoradiotherapy; CT: Chemotherapy; RT: Radiotherapy; 5-FU: 5-fluoruracil.

0; 95%CI: 0-0.85; Figure 3).

Ninety-day mortality

Data from four studies, encompassing 108 patients, were analyzed[38,40-42]. The OR was 0.71 (95%CI: 0.28-1.84). No significant difference was observed between nCRT and nCT (P = 0.34), with no between-study heterogeneity (I^2 value: 0; 95%CI: 0-0.85; Supplementary Figure 1).

Overall survival

The KM curves and logHR analysis conducted for eight studies encompassing 1540 patients did not reveal significant differences between the two groups in terms of overall survival (P = 0.82)[36-42,44]. The OR was 0.98 (95%CI: 0.77-1.23) and between-study heterogeneity was 0.35 (95%CI: 0-0.71; Figures 4 and 5).

Considering the 12-month overall survival (OS), nine studies including 1588 patients were selected for analysis[36-44]. The OR was 1.08 (95%CI: 0.8-1.46). No significant difference was observed between the two groups (P = 0.551). The between-study heterogeneity was 0.05 (95%CI, 0-0.67; Supplementary Figure 2). The log HR analysis revealed no

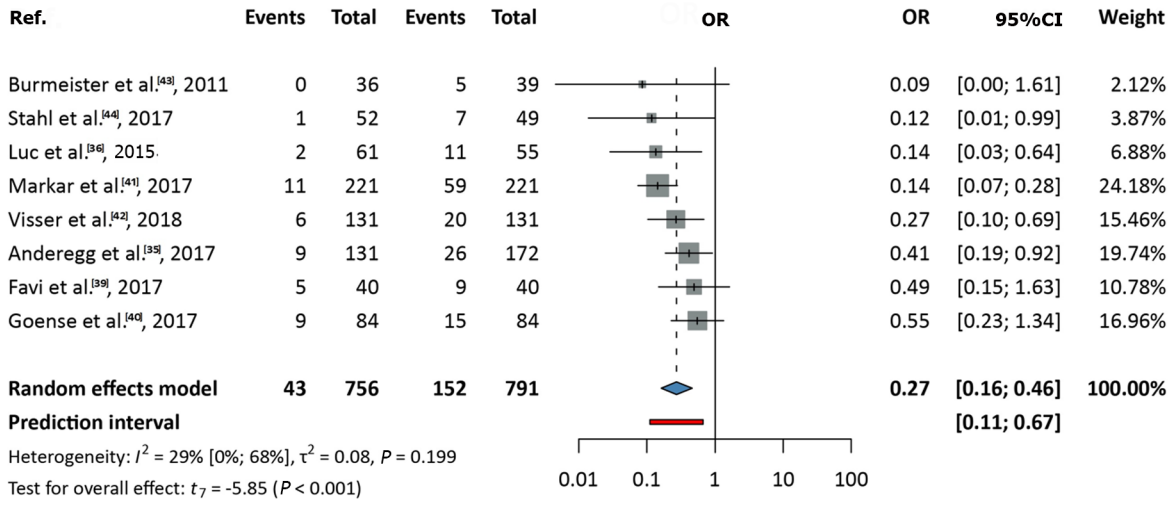

Figure 2 Analysis of pathological complete response. OR: Odds ratio.

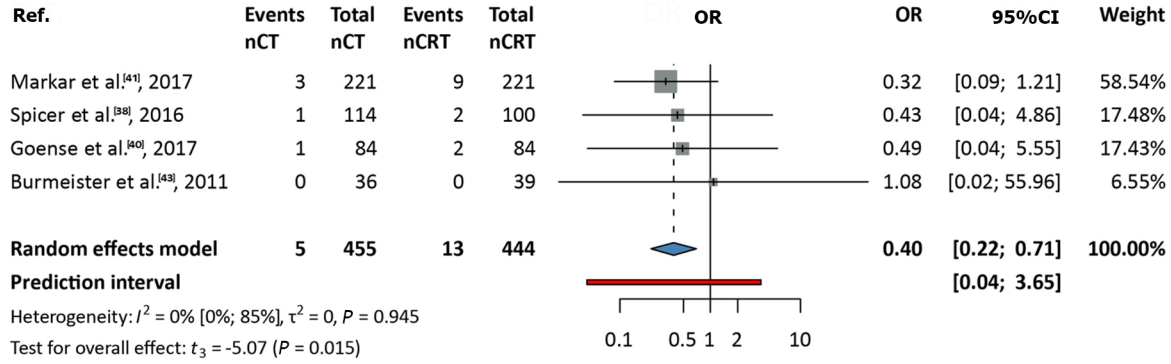

Figure 3 Analysis of the 30-d mortality. nCT: Neoadjuvant chemotherapy; nCRT: Neoadjuvant chemoradiotherapy; OR: Odds ratio.

significant differences between the groups (Supplementary Figure 3).

For the 24-month OS, the OR was 1.03 (95%CI: 0.73-1.45)[36-44]. No significant difference was observed between the two groups (P = 0.858). The between-study heterogeneity was 0.42 (95%CI: 0-0.73; Supplementary Figure 4). The log HR analysis revealed no significant differences between the groups (Supplementary Figure 5).

Considering the 36-month OS, the OR was 0.93 (95%CI: 0.54-1.6)[36-44]. No significant difference was observed between the two groups (P = 0.754). The between-study heterogeneity was 0.73 (95%CI: 0.47-0.86; Supplementary Figure 6). The logHR analysis revealed no significant differences between the groups (Supplementary Figure 7).

Considering the 48-month OS, seven studies including 1066 patients were selected for analysis[36-38,40,42-44]. The OR was 0.67 (95%CI: 0.27-0.85). No significant difference was observed between the two groups (P = 0.616). The between-study heterogeneity was 0.67 (95%CI: 0.27-0.85; Supplementary Figure 8). The log HR analysis revealed no significant differences between the groups (Supplementary Figure 9).

Considering the 60-month OS, the OR was 1.15 (95%CI: 0.56-2.35)[36-38,40,42-44]. No significant difference was observed between the two groups (P = 0.658). The between-study heterogeneity was 0.67 (95%CI: 0.27-0.85; Supplementary Figure 10).

Disease-free survival

The KM curves and logHR analysis conducted for two studies including 578 patients did not reveal significant differences in overall survival between the two groups (P = 0.85)[36,38,42]. The OR was 1.04 (95%CI: 0.5-2.16). The between-study heterogeneity was 0.49 (95%CI: 0-0.85; Supplementary Figures 11 and 12).

Considering the 12-month Disease-free survival (DFS), the OR was 0.93 (95%CI: 0.44-1.97)[36,38,42]. No significant difference was observed between the two groups (P = 0.702). The between-study heterogeneity was 0.07 (95%CI: 0-0.9; Supplementary Figure 13). The logHR analysis revealed no significant differences between the groups (Supplementary Figure 14).

Considering the 24-month DFS, the OR was 0.95 (95%CI: 0.49-1.86)[36,38,42]. No significant difference was observed between the two groups (P = 0.789). The between-study heterogeneity was 0 (95%CI: 0-0.9; Supplementary Figure 15). The logHR analysis revealed no significant differences between the groups (Supplementary Figure 16).

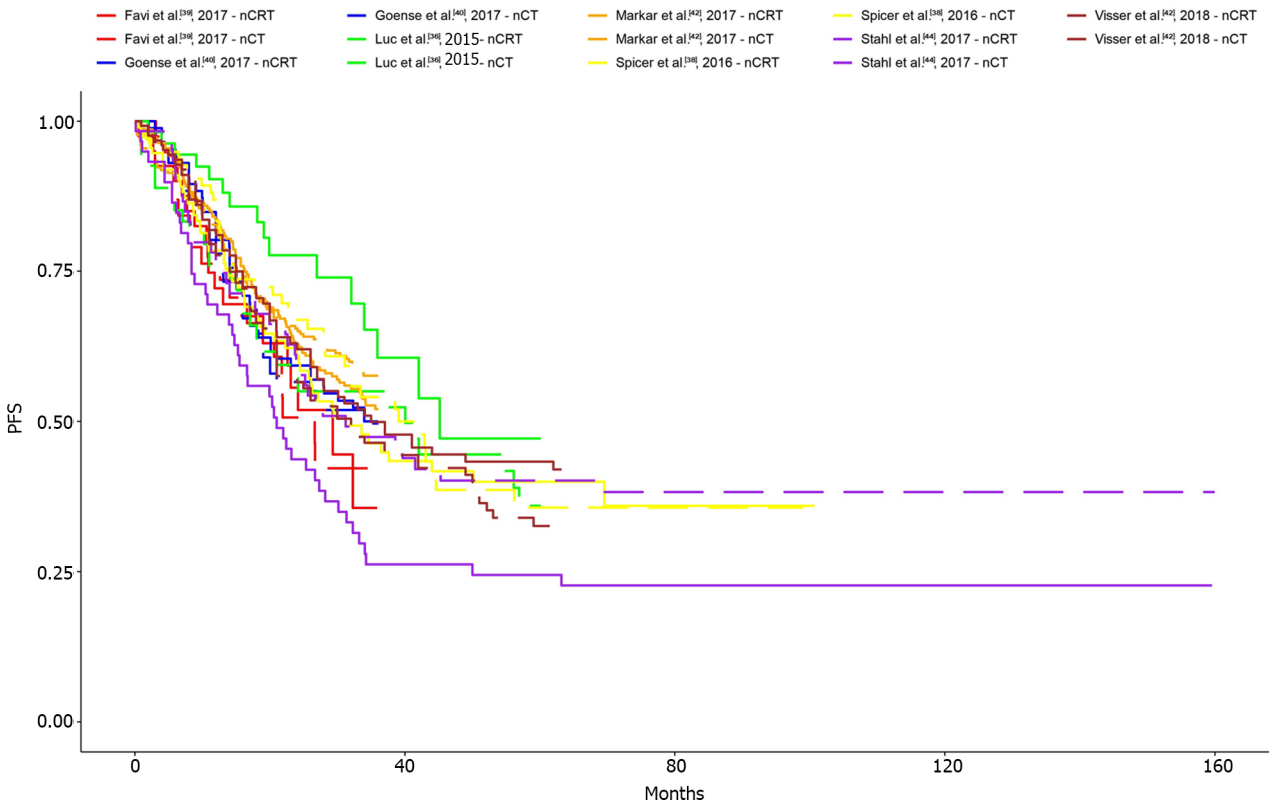

Figure 4 The Kaplan-Meier curves for the overall survival. The x-axis shows the time in month, the y-axis shows the number of patients in percentage. nCT: Neoadjuvant chemotherapy; nCRT: Neoadjuvant chemoradiotherapy; PFS: Progression-free survival.

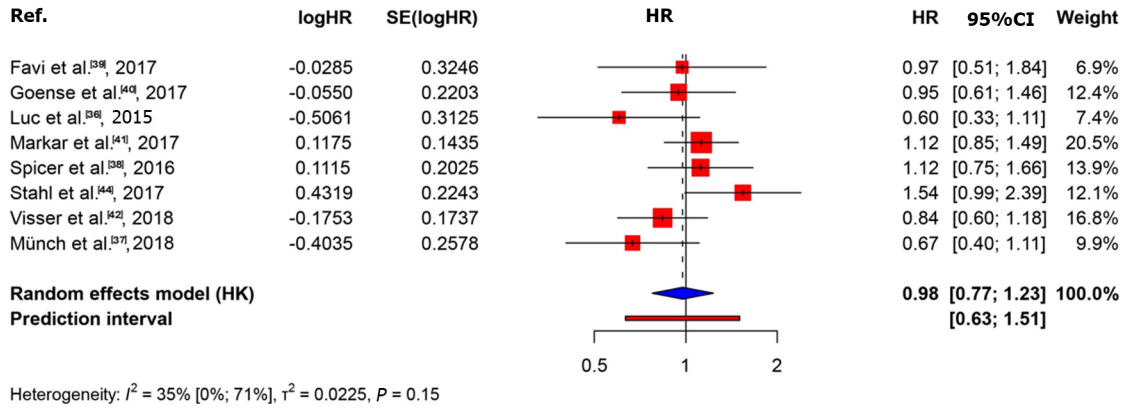

Figure 5 Pooled hazard ratio analysis of the overall mortality. HR: Hazard ratio; HK: Hoffman-Kringle random effect model.

Considering the 36-month DFS, the OR was 0.96 (95%CI: 0.4-2.28)[36,38,42]. No significant difference was observed between the two groups (P = 0.846). The between-study heterogeneity was 0.05 (95%CI: 0-0.9) was calculated (Supplementary Figure 17). The log HR analysis revealed no significant differences between the groups (Supplementary Figure 18).

Considering the 48-month DFS, the OR was 1.04 (95%CI: 0.31-3.51)[36,38,42]. No significant difference was observed between the two groups (P = 0.904). The between-study heterogeneity was 0.32 (95%CI: 0-0.93; Supplementary Figure 19). The log HR analysis revealed no significant differences between the groups (Supplementary Figure 20).

Considering the 60-month DFS, the OR was 1.04 (95%CI: 0.3-3.64)[36,38,42]. No significant difference was observed between the two groups (P = 0.913). The between-study heterogeneity was 0.32 (95%CI: 0-0.93) between the groups (Supplementary Figure 21).

Progression-free survival

For the 12-month progression-free survival (PFS), three studies including 340 patients were selected for analysis[40,43,44]. The OR was 0.73 (95%CI: 0.47-1.16). No statistically significant was observed difference between the two groups (P = 0.101). The between-study heterogeneity was 0 (95%CI: 0-0.9; Supplementary Figure 22).

Considering the 24-month PFS, the OR was 0.78 (95%CI: 0.1-6.18)[40,43,44]. No significant difference was observed between the two groups (P = 0.652). The between-study heterogeneity was 0.72 (95%CI: 0.04-0.92; Supplementary Figure 23).

Considering the 36-month PFS, the OR was 1.04 (95%CI: 0.1-11.05)[40,43,44]. No significant difference was observed between the two groups (P = 0.946). The between-study heterogeneity was 0.81 (95%CI: 0.39-0.94; Supplementary Figure 24).

Locoregional recurrence

Data from six studies including 1037 patients were analyzed, revealing locoregional recurrence in 12% of the patients[36,37,41-44]. The OR was 0.98 (95%CI: 0.35-2.77). No significant difference was observed between the two groups (P = 0.966). The between-study heterogeneity was 0.76 (95%CI: 0.47-0.89; Supplementary Figure 25).

Distant metastasis recurrence

Data from five studies including 910 patients were analyzed, revealing distal metastasis recurrence in 39% of the patients [37,41-44]. The OR was 1.12 (95%CI: 0.76-1.64). No significant difference was observed between the two groups (P = 0.462). The between-study heterogeneity was 0 (95%CI: 0-0.79; Supplementary Figure 26).

Thromboembolism events

Data from four studies including 818 patients were analyzed for the occurrence of thromboembolism events[35,40,42,43]. The OR was 1.93 (95%CI: 0.1-38.65). No significant difference was observed between the two groups (P = 0.535). The between-study heterogeneity was 0.72 (95%CI: 0.22-0.90; Supplementary Figure 27).

Cardiac complications

Data from seven studies including 1580 patients were analyzed for the occurrence of cardiac complications[35,36,38,40-43]. The OR was 0.8 (95%CI: 0.42-1.52). No significant difference between the two groups (P = 0.425). The between-study heterogeneity was 0.46 (95%CI: 0-0.77; Supplementary Figure 28).

Respiratory complications

Data from seven studies including 1580 patients were analyzed for the occurrence of respiratory complications[35,36,38,40-43]. The OR was 1.04 (95%CI: 0.66-1.64). No significant difference was observed between the two groups (P = 0.835). The between-study heterogeneity was 0.59 (95%CI: 0.04-0.82; Supplementary Figure 29).

Renal failure

Data from three studies including 650 patients were analyzed for the occurrence of renal failure[35,42,43]. The OR was 2.43 (95%CI: 1.12-5.28). A statistically significant difference was observed, favoring nCT over nCRT (P = 0.039). The between-study heterogeneity was 0 (95%CI: 0-0.9; Supplementary Figure 30).

Neutropenia

Data from three studies including 560 patients were analyzed for the occurrence of neutropenia[35,40,43]. The OR was 0.97 (95%CI: 0.09-10.29). No significant difference was observed between the two groups (P = 0.964). The between-study heterogeneity was 0.47 (95%CI: 0-0.84; Supplementary Figure 31).

Anastomotic leakage

Data from seven studies including 1580 patients were analyzed for the occurrence of anastomotic leakage[35,36,38,40-43]. The OR was 0.83 (95%CI: 0.41-1.68). No significant difference was observed between the two groups (P = 0.539). The between-study heterogeneity was 0.75 (95%CI: 0.48-0.88; Supplementary Figure 32).

Chyle leakage

Data from six studies including 1366 patients were analyzed for the occurrence of chyle leakage[35,36,40-43]. The OR was 0.99 (95%CI: 0.61-1.61). No significant difference was observed between the two groups (P = 0.961). The between-study heterogeneity was 0 (95%CI: 0.48-0.75; Supplementary Figure 33).

Wound infection

Data from five studies including 1022 patients were analyzed for the occurrence of wound infection[35,38,40,42,43]. The OR was 1.04 (95%CI: 0.36-3.02). No significant difference was observed between the two groups (P = 0.930). The between-study heterogeneity was 0.37 (95%CI: 0-0.76; Supplementary Figure 34).

Bleeding

Data from four studies including 849 patients were analyzed for the occurrence of bleeding[35,36,40,42]. The OR was 1.4 (95%CI: 0.425-7.79). No statistically significant difference was observed between the two groups (P = 0.581). The between-study heterogeneity was 0 (95%CI: 0-0.85; Supplementary Figure 35).

Vocal cord paresis

Data from three studies including 733 patients were analyzed for the occurrence of vocal cord paresis[35,40,42]. The OR was 1.21 (95%CI: 0.04-41.98). No significant difference was observed between the two groups (P = 0.537). The between-study heterogeneity was 0.5 (95%CI: 0-0.85; Supplementary Figure 36).

Leukopenia

Two studies including 485 patients were selected for descriptive analyses[35,40]. Leukopenia occurred in 8% and 12% of the patients in the nCT and nCRT groups, respectively.

Anemia

Two studies including 485 patients were selected for descriptive analyses[35,40]. Anemia occurred in 1% and 0.4% of the patients in the nCT and nCRT groups, respectively.

Nausea or vomiting

Three studies including 560 patients were selected for descriptive analyses[35,40,43]. Nausea or vomiting occurred in 9% and 3% of the patients in the nCT and nCRT groups, respectively.

Diarrhea

Two studies including 485 patients were selected for descriptive analyses[35,40]. Diarrhea occurred in 7% in the nCT group, whereas no cases were noted in the nCRT group.

Hospital stay

Two studies including 430 patients were selected for descriptive analyses[40,42]. The estimated mean hospital stay was 20 (range: 7-97) d in the nCT group and 18 (range: 7-75) d in the nCRT group.

Risk of bias

As we expected, the two RCTs demonstrated a low risk of bias. However, for other included trials, ROB2 indicated some concerns, mainly due to the randomization process (D1). In one trial, concerns were noted regarding the measurement process due to the utilization of a plot digitizer[17]. No instance of high risk of bias was identified across the included studies. Additional information is presented in Table 3.

GRADE approach

Employing the GRADE approach, our findings were determined to have low certainty for most outcomes; moderate certainty for 30-d mortality; very low certainty for 12-month OS, 36-month PFS, and the occurrence of thromboembolism events. The use of RoB2 indicated a moderate risk for all outcomes. High heterogeneity was reported for 36-month PFS and the occurrence of thromboembolic events. Imprecision was observed for pCR and 12-month OS. Additionally, a high variation in oncological treatments decreased the evidence quality, whereas a large effect size increased the quality of pCR and 30-d mortality[49] (Supplementary Table 4).

DISCUSSION

The benefits of neoadjuvant therapy have been previously reported[7-9]. Previous meta-analyses have examined the amplification of nCT and chemoradiotherapy in patients with AC or SCC. In the nCRT group, advantages were observed in terms of 3-year survival with R0 resection; however, the pCR rate had no effect on long-term survival. Perioperative mortality and cardiovascular complications are more common in patients with AC in the nCRT group[50]. A previous network meta-analysis showed that triplet-based chemotherapy increases overall survival and DFS in cases of AC of the stomach or GEJ[51].

pCR is defined as the lack of tumor in the resected specimen or lymph nodes (pT0 pN0 cM0)[15,36]. The 5-year survival rate is presumably 88% in patients with pCR compared to 39% in those without pCR[15,52]. According to a recent investigation comparing the long-term survival of the total population and patients with TRG grade 1-2 who underwent nCT or chemoradiotherapy before surgery revealed that tumor regression after neoadjuvant treatment is significantly associated with long-term survival, regardless of the treatment regimen[53]. Another retrospective cohort study revealed improved OS and DFS in patients who achieved pCR following nCT compared to those who achieved a lower rate of pCR following nCRT. The authors found a significant association between TRG and survival in both the groups. Additionally, patients who achieved pCR in the nCRT group did not have as good a survival rate as those in the nCT group, although their proportion was higher in the nCRT group. This finding suggests that esophageal AC should be considered a systemic disease and treated accordingly[53,54]. However, other trials have reported that a larger number of patients who achieved pCR do not have improved overall survival[55]. In this meta-analysis, we found a significantly higher pCR in the nCRT group; however, no differences were found in OS, DFS, or PFS, consistent with the findings of previous meta-analyses[50,55]. Based on this finding, we inferred that there is no association between pCR and OS; therefore, the use of pCR as a prognostic factor should be considered in cases of AC. These findings aligned with those of Gebauer *et al*'s study[56] reporting that high pCR after CROSS regimen is not clearly associated with longer overall survival[56]. Another study concluded that only clinically complete response without nodal metastasis is associated with

Table 3 Results using the risk of bias tool 2

Ref.	D1	D2	D3	D4	D5	Overall
Stahl *et al*[44], 2017	+	+	+	+	+	+
Burmeister *et al*[43], 2011	+	+	+	+	+	+
Visser *et al*[42], 2018	!	+	+	+	+	!
Markar *et al*[41], 2017	!	+	+	+	+	!
Goense *et al*[40], 2017	!	+	+	+	+	!
Favi *et al*[39], 2017	!	+	+	+	+	!
Anderegg *et al*[35], 2017	!	+	+	+	+	!
Spicer *et al*[38], 2016	!	+	+	+	+	!
Luc *et al*[36], 2015	!	+	+	+	+	!
Münch *et al*[37], 2018	!	+	+	!	+	!

+: Low risk; !: Some concerns; -: High risk. D1: Randomization process; D2: Deviation from the intended interventions; D3: Missing outcome data; D4: Measurement of the outcome; D5: Selection of the reported result.

long-term survival; therefore, the "watch-and-wait," strategies should be considered carefully and applied only to patients who have achieved pCR[57]. The utility of pCR as a prognostic indicator of neoadjuvant therapy remains questionable, indicating the need for large number of randomized studies in the future.

Our analysis revealed that none of the investigated groups were superior considering local recurrence, which aligns with the findings of a previous meta-analysis[50]. This indicates that the higher local control provided by radiotherapy does not reduce the incidence of local recurrence. Additionally, we did not detect a significant difference in terms of metastases, which occurred in 39% of the cases compared to 12% of local recurrence cases, suggesting that AC should be treated as a systematic disease, and therefore, the "watch-and-wait" strategies should be considered critically.

Our findings revealed a significantly higher 30-d mortality risk in the chemoradiotherapy group. This can be attributed to complications arising in the postoperative period. However, differences in the outcomes of surgical complications were not noted, consistent with the findings of a previous meta-analysis, in which no difference was reported in anastomotic leakage[50]. Additionally, a previous meta-analysis reported a higher risk of mortality in the postoperative period among patients with AC. Therefore, further investigation into the effects of nCRT on postoperative complications is warranted [50]. We only performed descriptive analysis, which revealed a comparable duration of postoperative hospitalization in both the groups[40,42].

We observed no difference in any of the clinical complications in both the groups; however, a previous meta-analysis reported a higher risk of cardiovascular complications in the nRCT group than in the nCT group, which could be a toxic side effect of this modality.

nCT and radiotherapy are also associated with adverse events, including thromboembolic events, neutropenia, leukopenia, anemia, nausea or vomiting, and diarrhea[35]. Renal failure occurred more often in the nCT group than in the nCRT group, indicating a toxic side effect of nCT. However, no difference was reported in terms of cardiac failure, in contrast to a former meta-analysis[50]. According to previous investigations, neutropenia is not associated with either neoadjuvant treatment modality. In the descriptive analysis, leukopenia occurred 4% more frequently in the nCRT group than in the nCT group, making them more vulnerable to developing infections. Additionally, a low number of anemia cases was observed in both the groups. The quality of life can be assessed using the EORTC QLQ-C30 questionnaire[58], which includes encompasses side effects including nausea, vomiting, and diarrhea. Notably, these side effects occurred approximately 7% more frequently in the nCT group than in the nCRT group.

Our meta-analysis provides the most comprehensive and recent summary of the data, particularly focusing on patients with esophageal AC. In addition, various outcomes were analyzed in a sufficient number of patients. The data from this study accurately reflect the esophageal AC population. No significant differences in demographic characteristics were reported between patients of the two groups.

Nevertheless, our study has some limitations. Deviating from the protocol, we included propensity score-matched studies and cohort trials, which are less reliable than RCTs and have potentially significant biases. Additionally, all trials were conducted in Western countries, reflecting a characteristic of AC, thus limiting the generalizability of the results to the Asian population or other countries. The use of various neoadjuvant regimens and some the lack of separation between preoperative and perioperative therapies in some included studies also pose some limitations. Furthermore, the evidence for most outcomes was deemed low; therefore, the true effect may differ substantially from the estimate.

In summary, one might question the lack of impact of radiotherapy on overall survival, despite improvements in measures of pathological regression, known to correlate with survival. This discrepancy can be attributed to modification of these crucial measures by local therapy. In the context of modern surgical techniques, the systemic component of the disease is the primary determinant of survival in esophageal and gastroesophageal junction ACs. Hence, the incorporation of systemic chemotherapy, new immunotherapies, and targeted treatments capable of addressing distant

diseases holds greater potential to enhance patient survival in the future.

CONCLUSION

In patients with esophageal AC, neoadjuvant chemoradiation increases pCR and 30-d mortality; however, it has no effect on long-term survival. nCT may be associated with side effects that can decrease the quality of life. Further randomized trials are required to address the limitations in the quality of the available studies.

ARTICLE HIGHLIGHTS

Research background

The incidence of adenocarcinoma (AC) in the esophagus is increasing, especially in the Western countries, in contrast to the incidence of squamous cell carcinomas (SCC). Neoadjuvant therapy before surgery can improve patient survival in advanced stages. The superiority of neoadjuvant modalities, especially for ACs, remains unclear. Previous meta-analyses have numerous limitations, including the pooled populations of AC and SCC, which makes the application of their results specifically to either subtype difficult.

Research motivation

The superiority of neoadjuvant therapy has been proven previously; however, determining which modality has a greater benefit, especially for esophageal AC, remains uncertain. In this study, we performed a comprehensive, up-to-date investigation to compare the efficacy of neoadjuvant chemotherapy (nCT) and neoadjuvant chemoradiotherapy (nCRT) in the surgical treatment of AC of the esophagus and esophageal junction.

Research objectives

To address the questions of this meta-analysis, we used the PICO protocol to evaluate data from patients with esophageal or cardiac AC, who underwent neoadjuvant therapy before surgery. Intervention was preoperative nCT, which was compared with nCRT. We investigated the following outcomes: Survival, remission rate, mortality, short- and long-term clinical and surgical complications, and quality of life.

Research methods

Following the PICO protocol, two authors independently performed a comprehensive search of multiple databases using the predefined criteria. Statistical analyses were performed by biostatisticians to calculate odds ratio and hazard ratio with the 95%CI. Results were visualized using forest plots and Kaplan-Meier curves. The Risk of Bias Tool 2 and GRADE approach were used to assess the quality of the results.

Research results

Ten articles were included after selection. After statistical analysis, we observed that 30-d mortality (P = 0.015) and pathological complete response (P < 0.001) were higher in the nCRT group than in the nCT group; however, no significant difference was observed for long-term survival. The risk of renal failure (P = 0.039) was higher in the nCT group, and the incidence of nausea or vomiting was 9% in the nCT group compared to 3% in the nCRT group. No significant difference was reported in other clinical or surgical complications.

Research conclusions

Although the superiority of neoadjuvant therapy has been previously demonstrated, nCRT may increase pathological complete response and 30-d mortality, without improving long-term survival. Furthermore, nCT may lead to some adverse effects, which can decrease the quality of life.

Research perspectives

The present study predominantly analyzed retrospective data, potentially introducing research bias; therefore, future randomized studies with more detailed data collection are warranted.

FOOTNOTES

Author contributions: Csontos A contributed to the design and implementation of the study and the writing of the manuscript; Fazekas A and Farkas N contributed to the statistical analyses and the writing of the manuscript; Szakó L contributed to the design of the study and the revision of the manuscript; Papp C and Ferenczi S contributed to the performance of the research; Bellyei S and Hegyi P contributed to the quality and professional revision; Papp A contributed to the quality and professional revision and the writing of the manuscript.

Conflict-of-interest statement: All the authors report no relevant conflicts of interest for this article.

PRISMA 2009 Checklist statement: The authors have read the PRISMA 2009 Checklist, and the manuscript was prepared and revised according to the PRISMA 2009 Checklist.

Country/Territory of origin: Hungary

ORCID number: Armand Csontos 0000-0002-0204-0642; Lajos Szakó 0000-0001-9783-4076; Nelli Farkas 0000-0002-5349-6527; Péter Hegyi 0000-0003-0399-7259; András Papp 0000-0002-2845-531X.

S-Editor: Li L
L-Editor: A
P-Editor: Cai YX

REFERENCES

1 **Liu CQ**, Ma YL, Qin Q, Wang PH, Luo Y, Xu PF, Cui Y. Epidemiology of esophageal cancer in 2020 and projections to 2030 and 2040. *Thorac Cancer* 2023; **14**: 3-11 [PMID: 36482832 DOI: 10.1111/1759-7714.14745]
2 **Tinusz B**, Szapáry LB, Paládi B, Papp A, Bogner B, Hegedűs I, Bellyei S, Vincze Á, Solt J, Micsik T, Dunás-Varga V, Pályu E, Vass T, Schnabel T, Farkas N, Hegyi P, Thrift AP, Erőss B. The Esophageal Adenocarcinoma Epidemic Has Reached Hungary: A Multicenter, Cross-Sectional Study. *Front Oncol* 2020; **10**: 541794 [PMID: 33425714 DOI: 10.3389/fonc.2020.541794]
3 **Rice TW**, Patil DT, Blackstone EH. 8th edition AJCC/UICC staging of cancers of the esophagus and esophagogastric junction: application to clinical practice. *Ann Cardiothorac Surg* 2017; **6**: 119-130 [PMID: 28447000 DOI: 10.21037/acs.2017.03.14]
4 **Liu F**, Wang W, Wang C, Peng X. Enhanced recovery after surgery (ERAS) programs for esophagectomy protocol for a systematic review and meta-analysis. *Medicine (Baltimore)* 2018; **97**: e0016 [PMID: 29465538 DOI: 10.1097/MD.0000000000010016]
5 **Sindler DL**, Mátrai P, Szakó L, Berki D, Berke G, Csontos A, Papp C, Hegyi P, Papp A. Faster recovery and bowel movement after early oral feeding compared to late oral feeding after upper GI tumor resections: a meta-analysis. *Front Surg* 2023; **10**: 1092303 [PMID: 37304183 DOI: 10.3389/fsurg.2023.1092303]
6 **Szakó L**, Németh D, Farkas N, Kiss S, Dömötör RZ, Engh MA, Hegyi P, Eross B, Papp A. Network meta-analysis of randomized controlled trials on esophagectomies in esophageal cancer: The superiority of minimally invasive surgery. *World J Gastroenterol* 2022; **28**: 4201-4210 [PMID: 36157121 DOI: 10.3748/wjg.v28.i30.4201]
7 **van Hagen P**, Hulshof MC, van Lanschot JJ, Steyerberg EW, van Berge Henegouwen MI, Wijnhoven BP, Richel DJ, Nieuwenhuijzen GA, Hospers GA, Bonenkamp JJ, Cuesta MA, Blaisse RJ, Busch OR, ten Kate FJ, Creemers GJ, Punt CJ, Plukker JT, Verheul HM, Spillenaar Bilgen EJ, van Dekken H, van der Sangen MJ, Rozema T, Biermann K, Beukema JC, Piet AH, van Rij CM, Reinders JG, Tilanus HW, van der Gaast A; CROSS Group. Preoperative chemoradiotherapy for esophageal or junctional cancer. *N Engl J Med* 2012; **366**: 2074-2084 [PMID: 22646630 DOI: 10.1056/NEJMoa1112088]
8 **Cunningham D**, Allum WH, Stenning SP, Thompson JN, Van de Velde CJ, Nicolson M, Scarffe JH, Lofts FJ, Falk SJ, Iveson TJ, Smith DB, Langley RE, Verma M, Weeden S, Chua YJ, MAGIC Trial Participants. Perioperative chemotherapy *vs* surgery alone for resectable gastroesophageal cancer. *N Engl J Med* 2006; **355**: 11-20 [PMID: 16822992 DOI: 10.1056/NEJMoa055531]
9 **Ychou M**, Boige V, Pignon JP, Conroy T, Bouché O, Lebreton G, Ducourtieux M, Bedenne L, Fabre JM, Saint-Aubert B, Genève J, Lasser P, Rougier P. Perioperative chemotherapy compared with surgery alone for resectable gastroesophageal adenocarcinoma: an FNCLCC and FFCD multicenter phase III trial. *J Clin Oncol* 2011; **29**: 1715-1721 [PMID: 21444866 DOI: 10.1200/JCO.2010.33.0597]
10 **Allum WH**, Stenning SP, Bancewicz J, Clark PI, Langley RE. Long-term results of a randomized trial of surgery with or without preoperative chemotherapy in esophageal cancer. *J Clin Oncol* 2009; **27**: 5062-5067 [PMID: 19770374 DOI: 10.1200/JCO.2009.22.2083]
11 **Ronellenfitsch U**, Schwarzbach M, Hofheinz R, Kienle P, Kieser M, Slanger TE, Burmeister B, Kelsen D, Niedzwiecki D, Schuhmacher C, Urba S, van de Velde C, Walsh TN, Ychou M, Jensen K. Preoperative chemo(radio)therapy *vs* primary surgery for gastroesophageal adenocarcinoma: systematic review with meta-analysis combining individual patient and aggregate data. *Eur J Cancer* 2013; **49**: 3149-3158 [PMID: 23800671 DOI: 10.1016/j.ejca.2013.05.029]
12 **Ronellenfitsch U**, Schwarzbach M, Hofheinz R, Kienle P, Kieser M, Slanger TE, Jensen K; GE Adenocarcinoma Meta-analysis Group. Perioperative chemo(radio)therapy *vs* primary surgery for resectable adenocarcinoma of the stomach, gastroesophageal junction, and lower esophagus. *Cochrane Database Syst Rev* 2013; CD008107 [PMID: 23728671 DOI: 10.1002/14651858.CD008107.pub2]
13 **Schuhmacher C**, Gretschel S, Lordick F, Reichardt P, Hohenberger W, Eisenberger CF, Haag C, Mauer ME, Hasan B, Welch J, Ott K, Hoelscher A, Schneider PM, Bechstein W, Wilke H, Lutz MP, Nordlinger B, Van Cutsem E, Siewert JR, Schlag PM. Neoadjuvant chemotherapy compared with surgery alone for locally advanced cancer of the stomach and cardia: European Organisation for Research and Treatment of Cancer randomized trial 40954. *J Clin Oncol* 2010; **28**: 5210-5218 [PMID: 21060024 DOI: 10.1200/JCO.2009.26.6114]
14 **Sjoquist KM**, Burmeister BH, Smithers BM, Zalcberg JR, Simes RJ, Barbour A, Gebski V; Australasian Gastro-Intestinal Trials Group. Survival after neoadjuvant chemotherapy or chemoradiotherapy for resectable oesophageal carcinoma: an updated meta-analysis. *Lancet Oncol* 2011; **12**: 681-692 [PMID: 21684205 DOI: 10.1016/S1470-2045(11)70142-5]
15 **Stahl M**, Walz MK, Stuschke M, Lehmann N, Meyer HJ, Riera-Knorrenschild J, Langer P, Engenhart-Cabillic R, Bitzer M, Königsrainer A, Budach W, Wilke H. Phase III comparison of preoperative chemotherapy compared with chemoradiotherapy in patients with locally advanced adenocarcinoma of the esophagogastric junction. *J Clin Oncol* 2009; **27**: 851-856 [PMID: 19139439 DOI: 10.1200/JCO.2008.17.0506]
16 **National Institute for Health and Care Research**. PROSPERO is fast-tracking registration of protocols related to COVID-19. [cited 23

February 2024]. Available from: https://www.crd.york.ac.uk/prospero/
17 **Plotdigitizer**. All-in-One Tool to Extract Data from Graphs, Plots & Images. [cited 23 February 2024]. Available from: https://plotdigitizer.com/app
18 **Guyot P**, Ades AE, Ouwens MJ, Welton NJ. Enhanced secondary analysis of survival data: reconstructing the data from published Kaplan-Meier survival curves. *BMC Med Res Methodol* 2012; **12**: 9 [PMID: 22297116 DOI: 10.1186/1471-2288-12-9]
19 **WebPlotDigitizer**. Extract data from XY charts, Bar graphs, Polar diagrams and much more! [cited 23 February 2024]. Available from: https://automeris.io/WebPlotDigitizer/
20 **Higgins JP**, Thompson SG. Quantifying heterogeneity in a meta-analysis. *Stat Med* 2002; **21**: 1539-1558 [PMID: 12111919 DOI: 10.1002/sim.1186]
21 **Harbord RM**, Harris RJ, Sterne JAC. Updated tests for small-study effects in meta-analyses. *The Stata Journal: Promoting Communications on Statistics and Stata* 2009; **9**: 197-210 [DOI: 10.1177/1536867X0900900202]
22 **Harrer M**, Cuijpers P, Toshi F, Ebert DD. Doing meta-analysis with R: a hands-on guide. 1st ed. New York: Chapman and Hall/CRC Press, 2021 [DOI: 10.1201/9781003107347]
23 **R Core Team**. R: a language and environment for statistical computing. Vienna, Austria: R Foundation for Statistical Computing. 2023. [cited 23 February 2024]. Available from: https://www.R-project.org/
24 **Schwarzer G**. Meta-Analysis in R. In: Systematic Reviews in Health Research: Meta-Analysis in Context, 3rd Ed. Egger M, Higgins JPT, Smith GD, editors. New York: John Wiley & Sons, 2022 [DOI: 10.1002/9781119099369.ch26]
25 **Cuijpers P**, Furukawa T, Ebert DD. Dmetar: companion R package for the guide doing meta-analysis in R. 2022. [cited 23 February 2024]. Available from: https://dmetar.protectlab.org
26 **Mantel N**, Haenszel W. Statistical aspects of the analysis of data from retrospective studies of disease. *J Natl Cancer Inst* 1959; **22**: 719-748 [PMID: 13655060]
27 **Robins J**, Greenland S, Breslow NE. A general estimator for the variance of the Mantel-Haenszel odds ratio. *Am J Epidemiol* 1986; **124**: 719-723 [PMID: 3766505 DOI: 10.1093/oxfordjournals.aje.a114447]
28 **Cooper HM**, Hedges LV, Valentine JC. The handbook of research synthesis and meta-analysis. 2nd ed. New York: Russell Sage Foundation, 2009
29 **Sweeting MJ**, Sutton AJ, Lambert PC. What to add to nothing? Use and avoidance of continuity corrections in meta-analysis of sparse data. *Stat Med* 2004; **23**: 1351-1375 [PMID: 15116347 DOI: 10.1002/sim.1761]
30 **Knapp G**, Hartung J. Improved tests for a random effects meta-regression with a single covariate. *Stat Med* 2003; **22**: 2693-2710 [PMID: 12939780 DOI: 10.1002/sim.1482]
31 **IntHout J**, Ioannidis JP, Borm GF. The Hartung-Knapp-Sidik-Jonkman method for random effects meta-analysis is straightforward and considerably outperforms the standard DerSimonian-Laird method. *BMC Med Res Methodol* 2014; **14**: 25 [PMID: 24548571 DOI: 10.1186/1471-2288-14-25]
32 **Paule RC**, Mandel J. Consensus Values and Weighting Factors. *J Res Natl Bur Stand (1977)* 1982; **87**: 377-385 [PMID: 34566088 DOI: 10.6028/jres.087.022]
33 **Veroniki AA**, Jackson D, Viechtbauer W, Bender R, Bowden J, Knapp G, Kuss O, Higgins JP, Langan D, Salanti G. Methods to estimate the between-study variance and its uncertainty in meta-analysis. *Res Synth Methods* 2016; **7**: 55-79 [PMID: 26332144 DOI: 10.1002/jrsm.1164]
34 **Shinyapps**. Estimating the sample mean and standard deviation. [cited 23 February 2024]. Available from: https://smcgrath.shinyapps.io/estmeansd
35 **Anderegg MCJ**, van der Sluis PC, Ruurda JP, Gisbertz SS, Hulshof MCCM, van Vulpen M, Mohammed NH, van Laarhoven HWM, Wiezer MJ, Los M, van Berge Henegouwen MI, van Hillegersberg R. Preoperative Chemoradiotherapy Versus Perioperative Chemotherapy for Patients With Resectable Esophageal or Gastroesophageal Junction Adenocarcinoma. *Ann Surg Oncol* 2017; **24**: 2282-2290 [PMID: 28424936 DOI: 10.1245/s10434-017-5827-1]
36 **Luc G**, Vendrely V, Terrebonne E, Chiche L, Collet D. Neoadjuvant chemoradiotherapy improves histological results compared with perioperative chemotherapy in locally advanced esophageal adenocarcinoma. *Ann Surg Oncol* 2015; **22**: 604-609 [PMID: 25169119 DOI: 10.1245/s10434-014-4005-y]
37 **Münch S**, Habermehl D, Agha A, Belka C, Combs SE, Eckel R, Friess H, Gerbes A, Nüssler NC, Schepp W, Schmid RM, Schmitt W, Schubert-Fritschle G, Weber B, Werner J, Engel J. Perioperative chemotherapy vs. neoadjuvant chemoradiation in gastroesophageal junction adenocarcinoma: A population-based evaluation of the Munich Cancer Registry. *Strahlenther Onkol* 2018; **194**: 125-135 [PMID: 29071366 DOI: 10.1007/s00066-017-1225-7]
38 **Spicer JD**, Stiles BM, Sudarshan M, Correa AM, Ferri LE, Altorki NK, Hofstetter WL. Preoperative Chemoradiation Therapy Versus Chemotherapy in Patients Undergoing Modified En Bloc Esophagectomy for Locally Advanced Esophageal Adenocarcinoma: Is Radiotherapy Beneficial? *Ann Thorac Surg* 2016; **101**: 1262-9; discussion 1969 [PMID: 26916717 DOI: 10.1016/j.athoracsur.2015.11.070]
39 **Favi F**, Bollschweiler E, Berlth F, Plum P, Hescheler DA, Alakus H, Semrau R, Celik E, Mönig SP, Drebber U, Hölscher AH. Neoadjuvant chemotherapy or chemoradiation for patients with advanced adenocarcinoma of the oesophagus? A propensity score-matched study. *Eur J Surg Oncol* 2017; **43**: 1572-1580 [PMID: 28666624 DOI: 10.1016/j.ejso.2017.06.003]
40 **Goense L**, van der Sluis PC, van Rossum PSN, van der Horst S, Meijer GJ, Haj Mohammad N, van Vulpen M, Mook S, Ruurda JP, van Hillegersberg R. Perioperative chemotherapy *vs* neoadjuvant chemoradiotherapy for esophageal or GEJ adenocarcinoma: A propensity score-matched analysis comparing toxicity, pathologic outcome, and survival. *J Surg Oncol* 2017; **115**: 812-820 [PMID: 28267212 DOI: 10.1002/jso.24596]
41 **Markar SR**, Noordman BJ, Mackenzie H, Findlay JM, Boshier PR, Ni M, Steyerberg EW, van der Gaast A, Hulshof MCCM, Maynard N, van Berge Henegouwen MI, Wijnhoven BPL, Reynolds JV, Van Lanschot JJB, Hanna GB. Multimodality treatment for esophageal adenocarcinoma: multi-center propensity-score matched study. *Ann Oncol* 2017; **28**: 519-527 [PMID: 28039180 DOI: 10.1093/annonc/mdw560]
42 **Visser E**, Edholm D, Smithers BM, Thomson IG, Burmeister BH, Walpole ET, Gotley DC, Joubert WL, Atkinson V, Mai T, Thomas JM, Barbour AP. Neoadjuvant chemotherapy or chemoradiotherapy for adenocarcinoma of the esophagus. *J Surg Oncol* 2018; **117**: 1687-1696 [PMID: 29806960 DOI: 10.1002/jso.25089]
43 **Burmeister BH**, Thomas JM, Burmeister EA, Walpole ET, Harvey JA, Thomson DB, Barbour AP, Gotley DC, Smithers BM. Is concurrent radiation therapy required in patients receiving preoperative chemotherapy for adenocarcinoma of the oesophagus? A randomised phase II trial. *Eur J Cancer* 2011; **47**: 354-360 [PMID: 21084184 DOI: 10.1016/j.ejca.2010.09.009]

44 **Stahl M**, Walz MK, Riera-Knorrenschild J, Stuschke M, Sandermann A, Bitzer M, Wilke H, Budach W. Preoperative chemotherapy *vs* chemoradiotherapy in locally advanced adenocarcinomas of the oesophagogastric junction (POET): Long-term results of a controlled randomised trial. *Eur J Cancer* 2017; **81**: 183-190 [PMID: 28628843 DOI: 10.1016/j.ejca.2017.04.027]

45 **Alderson D**, Langley RE, Nankivell MG, Blazeby JM, Griffin M, Crellin A, Grabsch HI, Okines AFC, Goldstein C, Falk S, Thompson J, Krysztopik R, Coxon FY, Pritchard S, Langer R, Stenning SP, Cunningham D. Neoadjuvant chemotherapy for resectable oesophageal and junctional adenocarcinoma: results from the UK Medical Research Council randomised OEO5 trial (ISRCTN 01852072). *J Clin Oncol* 2015; **33**: Abstr 4002 [DOI: 10.1200/jco.2015.33.15_suppl.4002]

46 **Shapiro J**, van Lanschot JJB, Hulshof MCCM, van Hagen P, van Berge Henegouwen MI, Wijnhoven BPL, van Laarhoven HWM, Nieuwenhuijzen GAP, Hospers GAP, Bonenkamp JJ, Cuesta MA, Blaisse RJB, Busch ORC, Ten Kate FJW, Creemers GM, Punt CJA, Plukker JTM, Verheul HMW, Bilgen EJS, van Dekken H, van der Sangen MJC, Rozema T, Biermann K, Beukema JC, Piet AHM, van Rij CM, Reinders JG, Tilanus HW, Steyerberg EW, van der Gaast A; CROSS study group. Neoadjuvant chemoradiotherapy plus surgery *vs* surgery alone for oesophageal or junctional cancer (CROSS): long-term results of a randomised controlled trial. *Lancet Oncol* 2015; **16**: 1090-1098 [PMID: 26254683 DOI: 10.1016/S1470-2045(15)00040-6]

47 **Lorenzen S**, Pauligk C, Homann N, Schmalenberg H, Jäger E, Al-Batran SE. Feasibility of perioperative chemotherapy with infusional 5-FU, leucovorin, and oxaliplatin with (FLOT) or without (FLO) docetaxel in elderly patients with locally advanced esophagogastric cancer. *Br J Cancer* 2013; **108**: 519-526 [PMID: 23322206 DOI: 10.1038/bjc.2012.588]

48 **Ferri LE**, Ades S, Alcindor T, Chasen M, Marcus V, Hickeson M, Artho G, Thirlwell MP. Perioperative docetaxel, cisplatin, and 5-fluorouracil (DCF) for locally advanced esophageal and gastric adenocarcinoma: a multicenter phase II trial. *Ann Oncol* 2012; **23**: 1512-1517 [PMID: 22039085 DOI: 10.1093/annonc/mdr465]

49 **Kirmayr M**, Quilodrán C, Valente B, Loezar C, Garegnani L, Franco JVA. The GRADE approach, Part 1: how to assess the certainty of the evidence. *Medwave* 2021; **21**: e8109 [PMID: 33830974 DOI: 10.5867/medwave.2021.02.8109]

50 **Han J**, Wang Z, Liu C. Survival and complications after neoadjuvant chemotherapy or chemoradiotherapy for esophageal cancer: a meta-analysis. *Future Oncol* 2021; **17**: 2257-2274 [PMID: 33739165 DOI: 10.2217/fon-2021-0021]

51 **Grizzi G**, Petrelli F, Di Bartolomeo M, Viti M, Texeira Moraes M, Luciani A, Passalacqua R, Ghidini M, Tomasello G, Baiocchi GL, Celotti A. Preferred neoadjuvant therapy for gastric and gastroesophageal junction adenocarcinoma: a systematic review and network meta-analysis. *Gastric Cancer* 2022; **25**: 982-987 [PMID: 35704113 DOI: 10.1007/s10120-022-01314-9]

52 **Barbour AP**, Jones M, Gonen M, Gotley DC, Thomas J, Thomson DB, Burmeister B, Smithers BM. Refining esophageal cancer staging after neoadjuvant therapy: importance of treatment response. *Ann Surg Oncol* 2008; **15**: 2894-2902 [PMID: 18663531 DOI: 10.1245/s10434-008-0084-y]

53 **Sciuto M**, Capovilla G, Scarton A, Tagkalos E, Uzun E, Moletta L, Hadzijusufoviç Edin, Provenzano L, Salvador R, Pierobon E, Zanchettin G, Berlth F, Lang H, Grimminger P, Valmasoni M. 462. Major pathologic response in esophageal adenocarcinoma: should we adopt a new paradigm in defining response to treatments? *Diseases of the Esophagus* 2003; **36** [DOI: 10.1093/dote/doad052.246]

54 **Scarton A**, Capovilla G, Tagkalos E, Uzun E, Moletta L, Hadzijusufoviç E, Provenzano L, Salvador R, Pierobon E, Zanchettin G, Berlth F, Grimminger P, Valmasoni M. 463. The impact of pathological tumor response following neoadjuvant chemotherapy and chemoradiotherapy for esophageal adenocarcinoma. A retrospective multicenter cohort study. *Diseases of the Esophagus* 2003; **36** [DOI: 10.1093/dote/doad052.247]

55 **Klevebro F**, Alexandersson von Döbeln G, Wang N, Johnsen G, Jacobsen AB, Friesland S, Hatlevoll I, Glenjen NI, Lind P, Tsai JA, Lundell L, Nilsson M. A randomized clinical trial of neoadjuvant chemotherapy *vs* neoadjuvant chemoradiotherapy for cancer of the oesophagus or gastro-oesophageal junction. *Ann Oncol* 2016; **27**: 660-667 [PMID: 26782957 DOI: 10.1093/annonc/mdw010]

56 **Gebauer F**, Plum PS, Damanakis A, Chon SH, Popp F, Zander T, Quaas A, Fuchs H, Schmidt T, Schröder W, Bruns CJ. Long-Term Postsurgical Outcomes of Neoadjuvant Chemoradiation (CROSS) Versus Chemotherapy (FLOT) for Multimodal Treatment of Adenocarcinoma of the Esophagus and the Esophagogastric Junction. *Ann Surg Oncol* 2023; **30**: 7422-7433 [PMID: 37210683 DOI: 10.1245/s10434-023-13643-9]

57 **Schroeder W**, Ghadimi MPH, Schloesser H, Loeser H, Schiller P, Zander T, Gebauer F, Fuchs H, Quaas A, Bruns CJ. Long-Term Outcome After Histopathological Complete Response with and Without Nodal Metastases Following Multimodal Treatment of Esophageal Cancer. *Ann Surg Oncol* 2022 [PMID: 35403919 DOI: 10.1245/s10434-022-11700-3]

58 **Adenis A**, Kulkarni AS, Girotto GC, de la Fouchardiere C, Senellart H, van Laarhoven HWM, Mansoor W, Al-Rajabi R, Norquist J, Amonkar M, Suryawanshi S, Bhagia P, Metges JP. Impact of Pembrolizumab Versus Chemotherapy as Second-Line Therapy for Advanced Esophageal Cancer on Health-Related Quality of Life in KEYNOTE-181. *J Clin Oncol* 2022; **40**: 382-391 [PMID: 34730989 DOI: 10.1200/JCO.21.00601]

World Journal of Gastroenterology

Submit a Manuscript: https://www.f6publishing.com

World J Gastroenterol 2024 March 21; 30(11): 1636-1643

DOI: 10.3748/wjg.v30.i11.1636

ISSN 1007-9327 (print) ISSN 2219-2840 (online)

CASE REPORT

Myocardial metastasis from ZEB1- and TWIST-positive spindle cell carcinoma of the esophagus: A case report

Yoshihiro Shibata, Hirofumi Ohmura, Kazuki Komatsu, Kosuke Sagara, Atsuji Matsuyama, Ryuji Nakano, Eishi Baba

Specialty type: Gastroenterology and hepatology

Provenance and peer review: Unsolicited article; Externally peer reviewed.

Peer-review model: Single blind

Peer-review report's scientific quality classification

Grade A (Excellent): 0
Grade B (Very good): B
Grade C (Good): 0
Grade D (Fair): 0
Grade E (Poor): 0

P-Reviewer: Huang LQ, China

Received: January 19, 2024
Peer-review started: January 19, 2024
First decision: January 31, 2024
Revised: February 2, 2024
Accepted: March 7, 2024
Article in press: March 7, 2024
Published online: March 21, 2024

Yoshihiro Shibata, Kosuke Sagara, Department of Medical Oncology, Fukuoka Wajiro Hospital, Fukuoka 811-0213, Japan

Hirofumi Ohmura, Eishi Baba, Department of Oncology and Social Medicine, Kyushu University Graduate School of Medical Sciences, Fukuoka 812-8582, Japan

Kazuki Komatsu, Department of Pathology and Oncology, University of Occupational and Environmental Health, Kitakyushu 807-8555, Japan

Atsuji Matsuyama, Ryuji Nakano, Department of Diagnostic Pathology, Fukuoka Wajiro Hospital, Fukuoka 811-0213, Japan

Corresponding author: Eishi Baba, MD, PhD, Professor, Department of Oncology and Social Medicine, Kyushu University Graduate School of Medical Sciences, 3-1-1 Maidashi, Higashi-ku, Fukuoka 812-8582, Japan. baba.eishi.889@m.kyushu-u.ac.jp

Abstract

BACKGROUND

Metastatic cardiac tumors are known to occur more frequently than primary cardiac tumors, however, they often remain asymptomatic and are commonly discovered on autopsy. Malignant tumors with a relatively high frequency of cardiac metastasis include mesothelioma, melanoma, lung cancer, and breast cancer, whereas reports of esophageal cancer with cardiac metastasis are rare.

CASE SUMMARY

The case of a 60-year-old man who complained of dysphagia is presented. Upper gastrointestinal endoscopy showed a submucosal tumor-like elevated lesion in the esophagus causing stenosis. Contrast-enhanced computed tomography showed left atrial compression due to the esophageal tumor, multiple liver and lung metastases, and a left pleural effusion. Pathological examination of a biopsy specimen from the esophageal tumor showed spindle-shaped cells, raising suspicion of esophageal sarcoma. The disease progressed rapidly, and systemic chemotherapy was deemed necessary, however, due to his poor general condition, administration of cytotoxic agents was considered difficult. Given his high Combined Positive Score, nivolumab was administered, however, the patient soon died from the disease. The autopsy confirmed spindle cell carcinoma (SCC) of the esophagus and cardiac metastasis with similar histological features. Cancer stem cell markers, ZEB1 and TWIST, were positive in both the primary tumor and the

cardiac metastasis.

CONCLUSION
To the best of our knowledge, there have been no prior reports of cardiac metastasis of esophageal SCC. This case highlights our experience with a patient with esophageal SCC who progressed rapidly and died from the disease, with the autopsy examination showing cardiac metastasis.

Key Words: Spindle cell carcinoma; Esophagus; Myocardial metastasis; Epithelial-mesenchymal transition; Case report

Core Tip: Spindle cell carcinoma (SCC) is rare, accounting for about 0.1%-1.5% of esophageal cancers. Tumor cells show sarcomatoid differentiation with spindle cells and are accompanied by components of conventional carcinoma including squamous cell carcinoma in some cases. Many of cardiac metastatic tumors are asymptomatic and are typically discovered through pathological autopsy, with metastatic cardiac tumors being identified in 2% to 18% of cancer patients undergoing autopsy. There has been no report of cardiac metastasis in esophageal SCC.

Citation: Shibata Y, Ohmura H, Komatsu K, Sagara K, Matsuyama A, Nakano R, Baba E. Myocardial metastasis from ZEB1- and TWIST-positive spindle cell carcinoma of the esophagus: A case report. *World J Gastroenterol* 2024; 30(11): 1636-1643
URL: https://www.wjgnet.com/1007-9327/full/v30/i11/1636.htm
DOI: https://dx.doi.org/10.3748/wjg.v30.i11.1636

INTRODUCTION

Cardiac tumors are classified into primary tumors, originating within the heart, and metastatic tumors from other organs. Primary cardiac tumors include benign tumors, represented by myxoma, and malignant tumors, including sarcomas and lymphomas. Primary cardiac tumors are extremely rare, with prevalence rates ranging from 0.001% to 0.3% in autopsy studies. Furthermore, the proportion of malignant tumors among primary cardiac tumors is approximately 10%. On the other hand, metastatic cardiac tumors are much more frequent than primary cardiac tumors, with an estimated occurrence rate that is approximately 20 to 40 times higher. Many of these cases remain asymptomatic and are typically discovered on autopsy, with metastatic cardiac tumors being identified in 2% to 18% of cancer patients undergoing autopsy examination[1-3]. Excluding direct infiltration from adjacent organs, the mechanisms of cardiac metastasis are considered to include lymphatic or hematogenous metastasis, as well as composite types. In cases with cardiac metastasis, 69.4% had pericardial metastasis, 34.2% had epicardial metastasis, 31.8% had myocardial metastasis, and endocardial metastasis was uncommon, at 5%. Malignant tumors reported to have a relatively high frequency of cardiac metastasis include malignant pleural mesothelioma, melanoma, lung cancer, and breast cancer, however, reports of cardiac metastasis in esophageal cancer are rare[2]. Spindle cell carcinoma (SCC) is rare, accounting for about 0.1%-1.5% of esophageal cancers. Tumor cells show sarcomatoid differentiation with spindle cells and are accompanied by components of conventional carcinoma, including squamous cell carcinoma in some cases. There are reports of a high frequency of lymphatic metastasis and of a higher frequency of hematogenous metastasis[4].

The efficacy of 5-fluorouracil + cisplatin + anti-programmed cell death 1 antibody (nivolumab or pembrolizumab) and anti-programmed cell death 1 antibody + anti- cytotoxic T lymphocyte-associated antigen-4 antibody (nivolumab + ipilimumab) as first-line treatment has been demonstrated for metastatic/recurrent esophageal squamous cell carcinoma and adenocarcinoma, and they are standard treatments[5,6]. However, a standard treatment for advanced SCC has not been established. There have been no previous reports of myocardial metastasis from esophageal SCC. A case of esophageal SCC with rapid disease progression leading to death that showed myocardial metastasis on autopsy is presented.

CASE PRESENTATION

Chief complaints

A 60-year-old man was admitted to our hospital with complaints of difficulty in swallowing and left chest pain.

History of present illness

The patient had a 6-month history of persistent, worsening difficulty in swallowing since December 2023.

History of past illness
The patient had no significant history.

Personal and family history
Mother of the patient had the history of uterine cancer.

Physical examination
The patient showed a poor general condition, with Eastern Comprehensive Oncology Group Performance Status (ECOG PS 3).

Laboratory examinations
Blood tests showed preserved bone marrow, liver, and kidney functions, without coagulation abnormalities. Serum levels of tumor markers (carcinoembryonic antigen, SCC) were not increased.

Imaging examinations
Upper gastrointestinal endoscopy showed a submucosal tumor-like protruding lesion, occupying nearly the entire lumen from the mid to lower thoracic esophagus, causing stenosis (Figure 1). Contrast-enhanced computed tomography (CT) showed esophageal tumor invasion into the left atrium, multiple liver and lung metastases, and a left pleural effusion (Figure 2). The biopsy specimen of the esophageal tumor showed spindle cells, positive for the mesenchymal marker vimentin and negative for epithelial markers including AE1/AE3, CAM5.2, p40, and cytokeratin 7, leading to a suspicion of esophageal sarcoma, and the patient was referred to our hospital for treatment. Cardiac ultrasonography showed a tumorous lesion on the posterior side of the left atrium, however, no invasion into the heart or intramyocardial tumor was observed. Chest X-ray and ultrasonography showed a pleural effusion, and thoracentesis was performed to alleviate symptoms and make a diagnosis, draining 1000 mL of slightly turbid, bloody pleural fluid. However, chest X-ray the next day showed re-accumulation of pleural fluid to the same degree as before drainage. Upper gastrointestinal endoscopy allowed passage of a slim scope, and biopsy of the primary lesion was performed. Histopathologically, atypical spindle cells and polymorphic cells, however, no epithelial components, were observed and immunohistological staining was negative for AE1/AE3, CAM5.2, cytokeratin 5/6, and p63, similar to the previous pathological report; thus, an epithelial malignant tumor could not be confirmed. The programmed death-ligand 1 Combined Positive Score (CPS) was ≥ 10. Pleural fluid cytology showed malignant cells, and cell block immunostaining showed similar findings to those of the primary lesion. Cancer stem cell markers including ZEB1 and TWIST were positive in both the primary and metastatic cardiac lesions (Figure 3).

FINAL DIAGNOSIS
Histopathologically, advanced esophageal squamous cell carcinoma or non-small round cell sarcoma was considered.

TREATMENT
Disease progression was aggressive; thus, systemic chemotherapy for advanced esophageal squamous cell carcinoma or non-small round cell sarcoma was considered, however, it was deemed infeasible due to the patient's poor general condition (ECOG PS 3). Expecting efficacy of nivolumab monotherapy given the high CPS, administration of nivolumab was started in January 2023.

OUTCOME AND FOLLOW-UP
However, on the day of administration of nivolumab, the patient lost consciousness, developed lower jaw breathing, and then developed respiratory and cardiac arrest resulting in death. Pathological autopsy examination was performed with the prior written, informed consent from the patient and family to investigate the cause of death. In the pathological autopsy examination, A whitish, protruding lesion was observed from the mid to lower esophagus, mainly on the lateral to posterior walls, bulging into the lumen with severe stenosis of the esophageal lumen. Histologically, atypical epithelioid cells were densely proliferating with poor cohesion admixed with spindle cells and pleomorphic cells. Numerous mitotic figures were observed. The presence of an area considered to be carcinoma in situ at the border between tumor and non-tumor areas in the anterior and lateral esophageal walls, and partial positivity of the atypical cells for AE1/AE3 and cytokeratin 5/6 on immunohistochemistry, along with negative smooth muscle actin, desmin, c-kit, and no other distinct differentiation, led to a diagnosis of spindle cell squamous cell carcinoma arising from esophageal squamous cell carcinoma. The mediastinal lymph nodes were fused into a single mass by tumor metastases, with indistinct original nodal structures. Widespread tumor metastasis was observed in both lungs and the liver, accompanied by marked vascular invasion. In addition to a 15 mm × 12 mm nodular lesion in the left ventricular lateral wall, microscopic metastases were also observed in the left ventricular lateral and posterior walls and interventricular

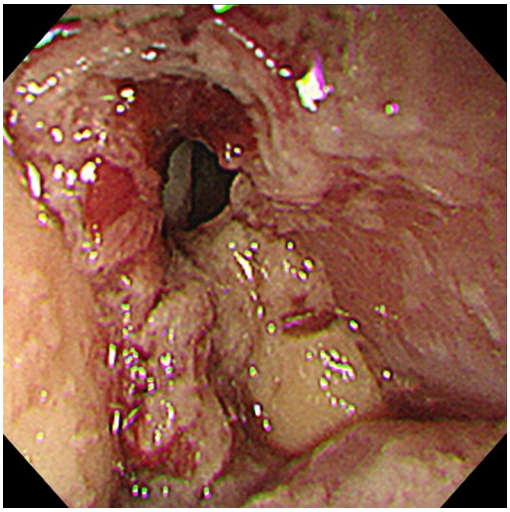

Figure 1 Imaging of primary lesion by upper gastrointestinal endoscopy. Upper gastrointestinal endoscopy shows a submucosal tumor-like protruding lesion occupying nearly the entire lumen from the mid to lower thoracic esophagus, causing stenosis.

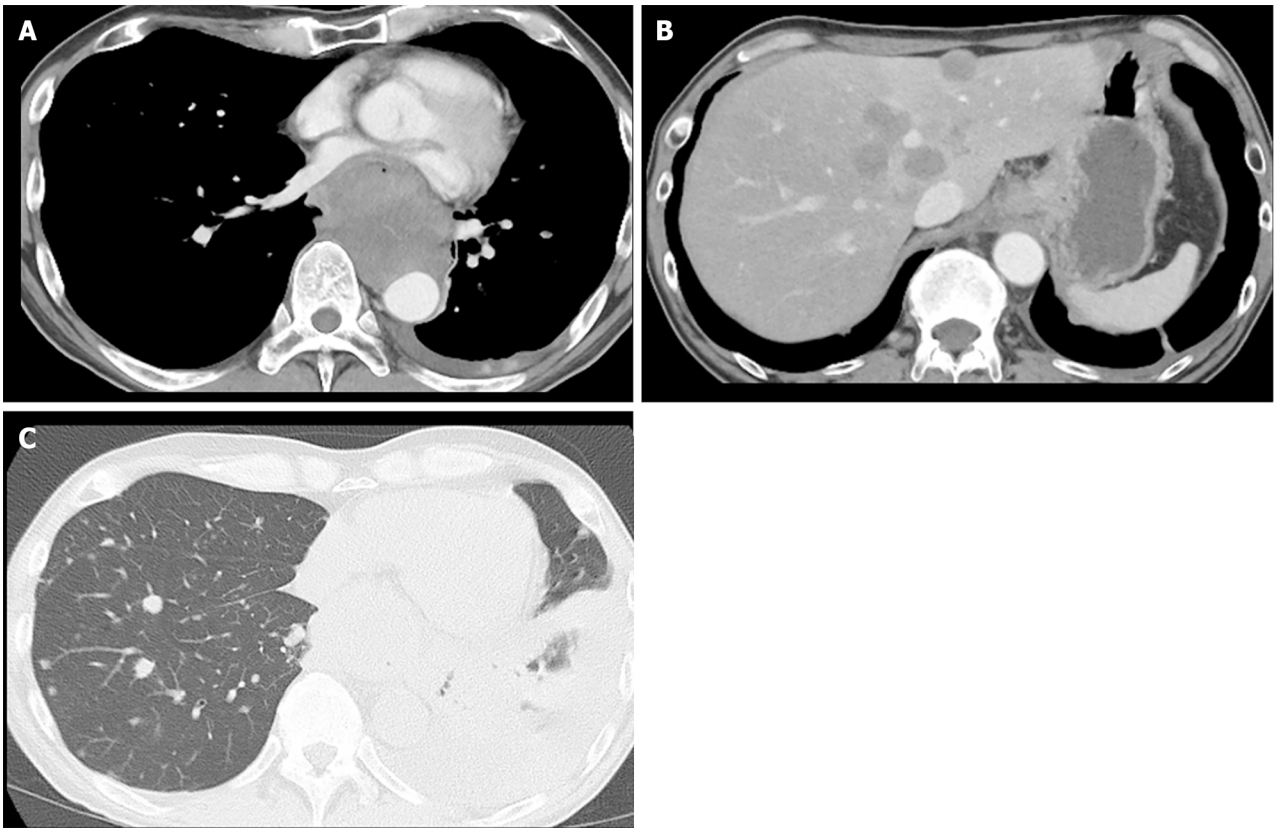

Figure 2 Imaging of primary and metastatic lesions by computed tomography. A: Contrast-enhanced computed tomography shows left atrial compression due to the esophageal tumor; B: Multiple liver metastases; C: Multiple lung metastases and left pleural effusion.

septum. Histologically, pleomorphic to spindle-shaped atypical cells with hyperchromatic nuclei, distinct nucleoli, and eosinophilic cytoplasm showed poorly cohesive proliferation, often admixed with polymorphic cells. There was no major histological difference between the primary and metastatic lesions. Numerous disseminated nodules were also observed in the left pleural cavity, with accumulation of a bloody pleural effusion. Death was ascribed to multi-organ tumor metastases, with respiratory failure due to pleural effusion also potentially contributing as a cause of death (Figure 4).

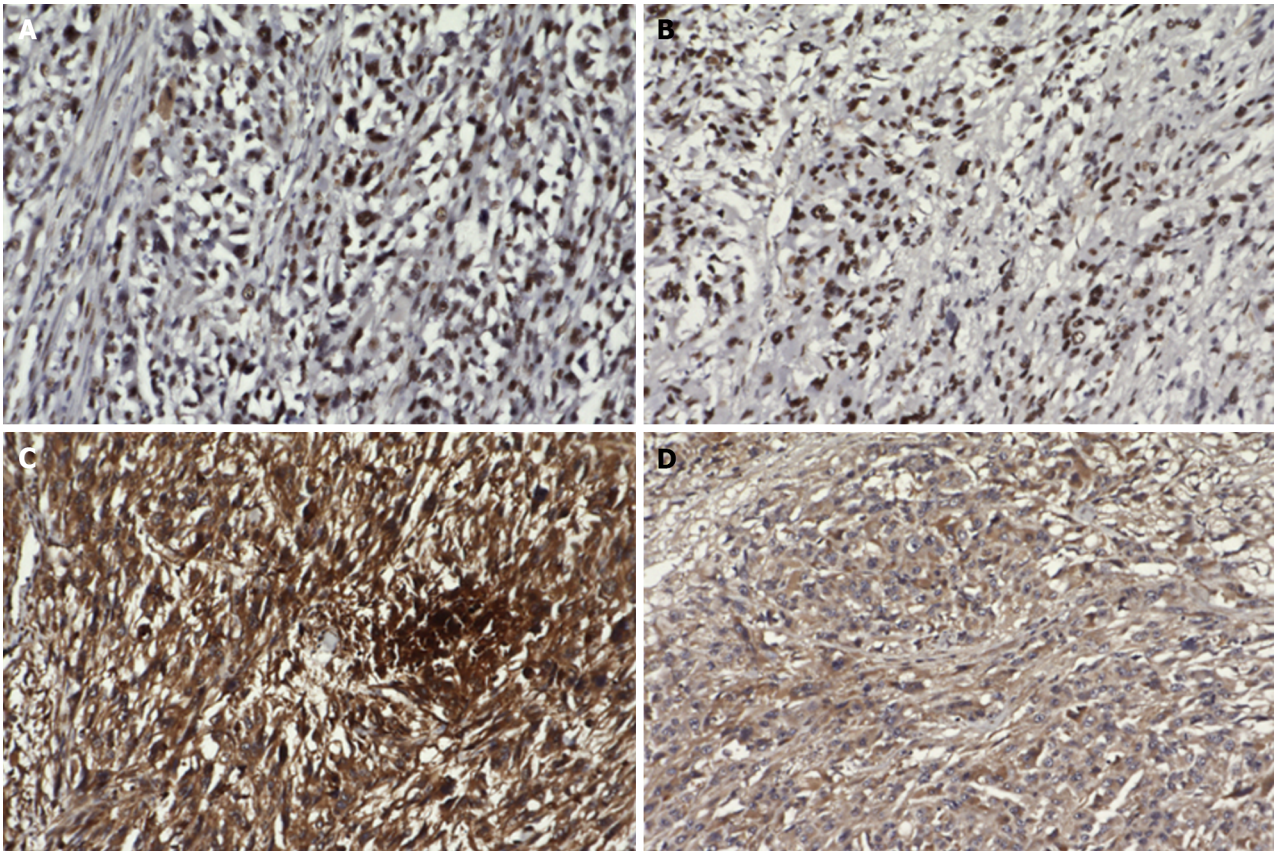

Figure 3 ZEB1 and TWIST in primary and metastatic cardiac lesions. Cancer stem cell markers ZEB1 and TWIST are immunohistologically positive in both the primary and metastatic cardiac lesions. A: ZEB1 staining of the primary lesion; B: ZEB1 staining of the cardiac lesion; C: TWIST staining of primary lesion; D: TWIST staining of the cardiac lesion.

DISCUSSION

Cardiac metastasis occurs more often than primary cardiac tumors. In an autopsy study of 18751 cases, malignant tumors were identified in 7289 cases, of which 622 (9.1%) had cardiac metastases[2]. The most common metastases to the pericardium are from mesothelioma, lung cancer, uterine cancer, gastric cancer, and prostate cancer. Metastases to the epicardium are most common from melanoma, squamous cell carcinoma, and adenocarcinoma of the lung. Myocardial metastases occur most often from melanoma and hematological malignancies, whereas endocardial metastases are most common from melanoma, renal cell carcinoma, and hepatocellular carcinoma. In a study of 111 autopsies of esophageal cancer patients, epicardial metastases were found in 13%, and no myocardial metastases or endocardial metastases were identified[7]. Besides direct invasion, the mechanisms of cardiac metastasis are thought to include lymphatic spread, hematogenous spread, and their combination. Pericardial metastases, excluding direct invasion from intrathoracic or mediastinal tumors, are considered to arise from retrograde lymphatic spread from the trachea and mediastinal lymph nodes. Myocardial metastases and epicardial metastases may result from lymphatic spread and seeding from pericardial metastases. Hematogenous spread *via* the coronary arteries also contributes to myocardial metastases. In the present case, direct invasion and pericardial metastases were absent, and myocardial metastasis due to hematogenous spread was presumed.

SCC often shows positivity for vimentin and p53 on immunohistochemistry, whereas the epithelial component is frequently positive for pan cytokeratin (AE1/AE3). Li *et al*[8] reported that, in 23.2% of cases of primary esophageal SCC, both the spindle cells and the epithelial cells were positive for AE1/AE3, and in 8.5% of cases, both components were also positive for vimentin. In the present case, AE1/AE3 expression was limited to only a small portion, with loss of epithelial characteristics in the majority, suggesting difficulty in making a definitive diagnosis on biopsy. ZEB1 and TWIST positivity in primary esophageal SCC has been reported, implicating the epithelial-mesenchymal transition in its pathogenesis. Both the primary and metastatic cardiac tumors in the present case were positive for ZEB1 and TWIST[9]. To the best of our knowledge, this is the first analysis of these molecules in the rare occurrence of cardiac metastasis from primary esophageal SCC.

A previous report showed that primary esophageal SCC had a better prognosis than squamous cell carcinoma[10]. SCC often forms intraluminal protruding lesions, leading to early symptoms of dysphagia, which may account for its detection at an early stage. It is usually diagnosed as early cancer, with a lower frequency of lymph node metastasis. Iyomasa *et al*[11] compared 20 cases of carcinosarcoma to 773 cases of squamous cell carcinoma, reporting 3-year survival rates of 62.8% *vs* 28.1%, however, similar 5-year survival rates of 26.7% *vs* 22.4%, respectively[11]. Most cases are diagnosed and surgically resected before developing distant metastases, and surgery remains the only curative treatment of SCC. Other

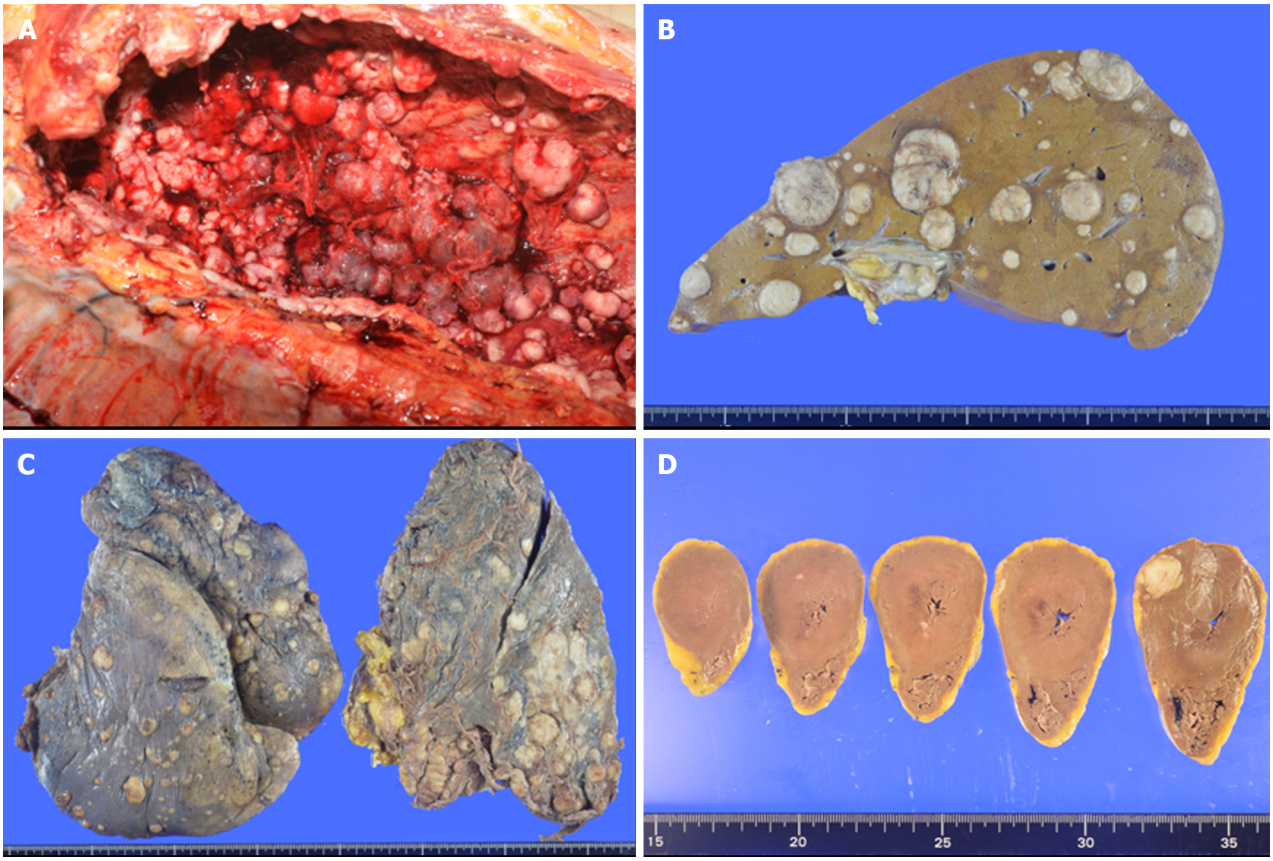

Figure 4 Autopsy examination findings. A: Numerous disseminated nodules are observed in the left pleural cavity; B: Multiple metastases in the liver; C: Multiple metastases in the lung; D: Multiple metastases in the heart.

therapies including radiation and chemotherapy have been reported, however, the roles of radiation therapy and chemotherapy are unclear because of insufficient evidence. Schizas *et al*[12] reported that perioperative chemotherapy did not improve survival. Iwaya *et al*[13] described failure to control tumor progression with radiation therapy. In contrast, Sanada *et al*[14] reported tumor shrinkage with chemoradiation. Yamauchi *et al*[15] observed tumor reduction with chemoradiotherapy followed by rapid regrowth, speculating that the squamous component responded to the therapy, however, the sarcomatous component did not[12-15]. In the present case, biopsy pathology and the cell block of pleural fluid showed no epithelial component, suggesting sarcoma, and carcinosarcoma could not be ruled out. Standard therapy for sarcoma with doxorubicin alone or doxorubicin + ifosfamide could not be administered due to the patient's poor general condition. A high CPS has been associated with response to immune checkpoint inhibitors (ICIs) in several cancers[16-18], and the CPS was greater than 10 in the present case, and a response to ICI therapy was expected. However, the disease progressed rapidly, and the patient died before a response to ICI therapy could be obtained. Although death on the day of ICI administration raises the possibility of a drug-related event, the patient's vital signs were normal at the time of administration, without signs of allergy or anaphylaxis. Autopsy findings of rapid tumor progression and widespread dissemination support cancer death as the cause. Cardiac metastases are often asymptomatic and found incidentally on postmortem examination. Fluorodeoxyglucose positron emission tomography/CT has also shown asymptomatic myocardial metastases prior to death[19]. When symptomatic, widespread metastases to other sites are usually present, and death more commonly results from metastases elsewhere rather than the cardiac metastasis. However, pericardial metastases can cause cardiac tamponade requiring emergency drainage[20]. Myocardial metastases may cause symptoms mimicking myocardial infarction[21]. Endocardial metastasis causing an intracavitary cardiac mass from esophageal cancer has been resected to prevent sudden death and potentially prolong survival[22,23]. In the present case, the patient died before response assessment, and myocardial metastasis was found at autopsy, however, it did not appear to cause symptoms or affect prognosis.

CONCLUSION

Myocardial metastasis from esophageal cancer is rare, and among esophageal cancers, SCC is uncommon, so its metastatic patterns are unclear with no prior reports of myocardial metastasis. This report presents the first case of myocardial metastasis from ZEB1- and TWIST-positive esophageal SCC and characterizes its immunohistochemical profile.

ACKNOWLEDGEMENTS

The authors are grateful to the patient for granting us permission for this case report.

FOOTNOTES

Author contributions: Shibata Y, Ohmura H, and Baba E contributed to the design of the report and drafted the manuscript; Komatsu K, Sagara K, Matsuyama A, and Nakano R critically revised the manuscript.

Informed consent statement: Written, informed consent was obtained from the patient's next of kin for publication of the details of the patient's medical case and any accompanying images.

Conflict-of-interest statement: Hirofumi Ohmura has received speakers' bureau from Ono Pharmaceutical; Eishi Baba has received honoraria from Ono Pharmaceutical and Bristol-Myers Squibb; All other authors have no conflicts of interest to report.

CARE Checklist (2016) statement: The authors have read CARE Checklist (2016), and the manuscript was prepared and revised according to CARE Checklist (2016).

Country/Territory of origin: Japan

ORCID number: Hirofumi Ohmura 0000-0003-4650-9120; Eishi Baba 0000-0001-9428-6772.

S-Editor: Li L
L-Editor: A
P-Editor: Cai YX

REFERENCES

1 **Glancy DL**, Roberts WC. The heart in malignant melanoma. A study of 70 autopsy cases. *Am J Cardiol* 1968; **21**: 555-571 [PMID: 5650736 DOI: 10.1016/0002-9149(68)90289-0]
2 **Centofanti P**, Di Rosa E, Deorsola L, Dato GM, Patanè F, La Torre M, Barbato L, Verzini A, Fortunato G, di Summa M. Primary cardiac tumors: early and late results of surgical treatment in 91 patients. *Ann Thorac Surg* 1999; **68**: 1236-1241 [PMID: 10543485 DOI: 10.1016/S0003-4975(99)00700-6]
3 **Silverman NA**. Primary cardiac tumors. *Ann Surg* 1980; **191**: 127-138 [PMID: 7362282 DOI: 10.1097/00000658-198002000-00001]
4 **Raza MA**, Mazzara PF. Sarcomatoid carcinoma of esophagus. *Arch Pathol Lab Med* 2011; **135**: 945-948 [PMID: 21732788 DOI: 10.5858/2010-0074-RSR.1]
5 **Sun JM**, Shen L, Shah MA, Enzinger P, Adenis A, Doi T, Kojima T, Metges JP, Li Z, Kim SB, Cho BC, Mansoor W, Li SH, Sunpaweravong P, Maqueda MA, Goekkurt E, Hara H, Antunes L, Fountzilas C, Tsuji A, Oliden VC, Liu Q, Shah S, Bhagia P, Kato K; KEYNOTE-590 Investigators. Pembrolizumab plus chemotherapy versus chemotherapy alone for first-line treatment of advanced oesophageal cancer (KEYNOTE-590): a randomised, placebo-controlled, phase 3 study. *Lancet* 2021; **398**: 759-771 [PMID: 34454674 DOI: 10.1016/S0140-6736(21)01234-4]
6 **Doki Y**, Ajani JA, Kato K, Xu J, Wyrwicz L, Motoyama S, Ogata T, Kawakami H, Hsu CH, Adenis A, El Hajbi F, Di Bartolomeo M, Braghiroli MI, Holtved E, Ostoich SA, Kim HR, Ueno M, Mansoor W, Yang WC, Liu T, Bridgewater J, Makino T, Xynos I, Liu X, Lei M, Kondo K, Patel A, Gricar J, Chau I, Kitagawa Y; CheckMate 648 Trial Investigators. Nivolumab Combination Therapy in Advanced Esophageal Squamous-Cell Carcinoma. *N Engl J Med* 2022; **386**: 449-462 [PMID: 35108470 DOI: 10.1056/NEJMoa2111380]
7 **Mandard AM**, Chasle J, Marnay J, Villedieu B, Bianco C, Roussel A, Elie H, Vernhes JC. Autopsy findings in 111 cases of esophageal cancer. *Cancer* 1981; **48**: 329-335 [PMID: 6453643 DOI: 10.1002/1097-0142(19810715)48:2<329::AID-CNCR2820480219>3.0.CO;2-V]
8 **Li XM**, Song X, Zhao XK, Hu SJ, Cheng R, Lv S, Du DF, Zhang XY, Lu JL, Ku JW, Zhang DY, Zhang Y, Fan ZM, Wang LD. The alterations of cytokeratin and vimentin protein expressions in primary esophageal spindle cell carcinoma. *BMC Cancer* 2018; **18**: 356 [PMID: 29609569 DOI: 10.1186/s12885-018-4301-1]
9 **Nakazawa T**, Nobusawa S, Ikota H, Kuwano H, Takeyoshi I, Yokoo H. Wide expression of ZEB1 in sarcomatous component of spindle cell carcinoma of the esophagus. *Pathol Int* 2015; **65**: 635-643 [PMID: 26515382 DOI: 10.1111/pin.12354]
10 **McCort JJ**. Esophageal carcinosarcoma and pesudosarcoma. *Radiology* 1972; **102**: 519-524 [PMID: 5060153 DOI: 10.1148/102.3.519]
11 **Iyomasa S**, Kato H, Tachimori Y, Watanabe H, Yamaguchi H, Itabashi M. Carcinosarcoma of the esophagus: a twenty-case study. *Jpn J Clin Oncol* 1990; **20**: 99-106 [PMID: 2319703]
12 **Schizas D**, Mastoraki A, Bagias G, Ioannidi M, Kanavidis P, Moris D, Tsilimigras DI, Spartalis E, Arkadopoulos N, Liakakos T. Carcinosarcomas of the esophagus: systematic review of a rare nosologic entity. *J BUON* 2018; **23**: 1432-1438 [PMID: 30570870]
13 **Iwaya T**, Maesawa C, Uesugi N, Kimura T, Ogasawara S, Ikeda K, Kimura Y, Mitomo S, Ishida K, Sato N, Saito K, Masuda T. True carcinosarcoma of the esophagus. *Dis Esophagus* 2006; **19**: 48-52 [PMID: 16364045 DOI: 10.1111/j.1442-2050.2006.00538.x]

14 **Sanada Y**, Hihara J, Yoshida K, Yamaguchi Y. Esophageal carcinosarcoma with intramural metastasis. *Dis Esophagus* 2006; **19**: 119-131 [PMID: 16643182 DOI: 10.1111/j.1442-2050.2006.00551.x]

15 **Yamauchi T**, Taniyama Y, Fujishima F, Sasano H, Unno M, Kamei T. Rapidly growing carcinosarcoma of the esophagus following definitive chemoradiotherapy: A case report and the literature review. *Int J Surg Case Rep* 2022; **94**: 107116 [PMID: 35468385 DOI: 10.1016/j.ijscr.2022.107116]

16 **Ulas EB**, Hashemi SMS, Houda I, Kaynak A, Veltman JD, Fransen MF, Radonic T, Bahce I. Predictive Value of Combined Positive Score and Tumor Proportion Score for Immunotherapy Response in Advanced NSCLC. *JTO Clin Res Rep* 2023; **4**: 100532 [PMID: 37681219 DOI: 10.1016/j.jtocrr.2023.100532]

17 **Shin M**, Ahn S, Jung J, Hyung S, Kim KM, Kim ST, Kang WK, Lee J. Impact of programmed death-ligand 1 (PD-L1) positivity on clinical and molecular features of patients with metastatic gastric cancer. *Cancer Med* 2023; **12**: 18633-18642 [PMID: 37654198 DOI: 10.1002/cam4.6472]

18 **Burtness B**, Harrington KJ, Greil R, Soulières D, Tahara M, de Castro G Jr, Psyrri A, Basté N, Neupane P, Bratland Å, Fuereder T, Hughes BGM, Mesía R, Ngamphaiboon N, Rordorf T, Wan Ishak WZ, Hong RL, González Mendoza R, Roy A, Zhang Y, Gumuscu B, Cheng JD, Jin F, Rischin D; KEYNOTE-048 Investigators. Pembrolizumab alone or with chemotherapy versus cetuximab with chemotherapy for recurrent or metastatic squamous cell carcinoma of the head and neck (KEYNOTE-048): a randomised, open-label, phase 3 study. *Lancet* 2019; **394**: 1915-1928 [PMID: 31679945 DOI: 10.1016/S0140-6736(19)32591-7]

19 **Puranik AD**, Purandare NC, Sawant S, Agrawal A, Shah S, Jatale P, Rangarajan V. Asymptomatic myocardial metastasis from cancers of upper aero-digestive tract detected on FDG PET/CT: a series of 4 cases. *Cancer Imaging* 2014; **14**: 16 [PMID: 25608865 DOI: 10.1186/1470-7330-14-16]

20 **Kishino T**, Kumamoto K, Matsukawa H, Kondo A, Ando Y, Uemura J, Suto H, Asano E, Oshima M, Chiba Y, Ueno M, Nakagawa S, Kitamoto S, Yamashita Y, Horii T, Okano K. Constrictive pericarditis caused by pericardial metastasis from esophageal squamous cell carcinoma: a case report. *Int Cancer Conf J* 2022; **11**: 172-177 [PMID: 35669905 DOI: 10.1007/s13691-022-00543-0]

21 **Oliveira SM**, Gonçalves A, Cruz C, Almeida J, Madureira AJ, Amendoeira I, Maciel MJ. Cardiac metastasis from epidermoid esophageal cancer mimicking anterior myocardial infarction. *Rev Port Cardiol* 2012; **31**: 163-166 [PMID: 22222060 DOI: 10.1016/j.repc.2011.12.011]

22 **Yamazaki I**, Yanagi H, Goda M, Suzuki S, Masuda M. Isolated intracavitary metastatic esophageal cancer of the right atrium and right ventricle. *Jpn J Cardiovasc Surg* 2011; **40**: 310-313 [DOI: 10.4326/jjcvs.40.310]

23 **Kiryu K**, Kadohama T, Yamaura G, Chida Y, Tanaka F, Takagi D, Itagaki Y, Yamamoto H. Tumorectomy to avoid sudden death by pulmonary embolism in a patient with a cardiac tumor originating from the esophagus. *Jpn J Cardiovasc Surg* 2019; **48**: 170-172 [DOI: 10.4326/jjcvs.48.170]

Published by **Baishideng Publishing Group Inc**
7041 Koll Center Parkway, Suite 160, Pleasanton, CA 94566, USA
Telephone: +1-925-3991568
E-mail: office@baishideng.com
Help Desk: https://www.f6publishing.com/helpdesk
https://www.wjgnet.com